UNIVERSAL
LIBRARY

OU_164137

UNIVERSAL
LIBRARY

# DYNAMIC METEOROLOGY

By JÖRGEN HOLMBOE
GEORGE E. FORSYTHE
and WILLIAM GUSTIN

DEPARTMENT OF METEOROLOGY, UNIVERSITY OF CALIFORNIA AT LOS ANGELES

New York - JOHN WILEY AND SONS, INC.
London - CHAPMAN AND HALL, LIMITED

THIS BOOK HAS BEEN MANUFACTURED IN ACCORDANCE WITH THE RECOMMENDATIONS OF THE WAR PRODUCTION BOARD IN THE INTEREST OF THE CONSERVATION OF PAPER AND OTHER IMPORTANT WAR MATERIALS.

COPYRIGHT, 1945, BY
JÖRGEN HOLMBOE, WILLIAM SHARP GUSTIN,
AND GEORGE E. FORSYTHE

*All Rights Reserved*

*This book or any part thereof must not be reproduced in any form without the written permission of the publisher.*

PRINTED IN THE UNITED STATES OF AMERICA

# PREFACE

This book is intended as a basic textbook in theoretical meteorology for students who are preparing for a professional career in meteorology. It may be helpful to students of such applied sciences as geophysics, aerodynamics, and hydrology, and to students of various branches of pure physics.

The aim of the book is to provide the theoretical background for the understanding of the physical behavior of the atmosphere and its motions. Only material which is considered indispensable for the practical meteorologist and weather forecaster has been includ The book is self-contained and presupposes only some general knowledge of physics and calculus. Starting from the fundamental concepts of physics, it develops the thermodynamical and hydrodynamical principles by which atmospheric phenomena and the evolution of the weather may be explained.

The theory of atmospheric motion is most naturally and conveniently developed in vector notation. The methods of vector algebra and some simple operations of vector calculus are therefore consistently used. No previous knowledge of vector methods is assumed; the vector operations are introduced and explained gradually as the need arises as part of the general development of the subject.

Since the book is intended as a basic introduction to the subject, few references to original papers are given.

The book originated from my lectures on dynamic meteorology given at the Massachusetts Institute of Technology from 1936 to 1940 and at the University of California at Los Angeles after 1940. In the selection and organization of the material I have been greatly aided by studies pursued under Professor V. Bjerknes at Oslo University in 1926–30, and under Professor C.-G. Rossby during my years at the Massachusetts Institute of Technology. In connection with the extensive training programs for weather officers for the armed forces my two co-authors, Messrs. Forsythe and Gustin, joined the department as instructors in dynamic meteorology. During the subsequent joint instruction of the course by the three authors the earlier mimeographed lecture material was revised and reorganized several times, and much new material was added, before the final version of the book was written.

I am much indebted to Professor J. Bjerknes for his permission to

include in chapter 10 a large part of our joint paper, "On the Theory of Cyclones," *Journal of Meteorology*, Vol. 1, Nos. 1 and 2, 1944. I am also greatly obliged to Professor H. G. Houghton of the Massachusetts Institute of Technology, whose unpublished lecture material on meteorological thermodynamics was a great help when the first outline of chapters 2 and 3 was written.

On behalf of the three authors I wish to extend sincere thanks to all those friends who have given us help and encouragement in our work. We are very grateful to Professor J. Kaplan, former chairman of the meteorological department at the University of California at Los Angeles, for his unfailing support during the preparation of the manuscript and illustrations. We also are much indebted to Professor H. U. Sverdrup and Professor M. Neiburger, who have read parts of the manuscript and made many helpful suggestions.

JÖRGEN HOLMBOE

UNIVERSITY OF CALIFORNIA
AT LOS ANGELES
*January 1945*

# CONTENTS

PAGES

SYMBOLS AND CONSTANTS ..... ix–xvi

CHAPTER ONE. DIMENSIONS AND UNITS

1·01 The goal of dynamic meteorology. 1·02 The tools of dynamic meteorology. 1·03 The fundamental variables and their dimensions. 1·04 Mts units. 1·05 Comparison with cgs units. 1·06 Comparison with English units. 1·07 Pressure measurement and units..... 1–8

CHAPTER TWO. THERMODYNAMICS OF A PERFECT GAS

2·01 Thermodynamical systems. 2·02 The physical variables. 2·03 Volume. 2·04 Pressure. 2·05 Temperature. 2·06 Meteorological temperature scales. 2·07 Equation of state. 2·08 The perfect gas. 2·09 Equation of state of a perfect gas. 2·10 Molecular weights. 2·11 Universal gas constant. 2·12 Mixtures of perfect gases. 2·13 Molecular weight of dry air. 2·14 Work in thermodynamics. 2·15 $(\alpha,-p)$-diagram. 2·16 Isotherms of a perfect gas. 2·17 Heat. 2·18 The first law of thermodynamics. 2·19 Specific heats of gases. 2·20 Internal energy of a perfect gas. 2·21 Specific heats of a perfect gas. 2·22 Energy equations in logarithmic form. 2·23 Atmospheric processes. 2·24 Adiabatic processes of a perfect gas. 2·25 Adiabats on diagrams. 2·26 Potential temperature. 2·27 Differentials and functions of state. 2·28 Entropy. 2·29 Thermodynamic diagrams. 2·30 Important criteria of the diagram. 2·31 Stüve diagram. 2·32 Emagram. 2·33 Tephigram..... 9–39

CHAPTER THREE. THERMAL PROPERTIES OF WATER SUBSTANCE AND MOIST AIR

3·01 Isotherms of water substance. 3·02 $(\alpha,e)$-diagram and the triple state. 3·03 The critical state. 3·04 Thermal properties of ice. 3·05 Thermal properties of water. 3·06 Equation of state of water vapor. 3·07 Specific heats of water vapor. 3·08 Changes of phase. 3·09 Variation of the latent heats with temperature. 3·10 Clapeyron's equation. 3·11 Saturation vapor pressure over water. 3·12 Saturation vapor pressure over ice. 3·13 Pressure and temperature of melting. 3·14 Complete $(T,e)$-diagram. 3·15 Supercooled water. 3·16 Thermodynamic surface of water substance. 3·17 Moist air. 3·18 Moisture variables. 3·19 Relative humidity. 3·20 Relations among the humidity variables. 3·21 Numerical determination of mixing ratio. 3·22 Vapor lines on the diagrams. 3·23 Graphical determination of $w$, $q$, and $e$. 3·24 Thermal properties of moist air. 3·25 Equation of state of moist air; virtual temperature. 3·26 Specific heats of moist air. 3·27 Adiabatic process of unsaturated air. 3·28 Virtual potential temperature; characteristic point.

3·29 Useful approximate formulas. 3·30 The adiabatic processes of saturated air. 3·31 Exact equation of the pseudo-adiabatic process. 3·32 Exact equation of the reversible saturation-adiabatic process. 3·33 Critique of the two equations. 3·34 Simplified equation of the adiabatic process of saturated air. 3·35 Isobaric warming and cooling. 3·36 Graphical construction of the saturation adiabats. 3·37 Nomenclature. 3·38 Definitions of $\theta_w$, $\theta_e$, $T_{aw}$, $T_{ae}$, $T_d$. 3·39 Definitions of $T_{ie}$ and $T_{iw}$. 3·40 Surface observations. 3·41 Example..... 40–80

CHAPTER FOUR. HYDROSTATIC EQUILIBRIUM

4·01 The hydrostatic problem. 4·02 The fields of the physical variables. 4·03 The coordinate system. 4·04 Analytical expression for scalar quantities. 4·05 Vectors. 4·06 Vector sum. 4·07 Scalar product. 4·08 Mechanical equilibrium. 4·09 The force of gravity. 4·10 The field of geopotential. 4·11 Dynamic height. 4·12 Analytical expression for the force of gravity. 4·13 Potential vector; ascendent; gradient. 4·14 The pressure field in equilibrium. 4·15 The pressure gradient. 4·16 The hydrostatic equation. 4·17 Distribution of pressure and mass in equilibrium. 4·18 The atmosphere with constant lapse rate. 4·19 The homogeneous atmosphere. 4·20 The dry-adiabatic atmosphere. 4·21 The isothermal atmosphere. 4·22 Atmospheric soundings. 4·23 Graphical representation of dynamic height. 4·24 Adiabatic and isothermal layers. 4·25 The Bjerknes hydrostatic tables. 4·26 U. S. Weather Bureau hydrostatic tables. 4·27 Height evaluation on a diagram. 4·28 Example of height computation on the diagram. 4·29 Further remarks. 4·30 U. S. standard atmosphere. 4·31 The pressure altimeter. 4·32 Altimeter errors..... 81–124

CHAPTER FIVE. STABILITY OF HYDROSTATIC EQUILIBRIUM

5·01 The parcel method. 5·02 Stability criteria. 5·03 The individual lapse rate. 5·04 The lapse rate in the environment. 5·05 Stability criteria for adiabatic processes. 5·06 Stable oscillation. 5·07 Finite displacement. 5·08 Latent instability. 5·09 The slice method. 5·10 Formulas for $\gamma_u$ and $\gamma_s$. 5·11 Rate of precipitation. 5·12 Precipitation lines on the emagram..... 125–144

CHAPTER SIX. THE EQUATION OF MOTION

6·01 Kinematics. 6·02 Velocity. 6·03 Differentiation of a vector. 6·04 Acceleration. 6·05 Curvature. 6·06 Reference frames. 6·07 Dynamics. 6·08 The force of gravitation. 6·09 The equation of absolute motion. 6·10 The acceleration of a point of the earth. 6·11 Zonal flow. 6·12 Angular velocity. 6·13 The vector product. 6·14 The scalar triple product. 6·15 The velocity of a point of the earth. 6·16 Absolute and relative velocity. 6·17 Absolute and relative acceleration. 6·18 Absolute and relative zonal flow. 6·19 The equation of relative motion..... 145–172

CHAPTER SEVEN. HORIZONTAL FLOW

7·01 Horizontal flow. 7·02 Natural coordinates for horizontal flow. 7·03 Standard and natural components. 7·04 The acceleration. 7·05 Cyclic sense. 7·06 Angular radius of curvature. 7·07 Horizontal curvature. 7·08 Geodesic curvature. 7·09 Vertical curvature. 7·10 The angular velocity of the earth. 7·11 The Coriolis force. 7·12 The pressure force and the force of gravity. 7·13 The component equations of relative motion. 7·14 The vertical equation. 7·15 The tangential equation. 7·16 The normal equation. 7·17 Geostrophic flow. 7·18 Inertial flow. 7·19 Cyclostrophic flow. 7·20 Arbitrary horizontal flow. 7·21 Maximum speed. 7·22 Solution of the normal equation. 7·23 Horizontal curvature of the streamlines..... 173–209

CHAPTER EIGHT. WIND VARIATION ALONG THE VERTICAL

8·01 Geostrophic gradient flow. 8·02 Isobaric slope. 8·03 The thermal wind equation. 8·04 Isothermal slope. 8·05 The approximate thermal wind equation. 8·06 Analysis of the shear hodograph. 8·07 Fronts. 8·08 The dynamic boundary condition. 8·09 Application of the dynamic boundary condition. 8·10 The kinematic boundary condition. 8·11 Front separating two arbitrary currents. 8·12 The zonal front. 8·13 The geostrophic front..... 210–232

CHAPTER NINE. WIND VARIATION ALONG THE VERTICAL IN THE SURFACE LAYER

9·01 Dynamics of friction. 9·02 Steady great circle flow. 9·03 The viscous stress. 9·04 The viscosity of a perfect gas. 9·05 Viscosity of air and water. 9·06 The frictional force. 9·07 Total mass transport in the surface layer. 9·08 Wind distribution in the surface layer. 9·09 Relation between surface velocity and geostrophic velocity. 9·10 The geostrophic wind level. 9·11 The eddy viscosity..... 233–249

CHAPTER TEN. MECHANISM OF PRESSURE CHANGES

10·01 Equation of continuity. 10·02 Divergence. 10·03 Horizontal divergence. 10·04 Individual and local change. 10·05 Relative change in a moving pressure field. 10·06 The pressure tendency. 10·07 The tendency equation. 10·08 The advective pressure tendency. 10·09 Relation between the horizontal divergence and the field of pressure. 10·10 Longitudinal divergence in wave-shaped isobar patterns. 10·11 Critical speed in sinusoidal waves. 10·12 Transversal divergence in wave-shaped isobar patterns. 10·13 Total horizontal divergence associated with wave-shaped isobar patterns. 10·14 Barotropic waves in a westerly current. 10·15 The relative streamlines. 10·16 Stable baroclinic waves. 10·17 The first formation of the baroclinic wave. 10·18 Horizontal divergence in closed cyclonic isobar patterns. 10·19 Closed cyclonic isobar patterns surmounted by wave-shaped patterns. 10·20 Closed anticyclonic isobar patterns..... 250–294

CHAPTER ELEVEN. CIRCULATION AND VORTICITY

11·01 Method of line integrals. 11·02 Line integral of a vector. 11·03 Line integrals of the equation of absolute motion. 11·04 Primitive circulation theorems in absolute motion. 11·05 The theorem of solenoids. 11·06 Practical forms of the theorem of solenoids. 11·07 Dynamic balance of steady zonal motion. 11·08 Thermal wind in zonal motion. 11 09 Circulation theorems in developed form. 11·10 Transformation of the acceleration integral for closed individual curves. 11·11 Individual circulation in absolute motion. 11·12 Circulation of the latitude circles in zonal motion. 11·13 Relation between absolute and relative circulation. 11·14 Individual circulation relative to the earth. 11·15 Circulation of the circles in a local vortex. 11·16 Vorticity. 11·17 The vorticity in rectangular coordinates. 11·18 The vorticity in natural coordinates. 11·19 Absolute and relative vorticity. 11·20 The theorem of absolute vorticity. 11·21 The theorem of relative vorticity. 11·22 Air current crossing the equator. 11·23 Air current crossing a mountain range. 11·24 Non-diverging wave-shaped flow pattern. 11·25 Export. 11·26 Irrotational vectors. 11·27 Velocity potential. 11·28 Stream function..... 295–336

CHAPTER TWELVE. THEORY OF WAVES IN A ZONAL CURRENT

12·01 The atmospheric equations. 12·02 Autobarotropy. 12·03 Boundary conditions. 12·04 Sinusoidal waves in a westerly current. 12·05 Waves in a barotropic current. 12·06 The pressure field in the barotropic wave. 12·07 The speed of propagation of the barotropic wave. 12·08 Waves in a baroclinic current..... 337–363

INDEX..... 365–378

# SYMBOLS AND CONSTANTS

(All numerical values are in mts mechanical units.)

## 1. Scalars

$a = 6.371 \times 10^6$ Mean radius of earth (6·08).

$a_E = 6.378 \times 10^6$ Equatorial radius of earth (6·08).

$a_P = 6.357 \times 10^6$ Polar radius of earth (6·08).

1 atm = 101.33 Normal atmosphere (1·07).

$A$ Area.

$A, A_S, A_R$ Amplitude of wave-shaped path (11·24), streamline (10·11), relative streamline (10·15).

$A_{S0}$ Amplitude factor (12·05).

$b_n$ Horizontal normal component of pressure force (7·16).

$c$ Curve; closed curve.

$c$ Specific heat (2·17).

$c$ Average speed of heat motion (9·04).

$c$ Speed of propagation (10·14); *see also* **c**.

$c_H$ Horizontal path (7·07).

$c_p, c_v$ Specific heat at constant pressure, constant volume: of perfect gas (2·19); of moist air (3·26).

$c_{pd} = 1004$ Specific heat of dry air at constant pressure (2·21).

$c_{vd} = 717$ Specific heat of dry air at constant volume (2·21).

$c_{pv} = 1911$ Specific heat of water vapor at constant pressure (3·07).

$c_{vv} = 1450$ Specific heat of water vapor at constant volume (3·07).

$c_w = 4185$ Specific heat of water (3·05).

$c_i = 2060$ Specific heat of ice (3·04).

cb Centibar (1·04).

$C$ Heat capacity (2·17).

$C$ Circulation: general (11·02); relative to earth (11·13).

$C_a$ Absolute circulation (11·11).

$d$ Individual (process) differentiation symbol (4·10, 10·04).

dyn Dynamic (4·11).

$D$ Displacement in 12 hours (7·17).

$\partial$ Partial (local) differentiation symbol (2·20, 10·04).

$e$ 2.71828 · · · .

$e$ Vapor pressure (3·01, 3·18).

$e_s$ Saturation vapor pressure (3·08, 3·19); saturation pressure between any two phases (3·10).

$E$ Export (11·25).

$F$ Transport capacity (10·09, 10·10).

$g$ Acceleration of gravity (4·09); *see also* **g**.

$g_a$ Acceleration of gravitation (6·08).

$g_A$, $g^*$ Apparent gravity (8·12); virtual gravity (7·14).

$g_E = 9.78$ Acceleration of gravity at the equator (4·09).

$g_P = 9.83$ Acceleration of gravity at the poles (4·09).

$g_{45} = 9.80617$ Acceleration of gravity at 45° latitude (4·09).

$g_n = 9.80665$ Standard value of acceleration of gravity (1·07).

$G = 6.658 \times 10^{-8}$ Gravitational constant (6·08).

$h$ Heat per unit mass (2·17).

$h_\phi$, $h_p$ Thickness: of geopotential unit layer (4·10); of isobaric unit layer (4·15).

$H$ Heat (2·17).

$H$ Height in dynamic meters.

$H$ Subscript denoting horizontal component.

$H_n$ Distance between 5-millibar isobars (7·17).

$H_T$ Distance between 5-degree isotherms (8·05).

$k$ Wave number (10·11).

$k$ Constant used in computing dynamic height (4·27).

| | |
|---|---|
| kj | Kilojoule (1·04). |
| $K$ | Curvature (6·05); horizontal curvature of path (10·10). |
| $K_g$ | Geodesic curvature (7·08). |
| $K_H$ | Horizontal curvature of path (7·07). |
| $K_{HS}$, $K_S$ | Horizontal curvature of streamline (7·23, 10·10). |
| $l$ | Arbitrary linear coordinate or line (4·05). |
| $l$ | Subscript denoting component along l. |
| $l$ | Mixing length (9·11). |
| ln | Natural logarithm (2·22). |
| log | Logarithm to base 10. |
| $L$ | Mean free path (9·04). |
| $L$, $L_S$ | Wave length: of path (11·24); of streamline (10·11). |
| [L] | Dimension of length (1·03). |
| $L = 2.500 \times 10^6$ | Latent heat of evaporation (3·08). |
| $L_{iv} = 2.834 \times 10^6$ | Latent heat of sublimation (3·08). |
| $L_{iw} = 0.334 \times 10^6$ | Latent heat of melting (3·08). |
| $L_{12}$ | Any one of $L$, $L_{iv}$, $L_{iw}$ (3·08). |
| $m$ | Molecular weight (2·10). |
| $m$ | Mass of molecule (9·04). |
| $m_d = 28.97$ | Molecular weight of dry air (2·13). |
| $m_v = 18.016$ | Molecular weight of water vapor (3·06). |
| m | Meter (1·04). |
| mts | Meter-ton-second (1·04). |
| [M] | Dimension of mass (1·03). |
| $M$ | Mass. |
| $M = 5.988 \times 10^{21}$ | Mass of the earth (6·08). |
| $n$ | Horizontal coordinate normal to path, increasing to left (7·02). |
| $n$ | Subscript denoting component along n. |
| $n$ | $\gamma_s/\gamma_u$ (5·10). |
| $n$ | Angular wave number (10·11). |
| $N$ | Number of solenoids (11·05). |
| $N$ | Number of molecules per unit volume (9·04). |
| $O$ | Origin (6·01). |
| $p$ | Pressure (2·04). |
| $p_d$ | Partial pressure of dry air (3·20). |

| | |
|---|---|
| $p_s$ | Pressure at characteristic point (3·28). |
| $P$ | Point. |
| $P$ | Procession (11·02). |
| $P$ | Rate of precipitation (5·11). |
| $q$ | Specific humidity (3·18). |
| $q_s$ | Saturation specific humidity (3·19). |
| $r$ | Length of position vector **r** (6·01). |
| $r$ | Distance from center of earth (4·09, 6·08). |
| $r$ | Relative huimdity (3·19). |
| rad | Radian (1·04). |
| $R$ | Radius of curvature (6·05). |
| $R_H$ | Radius of horizontal curvature (7·07). |
| $R_S$ | Radius of horizontal curvature of streamline (11·18). |
| $R$ | Specific gas constant: of perfect gas (2·09); of moist air (3·25). |
| $R^* = 8313.6$ | Universal gas constant (2·11). |
| $R_d = 287.0$ | Specific gas constant for dry air (2·09). |
| $R_v = 461.5$ | Specific gas constant for water vapor (3·06). |
| $s$ | Arc length (6·02); horizontal coordinate along path (7·02). |
| $s$ | Specific entropy (2·28). |
| $s$ | Subscript denoting component along **t**. |
| s | Second of time (1·04). |
| $s, n, z$ | Natural coordinates (7·02). |
| $t$ | Time. |
| $t$ | Temperature in degrees centigrade (2·05). |
| t | (Metric) ton (1·04). |
| $T$ | Temperature in degrees absolute (2·05). |
| [T] | Dimension of time (1·03). |
| $T^*$ | Virtual temperature (3·25). |
| $T_s, T_d, T_{aw}, T_{iw}, T_{ie}, T_{ae}$ | Temperature parameters of moist air (3·28, 3·38, 3·39). |
| $T_p$ | Standard temperature (4·30). |
| $T_p$ | Temperature on isobaric surface (8·03). |
| $u$ | Magnitude of geostrophic deviation velocity (9·08). |
| $u$ | Specific internal energy (2·18). |
| $U$ | Internal energy (2·18). |

$v$ Molar volume (2·10).

$v_0 = 22{,}414$ Molar volume at 1 atm, 0° C (2·10).

$v$ Speed, magnitude of velocity (6·02).

$v_e$ Absolute speed of a point of the earth (6·15).

$v_g$ Geostrophic speed (7·17).

$v_i$ Inertial speed (7·18).

$v_c$ Cyclostrophic speed (7·19).

$v_g, v_i, v_c$ Speed parameters in horizontal flow (7·22).

$v_c$ Critical speed (10·10).

$\bar{v}$ Mean zonal wind speed (10·10).

$\Delta v$ Parameter of wave-shaped flow pattern (10·10).

$V$ Volume.

$w$ Specific work (2·14).

$w$ Mixing ratio (3·18).

$w_s$ Saturation mixing ratio (3·19).

$W$ Work (2·14).

$x, y, z$ Rectangular (Cartesian) coordinates; standard coordinates with $x$ axis toward the east, $y$ axis toward the north, $z$ axis toward the zenith (4·03).

$x, y, z$ Subscripts denoting components along $x$, $y$, $z$ axes.

$z_p$ Standard altitude (4·30).

$z_p$ Altitude of isobaric surface (8·02).

$\alpha$ Specific volume (2·03).

$\alpha_0 = 773$ Specific volume of dry air at 1 atm, 0° C (2·09).

$\gamma$ Lapse rate of temperature.

$\gamma^*$ Lapse rate of virtual temperature (4·18).

$\gamma_d = 0.000996$ Dry-adiabatic lapse rate (4·20).

$\gamma_h = 0.00348$ Lapse rate in homogeneous atmosphere (4·19).

$\gamma_s$ Saturation-adiabatic lapse rate (5·03).

$\gamma_w$ Unsaturated-adiabatic lapse rate (5·03).

$\delta$ Geometric differentiation symbol (4·10).

$\epsilon = 0.622$ $m_v/m_d$ (3·06).

$\zeta$ Vertical component of vorticity: general (11·16); relative to earth (11·19).

$\zeta_a$ Vertical component of absolute vorticity (11·19).

$\eta$ Acoustical constant $c_p/c_v$: for perfect gas (2·24); for moist air (3·27).

$\eta_d = 1.400$ Acoustical constant for dry air (2·24).

$\theta$ Angle.

$\theta$ Angular radius of curvature (7·06).

$\theta$ Potential temperature (2·26, 3·27).

$\theta_w$, $\theta_e$ Potential temperature parameters of moist air (3·38).

$\theta_p$, $\theta_T$, $\theta_F$ Angle of inclination between level surface and: isobaric surface (8·02); isothermal surface (8·04); frontal surface (8·09).

$[\Theta]$ Dimension of temperature (1·03).

$\kappa$ Poisson's constant $R/c_p$: for perfect gas (2·24); for moist air (3·27).

$\kappa_d = 0.286$ Poisson's constant for dry air (2·24).

$\kappa$ Roughness parameter (9·09).

$\lambda_S$ Angular wave length of streamline (10·11).

$\mu$, $\mu_e$ Viscosity (9·03); eddy viscosity (9·10).

$\nu$ Circular frequency (5·06).

$\pi$ 3.14159 · · · .

$\pi$ Barotropic pressure function (12·06).

$\pi$, $\pi_H$ Osculating plane (7·07); horizontal plane (7·07).

$\rho$ Density (2·03).

$\sigma_S$, $\sigma_p$ Angular amplitude of wave-shaped streamline (10·11), isobar (10·10).

$\Sigma$ Equatorial projection of area enclosed by closed fluid curve (11·13).

$\tau$, $\tau_i$, $\tau_p$ Period (5·06); inertial period (7·18); pendulum day (7·18).

$\varphi$ Thermodynamic potential (3·10).
$\varphi$ Velocity potential (11·27).
$\varphi$ Latitude (7·10).
$\phi$ Geopotential; dynamic height in dynamic decimeters (4·10).
$\phi_d$, $\phi_h$, $\phi_l$ Dynamic height of: dry-adiabatic atmosphere (4·20); homogeneous atmosphere (4·19); atmosphere with linear lapse rate (4·18).
$\phi_a$ Gravitational potential (6·08).
$\phi_e$ Centrifugal potential (6·10).

$\psi$ Angle indicating orientation of tangent to a curve (6·05).
$\psi$ Stream function (11·28).

$\omega$ Angular speed: general (6·05); relative to earth (6·11).
$\omega_a$ Absolute angular speed (6·11).
$\Omega = \pm 7.292 \times 10^{-5}$ Angular speed of the earth (6·10, 7·10).
$\Omega_z$ $|\Omega| \sin\varphi$ (7·10).

## 2. Vectors

$|\mathbf{a}|$ Magnitude of vector **a** (4·05).
$\mathbf{a}\cdot\mathbf{b}$ Scalar product (4·07).
$\mathbf{a}\times\mathbf{b}$ Vector product (6·13).
$\mathbf{A}$ Vector area (10·08).

$\mathbf{b}$ Pressure force per unit mass (6·09).

$\mathbf{c}$ Coriolis force (6·19).
$\mathbf{c}$ Velocity of propagation (10·05).

$\nabla$ Del (4·12, 10·01).
$\nabla\varepsilon$ Ascendent of scalar $\varepsilon$ (4·13).
$\nabla_H\varepsilon$ Horizontal ascendent of scalar $\varepsilon$ (4·15).
$\nabla\cdot\mathbf{a}$ Divergence of vector **a** (10·01).
$\nabla_H\cdot\mathbf{a}$ Horizontal diyergence of vector **a** (10·03).

$\mathbf{f}_a$ Inertial force (6·09).
$\mathbf{f}_e$ Centrifugal force of the earth (6·10).
$\mathbf{F}$ Mass transport (9·07).
$\mathbf{F}$ Vector perpendicular to frontal surface (8·08).

$\mathbf{g}$ Force of gravity (4·09, 6·10).
$\mathbf{g}_a$ Force of gravitation (4·09, 6·08).

$\mathbf{i}, \mathbf{j}, \mathbf{k}$ Rectangular (Cartesian) system of unit vectors along $x$, $y$, $z$ axes (4·06).

$\mathbf{K}$ Vector curvature (6·05).

$\mathbf{l}$ Unit vector along arbitrary line (4·05).

$\mathbf{m}$ Frictional force per unit mass (9·01).

$\mathbf{n}$ Horizontal unit normal, pointing to left of path (7·02).
$\mathbf{N}$ Unit normal toward center of curvature (6·05).
$\mathbf{n}_F, \mathbf{n}_T$ Horizontal unit vector normal to: front (8·09); isotherm (8·04).

$\mathbf{0}$ Zero-vector (4·06).

$\mathbf{r}$ Position vector (6·01).
$\mathbf{R}$ Vector radius of curvature (4·09, 6·05).

$\mathbf{t}$ Unit tangent vector (6·02).
$\mathbf{t}, \mathbf{n}, \mathbf{k}$ Natural system of unit vectors along $s$, $n$, $z$ directions (7·02).

$\mathbf{u}$ Geostrophic deviation velocity (9·02).

$\mathbf{v}$ Velocity: general (6·02); relative to earth (6·16).
$\mathbf{v}_a$ Absolute velocity (6·16).
$\mathbf{v}_e$ Velocity of a point of the earth (6·15).
$\mathbf{v}_g$ Geostrophic velocity (8·01).
$\dot{\mathbf{v}}$ Acceleration (6·05); acceleration relative tc earth (6·17).

$\boldsymbol{\tau}$ Viscous stress (9·03, 9·04).

$\boldsymbol{\omega}$ Angular velocity (6·12).
$\boldsymbol{\Omega}$ Angular velocity of the earth (6·12).
$\boldsymbol{\Omega}_z$ Local angular velocity (7·11).

CHAPTER ONE

# DIMENSIONS AND UNITS

**1·01. The goal of dynamic meteorology.** It is customary to divide meteorology into several fields, of which dynamic meteorology is one. Dynamic meteorology starts from pure physical theory and attempts to give a systematic and quantitative description of the composition and physical behavior of the atmosphere. The goal is the complete explanation in physical terms of the atmospheric phenomena constituting the weather. Synoptic meteorology (another of the fields) starts from weather observations and attempts to describe the current state of the weather in such terms that its future development may be predicted. The goal is to forecast the weather without error.

It is clear that the ultimate goals of dynamic and synoptic meteorology can only be attained simultaneously: the first perfect forecaster would be the first man who could explain completely the physical behavior of the atmosphere, and vice versa.

In the present stage of meteorological development certain steps have been taken in the direction of these goals. It must be understood that these steps are only a beginning; for the most part the goals still remain unattained. Nevertheless it is already clear that an understanding of the atmosphere in physical terms is absolutely essential for the synoptic meteorologist.

**1·02. The tools of dynamic meteorology.** Knowing the goal of dynamic meteorology, we first select the branches of physics which furnish suitable tools. These seem at present to be thermodynamics and hydrodynamics. Accordingly, chapters 2 and 3 are devoted to thermodynamics, and chapters 4 and 6 to hydrodynamics. The other chapters are devoted to more properly meteorological topics.

The presentations will presuppose a certain knowledge of general physics and of the calculus. We will start from elementary physical principles and build up all the thermodynamics, vector analysis, and hydrodynamics used in this book. From the beginning the notation and subject matter will be adapted exclusively to the needs of meteorology. This physical material constitutes a background indispensable for the understanding of even the most elementary atmospheric phenomena.

In chapter 1 are introduced some important mechanical variables of general physics, together with their dimensions and units.

**1·03. The fundamental variables and their dimensions.** A mechanical system is measured by various quantities, such as force and energy. All these quantities are reducible to three *fundamental* quantities, namely, *mass*, *length*, and *time*. All other mechanical quantities can be expressed in terms of these three fundamental quantities and are called *derived* quantities. (It should be understood that the selection of fundamental quantities is by no means unique, but our choice has the advantage of simplicity.)

The method by which the derived quantities are built up from the fundamental quantities is best expressed in terms of algebraic expressions called *dimensions*. There is assigned to each of the fundamental quantities a dimensional letter in brackets, as follows:

$$[\text{mass}] = [\text{M}]; \tag{1}$$

$$[\text{length}] = [\text{L}]; \tag{2}$$

$$[\text{time}] = [\text{T}]. \tag{3}$$

For completeness, we include a fourth fundamental quantity which we will need in thermodynamics, namely, *temperature:*

$$[\text{temperature}] = [\Theta]. \tag{4}$$

A pure number, for example, an angle expressed in radians or a molecular weight, is assigned the dimension unity:

$$[\text{pure number}] = [1] = [\text{L}^0\text{M}^0\text{T}^0]. \tag{5}$$

Since M, L, and T not enclosed in brackets will have other meanings in this book, *it is essential that dimensional formulas always be enclosed in brackets.*

The derived quantities are assigned dimensions which are algebraic monomials in M, L, T, and Θ. The exponents represent the powers of fundamental quantities contained in the derived quantity. It is assumed that the reader is familiar with the derived quantities of elementary mechanics, but for convenience we give brief definitions and the dimensions of those of especial use in dynamic meteorology. Many of these will also be discussed later; those involving temperature will be introduced in chapters 2 and 3.

*Area* is ultimately reduced to the area of a rectangle, which is the product of the lengths of its sides:

$$[\text{area}] = [\text{length}] \times [\text{length}] = [\text{L}^2]. \tag{6}$$

*Volume* is ultimately reduced to the volume of a rectangular prism, which is the product of the base area and an altitude:

$$[\text{volume}] = [\text{area}] \times [\text{length}] = [\text{L}^3]. \tag{7}$$

*Density* is defined as the mass of an object per unit volume occupied by the object:

(8) $$[\text{density}] = [\text{mass}] \div [\text{volume}] = [ML^{-3}].$$

*Specific volume* is defined as the volume occupied by an object per unit mass of the object (" specific " always stands for " per unit mass "):

(9) $$[\text{specific volume}] = [\text{volume}] \div [\text{mass}] = [M^{-1}L^3].$$

*Velocity* is the distance traversed per unit of time:

(10) $$[\text{velocity}] = [\text{length}] \div [\text{time}] = [LT^{-1}].$$

*Acceleration* is the change of velocity per unit of time:

(11) $$[\text{acceleration}] = [\text{velocity}] \div [\text{time}] = [LT^{-2}].$$

*Force* is sometimes taken as a fundamental quantity, but is always found to be proportional to the mass of an object multiplied by the acceleration of the object produced by the force:

(12) $$[\text{force}] = [\text{mass}] \times [\text{acceleration}] = [MLT^{-2}].$$

*Pressure* is defined to be the force exerted on a surface per unit area of surface:

(13) $$[\text{pressure}] = [\text{force}] \div [\text{area}] = [ML^{-1}T^{-2}].$$

The *work* done by a force is the product of the force and the length through which the force moves something:

(14) $$[\text{work}] = [\text{force}] \times [\text{length}] = [ML^2T^{-2}].$$

*Energy* is the measure of the work which can be gotten out of a system by some procedure. It then has the same dimensions as work:

(15) $$[\text{energy}] = [ML^2T^{-2}].$$

*Specific work* is the work done per unit mass:

(16) $$[\text{specific work}] = [L^2T^{-2}].$$

*Specific energy* is the energy per unit mass:

(17) $$[\text{specific energy}] = [L^2T^{-2}].$$

*Angular velocity* is the angular distance traveled per unit of time. Since [angle] = [1], we have:

(18) $$[\text{angular velocity}] = [\text{angle}] \div [\text{time}] = [T^{-1}].$$

*Momentum* is the mass of something times its velocity:

(19) $$[\text{momentum}] = [\text{mass}] \times [\text{velocity}] = [MLT^{-1}].$$

Other quantities will be introduced later as the need for them arises. It should be remarked that a quantity expressed as a vector will be assigned the same dimensions as the same quantity expressed as a scalar.

Any physical equation can be interpreted as a relation between dimensional quantities. *The dimensions of the variables in an equation must satisfy the algebraic relation expressed by the equation.* For example, the relation *force = change of momentum per unit time* can be expressed dimensionally by

$$[MLT^{-2}] = [MLT^{-1}] \div [T].$$

The habit of checking the dimensions of every equation should be developed. If the dimensions do not balance, the formula is definitely wrong. If the dimensions do balance, the formula is probably correct up to a numerical constant or other quantity of dimension unity. In certain fields, dimensional analysis is used even to derive physical relations and is a tool of great power.

**1·04. Mts units.** The definitions of the physical quantities of 1·03 are independent of the particular choice of units used to measure them. Their dimensions are also independent of the system of units; that is the peculiar advantage of dimensional analysis.

But as soon as we desire to measure and assign numerical values to those quantities of 1·03, we must have a system of units. The usual procedure is first to define the *fundamental units* — the units of length, mass, and time. Each derived unit is then defined by compounding its component fundamental units according to the dimensional definition of the derived unit.

The standard centimeter-gram-second or cgs system of units is universal and convenient in experimental physics, where the systems generally considered are of the same order of magnitude as the units. In meteorology the system under consideration is the atmosphere, whose magnitude is enormous compared with the cgs units. Hence it is logical to introduce units which are of atmospheric magnitude, and which at the same time are easily translatable into the comparable cgs units. The system adopted by the International Meteorological Conference in 1911 is the meter-ton-second or mts system, and we shall use it exclusively in this book. The units are defined as follows:

*a.* The unit of length is one *meter*, abbreviated 1 m. This was intended to be one ten-millionth of the length of the meridian from the pole to the equator at sea level. Since the meridian is divided into 90 degrees of latitude, each degree of latitude was to be a length unit equal to $\frac{1}{9} \times 10^6$ m, or $111\frac{1}{9}$ km. Although the original computation had

a small error, the relation

(1) 1 degree of latitude = 111.1 km

is correct and often used in synoptic work. The meter is now fixed by a standard in Paris, but may always be reproduced in terms of the wave length of a certain line in the spectrum of cadmium.

*b.* The unit of mass is one (*metric*) *ton*, abbreviated 1 t. It is the mass of one cubic meter of pure water at its maximum density (near 4°C).

*c.* The unit of time is one (*solar*) *second*, defined as $1/(24 \cdot 60 \cdot 60)$ of the mean time interval between consecutive upper transits of the sun across the same meridian.

The derived units are obtained as follows: The units of area and volume are one square meter (1 $m^2$) and one cubic meter (1 $m^3$) respectively. The units of density and specific volume are one ton per cubic meter (1 $t\ m^{-3}$) and one cubic meter per ton (1 $m^3\ t^{-1}$), respectively. The units of velocity and acceleration are one meter per second (1 $m\ s^{-1}$) and one meter-per-second-per-second (1 $m\ s^{-2}$), respectively.

The unit of force is the force which gives a mass of one ton an acceleration of 1 $m\ s^{-2}$. Unfortunately it has no more specific name than one ton-meter-per-second-per-second (1 $t\ m\ s^{-2}$) or one mts unit of force. The unit of pressure is the pressure developed by an mts unit of force acting on each square meter and is called one *centibar* (1 cb). The unit of work is the work done by one mts unit of force acting through a distance of one meter, and is called one *kilojoule* (1 kj). The kilojoule serves also as the unit of energy. The unit of specific work and specific energy is one kilojoule per ton (1 $kj\ t^{-1}$). The origin of the names centibar and kilojoule will be explained in 1·05.

Angles will be expressed in radians (rad), where $2\pi$ radians equals 360°. The unit of angular velocity is one radian per second (1 $rad\ s^{-1}$).

**1·05. Comparison with cgs units.** It is presumed that the reader is familiar with the cgs units, whose definitions are completely analogous to the mts units. They start from the fundamental units:

(1) 1 centimeter (1 cm) = $10^{-2}$ meter;

(2) 1 gram (1 gm) = $10^{-6}$ ton;

(3) 1 second (1 s) = 1 second.

The cgs unit of force, in contrast to the corresponding mts unit, has a name — the *dyne*. The cgs unit of pressure is the *barye*. The cgs unit of work or energy is the *erg*. Because of the small size of the barye and erg, the following alternate measures are often introduced, *but they are*

*not strictly speaking units in the cgs system:*

pressure: 1 bar $= 10^6$ baryes;

work or energy: 1 joule $= 10^7$ ergs.

It is from these names that the mts units get their names. It will be shown presently that in accordance with their names:

(4) 1 centibar $= 10^{-2}$ bar;

(5) 1 kilojoule $= 10^3$ joules.

Despite their prefixes, it must be understood that the *centibar and kilojoule are actually the units of pressure and work in the mts system.*

In order to make a convenient reference page, we will tabulate (table 1·05) the quantities so far considered. For each quantity, we give: (i) its name, (ii) its dimensions, (iii) its mts unit, (iv) its cgs unit, (v) the number $N$ of cgs units contained in one mts unit of that quantity. For all the derived quantities used in this book the mts unit is equal to or larger in magnitude than the corresponding cgs unit; so that in table 1·05, $N \geqq 1$.

TABLE 1·05

(Mts unit = cgs unit × $N$)

| Quantity | Dimensions | Mts Unit | Cgs Unit | $N$ |
|---|---|---|---|---|
| Length | [L] | 1 m | 1 cm | $10^2$ |
| Mass | [M] | 1 t | 1 gm | $10^6$ |
| Time | [T] | 1 s | 1 s | 1 |
| Area | $[L^2]$ | 1 $m^2$ | 1 $cm^2$ | $10^4$ |
| Volume | $[L^3]$ | 1 $m^3$ | 1 $cm^3$ | $10^6$ |
| Density | $[ML^{-3}]$ | 1 t $m^{-3}$ | 1 gm $cm^{-3}$ | 1 |
| Specific volume | $[M^{-1}L^3]$ | 1 $m^3$ $t^{-1}$ | 1 $cm^3$ $gm^{-1}$ | 1 |
| Velocity | $[LT^{-1}]$ | 1 m $s^{-1}$ | 1 cm $s^{-1}$ | $10^2$ |
| Acceleration | $[LT^{-2}]$ | 1 m $s^{-2}$ | 1 cm $s^{-2}$ | $10^2$ |
| Force | $[MLT^{-2}]$ | 1 t m $s^{-2}$ | 1 gm cm $s^{-2}$ = 1 dyne | $10^8$ |
| Pressure | $[ML^{-1}T^{-2}]$ | 1 t $m^{-1}$ $s^{-2}$ = 1 cb | 1 gm $cm^{-1}$ $s^{-2}$ = 1 barye | $10^4$ |
| Work / Energy | $[ML^2T^{-2}]$ | 1 t $m^2$ $s^{-2}$ = 1 kj | 1 gm $cm^2$ $s^{-2}$ = 1 erg | $10^{10}$ |
| Specific work / Specific energy | $[L^2T^{-2}]$ | 1 kj $t^{-1}$ | 1 erg $gm^{-1}$ | $10^4$ |
| Angular velocity | $[T^{-1}]$ | 1 rad $s^{-1}$ | 1 rad $s^{-1}$ | 1 |
| Momentum | $[MLT^{-1}]$ | 1 t m $s^{-1}$ | 1 gm cm $s^{-1}$ | $10^8$ |

To obtain $N$ readily, we start from the relations (1), (2), and (3). Thus for length [L], $N = 10^2$; for mass [M], $N = 10^6$; and for time [T], $N = 1$. To obtain $N$ for any derived quantity, we multiply together the component $N$'s according to the dimensional formula. For example,

pressure = $[ML^{-1}T^{-2}]$. Hence, for pressure, $N = 10^6 \cdot (10^2)^{-1} \cdot (1)^{-2} = 10^4$. This means that 1 cb = $10^4$ baryes (= $10^{-2}$ bar), which proves (4). For work, $N = 10^6 \cdot (10^2)^2 \cdot (1)^{-2} = 10^{10}$. Thus 1 kj = $10^{10}$ ergs (= $10^3$ joules), which proves (5).

It should be noted that density and specific volume have the same numerical values in both cgs and mts units, and that water has unit density and unit specific volume.

**1·06. Comparison with English units.** Even in countries where the metric system is not in general use, the weather services use metric units to a very large degree. Hence the reader should become familiar with the units of table 1·05 to the point where he can use them in everyday life. To help in this, we give a few comparisons with English units:

Length: 1 m = 39.37 in.;
10,000 ft = 3048 m;
1 km = 0.6214 mile $\approx \frac{5}{8}$ mile;

Mass: 1 t = 2205 (lb mass);

Density: 1 t $m^{-3}$ = 62.43 (lb mass) $ft^{-3}$;

Velocity: 1 m $s^{-1}$ = 2.237 miles $hr^{-1} \approx 2\frac{1}{4}$ miles $hr^{-1}$;

Pressure: 1 cb = 0.1450 (lb force) $in.^{-2} \approx \frac{1}{7}$ (lb force) $in.^{-2}$;

Work: 1 kj = 737.6 ft-(lb force).

**1·07. Pressure measurement and units.** Besides the centibar the meteorologist must know several other pressure units. In the weather services pressure is represented in millibars (mb):

(1) 1 cb = 10 mb.

For this reason it is necessary to caution students repeatedly *to convert pressure to centibars when computing with mts units.*

The standard pressure-measuring instrument of meteorology is the mercury barometer. This instrument is so designed that the pressure of the air is balanced against a column of mercury (Hg) whose length can be measured very accurately. The pressure is expressed as the length of the mercury column, in either millimeters or inches. The pressure of the mercury column is determined by its weight per unit cross section, which for a column of constant height varies with both the density and the acceleration of gravity. To compare pressure readings made with mercury barometers at different temperatures and at points where gravity is different, all readings are reduced to a standard temperature and a standard value of gravity. For millimeter barometers, the

standard temperature is 0°C, at which the density $\rho_0$ of mercury is 13.5955 t $m^{-3}$. The standard value of the acceleration of gravity is $g_n = 9.80665$ m $s^{-2}$, which is approximately the sea-level value of gravity at 45° latitude.

The pressure of one *normal atmosphere* (1 atm) is that balanced by a column of mercury 760 mm = 0.760 m long, under the above standard conditions. It is the reference pressure of physical chemistry. To evaluate it, we find that

$$1 \text{ atm} = (0.76 \text{ m}) \times (13.5955 \text{ t m}^{-3}) \times (9.80665 \text{ m s}^{-2}) = 101.33 \text{ cb}.$$

Thus the normal atmosphere is expressed in mechanical units. We have

(1) 1 atm = 760 mm Hg = 29.92 in. Hg = 101.33 cb = 1013.3 mb.

Another reference pressure frequently used in meteorology is *standard pressure*, which is defined to be exactly 100 cb. Thus

(2) 750.04 mm Hg = 29.53 in. Hg = 100.00 cb = 1000.0 mb.

From either (1) or (2), tables are computed to convert pressure from inches of mercury or millimeters of mercury to millibars. The conversion factor

(3) $$1 \text{ mb} = \tfrac{3}{4} \text{ mm Hg}$$

is easy to remember and yields all the accuracy usually required for converting millibars into millimeters of mercury.

CHAPTER TWO

# THERMODYNAMICS OF A PERFECT GAS

**2·01. Thermodynamical systems.** Thermodynamics deals with systems which, in addition to certain mechanical parameters to be mentioned later, require for their description a thermal parameter, the temperature. The very definition of temperature requires that a system be in equilibrium. Thus of necessity thermodynamics is the study of systems *in equilibrium* and of processes which can take place in states differing only slightly from the state of equilibrium. The fact is that the actual atmosphere is not in equilibrium. Dynamic meteorology is compelled to make the pretense that equilibrium exists, in order to make an analysis. We should therefore expect the results to have some slight disagreements with conditions in the real atmosphere.

The systems considered mostly in dynamic meteorology are infinitesimal parcels of: (i) dry air, which can for practical purposes be considered as one *substance;* (ii) pure *water substance* in any one, two, or three of the *phases* solid (ice), liquid (water), or gas (water vapor); (iii) a mixture of dry air with some water vapor, called *moist air;* (iv) a mixture of moist air with some water droplets or ice crystals.

**2·02. The physical variables.** The infinitesimal systems considered will be described thermodynamically by the four parameters mass ($\delta M$), volume ($\delta V$), pressure ($p$), and temperature ($T$). One system will be defined so as always to consist of the same particles. Hence its mass $\delta M$ and composition will remain constant, and the other parameters, volume, pressure, and temperature, will be called the *physical variables.* The values of the physical variables will completely describe the *state* of the system.

**2·03. Volume.** The actual volume $\delta V$ is conveniently replaced by the *specific volume* $\alpha = \delta V/\delta M$. See 1·03(9). Since the mass $\delta M$ remains constant, $\alpha$ is directly proportional to the actual volume $\delta V$. An alternative mass-volume variable is the density $\rho = \delta M/\delta V$. See 1·03(8). The two variables are related by the equation

$$\alpha\rho = 1. \tag{1}$$

By means of (1), one of the variables may be replaced by the other in any physical equation. Either of them may with equal right be taken as the mass variable in dynamics, but we shall usually prefer $\alpha$.

**2·04. Pressure.** To define the pressure $p$ of a thermodynamic system, we must first consider any fixed point $P$ in the system, and any fixed direction $l$ at $P$. We assume it possible to place a testing surface of small plane area $\delta A$ at the point $P$, and orient the testing surface normal to the direction $l$. The molecules of that part of the system on *one side* of the testing surface will bombard the area $\delta A$, giving rise to a force $\delta F$ in the direction $l$. (The molecules on the *other* side of $\delta A$ must be disregarded in computing $\delta F$.)

Experiment shows that $\delta F$ is proportional to $\delta A$ for a range of areas $\delta A$ which are neither so large as to exceed the size of the system, nor so small as to be of molecular dimensions. The proportionality factor is called the *pressure $p(P,l)$ at the point $P$ in the direction $l$.* Thus

$$p(P,l) = \frac{\delta F}{\delta A}.$$

Pressure is hence a force per unit area, as in 1·03(13).

Now the important points follow: First, experiment and theory show that $p(P,l)$ has the same value in each direction $l$. Thus $p$ depends on $P$ alone. Second, since our systems are infinitesimal in size, and since they are in equilibrium, the variation of $p$ with $P$ is negligible throughout one system.

We are thus able to define *the pressure $p$ of a system as the common value of $p(P,l)$ for all points $P$ and directions $l$ in the system.* The pressure (in mts units) gives rise to a net force of $p$ mts force units normal to the boundary surface, per square meter of boundary surface.

Although the infinitesimal *variation* of $p$ throughout a system is negligible in so far as the value of $p$ is concerned, the *pressure gradient* or *rate of change of $p$ with respect to distance across the system* is of vital importance in dynamics. The pressure gradient may assume a large value, being the quotient of two infinitesimals. This will be discussed in chapter 4.

**2·05. Temperature.** The rigorous definition of temperature is one of the major *results* of thermodynamics, rather than being a simple *presupposition* of this branch of physics. Thus a logical treatise on thermodynamics will omit temperature until well into the book, and then introduce it by a theorem. (See 2·28.) Such a treatment is bewildering to the ordinary student, and we prefer to follow a less rigorous but more convincing procedure.

We start from the evidence of our senses that we may distinguish between warm and cold bodies. Experiments reveal that when a warm and a cold body are put in contact, the former gets colder and the latter gets warmer. This continues until a state of *thermal equilibrium* is

reached, by which we mean that there is no further flow of heat. In thermodynamics we shall discuss only systems which are in thermal equilibrium.

Any substance which may be brought into thermal equilibrium with a mixture of ice and pure water at a pressure of 1 atm (see 1·07) is said to have the temperature 0° centigrade (0°C). Any substance which may be brought into thermal equilibrium with steam immediately over water boiling at a pressure of 1 atm is said to have the temperature 100°C. No *other* temperatures are yet defined.

Now consider any gas which will not liquefy in the following experiment. Let its pressure be kept constant at any fixed value $p_0$. Let its specific volume at 0°C be $\alpha_0$. Let $\alpha_{100}$ be its specific volume at 100°C. It will be found that $\alpha_{100} > \alpha_0$.

When the specific volume has any other value $\alpha_t$, we will define the *centigrade temperature* $t$ (0°C) by the linear interpolation formula

$$t = 100\,\frac{\alpha_t - \alpha_0}{\alpha_{100} - \alpha_0}. \tag{1}$$

Of course, this makes temperature dependent on the gas used. All that can be said in this treatment is that, for the " permanent gases " like helium and hydrogen, the temperatures so defined are consistent to within a very small error. This gives us a very reliable " gas thermometer " from which a mercury or spirit thermometer may be calibrated.

It is desirable to introduce an absolute scale of temperature, whereby the temperature of a gas is proportional to its specific volume. To do this we let

$$T_0 = \frac{100\alpha_0}{\alpha_{100} - \alpha_0}. \tag{2}$$

We find empirically that $T_0 = 273.18$ for all the permanent gases, meaning that they all have about the same coefficient of expansion $1/T_0$. We then define the *absolute temperature* $T$ (°K) of a system in terms of $t$ by the relation

$$T = T_0 + t. \tag{3}$$

(The K stands for Kelvin.) Let $\alpha_T$ be the specific volume at the absolute temperature $T$ of the gas in the experiment above (i.e., $\alpha_T = \alpha_t$). Then from (3), (2), and (1) we get

$$T = T_0\,\frac{\alpha_T}{\alpha_0}, \quad \text{or}$$

$$\frac{\alpha_T}{T} = \frac{\alpha_0}{T_0}. \tag{4}$$

Equation (4), representing the proportionality of $\alpha$ and $T$ at the fixed pressure $p_0$, is called *Charles's law.*

**2·06. Meteorological temperature scales.** The exact value of the $T_0$ of 2·05 requires careful experiment, and as a result physicists have changed the accepted value from time to time. To standardize the usage in meteorology, which does not require greater accuracy, it is customary to use the relation

$$0°C = 273°K. \tag{1}$$

This practice will be followed throughout this book. The symbol $T_0$ will often be used for 273 (°K).

It is presumed that the reader is familiar with the Fahrenheit scale and knows how to convert it to centigrade by the relation

$$t_f\ (°F) = \tfrac{9}{5}t\ (°C) + 32.$$

Every meteorologist using Fahrenheit on synoptic maps should know the following corresponding values, or a similar table:

| | | | | | | | | |
|---|---|---|---|---|---|---|---|---|
| $t$ (°C) | −40 | −10 | 0 | 10 | 20 | 30 | 37 | 100 |
| $t_f$ (°F) | −40 | 14 | 32 | 50 | 68 | 86 | 98.6 | 212 |

In dimensional formulas we shall use

$$[\text{temperature}] = [\Theta]. \tag{2}$$

**2·07. Equation of state.** In 2·05 we observed that absolute temperature $T$ is measured by the volume change of a suitable substance. The reason why this is possible lies in a fundamental property of any of the thermodynamical systems of 2·01.

This property is that between the physical variables $p$, $\alpha$, and $T$ defining the state of a system there exists a functional relation. The relation may be written

$$f(p,\alpha,T) = 0, \tag{1}$$

and is called the *equation of state* of the system. It may be determined empirically for real systems to any obtainable degree of accuracy, or it may be prescribed for an idealized system like a " perfect gas."

Except at certain transition states the equation of state can be used to determine the value of any one of the physical variables from the values of the other two physical variables.

**2·08. The perfect gas.** The so-called permanent gases follow to a close approximation a number of well-known laws. One of these is *Charles's law*, given by 2·05(4). Another is *Boyle's law*, which says that at a constant temperature the pressure $p$ and specific volume $\alpha$ are

related by the formula

$$p\alpha = \text{const}, \tag{1}$$

where the value of the constant depends on the temperature. Two other laws, known as *Avogadro's law* and *Dalton's law*, will be stated in 2·10 and 2·12.

We define a *(thermally) perfect gas* as a gas which obeys Charles's and Boyle's laws exactly. No such gas exists, but the purely gaseous systems considered in meteorology (see 2·01) are so nearly perfect that it is most convenient to treat them as perfect gases.

**2·09. Equation of state of a perfect gas.** We shall show that *a perfect gas has an equation of state of form*

$$p\alpha = RT, \tag{1}$$

where $R$ is the *specific gas constant*, which depends on the particular perfect gas considered. To balance dimensions we must have

$$[R] = [\mathrm{L}^2\mathrm{T}^{-2}\Theta^{-1}].$$

Thus from table 1·05 it is seen that $R$ is measured in kj $\mathrm{t}^{-1}$ $\mathrm{deg}^{-1}$ in the mts system.

To prove (1), let $\alpha = \alpha(T,p)$ be the specific volume at temperature $T$ and pressure $p$. Let $T_0$ be a fixed temperature, and let $p_0$ be the fixed pressure of the gas as in 2·05. By Charles's law, 2·05(4),

$$\frac{\alpha(T,p_0)}{T} = \frac{\alpha(T_0,p_0)}{T_0}. \tag{2}$$

By Boyle's law, 2·08(1),

$$p\alpha(T,p) = p_0\alpha(T,p_0). \tag{3}$$

Eliminating $\alpha(T,p_0)$ between (2) and (3), we get

$$p\alpha(T,p) = \frac{p_0\alpha(T_0,p_0)}{T_0}\,T. \tag{4}$$

Writing $\alpha(T,p)$ as simply $\alpha$, and letting $R$ stand for $p_0\alpha(T_0,p_0)/T_0$, we get (1), as desired.

From (4) we also see that, to determine the numerical value of $R$, we need only measure $\alpha$ at say $T_0 = 273°\mathrm{K}$ and $p_0 = 101.33$ cb. Then

$$R = \frac{p_0\alpha(T_0,p_0)}{T_0} \text{ kj } \mathrm{t}^{-1} \mathrm{deg}^{-1}.$$

For example, dry air is considered a perfect gas in meteorology. At

$p_0 = 101.33$ cb and $T_0 = 273°K$, measurements on dry air give for its specific volume $\alpha_0$:

(5) $$\alpha_0 = 773 \text{ m}^3 \text{ t}^{-1} \qquad (1 \text{ atm}, 273°K).$$

Then the specific gas constant $R_d$ for dry air is:

(6) $$R_d = \frac{p_0\alpha_0}{T_0} = \frac{(101.33)(773)}{273} = 287 \text{ kj t}^{-1} \text{ deg}^{-1}.$$

**2·10. Molecular weights.** The numerical value of the specific gas constant for each perfect gas can be obtained directly from considerations of molecular weight, without actually measuring $\alpha(T_0,p_0)$ for the individual gas.

Each pure gas has assigned to it in chemistry a *pure number* called the *molecular weight*, denoted by $m$. For our purposes the molecular weight may be thought of as simply a relative density at uniform pressure and temperature, based on 32.000 for oxygen. The molecular weights used in meteorology are given in tables 2·10 and 2·13.

TABLE 2·10

MOLECULAR WEIGHTS

| | |
|---|---|
| Helium | 4.003 |
| Hydrogen | 2.016 |
| Water vapor | 18.016 |

If $m$ denotes the molecular weight of a given gas, then $m$ tons of the gas constitute a *ton mole*, with dimension [M]. The volume occupied by a ton mole is called the *molar volume*, and is denoted by $v$, with dimensions $[M^{-1}L^3]$.

An empirical law called *Avogadro's law* states that at a fixed temperature and pressure the molar volume, within a close approximation, is the same for all permanent gases. At $p_0 = 1$ atm and $T_0 = 0°C$, the molar volume is denoted by $v_0$:

(1) $$v_0 = 22{,}414 \text{ cubic meters (ton mole)}^{-1}.$$

The value (1) is assumed exact for perfect gases.

**2·11. Universal gas constant.** Consider a mass of $M$ tons of any perfect gas, at any pressure and temperature, occupying the volume $V$. Its specific volume $\alpha$ is $V/M$. From the equation of state 2·09(1), we get

(1) $$pV = MRT.$$

In particular, if the mass is one ton mole, i.e., $m$ tons, then the volume is $v$ and (1) takes the form

$$pv = mRT. \tag{2}$$

Letting $p_0 = 1$ atm and $T_0 = 0°C$, we have

$$p_0 v_0 = mRT_0 \quad \text{or} \quad mR = \frac{p_0 v_0}{T_0},$$

where $v_0$ is given by 2·10(1). Hence $mR = p_0 v_0 / T_0$ has the same value for all gases. It is called the *universal gas constant* and is denoted by $R^*$. $R^*$ has the dimensions $[L^2T^{-2}\Theta^{-1}]$, and in mts units has the value

$$R^* = \frac{(101.33)(22{,}414)}{273.18} = 8313.6 \text{ kj (ton mole)}^{-1} \text{ deg}^{-1}. \tag{3}$$

Since $R^* = mR$, we get the formula for the specific gas constant for any perfect gas in terms of the molecular weight $m$ of the gas:

$$R = \frac{1}{m} R^* \text{ kj t}^{-1} \text{ deg}^{-1}. \tag{4}$$

This is the formula used to get the numerical value of $R$ for the equation of state 2·09(1) of any pure gas.

**2·12. Mixtures of perfect gases.** Dry and moist air are both mixtures of several gases, each of which is treated as perfect. Therefore we must learn how to get the specific gas constant for mixtures.

Let a mixture of volume $V$ cubic meters contain $M_1$ tons of gas 1, $M_2$ tons of gas 2, $\cdots$, $M_s$ tons of gas $s$. Let the total mass be $M = \sum M_k$. Let the respective molecular weights be $m_1, m_2, \cdots, m_s$. Let the respective specific gas constants be $R_1, R_2, \cdots, R_s$, where each $R_k = R^*/m_k$, according to 2·11(4). Assume each constituent is perfect.

According to a fourth empirical law, *Dalton's law*, each individual constituent gas will obey its equation of state as though the other constituents were not present. Let $p_1, p_2, \cdots, p_s$ be the *partial pressures* of the constituents. Then by Dalton's law and 2·11(1),

$$p_k V = M_k R_k T, \qquad (k = 1, 2, \cdots, s). \tag{1}$$

The total pressure $p$ of the mixture is given by $p = \sum p_k$. Summing equation (1) from $k = 1$ to $s$, we get

$$pV = \left( \sum_{k=1}^{s} M_k R_k \right) T. \tag{2}$$

Now, if we pick $R$ such that

$$MR = \sum_{k=1}^{s} M_k R_k, \tag{3}$$

then by (2),

$$pV = MRT. \tag{4}$$

But (4) is simply 2·11(1) over again. Thus we have the rule that *if we define $R$ according to* (3) *above, then a mixture of perfect gases will also have the equation of state of a perfect gas.* The formula (3) says in words that $R$ is simply a weighted average of the $R_k$'s, each $R_k$ being weighted according to the mass of gas $k$ present in the mixture. Thus we say that the specific gas constant is *mass-additive* in mixtures.

**2·13. Molecular weight of dry air.** The composition of dry air varies only slightly. Table 2·13 presents the computation of the specific gas constant $R = R_d$ of dry air by the method of 2·12. In the first column are the principal constituents of dry air. In the second column are their molecular weights ($m_k$). In the third column are their individual specific gas constants ($R_k$) as computed from 2·11(4). In the fourth column are the masses ($M_k$) of the constituents in one ton of dry air (so that $M = 1$). In the fifth column are the values of $M_k R_k$, the total of which is equal to $R_d$, according to 2·12(3). The computation shows that, to four figures, $R_d = 287.0$ kj $t^{-1}$ $deg^{-1}$, in accordance with 2·09(6).

TABLE 2·13

| Gas | Mol. Wt. ($m_k$) | Gas Const. ($R_k$) | Part by Mass ($M_k$) | $M_k R_k$ |
|---|---|---|---|---|
| Nitrogen | 28.016 | 296.74 | 0.7552 | 224.10 |
| Oxygen | 32.000 | 259.80 | 0.2315 | 60.14 |
| Argon | 39.944 | 208.13 | 0.0128 | 2.66 |
| Carbon dioxide | 44.010 | 188.90 | 0.0005 | 0.09 |
| Dry air | | | $1.0000 = M$ | $286.99 = R_d$ |

It was shown in 2·12 that a mixture of perfect gases is a perfect gas. The molecular weights of the constituents have been used here only as relative densities, and not as relating to the structure of the gas molecules. It is thus permissible to define a "molecular weight" for a mixture, if we choose. The defining relation is 2·11(4), in order that the molecular weight may still be a relative density.

Thus meteorologists define the *molecular weight $m_d$ of dry air* by

$$m_d = \frac{R^*}{R_d} = \frac{8313.6}{287.0} = 28.97 \quad \text{(pure number)}. \tag{1}$$

With this definition, we have from 2·09(1) for dry air that

$$p\alpha = \frac{1}{m_d} R^*T, \tag{2}$$

just as for any other gas of molecular weight $m$,

$$p\alpha = \frac{1}{m} R^*T. \tag{3}$$

With this definition we may treat dry air as though it were one " substance " with the molecular weight $m_d$. In particular, we may treat dry air as a " pure gas " by the method of 2·12, whenever it is in turn mixed with water vapor or other pure substances.

The reader may prove for himself that in the notation of 2·12 the molecular weight $m$ of a mixture is given by the formula:

$$M \frac{1}{m} = \sum_{k=1}^{s} M_k \left(\frac{1}{m_k}\right). \tag{4}$$

*Thus the reciprocals of molecular weights are mass-additive in mixtures.*

**2·14. Work in thermodynamics.** The definition of work in 1·03(14) is more precisely formulated in mechanics as follows. When a material particle under the action of a force $F$ moves through the distance $ds$ in the direction of the force, the work $dW$ done by the force is $Fds$. When the direction of movement makes an angle $\theta$ with the force, only the component $F \cos \theta$ of $F$ in the direction of the motion contributes to the work, and the work is given by the expression

$$dW = Fds \cos \theta. \tag{1}$$

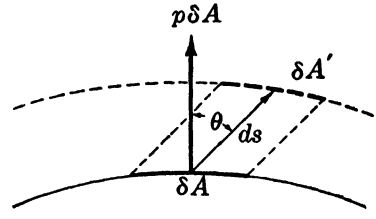



FIG. 2·14.

When the system considered is an infinitesimal element of fluid, the only force with which this element can do work upon its environment is that arising from the pressure $p$ on its surface. On each area element $\delta A$ of the surface there is a force $p\delta A$ pushing normal to the surface, by 2·04. Suppose that under the action of the force, the surface element $\delta A$ moves a distance $ds$ in a direction making the angle $\theta$ with the normal direction, thus arriving at a new position $\delta A'$ (see fig. 2·14). Then by (1) the work done by the force acting on $\delta A$ is equal to $p\delta A ds \cos \theta$.

It is seen that $\delta A ds \cos\theta$ is equal to the volume swept out by the motion of the area element $\delta A$ to its new position $\delta A'$. Consider now the work $dW$ done by the pressure force in the expansion of a system of volume $V$, surface area $A$, and mass $M$. Let $dV$ be the total change in volume of the system, being the sum over the complete area $A$ of the cylinders swept out by the area elements $\delta A$ mentioned above. We see that

$$dW = pdV. \tag{2}$$

We shall usually use capital letters to denote quantities referring to the total mass of a system, and the corresponding small letters to denote the value of the same quantities referred to unit mass (specific quantities). Dividing (2) by the mass $M$, we obtain the expression for the *specific work dw done by the system:*

$$dw = pd\alpha. \tag{3}$$

Our sign convention is such that if an element expands under its pressure forces, i.e., does work on the environment, then $dw$ is positive. If the element is compressed by the external pressure force, i.e., has work done on it by the environment, $dw$ is negative. *A system unchanged in volume can do no work of the type considered here.*

**2·15. $(\alpha,-p)$-diagram.** A convenient diagram for many purposes in thermodynamics is the $(\alpha,-p)$-diagram, which is a graph of pressure against specific volume, both variables having linear scales. On account of its frequent application to atmospheric problems, where pressure variations are mainly due to vertical displacements of an air element, the diagram is drawn with pressure increasing downward. Consider any one perfect gas. Its state (see 2·02) is defined by any two of the variables $p$, $\alpha$, $T$ — the third being obtained from the equation of state 2·09(1). Each point on the $(\alpha,\ p)$-diagram represents by its coordinates a unique pair of values of $\alpha$ and $p$. It consequently represents a unique state; conversely, each state is uniquely represented by a point on the diagram.

Any change of state from $(\alpha,p)$ to $(\alpha + d\alpha, p + dp)$ is called an *elementary physical process* and is, of course, represented by an infinitesimal line on the $(\alpha,-p)$-diagram. A *finite process* is composed of a succession of elementary ones, and is thus represented by a continuous curve on the diagram — the *path* of the process.

Let a gas perform an arbitrary process represented in the $(\alpha,-p)$-diagram by the curve $DD'E$ (fig. 2·15*a*). The specific work $dw$ performed during the elementary process of expansion $DD'$ is $pd\alpha$, which is

measured by the area of the dotted strip. For the finite expansion process $D$ to $E$, the total specific work $w$ is equal to the integral of 2·14(3):

$$w = \int_D^E p d\alpha. \tag{1}$$

This is measured by the whole shaded area under the curve $DE$.

Of particular importance is the *cyclic* process where the system returns to its initial state (fig. 2·15*b*). While expanding ($DIIE$) the element does positive work. During the subsequent compression ($EGD$) work

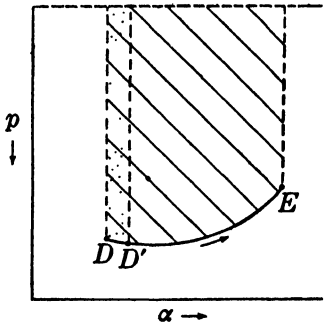


FIG. 2·15*a*.

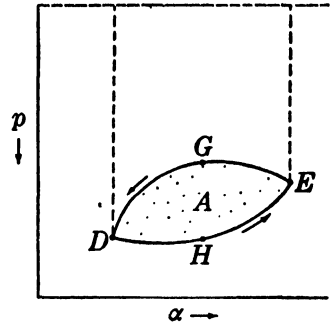


FIG. 2·15*b*.

is done on the element and is negative. It must hence be subtracted. The net work done by the element in the complete cycle is therefore equal to the area $A$ enclosed by the path representing the cycle in the $(\alpha, -p)$-diagram. Denoting the cyclic path by $c$ we have

$$w = \int_c p d\alpha = A. \tag{2}$$

The unit of area on the diagram must of course be that of a rectangle whose base is the length of a unit ($m^3\ t^{-1}$) of $\alpha$ and whose height is the length of a unit (cb) of $p$. Multiplying the dimensions of pressure by those of specific volume, we see that area on the $(\alpha,-p)$-diagram has the dimensions $[L^2T^{-2}]$ of specific work. From (2) we have the rule:

*The work performed by unit mass in a cyclic process equals the area enclosed by the path in the $(\alpha,-p)$-diagram; the work is positive when the cycle is taken counterclockwise, and negative when the sense is clockwise.*

**2·16. Isotherms of a perfect gas.** As an example of a process represented on the $(\alpha,-p)$-diagram by a curve, we consider the isothermal process of a perfect gas. For a particular gas at any constant value $T_1$ of $T$, the product $RT_1$ is a definite, known constant.

Then the equation of state 2·09(1) becomes

$$p\alpha = RT_1 = \text{const}, \tag{1}$$

whose graph is a rectangular hyperbola in the $(\alpha,-p)$-diagram (fig. 2·16). The hyperbola is called the *isotherm* $T = T_1$. It passes through just those points $(\alpha,-p)$ which represent states with temperature $T_1$.

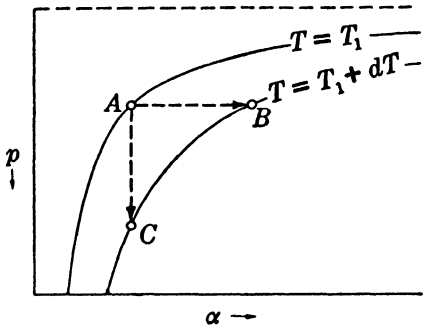


FIG. 2·16.

In fig. 2·16 there is also drawn the isotherm $T = T_1 + dT$.

Now suppose a system is in the state represented by the point $A$ in the figure. Suppose it is desired to heat the system from temperature $T_1$ to $T_1 + dT$. This may be done by any of an infinite number of processes, each of which can be represented by a line segment starting from $A$ and ending on the isotherm $T_1 + dT$.

We have here pictured just two of these processes. $AB$ is a process taking place at constant pressure. This is called an *isobaric* process. $AC$ is a process taking place at constant volume. This is called an *isosteric* process. Note that in the process $AC$ no work is done. In the process $AB$, work is done by the system. This will be of significance in the evaluation of the specific heats in 2·21.

**2·17. Heat.** It was mentioned in 2·05 that when two systems at different temperatures are brought in contact, the warmer gets colder, and the colder gets warmer. A *calorimeter* is a standard system with which different bodies are brought in contact in order to compare their various temperature changes with those of the calorimeter. Let the calorimeter have the initial temperature $T_1$, and let a body to be tested have the initial temperature $T_2 > T_1$. Let the final temperature of the combined systems be $T'$. Then $T_1 < T' < T_2$. Experiments with the same body under varying temperatures show that the final temperature $T'$ is determined invariably by the same equation:

$$C(T' - T_2) + C_w(T' - T_1) = 0, \tag{1}$$

where $C$ and $C_w$ are constants.

Comparing different masses of the same substance in the same calorimeter, it is found that $C_w$ remains unchanged, and that the constant $C$ is proportional to the mass $M$ of the body: $C = cM$, where $c$ is a constant for the substance. The equation (1) has the form of an equation of conservation, in that the term relating to the body is equal but opposite

in sign to the term relating to the calorimeter. The equation suggests that there is something which does not change in the process, and which flows from the hotter to the colder body. This something is called *heat* and will be denoted by $\Delta H$. Both terms of (1) have the form

$$\Delta H = C(T' - T), \tag{2}$$

where $T'$ is the final temperature. The constant $C$ is called the *heat capacity* of the system.

Modern measurements have verified the fact that there is conservation of heat in all processes of thermal conduction. However, it turns out that the heat capacity is not strictly constant, but rather depends upon the temperature interval. It is therefore defined by an infinitesimal process. When $dH$ is the amount of heat required to raise the temperature of a substance from $T$ to $T + dT$, we define the *heat capacity $C$ at the temperature $T$* as the ratio

$$C = \frac{dH}{dT}. \tag{3}$$

It was mentioned that $C = cM$. The quantity $c$ is the heat capacity per unit mass, or *specific heat* of the substance. Let $dh = dH/M$ stand for the *heat imparted per unit mass*. Then from (3):

$$c = \frac{dh}{dT}. \tag{4}$$

The accepted unit of heat in physics is the *15° gram calorie* = 1 cal, defined as the heat required to raise the temperature of one gram of pure water from 14.5°C to 15.5°C. We shall, however, always express heat in mts mechanical units of energy (see 2·18).

**2·18. The first law of thermodynamics.** The concept of mechanical energy and its conservation was established by Leibnitz (1693). He showed that in an isolated system the sum of the potential and kinetic energies is constant. If a system is not isolated, any loss (or gain) of energy is compensated for by the accomplishment of an exactly equivalent amount of work by (or on) the system. The conservation of heat in all processes of thermal conduction, as formulated in 2·17, was established about seventy years later.

The role of the first law of thermodynamics is to bring these two separate kinds of conservation into one statement by asserting that *mechanical energy and heat are equivalent to each other and interconvertible.* This law was first suggested by Count Rumford (1798). However, the credit for having set the principle of the conservation of energy upon a firm

experimental foundation is due to Joule. In a classical experiment in 1849, Joule produced heat by churning water and other liquids with paddle wheels and thus determined directly the *mechanical equivalent of heat.* He found that

(1) $$1 \text{ cal} = 4.185 \times 10^{-3} \text{ kj},$$

and the joule was named in his honor. Séguin (1839), Mayer (1842), and particularly Helmholtz (1848) are regarded with Joule as also being founders of the first law, because of their important contributions to the understanding of its fundamental physical significance.

Since, according to the first law, heat is equivalent to mechanical energy, we shall always express heat in kilojoules, with dimensions $[ML^2T^{-2}]$. The conversion to calorie units can always be accomplished with (1), if desired.

We shall apply the first law to the thermodynamical systems of 2·01. We shall determine the fate of an infinitesimal amount of heat $dII$ introduced into the system from its environment. Since we are dealing with systems which are in equilibrium, there is no conversion of $dII$ into kinetic or potential energy. The heat $dH$ will in part cause the system to expand, and thereby do the work $dW$ against external pressure forces. In part the heat will be used to raise the temperature of the system, and perhaps also to overcome the resistance of inner forces of attraction between the molecules. This second portion will be denoted by $dU$ and is called the change of *internal energy* of the system. The first law says in symbols that

(2) $$dII = dU + dW.$$

Equation (2) is called the *energy equation* and is the complete mathematical description of an elementary process performed by a system in equilibrium.

The internal energy $U$ is a measure of the random molecular excitation of the system. Its value is found to depend only on the state of the system; that is, *$U$ is a function only of the mass and of the physical variables $p$, $\alpha$, and $T$.*

If we divide each term of (2) by the mass of the system, we obtain the energy equation in the form

(3) $$dh = du + dw = du + pd\alpha.$$

Here $u$ is the *internal energy per unit mass;* $dw$ is replaced by $pd\alpha$ from 2·14(3). Each term in (3) has the dimensions $[L^2T^{-2}]$ of specific energy.

**2·19. Specific heats of gases.** The specific heat of a substance was defined in 2·17 as the ratio $dh/dT$. This definition is adequate for a solid or liquid. For a gas, however, we must proceed carefully. Let a gase-

ous system at temperature $T_1$ be in the state represented by the point $A$ in fig. 2·16. As remarked in section 2·16, there are an infinite number of processes whereby the system can be warmed to the temperature $T_1 + dT$. Each one requires the absorption of a different amount of heat $dh$. Thus each process defines a different specific heat $dh/dT$.

From this multitude we select two specific heats of particular practical interest: (i) *the specific heat at constant volume* ($c_v$), defined by the isosteric process ($d\alpha = 0$) $AC$ of fig. 2·16; (ii) *the specific heat at constant pressure* ($c_p$), defined by the isobaric process ($dp = 0$) $AB$ of fig. 2·16. Thus we have

$$(1) \qquad c_v = \left(\frac{dh}{dT}\right)_{d\alpha=0}; \qquad c_p = \left(\frac{dh}{dT}\right)_{dp=0}.$$

The dimensions of specific heat are $[L^2T^{-2}\Theta^{-1}]$.

The two processes selected here must each satisfy the energy equation 2·18(3). This will lead in the next sections to several relations among the specific heats and the internal energy.

**2·20. Internal energy of a perfect gas.** The (specific) internal energy $u$ is a function only of $p$, $\alpha$, and $T$. By means of the equation of state 2·09(1), we may eliminate any one of these three variables, for example $p$. Then $u$ becomes a function of two independent variables $T$ and $\alpha$, and may be treated by the calculus as such. The change of internal energy $du$ from any given state may always be expressed in terms of the changes $d\alpha$ and $dT$ from that state. In the notation of the calculus:

$$(1) \qquad du = \frac{\partial u}{\partial T} dT + \frac{\partial u}{\partial \alpha} d\alpha.$$

The symbol $\partial u/\partial T$ is here interpreted to be the rate of change of $u$ with respect to $T$, in a process for which $\alpha$ is constant. Introducing the expression (1) into the energy equation 2·18(3), we get

$$(2) \qquad dh = \frac{\partial u}{\partial T} dT + \left(\frac{\partial u}{\partial \alpha} + p\right) d\alpha.$$

This equation is valid for any process. Specializing to the case of the isosteric process ($d\alpha = 0$), we obtain immediately from (2) and 2·19(1):

$$(3) \qquad c_v = \left(\frac{dh}{dT}\right)_{d\alpha=0} = \frac{\partial u}{\partial T}.$$

Comparing (1) and (3), we see that

$$(4) \qquad du = c_v dT + \frac{\partial u}{\partial \alpha} d\alpha.$$

To evaluate $\partial u/\partial\alpha$, i.e., to see how internal energy varies with a change in volume, we must have recourse to experiments. A suitable experiment is the so-called " expansion into the void." Two vessels, one of which contains the gas under high pressure, the other evacuated, are placed in communication by means of a pipe with a stopcock. The gas will then rush into the empty vessel without doing work $dw$, since it is pushing against no external forces. If the whole system is insulated, no heat $dh$ is imparted to the system. Applied to this process, the energy equation $dh = du + dw$ gives $du = 0$ for each step of the process. Denoting the finite changes during the complete expansion with a $\Delta$, we can write by means of (4):

$$\Delta u = c_v \Delta T + \frac{\partial u}{\partial \alpha}\Delta\alpha = 0 \quad \text{or} \quad \frac{\partial u}{\partial \alpha} = -c_v \frac{\Delta T}{\Delta \alpha}. \tag{5}$$

Joule performed this experiment and found $\Delta T = 0$ for all gases used. That is, there was no temperature increase during the expansion $\Delta\alpha$. He thus concluded from (5) that $\partial u/\partial\alpha = 0$ for all gases.

Later experiments permitting more accurate measurements showed an observable temperature change (Joule-Thomson effect). From such experiments, $\partial u/\partial\alpha$ is found to be small. The more nearly a given gas is " perfect " in the sense of 2·08, the nearer $\partial u/\partial\alpha$ is to 0. *It is therefore logical to include in the definition of a perfect gas the stipulation that its internal energy be entirely independent of volume*, or

$$\frac{\partial u}{\partial \alpha} = 0. \tag{6}$$

Combining (6) with (4), we obtain

$$du = c_v dT. \tag{7}$$

Now by (3) and (6)

$$\frac{\partial c_v}{\partial \alpha} = \frac{\partial}{\partial \alpha}\left(\frac{\partial u}{\partial T}\right) = \frac{\partial}{\partial T}\left(\frac{\partial u}{\partial \alpha}\right) = 0,$$

which shows that $c_v$ is a function of temperature alone. Experiments show that the variation of $c_v$ with temperature is the smaller, the nearer the gas approaches a perfect gas. *A third and last requirement of a perfect gas, therefore, is that $c_v$ be constant.*

The integral, $u = c_v T + \text{const}$, of (7) exhibits explicitly the functional dependence of $u$ on the state $(p, T, \alpha)$, but (7) itself is sufficient for our purposes.

**2·21. Specific heats of a perfect gas.** From 2·18(3) and 2·20(7), we may write the energy equation of a perfect gas in the form

$$dh = c_v dT + p d\alpha, \tag{1}$$

a very useful equation expressing the heat added in terms of the variation of the independent variables $T$ and $\alpha$. In order to compare the specific heats $c_p$ and $c_v$, we need an expression for $dh$ in terms of the variation of the independent variables $T$ and $p$. To get this, we differentiate the equation of state $p\alpha = RT$, whence

$$p d\alpha = R dT - \alpha dp. \tag{2}$$

Substituting for $pd\alpha$ in (1) we obtain

$$dh = (c_v + R)dT - \alpha dp. \tag{3}$$

But then we have for isobaric processes ($dp = 0$):

$$\left(\frac{dh}{dT}\right)_{dp=0} = c_v + R.$$

Comparing this with the definition 2·19(1) of $c_p$, we see that

$$c_p = c_v + R \quad \text{or} \quad c_p - c_v = R. \tag{4}$$

These equations (4) say with 2·20 that *for a perfect gas, $c_p$ and $c_v$ are both constants*, whose difference is equal to the specific gas constant $R$. It will be noted from 2·09 and 2·19 that equations (4) balance dimensionally.

That $c_p$ is larger than $c_v$ was already clear in 2·19, because in heating at constant pressure the gas must expand, thereby doing external work. The heat then is only partly used to raise the temperature. Thus more heat is required to raise it one degree isobarically than isosterically (where no work is done). See fig. 2·16.

For dry air, which is regarded as a perfect gas, we shall denote the specific heats by $c_{vd}$ and $c_{pd}$. From experiments their values are determined to be as follows:

$$c_{vd} = 717 \text{ kj t}^{-1} \text{ deg}^{-1}; \qquad c_{pd} = 1004 \text{ kj t}^{-1} \text{ deg}^{-1}. \tag{5}$$

Then by (5), $c_{pd} - c_{vd} = 287 \text{ kj t}^{-1} \text{ deg}^{-1} = R_d$, in accord with 2·09(6). These values should be remembered.

Actually $c_{vd}$ and $c_{pd}$ are found experimentally to vary slightly with temperature, but the variation may be disregarded in the atmospheric range of temperature.

**2·22. Energy equations in logarithmic form.** The energy equation is the starting point for most of the meteorological applications of thermodynamics. It is therefore desirable to express it in various useful ways. The basic expression is

$$dh = du + dw. \tag{2·18(3)}$$

To express $dh$ in terms of the independent variables $T$ and $\alpha$, we have

2·21(1) $$dh = c_v dT + p d\alpha.$$

To express $dh$ in terms of the independent variables $T$ and $p$, we can combine 2·21(3) and 2·21(4):

(1) $$dh = c_p dT - \alpha dp.$$

The last form will be used most often, since the variables $T$ and $p$ are those directly observed in the atmosphere.

The energy equation assumes a convenient form when both sides are divided by the temperature $T$, and the equation of state $p\alpha = RT$ is used. Equation 2·21(1) becomes

(2) $$\frac{dh}{T} = c_v \frac{dT}{T} + R \frac{d\alpha}{\alpha}.$$

Similarly, (1) becomes

(3) $$\frac{dh}{T} = c_p \frac{dT}{T} - R \frac{dp}{p}.$$

Now by differentiating the logarithm of the equation of state, called *logarithmic differentiation*, we get

(4) $$\frac{dp}{p} + \frac{d\alpha}{\alpha} = \frac{dT}{T}.$$

By means of (4) we can eliminate $dT$ from either (2) or (3). Then since by 2·21(4) $c_p = c_v + R$, we get

(5) $$\frac{dh}{T} = c_p \frac{d\alpha}{\alpha} + c_v \frac{dp}{p}.$$

The three forms (2), (3), and (5) of the energy equation may be written together in an order which makes them all easy to remember:

(6) $$\frac{dh}{T} = R\frac{d\alpha}{\alpha} + c_v \frac{dT}{T} = c_p \frac{dT}{T} - R\frac{dp}{p} = c_v \frac{dp}{p} + c_p \frac{d\alpha}{\alpha}.$$

Note that the variables in (6) are written in a certain cyclic order, starting with $\alpha$, $T$. The constants are written twice in order of magnitude, separated by a minus sign:

$$R, c_v, c_p, \; -R, c_v, c_p.$$

The symmetry of (6) is a superficial aspect of a far-reaching physical simplification which results from dividing the energy equation by $T$. This will be discussed in 2·28. For the present it suffices to note that

the expressions in (6) are differentials of functions of state. Thus we have:

$$(7) \qquad \frac{dh}{T} = d[\ln \alpha^R T^{c_v}] = d[\ln T^{c_p} p^{-R}] = d[\ln p^{c_v} \alpha^{c_p}].$$

By $\ln x$ we shall always mean the natural logarithm of $x$, i.e., the logarithm with base $e = 2.71828 \cdots$.

**2·23. Atmospheric processes.** The most fundamental process which adds or subtracts heat energy to or from a parcel of air in the atmosphere is radiation. Other important agencies for the exchange of heat are conduction, turbulent mixing, and internal friction. All these processes are continually influencing every element of the atmosphere in a complicated fashion, usually inaccessible to a detailed thermodynamic analysis. However, they all proceed quite slowly, compared with another important class of processes, which it will be our primary objective to analyze.

These other processes are those caused by the motion of the air and primarily by the vertical motion. They proceed with relative rapidity, so that they can profitably be investigated by neglecting the influences of the slow processes involving heat exchange between the system and its environment. We shall therefore concentrate our attention on processes for which there is assumed to be no heat exchange between the system and its environment. Such a process is called *adiabatic*.

Later, in chapter 3, we shall discuss processes which are not strictly adiabatic, but there the heat exchange will be small.

**2·24. Adiabatic processes of a perfect gas.** The condition which must be satisfied for an adiabatic process is by definition $dh = 0$. In 2·22 there are many expressions involving $dh$ and other variables. Each of them becomes a differential equation of the adiabatic process of a perfect gas, when $dh$ is replaced by 0. For reference, they are repeated here:

$$(1) \qquad du + dw = 0;$$

$$(2) \qquad c_v dT + p d\alpha = 0;$$

$$(3) \qquad c_p dT - \alpha dp = 0;$$

$$(4) \qquad R\frac{d\alpha}{\alpha} + c_v \frac{dT}{T} = c_p \frac{dT}{T} - R\frac{dp}{p} = c_v \frac{dp}{p} + c_p \frac{d\alpha}{\alpha} = 0;$$

$$(5) \qquad d[\ln \alpha^R T^{c_v}] = d[\ln T^{c_p} p^{-R}] = d[\ln p^{c_v} \alpha^{c_p}] = 0.$$

From the integration of (5), we get three equivalent relations between the variables of state in an adiabatic process:

$$\alpha^R T^{c_v} = \text{const}; \quad T^{c_p} p^{-R} = \text{const}; \quad p^{c_v} \alpha^{c_p} = \text{const}. \tag{6}$$

Defining two pure numbers $\kappa$ and $\eta$ by the relations

$$\kappa = \frac{R}{c_p} \quad \text{and} \quad \eta = \frac{c_p}{c_v}, \tag{7}$$

we can rewrite the more important two of the equations (6) in the form:

$$T = \text{const} \cdot p^{\kappa}; \tag{8}$$

$$p\alpha^{\eta} = \text{const}. \tag{9}$$

These are the equations derived by Poisson (1823), and generally bear his name. For this book, (8) is the more important, and $\kappa$ will be used often. Formula (9) will be discussed presently for illustration; the use of $\eta$ is not standard in meteorology. Both $\kappa$ and $\eta$ have dimension [1].

It must be understood that the constants of integration in (8) and (9) are fixed for one adiabatic process, but they will have different values for other adiabatic processes. They are each determined separately from the values of the physical variables at a given initial state, exactly as the constant in the equation of a straight line of slope 6,

$$y = 6x + \text{const},$$

is determined by knowing one point on the line.

We may also rewrite (8) and (9) in terms of the values $p_1$, $\alpha_1$, $T_1$ of the variables at an initial state:

$$\frac{T}{T_1} = \left(\frac{p}{p_1}\right)^{\kappa} \quad \text{or} \quad T = T_1 \left(\frac{p}{p_1}\right)^{\kappa}; \tag{10}$$

$$p\alpha^{\eta} = p_1 \alpha_1^{\eta}. \tag{11}$$

These equations are analogous to the point-slope equation of the straight line referred to above:

$$y - y_1 = 6(x - x_1).$$

For dry air, the Poisson constants $\kappa$ and $\eta$ have the following values:

$$\kappa_d = \frac{R_d}{c_{pd}} = 0.286, \qquad \eta_d = \frac{c_{pd}}{c_{vd}} = 1.400. \tag{12}$$

These values should be remembered.

**2·25. Adiabats on diagrams.** Each adiabatic process, like any other process, is represented by a definite curve on the $(\alpha,-p)$-diagram. The curve is called an *adiabat*, and its equation is 2·24(11). The whole

family of adiabats is given by 2·24(9)

$$p\alpha^{\eta} = \text{const},$$

as the constant varies. The family of *isotherms* was found in 2·16 to be given by the equation 2·16(1)

$$p\alpha = \text{const},$$

as the constant varies. The adiabats and the isotherms are distinct curves, since $\eta > 1$. The actual shape of the adiabats depends on the value of $\eta$. For dry air, when $\eta = \eta_d$, they are called *dry adiabats*.

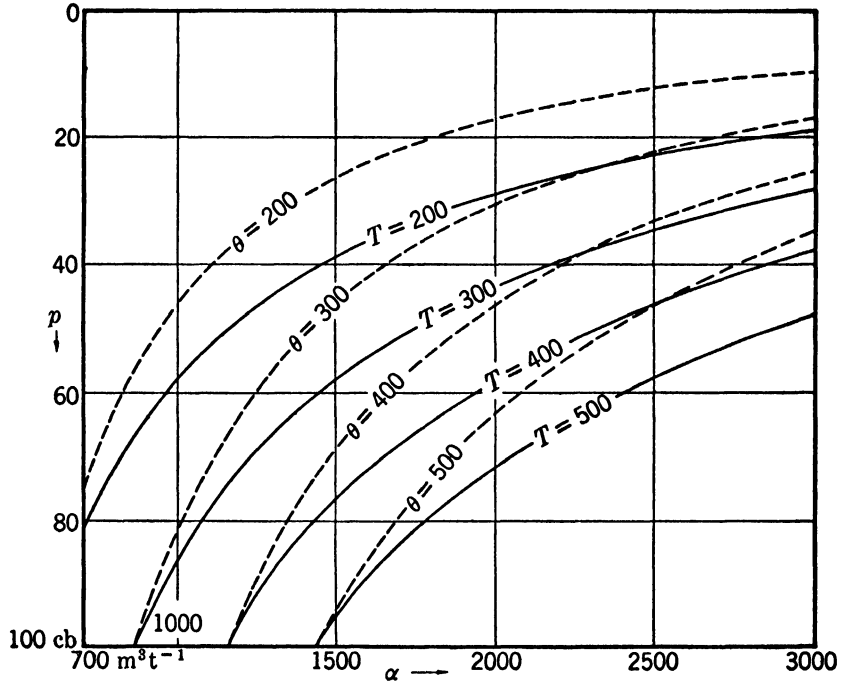



FIG. 2·25*a*. $(\alpha, -p)$-diagram.

In fig. 2·25*a* we have an $(\alpha, -p)$-diagram for the range of values of $\alpha$ and $p$ observed in the lower atmosphere. The isotherms $T = 200$, 300, 400, and 500 are drawn in solid lines; the dry adiabats $\theta = 200$, 300, 400, and 500 are drawn in dashed lines. $\theta$ is defined in 2·26. The adiabats have the same asymptotes as the isotherms, but their slope $(-dp/d\alpha = \eta p/\alpha)$ is steeper than the slope $(-dp/d\alpha = p/\alpha)$ of the isotherms.

The $(\alpha, -p)$-diagram is very suitable for a theoretical analysis of

atmospheric processes, since work is measured by an area on the diagram, as in 2·15(1). However, it is very inconvenient in actual practice for several reasons. First, neither the adiabatic nor the isothermal processes are represented by straight lines. Second, the variation of the variables requires that the adiabats and isotherms meet at too small an angle for easy discrimination. See fig. 2·25*a*. Third, the areas of most importance in meteorology are spread out inconveniently on the page, making it difficult to design this diagram as a well-shaped, large-scale chart for detailed use.

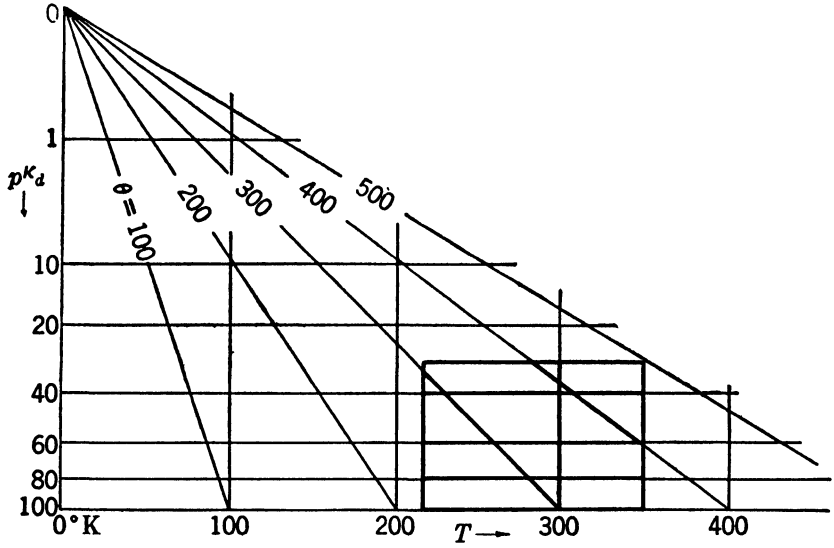



FIG. 2·25*b*. Stüve diagram.

Much better diagrams for practical purposes are those involving $p$ and $T$ as coordinate variables. These are more logical anyway, being those directly measured. The simplest of these diagrams is the Stüve diagram, which is the basic diagram on which the so-called pseudo-adiabatic chart is drawn. The Stüve diagram is designed to make the adiabats straight lines, while keeping $p$ and $T$ as the coordinate variables. This is accomplished by the device of using a linear temperature scale, but making the pressure coordinate represent pressures in terms of their $\kappa_d$th powers. Thus the isobar $p$ cb will be $p^{\kappa_d}$ units from the axis $p = 0$. The scale is for convenience still labeled in centibars. (See fig. 2·25*b*.) But now from 2·24(8) it will be seen that each dry adiabat will be a separate straight line through the origin ($p = 0$, $T = 0$). These are drawn in the figure, and finally the portion of the diagram of greatest

meteorological interest is drawn in heavy lines and enclosed in a frame. The rest is usually omitted from the meteorological charts.

The fact that in older books the value $\kappa_d = 0.288$ was used explains why this value occurs on many pseudo-adiabatic charts.

**2·26. Potential temperature.** The various dry adiabats on the Stüve diagram (or any other diagram) need to be *labeled.* The standard method is to *label each adiabat by the temperature $\theta$ at which it crosses the isobar $p = 100$ cb.* Any parcel of dry air is in some state $(p, T, \alpha)$, which is uniquely defined by $p$ and $T$. If we plot this state on the diagram, it will lie on some dry adiabat. The corresponding value of $\theta$ is the temperature read off the same dry adiabat at 100 cb. This temperature $\theta$ is defined to be the *potential temperature* of the parcel of air in the state $(p, T, \alpha)$. In physical language the potential temperature is the temperature which the air parcel assumes when compressed (or expanded) adiabatically to a pressure of 100 cb. $\theta$ is always expressed in degrees absolute and has the dimension $[\Theta]$ of temperature.

By 2·24(10) we see that the potential temperature $\theta$ of dry air can be computed from the formula

$$\theta = T\left(\frac{100}{p}\right)^{\kappa_d}. \tag{1}$$

The student should be able to use formula (1) readily, with the aid of logarithm tables, even though in practice $\theta$ is usually estimated from a diagram. When $\theta$ is given a constant value, (1) gives the variation of $T$ and $p$ in the dry-adiabatic process. It is equivalent in this respect to 2·24(8).

The potential temperature is an invaluable aid to the thermodynamical study of the atmosphere. The main reason for this is that, as mentioned in 2·23, short-term atmospheric processes are adiabatic. Unless the air is saturated, they are approximately dry adiabatic. But in a dry-adiabatic process, $\theta$ remains unchanged, even though $T$ and $p$ may change a great deal. Such a quantity, which remains invariant under dry-adiabatic processes, is called a *conservative* property of atmospheric air. Thus potential temperature is conservative, and as such may be used to identify air masses through a short interval of time (say 24 hours).

For dry air still another form of the energy equation can be obtained by logarithmic differentiation of (1). We get

$$\frac{d\theta}{\theta} = \frac{dT}{T} - \kappa_d \frac{dp}{p} = \frac{dT}{T} - \frac{R_d}{c_{pd}} \frac{dp}{p}, \tag{2}$$

where $\kappa_d$ has been removed by 2·24(12). Multiplying (2) by $c_{pd}$, v obtain

$$c_{pd}\frac{d\theta}{\theta} = c_{pd}\frac{dT}{T} - R_d\frac{dp}{p}. \tag{3}$$

Comparing (3) with 2·22(6), we see that

$$\frac{dh}{T} = c_{pd}\frac{d\theta}{\theta} = d(c_{pd}\ln\theta). \tag{4}$$

By (4) we see that when $dh = 0$, then $d\theta = 0$ (which we already knew We can also compute the magnitude of the change $d\theta$ of potenti temperature, due to the introduction of $dh$ kj $t^{-1}$ of heat.

*It must be emphasized that so far $\theta$ is defined only for dry air.*

**2·27. Differentials and functions of state.** A physical variable called a *function of state* if it can be expressed as a single-valued math matical function of two of the variables $\alpha$, $p$, $T$ defining the state: f example, as a function of $\alpha$ and $p$. In physical language, a variable a function of state whenever in th $(\alpha,-p)$-diagram it is possible t draw lines along which the var able assumes one constant valu Such lines are called *isopleths* of th variable. Some of the functior of state so far considered are no listed, together with the speci names (if any) of their isopleth $p$(isobars), $T$(isotherms), $\theta$(adi bats), $\alpha$(isosteres), $\rho$(isopycnics),

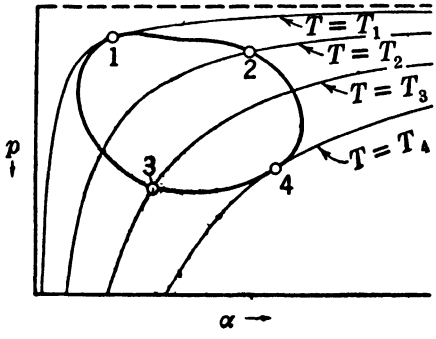


FIG. 2·27.

The differentials so far considered may be placed in two groups. I the first group are $dp$, $dT$, $d\theta$, $d\alpha$, $d\rho$, and $du$, all of which are differentia of the functions of state just mentioned. The differential of any fun tion of state is called an *exact differential.*

In the second group are $dw$ and $dh$, which are not differentials of fun tions of state, and are therefore called *inexact differentials.* That is, *n functions of state w and h exist whose differentials are dw and dh.* This wi be proved below.

We first quote a theorem from the calculus:

(1) *The integral of an exact differential around a closed path is zero.*

The rigorous proof of (1) may be found in any textbook of advance calculus. The general idea may be illustrated by considering $\int_c dI$ where $c$ is the closed path 13421 in the $(\alpha,-p)$-diagram of fig. 2·2

Starting the integration at 1, it turns out that the integral $\int dT$ along $c$ from 1 to 3 is equal to the net change of $T$ between 1 and 3. This can be measured by subtracting the $T$-value $T_1$ of the isotherm through 1 from the $T$-value $T_3$ of the isotherm through 3, giving $T_3 - T_1$. Let the integration be continued through points 4 and 2 back to the starting point 1 again. The value of $\int_c dT$ will be the net change of $T$ over the complete path. This will be obtained by subtracting the $T$-value $T_1$ from itself, giving zero.

Now let us integrate the energy equation 2·18(3) around a cyclic path $c$ enclosing the positive area $A$. By (1), $\int_c du = 0$. Using 2·15(2), we then have

$$(2) \qquad \int_c dh = \int_c du + \int_c dw = \int_c dw = A > 0.$$

From (2), we see that neither $\int_c dh$ nor $\int_c dw$ is zero. It then follows from (1) that $dh$ and $dw$ cannot be exact differentials, as asserted previously.

Exact differentials are very handy to deal with mathematically. The integral from 1 to 2 of any exact differential $d\varphi$ may be evaluated as the difference $\varphi_2 - \varphi_1$ in the values of the $\varphi$-isopleths between states 1 and 2. For an inexact differential like $dw$, on the other hand, there are no isopleths to draw, and $\int_1^2 dw$ depends entirely on the path of integration from 1 to 2. See 2·15.

**2·28. Entropy.** Equation 2·26(4) states that for dry air $dh/T$ is equal to the differential of the function of state $c_{pd} \ln \theta$. From 2·22(7) it is seen that for *any* perfect gas $dh/T$ is the differential of a function of state, namely, any of the functions in brackets in 2·22(7), which differ only by a constant. According to the definitions of 2·27, in these instances $dh/T$ is an exact differential.

The foregoing are but instances of a very general thermodynamical theorem, whose proof is given in any standard textbook on thermodynamics. This asserts for an arbitrary system, whether or not the equation of state and the internal energy function are known, that *the expression $dh/T$ is always an exact differential.* As such it is the differential of a function of state which is called the (*specific*) *entropy* of the system, denoted by $s$. The dimensions of specific entropy are those of specific heat, namely, $[L^2T^{-2}\Theta^{-1}]$. The *total entropy* $S$ is equal to $s$ times the mass of the system.

We have always

$$(1) \qquad ds = \frac{dh}{T} \quad \text{or} \quad s = \int \frac{dh}{T} + \text{const.}$$

Being defined differentially, $s$ is known only up to an arbitrary constant. For dry air, because of 2·26(4),

$$s = s_d = c_{pd} \ln \theta + \text{const.} \tag{2}$$

For any perfect gas, because of 2·22(7),

$$s = \ln [\alpha^R T^{c_v}] + \text{const} = \ln [T^{c_p} p^{-R}] + \text{const} = \ln [p^{c_v} \alpha^{c_p}] + \text{const.} \tag{3}$$

In general, for any system

$$s = \text{some function of } \alpha, p, \text{ and } T. \tag{4}$$

Since by (1) an adiabatic process ($dh = 0$) is a process for which entropy is constant ($ds = 0$), adiabatic processes are often called *isentropic.*

The factor $1/T$ is called an *integrating factor* for the inexact differential $dh$, since $dh/T$ is exact. It is this which yields the logical definition of temperature mentioned in 2·05: logically temperature is simply the reciprocal of the integrating factor for $dh$.

The fact that $ds$ is exact makes entropy very important as a heat variable in thermodynamics. Because of its abstract definition, however, entropy is rather bewildering to the student, and we shall use it as little as possible. For dry air, the concrete meteorological variable $\theta$ can completely replace entropy.

**2·29. Thermodynamic diagrams.** It has already been shown that thermodynamic processes can be represented and studied on a diagram whose coordinates are the independent variables of the system. Any such diagram is called a thermodynamic diagram, and the first example was the $(\alpha, -p)$-diagram of 2·15 and 2·25. Another was the Stüve diagram of 2·25. We shall conclude this chapter with a discussion of the emagram and tephigram.

A great deal of dispute is heard among meteorologists as to which are the best diagrams. The majority of problems can be worked theoretically with equal facility on all the basic diagrams, since they are all maps of each other. What really makes one diagram easy to use is the accuracy, clarity, and convenient scale with which its plate has been drawn. For certain special problems, special scales are required, and these can (usually) be put on any diagram, but in practice they are found only on special prints made for the purpose.

As for the basic diagrams in frequent use in the United States — the Stüve diagram, the emagram, and the tephigram — it is most important that the student first realize their *similarities*, not their differences. The fact is that all are " maps " of each other. Like all maps, all can show the same lines, if desired. Finally, like all maps, each bears the individuality of the particular projection.

**2·30. Important criteria of the diagram.** There are three criteria which we shall use to examine each diagram after it has been defined.

(i) How large an angle is there between the isotherms and the adiabats? A large angle is desirable, since soundings drawn on the diagrams will be analyzed on the basis of their slopes. The larger the angle, the easier it is to distinguish important changes of slope.

(ii) How many of the important isopleths (isobars, isotherms, adiabats, etc.) are straight lines? The more straight lines and the less curved lines, the easier the diagram is to use.

(iii) Is the work done in a cyclic process proportional to the area enclosed by the curve representing the process? This is an essential feature in theory, and it is important in practice for certain operations. On the whole, however, this feature has probably received too much emphasis in meteorology.

**2·31. Stüve diagram.** As it was discussed in 2·25, the Stüve diagram need not be defined again. The student should get a pseudo-adiabatic chart and make sure he can determine the pressure, temperature, and potential temperature of any point on it. The other lines will be introduced in chapter 3. As for the criteria of 2·30:

(i) Theoretically, by stretching the $T$ axis sufficiently, the angle between adiabats and isotherms in the atmospheric range could be made arbitrarily close to 90°. In practice, to keep the diagram more or less square and legible, the angle is near 45°. See fig. 2·25*b*.

(ii) Isobars, isotherms, and adiabats are all straight lines.

(iii) The work done is not proportional to the area enclosed but depends also on which pressures the area covers. The variation is rather gradual. For example, one square centimeter represents about 25% more energy at 40 cb than the same area at 100 cb.

**2·32. Emagram.** The emagram is a graph of $-\ln p$ against $T$. It was specifically designed to be a pressure-temperature graph having the work-area property (iii) of 2·30. From this property Refsdal gave the diagram its name, as an abbreviation for "energy-per-unit-mass diagram." It is sometimes also named after Hertz, Neuhoff, and Väisälä, who discussed the diagram and added features to it.

The emagram has a linear temperature scale on the horizontal axis, and a logarithmic pressure scale, increasing downward, as a vertical coordinate. Since as $p \to 0$, $\lim(-\ln p) = \infty$, the diagram must in practice be cut at some low pressure, usually 4 cb.

After the axis scales have been drawn (see fig. 2·32*a*) the adiabats are drawn in by formula 2·26(1), or else they are plotted from a Stüve diagram. The equation of any adiabat can be obtained by taking the

logarithm of 2·26(1) for $\theta = \text{const}$:

$$-\ln p = -\frac{1}{\kappa_d} \ln T + \text{const.} \tag{1}$$

Formula (1) shows two things. First, each adiabat is a logarithmic curve on the emagram, becoming steeper with decreasing $T$. Second,

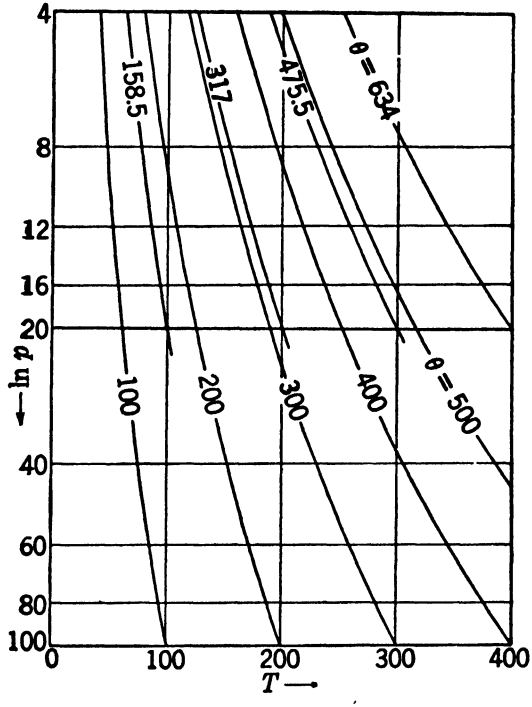



FIG. 2·32*a*. Emagram.

any two adiabats may be brought into coincidence by a displacement parallel to the ln $p$ axis, so that all adiabats are congruent. As for the criteria of 2·30:

(i) As in the Stüve diagram, the angle between adiabats and isotherms in the atmospheric range can be adjusted to any value short of 90°. But again the convenience of scale and economy of paper dictate that the angle be about 45°.

(ii) The isobars and isotherms are straight lines, but the adiabats are logarithmic curves.

(iii) The work $w$ done in a cyclic process $c$ is proportional to the area $A'$ enclosed by $c$ on the emagram. To see this, we recall from

2·21(2) that

$$dw = pd\alpha = R_d dT - \alpha dp.$$

Hence the work $w$ is given by

$$(2) \qquad \int_c dw = \int_c R_d dT - \int_c \alpha dp = -\int_c \alpha dp,$$

where one integral is 0 by 2·27(1). Now $\alpha = R_d T/p$ by the equation of state. Hence from (2)

$$(3) \qquad w = -\int_c \frac{R_d T}{p} dp = R_d \int_c T\, d(-\ln p) = R_d A'.$$

The last equality follows for the emagram, whose coordinates are $T$ and $-\ln p$, just as 2·15(2) is true for an $(\alpha, -p)$-diagram.

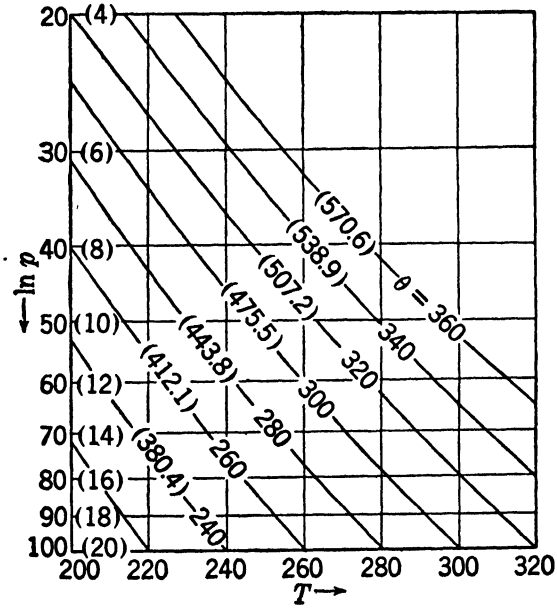



FIG. 2·32*b*. Emagram.

One other feature of the emagram as drawn in practice must be mentioned. Note in fig. 2·32*a* that the isobars for $p$ = 4, 8, 12, 16, and 20 cb appear to have exactly the same relative position and spacing as the isobars whose pressures are respectively five times as large, namely, $p$ = 20, 40, 60, 80, and 100 cb. Thus the portion of the coordinate grid on the emagram between 4 cb and 20 cb appears to be congruent to that

portion between 20 cb and 100 cb. If the graph were cut in two at 20 cb and the two halves superimposed as in fig. 2·32*b*, then each isobar would represent *two* pressures: (i) a " high " pressure above 20 cb; (ii) a " low " pressure under 20 cb, which is one-fifth of the corresponding high pressure.

The reason for the congruence of the high- and low-pressure scales is the logarithmic pressure scale. To draw a logarithmic scale, a base line is fixed, corresponding to the isobar $p = 1$ ($\ln p = 0$). A unit of length is fixed. The isobar for $p$ cb is drawn $\ln p$ units away from $p = 1$. Now $\ln 5p = \ln 5 + \ln p$. Hence the isobar for $5p$ cb is just $\ln 5 + \ln p$ units away from $p = 1$. Hence the isobar for $5p$ cb is found just $\ln 5$ units below the isobar for $p$ cb. This results in the congruence mentioned.

Not only the isobars do double duty in fig. 2·32*b*, but the adiabats also can serve with either the high pressures or the low pressures by simply changing the value of their label $\theta$. This follows from the fact that all adiabats are congruent to each other.

Fig. 2·32*b* is drawn with the low pressures in parentheses. The values of $\theta$ to be used with the low-pressure scale are also in parentheses. The high pressures and corresponding values of $\theta$ are without parentheses. The diagram has also been cut to the atmospheric temperature range. The student should get an emagram and become familiar with the scales introduced here.

*Exercise.* Prove that if an adiabat has the value $\theta = \theta_1$ on the high-pressure scale, then it has the value $\theta = 5^{\kappa_d} \cdot \theta_1$ on the low-pressure scale. Check fig. 2·32*b* by this formula.

**2·33. Tephigram.** The tephigram is a graph of $\ln \theta$ against $T$. This diagram has a linear temperature scale and a logarithmic $\theta$ scale which is a linear entropy scale, by 2·28(2). The diagram was adopted for meteorological use by Shaw (who used the symbol $\phi$ for entropy), and was called by him a $T$-$\phi$-gram or tephigram. The coordinates are shown in fig. 2·33*a*.

The equation for the isobars in terms of $T$ and $\theta$ as independent variables is given by 2·26(1). For each isobar, $p$ is constant, whence $\theta = \text{const} \cdot T$. Thus,

$$\ln \theta = \ln T + \text{const} \qquad \text{(isobar)}. \tag{1}$$

From (1) we see that each isobar is a logarithmic curve on the tephigram. Furthermore, *all isobars are congruent, and any two isobars may be brought into coincidence by a displacement parallel to the ln θ axis.* See fig. 2·33*a*. Equations 2·32(1) and 2·33(1) may be compared.

In fig. 2·33*a* the approximate range of variables commonly used is out-

lined with a rectangle. This rectangle is then rotated, so that the isobars are roughly horizontal. A sketch of the resulting diagram is shown in fig. 2·33*b*. As for the criteria of 2·30:

(i) The angle between the adiabats and isotherms is exactly 90°, since these lines are the coordinates of the tephigram. This 90° angle is probably the greatest advantage of this diagram.

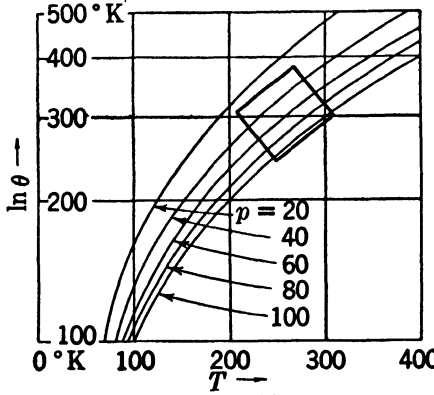



FIG. 2·33*a*. Tephigram.

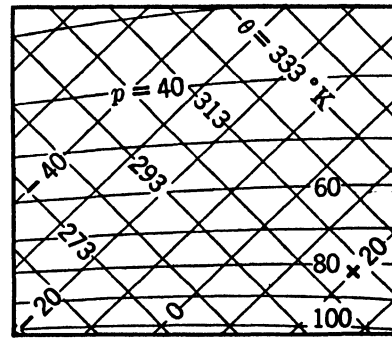



FIG. 2·33*b*. Tephigram.

(ii) The isotherms and adiabats are straight lines, whereas the isobars have a curvature which is slight in the atmospheric range.

(iii) The work $w$ done in a cyclic process $c$ is proportional to the area $A''$ enclosed by $c$ on the tephigram. To see this, note from 2·26(4) that

$$dh = c_{pd} T d(\ln \theta). \tag{2}$$

Now by (2) and 2·27(2),

$$w = \int_c dw = \int_c dh = c_{pd} \int_c T d(\ln \theta). \tag{3}$$

But the last integral is $c_{pd} A''$, whence $w$ is proportional to $A''$.

The student should get a tephigram, and become completely familiar with the coordinates so far introduced. Above all, he should see that the Stüve diagram, emagram, and tephigram are all minor distortions of each other.

CHAPTER THREE

# THERMAL PROPERTIES OF WATER SUBSTANCE AND MOIST AIR

**3·01. Isotherms of water substance.** The preceding chapter has treated the thermal properties of dry air in equilibrium as a special case of a perfect gas. Any real gas actually behaves nearly like a perfect gas in a temperature range where it can neither liquefy nor solidify. The isotherms of a real gas are therefore nearly rectangular hyperbolas

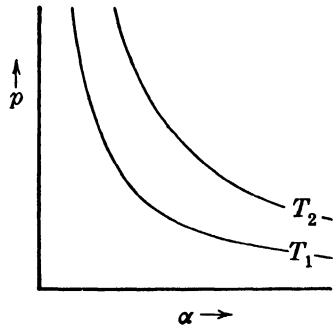



FIG. 3·01*a*.

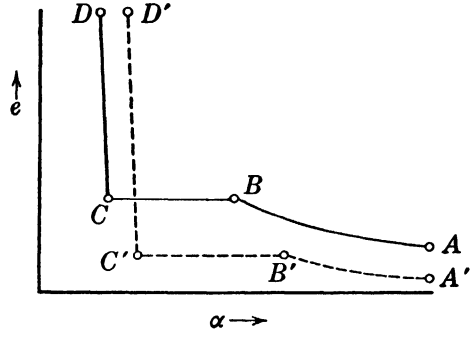



FIG. 3·01*b*.

in the $(\alpha,p)$-diagram. (See fig. 3·01*a* and compare fig. 2·16. Here we follow the practice of physicists in having pressure increase upward. This is convenient, since the system considered at present is not the atmosphere. Cf. 2·15.)

Water substance, however, does liquefy and freeze in the atmosphere. Its isotherms are therefore complicated. Consider a sample of pure water vapor in a cylinder. We shall denote the vapor pressure by $e$, reserving $p$ for pressure in the atmosphere. Let the vapor be compressed by a piston while the system remains at a constant temperature of say 300°K. We shall follow the true isotherm 300°K on an $(\alpha,e)$-diagram, as drawn from empirical evidence. See the schematic diagram in fig. 3·01*b*.

The specific volume $\alpha$ will roughly follow the perfect gas behavior from $A$ until the vapor becomes " saturated " at a definite pressure, depending on the temperature. This pressure is called the *saturation vapor*

*pressure*, and in the present instance equals 3.6 cb (see point $B$). Further compression by the piston does not change the pressure $e$. Instead, the vapor gradually condenses, and the isotherm proceeds from $B$ ($\alpha \approx 39{,}000$ m$^3$ t$^{-1}$) to $C$ ($\alpha \approx 1$ m$^3$ t$^{-1}$), where we have only liquid water. After this, further compression can reduce $\alpha$ but very little, since water is nearly incompressible. Thus the isotherm continues from $C$ nearly parallel to the $e$ axis to $D$ and beyond.

If we follow the isotherm 250°K in the same manner (see dotted line in fig. 3·01*b*), we get a similar pattern, except that no liquid stage occurs. The vapor starts to solidify directly to ice at $e = 0.077$ cb, $\alpha \approx 1.5 \times 10^6$ m$^3$ t$^{-1}$ (point $B'$). All the vapor is solidified into ice at the point $C'$ ($\alpha \approx 1.09$ m$^3$ t$^{-1}$). Further compression of the ice at ordinary high pressures results in no significant volume change.

**3·02. ($\alpha$,$e$)-diagram and the triple state.** The above considerations show that we must examine in some detail the behavior of water substance under equilibrium conditions. To a certain extent it is possible to describe the liquid and vapor phases of *all* fluids by one equation,

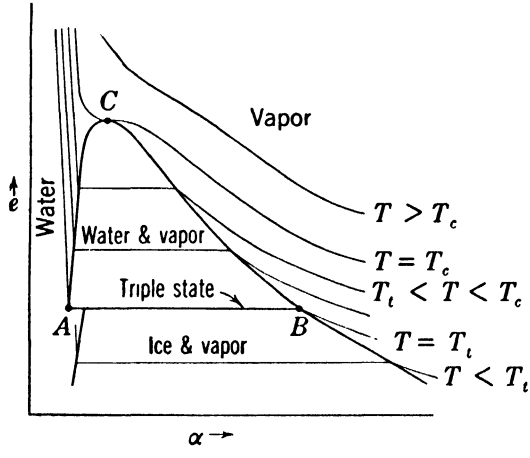



FIG. 3·02.

the van der Waals equation of state. Since the van der Waals formula is not very successful with water and water vapor, and since it does not even pretend to describe the solid phase, we will omit any such discussion. We prefer to give the ($\alpha$,$e$)-diagram obtained from experiments on water substance.

Fig. 3·02 shows a number of isotherms in the ($\alpha$,$e$)-diagram. For temperatures above the *critical temperature* $T_c$ (647°K for water substance), the vapor never condenses, and the isotherms are roughly like

those for a perfect gas. For temperatures between the *triple state temperature* $T_t$ (273°K for water) and $T_c$, the isotherms look like the solid line in fig. 3·01*b*. The significance of $T_t$ and $T_c$ is explained in this and the following sections. For $T < T_t$, the vapor condenses directly to ice on compression, as shown. On further compression the specific volume of the ice remains near 1.09 $m^3\ t^{-1}$, until at high enough pressures the ice melts to water, or else changes to a second crystalline form of ice. Neither of the last processes is represented in fig. 3·02, as it would unduly complicate the left side of the diagram. The ice ↔ water transition will be discussed in detail in section 3·13.

The empirical evidence thus shows that the $(\alpha,e)$-diagram is divided into several regions, each region representing one type of phase equilibrium for water substance. Some of these regions are outlined with heavy lines in fig. 3·02 and are labeled *vapor*, *water*, *water & vapor*, *ice & vapor*. The regions *ice* and *ice & water* have been omitted.

The line $AB$ represents all states where the three phases ice, water, and vapor can exist simultaneously in *equilibrium* in any relative proportions. This is the *triple state*. It is found to occur for water substance at

(1) $$e = 0.611 \text{ cb}; \qquad T_t - T_0 = 0.0075°\text{C}.$$

The corresponding specific volumes of ice, water, and vapor are respectively (in $m^3\ t^{-1}$)

(2) $$\alpha_i = 1.091; \qquad \alpha_w = 1.000; \qquad \alpha_v \approx 206{,}000.$$

One phenomenon has been entirely omitted in this discussion, the supercooling of water. The discussion of this topic is reserved in section 3·15.

**3·03. The critical state.** The point $C$ in fig. 3·02 is the point where the critical isotherm touches the *water & vapor* region. The corresponding state is called the *critical state*. For water substance, the critical state occurs at approximately*

(1) $$e_c = 22{,}100 \text{ cb} \approx 218 \text{ atm}; \qquad T_c = 647°\text{K}; \qquad \alpha_c = 3.1\ m^3\ t^{-1}.$$

*The critical temperature $T_c$ is the highest temperature at which water and vapor can co-exist in equilibrium.* The critical pressure $e_c$ is similarly the highest pressure at which water and vapor can co-exist in equilibrium. The critical specific volume $\alpha_c$ is the value of $\alpha$ observed at the critical temperature and pressure.

* N. Ernest Dorsey (comp.), *Properties of Ordinary Water-Substance*, Reinhold Publishing Corp., New York, 1940; p. 558.

It is seen from fig. 3·02 that it is possible to take a sample of vapor into the state labeled *water* without passing through any transition zone, for example, by keeping the pressure greater than $e_c$; i.e., there is no boundary curve in fig. 3·02 separating *water* from *vapor*. This corresponds to the experimental fact that vapor goes into water at these pressures without any abrupt transition.

It is arbitrary whether we call the fluid a vapor or a liquid in this region. For $\alpha < \alpha_c$, the critical isotherm is customarily taken as the boundary between vapor and liquid. We then have the following rule pertaining to all fluids: *It is impossible to liquefy a substance at temperatures higher than the critical.* This law explains why the permanent gases of the air are never liquefied at atmospheric temperatures: their critical temperatures are too low.

Table 3·03 gives the critical data* for some permanent gases and carbon dioxide.

TABLE 3·03

| Gas | $T_c$ (°K) | $p_c$ (cb) | $\alpha_c$ ($m^3\ t^{-1}$) |
|---|---|---|---|
| He | 5.2 | 230 | 14.4 |
| $H_2$ | 33.2 | 1300 | 32.2 |
| $N_2$ | 126.0 | 3390 | 3.2 |
| $O_2$ | 154.3 | 5040 | 2.3 |
| $CO_2$ | 304.1 | 7400 | 2.2 |

**3·04. Thermal properties of ice.** Beginning with ice, we shall discuss separately the thermal properties of the three phases of water substance and the various changes of phase.

Ice, the solid phase of water substance, is known to exist in several different crystalline states, each of which is properly a phase itself. Since only one of these phases occurs in the atmosphere, we shall ignore the others

At 0°C the specific volume $\alpha_i$ of ice is given by

$$\alpha_i = 1.091\ m^3\ t^{-1}. \tag{1}$$

On cooling below 0°C ice contracts so slowly that we may regard $\alpha_i$ as constant for our purposes.

The specific heat $c_i$ of ice (cf. 2·17) varies with temperature, but the 0°C value†

$$c_i = 2060\ kj\ t^{-1}\ deg^{-1} \tag{2}$$

is sufficiently accurate for atmospheric problems.

* Charles D. Hodgman (edit.), *Handbook of Chemistry and Physics*, 25th edition, Chemical Rubber Publishing Co., Cleveland, 1941; pp. 1703–1705.

† Edward W. Washburn (editor-in-chief), *International Critical Tables of Numerical Data*, McGraw-Hill Book Company, New York, 1926 ff., 7 vol. and index; vol. 5, p. 95.

**3·05. Thermal properties of water.** The specific volume $\alpha_w$ of (liquid) water assumes its least value $\alpha_w = 1.00\ \text{m}^3\ \text{t}^{-1}$ near 4°C. (This value will be recalled from section 1·04 as the definition of unit specific volume.) $\alpha_w$ increases somewhat at higher and lower temperatures, getting as high as $1.043\ \text{m}^3\ \text{t}^{-1}$ at 100°C. In the atmosphere we shall use

$$\alpha_w = 1.00\ \text{m}^3\ \text{t}^{-1} \tag{1}$$

in computations, regarding $\alpha_w$ as constant for practical purposes.

The specific heat of water is denoted by $c_w$, and it varies slightly with temperature. The gram calorie was defined in 2·17 as the heat required to heat one gram of water one degree at 15°C. Referring to the mechanical equivalent of heat, 2·18(1), we have at 15°C

$$c_w = 4185\ \text{kj}\ \text{t}^{-1}\ \text{deg}^{-1}. \tag{2}$$

In our subsequent work we shall treat $c_w$ as a constant with this value.

**3·06. Equation of state of water vapor.** As in section 3·01, the pressure exerted by water vapor will be denoted by $e$. The other physical variables relating to water vapor will be denoted by the subscript $v$, for example, $\alpha_v$. With the assumption that water vapor behaves closely enough like a perfect gas, its equation of state 2·09(1) has the form

$$e\alpha_v = R_v T. \tag{1}$$

The gas constant $R_v$ is computed from the relation 2·11(4), $R^* = m_v R_v$, where $m_v$ (= 18.016) is the molecular weight of water vapor. This gives

$$R_v = \frac{R^*}{m_v} = \frac{8313.6}{18.016} = 461.5\ \text{kj}\ \text{t}^{-1}\ \text{deg}^{-1}. \tag{2}$$

For later work it is convenient to express $R_v$ in terms of $R_d$, using the relation $R^* = m_v R_v = m_d R_d$, where by 2·13(1) $m_d$ (= 28.97) is the molecular weight of dry air. Thus

$$R_v = \frac{m_d}{m_v} R_d = \frac{1}{\epsilon} R_d, \tag{3}$$

where

$$\epsilon = \frac{m_v}{m_d} = 0.622. \tag{4}$$

By introducing in (1) the expression (3) for $R_v$, the equation of state for water vapor takes the form in which we will generally write it:

$$e\alpha_v = \frac{1}{\epsilon} R_d T. \tag{5}$$

It will be useful later to know the magnitude of $\alpha_v$ under certain special conditions. The following values are computed from (5). At the normal boiling point

(6) $$(\alpha_v)_{1\text{ atm},\,373^\circ} = 1699\ \text{m}^3\ \text{t}^{-1}.$$

Saturated vapor at the triple state (nearly 0°C) has

(7) $$(\alpha_v)_{0.611\text{ cb},\,273^\circ} = 206{,}200\ \text{m}^3\ \text{t}^{-1}.$$

Saturated atmospheric air seldom is warmer than 35°C. The corresponding saturation vapor pressure (5.62 cb) is therefore the highest, and the corresponding value of $\alpha_v$ is the lowest, value which normally occurs in the atmosphere. This value is

(8) $$(\alpha_v)_{5.62\text{ cb},\,308^\circ} = 25{,}290\ \text{m}^3\ \text{t}^{-1}.$$

As a check on the accuracy of (5), we give the values of $\alpha_v$ in the three cases above, as taken from experimental data in the *Handbook of Chemistry and Physics*:*

$$\left.\begin{aligned}(\alpha_v)_{1\text{ atm},\,373^\circ} &= 1671\ \text{m}^3\ \text{t}^{-1}\\ (\alpha_v)_{0.611\text{ cb},\,273^\circ} &= 206{,}300\ \text{m}^3\ \text{t}^{-1}\\ (\alpha_v)_{5.62\text{ cb},\,308^\circ} &= 25{,}250\ \text{m}^3\ \text{t}^{-1}\end{aligned}\right\}\quad\text{(empirical)}.$$

Thus it will be seen that at atmospheric temperatures (5) gives all accuracy possible from the data. At the boiling point a 2% error is found. For temperatures and pressures approaching the critical, it is found necessary to use a more refined equation of state.

**3·07. Specific heats of water vapor.** For ice and liquid water the specific heats $c_i$ and $c_w$ are practically independent of the type of process used to heat the substance. For water vapor, however, as in section 2·19, we must distinguish various specific heats. The specific heat of water vapor at constant pressure will be denoted by $c_{pv}$. The specific heat of water vapor at constant volume will be denoted by $c_{vv}$.

The variation of $c_{pv}$ and $c_{vv}$ with temperature is quite considerable. Furthermore, there are few data available as to their values at atmospheric temperatures. Simply to fix the magnitudes of these quantities for our calculations, we shall regard $c_{pv}$ and $c_{vv}$ as constants in the atmosphere, with the following values:†

(1) $$c_{pv} = 1911\ \text{kj}\ \text{t}^{-1}\ \text{deg}^{-1};\qquad c_{vv} = 1450\ \text{kj}\ \text{t}^{-1}\ \text{deg}^{-1}.$$

* *Op. cit.*, pp. 1772–1777.

† $c_{pv}$ is converted to mechanical units from an estimated value given in Dorsey, *op. cit.*, p. 599, line 4. The value of $c_{vv}$, chosen so that our equation 3·07 (2) is satisfied, is near the mean of two determinations reported by Dorsey, *op. cit.*, p. 105.

These values may be as much as 2% in error. With the chosen values, we have

$$c_{pv} - c_{vv} = 461 \approx R_v, \tag{2}$$

which agrees with 2·21(4). Since water vapor is in some ways far from being a perfect gas, $c_{pv} - c_{vv}$ may actually differ from $R_v$, but the order of magnitude is correct.

**3·08. Changes of phase.** In sections 3·01 and 3·02 it was stated that at certain pressures and temperatures an equilibrium may exist between any two phases, for example, between liquid water and water vapor. To make the following discussion apply to all three phase-equilibria, we shall denote the phases by 1 and 2. The pressure at which the two phases are in equilibrium will be denoted by $e_s$. This notation will be used throughout the chapter.

Consider now a process where a unit of mass transforms at equilibrium from phase 1 to phase 2. The equation of energy 2·18(3) can be written in the following form, since $dh = Tds$ by 2·28(1):

$$dh = Tds = du + e_s d\alpha. \tag{1}$$

Here $s$ is the specific entropy of the system. The complete change of phase will be represented by integrating (1) from phase 1 to phase 2:

$$\int_1^2 dh = \int_1^2 Tds = \int_1^2 du + \int_1^2 e_s d\alpha. \tag{2}$$

The first integral represents the total amount of heat *absorbed* by the unit mass in phase 1 in order to cause it to transform completely into phase 2. It is known as the *latent heat of the transformation 1 to 2*, and will be denoted by $L_{12}$. Latent heat has the dimensions $[L^2T^{-2}]$ of specific energy. The pressure and temperature remain constant during the transformation (see fig. 3·01*b*), so that (2) may be integrated:

$$L_{12} = T(s_2 - s_1) = (u_2 - u_1) + e_s(\alpha_2 - \alpha_1). \tag{3}$$

The equation (3) will be used in later work.

For the present it suffices to realize that, at each pressure $e_s$ and corresponding temperature $T$ where two phases can co-exist, there is a definite latent heat $L_{12}$. $L_{12}$ varies with temperature, and it is different for each of the three phase transformations. Also, $L_{12}$ is equal to the amount of heat *released* by a unit mass in phase 2 when it transforms to phase 1. (That is to say, $L_{12} = -L_{21}$.)

The three possible phase transformations of water substance are: water↔vapor (*wv*), ice↔vapor (*iv*), and ice↔water (*iw*). The corre-

sponding latent heats are called respectively: latent heat of *evaporation* ($L_{wv}$, always written $L$), latent heat of *sublimation* ($L_{iv}$), and latent heat of *melting* ($L_{iw}$). All these transformations will be discussed in detail later.

For reference we give the values of the latent heats at 0°C for water substance.*

$$L = 2.500 \times 10^6 \text{ kj t}^{-1}; \tag{4}$$

$$L_{iv} = 2.834 \times 10^6 \text{ kj t}^{-1}; \tag{5}$$

$$L_{iw} = 0.334 \times 10^6 \text{ kj t}^{-1}. \tag{6}$$

These values will be used for most purposes as constants in the atmospheric range of temperatures.

**3·09. Variation of the latent heats with temperature.** The variations of the latent heats with temperature are relatively small but can be obtained from theory. We shall give the argument for $L$. For the case of the latent heat of evaporation 3·08(3) takes the form

$$L = e_s(\alpha_v - \alpha_w) + (u_v - u_w). \tag{1}$$

At atmospheric temperatures we may neglect $\alpha_w (= 1)$ against $\alpha_v$, which was seen in 3·06(8) to exceed 25,000. By replacing $e_s\alpha_v$ by $R_vT$ from 3·06(1), (1) becomes:

$$L = R_vT + u_v - u_w,$$

or in differential form

$$dL = R_vdT + du_v - du_w. \tag{2}$$

Since the vapor behaves nearly like a perfect gas, we note from 2·20(7) that $du_v = c_{vv}dT$. Since $\alpha_w$ is practically constant, the energy equation 2·18(3) for the liquid reduces to $dh = du_w$. And from the definition of $c_w$, we see that $dh = c_wdT$. Thus $du_w = c_wdT$, which when introduced in (2) yields

$$dL = (R_v + c_{vv} - c_w)dT = (c_{pv} - c_w)dT.$$

The last step is according to 3·07(2). Finally, dividing by $dT$ we get

$$\frac{dL}{dT} = c_{pv} - c_w, \tag{3}$$

which contains the following simple rule: *The rate of change of the latent heat L with temperature is equal to the change of the specific heat at constant pressure from the liquid to the vapor phase.* Note that (3) checks dimensionally.

* Dorsey, *op. cit.*, pp. 616–617. We assume $L_{iv} = L + L_{iw}$.

Integrating (3) and using the values of the specific heats in 3·05 and 3·07, we have in the atmospheric range $-40°C$ to $40°C$ the good approximation:

$$L = L_0 + (T - T_0)(c_{pv} - c_w) = L_0 - 2274(T - 273),$$

where $L_0$ is the value of $L$ at 0°C in 3·08(4). Introducing this value, we get the final formula

(4) $L = (2.500 - 0.002274t°C) \times 10^6$ kj t$^{-1}$ (in the atmosphere).

Inspection of (4) justifies the ordinary approximation that $L$ is constant in the atmosphere.

The reader may show similarly that

(5) $L_{iv} = (2.834 - 0.000149t°C) \times 10^6$ kj t$^{-1}$ (near 0°C).

Thus $L_{iv}$ has a variation with temperature only 7% as large as that of $L$. Hence $L_{iv}$ is still more appropriately taken to be constant.

For $L_{iw}$ an essential modification of the above argument is required. Since, however, the melting temperature of ice is almost constant in the atmosphere (see 3·13), the dependence of $L_{iw}$ on temperature is unimportant to meteorology. On the other hand, (4) and (5) are sometimes used in meteorological investigations requiring accuracy.

**3·10. Clapeyron's equation.** Consider water substance in two phases, called 1 and 2 as in 3·08. For each temperature $T$ less than $T_c$, there is one *saturation pressure* $e_s$ at which the phases 1 and 2 are in equilibrium. Conversely, for each pressure $e$ less than $e_c$, there is one *transformation temperature* at which the equilibrium exists. Let the two phases be numbered so that in equilibrium $s_2 > s_1$, i.e., so that heat must be added to phase 1 to convert it to phase 2.

It is now our purpose to obtain a differential relationship between the saturation pressure $e_s$ and the transformation temperature $T$ just defined. From the latter equality of 3·08(3), we have at the state $(T,e_s)$:

(1) $$u_1 + e_s\alpha_1 - Ts_1 = u_2 + e_s\alpha_2 - Ts_2,$$

where the subscripts refer to the two phases. Both sides of (1) have the same form, showing that the function

(2) $$\varphi = u + e_s\alpha - Ts$$

remains constant during the isothermal-isobaric change of phase. The function $\varphi$ is known as the *thermodynamic potential*, and it is a function of state alone. It has the dimensions $[L^2T^{-2}]$ of specific energy.

We now consider the isothermal change of phase at the temperature $T + dT$ and the corresponding pressure $e_s + de_s$. As above, the thermo-

dynamic potential will be constant throughout the change of phase at $T + dT$. Let its value be $\varphi + d\varphi$. By differentiating (2), we get

$$d\varphi = du + e_s d\alpha - Tds + \alpha de_s - sdT.$$

But the first three terms on the right are zero, according to the energy equation 3·08(1). Thus

$$d\varphi = \alpha de_s - sdT. \tag{3}$$

Since $\varphi$ remains constant in the change of phase at $(T,e_s)$, and since $\varphi + d\varphi$ is constant in the change of phase at $(T + dT, e_s + de_s)$, it follows that $d\varphi$ remains constant during the transformation from the phase 1 to the phase 2. We have therefore from (3):

$$\alpha_1 de_s - s_1 dT = \alpha_2 de_s - s_2 dT,$$

or by rearrangement:

$$\frac{de_s}{dT} = \frac{s_2 - s_1}{\alpha_2 - \alpha_1}. \tag{4}$$

But $s_2 - s_1 = L_{12}/T$, from 3·08(3). Hence we get the desired final differential relationship between $e_s$ and $T$:

$$\frac{de_s}{dT} = \frac{L_{12}}{T(\alpha_2 - \alpha_1)}. \tag{5}$$

Equation (5) is *Clapeyron's equation*, found by Clapeyron in 1832 and later derived from the modern point of view by Clausius.

Since Clapeyron's equation holds for any two phases, we may write down the three forms it takes:

$$\frac{de_s}{dT} = \frac{L}{T(\alpha_v - \alpha_w)} \qquad \text{(water}\leftrightarrow\text{vapor)}; \tag{6}$$

$$\frac{de_s}{dT} = \frac{L_{iv}}{T(\alpha_v - \alpha_i)} \qquad \text{(ice}\leftrightarrow\text{vapor)}; \tag{7}$$

$$\frac{de_s}{dT} = \frac{L_{iw}}{T(\alpha_w - \alpha_i)} \qquad \text{(ice}\leftrightarrow\text{water)}. \tag{8}$$

For equilibrium between each pair of phases the pressure $e_s$ and temperature $T$ satisfy the corresponding Clapeyron equation. Each of the equations may be integrated to give a curve in the $(T,e)$-diagram, which we shall call respectively the *evaporation curve*, the *sublimation curve*, and the *melting curve*. Along the evaporation curve there exists equilibrium between water and vapor. Along the sublimation curve there exists equilibrium between ice and vapor. At the point where these two curves

intersect there is equilibrium among all three phases. It follows therefore that the melting curve, representing equilibrium between ice and water, must pass through the intersection of the other two curves. This common point on all three curves is the *triple point*, and the correspond-

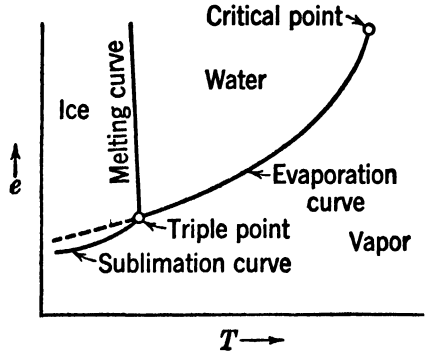



FIG. 3·10.

ing state is the triple state mentioned in 3·02. A schematic $(T,e)$-diagram is given in fig. 3·10.

In the next sections we shall give a more detailed discussion of each of the three changes of phase of water substance.

**3·11. Saturation vapor pressure over water.** In the case of the water↔vapor transformation, the pressure $e_s$ is called the *saturation vapor pressure (over water)*. The corresponding temperature $T$ at which the transformation takes place is called the *evaporation temperature* (or, sometimes, boiling temperature). The curve showing the variation of $e_s$ with $T$ on a $(T,e)$-diagram is the evaporation curve, and 3·10(6) is the differential equation of this curve. The evaporation curve is known to pass through these three points:

(1) $e_s = 0.611$ cb, $T = 273°K$ (triple point);

(2) $e_s = 101.33$ cb, $T = 373°K$ (normal boiling point);

(3) $e_s = 22{,}100$ cb, $T = 647°K$ (critical point).

The critical point is of course one end of the evaporation curve.

Now $\alpha_w = 1$ and $\alpha_v > 25{,}000$ in the atmosphere (see 3·06). Using the equation of state 3·06(5), we can therefore replace $\alpha_v - \alpha_w$ by $\alpha_v = R_d T/(\epsilon e_s)$, with sufficient accuracy. Then 3·10(6) takes the form

$$\frac{1}{e_s}\frac{de_s}{dT} = \frac{\epsilon L}{R_d T^2} \qquad \text{(water↔vapor)}, \tag{4}$$

an important form of Clapeyron's equation. Equation (4) can also be written

$$d(\ln e_s) = -\frac{\epsilon L}{R_d} d\left(\frac{1}{T}\right). \tag{5}$$

In 3·09 it was shown that in a limited range of temperatures (such as the atmospheric range) $L$ may be regarded as constant. With this assumption (5) represents a straight line on a $(-1/T, \ln e)$-diagram. By using the value $L = 2.500 \times 10^6$ kj $t^{-1}$, (5) becomes

$$d(\ln e_s) = -5418\, d\left(\frac{1}{T}\right) \qquad \text{(water}\leftrightarrow\text{vapor, } -40°\text{C to } 40°\text{C)}. \tag{6}$$

Or in base 10 logarithms:

$$d(\log e_s) = -2353\, d\left(\frac{1}{T}\right) \qquad \text{(water}\leftrightarrow\text{vapor, } -40°\text{C to } 40°\text{C)}. \tag{7}$$

Integrating (7), with the initial condition (1), gives

$$\log e_s = 8.4051 - \frac{2353}{T} \qquad \text{(water}\leftrightarrow\text{vapor, } -40°\text{C to } 40°\text{C)}. \tag{8}$$

Equation (8) provides a convenient graphical method of determining $e_s$ in the atmospheric range. Fig. 3·11*a* shows a graph of log $e$ against $-1/T$, for temperatures up to the critical. In the atmospheric range, the slope of the evaporation curve is 2353, which is represented by the

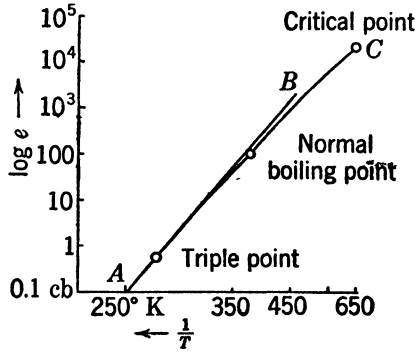



FIG. 3·11*a*.

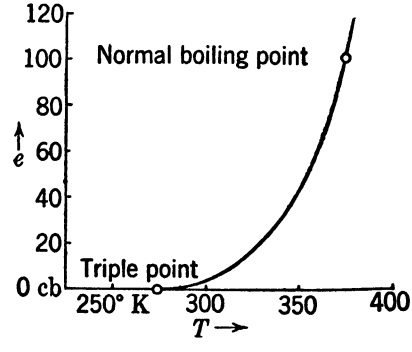



FIG. 3·11*b*.

line $AB$ in the figure. The variation of $L$ at high temperatures causes the true evaporation curve to bend slightly (curve $AC$), so as to go to the critical point. The evaporation curve may then be transferred to a linear $(T,e)$-diagram, where the curve shows extreme curvature (see fig. 3·11*b*). All physical and meteorological handbooks contain tables giving $e_s$ as a function of $T$, as determined from experiments.

If the formula 3·09(4) for $L$ is introduced into 3·11(4), an integration can be carried out to yield the *Magnus formula* for $e_s$:

$$(9)\quad \log e_s = -\frac{2937.4}{T} - 4.9283 \log T + 22.5518$$

(water↔vapor, −40°C to 40°C).

Table 3·11 shows in parallel rows the values of $e_s$ from the simple formula (8), from (9), and from empirical data. (The observed values at temperatures below −20°C are unreliable, since the water tends to freeze.) As might be expected, the values derived from (9) show closer agreement

TABLE 3·11

| $T - T_0$ | −30°C | −20°C | −10°C | 0°C | 10°C | 20°C | 30°C |
|---|---|---|---|---|---|---|---|
| $e_s$ from (8), cb | 0.0527 | 0.1273 | 0.2873 | 0.611 | 1.232 | 2.37 | 4.36 |
| $e_s$ from (9) | 0.0509 | 0.1254 | 0.2862 | 0.611 | 1.228 | 2.339 | 4.247 |
| $e_s$ observed | ..... | ..... | 0.2865 | 0.611 | 1.228 | 2.338 | 4.243 |

with the observed values than those derived from (8), but the difference is less than one millibar throughout the atmospheric range, and for the most common temperatures the simple formula (8) gives all the accuracy needed.

**3·12. Saturation vapor pressure over ice.** The ice↔vapor transformation can be treated in complete analogy to 3·11. Since the resemblance is so close, and since the transformation is less important, we shall go over it rapidly.

In the case of the ice↔vapor transformation, the pressure $e_s$ is called the *saturation vapor pressure over ice.* The transformation temperature $T$ is called the *sublimation temperature* at the pressure $e_s$. The curve giving $e_s$ as a function of $T$ is the sublimation curve. As stated in 3·10, the sublimation curve is known to pass through the triple point of 3·11(1).

Clapeyron's equation 3·10(7) is the differential equation of the sublimation curve. Repeating the argument which led to 3·11(4), we may obtain the differential equation in the form

$$(1)\quad \frac{1}{e_s}\frac{de_s}{dT} = \frac{\epsilon L_{iv}}{R_d T^2} \qquad \text{(ice↔vapor)}.$$

In the atmospheric range $L_{iv}$ may be regarded as constant. Taking its value from 3·08(5), we get the analog of 3·11(8):

$$(2)\quad \log e_s = 9.5553 - \frac{2667}{T} \qquad \text{(ice↔vapor)}.$$

The sublimation curve plotted on a graph of log $e$ against $-1/T$ is a straight line (fig. 3·12$a$). For comparison the evaporation curve is drawn as a broken line. The sublimation curve is steeper than the evaporation curve and lies at slightly lower pressures. It should be

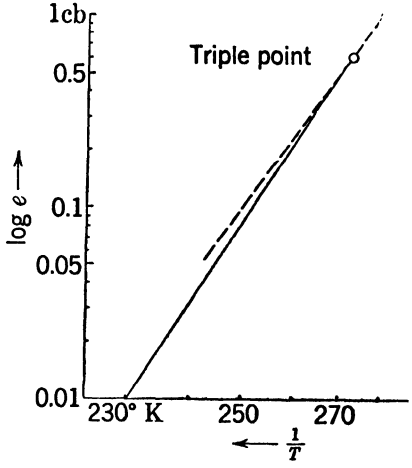



FIG. 3·12$a$.

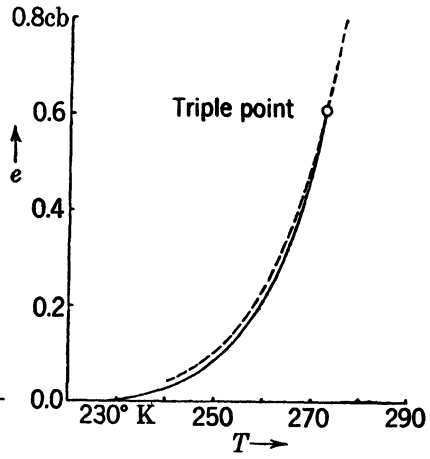



FIG. 3·12$b$.

noted that the sublimation curve does not extend above the triple point, since ice cannot be heated above this temperature. However, water can be cooled below its freezing point, and such supercooled water is usually found in the atmosphere. (See 3·15.) Consequently the evaporation curve must be drawn to about $-30$°C.

In fig. 3·12$b$ the same curves are drawn on a linear $(T,e)$-diagram.

**3·13. Pressure and temperature of melting.** The treatment of the ice↔water transformation is similar to that of 3·11 and 3·12, but it differs in that the equation of state for water vapor does not enter into it. In the case of the ice↔water transformation, the pressure $e_s$ is called the *melting pressure* of ice, and the corresponding temperature $T$ is called the *melting temperature* of ice. Whenever ice and water are in equilibrium with each other at a surface of mutual contact, the hydrostatic pressure of the water on the surface is the melting pressure and the temperature is the corresponding melting temperature.

The curve giving $e_s$ as a function of $T$ is the melting curve. It passes through the triple point

(1) $$e_s = 0.611 \text{ cb}, \qquad T - T_0 = 0.0075°\text{C},$$

and also through the *normal melting point*

(2) $$e_s = 101.33 \text{ cb}, \qquad T - T_0 = 0°\text{C}.$$

The differential equation of the melting curve is Clapeyron's equation in the form 3·10(8):

$$\frac{de_s}{dT} = \frac{L_{iw}}{T(\alpha_w - \alpha_i)} \qquad \text{(ice}\leftrightarrow\text{water)}.$$

Introducing the practically constant values: $L_{iw} = 0.334 \times 10^6$ from 3·08(6), $\alpha_i = 1.091$ from 3·04(1), and $\alpha_w = 1.00$ from 3·05(1), we get at $T = 273°\text{K}$:

$$\frac{de_s}{dT} = -13{,}440 \text{ cb deg}^{-1} \qquad \text{(ice}\leftrightarrow\text{water)}. \tag{3}$$

We note from (3) that the melting curve is the only one of the three phase-transformation curves which has a negative slope in the $(T,e)$-diagram; i.e., the melting temperature *decreases* with increasing pressure. We note also that the curve is very steep, being nearly isothermal (see fig. 3·10).

As a verification of (3), we may compute the theoretical pressure difference between the normal melting point (1) and the triple point (2). Introducing $dT = 0.0075°$ in (3), we get $de_s = 100.8$. The empirical value is 100.7 cb, from (1) and (2).

The drop in melting point with increasing pressure has the following effect. When ice at a temperature slightly below 0°C is subjected to high pressure, it is brought into a state above its melting point. It is therefore converted into water but freezes again as soon as the pressure is released. This phenomenon is called *regelation*, and it accounts for the plasticity of ice which permits the flow of glaciers.

**3·14. Complete $(T,e)$-diagram.** In fig. 3·10 are combined into one schematic diagram the three transformation curves just discussed. Forgetting about the dotted extension of the evaporation curve below the triple point, we see that the $(T,e)$-diagram is divided into three regions. These represent the ice, water, and vapor phases; they are labeled accordingly. The phase of water substance is uniquely determined by its temperature $T$ and pressure $e$, except along the curves where two phases can exist in equilibrium.

Any equilibrium process must have a continuous path on the $(T,e)$-diagram. Thus a change of phase must occur on one of the transformation curves and ordinarily will occur only on these curves. An exception is found when we pass from the vapor region to the water region through pressures higher than the critical. This corresponds to a continuous physical process with none of the usual properties of a change of

phase. There is probably likewise a critical point on the melting curve with similar properties. There is, however, no critical point on the sublimation curve, which must extend to absolute zero.

**3·15. Supercooled water.** The dotted extension below 0°C of the evaporation curve has a physical significance. Suppose that we have vapor and water in equilibrium, and cool them carefully. At the triple point the water ordinarily freezes but, if the water is pure, the ice phase may fail to appear. The vapor-water combination continues to cool and follows the evaporation curve. This *supercooled* state is thermodynamically unstable, and the slightest disturbance will make the system jump into the stable state on the sublimation curve.

The droplets in clouds and fogs which are formed by condensation above 0°C will usually assume the supercooled liquid state on cooling below 0°C. According to experience most cloud elements are still liquid at −10°C, and water droplets may be found down to −30°C. When ice particles are brought into a cloud of supercooled drops at a fixed temperature, the system is no longer in equilibrium. The vapor is saturated with respect to the water drops, but is *supersaturated* with respect to the ice particles; i.e., $e$ is *larger* than the saturation vapor pressure over *ice* (see fig. 3·12*b*). The result is condensation of vapor on the ice particles. But the loss of vapor means that $e$ becomes *less* than the saturation vapor pressure over *water*. Thus water evaporates. The net result of the two processes is a growth of the ice crystals at the expense of the water droplets. This goes on until all the water drops have evaporated. This process goes on most rapidly near −12°C, where the saturation vapor pressure over water most greatly exceeds that over ice.

Two important meteorological applications of the above phenomena may be mentioned: (i) When a supercooled fog moves over a snow-covered surface, it tends to dissolve; (ii) when a relatively small number of ice crystals are present in a cloud of supercooled water droplets, the ice crystals grow enormously. They can therefore no longer remain suspended in the air, and they start falling. Bergeron assumes that tiny ice crystals are always present above a certain level as the end product of dissipated cirrus clouds. When a cloud grows in thickness precipitation may be expected from it when its top has reached the ice crystal level. Although the indications are that other factors also contribute to the formation of precipitation, the effect mentioned here is undoubtedly an important one.

**3·16. Thermodynamic surface of water substance.** The fact that there are three variables of state, namely, $e$, $T$, and $\alpha$, suggests a three-

dimensional representation of the state of water substance. Let three coordinate axes measure $e$, $T$, and $\alpha$, respectively. Each state $(e,T,\alpha)$ of water substance is then represented by a unique point in space.

As shown in 2·07, water substance cannot assume an arbitrary state $(e,T,\alpha)$, but only those states $(e,T,\alpha)$ which satisfy an equation of state of type

$$f(e,T,\alpha) = 0. \tag{1}$$

It is not possible to express relation (1) exactly in terms of one elementary function. The equation of state can, however, be expressed approximately in a restricted range of states. See 3·06(5), for example.

The nature of the equation of state is such that all the points $(e,T,\alpha)$ satisfying (1) lie on a continuous surface. This is called the thermodynamic surface for water substance and is a representation of all possible states of water substance. This surface is shown in fig. 3·16. Each

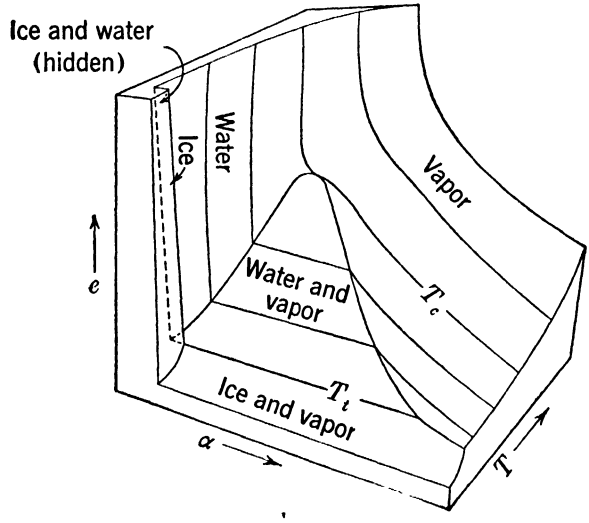



FIG. 3·16. Thermodynamic surface of water substance.

phase is represented by an area on the surface. Each region of equilibrium between two phases is represented on the surface by an area where the isotherms are parallel to the $\alpha$ axis. The thermodynamic surface reduces to fig. 3·02 when projected on the $(\alpha,e)$-plane, i.e., when viewed parallel to the $T$ axis. It reduces to fig. 3·10 when projected on the $(T,e)$-plane, i.e., when viewed parallel to the $\alpha$ axis.

The construction and study of a model of the thermodynamic surface will greatly enhance the understanding of the thermodynamic properties of water substance.

**3·17. Moist air.** Thus far in chapter 3 we have treated the thermodynamics of pure water substance. The real atmospheric air with its variable admixture of water vapor will be called *moist air*. Its thermal properties are obtained by combining the thermal properties of the dry air and the water vapor. The question arises whether the presence of the dry air constituents in any way influences the thermal behavior of the water vapor. As long as the vapor is unsaturated it behaves very closely as a perfect gas and, according to Dalton's law (see section 2·12), its state is unaffected by the presence of the dry air. When moist air is brought in contact with a water surface, equilibrium is reached when there is equilibrium between the water vapor in the air and the liquid water. This situation is of course not identical with the one discussed in section 3·11 where no foreign substance was present. We have no right to assume a priori that the saturation vapor pressure will be the same in the two cases. However, it has been found that for practical purposes the *atmosphere does not influence the saturation vapor pressure;* i.e., the partial pressure of water vapor in saturated air is equal to the saturation pressure of pure water vapor.

**3·18. Moisture variables.** Dry air is treated as an invariable perfect gas, according to section 2·13. Since, however, the proportion of water vapor in the atmosphere varies greatly, we must introduce variables measuring the moisture content of a parcel of air.

The first of these is the (partial) *vapor pressure e* of water vapor in the parcel. Here $e$ has the same meaning as heretofore in chapter 3. It has the dimensions $[ML^{-1}T^{-2}]$ of pressure.

Two other moisture variables are the *dimensionless ratios w* and $q$ now to be defined. Let the parcel of moist air with total mass $M$ consist of $M_d$ tons of dry air mixed with $M_v$ tons of water vapor. Thus $M_d + M_v = M$. Then the *mixing ratio w* is defined by:

$$w = \frac{M_v}{M_d} \qquad \text{(pure number)}. \tag{1}$$

*Thus w is the mass of water vapor per ton of* **dry** *air.*

A closely related variable is the *specific humidity q* defined by:

$$q = \frac{M_v}{M} \qquad \text{(pure number)}. \tag{2}$$

*Thus q is the mass of water vapor per ton of* **moist** *air.*

Now we see that

$$\frac{1}{q} = \frac{M}{M_v} = \frac{M_v + M_d}{M_v} = 1 + \frac{M_d}{M_v} = 1 + \frac{1}{w},$$

whence by solving for $q$ and $w$:

$$(3) \qquad q = \frac{w}{1+w} \quad \text{and} \quad w = \frac{q}{1-q}.$$

For absolutely dry air, $w = q = 0$. For pure water vapor, $w = \infty$ and $q = 1$. $q$ is always less than $w$. It will be shown in 3·20 that in the atmosphere usually $w < 0.04$. Then from (3) we see that $q/w > (1.04)^{-1} \approx 0.96$. Thus $q$ and $w$ differ by at most 4%, and usually much less. *For most practical purposes, we can use* $w = q$. For this reason the names of $w$ and $q$ have been confused in meteorological literature. Logically one of the two variables could well be omitted, but current usage makes it necessary to know both.

The numerical values of $w$ and $q$ are found between 0 and 0.04. We shall usually express these numbers as parts per thousand. For example, the value 0.0154 will be written $15.4 \times 10^{-3}$. Some authors omit the factor $10^{-3}$, and speak of " 15.4 per mille " (15.4 $^0/_{00}$) or " 15.4 grams per kilogram." In applying these numbers to thermodynamical formulas, the factor $10^{-3}$ must be added.

**3·19. Relative humidity.** The maximum vapor pressure obtainable at a given temperature is the *saturation vapor pressure over water* (not over ice). This will be denoted by $e_s$ throughout this discussion. In 3·11 it was shown that $e_s$ depends only on the temperature, and in 3·17 we mentioned that the presence of dry air leaves this property of $e_s$ unchanged. Any attempt to raise $e$ above $e_s$ will usually cause condensation to liquid water.

The values of $w$ and $q$ for saturated air are called the *saturation mixing ratio* ($w_s$) and the *saturation specific humidity* ($q_s$) respectively. Thus we have

$$(1) \qquad e \leqq e_s; \qquad w \leqq w_s; \qquad q \leqq q_s.$$

Many meteorological and physiological phenomena involving the " wetness " of the air depend not on the quantity ($w$) of vapor present but rather on the degree of saturation. This is true of the hair hygrometer used in meteorographs to measure vapor content. It is also true of the comfort of a person living in the air. The degree of saturation could be measured by any of the quantities $w/w_s$, $q/q_s$, or $e/e_s$. It is the universal practice to use the third, called the *relative humidity* ($r$). We have

$$(2) \qquad r = \frac{e}{e_s}.$$

Thus $r$ lies between 0 and 1.00. In practice it is expressed as a per cent. If $r = 22\%$, then $r$ is to be given the value 0.22 in our formulas. In

words, *r indicates what per cent the actual vapor pressure is of the saturation vapor pressure over water at the same temperature.*

The meteorograph reports relative humidity as a primary measurement. Thus the state of the upper air is originally described by total pressure $p$, temperature $T$, and relative humidity $r$. The main problem of the next sections is to obtain the values of $w$, $q$, and $e$ from $p$, $T$, and $r$. This will be done both numerically and graphically.

**3·20. Relations among the humidity variables.** The first task is to express $w$ in terms of $e$. The total pressure $p$ of a parcel of air is by Dalton's law (2·12) the sum of the *partial pressure* $p_d$ of the dry air and the vapor pressure $e$ of the water vapor. Thus

$$p_d = p - e. \tag{1}$$

Let $M_d$ tons of dry air and $M_v$ tons of vapor separately fill an entire volume $V$. We write the equations of state of each component separately in the form 2·11(1):

$$eV = M_v R_v T \qquad \text{(water vapor)};$$

$$p_d V = M_d R_d T \qquad \text{(dry air)}.$$

We take the ratio of these equations, and introduce $M_v/M_d = w$ from 3·18(1) and $R_v/R_d = 1/\epsilon$ from 3·06(3). We then have

$$\frac{e}{p_d} = \frac{w}{\epsilon}. \tag{2}$$

Solving for $w$ and using (1), we get

$$w = \frac{\epsilon e}{p - e} \qquad \text{(exact)}. \tag{3}$$

Thus $w$ is obtained from $p$ and $e$. This is a very important formula to know. If the air is saturated, we get as a special case of (3):

$$w_s = \frac{\epsilon e_s}{p - e_s} \qquad \text{(exact)}. \tag{4}$$

We can now estimate the largest value of $w_s$ likely to occur in the atmosphere, say that for saturated air at 36°C and 100 cb. From 3·11(8) we determine that $e_s \approx 6$ cb. Then from (4)

$$w_s \approx \frac{(0.622)6}{100 - 6} \approx 40 \times 10^{-3}.$$

In everyday synoptic work, $w$ rarely exceeds $20 \times 10^{-3}$.

Solving (3) and (4) for the vapor pressure, we get the occasionally

useful relations:

$$(5) \qquad e = \frac{wp}{\epsilon + w}; \qquad e_s = \frac{w_s p}{\epsilon + w_s} \qquad \text{(exact)}.$$

The relations (5) can be replaced for most practical purposes by the important approximate formulas

$$(6) \qquad e \approx \frac{p}{\epsilon} w; \qquad e_s \approx \frac{p}{\epsilon} w_s \qquad \text{(approximate)}.$$

Formulas (6) are obtained by ignoring $w$ and $w_s$ in the denominators of (5), since these are quite small in comparison with $\epsilon$. Formulas (6) are the more accurate, the smaller $w$ and $w_s$ are. The error in (6) rarely exceeds 3%.

**3·21. Numerical determination of mixing ratio.** Now suppose $p$, $T$, and $r$ are known, and $w$ is desired. The following calculation is carried out: (i) The saturation vapor pressure $e_s$ is obtained from $T$ alone, according to formula 3·11(8); (ii) we get $e = re_s$, from 3·19(2); (iii) we get $w$ from $p$ and $e$, by 3·20(3). If desired, $q$ can be obtained from 3·18(3), or with a small error $q = w$. Thus the problem stated above is solved in principle. This should be carefully understood.

However, this algebraic procedure involves laborious numerical computations for each determination of $w$. For all the accuracy required in practice, a graphical procedure is much quicker. This will be described in section 3·23.

Another important problem is one that will arise in the use of the diagram: *given $w_s$ and $r$, to determine $w$.* The exact solution is independent of $p$ and could be obtained as follows: (i) Get $e_s$ from 3·20(5); (ii) then get $e$ from 3·19(2); (iii) then get $w$ from 3·20(3). The result of this algebra would be

$$(1) \qquad w = \frac{rw_s}{1 + (1 - r)\, w_s/\epsilon} \qquad \text{(exact)}.$$

The following approximate solution is the one invariably used in practice: Take the ratio of the two equations 3·20(6), obtaining

$$\frac{w}{w_s} \approx \frac{e}{e_s} = r.$$

Hence

$$(2) \qquad w \approx rw_s \qquad \text{(approximate)}.$$

A comparison of (2) and (1) shows that (2) is exact when $r = 0$ and also when $r = 100\%$. It can be shown that $w$ obtained from (2) is usually in error by not more than $0.2 \times 10^{-3}$, which is accurate enough for most

purposes. The error can be as much as $0.6 \times 10^{-3}$, when $w_s = 40.0 \times 10^{-3}$ and $r = 50\%$.

**3·22. Vapor lines on the diagrams.** Since $e_s$ is a function of $T$ alone (see 3·11), it follows from 3·20(4) *that $w_s$ is a function of $p$ and $T$.* Since all the meteorological diagrams contain the variables $p$ and $T$, it is possible to draw curves of constant $w_s$ on each diagram. These curves should properly be called mixing ratio lines for saturated air, but we shall refer to them simply as vapor lines.

The shape of the vapor lines depends on the diagram. The differential equation of a vapor line may be obtained as follows: From 3·20(5) if $w_s = \text{const}$, then $e_s = (\text{const}) \cdot p$. Hence $d(\log p) = d(\log e_s)$. Introducing the expression 3·11(7) for $d(\log e_s)$, we have

$$(1) \qquad d(\log p) = -2353\, d\left(\frac{1}{T}\right) \qquad \text{(vapor line)}.$$

By integrating (1) it is seen that on the emagram each vapor line is a segment of a hyperbola, and that all vapor lines are congruent.

In the atmospheric range, the vapor lines are nearly straight lines on all diagrams. They always have a slope between that of the dry adiabats and that of the isotherms. That is, on each vapor line as $p$ decreases, $T$ decreases but $\theta$ increases. The vapor lines on a tephigram are shown in fig. 3·36. The student should study the vapor lines on all the diagrams at his disposal. See 3·18 for the usual method of labeling them.

**3·23. Graphical determination of $w$, $q$, and $e$.** We now consider the graphical solution of the problem mentioned at the end of 3·19: given $p$, $T$, and $r$, to determine $w$, $q$, and $e$.

(i) To determine $w$, first plot the point $(T,p)$ on any thermodynamic diagram. Interpolating between the vapor lines, find the value of $w_s$; this should be accurate to $0.1 \times 10^{-3}$. Finally, multiply $w_s$ by $r$ to obtain $w$, according to 3·21(2).

(ii) To determine $q$, simply take $q = w$. More accuracy is neither necessary nor compatible with the approximation already made in (i).

(iii) To determine $e$, first obtain the value of $e_s$. Since $e_s$ depends on temperature alone, it will be the same at the point ($T$, 62.2 cb) as it is at the point $(T,p)$. Read the value $w_s'$ of the saturation mixing ratio at the point ($T$, 62.2 cb). Then by 3·20(6),

$$(1) \qquad e_s \approx \frac{62.2}{0.622}\, w_s' = 100 w_s' = \frac{1}{10}\,(10^3 w_s') \qquad \text{(cb)}.$$

Hence $e_s \approx 10^3 w_s'$ *millibars*. Finally, the value of $e$ is equal to $re_s$. This completes the graphical solution of the problem mentioned.

The rule for getting $e_s$ at any temperature can be expressed in words: *The value in millibars of the saturation vapor pressure $e_s$ at the temperature $T$ is approximately equal to the value in parts per thousand of the saturation mixing ratio at the temperature $T$ and pressure 622 mb.* Thus a diagram can replace a table of vapor pressures, with an error rarely exceeding 4%.

One additional step will correct practically all this inaccuracy in $e_s$. Having found $w_s'$ above, express it in parts per thousand, and add it to 622, to get a pressure $p_1$ in millibars. Then go to the point $(T,p_1)$ and read the value $w_s''$ of the saturation mixing ratio. This will be almost exactly $e_s$ in millibars. The reason follows from the exact formula 3·20(5):

$$e_s = \frac{p_1}{\epsilon + w_s''} w_s'' \approx \frac{p_1}{\epsilon + w_s'} w_s'' = \frac{62.2 + 10^2 w_s'}{0.622 + w_s'} w_s'' = \frac{1}{10} (10^3 w_s'').$$

The error committed here is negligible, compared with that in (1).

**3·24. Thermal properties of moist air.** Moist air for which the relative humidity is 100%, i.e., $e = e_s$, is called *saturated.* Otherwise the moist air is called *unsaturated* ($e < e_s$). We have seen that the water vapor seldom comprises more than a few per cent of the air. As a result, during any process which does not lead to condensation, moist air behaves like a perfect gas whose thermal properties differ only slightly from those of dry air.

In 3·25 and 3·26 will be given the equation of state and the values of the specific heats for moist air, using the general theory of chapter 2. There will be given explicitly the small deviations from dry air caused by the presence of vapor. These deviations will be expressed in terms of the parameters $w$ and $q$ expressing the variable vapor content of moist air.

In section 3·27 the adiabatic process for unsaturated air is considered. This also is nearly the same as that for dry air. However, as soon as saturation is reached in the adiabatic process, any further cooling leads to condensation with consequent release of relatively large amounts of latent heat. As a result there is a sudden transition to new types of adiabatic processes, to be discussed in sections beginning with 3·30. Thus it is vitally important to distinguish between the behavior of air in its so-called *unsaturated stage* and its behavior in the *saturated stage.* The unsaturated stage is called by some authors the *dry stage,* although it does not deal with truly dry air.

The notation used here is *in so far as possible* governed by the following principles. For dry air the constants and variables are given the

subscript $d$. For water vapor they are given the subscript $v$. For moist air and hence for the atmosphere in general they are given no subscript. However, the adoption of a notation is always limited by the usage well established by previous writers. There are also difficulties inherent in the nature of a science. As a result, there will always be certain inconsistencies. For example, the vapor pressure might well be denoted by $p_v$, but $e$ is always used. The temperature $T$ is the same for all components of a system in equilibrium; hence no symbols $T_d$ or $T_v$ are needed.

**3·25. Equation of state of moist air; virtual temperature.** Let a parcel of one ton of moist air have the specific humidity $q$. Then the parcel contains $M_d = 1 - q$ tons of dry air and $M_v = q$ tons of water vapor. According to 2·12(3), the specific gas constant $R$ of the mixture is given by

$$1 \cdot R = M_d R_d + M_v R_v, \quad \text{or}$$
$$R = (1 - q)R_d + qR_v. \tag{1}$$

But by 3·06(3) we can write $R_v = R_d/\epsilon$. Hence

$$R = (1 - q)R_d + \frac{q}{\epsilon} R_d = R_d\left[1 + \left(\frac{1}{\epsilon} - 1\right)q\right].$$

Evaluating $(1/\epsilon) - 1$ and using $q \approx w$, we get the important formulas

$$R = (1 + 0.61q)R_d \approx (1 + 0.61w)R_d. \tag{2}$$

Thus the presence of water vapor will *raise* the specific gas constant of atmospheric air from the value $R_d = 287$ up to a maximum of 294 (corresponding to $q = 40 \times 10^{-3}$).

Using (2), we can write the equation of state of moist air:

$$p\alpha = RT = R_d(1 + 0.61q)T. \tag{3}$$

We see from (3) that moist air of specific humidity $q$ in the state $(p,T)$ has the same specific volume as dry air would have in the state $(p,T^*)$, where

$$T^* = (1 + 0.61q)T \approx (1 + 0.61w)T. \tag{4}$$

The temperature $T^*$ is called the *virtual temperature* of the moist air and is by definition *the temperature of dry air having the same pressure and specific volume as the moist air.*

The expressions (3) and (4), when combined, give an alternative form of the equation of state for moist air:

$$p\alpha = R_d T^*. \tag{5}$$

Thus to compute $\alpha$ we have our choice of using the real temperature $T$ with an altered gas constant $R$, or of using a fictitious temperature $T^*$ with the dry air gas constant $R_d$. The former method of equation (3) is perhaps simpler for computations. The use of virtual temperature and (5) affords a great simplification of later dynamical theory.

**3·26. Specific heats of moist air.** Consider the one-ton parcel of moist air described in 3·25 above. Let there be introduced the quantity $dh$ of heat into the parcel. As a result the parcel is heated from temperature $T$ to $T + dT$. This temperature rise $dT$ is experienced by both the dry air and the water vapor. Let $dh_d$ be the amount of heat received by the dry air, per ton of dry air. Let $dh_v$ be the amount of heat received by the water vapor, per ton of water vapor. Then in the notation at the start of 3·25:

$$dh = M_d dh_d + M_v dh_v. \tag{1}$$

By dividing both sides of (1) by $dT$ and writing $M_d$ and $M_v$ in terms of $q$, we have

$$\frac{dh}{dT} = (1 - q)\frac{dh_d}{dT} + q\frac{dh_v}{dT}. \tag{2}$$

Now (2) holds for an arbitrary process in which $q$ (and hence $w$) are constant. If the process is at constant pressure $p$ for the whole parcel, then from 3·20(5) we find that it proceeds at a constant partial pressure $e$ for the water vapor and hence at a constant partial pressure $p_d = p - e$ for the dry air. At constant $p$, $dh/dT$ becomes by 2·19(1) the specific heat $c_p$ of moist air at constant pressure. Since $e$ and $p_d$ are constant, the other two quotients in (2) are specific heats at constant pressure. Hence from (2) we have

$$c_p = (1 - q)c_{pd} + q\,c_{pv} = c_{pd}\left[1 + \left(\frac{c_{pv}}{c_{pd}} - 1\right)q\right].$$

Evaluating $c_{pv}/c_{pd}$ from 3·07(1) and 2·21(5), we have the important formulas

$$c_p = (1 + 0.90q)c_{pd} \approx (1 + 0.90w)c_{pd}. \tag{3}$$

Thus the presence of water vapor will *raise* the specific heat of air from $c_{pd} = 1004$ to a maximum of 1040. A similar analysis for the specific heat $c_v$ of moist air at constant volume gives the less used formulas

$$c_v = (1 + 1.02q)c_{vd} \approx (1 + 1.02w)c_{vd}. \tag{4}$$

**3·27. Adiabatic process of unsaturated air.** The adiabatic process of unsaturated air (*the unsaturated stage* of 3·24) is a special case of the

adiabatic process of any perfect gas. A certain parcel of moist air is under consideration. Since no condensation takes place in the unsaturated stage, the value of $q$ is constant. Then $R$, $c_v$, and $c_p$ have the numerical values given by 3·25(2), 3·26(3), and 3·26(4). With these values, the equations of section 2·24 define the adiabatic process exactly.

There only remains in theory to evaluate the constants $\kappa = R/c_p$ and $\eta = c_p/c_v$ of 2·24. We have

$$\kappa = \frac{(1 + 0.61q)R_d}{(1 + 0.90q)c_{pd}} = \frac{1 + 0.61q}{1 + 0.90q}\kappa_d = (1 + 0.61q)(1 + 0.90q)^{-1}\kappa_d,$$

where $\kappa_d = 0.286$ by 2·24(12). Since $q$ is always small, we can expand $(1 + 0.90q)^{-1}$ in a power series and then can neglect squares and higher powers of $q$. We finally obtain with all necessary accuracy the important formula

$$\kappa \approx (1 - 0.29q)\kappa_d \approx (1 - 0.29w)\kappa_d. \tag{1}$$

A similar derivation gives a formula important in acoustics, but not used by us:

$$\eta \approx (1 - 0.12q)\eta_d \approx (1 - 0.12w)\eta_d.$$

We see from (1) that the presence of water vapor will *lower* Poisson's constant $\kappa$ from its dry air value of 0.286 to a minimum of 0.283.

Let a parcel of moist air be in the initial state $(T,p)$, where $p < 100$ cb. According to 2·24(10), the temperature $T_1$ and pressure $p_1$ at any other state in the unsaturated adiabatic process will be given by:

$$T_1 = T\left(\frac{p_1}{p}\right)^{\kappa}. \tag{2}$$

The equation (2) defines a curve which might be plotted on any meteorological diagram, to be called an *unsaturated adiabat*. Since $\kappa$ varies with $q$, *through* $(T,p)$ *there would be a different unsaturated adiabat for each value of* $q$. Let $q$ be fixed, and consider the corresponding adiabat (2). This curve will intersect the 100-cb isobar at a temperature $\theta_u$, where

$$\theta_u = T\left(\frac{100}{p}\right)^{\kappa}. \tag{3}$$

Now on the diagram there is a dry adiabat through $(T,p)$ with the potential temperature $\theta$, where by 2·26(1):

$$\theta = T\left(\frac{100}{p}\right)^{\kappa_d}. \tag{4}$$

This $\theta$ is the temperature which *dry* air in the state $(T,p)$ would attain after adiabatic warming to 100 cb. Comparing (3) with (4) and remem-

bering that $\kappa$ is slightly less than $\kappa_d$, we see that $\theta_u$ is slightly less than $\theta$. *Thus the adiabatic change of temperature with pressure is slightly less for moist air than for dry air.* This rule holds for adiabatic cooling in the unsaturated stage, as well as for warming. It is ultimately a consequence of the water vapor's greater heat capacity.

From (3) and (4), it can be shown that the dry adiabat and the steepest unsaturated adiabat through the same point at 40 cb will have a temperature difference of about one degree at 100 cb. *Hence in practical problems the dry adiabats can safely be used for moist unsaturated air without committing a significant error.* This is invariably done in practice, and the unsaturated adiabats are never drawn on a diagram.

The potential temperature $\theta$ has so far been defined only for dry air. For moist air in the state $(T,p)$ we have the *choice* between defining $\theta$: (i) by (4) above; or (ii) as equal to the $\theta_u$ of (3) above. Definition (i) permits $\theta$ to be read directly from the dry adiabats of the meteorological diagram. Definition (ii) would preserve the property that $\theta$ is equal to the temperature of the parcel after adiabatic compression to 100 cb. No definition can do both of these things.

In order to keep our theory in the closest harmony with meteorological practice, definition (i) has been chosen, so that *for moist or dry air, potential temperature $\theta$ is defined by the equation* (4) *above*, i.e., by 2·26(1). For practical purposes we shall assume that the moist unsaturated adiabatic process is represented by the dry adiabats $\theta$ = const.

**3·28. Virtual potential temperature; characteristic point.** According to the formula 3·27(4), every point $(T,p)$ on a meteorological diagram has a definite value of $\theta$ assigned to it, which may be read directly from a diagram by interpolation between the dry adiabats. It is sometimes convenient to use the so-called *virtual potential temperature* $\theta^*$. This $\theta^*$ is the value of $\theta$ for the point $(T^*,p)$. According to 3·27(4),

$$\theta^* = T^* \left(\frac{100}{p}\right)^{\kappa_d}. \tag{1}$$

For moist air in the state $(T,p)$, $T^*$ is determined from 3·25(4), and $\theta$ from 3·27(4). Introducing these into (1), we get

$$\theta^* = (1 + 0.61q)\theta \approx (1 + 0.61w)\theta. \tag{2}$$

Thus $\theta^*$ bears the same relation to $\theta$ that $T^*$ bears to $T$.

Consider now unsaturated air in the initial state $(T,p)$ and having the mixing ratio $w$. The point $(T,p)$ plotted on a diagram is called the *image point* of the air. When this air performs an adiabatic process its image point moves nearly (see 3·27) along the dry adiabat through the

point $(T,p)$. For an adiabatic compression the air will always remain unsaturated, and its image point continues along the dry adiabat. When the process is an adiabatic expansion the image point will move along the adiabat to the point $(T_s,p_s)$ where saturation is reached. (See fig. 3·38). Rossby has named this the *characteristic point*, and it is conveniently determined as the point where the dry adiabat $\theta$ through the image point intersects the vapor line $w_s = w$. Thus the coordinates of the characteristic point may be thought of as $(\theta,w)$, where $\theta$ and $w$ are the values of these respective variables at the image point. Note that $\theta$ and $w$ remain unchanged throughout the adiabatic process from image point to characteristic point.

The point $(T_s,p_s)$ marks the end of the *unsaturated stage*. Further adiabatic expansion results in condensation of part of the water vapor with the release of latent heat which is added to the air. This requires a separate investigation, to be given in the sections beginning with 3·30.

**3·29. Useful approximate formulas.** If a meteorologist has frequent occasion to use the virtual temperature $T^*$ or the moist air constants $R$, $c_p$, and $\kappa$, the following formulas are recommended. The formula (1) for the virtual temperature is especially useful in working on a diagram.

In using formula 3·25(4) in the lower atmosphere we can use the average value 273°K for $T$. Thus we have

$$T^* \approx T + 0.61Tw \approx T + (0.61)(273)w \approx T + \tfrac{1}{6}(10^3w).$$

This gives the formula

$$T^* \approx T + \tfrac{1}{6}(10^3w). \tag{1}$$

Formula (1) is almost exact at $T = 273$°K, and is good enough for most purposes in the atmosphere.

For $R$, we have by 3·25(2) that $R \approx R_d + 0.61R_dw = 287 + 0.175\ (10^3w)$. For many purposes we can use

$$R \approx 287 + \tfrac{1}{6}(10^3w). \tag{2}$$

For $c_p$ we have similarly from 3·26(3),

$$c_p \approx 1004 + \tfrac{9}{10}\ (10^3w). \tag{3}$$

For $\kappa$ we get from 3·27(1) a similar, but less accurate, formula

$$\kappa \approx 0.286 - \frac{1}{10{,}000}\ (10^3w). \tag{4}$$

All these formulas can be used mentally.

**3·30. The adiabatic processes of saturated air.** When saturated air expands adiabatically it will continue to remain saturated during the

process, and some of the vapor will condense to water or ice. If the air were enclosed in an adiabatic container during the expansion, the products of condensation would remain in the system and would evaporate again if the process were reversed into an adiabatic compression. This process which is both *reversible* and *adiabatic* is called the *reversible saturation-adiabatic process*.

In the atmosphere the above conditions are not usually satisfied. Condensation is in most cases followed by precipitation, so that some of the condensed water or ice is removed from the system. The extreme case where all the products of condensation fall out of the air is called the *pseudo-adiabatic process*. This process is evidently *not reversible*, and *neither is it strictly adiabatic*, since the condensation products remove some heat from the system when they fall out. (In fact, the system itself is constantly changing in mass and composition.) The real atmospheric processes lie somewhere between the two extremes just described.

The reversible saturation-adiabatic process is divided into three *stages:* (i) At temperatures above 0°C there is the *rain stage*, where the vapor condenses to water, and the water vapor has the saturation vapor pressure over water; (ii) at 0°C there is the *hail stage*, where the condensed water freezes to ice; (iii) at temperatures below 0°C there is the *snow stage*, where the vapor condenses directly to ice, and the water vapor has the saturation vapor pressure over ice. The pseudo-adiabatic process has only a rain stage and a snow stage, since no water is retained to be frozen in a hail stage.

In the real atmospheric process, the temperature of the transition between the rain and snow stages is usually below 0°C, owing to the tendency of the water droplets to remain in the supercooled liquid stage. The snow stage differs relatively little from the rain stage. The hail and snow stages would require a separate discussion, but are meteorologically less important than the rain stage. The effect of an unknown amount of mixing makes the true atmospheric processes differ somewhat from the ideal processes described above. For all these reasons we shall confine our discussion to the rain stage and make the approximation that the entire adiabatic process is in the rain stage.

The adiabatic expansion of saturated air was first investigated by Hann, and by Guldberg and Mohn. A more nearly complete discussion was given by Hertz (1884) and Neuhoff (1901). The distinction between the reversible saturation-adiabatic and the pseudo-adiabatic process was made by von Bezold (1888). A thorough discussion of both processes with numerical comparisons between them was made by Fjeldstad (1925).

Both the reversible saturation-adiabatic and the pseudo-adiabatic

processes can be expressed in the form of differential equations involving $dT$, $dp$, and $dw_s$. By $w_s$ we mean the saturation mixing ratio over water in the state $(T,p)$. Since the air is always saturated, $w_s$ is also the *actual* mixing ratio of the air. Immediately upon expansion from the characteristic point, the temperature starts to decrease. This causes $w_s$ to decrease. Hence some water vapor condenses to liquid water, releasing some latent heat. This heat is used to warm the whole system, including the moist air. Hence the cooling proceeds at a slower rate than in the dry-adiabatic process. As a result of this argument, it follows that *the adiabats for saturated air must have a slope between that of the dry adiabats and the vapor lines.* See fig. 3·31.

If the reader is interested only in an approximate equation for these adiabatic processes, he should go to section 3·34 at once.

**3·31. Exact equation of the pseudo-adiabatic process.** To derive the exact equation for the pseudo-adiabats, let the saturated air be in the state $(T,p,w_s)$ represented by $A$ in fig. 3·31. After a small pseudo-adiabatic expansion, the air is in the state $(T + dT, p + dp, w_s + dw_s)$ represented by $B$ in the figure. Note that $dT$, $dp$, and $dw_s$ are all negative. Let us consider a mass of $1 + w_s$ tons of moist air, made up of one ton of dry air and $w_s$ tons of water vapor. In the pseudo-adiabatic process $AB$, the quantity $-dw_s$ of water vapor condenses and drops out as precipitation. The condensation releases the quantity of heat

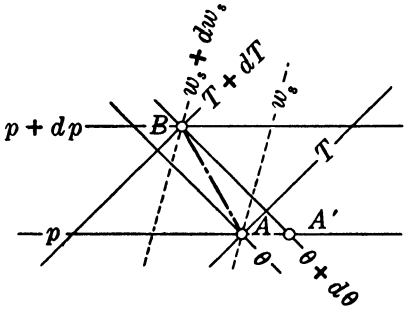



FIG. 3·31.

$$dH = -L dw_s, \tag{1}$$

which is used to heat the moist air. From 2·22(3) the heat $dh$ absorbed by the moist air *per unit mass* is related to the temperature change $dT$ and pressure change $dp$ as follows:

$$dh = c_p dT - RT\frac{dp}{p}. \tag{2}$$

Here $c_p$ and $R$ are the thermal constants for moist air. Since the mass of moist air is $1 + w_s$, we see that

$$dH = (1 + w_s)dh. \tag{3}$$

Combining (1), (2), and (3) we have

$$-L dw_s = (1 + w_s)\left[c_p dT - RT\frac{dp}{p}\right]. \tag{4}$$

Equation (4) is an *exact* form of the differential equation for the pseudo-adiabatic process.

It is convenient to express (4) in terms of the constants $c_{pd}$ and $R_d$ for dry air. We substitute for $R$ from 3·25(2) and for $c_p$ from 3·26(3). Multiplying through by $(1 + w_s)$ and ignoring squares of $w_s$, we get

$$(5) \qquad -Ldw_s = (1 + 1.90w_s)c_{pd}dT - (1 + 1.61w_s)R_dT\frac{dp}{p}.$$

Equation (5) can be shown to be equivalent to that derived by Fjeldstad.

**3·32. Exact equation of the reversible saturation-adiabatic process.** As stated in 3·30, in the reversible saturation-adiabatic process the condensed water is retained in the system in the form of cloud droplets. Let $w$ be the total mass of water substance in a saturated parcel containing unit mass of dry air. The system will then consist of $1 + w_s$ tons of moist air and $w - w_s$ tons of liquid water. Let the air be in the state $(T,p,w_s)$ represented by point $A$ in fig. 3·31. Let the expansion to the state $(T + dT, p + dp, w_s + dw_s)$ take place. As in 3·31 the quantity $-dw_s$ tons of vapor will condense and release the quantity of heat

$$(1) \qquad dH_1 = -Ldw_s.$$

A second source of heat is the cooling of the $w - w_s$ tons of water through $dT$ degrees. This provides the quantity of heat

$$(2) \qquad dH_2 = -c_w(w - w_s)dT,$$

where $c_w$ is the specific heat of water. The total heat $dH_1 + dH_2$ released by the process is absorbed by the moist air. For the $1 + w_s$ tons of moist air this heat is equal to

$$(3) \qquad (1 + w_s)\left[c_pdT - RT\frac{dp}{p}\right].$$

Equating the total heat released in (1) and (2) to the heat absorbed in (3), we get

$$-Ldw_s - c_w(w - w_s)dT = (1 + w_s)\left[c_pdT - RT\frac{dp}{p}\right].$$

Introducing $R_d$ and $c_{pd}$ and transposing the term $-c_w(w - w_s)dT$ give

$$-Ldw_s = \left[1 + 1.90w_s + \frac{c_w}{c_{pd}}(w - w_s)\right]c_{pd}dT - (1 + 1.61w_s)R_dT\frac{dp}{p}.$$

Putting in the value $c_w/c_{pd} = 4185/1004$, we get the final form

$$(4) \qquad -Ldw_s = [1 + 1.90w_s + 4.17(w - w_s)]c_{pd}dT - (1 + 1.61w_s)R_dT\frac{dp}{p}.$$

Equation (4) is an *exact* form of the differential equation for the reversible saturation-adiabatic process. It will be noted from (4) that there is a different reversible saturation adiabat through $(T,p)$ for each value $w$ of the total water content. They differ only slightly from each other and from the pseudo-adiabat.

**3·33. Critique of the two equations.** Equations 3·31(5) and 3·32(4) cannot be integrated directly in their present form. The latter can be written in terms of the variables $w_s$, $p_d$, and $T$ and is directly integrable in that form, a fact of questionable practical value, since $p_d$ is not a convenient variable to use. The former equation seems non-integrable in terms of elementary functions, a consequence of its representing a non-adiabatic process.

Either equation may be integrated numerically to any desired degree of accuracy by a series of small steps. To do this, a second relation between $dw_s$, $dT$, and $dp$ is obtained by differentiating 3·20(4), which expresses the physical condition that the air remains saturated. See 5·10(6). This second relation may be combined with the equation of either saturation process, and the two can be solved simultaneously for $dT$ and $dp$ in terms of $dw_s$. The work is very laborious in practice.

This numerical integration shows that the pseudo-adiabatic process cools slightly faster than the reversible saturation-adiabatic process. This is due to the loss of the heat content of the precipitated water. The difference is very slight and, in comparison with the effects of radiation and turbulent exchange of heat, may be neglected in practical problems.

It is therefore immaterial for practical purposes whether the adiabatic process of saturated air is calculated from the reversible saturation-adiabatic or from the pseudo-adiabatic equation, provided the process is an expansion. The practical difference between the two appears when the process is reversed. When the condensed water remains in the air, the process is reversible, and the compression returns along its path of expansion. However, when a pseudo-adiabatic expansion is followed by compression, the compression nearly follows a dry adiabat.

**3·34. Simplified equation of the adiabatic process of saturated air.** Let a parcel of $1 + w_s$ tons of saturated moist air be in the state $(p,T,w_s)$ represented by $A$ in fig. 3·31. The parcel thus contains one ton of dry air and $w_s$ tons of water vapor. After a small adiabatic expansion the air is in the state $(T + dT, p + dp, w_s + dw_s)$ represented by $B$ in that figure. Note that $dT$, $dp$, and $dw_s$ are all negative.

Now the condensation of $-dw_s$ tons of water vapor will release the quantity of heat $-L dw_s$. Let us make the slightly incorrect assumption

that this latent heat is used exclusively to heat the ton of dry air; i.e., we ignore the heating of the $w_s$ tons of water vapor. Then by 2·22(3) the heat $dh$ absorbed by the dry air is related to the temperature change $dT$ and pressure change $dp$ as follows:

$$dh = c_{pd}dT - R_dT\frac{dp}{p}.$$

Equating $dh$ to $-Ldw_s$, we arrive at an important approximate equation:

$$-Ldw_s = c_{pd}dT - R_dT\frac{dp}{p}. \tag{1}$$

It will be observed that the exact equations 3·31(5) and 3·32(4) both reduce to (1) when the small correction factors to $c_{pd}$ and $R_d$ are neglected. The solutions of (1) are found to lie very close to the exact solutions of 3·31(5) and 3·32(4). In view of the element of uncertainty in atmospheric problems, we are quite justified in using the equation (1) as an acceptable formula for the adiabatic process of saturated air. This will be done, and the process described by (1) will in the following be called the *saturation-adiabatic* process. The corresponding lines on the diagram will hereafter be called *saturation adiabats*. It will be shown in section 3·36 how these lines are constructed on the diagram.

From 2·26(3), we may write (1) in the form

$$-\frac{Ldw_s}{T} = c_{pd}\frac{d\theta}{\theta}. \tag{2}$$

From (2) the change $d\theta$ of potential temperature in fig. 3·31 can be expressed in terms of $dw_s$.

**3·35. Isobaric warming and cooling.** For two later sections (3·36 and 3·39) it is necessary to compute the temperature change resulting from isobaric evaporation from, or condensation into, a parcel of air. Let a parcel of moist air, saturated or not, be in the state $(T,p,w)$. Suppose that some vapor is condensed from the parcel, or that some water is evaporated into the parcel. Let either process take place at constant pressure, *the latent heat being supplied to or taken from the air.* In the case of condensation the resulting change $dw$ of mixing ratio is negative, and the air absorbs the latent heat by warming. In the case of evaporation $dw$ is positive, and the air provides the latent heat by cooling. Let $(dT)_p$ be the resulting isobaric change in the temperature of the air. The air thus finishes in the state $[T + (dT)_p,p,w + dw]$.

The expression giving $(dT)_p$ in terms of $dw$ is easy to obtain. In the case of condensation, the latent heat made available to the moist air (per

ton of dry air) is $-Ldw$. We shall, as in 3·34, assume that this heat is used exclusively to heat the ton of dry air. Since the process is isobaric, the heat $dh$ absorbed by the air is from 2·22(3)

$$dh = c_{pd}(dT)_p.$$

Equating the heat $-Ldw$ released to the heat $dh$ absorbed by the air, we get

$$-Ldw = c_{pd}(dT)_p. \tag{1}$$

It will be seen that (1) is valid for either condensation or evaporation. It should be noted that formula (1) is mathematically equivalent to the special case $dp = 0$ of formula 3·34(1).

For easy computation, we solve (1) for $(dT)_p$ and substitute for $L$ and $c_{pd}$ their values from 3·08(4) and 2·21(5). The result is

$$(dT)_p = -2.5(10^3 dw). \tag{2}$$

By grouping $10^3$ with $dw$ we have expressed $dw$ in parts per thousand, as on a diagram. Equation (2) can thus be expressed in words:

*At constant pressure, adiabatic condensation of one part per thousand of vapor will warm moist air two and one-half degrees. At constant pressure, adiabatic evaporation of the same amount of water into air will cool the air two and one-half degrees.*

**3·36. Graphical construction of the saturation adiabats.** The construction of the saturation adiabats can be carried out on a diagram very quickly by using 3·35(2). The method is equivalent to a numerical integration of the equation 3·34(1). Suppose saturated air is in the state $(T,p,w_s)$ represented by $A$ in fig. 3·31. Let $dw_s$ be fixed at some convenient small negative value, generally $-1 \times 10^{-3}$ or $-2 \times 10^{-3}$. It is desired to find the point $B$ (see fig. 3·31) where the saturation adiabat through $A$ crosses the vapor line $w_s + dw_s$. For this construction we replace the saturation-adiabatic process $AB$ by another adiabatic process $AA'B$ consisting of two parts: (i) The latent heat released by the condensation of $-dw_s$ tons of vapor is used to warm the air at constant pressure along the path $AA'$; (ii) the now unsaturated air is brought back to saturation by a dry-adiabatic expansion $A'B$. Both (i) and (ii) are easily performed graphically.

According to 3·35(2) the warming $AA'$ will amount to 2.5 degrees for each part per thousand of vapor condensed. Thus $A'$ is easily plotted. The point $B$ is found at the intersection of the dry adiabat through $A'$ with the vapor line $w_s + dw_s$. When $B$ has been obtained, the same procedure can be repeated from that point, and so on. We thus obtain a series of points $A$, $B$, $C$, $D$, $\cdots$ on the saturation adiabat. A smooth

curve can be put through these points for as long a distance as we choose to carry out the process.

The approximation 3·35(2) is consistent for infinitesimal $dw_s$ with the approximate equation 3·34(1) defining the saturation-adiabatic process. The adiabatic process $AA'B$ described above is therefore equivalent to the saturation-adiabatic process $AB$ of 3·34, as long as $dw_s$ is infinitesimal. For finite values of $dw_s$, however, the method of the present section has a small error. The smaller the numerical values chosen for $dw_s$, the more accurate the method is in practice. In this way it is limited only by one's ability to read the diagrams.

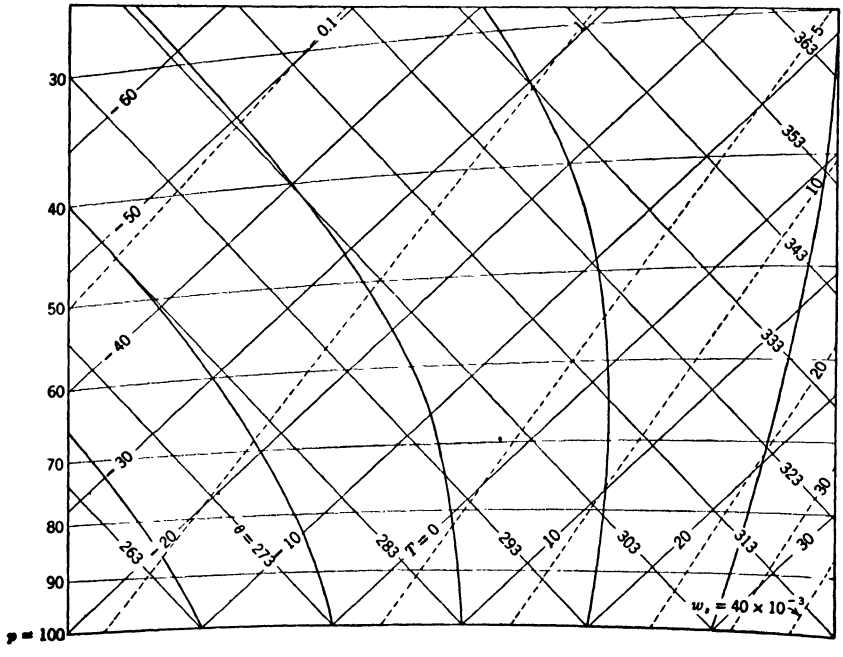



FIG. 3·36.

As an example we will compute the saturation adiabat through $T = 20°C$, $p = 100.0$ cb. This and other saturation adiabats are shown on the tephigram in fig. 3·36. A calculation yields $w_s = 14.9 \times 10^{-3}$. The remaining steps have been done on a large tephigram and are shown in table 3·36. The student should follow the calculations on some legible diagram.

There will be discrepancies on another diagram, of course, because of the human factor and the fact that few meteorological diagrams are made from strictly accurate plates. The point is that this method is

convenient and reliable. More will be said in 3·38 about the asymptotic dry adiabat mentioned in table 3·36. It is labeled $\theta = \theta_e$.

TABLE 3·36

| POINT | $T$(°C) | $p$(cb) | $10^3 w_s$ | $10^3 dw_s$ | $(dT)_p$ | $\theta$(°K) |
|---|---|---|---|---|---|---|
| $A$ | 20.0 | 100.0 | 14.9 | −0.9 | 2.25 | 293.0 |
| $A'$ | 22.2 | 100.0 | .... | ..... | .... | 295.2 |
| $B$ | 18.4 | 95.8 | 14.0 | −2.0 | 5.0 | 295.2 |
| $B'$ | 23.4 | 95.8 | .... | ..... | .... | 300.4 |
| $C$ | 14.4 | 85.8 | 12.0 | −2.0 | 5.0 | 300.4 |
| $C'$ | 19.4 | 85.8 | .... | ..... | .... | 305.7 |
| $D$ | 9.8 | 76.3 | 10.0 | −2.0 | 5.0 | 305.7 |
| $D'$ | 14.8 | 76.3 | .... | ..... | .... | 311.2 |
| $E$ | 4.9 | 67.7 | 8.0 | −2.0 | 5.0 | 311.2 |
| $E'$ | 9.9 | 67.7 | .... | ..... | .... | 316.8 |
| $F$ | −1.0 | 59.2 | 6.0 | −2.0 | 5.0 | 316.8 |
| $F'$ | 4.0 | 59.2 | .... | ..... | .... | 322.8 |
| $G$ | −8.4 | 50.2 | 4.0 | −2.0 | 5.0 | 322.8 |
| $G'$ | −3.4 | 50.2 | .... | ..... | .... | 329.2 |
| $H$ | −19.7 | 40.3 | 2.0 | −1.0 | 2.5 | 329.2 |
| $H'$ | −17.2 | 40.3 | .... | ..... | .... | 332.6 |
| $I$ | −29.2 | 34.0 | 1.0 | −0.5 | 1.25 | 332.6 |
| $I'$ | −28.0 | 34.0 | .... | ..... | .... | 334.6 |
| $J$ | −37.8 | 29.5 | 0.5 | −0.5 | 1.25 | 334.6 |
| $J'$ | −36.5 | 29.5 | .... | ..... | .... | 336.2 |

(asymptotic dry adiabat: $\theta$ = 336.2)

**3·37. Nomenclature.** A number of temperatures and potential temperatures of moist air are used by meteorological writers. There is fair agreement on the definitions of the variables to be introduced, but there is very little agreement on the names to be given them. It is therefore important to learn the variables in terms of definite operations on a diagram. By means of the operations themselves it is possible to distinguish what an author means by a certain complicated name.

Concerning our own terminology the word *wet bulb* or subscript $w$ always refers to temperatures attained by a parcel after it has been completely saturated. The word *equivalent* or subscript $e$ always refers to temperatures attained by a parcel after it has been completely dried out. The word *potential* (or letter $\theta$) always refers to a temperature attained after some kind of adiabatic compression to 100 cb.

Any temperature with the prefix *isobaric* or subscript $i$ is that attained by a parcel after being saturated or dried out at constant pressure. These are in contrast to temperatures labeled by a prefix *adiabatic* or subscript $a$. The latter are temperatures attained after a parcel has been saturated or dried out along dry and saturation adiabats.

**3·38. Definitions of $\theta_w, \theta_e, T_{aw}, T_{ae}, T_d$.** The method of labeling dry adiabats can be applied to the saturation adiabats. Every saturation adiabat intersects the isobar $p = 100$ cb. The value of the temperature at this intersection is called the *wet bulb potential temperature*, and is denoted by $\theta_w$. See fig. 3·38. The value of $\theta_w$ uniquely labels the saturation adiabats. On many diagrams the saturation adiabats are drawn at intervals for $\theta_w$ of 2°C.

*A parcel of moist air is said to have the wet bulb potential temperature $\theta_w$ of the saturation adiabat through the characteristic point (see 3·28) of the parcel.*

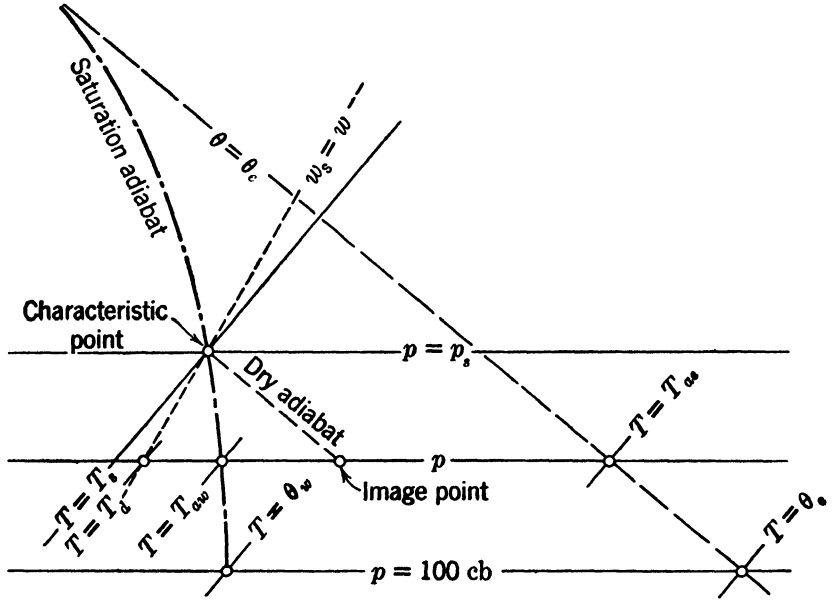



FIG. 3·38.

Another way of labeling the saturation adiabats is obtained from the fact that as $w_s$ approaches 0, the saturation adiabat approaches asymptotically a certain dry adiabat. (This is not proved here but is plausible from a diagram.) The potential temperature of this asymptotic dry adiabat is called the *equivalent potential temperature* and is denoted by $\theta_e$. This value of $\theta_e$ uniquely labels the saturation adiabat. On some diagrams the value of $\theta_e$ is given at the low-pressure end of each saturation adiabat. On other diagrams $\theta_e$ must be computed according to the method described in 3·41.

*A parcel of moist air is said to have the equivalent potential temperature $\theta_e$ of the saturation adiabat through the characteristic point of the parcel.*

The two potential temperatures $\theta_w$ and $\theta_e$ are both used in the literature and both must be familiar to the meteorologist, even though either one of the two would be quite sufficient in theory.

Consider any parcel of moist air with pressure $p$, wet bulb potential temperature $\theta_w$, and equivalent potential temperature $\theta_e$. The temperature at the point where the saturation adiabat $\theta_w$ crosses the initial isobar $p$ is called the *adiabatic wet bulb temperature* and is denoted by $T_{aw}$. See fig. 3·38. The temperature at the point where the dry adiabat $\theta = \theta_e$ crosses the initial isobar is called the *adiabatic equivalent temperature* and is denoted by $T_{ae}$.

The *dew point temperature* $T_d$ of a parcel of moist air is the temperature at which the air would become saturated if it were cooled isobarically without change of mixing ratio. This temperature is that of the intersection of the initial isobar with the vapor line $w_s = w$. See fig. 3·38. The cooling process defining $T_d$ is not an adiabatic process.

Each of the temperatures just defined has found theoretical and practical applications to meteorology, and should be known. Each can be defined by an ideal physical process on the initial parcel, and the student should have no trouble in stating the processes needed. For example, $T_{ae}$ is attained by a parcel from the successive application of three processes: (i) expanding the parcel by a dry-adiabatic process until it becomes saturated at the characteristic point; (ii) completely drying the parcel out by a saturation-adiabatic expansion to very low pressure; (iii) compressing the resulting dry air dry adiabatically to the initial pressure.

**3·39. Definitions of $T_{ie}$ and $T_{iw}$.** Consider the fictitious process where a parcel of moist air is dried out by an isobaric process which is also adiabatic. That is, we suppose that all the water vapor is condensed out of the parcel, the latent heat released being used to heat the air itself. The resulting temperature is called the *isobaric equivalent temperature* and is denoted by $T_{ie}$. It can be shown that for moist air we always have

$$T_{ie} < T_{ae}. \tag{1}$$

Both the processes which define $T_{ae}$ and $T_{ie}$ are adiabatic, and the amount of latent heat released is the same in both of them. The final temperatures are, however, different, since the two processes follow different paths in the diagram and therefore perform different amounts of work.

In contrast to the temperatures defined in 3·38, which are usually obtained graphically, $T_{ie}$ is obtained by a simple calculation. From 3·35(2) each part per thousand of vapor condensed will heat the air

2.5°C. Hence with good accuracy,

$$T_{ie} = T + 2.5(10^3 w), \tag{2}$$

where $w$ is the mixing ratio of the air.

The corresponding wet bulb temperature is obtained from the initial parcel by evaporating water vapor into the parcel isobarically and obtaining the necessary latent heat by cooling the parcel. This process may be assumed to take place when precipitation falls through a layer of unsaturated air. Thus the mixing ratio rises from its initial value $w$, while the temperature falls from its initial value $T$. The temperature where the air becomes saturated is called the *isobaric wet bulb temperature* and is denoted by $T_{iw}$. The corresponding saturation mixing ratio is denoted by $w_{iw}$. It can be shown that for unsaturated air we always have

$$T_{aw} < T_{iw},$$

for the same reason as in the case of the equivalent temperatures. *The difference $T_{iw} - T_{aw}$ rarely exceeds a few tenths of a degree.* For this reason many authors lump the two into a single " wet bulb temperature."

$T_{iw}$ can be very accurately obtained by a combination of reading a diagram and numerical interpolation, as follows. Integrating 3·35(2) between the initial state and the saturated state, we get

$$T_{iw} - T = -2.5 \times 10^3 (w_{iw} - w).$$

This may be written in the form

$$T_{iw} + 2.5(10^3 w_{iw}) = T + 2.5(10^3 w) = T_{ie}. \tag{3}$$

Since both $T_{iw}$ and $w_{iw}$ are unknown, (3) cannot be solved directly.

For *any* temperature $T$ on the initial isobar, the corresponding *saturation mixing ratio* $w_s$ can be read from a diagram. Then the variable quantity

$$a_T = T + 2.5(10^3 w_s)$$

can easily be computed. Now the solution $T_{iw}$ of (3) is the value of $T$ such that $a_T = T_{ie}$. This is most easily found by choosing a $T$ likely to be a little too low, for example $T_{aw}$, and another $T$ likely to be a little too high. On computing $a_T$ for both of these guesses, a direct interpolation will yield the $T$ for which $a_T = T_{ie}$. This $T$ is $T_{iw}$. All temperatures may be expressed in centigrade in this computation.

A more important problem in practice is to obtain $w$, being given $T$ and $T_{iw}$. This is much easier, since from a diagram we can get $w_{iw}$ at once.

Then (3) can be solved for $w$, yielding the so-called *psychrometric formula*

$$10^3 w = 10^3 w_{iw} + \frac{T - T_{iw}}{2.5}. \tag{4}$$

The importance of this formula will appear in the next section.

It can be shown that the temperatures defined so far stand in the following relation for moist unsaturated air:

$$T_s < T_d < T_{aw} < T_{iw} < T < T_{ie} < T_{ae}.$$

This can be used as a check on the computations.

**3·40. Surface observations.** The humidity is obtained in surface observations by measuring the "wet bulb temperature" with a psychrometer. The evaporation from the damp cloth lowers the temperature by a very complex process, which probably cannot be adequately described. Though it is an isobaric process, it certainly is not adiabatic, so that the temperatures of 3·39 do not strictly apply. *However, it is found that with very little error we can assume the wet bulb temperature to be equal to* $T_{iw}$.

With this assumption, we can regard the raw data of a surface observation as being the values of $T$, $T_{iw}$, and $p$. From the psychrometric formula 3·39(4) we can get $w$. Thus we have the state of the air in terms of $T$, $p$, and $w$. From this point on all other desired quantities can be obtained as outlined previously.

In particular: $r$ can be obtained from 3·21(2); $T_d$, from the method of 3·38; and $e$, from the method of 3·23. These are the moisture variables usually reported in a surface observation and obtained from psychrometric tables. The present discussion has shown how a surface observation report can be prepared independently of such tables by methods which are rapid and practical, requiring only a diagram.

**3·41. Example.** The following example will show how the formulas and processes described in this chapter are used to evaluate the different variables. The graphical operations are done on a tephigram like that of fig. 3·36.

Given air in the initial state $T = 13.5°\text{C}$, $p = 90.0$ cb, $w = 3.0 \times 10^{-3}$. The following quantities are obtained immediately by calculation: $T^*$, $R$, $c_p$, $\kappa$, $\alpha$:

By 3·29(1), $T^* = 13.5 + \frac{1}{6}3 = 14.0°\text{C} = 287.0°\text{K}$.
By 3·29(2), $R = 287 + \frac{1}{6}3 = 287.5$ kj $\text{t}^{-1}$ $\text{deg}^{-1}$.
By 3·29(3), $c_p = 1004 + \frac{9}{10}3 = 1006.7$ kj $\text{t}^{-1}$ $\text{deg}^{-1}$.
By 3·29(4), $\kappa = 0.286 - 3(0.0001) = 0.286$.
By 3·25(5), $\alpha = (287)(287)/(90) = 915$ $\text{m}^3$ $\text{t}^{-1}$.

The following quantities are usually obtained from a diagram: $w_s$, $\theta$, $p_s$, $T_s$, $\theta_w$, $T_{aw}$, $\theta_e$, $T_{ae}$, $T_d$, $e_s$.

Plotting the image point (13.5°C, 90.0 cb) on a diagram, we read $w_s = 11.0 \times 10^{-3}$ and we interpolate $\theta = 295.5$°K between the dry adiabats. Following this same interpolated adiabat to the point where it intersects the vapor line $w_s = 3.0 \times 10^{-3}$, we read the pressure $p_s = 68.3$ cb and temperature $T_s = -8.2$°C. This point is the characteristic point. The saturation adiabat through this point intersects the 100-cb isobar at the temperature $\theta_w = 10.0$°C = 283.0°K.

Going back up the same saturation adiabat, we read the temperature $T_{aw}$ where it crosses 90.0 cb, getting $T_{aw} = 5.0$°C. We continue on the saturation adiabat to the point (−24.9°C, 51.2 cb) where it crosses the vapor line $w_s = 1 \times 10^{-3}$. We get $\theta_e$ by following the construction of section 3·36. Since $10^3 w_s = 1$, we add 2.5°C isobarically to the last point mentioned and get (−22.4°C, 51.2 cb). We read the potential temperature $\theta_e = 304$°K. (This is the only safe method on most diagrams, as it is impossible to estimate which dry adiabat the saturation adiabat is approaching.) Following the dry adiabat $\theta = \theta_e$ to 90.0 cb, we read $T_{ae} = 21.8$°C.

We now read the dew point temperature $T_d = -4.7$°C at the intersection of the vapor line $w_s = 3.0 \times 10^{-3}$ with the initial isobar $p = 90.0$ cb.

To get $e_s$, we follow the isotherm $T = 13.5$°C to its intersection with the pressure 622 mb (see section 3·23). Here $10^3 w_s' = 16$, which when added to 622 gives 638. At (13.5°C, 638 mb) we read $10^3 w_s'' = 15.5$, so that $e_s = 15.5$ mb = 1.55 cb.

At this stage, we can obtain $r$, $e$, $T_{ie}$, and $T_{iw}$ by calculation. By 3·21(2), $r \approx w/w_s = 3.0/11.0 = 27\%$. Then by 3·19(2), $e = re_s = (0.27)(1.55) = 0.418$ cb. From 3·39(2), $T_{ie} = 13.5 + 2.5(3) = 21.0$°C. To get $T_{iw}$ we follow the method of section 3·39. We use $T_{aw} = 5.0$°C as the first guess. From the diagram at (5.0°C, 90.0 cb), $w_s = 6.1 \times 10^{-3}$. Thus

$$a_5 = 5.0 + (2.5)(6.1) = 20.25.$$

Similarly, trying 6.0°C as a second guess, with the corresponding value $w_s = 6.5 \times 10^{-3}$, we have

$$a_6 = 6.0 + (2.5)(6.5) = 22.25.$$

Interpolating between 5° and 6° to get $a_T = T_{ie} = 21.0$, we get

$$T_{iw} = 5.0 + \frac{21.0 - 20.25}{22.25 - 20.25} = 5.4\text{°C}.$$

Several of the graphical operations can be checked by use of formulas, if desired, but unless exceptional accuracy is desired this is unnecessary.

CHAPTER FOUR

# HYDROSTATIC EQUILIBRIUM

**4·01. The hydrostatic problem.** The preceding chapters have treated the physical behavior of individual air elements. We shall now proceed to discuss the distribution of air elements in space. In the present chapter the case will be considered where the atmosphere is in equilibrium. Although this case never holds in practice, there are several reasons why it is important to examine the atmosphere in this state. First, it serves as the natural introduction to the more complicated general problem of the atmosphere in motion. Second, the analysis of a resting atmosphere will provide useful insight into the general laws for the distribution of mass and pressure. Third, it will be shown later (see 7·14) that an important practical problem can be solved with sufficient accuracy by assuming the atmosphere at rest.

This so-called hydrostatic problem consists in determining the distribution in space of the physical properties of the air elements, i.e., their pressure, temperature, specific volume, and density. Our knowledge of this distribution is in practice obtained by a series of meteorological observations, which are taken simultaneously at the surface of the earth and, to a less extent, from the free atmosphere. The surface observations give values of the atmospheric variables at fixed points. The upper air observations on the other hand are made by sounding instruments which give simultaneous values of the atmospheric variables, pressure, temperature, and humidity. The soundings give no direct information about the position in space where the various values occur. Thus the problem to be solved in order to determine the distribution in space of mass and pressure is to refer the upper air observations to geometric points, or more specifically to determine the heights which correspond to the various pressure values along an aerological ascent. The solution of this problem is the practical aim of this chapter.

**4·02. The fields of the physical variables.** Each geometrical point within the region of the atmosphere is occupied by an infinitesimal element of air in a certain physical state, characterized by certain definite values of the physical variables $p$, $\alpha$, $T$. A region where every point has a definite value of a physical property assigned to it is known as a field of that property.

Let us consider any one of the physical variables, for instance, the pressure. Apart from certain singular points the pressure will from every point in space increase in certain directions and decrease in others. Thus, through every point there is a surface on which the pressure does not change, which separates the region of increase from the region of decrease. This surface does not terminate anywhere in the interior of the atmosphere; it either is closed or continues until it intersects the surface of the earth. This surface is called an *isobaric surface.* It divides space into a region of higher pressures on one side and a region of lower pressures on the other side. Consider now two isobaric surfaces characterized by the pressures $p$ and $p + \delta p$. These surfaces do not intersect, for the pressure has only one value at a point. The normal distance between the two surfaces is everywhere small if the pressure interval $\delta p$ is sufficiently small. The two surfaces bound a thin layer which is known as an *infinitesimal isobaric layer.* The whole atmosphere may accordingly be divided into a large number of thin isobaric layers. In practice it is unnecessary to draw many surfaces, since a small number gives a sufficiently clear picture of the pressure field. Generally the surfaces $p = 0, 1, 2, \cdots$ cb are selected. The layers defined by these surfaces are called the *isobaric unit layers.* This method of representation is essentially the one used in practical meteorology. The *isobars* which are drawn on the synoptic weather map are the intersections between the isobaric surfaces and mean sea level. If similar isobars are drawn in a number of level surfaces sufficiently close together, one obtains in practice the three-dimensional picture. We shall in the following discussion only occasionally make use of the two-dimensional isobars in the level surfaces, and generally think of the pressure field in terms of its isobaric unit layers.

A similar geometrical representation of the temperature field is given by the isothermal surfaces and the isothermal unit layers. The mass field may be represented either by the specific volume or by the density. According to 2·03(1), a surface $\alpha = \text{const}$ is always a surface $\rho = \text{const}$, so these two variables define the same family of surfaces. However, the selection of unit surfaces and unit layers is different, depending upon which of the two is used for the description of the mass field. When the specific volume is used, the mass field is geometrically represented by the *isosteric* surfaces and unit layers. The surfaces and unit layers of density are called *isopycnic.*

Any physical quantity whose field can be described by one single numerical value in each point in space may be given a similar geometrical representation. There is no essential difference between such fields, and accordingly they may be treated mathematically as quantities of the

same kind. It is then unnecessary to derive the mathematical rules for such quantities more than once. Physical quantities of this kind are known in mathematical physics as *scalars*, and their fields as *scalar fields*. We shall presently meet other physical quantities which for their description require more than one number in each point. Before these quantities are discussed we shall introduce analytical expressions for the scalars.

**4·03. The coordinate system.** The fundamental tool which is used to describe geometrical quantities in analytical terms is the coordinate system. The ideal system for atmospheric problems would of course be one with spherical coordinates. For most purposes, however, the Cartesian or rectangular system is satisfactory, and is preferable because of its great simplicity. The Cartesian system generally adopted in mathematical physics is the so-called right-handed system, which by definition is such that a rotation in the $xy$ plane from the positive $x$ axis to the positive $y$ axis will drive a right-handed screw in the direction of the positive $z$ axis. See fig. 4·03. It then follows that the rotations $y$ to $z$ and $z$ to $x$ will also give the right-handed screw displacements along the positive $x$ axis and $y$ axis respectively. We shall later apply this *right-handed screw rule* whenever the rotation in a plane is associated with a positive direction along the axis of rotation.

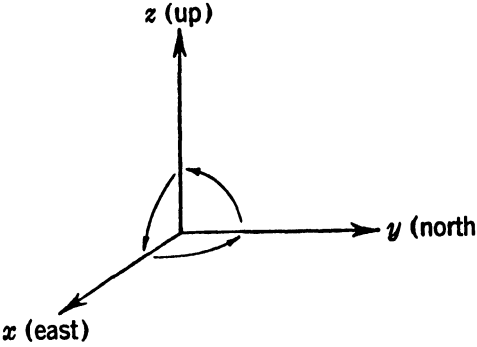


FIG. 4·03. The standard system of coordinates.

In meteorology this system of coordinates is generally given a fixed position and orientation with reference to the earth. The origin is placed at some special point, fixed in the earth's surface. The $xy$ plane is chosen as the plane tangent to the surface of the earth at the origin, with the $x$ axis to the east and the $y$ axis to the north. This choice automatically fixes the direction of the $z$ axis as pointing vertically upward. This system will be referred to as the *standard system*.

**4·04. Analytical expression for scalar quantities.** It was shown in section 4·02 that any scalar quantity may be represented geometrically by its surfaces of constant value of the scalar, or more specifically by its *equiscalar* unit layers. Let the scalar be denoted by $\varepsilon$, and consider first one of its surfaces defined by the value $\varepsilon_1$. The equation for this surface

in a rectangular system of coordinates will be of the form $\varepsilon_1 = \varepsilon(x,y,z)$, where $\varepsilon(x,y,z)$ is a certain definite mathematical function of the variables $x, y, z$. If this function is put equal to another constant value $\varepsilon_2$ close to $\varepsilon_1$, we obtain the equation for another surface: $\varepsilon_2 = \varepsilon(x,y,z)$, which generally is close to the surface $\varepsilon_1$, and so on. Thus the whole scalar field may be described analytically by the expression

$$\varepsilon = \varepsilon(x,y,z). \tag{1}$$

By successively giving $\varepsilon$ the values 0, 1, 2, $\cdots$ this expression gives the equations for the equiscalar unit surfaces.

The expression (1) cannot, of course, be specified further, since it represents all possible functions. Under real conditions in the atmosphere the distribution and shape of the equiscalar surfaces of the physical variables are in general so complicated that it is impossible to express the corresponding functions (1) in terms of explicit mathematical expressions. Nevertheless we know that the functions exist, and that they are continuous and single valued in space, except along frontal surfaces. This information is sufficient for the theoretical analysis of their dynamical behavior.

The fields of the three scalar quantities with which we are primarily concerned are expressed mathematically as follows:

$$p = p(x,y,z); \qquad \alpha = \alpha(x,y,z); \qquad T = T(x,y,z). \tag{2}$$

These expressions, or the equivalent geometrical representation by unit layers, define the fields of these quantities at a certain fixed time. In the case of equilibrium this representation is complete. If the atmosphere is in motion, however, the fixed points $(x,y,z)$ will continually be occupied by new particles, bringing their physical properties along with them. For each new instant we would have a new distribution in space of the unit layers and a new set of functions (2). This is analytically expressed by introducing the time $t$ as an additional variable, which gives:

$$p = p(x,y,z,t); \qquad \alpha = \alpha(x,y,z,t); \qquad T = T(x,y,z,t). \tag{3}$$

When $t$ here is given a constant value $t_0$, we are back to the expressions (2) for a given instant. When $t$ changes, the expressions (3) describe how the surfaces change their position with time.

**4·05. Vectors.** The physical condition for the equilibrium of a system is that the forces acting upon it are in balance, or that their *resultant* is zero. Thus the study of equilibrium brings in a new physical concept, force. Force belongs to a class of physical quantities differ-

ent from the scalars. Whereas a scalar is characterized by magnitude only, and can be represented by one number when the units are chosen, *force has direction as well as magnitude.* Other physical quantities belonging to this class are displacement, velocity, acceleration, etc. These directed quantities are known as *vectors.*

Any vector may be represented geometrically by an arrow, pointing in the assigned direction, whose length is equal to the magnitude of the vector. Since all vectors thus have the same geometrical representation, the mathematical rules which apply to one of them apply to them all. These rules may be developed without specification of the physical nature of the vectors.

The vectors will in the following be denoted by bold-face letters, and their magnitudes by the corresponding letters in ordinary type. Thus if a vector is denoted by **a**, we have by definition $|\mathbf{a}| = a$. We shall often deal with vectors of unit length. Thus if **l** is a *unit vector* we have by definition $|\mathbf{l}| = 1$.

Consider an arbitrary vector **a** and an arbitrary straight line $l$ with an assigned positive direction determined by a unit vector **l** (fig. 4·05). It is always possible to pass planes normal to $l$ through the two endpoints of the vector **a**. The projection of the vector on the line, defined by this operation, is called its *component* along the direction $l$ and will be denoted by $a_l$. The component is a pure number, and hence a scalar. It is positive when the projection extends in the direction of **l**, and negative when it extends in the opposite direction. When the operation illustrated in fig. 4·05 is applied to the three axes of the coordinate system we obtain the rectangular components $a_x$, $a_y$, $a_z$ of the vector **a**.

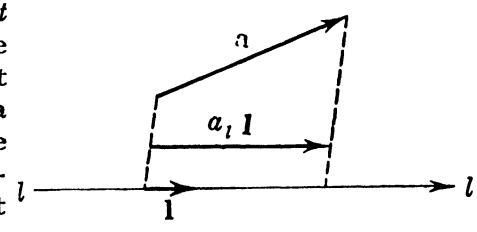



FIG. 4·05.

If $\epsilon$ is a scalar and **a** is a vector, the expression $\epsilon\mathbf{a}$ is used to represent a vector $\epsilon$ times as long as **a**, having the same direction if $\epsilon$ is positive, the opposite direction if $\epsilon$ is negative. In particular, if $\epsilon = -1$, then $\epsilon\mathbf{a} = -\mathbf{a}$ is a vector equal in magnitude to **a**, but having the opposite direction. If **A** is a unit vector in the direction of the vector **a**, then $\mathbf{a} = a\mathbf{A}$. It is important to note that the component $a_l$ is *not* a vector, but that $a_l\mathbf{l}$ *is* a vector.

Before we take up the discussion of the state of equilibrium, it is necessary to derive a few simple mathematical rules for vectors which will be needed in this discussion. The immediate need will be the expression for the resultant of the acting forces.

**4·06. Vector sum.** The resultant of two forces acting on the same particle is by physical definition a third force whose effect on the particle is identical to the joint effect of the two forces. Experiments show that when the two forces are represented by arrows (fig. 4·06*a*), their resultant is geometrically represented by the diagonal in the parallelogram

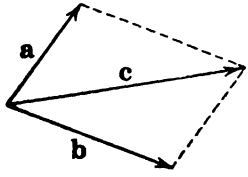



FIG. 4·06*a*.

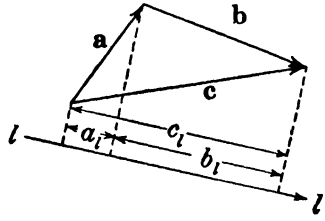



FIG. 4·06*b*.

defined by the two arrows. This *law of the parallelogram* is also valid for displacements, velocities, accelerations, etc., or more generally for all vectors.

The parallelogram is conveniently replaced by the triangle (fig. 4·06*b*) defined by the two vectors. Their resultant is the third side of this triangle. We shall introduce for the resultant $\mathbf{c}$ of the vectors $\mathbf{a}$ and $\mathbf{b}$ the notation

$$\mathbf{c} = \mathbf{a} + \mathbf{b}, \tag{1}$$

and call $\mathbf{c}$ the *vector sum* of the two vectors. Similarly the sum of three or more vectors is obtained by constructing a polygon of the vectors, and drawing a vector from the initial point of the first to the terminal point of the last. By inspecting this polygon it is easily verified that the commutative and associative laws are valid for vector addition.

If the polygon representing the sum of two or more vectors is closed, the vector sum is the *zero-vector*, denoted by $\mathbf{0}$. Thus the vector sum of $\mathbf{a}$ and $-\mathbf{a}$ is $\mathbf{0}$:

$$\mathbf{0} = \mathbf{a} - \mathbf{a}.$$

The zero-vector, being a vector of zero magnitude, should be distinguished from the scalar zero.

An important example of the vector sum is the representation of a vector $\mathbf{a}$ in a rectangular system of coordinates. The three unit vectors along the positive axes of $x$, $y$, $z$ will be denoted by $\mathbf{i}$, $\mathbf{j}$, $\mathbf{k}$. If the operation illustrated in fig. 4·05 is applied to the three axes of the system, we obtain the three vectors $a_x\mathbf{i}$, $a_y\mathbf{j}$, $a_z\mathbf{k}$. According to the above rule their sum is equal to the vector $\mathbf{a}$; hence

$$\mathbf{a} = a_x\mathbf{i} + a_y\mathbf{j} + a_z\mathbf{k}. \tag{2}$$

A similar expression may be derived for the vector **b**. When these expressions are introduced in (1), we obtain

$$\mathbf{c} = \mathbf{a} + \mathbf{b} = (a_x + b_x)\mathbf{i} + (a_y + b_y)\mathbf{j} + (a_z + b_z)\mathbf{k}. \tag{3}$$

The rectangular components of $\mathbf{a} + \mathbf{b}$ are obtained by adding corresponding components of **a** and **b**. This rule also follows directly from fig. 4·06*b*, by projecting the triangle upon an arbitrary straight line $l$ by planes normal to $l$.

**4·07. Scalar product.** Another important vector operation is exemplified by the element of work 2·14(1), where the two vectors in question are the force and the infinitesimal displacement. Let **a** and **b** be any

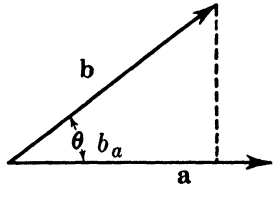



FIG. 4·07*a*.

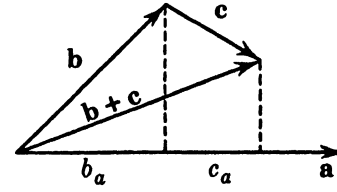



FIG. 4·07*b*.

two vectors, and let $\theta$ be the angle between them (fig. 4·07*a*). The scalar quantity $ab \cos\theta$ is defined as the *scalar product* or dot product of the two vectors, and is indicated by placing a dot between the factors. Hence by definition,

$$\mathbf{a}\cdot\mathbf{b} = ab \cos\theta = ab_a. \tag{1}$$

In the third expression we have used the notation $b_a$ for the component of **b** along **a**. *Thus the scalar product of two vectors is a scalar.* Obviously

$$\mathbf{a}\cdot\mathbf{b} = \mathbf{b}\cdot\mathbf{a};$$

i.e., scalar multiplication obeys the commutative law.

Let $b_a$ and $c_a$ be the components of **b** and **c** along **a**. From fig. 4·07*b* it is clear that $b_a + c_a$ is the component of $\mathbf{b} + \mathbf{c}$ along **a**. From the equation

$$a(b_a + c_a) = ab_a + ac_a \tag{2}$$

it follows by using the rule (1) on each term that

$$\mathbf{a}\cdot(\mathbf{b} + \mathbf{c}) = \mathbf{a}\cdot\mathbf{b} + \mathbf{a}\cdot\mathbf{c}. \tag{3}$$

This proves that the distributive law is valid for scalar multiplication.

If two vectors are parallel and have the same sense, $\cos\theta = 1$, and their scalar product is equal to the regular product of their lengths. If the

two vectors are perpendicular, $\cos\theta = 0$ and their scalar product is zero. Conversely, *if a scalar product is zero, one of the vectors is zero or else the two are perpendicular.*

Applying the definition (1) to the unit vectors **i**, **j**, **k**, we obtain

$$\begin{aligned} &\mathbf{i}\cdot\mathbf{i} = \mathbf{j}\cdot\mathbf{j} = \mathbf{k}\cdot\mathbf{k} = 1; \\ &\mathbf{i}\cdot\mathbf{j} = \mathbf{j}\cdot\mathbf{k} = \mathbf{k}\cdot\mathbf{i} = 0. \end{aligned} \tag{4}$$

To obtain another expression for $\mathbf{a}\cdot\mathbf{b}$, we first write **a** and **b** in component form, as in 4·06(2). Then, according to (3), we take the scalar product of each term of **a** with each term of **b**. Finally, applying (4), we see that

$$\mathbf{a}\cdot\mathbf{b} = a_x b_x + a_y b_y + a_z b_z = ab\cos\theta. \tag{5}$$

All three equivalent expressions in (5) for the scalar product are useful, according to the nature of the theoretical problem. We shall generally use the compact expression to the left, and only make use of the expanded forms in practical applications.

**4·08. Mechanical equilibrium.** A system is in mechanical equilibrium when the resultant of the forces acting upon it is equal to zero. Applied to the atmosphere, this principle can be formulated as follows: *The atmosphere is in equilibrium when for any arbitrary part of the atmosphere (not necessarily infinitesimal) the resultant of all the acting forces is zero.* There are two sets of forces to be considered in the atmosphere: the external forces acting upon the air elements from without, and the internal forces arising from the interaction between the air particles themselves. The only external force in the atmosphere is the force of *gravity*. In the case of equilibrium the only internal force is the *pressure force*. In order to formulate the equilibrium condition mathematically it is necessary to know the analytical expressions for these two forces.

**4·09. The force of gravity.** By the force of gravity we mean the force imparted by the earth to a unit mass which is at rest relative to the earth, i.e., which rotates with the earth. Since it is a force per unit mass, it has the dimensions $[LT^{-2}]$ of acceleration and indeed is sometimes called the acceleration of gravity. The force of gravity is a vector denoted by **g**, whose magnitude is therefore $g$.

If the earth had no rotation, the force of gravity would be identical to the force $\mathbf{g}_a$ of pure gravitational attraction, directed toward the center of the earth. The earth would be a perfect sphere whose gravity would have the same magnitude everywhere on its surface. According to Newton's law of universal gravitation, the magnitude $g_a$ of the *force of gravitation* on a unit mass situated at the distance $r$ from the earth's

center is $K/r^2$. Here $K$ is a constant fixed by the mass of the earth. See 6·08.

Since the earth is actually rotating, the force observed as gravity is the resultant of $\mathbf{g}_a$ and the *centrifugal force* arising from this rotation. (This will be discussed in more detail in section 6·10, in connection with motion relative to the earth.) The centrifugal force is directed outward,

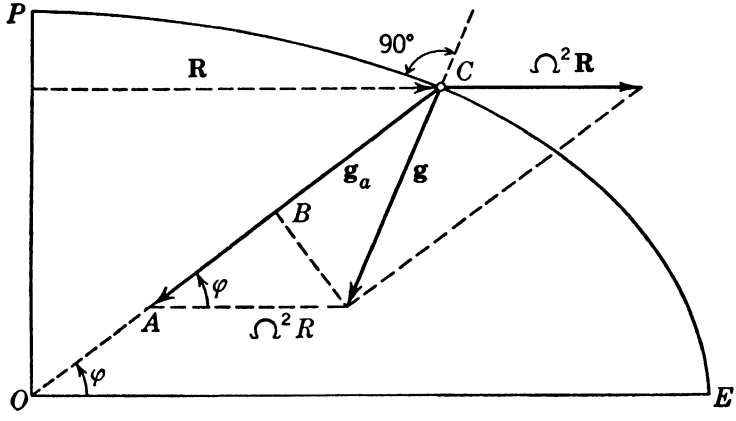



FIG. 4·09. The force of gravity.

normal to the axis of the earth. Its magnitude is numerically equal to $\Omega^2 R$, where $\Omega$ is the angular speed of the earth and $R$ is the distance from the axis. Let $\mathbf{R}$ be the vector from the axis of the earth, extending normal to the axis and ending on the point in question. Then the centrifugal force is $\Omega^2\mathbf{R}$. Fig. 4·09 is a schematic diagram of these forces in which the eccentricity of the earth has been exaggerated.

The force of gravity $\mathbf{g}$ is the vector sum of $\mathbf{g}_a$ and $\Omega^2\mathbf{R}$. It is important to note that the motion of the earth enters into the definition of gravity. Thus the equilibrium we are considering is no real equilibrium, but rather a state where the earth and the atmosphere rotate together as a rigid system. We shall call this state *relative equilibrium*. It will be explained in section 6·10 why this state can be investigated as though it were a real equilibrium.

At present we wish to derive an expression for the dependence of $g$ upon the latitude $\varphi$ and height $z$ above the surface of the earth. The angle between $\mathbf{g}_a$ and $\mathbf{g}$ is very small. Hence the magnitude of $\mathbf{g}$ can be closely approximated by subtracting from $g_a$ the length of the projection $AB$ of $\Omega^2\mathbf{R}$ on $\mathbf{g}_a$. But the length of $AB$ is equal to $\Omega^2 R \cos\varphi$. See fig. 4·09. Since $R = r\cos\varphi$, we can write

$$\text{(1)} \qquad \text{length of } AB = \Omega^2 r \cos^2\varphi.$$

As above, we have for the magnitude of $\mathbf{g}_a$:

$$g_a = \frac{K}{r^2}. \tag{2}$$

Subtracting (1) from (2), we get an approximate expression for the magnitude $g_\varphi$ of the force of gravity at latitude $\varphi$:

$$g_\varphi = \frac{K}{r^2} - \Omega^2 r \cos^2 \varphi. \tag{3}$$

Letting $g_{45}$ be the value of $g$ at 45° latitude, we have, from (3),

$$g_{45} = \frac{K}{r^2} - \tfrac{1}{2}\Omega^2 r. \tag{4}$$

Eliminating $K/r^2$ between (3) and (4), we find

$$g_\varphi = g_{45} - \tfrac{1}{2}\Omega^2 r \cos 2\varphi. \tag{5}$$

Now $r$ is approximately constant on the earth's surface. Hence the expression $\Omega^2 r$ is nearly constant, and (5) suggests that a formula for $g_\varphi$ should take the form

$$g_\varphi = g_{45}(1 - a_1 \cos 2\varphi) \qquad (a_1 = \text{const}). \tag{6}$$

To get an expression for the variation of gravity with elevation $z$, we fix our attention on the poles, where the centrifugal force vanishes. At the height $z$ above the pole, the distance from the center of the earth is $r + z$, whence from (3) the gravity $g_z$ becomes

$$g_z = \frac{K}{(r+z)^2}. \tag{8}$$

At the ground we have the value $g_0$ of gravity

$$g_0 = \frac{K}{r^2}. \tag{9}$$

Dividing (8) by (9), we get

$$\frac{g_z}{g_0} = \left(\frac{r}{r+z}\right)^2 = \left(1 + \frac{z}{r}\right)^{-2} = \left(1 - \frac{2}{r}z + \cdots\right).$$

Hence to a good approximation

$$\frac{g_z}{g_0} \approx \left(1 - \frac{2}{r}z\right). \tag{10}$$

Since $r$ is approximately constant, formula (10) suggests that a formula for $g_z$ at any height should take the form

$$g_z = g_0(1 - a_2 z) \qquad (a_2 = \text{const}). \tag{11}$$

Putting (6) and (11) together, we have a suggested type of formula for the value $g_{\varphi,z}$ of gravity at latitude $\varphi$ and elevation $z$:

$$g_{\varphi,z} = g_{45,0}(1 - a_1 \cos 2\varphi)(1 - a_2 z). \tag{12}$$

The actual best values of $a_1$ and $a_2$ in (12) can be found only by statistical methods, based on measurements of gravity. These measurements are obtained from pendulum experiments all over the earth, and they yield the formula

$$g_{\varphi,z} = 9.80617(1 - 0.00259 \cos 2\varphi)(1 - 3.14 \times 10^{-7} z), \tag{13}$$

where $z$ is the elevation in meters. The value of $a_2$ in (13) can be obtained from (10), but the value of $a_1$ is some 50% larger than that computable from (5).

Denoting the sea level value of gravity at the pole by $g_P$, and the value at the equator by $g_E$, we get approximately in m $s^{-2}$:

$$g_E = 9.78; \qquad g_{45} = 9.81; \qquad g_P = 9.83. \tag{14}$$

It is sufficient to remember these values for our later discussions.

Now that the physical nature of the force of gravity has been established, our next task will be to derive a suitable analytical expression for it. Equation (13) cannot be used for this purpose, since it gives no information about its direction. The first step toward the analytical expression is to find a geometrical representation of the force of gravity. A very simple and convenient representation is obtained by means of the geopotential.

**4·10. The field of geopotential.** Consider an isolated particle of unit mass moving through the field of gravity along an arbitrary path. Let $d\mathbf{r}$ be an infinitesimal vector displacement of length $ds$ along this path, and let $\theta$ be the angle between the force of gravity and $d\mathbf{r}$. The work $dw$ of gravity on the particle during this displacement is, according to 2·14(1) and 4·07(1),

$$dw = g\,ds \cos\theta = \mathbf{g}\cdot d\mathbf{r}. \tag{1}$$

The work is positive if the angle is acute, and negative for an obtuse angle. This work can, according to the principle of the conservation of mechanical energy (section 2·18), be provided only through some expenditure of energy. Since the particle is isolated and undergoes no physical changes during the motion, the energy must be stored in the particle as a consequence of its position in the gravitational field. This form of energy which is released whenever a particle moves in the field of gravity is called *potential energy*. Denoting the change in the poten-

tial energy of unit mass during its displacement $d\mathbf{r}$ by $d\phi$, the conservation of energy gives $dw + d\phi = 0$, which introduced in (1) gives

$$d\phi = -\mathbf{g}\cdot d\mathbf{r}. \tag{2}$$

We see that $d\phi$ is an *exact differential* (section 2·27) by letting the particle return to its initial position after having moved in an arbitrary closed path. The final state is then in every respect identical to the initial, and the conservation of mechanical energy requires that the total amount of energy gained during this motion is zero. Thus $\phi$ is a function only of the position in space, i.e., a function of the coordinates $x,y,z$. Hence

$$\phi = \phi(x,y,z). \tag{3}$$

We shall now introduce the letter $\delta$ to denote differentials which represent the *difference* in value of some physical variable between two points in space, the difference being computed at a fixed time. Differentials denoted with $\delta$ are called " geometrical differentials." We shall reserve the letter $d$ for differentials representing the *change* in value of some physical property of a particle during a process on that particle. Such a process will consume a certain amount of time $dt$, in contrast to the instantaneous nature of the geometrical differentials. Differentials denoted with $d$ are called " process differentials." As an example of the distinction made here, the thickness of a falling leaf would be $\delta z$, but the distance the leaf dropped during a certain time would be $dz$.

An example of the geometrical differential is the variation in $\phi$ between two points in space separated by a small distance. The distance is denoted by $\delta\mathbf{r}$, and the corresponding variation in $\phi$ is $\delta\phi$. We have from the above argument that

$$\delta\phi = -\mathbf{g}\cdot\delta\mathbf{r}. \tag{4}$$

Equation (4) refers to $\phi$ as a function of position in space; equation (2) refers to the change of potential energy of a moving particle. Since $\phi$ is a function only of position in space, $\delta\phi$ is according to section 2·27 an exact differential of the three variables $x,y,z$.

We notice that when the angle $\theta$ between $\mathbf{g}$ and $\delta\mathbf{r}$ is acute $\delta\phi$ is negative and the potential energy decreases in the direction of $\delta\mathbf{r}$; when $\theta$ is obtuse $\delta\phi$ is positive and the potential energy increases in this direction. For displacements normal to the force of gravity ($\theta = 90°$), $\delta\phi$ equals 0, so any such displacement is contained in a surface $\phi = \text{const}$. These surfaces, which are defined analytically by giving constant values to $\phi$ in (3), define the horizontal in each locality and are called *level surfaces*. To examine the variation in $\phi$ from level to level we consider a displacement in the direction opposite to gravity and hence normal to the level.

Denoting this displacement by $\delta z$ we have from (4), since $\cos\theta = -1$:

$$\delta\phi = g\delta z. \tag{5}$$

Thus the variation in $\phi$ is equal to $g$ per unit displacement normal to the level. Therefore if the potential energy is known at one level, its value can be computed for any other level by integration of (5). Let this known value at the reference level $z_0$ be $\phi_0$. Its value at any other level $z_1$ is then $\phi_1$, where

$$\phi_1 - \phi_0 = \int_{z_0}^{z_1} g\delta z. \tag{6}$$

We are never concerned with absolute values of energy, but only with its variations. Therefore we may choose our reference level as we please and give this level an arbitrary value of potential energy. The simplest choice is the surface of mean sea level as reference level. We shall assign to this level the potential energy value zero. Once this choice has been made, the potential energy throughout space is prescribed and is given at the elevation $z$ by the expression

$$\phi = \int_0^z g\delta z. \tag{7}$$

The integration is taken along a vertical from sea level to the point in question, i.e., along a path normal to the level surfaces. The integral is easily evaluated when the expression 4·09(13) for $g$ is introduced. To obtain the complete three-dimensional distribution of $\phi$ the integral must be computed for each latitude $\varphi$. The function in (3) may accordingly be considered a known function. Since this function is physically derived from the concept of potential energy in the field of gravity, it is known as the potential of gravity or the *geopotential*. We shall usually write it in the general form (3) and in our imagination represent this function by its surfaces for unit values of $\phi$.

These surfaces not only give a clear geometrical picture of the function $\phi$. They also can be used to define the *force of gravity*. Denoting the thickness of the unit layer by $h_\phi$, we have from (5), when the variation of $g$ through the layer is neglected,

$$g = \frac{\delta\phi}{\delta z} = \frac{1}{h_\phi}. \tag{8}$$

From this expression and the previous discussion we may formulate the following simple rule:

*The force of gravity is normal to the surfaces $\phi$ = const, is directed toward decreasing values of $\phi$, and its magnitude is equal to the reciprocal of the thickness of the unit layer of $\phi$.* The geopotential unit layers provide a convenient geometrical representation of the force of gravity. The corresponding analytical relation will give us the mathematical expression for this force. Before proceeding to derive this expression it will be useful to examine the distribution of the geopotential unit layers quantitatively.

**4·11. Dynamic height.** Geopotential was defined physically as the potential energy per unit mass. It is therefore measured in specific energy units (see table 1·05), and has the dimensions $[L^2T^{-2}]$. In the mts system this unit is 1 kilojoule per ton. We can therefore give 4·10(8) the following quantitative interpretation: When the level surfaces are drawn at intervals of 1 kilojoule per ton, the thickness of the layers is $h_\phi = 1/g$ meter, or approximately 1 decimeter. This means that if 1 ton of mass is lifted this vertical distance its potential energy increases by the amount of 1 kilojoule. We can therefore now obtain a clear quantitative picture of the distribution of the geopotential unit layers. The bottom layer has the mean sea level as its base, and its thickness is approximately 1 decimeter. The layer has its maximum thickness at the equator ($h_\phi$ = 1/9.78 meter $\approx$ 1.022 dm), and becomes gradually thinner toward the pole where it has its minimum thickness ($h_\phi$ = 1/9.83 meter $\approx$ 1.017 dm). The next layer follows on top of this, with practically the same thickness as the bottom layer in each latitude, and so on. For practical estimates it is sufficient to remember that the thickness of the geopotential unit layer is roughly 2% thicker than 1 decimeter and that its equatorial thickness is $\frac{1}{2}$% larger than its polar thickness.

Since the field of gravity is constant, the level surfaces are fixed surfaces in space, and can therefore be used as reference surfaces indicating the vertical distance between a point in space and sea level. This distance is uniquely determined by the value of the geopotential at the point, i.e., by the number of geopotential unit layers between the point and sea level. It is for this purpose convenient to introduce a terminology which is more suggestive of height than the energy expression kilojoule per ton. Since now the unit increase of geopotential roughly corresponds to a height of 1 decimeter, we are led to introduce for the geopotential unit the name *dynamic decimeter* (abbreviated dyn dm). We therefore have by definition

(1) $$1 \text{ kj } t^{-1} = 1 \text{ dyn dm}.$$

With the same terminology the geopotential of a unit mass at a point in space is referred to as the *dynamic height* of the point. When, for instance, a point has the dynamic height $\phi = 100$ dyn dm, this means both that its vertical distance above the ground is roughly 102 dm, and that the potential energy of 1 ton at this point is 100 kj. The dynamic decimeter has of course the dimensions $[L^2T^{-2}]$ of specific energy.

A measure in frequent use is the *dynamic meter* (abbreviated dyn m), defined by

(2) $$1 \text{ dyn m} = 10 \text{ dyn dm}.$$

The dynamic meter is thus approximately 2% longer than the true meter.

**4·12. Analytical expression for the force of gravity.** The expression for the force of gravity is derived from its relation to the geopotential. We return to 4·10(4), which defines the concept of geopotential. This equation has, from 4·07(5), the following alternative forms:

(1) $$-\delta\phi = g_x\delta x + g_y\delta y + g_z\delta z = \mathbf{g}\cdot\delta\mathbf{r}.$$

The geopotential is according to 4·10(3) a single-valued function. Its variation $\delta\phi$ from the point $(x,y,z)$ to the point $(x + \delta x, y + \delta y, z + \delta z)$ is

(2) $$\delta\phi = \frac{\partial\phi}{\partial x}\delta x + \frac{\partial\phi}{\partial y}\delta y + \frac{\partial\phi}{\partial z}\delta z = \delta\mathbf{r}\cdot\nabla\phi,$$

where $\delta\mathbf{r} = \mathbf{i}\delta x + \mathbf{j}\delta y + \mathbf{k}\delta z$. The expression in the middle is the scalar product of the vector $\delta\mathbf{r}$ and the vector $\mathbf{i}(\partial\phi/\partial x) + \mathbf{j}(\partial\phi/\partial y) + \mathbf{k}(\partial\phi/\partial z)$, whose rectangular components are the three partial derivatives of $\phi$. We introduce for this important vector the more convenient notation $\nabla\phi$ (read " del $\phi$ "). Hence by definition

(3) $$\nabla\phi = \mathbf{i}\frac{\partial\phi}{\partial x} + \mathbf{j}\frac{\partial\phi}{\partial y} + \mathbf{k}\frac{\partial\phi}{\partial z}.$$

This notation has already been introduced in the last expression on the right in (2). The expressions (1) and (2) are equal but opposite in sign. Hence, comparing the two scalar products, it follows that

$$\delta\mathbf{r}\cdot\mathbf{g} = -\delta\mathbf{r}\cdot\nabla\phi \quad \text{or} \quad \delta\mathbf{r}\cdot(\mathbf{g} + \nabla\phi) = 0.$$

Since their scalar product is zero, one of the two vectors $\delta\mathbf{r}$ and $(\mathbf{g} + \nabla\phi)$ must be zero, or else they are perpendicular. The vector $\delta\mathbf{r}$ is by definition different from zero, and its direction is arbitrary. The only possibility is then $\mathbf{g} + \nabla\phi = \mathbf{0}$, or

(4) $$\mathbf{g} = -\nabla\phi.$$

This is the analytical expression for the force of gravity.

The rectangular components of **g** are obtained by introducing in (4) the explicit form (3) of $\nabla\phi$. Since the coordinate system is arbitrary the component of **g** along an arbitrary direction $l$ is:

$$g_l = -\frac{\partial \phi}{\partial l}. \tag{5}$$

In the standard system defined in section 4·03 the $xy$ plane is tangential to the level surface. Therefore

$$g_x = 0; \quad g_y = 0; \quad g_z = -\frac{\partial \phi}{\partial z} = -g. \tag{6}$$

The analytical expression (4) and the geometrical connection between the force of gravity and the geopotential unit layers (section 4·10) are completely interrelated, and the nature of this relationship is entirely mathematical. The physical meaning of the vector **g** and the function $\phi$ is purely incidental. Any vector which is analytically defined by one single scalar function through an expression like (4) is geometrically related to the unit layers of the function in the same way. A vector of this kind is called a *potential vector*, and the corresponding scalar function is called the *potential* of the vector. It will be shown presently that the pressure force is a vector of this kind. Owing to their fundamental importance in atmospheric dynamics, the geometrical properties of these vectors should be well known. We shall therefore derive these properties once more without any reference to the special case of the field of gravity.

**4·13. Potential vector; ascendent; gradient.** Let $\varepsilon = \varepsilon(x,y,z)$ be any scalar function of the type discussed in section 4·04. This function may be represented by its unit layers, defined by the surfaces $\varepsilon = 0, 1, 2, \cdots$. The vector $\nabla\varepsilon$ which has the function $\varepsilon$ as its potential is defined by an equation similar to 4·12(2):

$$\delta\varepsilon = \delta\mathbf{r}\cdot\nabla\varepsilon = |\delta\mathbf{r}|\ |\nabla\varepsilon| \cos\theta. \tag{1}$$

By using the rules for the scalar product (section 4·07), we may derive the geometrical relation between the vector $\nabla\varepsilon$ and the unit layers of $\varepsilon$. The displacement $\delta\mathbf{r}$ is at our disposal and may be given an arbitrary direction in the field. If $\delta\mathbf{r}$ is chosen perpendicular to $\nabla\varepsilon$, their scalar product is zero. Hence from (1) $\delta\varepsilon = 0$; the displacement $\delta\mathbf{r}$ is in a direction where the function $\varepsilon$ has no changes, i.e., in a surface $\varepsilon = \text{const.}$ *The vector $\nabla\varepsilon$ is therefore directed normal to the equiscalar surfaces.* To investigate its sense we shall give the displacement $\delta\mathbf{r}$ the same direction as the vector $\nabla\varepsilon$. Denoting the magnitude of this displacement with

$\delta n$, it follows from (1), since $\cos\theta = 1$ for this displacement, that

$$\delta\varepsilon = \delta n|\nabla\varepsilon|. \tag{2}$$

The quantities on the right are the numerical values of the two vectors, and their product is therefore a positive quantity. The variation $\delta\varepsilon$ in the direction of $\nabla\varepsilon$ is thus a positive quantity; in other words *the vector $\nabla\varepsilon$ is directed toward increasing values of its potential.* Its magnitude as obtained from (2) is

$$|\nabla\varepsilon| = \frac{\delta\varepsilon}{\delta n} = \frac{1}{h_\varepsilon}, \tag{3}$$

where $h_\varepsilon$ denotes the thickness of the unit layer. The geometrical relation between the vector $\nabla\varepsilon$ and the function $\varepsilon$ is thus identical to the relation derived in section 4·10 between gravity and geopotential, except for the sign. The vector $\nabla\varepsilon$ is known as the *ascendent* of the function $\varepsilon$; the opposite vector $-\nabla\varepsilon$ is called the *gradient* of $\varepsilon$. The former is the mathematically convenient vector, whereas the latter generally is the physically important vector. With this new terminology the force of gravity is the geopotential gradient, which is a vector normal to the level surfaces, directed toward decreasing geopotential, and numerically equal to the reciprocal of the thickness of the geopotential unit layer.

**4·14. The pressure field in equilibrium.** The force which balances the force of gravity and thus determines the state of equilibrium is the so-called *pressure force*, arising from the interaction between the air particles. It will be shown that there exists a relation between this force and the pressure field similar to that connecting the force of gravity and the geopotential field.

To investigate the pressure field in equilibrium we shall apply the principle mentioned in section 4·08 to certain selected parts of the fluid, defined by closed boundaries, which in each case will be specified. In all cases the pressure forces in the interior of the selected part will appear in pairs, and hence give no contribution to the resultant. The only pressure forces left are those acting on the surface which encloses the fluid part. If the pressure at a certain point in this surface is $p$, the pressure force on an infinitesimal element $\delta A$ of the surface has, according to the definition 1·03(13), the magnitude $p\delta A$ and is directed normal to the surface element. As stated in 2·04, the pressure at a point is independent of the orientation of the surface element on which it acts. Therefore, although defined as a force per unit area, it can at each point in space be expressed by a single numerical value. Thus pressure is a scalar quantity.

To find the distribution of pressure, we apply the equilibrium condition to a thin cylindric fluid element situated with its axis in a level surface (fig. 4·14*a*). The end faces of the cylinder are normal cross sections with area $\delta A$. Since the resultant of the forces acting upon this

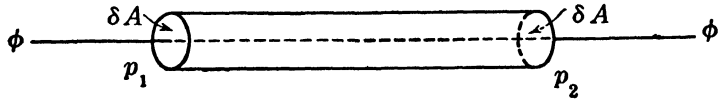



FIG. 4·14*a*.

fluid element is zero, its component along the axis of the cylinder is also zero. The force of gravity has no component in this direction, and neither have the pressure forces acting on the side wall. There remain only the pressure forces on the two end faces. Hence

$$p_1\delta A - p_2\delta A = 0 \quad \text{or} \quad p_1 = p_2. \tag{6}$$

This holds regardless of the length or orientation of the cylinder; *consequently any equipotential surface* is also a surface $p = \text{const}$, an *isobaric surface.*

In order to study the variation in pressure from level to level, we consider a cylindric fluid element whose axis is normal to the levels, and whose base and top are contained in two levels with the respective geopotential values $\phi$ and $\phi + \delta\phi$ (fig. 4·14*b*). It has just been shown that these levels also are isobaric surfaces defining certain definite pressure values $p$ and $p + \delta p$. We shall apply the equilibrium principle to this cylindric element and find the component of the resultant force along the axis. Let the mass of the cylinder be $\delta M$. The force of gravity contributes to this component with its full amount $g\delta M$. The pressure forces acting upon the side wall of the cylinder have no component along the axis, whereas the pressure forces on the top and bottom faces contribute with their full amount. Let $\delta z$ be the height of the cylinder and $\delta A$ its cross-section area. Its volume $\delta V$ and its mass $\delta M$ are then

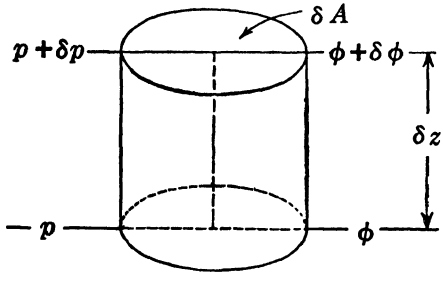



FIG. 4·14*b*.

$$\delta V = \delta A\,\delta z, \qquad \delta M = \rho\delta V. \tag{7}$$

Using the expression 4·10(8) for $g$ and choosing the positive direction along the axis upward, we have for the component of the resultant force

along this direction

$$-\left(\frac{\delta\phi}{\delta z}\right)\rho\delta V-(p+\delta p)\delta A+p\delta A=-\rho\left(\frac{\delta\phi}{\delta z}\right)\delta V-\delta p\delta A.$$

The equilibrium principle requires that the resultant be zero. Thus, when we introduce $\delta A=\delta V/\delta z$ in the last term, we have

$$-\rho\left(\frac{\delta\phi}{\delta z}\right)\delta V-\left(\frac{\delta p}{\delta z}\right)\delta V=0. \tag{8}$$

This equation can be used directly to discuss the distribution of pressure and mass in equilibrium. Before this discussion is taken up, the equation will be used to derive the analytical expression for the resultant pressure force upon the cylindric element.

**4·15. The pressure gradient.** The first term on the left in 4·14(8) is the *total* resultant of gravity acting upon the cylindric element. The total resultant of gravity is balanced by the total resultant of the pressure forces upon the boundary enclosing the element. It follows therefore that the resultant pressure force is directed upward, so the pressure on the bottom face of the cylinder is greater than the pressure on the top face. In other words $\delta p$ is a negative quantity, and the pressure decreases upward. The resultant pressure force is thus a vector normal to the isobaric surfaces and directed toward decreasing pressure. Its magnitude is given by the second term on the left in 4·14(8). Since this is the pressure force on an element which has the volume $\delta V$, the magnitude of the pressure force per unit volume is

$$\left|\frac{\delta p}{\delta z}\right|=\frac{1}{h_p}, \tag{1}$$

where $h_p$ denotes the thickness of the isobaric unit layer. According to the discussion in section 4·13 the pressure force per unit volume is therefore a potential vector, whose potential is the pressure. Since it is directed toward decreasing pressure, *the pressure force per unit volume is the gradient of the pressure*, or simply the *pressure gradient*. Using the notation of section 4·13 we can therefore write:

$$\text{the pressure force per unit volume} = -\nabla p. \tag{2}$$

The expression (2) for the pressure force has been derived here for the state of equilibrium. However, this expression is completely determined by the pressure field and is thus entirely independent of the field of gravity, or of the simple relation between the two fields in the state of equilibrium. We may thus conclude that the expression (2) for the

pressure force is valid for any state of motion of the fluid. This statement can be proved rigorously by more advanced mathematical methods. We will, however, accept it here on the strength of the physical evidence and use the expression (2) when the equation of motion is derived.

The rectangular components of the pressure force are obtained by introducing in (2) the explicit form of $\nabla p$ from 4·12(3):

$$-\nabla p = -\mathbf{i}\frac{\partial p}{\partial x} - \mathbf{j}\frac{\partial p}{\partial y} - \mathbf{k}\frac{\partial p}{\partial z}. \tag{3}$$

Since the system $(x,y,z)$ is arbitrary, we conclude that the component of $-\nabla p$ along an arbitrary direction $l$ defined by the unit vector $\mathbf{l}$ is

$$(-\nabla p)_l = -\mathbf{l}\cdot\nabla p = -\frac{\partial p}{\partial l}. \tag{4}$$

In practical problems we shall generally want to distinguish between the vertical component $-(\partial p/\partial z)\mathbf{k}$ and the horizontal component

$$-\nabla_H p = -\mathbf{i}\frac{\partial p}{\partial x} - \mathbf{j}\frac{\partial p}{\partial y} \tag{5}$$

of the pressure gradient. We have accordingly

$$-\nabla p = -\nabla_H p - \mathbf{k}\frac{\partial p}{\partial z}. \tag{6}$$

Since the vector $-\nabla p$ is normal to the isobaric surface, the horizontal vector $-\nabla_H p$ is normal to the lines of intersection between the isobaric surfaces and the level. These lines are the horizontal isobars in the constant-level maps. If $\delta n_H$ is an infinitesimal horizontal distance normal to the isobars, and $h_{pH}$ is the normal distance between unit isobars, it follows from (4)

$$\left|\nabla_H p\right| = \frac{\delta p}{\delta n_H} = \frac{1}{h_{pH}}. \tag{7}$$

Thus the two-dimensional relation (7) between the horizontal pressure gradient and the *isobaric unit channels* in a level surface corresponds to the three-dimensional relation (1) between the pressure gradient and the isobaric unit layers. In mts units (7) has the following meaning: If the normal distance between two isobars with a pressure difference of 1 cb (10 mb) is $h_{pH}$ m, the horizontal pressure force per cubic meter is $1/h_{pH}$ mts units of force.

**4·16. The hydrostatic equation.** From the expressions for the two forces which act upon the atmospheric elements the equation of relative

equilibrium can be written down directly. Consider an infinitesimal element of air which has the mass $\delta M$ and the volume $\delta V$. From 4·12(4) the force of gravity on the element $\delta M$ is $-\delta M \nabla\phi$. From 4·15(2) the force of pressure per unit volume is $-\nabla p$, and therefore the pressure force on the volume $\delta V$ is $-\delta V \nabla p$. In equilibrium the resultant of these forces is zero; hence

$$0 = -\delta M \nabla\phi - \delta V \nabla p. \tag{1}$$

This equation may be referred to unit mass by dividing it by $\delta M$, or to unit volume by dividing by $\delta V$. Thus we obtain the *equation of relative equilibrium* in two equivalent forms

$$0 = -\nabla\phi - \alpha\nabla p; \qquad 0 = -\rho\nabla\phi - \nabla p. \tag{2}$$

These equations are valid for every air element in a resting atmosphere. For the further discussion of the hydrostatic state the vector equations (2) are most conveniently transformed into scalar equations. For this purpose we consider an arbitrary infinitesimal displacement $\delta\mathbf{r}$. The corresponding variations of geopotential and pressure are, according to 4·13(1),

$$\delta\phi = \delta\mathbf{r}\cdot\nabla\phi; \qquad \delta p = \delta\mathbf{r}\cdot\nabla p.$$

Thus by performing scalar multiplication of the two vectors in (2) by the line element $\delta\mathbf{r}$ we obtain

$$\delta\phi = -\alpha\delta p; \qquad \delta p = -\rho\delta\phi. \tag{3}$$

The second equation in (3) could incidentally have been derived directly from 4·14(8) by dividing out the two common factors $\delta V$ and $\delta z$. It will be shown presently that either of the equations (3) gives a complete dynamical description of equilibrium, and therefore both are equivalent forms of what is known as the *hydrostatic equation*.

It was shown in section 4·14 that the isobaric surfaces coincide with the level surfaces in equilibrium. This fact is expressed mathematically by the equations (2), since the two gradient vectors are normal to their respective equiscalar surfaces. A geopotential layer of the dynamic thickness $\delta\phi$ will thus define an isobaric layer through which the pressure varies by the amount $\delta p$, so the variations $\delta\phi$ and $\delta p$ are characteristic for the whole layer. It follows then from (3) that the mass variables

$$\alpha = -\frac{\delta\phi}{\delta p} \quad \text{and} \quad \rho = -\frac{\delta p}{\delta\phi} \tag{4}$$

are constants throughout the layer. If the layer is of finite thickness, these equations define certain mean values of $\alpha$ and $\rho$ within the layer. For an infinitesimal layer ($\delta\phi \to 0$) the equations (4) give the values of $\alpha$

and $\rho$ on the level surface, and these values are constant on the level. Thus in the state of equilibrium the isosteric and the isopycnic surfaces also coincide with the level surfaces, and we can formulate the following important rule: *The state of equilibrium is characterized by complete coincidence between the surfaces of constant pressure and constant mass, both sets of surfaces being horizontal throughout the atmosphere.*

After the discussion of motion is taken up, it will be shown that certain states of *motion* are also characterized by the coincidence between the surfaces of constant pressure and constant mass. (However, only in the hydrostatic state are they also horizontal.) Whenever the state of the atmosphere is such that the isosteric surfaces coincide with the isobaric surfaces, the mass field is said to be *barotropic* (meaning: directed in accordance with the pressure field). In general the terminology is further simplified by omitting " the mass field," and thus the atmosphere itself is said to be barotropic when the above condition exists. In the usual case, where the isosteric surfaces intersect the isobaric surfaces, the atmosphere is said to be *baroclinic*. With this terminology we have the rule: *In the state of equilibrium the atmosphere is barotropic.*

The equations (2) can be given a simple geometrical interpretation by means of the unit layers, here given only for the first equation. Both vectors are numerically equal to the reciprocal of the thickness of their respective unit layers, by 4·13(3), so that

$$\frac{1}{h_\phi} = \alpha\left(\frac{1}{h_p}\right), \quad \text{or} \quad h_p = \alpha h_\phi. \tag{5}$$

Thus the isobaric unit layer contains $\alpha$ geopotential unit layers. Explicitly in mts units this rule may be expressed as follows: *An isobaric layer of 1 centibar has a dynamic thickness of $\alpha$ dynamic decimeters.* (If the variation of specific volume through the layer is appreciable, the mean value of $\alpha$ in the layer must be taken.)

To get a rough idea of the order of magnitude of this thickness, consider a layer of dry air next to the ground, whose temperature at the 100-cb level is 273°K. The corresponding value of $\alpha$ from the equation of state 2·09(1) is $287 \cdot 273/100 = 784$ m$^3$ t$^{-1}$. If the specific volume has this constant value throughout the isobaric unit layer 100–99 cb, the thickness of this layer is 784 dyn dm or approximately 800 dm. This gives the approximate rule that near the ground an increase in height of 80 m corresponds to a pressure drop of about 10 mb, or *8 m to a drop of 1 mb.*

By a *homogeneous atmosphere* is meant an atmosphere of constant density (and hence constant specific volume). If the above value $\alpha = 784$ m$^3$ t$^{-1}$ prevailed throughout the atmosphere, the pressure at the

height of 8000 m would be 1000 mb less than at the ground, or practically zero. Thus the height of a homogeneous atmosphere whose pressure and temperature at sea level are 100 cb, 273°K is approximately 8000 m.

**4·17. Distribution of pressure and mass in equilibrium.** It was shown in the preceding section that the mass field is barotropic in equilibrium, and that the equiscalar surfaces of mass and pressure are both horizontal. The distribution of pressure and mass is known throughout the atmosphere if it is known along one single vertical. The distribution along a vertical is obtained by integration of the equations 4·16(3), yielding

$$(1) \qquad \phi_b - \phi_a = -\int_a^b \alpha \delta p; \qquad p_b - p_a = -\int_a^b \rho \delta \phi.$$

The second of the equations (1) has mainly theoretical interest. It reveals the physical cause or origin of atmospheric pressure. By 4·10(5) we substitute $\delta\phi = g\delta z$ and have

$$(2) \qquad p_b - p_a = -\int_a^b \rho g \delta z.$$

Now $\rho g \delta z$ is the weight of an air column of unit cross section and height $\delta z$. Thus (2) says that the pressure difference between any two levels $a$ and $b$ is the weight $\int_a^b \rho g \delta z$ of the column of air of unit cross section extending between the two levels. Hence *the pressure at any level is the total weight of a vertical column of unit cross section extending from this level to the top of the atmosphere.* This is a principle to remember in all meteorological work.

The first equation (1) is known as the *barometric height formula.* It solves the fundamental problem of hydrostatics referred to at the beginning of the chapter — to determine the dynamic heights which correspond to the various pressure values along an aerological ascent. Most of the remainder of this chapter will be devoted to a discussion of this equation.

The aerological sounding gives simultaneous values of pressure, temperature, and relative humidity. According to sections 3·21 and 3·23, from these data we can obtain the mixing ratio $w$. Thus for every point along the ascent we have the values of $p$, $T$, $w$. The corresponding value of $\alpha$ is found from the equation of state for moist air 3·25(5):

$$(3) \qquad \alpha = \frac{R_d T^*}{p},$$

where $T^*$ is the virtual temperature 3·25(4), and $R_d$ is the specific gas constant for dry air. When this expression for $\alpha$ is introduced in (1), the integrand becomes $-R_dT^*\delta p/p = -R_dT^*\delta(\ln p)$. Then (1) takes the form

$$\phi_b - \phi_a = -R_d \int_a^b T^*\delta(\ln p), \tag{4}$$

which is the barometric height formula adapted for practical use.

Several graphical methods can be used to evaluate the dynamic height from formula (4) when simultaneous values of pressure and virtual temperature are known along a vertical. Before discussing these methods it is useful to investigate the state of equilibrium when the virtual temperature is a linear function of the geopotential. This simple temperature distribution is not only of great theoretical interest, but it also serves as a useful approximation of real atmospheric conditions.

**4·18. The atmosphere with constant lapse rate.** It is evident from 4·17(4) that in hydrostatic problems the moist air may be treated as though it were dry air by replacing the real temperature by the virtual temperature. (This is one of the great advantages of virtual temperature.) We shall systematically use virtual temperature in this chapter. In the special case of a dry atmosphere the virtual temperature automatically becomes the real temperature.

By combining 4·16(3) and 4·17(3) the hydrostatic equation takes the form

$$\delta\phi = -R_dT^*\frac{\delta p}{p}. \tag{1}$$

To integrate this equation the distribution of virtual temperature must be known, either as a function of pressure or as a function of the dynamic height $\phi$. The integration is particularly simple when $T^*$ is a linear function of $\phi$.

We define the *lapse rate of virtual temperature* $\gamma^*$ at any point in the atmosphere by the equation

$$\gamma^* = -\frac{\delta T^*}{\delta\phi}. \tag{2}$$

Thus $\gamma^*$ has the dimensions $[\Theta L^{-2}T^2]$, and in mts units is measured in *degrees per dynamic decimeter.* To say that $T^*$ is a linear function of $\phi$ is equivalent to saying that $\gamma^*$ is a constant or that the atmosphere has a *constant lapse rate* (of virtual temperature).

We shall now determine the relations between $T^*$, $p$, and $\phi$ when the

lapse rate has the constant value $\gamma^*$. We shall assume for the present that $\gamma^* > 0$, i.e., that temperature decreases with height. We denote the arbitrary initial conditions at sea level by the notations:

$$T^* = T_0^*; \qquad p = p_0; \qquad \phi = 0. \tag{3}$$

Integration of (2) with the initial condition (3) gives

$$T^* = T_0^* - \gamma^* \phi \quad \text{or} \quad \frac{T^*}{T_0^*} = 1 - \frac{\gamma^* \phi}{T_0^*}. \tag{4}$$

When $\delta\phi$ is eliminated between (1) and (2), we get

$$\frac{\delta T^*}{T^*} = R_d \gamma^* \frac{\delta p}{p}. \tag{5}$$

Integrating (5) with the initial condition (3), we have finally

$$\frac{T^*}{T_0^*} = \left(\frac{p}{p_0}\right)^{R_d \gamma^*}. \tag{6}$$

From (2) and (6) we obtain the following important rule: *When, in the state of equilibrium, the virtual temperature is a linear function of the geopotential with the constant lapse rate $\gamma^*$, it is also proportional to the power $R_d\gamma^*$ of the pressure.*

Elimination of $T^*/T_0^*$ between (4) and (6) gives

$$p = p_0 \left[1 - \frac{\gamma^*}{T_0^*} \phi\right]^{\frac{1}{R_d \gamma^*}}. \tag{7}$$

Equations (4, 6, 7) summarize the relations between $T^*$, $p$, and $\phi$. We note from (4) and (7) that both $p$ and $T^*$ vanish at the level

$$\phi_l = \frac{T_0^*}{\gamma^*}. \tag{8}$$

This level $\phi_l$ is called the *dynamic height of the atmosphere of constant lapse rate.* For $\phi > \phi_l$ there is no more air. We note that $\phi_l$ depends only on $T_0^*$ and $\gamma^*$.

When $\gamma^*$ is given certain particular values, we obtain three important special cases to be discussed in the next three sections.

**4·19. The homogeneous atmosphere.** When $\gamma^*$ is given the special value $1/R_d$, then $R_d\gamma^* = 1$, and the formula 4·18(5) becomes

$$\frac{\delta T^*}{T^*} = \frac{\delta p}{p}. \tag{1}$$

If we differentiate logarithmically the equation of state 3·25(5),

$p\alpha = R_d T^*$, we get

$$\frac{\delta T^*}{T^*} = \frac{\delta p}{p} + \frac{\delta \alpha}{\alpha}. \tag{2}$$

Comparing (1) and (2), we see that in the present case $\delta\alpha = 0$, or $\alpha = \text{const}$. Thus when $\gamma^* = 1/R_d$ we are dealing with a homogeneous atmosphere (defined in 4·16). Conversely, for a homogeneous atmosphere,

$$\gamma^* = \gamma_h = \frac{1}{R_d} = 0.00348 \text{ deg (dyn dm)}^{-1}, \tag{3}$$

amounting to a temperature drop of about 35°C per dynamic kilometer.

For a homogeneous atmosphere the equations 4·18(4, 6, 7) simplify to

$$T^* = T_0^* - \frac{\phi}{R_d}; \quad \frac{T^*}{T_0^*} = \frac{p}{p_0}; \quad p = p_0\left(1 - \frac{\phi}{R_d T_0^*}\right). \tag{4}$$

The dynamic height $\phi_h$ of the homogeneous atmosphere is obtained from either (4) or 4·18(8):

$$\phi_h = R_d T_0^*. \tag{5}$$

(This formula could have been obtained immediately by integrating 4·17(1) for $\alpha = \text{const}$, and using the equation of state.) In the special case $T_0^* = 273°\text{K}$, $\phi_h = 78{,}351$ dyn dm ($\approx 8000$ m, as shown at the end of 4·16).

In the real atmosphere the lapse rate never is as large as $\gamma_h$, except possibly in thin layers near the ground. The reason is that such an atmosphere would be too unstable, as will be shown in chapter 5. Still, the homogeneous atmosphere is a useful concept for theoretical discussion.

When $\gamma^* > 1/R_d$, the density increases with height, giving even stronger instability than for the isosteric mass distribution just considered. When $\gamma^*$ decreases from $1/R_d$, one gradually approaches conditions similar to those generally encountered in the real atmosphere. Another ideal case is the following.

**4·20. The dry-adiabatic atmosphere.** When $\gamma^*$ is given the special value $1/c_{pd}$, then $R_d\gamma^* = R_d/c_{pd} = \kappa_d$, and 4·18(6) takes the form

$$T^* = T_0^*\left(\frac{p}{p_0}\right)^{\kappa_d}. \tag{1}$$

By substituting this expression for $T^*$ in 3·28(1), we see that the virtual

potential temperature $\theta^*$ at all levels is given by

$$\theta^* = T_0^* \left(\frac{100}{p_0}\right)^{\kappa_d} = \text{const.} \tag{2}$$

Thus an atmosphere with $\gamma^* = 1/c_{pd}$ is characterized by constant virtual potential temperature, meaning that all points $(T^*,p)$ lie on the same dry adiabat. From this property such an atmosphere is called a *dry-adiabatic atmosphere.* It has the lapse rate

$$\gamma^* = \gamma_d = \frac{1}{c_{pd}} = 0.000996 \text{ deg (dyn dm)}^{-1}, \tag{3}$$

amounting to a temperature drop of about 10°C per dynamic kilometer.

For a dry-adiabatic atmosphere, the equations 4·18(4, 6, 7) take the form:

$$T^* = T_0^* - \frac{\phi}{c_{pd}}; \quad \frac{T^*}{T_0^*} = \left(\frac{p}{p_0}\right)^{\kappa_d}; \quad p = p_0 \left(1 - \frac{\phi}{c_{pd} T_0^*}\right)^{\frac{1}{\kappa_d}}. \tag{4}$$

The dynamic height $\phi_d$ of the dry-adiabatic atmosphere is obtained from either (4) or 4·18(8):

$$\phi_d = c_{pd} T_0^*. \tag{5}$$

In the special case $T_0^* = 273$°K, $\phi_d = 274{,}100$ dyn dm, or almost 28,000 m.

When in the dry-adiabatic atmosphere the virtual temperatures at the levels $\phi_a$ and $\phi_b$ are respectively $T_a^*$ and $T_b^*$, we have from the first equation (4):

$$\phi_b - \phi_a = c_{pd}(T_a^* - T_b^*) = 1004(T_a^* - T_b^*). \tag{6}$$

It will be shown in 4·24 how this formula permits a quick evaluation of height when little accuracy is required.

The transition from the homogeneous to the dry-adiabatic atmosphere corresponds to the decrease of $\gamma^*$ from approximately 0.0035 to approximately 0.0010, with a corresponding increase of the top of the atmosphere from near 8 km to nearly 28 km. When $\gamma^*$ is decreased to 0, it is evident from 4·18(8) that the height of the atmosphere becomes infinite. This limiting case is discussed next.

**4·21. The isothermal atmosphere.** When $\gamma^* = 0$, we have immediately from 4·18(2) that $T^*$ has the constant value $T_0^*$ throughout, so the atmosphere is *isothermal.* In this case the integrations of 4·18 no longer remain valid. However, we can in this case integrate 4·17(4) directly, obtaining

$$\phi = -R_d T_0^* \ln \frac{p}{p_0}. \tag{1}$$

Solving for $p$, we get

$$p = p_0 e^{-\phi/RT_0^*}. \tag{2}$$

Thus the pressure decreases exponentially upward, but never vanishes. This verifies the statement that the upper limit of the isothermal atmosphere is at infinity.

When in the atmosphere the virtual temperature between the levels $\phi_a$ and $\phi_b$ has the constant value $T_m^*$, we have from (1) that

$$\phi_b - \phi_a = R_d T_m^* \ln \frac{p_a}{p_b}. \tag{3}$$

It will be shown in 4·24 how this formula is used for the accurate evaluation of height.

The real atmospheric distribution of pressure and virtual temperature is rather complex and variable. However, within a thin layer the lapse rate may always be treated with good approximation as constant. Such a thin layer may therefore be considered as part of an atmosphere of constant lapse rate.

**4·22. Atmospheric soundings.** An aerological sounding provides, as stated in 4·17, a set of simultaneous values of $T^*$ and $p$. These values can be plotted on any thermodynamic diagram of chapter 2. The points are customarily joined with straight lines, and the result is a polygonal curve representing a vertical column of the atmosphere. The curve is briefly called the (*virtual temperature*) *sounding*.

The sounding should be distinguished from the *process curves* so far discussed on the diagram (for example, the adiabats). The process curves represent the change in the physical properties of one parcel of air during a process in which the parcel changes its state. These were much discussed in chapter 2. The sounding is an instantaneous picture of the state of a whole geometrical column of air. The distinction is analogous to that made in section 4·10 between the differentials $\delta$ and $d$. A small variation of pressure on a sounding would be $\delta p$; a small change of pressure during a process would be $dp$.

**4·23. Graphical representation of dynamic height.** We shall now return to the practical problem of evaluating the dynamic height when a sounding is presented. The theoretical basis for this evaluation is the barometric height formula 4·17(4), which we repeat here in slightly modified form:

$$\phi_b - \phi_a = R_d \int_a^b T^* \delta(-\ln p). \tag{1}$$

This has a simple graphical representation on the emagram. Let the virtual temperature sounding between the levels $a$ and $b$ be plotted on an emagram. Let $A$ denote the area bounded by the sounding, the isobar $p = p_a$, the isobar $p = p_b$, and the isotherm $T = 0°K$. See fig. 4·23. Since the emagram is a graph of $-\ln p$ against $T$, the area $A$ is given by

$$A = \int_a^b T^* \delta(-\ln p), \tag{2}$$

just as an analogous formula, 2·32(3), held for the process curves of chapter 2. (The boundary of $A$ in (2) is *not* a process curve, and the area $A$ is *not* to be thought of as work or heat.) Combining (1) with (2), we see that $\phi_b - \phi_a = R_d A$. Thus the dynamic thickness of any layer in the atmosphere is proportional to the area $A$ of fig. 4·23.

Any diagram with the property (iii) of 2·32 is (up to a factor of proportionality) an area-preserving transformation of the emagram. This includes the tephigram, the $(\alpha, -p)$-diagram, and certain other diagrams — *not* however including the Stüve diagram. Hence for any of these included diagrams we have the following rule: *The dynamic height between the pressure levels a and b is (up to a proportionality factor fixed by the diagram) equal to the area enclosed by the virtual temperature sounding, the isobar $p = p_a$, the isobar $p = p_b$, and the isotherm $T = 0$.*

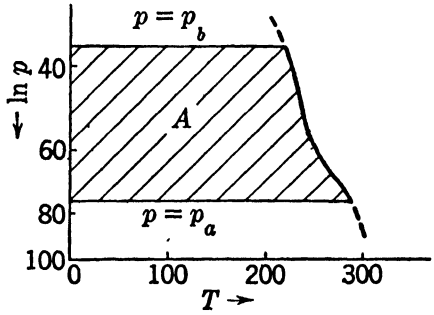


FIG. 4·23. Dynamic height on emagram.

Fig. 4·23 demonstrates how the dynamic thickness depends on the sounding. The warmer the sounding, the thicker must be a given isobaric layer, since the sounding encloses a larger area. This is physically obvious. The warmer air is less dense, and it takes a longer unit column between levels $a$ and $b$ to build up the weight of air which, according to 4·17, is responsible for the given pressure difference $p_a - p_b$. The same fact may be seen from 4·16(5), according to which the thickness of an isobaric layer is directly proportional to its specific volume.

**4·24. Adiabatic and isothermal layers.** According to the rule of 4·23, two different soundings between the pressure levels $a$ and $b$ will have the same dynamic thickness whenever they have equal areas $A$. To evaluate the thickness of an arbitrary layer, we replace the real

sounding between $a$ and $b$ by a fictitious sounding which has an equal area. We give the fictitious sounding such a temperature distribution that its dynamic thickness is easy to evaluate. In practice either *dry-adiabatic* or *isothermal* layers are chosen, since their evaluation was shown in 4·20 and 4·21 to be simple. Both give useful methods for the evaluation of height.

*a. Determination of height by dry-adiabatic layers.* The real virtual temperature sounding between the levels $a$ and $b$ is represented by the heavy curve in fig. 4·24*a*. It defines an area $A$ like that shaded in fig. 4·23. Each adiabat between the levels $a$ and $b$ defines a certain area $A'$ of the same type. In order to make $A'$ equal $A$, we choose the adiabat for which the areas $A_1$ and $A_2$ in fig. 4·24*a* are equal. This is easily estimated by the eye. Then the fictitious dry-adiabatic layer between the levels $a$ and $b$ is equivalent in dynamic thickness to the real layer.

According to 4·20(6), the dynamic thickness of the dry-adiabatic layer is given by

$$\phi_b - \phi_a = 1004(T_a^* - T_b^*) \qquad \text{(in dyn dm)}. \tag{1}$$

Here $T_a^*$ and $T_b^*$ are the virtual temperatures where the dry adiabat crosses the isobars $p = p_a$ and $p = p_b$, respectively. See fig. 4·24*a*. In

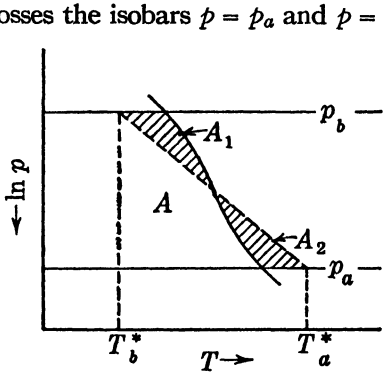



FIG. 4·24*a*. Equivalent adiabatic layer.

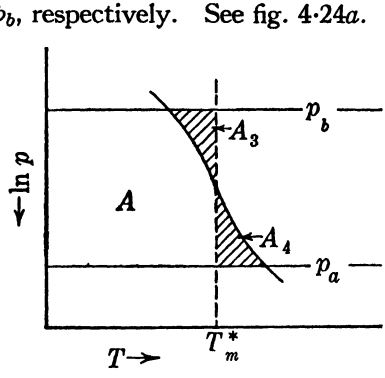



FIG. 4·24*b*. Equivalent isothermal layer.

practical work heights are generally measured in dynamic meters. Using the symbol $H$ for dynamic height measured in dynamic meters, we have the following approximate formula for the dynamic thickness:

$$H_b - H_a \approx 100(T_a^* - T_b^*) \qquad \text{(in dyn m)}. \tag{2}$$

Formula (2), first suggested by Stüve, is very convenient for rapid work when only approximate values are needed. Each 0.1°C error in reading $T_a^*$ or $T_b^*$ yields an error of 10 dyn m in $H_b - H_a$. For accurate height

evaluation a second method based on the isothermal layer is therefore needed.

*b. Determination of height by isothermal layers.* The real virtual temperature sounding between the levels $a$ and $b$ is represented by the heavy curve in fig. 4·24*b*. By visual estimation a mean isotherm $T = T_m^*$ is drawn so that $A_3 = A_4$. By the construction the fictitious isothermal layer $T = T_m^*$ has the same area $A$ as the real layer. Hence by the rule of 4·23 this fictitious layer has the same dynamic thickness as the real layer. But, according to 4·21(3), the dynamic thickness of the isothermal layer is given by

$$\phi_b - \phi_a = R_d T_m^* \ln \frac{p_a}{p_b}. \tag{3}$$

For practical purposes we prefer to express the mean virtual temperature in centigrade and the height in dynamic meters. Then (3) becomes:

$$H_b - H_a = 28.7(273 + t_m^*) \ln \frac{p_a}{p_b}, \tag{4}$$

where $t_m^*$ is the mean virtual temperature in degrees centigrade.

Formula (4) is the basis of all accurate height computations. For routine work tables have been constructed from (4), based on the tables of V. Bjerknes (1912).

**4·25. The Bjerknes hydrostatic tables.** Since the three variables $t_m^*$, $p_a$, and $p_b$ in formula 4·24(4) vary within wide limits, no direct tabulation of $H_b - H_a$ is possible in one single table. Bjerknes invented four tables* which conveniently solve all problems of determining dynamic height. In the tables pressures are expressed in millibars. The tables are referred to by their original numbers to facilitate reference. In section 4·26 we shall discuss the U.S. Weather Bureau's adaptation of these tables.

The *standard isobaric surfaces* are the surfaces for which $p = 1000, 900, \cdots, 100$ mb. The *standard isobaric layers* are the layers between adjacent standard isobaric surfaces, for example, between 800 mb and 700 mb.

*Table 9M* is computed directly from 4·24(4) by giving $p_a/p_b$ successively the values 10/9, 9/8, $\cdots$, 2/1, and $t_m^*$ integral values in various ranges between −109°C and 49°C. For each value of $p_a/p_b$ and each tabulated value of $t_m^*$, the table gives $H_b - H_a$ in dynamic meters. Having obtained $t_m^*$ from an emagram for a standard isobaric layer, table 9M gives directly the dynamic thickness of the layer. The part of table 9M covering the layer between 1000 mb and 900 mb is given here.

* V. Bjerknes, *Dynamic Meteorology and Hydrography*, Washington, 1912.

TABLE 9M

DISTANCE BETWEEN STANDARD ISOBARIC SURFACES IN DYNAMIC METERS

| 900 mb | $t_m^*$ | 0 | 1 | 2 | 3 | 4 | 5 | 6 | 7 | 8 | 9 |
|---|---|---|---|---|---|---|---|---|---|---|---|
| | −40 | 705 | 702 | 699 | 696 | 693 | 690 | 687 | 684 | 680 | 677 |
| | −30 | 735 | 732 | 729 | 726 | 723 | 720 | 717 | 714 | 711 | 708 |
| | −20 | 765 | 762 | 759 | 756 | 753 | 750 | 747 | 744 | 741 | 738 |
| | −10 | 795 | 792 | 789 | 786 | 783 | 780 | 777 | 774 | 771 | 768 |
| | − 0 | 826 | 823 | 820 | 817 | 814 | 811 | 808 | 804 | 801 | 798 |
| | + 0 | 826 | 829 | 832 | 835 | 838 | 841 | 844 | 847 | 850 | 853 |
| | 10 | 856 | 859 | 862 | 865 | 868 | 871 | 874 | 877 | 880 | 883 |
| | 20 | 886 | 889 | 892 | 895 | 898 | 901 | 904 | 907 | 910 | 913 |
| | 30 | 916 | 919 | 922 | 925 | 928 | 931 | 935 | 938 | 941 | 944 |
| | 40 | 947 | 950 | 953 | 956 | 959 | 962 | 965 | 968 | 971 | 974 |
| 1000 mb | | | | | | | | | | | |

The derivation of the other three tables is best understood after a simple transformation of the fundamental formula 4·24(4). This formula can be expanded into two terms. The first term is

$$(1) \qquad (H_b - H_a)_0 = (28.7)(273) \ln \frac{p_a}{p_b},$$

which is the dynamic thickness of the layer when $t_m^* = 0°C$. The second term may be written

$$(2) \qquad \Delta H = (H_b - H_a)_0 \frac{t_m^*}{273},$$

which becomes a temperature correction to (1). When these two expressions are introduced into 4·24(4), we have

$$(3) \qquad H_b - H_a = (H_b - H_a)_0 + \Delta H.$$

Thus when $(H_b - H_a)_0$ and $\Delta H$ are obtained separately, the true dynamic thickness $H_b - H_a$ is obtained by algebraic addition.

*Table 10M* is computed from (1) by giving $p_a$ successively the standard pressure values 1000, 900, · · ·, 100 mb. For each of those values, $p_b$ is given pressure values for each millibar from 100 mb above $p_a$ to 100 mb below $p_a$. For each value of $p_a$ and $p_b$, table 10M gives the dynamic thickness $(H_b - H_a)_0$ when $t_m^* = 0°C$. A sample of the part of table 10M for $p_a = 1000$ mb is given here, covering $p_b$ between 1000 mb and 1049 mb. All distances are negative, since $p_b > p_a$:

*Table 11M* is† computed from (1) by giving $p_a$ the value 1100 mb, a value chosen to avoid negative heights. The pressure $p_b$ is here ex-

† Called table 11*M in the original tables. The orginal table 11M is a seldom used combination of tables 9M and 10M, set up in different form.

TABLE 10M

DISTANCES FROM THE 1000-MB SURFACE AT 0°C IN DYNAMIC METERS

| 1000 mb Pressure (mb) | 0 | 1 | 2 | 3 | 4 | 5 | 6 | 7 | 8 | 9 |
|---|---|---|---|---|---|---|---|---|---|---|
| 1000 | 0 | −8 | −16 | −23 | −31 | −39 | −47 | −55 | −62 | −70 |
| 1010 | −78 | −86 | −93 | −101 | −109 | −117 | −124 | −132 | −140 | −147 |
| 1020 | −155 | −163 | −171 | −178 | −186 | −193 | −201 | −209 | −216 | −224 |
| 1030 | −232 | −239 | −247 | −254 | −262 | −270 | −277 | −285 | −292 | −300 |
| 1040 | −307 | −315 | −322 | −330 | −337 | −345 | −352 | −360 | −367 | −375 |

tended over all values from 1099 mb to 1 mb, and the table gives the dynamic thickness $(H_b - H_a)_0$ of a layer between $p_a$ and $p_b$ when $t_m^* = 0°C$. By using this table for any two pressure levels $p_b$ and $p_b'$, we can obtain by subtraction the dynamic thickness of a 0°C layer between the two levels $p_b$ and $p_b'$. As table 11M is seldom used in practice, no sample of this table is given.

*Table 12M* gives the temperature correction $\Delta H$ which is applied to all heights obtained from tables 10M and 11M. It is computed from formula (2) with $(H_b - H_a)_0$ as one argument and $t_m^*$ as the other. The correction has the same sign as $t_m^*$. A sample of table 12M is given here for $(H_b - H_a)_0$ between 150 and 190 dyn m and for $t_m^*$ between 0° and 49°:

TABLE 12M

TEMPERATURE CORRECTION FOR TABLES 10M AND 11M

| $(H_b - H_a)_0$ (dyn m) | $t_m^*$(°C) | | | | | | | | | | | | | |
|---|---|---|---|---|---|---|---|---|---|---|---|---|---|---|
| | 0 | 10 | 20 | 30 | 40 | 1 | 2 | 3 | 4 | 5 | 6 | 7 | 8 | 9 |
| 150 | 0 | 5 | 11 | 16 | 22 | 1 | 1 | 2 | 2 | 3 | 3 | 4 | 4 | 5 |
| 160 | 0 | 6 | 12 | 18 | 23 | 1 | 1 | 2 | 2 | 3 | 4 | 4 | 5 | 5 |
| 170 | 0 | 6 | 12 | 19 | 25 | 1 | 1 | 2 | 2 | 3 | 4 | 4 | 5 | 6 |
| 180 | 0 | 7 | 13 | 20 | 26 | 1 | 1 | 2 | 3 | 3 | 4 | 5 | 5 | 6 |
| 190 | 0 | 7 | 14 | 21 | 28 | 1 | 1 | 2 | 3 | 3 | 4 | 5 | 6 | 6 |

The temperature correction $\Delta H$ for $(H_b - H_a)_0 = 173$ dyn m and $t_m^* = 34°$ is calculated as follows: For 170 dyn m and 30°C, we read 19 dyn m. For 170 dyn m and 4°C, we read 2 dyn m. Hence $\Delta H = 19 + 2 = 21$ dyn m.

Tables 10M and 12M, according to (3), determine the height above or below the nearest standard surface of any salient point of the sounding curve (highest point, tropopause, inversion, front, etc.). Tables 11M and 12M determine by double operation and a subtraction the height between any two salient points, for example, between the surface of the earth and the top of the ascent. Table 11M should only be used for rather rough estimates of the total height, since appreciable errors may

be brought in by the graphical estimate of the mean virtual temperature of a thick layer.

Greater accuracy is obtained when the total layer is divided into the standard layers, and its thickness measured as the sum of the thicknesses of these layers. Thus the accurate determination of height by means of the tables is performed by the following three operations:

1. Determination of the dynamic height of the 1000-mb surface. This is done with the aid of table 10M and the correction table 12M.

2. Determination of the dynamic thicknesses of each of the standard layers. These are obtained directly from table 9M.

3. Determination of the dynamic height of the top of the ascent above the highest standard isobaric surface. This is done with the aid of table 10M and the correction table 12M.

When the results of 1, 2, and 3 are added we obtain the total dynamic height of the sounding, and also the dynamic heights of the standard isobaric surfaces. The heights of other salient points along the ascent curve can be found from tables 10M and 12M. These points are, however, determined more conveniently and with sufficient accuracy through an interpolation on a *pressure dynamic height* curve. This curve can be drawn on the same emagram where the original virtual temperature sounding curve was plotted for the determination of the values of $t_m^*$ (see fig. 4·27). It is constructed from the dynamic heights of the standard isobaric surfaces. We use the pressure scales of the emagram and introduce a horizontal scale of dynamic height, increasing from right to left, with 0 at sea level. In an isothermal layer the pressure dynamic height curve is a straight line, according to 4·21(1). Elsewhere it is slightly and smoothly curved. The lack of smoothness of the curve indicates errors in the height computation. The height of any salient point is found by following the isobar from the sounding curve to the pressure dynamic height curve, and reading the corresponding dynamic height on this curve.

**4·26. U.S. Weather Bureau hydrostatic tables.** The U.S. Weather Bureau has published hydrostatic tables used in all official height evaluations in this country. They are computed from Bjerknes' tables, but they are different in two respects: First, all heights are expressed in terms of the unit *0.98 dyn m*. This is a unit nearly equivalent to the geometric meter. All dynamic height values in these tables are thus 2% larger than those in Bjerknes' original tables. Second, there have been added a number of interpolated standard isobaric surfaces for greater accuracy, namely, the 350, 250, 175, 150, 125, 80, 60, 50, 40, 30, 20, 15, 10, and 5-mb surfaces. Having noted these general differences, we describe these tables briefly:

*Table 1* is Bjerknes' table 9M, with some unimportant reductions in the tabulated range of $t_m^*$.

*Tables 2 and 2a* are Bjerknes' table 10M. Except at pressures above 800 mb the arbitrary pressure levels $p_b$ are referred only to the next higher standard pressure $p_a > p_b$.

*Table 3* is Bjerknes' table 12M, made longer and simpler by tabulating directly for every degree of $t_m^*$.

There is no table corresponding to Bjerknes' table 11M.

**4·27. Height evaluation on a diagram.** An accurate graphical method for height determination has been invented by Väisälä. It combines the emagram with certain scales which are equivalent to Bjerknes' tables. The scales will be described in the same order as the tables in 4·25, in order to facilitate comparison. An emagram with Väisälä's scales is drawn in fig. 4·27. The dry adiabats and other curves are omitted for clearer reading.

1. The first scales to observe are those located along isobars in the middle of each standard layer. These scales correspond to table 9M, from which they have been plotted, and on a large-scale diagram can be read to an accuracy of nearly one dynamic meter. To get the thickness in dynamic meters of any standard isobaric layer, we simply read this scale at the point where the mean virtual temperature isotherm crosses this scale.

2. The double scale labeled $B$ at the bottom of the diagram gives the dynamic thickness $(H_{1000} - H_p)_0$ of the layer between the 1000-mb level and the pressure $p$. It assumes the mean virtual temperature 0°C. This replaces the most commonly used part of table 10M. It has an accuracy of about one dynamic meter on a larger diagram showing more detailed scales. It is used to get the dynamic height of the 1000-mb level above or below the station for stations not too far from sea level.

3. A scale on the right edge of the diagram gives directly the dynamic height in dynamic kilometers from the 1000-mb level to any other pressure level $p$, when the mean virtual temperature of the column is 0°C. This scale replaces table 11M, except that Väisälä has used 1000 mb instead of 1100 mb as the reference level. By means of this scale and a subtraction the dynamic thickness may be determined between two arbitrary pressure levels in an atmosphere where $t_m^* = 0$°C. The accuracy is about 10 dynamic meters on a detailed scale.

4. The scale labeled $A$ at the bottom of the diagram gives the factor $k$ by which the heights derived in 2 and 3 above must be *multiplied*, when the mean virtual temperature is different from 0°C. Scale $A$ uses the temperature scale of the emagram. This temperature correction does

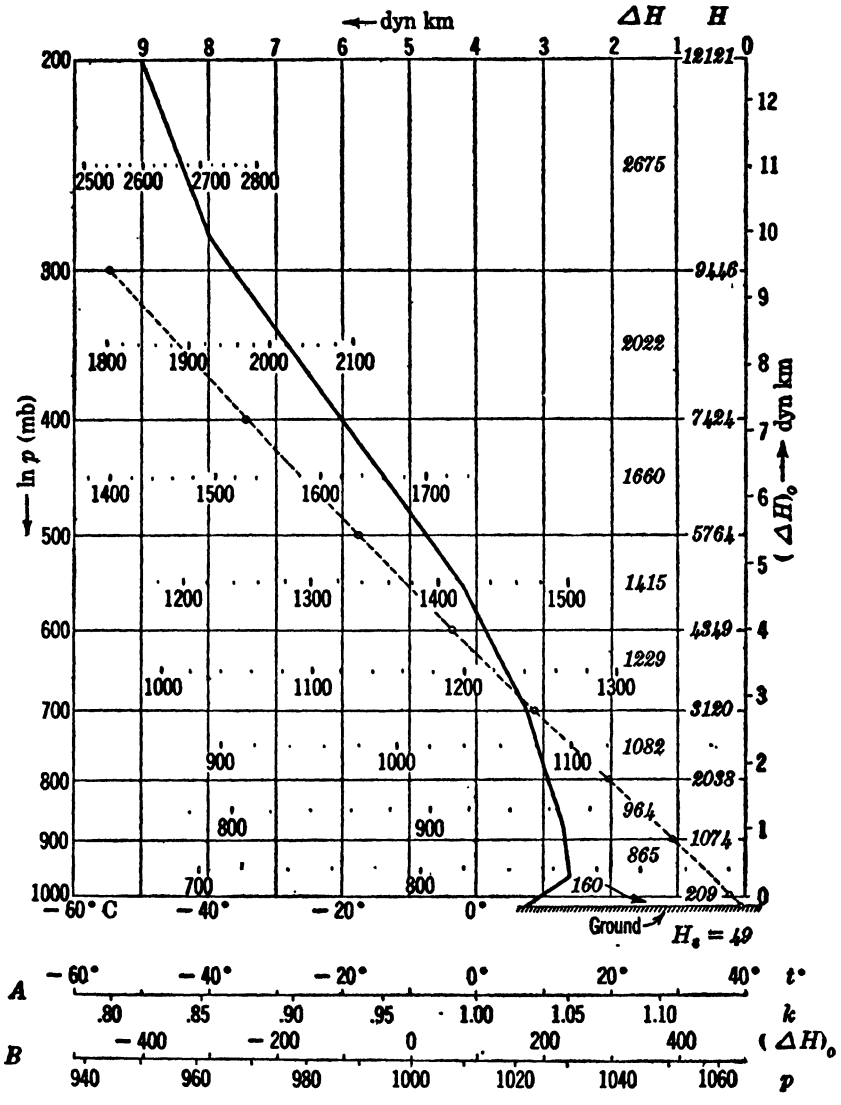



FIG. 4·27. Computation of height on emagram.

the same job as table 12M, but is designed for slide rule computation. If the mean virtual temperature is $t$°C, then the dynamic thickness $(H_b - H_a)_t$ at $t$°C is given by

$$(H_b - H_a)_t = k(H_b - H_a)_0. \tag{1}$$

From 4·25(2, 3) we see that $k = 1 + (t/273)$.

By the use of the scales described in 1, 2, and 4 we can determine the heights for a sounding beginning at any pressure within the range of scale $B$. This method is quite as accurate as the use of Bjerknes' tables. The errors in either method are less than the instrumental errors. For pressures below 200 mb, Väisälä's diagram contains a low-pressure scale (described in 2·32), but this has been omitted in fig. 4·27. There is customarily a scale of the type described in 1 above associated with these low pressures.

**4·28. Example of height computation on the diagram.** We suppose that a radiosonde observation has been received for a station whose elevation is 50 m (49 dyn m) above sea level. By some procedure the virtual temperatures $t^*$ have been computed at the pressures $p$ received in the ascent, and we have the following table for $p$ and $t^*$. The highest pressure is at the ground.

TABLE 4·28

| $p$ (mb) | $t^*$ (°C) | $p$ (mb) | $t^*$ (°C) |
|---|---|---|---|
| 1020 | 8 | 540 | −3 |
| 960 | 14 | 400 | −20 |
| 870 | 13 | 280 | −40 |
| 700 | 8 | 200 | −50 |

This virtual temperature sounding is plotted as a solid line in fig. 4·27, with the customary linear interpolation between the points received. The following steps are carried out in order. They have been performed on a larger diagram with more detailed scales than fig. 4·27, but the reader can follow the work on that figure.

1. The *dynamic height* $H_s$ in dynamic meters of the station is written in the right-hand corner of the diagram: 49.

2. The dynamic thickness $(H_{1000} - H_s)_t$ of the layer up to 1000 mb is obtained as follows: Opposite the ground pressure 1020 mb on scale $B$ is read $(H_{1000} - H_s)_0 = 155$ dyn m. From the sounding we see that the mean virtual temperature for the layer 1020 mb to 1000 mb is 9°C. Opposite 9°C on scale $A$ is read $k = 1.033$. According to equation 4·27(1), $(H_{1000} - H_s)_t = (155) \cdot (1.033) = 160$ dyn m. The number 160 is written between 1020 mb and 1000 mb in a column to the left of the station elevation.

The reader can obtain $(H_{1000} - H_s)_0 = 155$ from our sample of table 10M, with an additive correction $\Delta H = 5$ from our sample of table 12M. This gives $(H_{1000} - H_s)_t = 160$, confirming the above graphical work.

3. The dynamic height $H_{1000}$ of the 1000-mb level is obtained by

adding 160 to 49, giving 209 dyn m; 209 is written above 49, on the 1000-mb isobar.

4. The dynamic thickness $H_{900} - H_{1000}$ of the layer from 1000 mb to 900 mb is obtained as follows: A mean isotherm $t_m^*$ is found for this part of the sounding in fig. 4·24*b*. (A transparent ruler is usually used for this.) In this case $t_m^* = 13°C$, and this isotherm crosses the height scale for this layer at 865 dyn m. This is the dynamic thickness of the layer in question; it is posted in this layer above the figure 160.

The reader can also obtain $H_{900} - H_{1000} = 865$ from our sample of table 9M.

5. 865 is added to 209 to give the dynamic height 1074 dyn m for the 900-mb level.

6. In similar fashion the dynamic thickness $H_b - H_a$ is found for each of the standard isobaric layers, and the values are posted in the same column above 160.

7. The dynamic heights of the standard pressure levels are posted in the column above 49. They are always the cumulative totals of the $H_b - H_a$ for lower layers, plus the dynamic height of the ground. All these heights have been posted in fig. 4·27, ending with $H = 12{,}121$ dyn m at 200 mb.

8. A pressure dynamic height curve is drawn as follows: The same pressure scale is used, but the horizontal axis is now converted into a dynamic height scale. It increases from right to left and is labeled in dynamic kilometers at the top of fig. 4·27. With these scales the ground pressure and each of the standard pressure values are plotted against the corresponding dynamic heights from the last column. For example: at $p = 1020$ mb is plotted $H = 49$ dyn m; at $p = 1000$ mb is plotted $H = 209$ dyn m; etc. In fig. 4·27 the last point plotted is 9446 dyn m at 300 mb. These points are drawn as circles in the figure.

The points just plotted are joined with straight line segments to form the pressure dynamic height curve (the broken curve in fig. 4·27). This curve should show no marked irregularities; if such exist all the work should be checked. The curve should be more or less parallel to a dry adiabat (see fig. 2·32*b*).

From the pressure dynamic height curve and the sounding one can obtain all necessary information about the ascent. For example, the pressure at 10,000 ft (2990 dyn m) can be read as the pressure opposite 2.99 dyn km on the pressure dynamic height curve. It is 716 mb in this case, and the error should never exceed 1 mb. The virtual temperature at 10,000 ft can be read as the temperature where the sounding crosses the pressure 716 mb. It is 8.3°C in this case, and the accuracy is limited only by the original data.

**4·29. Further remarks.** The steps 2 and 3 of the method of 4·28 are modified slightly in case the ground pressure is less than 1000 mb. As long as the pressure is within the range of scale $B$ in fig. 4·27, the idea is to introduce a fictitious isothermal column down to 1000 mb. The thickness $H_{1000} - H_s$ of this fictitious column is obtained from scale $B$. This number will be *negative*, and it is therefore *subtracted* from the ground elevation to give the dynamic height of the fictitious 1000-mb level. By using the fictitious and the real columns, the thickness of the layer between 1000 mb and 900 mb is then determined, and the process of 4·28 is continued.

If the ground pressure is too low for scale $B$, it is necessary to compute the dynamic height from the ground up to the next standard pressure level by use of 4·24(4), or from Bjerknes' tables. After that the method of 4·28 can be applied.

The scale described in 3 of 4·27 is never used for accurate height evaluations; it is used only for rough estimates of height.

Väisälä's diagram contains two other scales not mentioned so far and not shown in fig. 4·27. The first gives immediately the difference between the actual temperature $t$ and the virtual temperature $t^*$ for saturated air. If the air is unsaturated the correction is mentally multiplied by $r$. With these scales the virtual temperature sounding may be plotted readily from the true temperature sounding. The other scale is designed to give directly the height correction in dynamic meters for saturated air due to the difference between $t^*$ and $t$. If these scales are used, the true temperature sounding is plotted instead of the virtual temperature sounding. The procedure of 4·28 is then carried out on the sounding as plotted. Before each height is posted, however, there is added to it the height correction for saturated air (from the scale) multiplied by $r$. This yields the same values of $H_b - H_a$ as the method of 4·28. The two methods give equally accurate results, and the choice between them is a matter of taste.

**4·30. U.S. standard atmosphere.** The U.S. standard atmosphere (also called the N.A.C.A. atmosphere) was adopted in 1925 by the N.A.C.A.* to serve as a standard for all aeronautic work. The standard atmosphere is conveniently described by letting the pressure $p$ be the independent variable, and considering *standard temperature* $T_p$ and *standard altitude* $z_p$ as unique functions of $p$. These functions may be obtained by a pressure-height calculation on a fictitious column of *dry air* with the following properties:

* National Advisory Committee for Aeronautics, *Technical Reports* 147, 218, 246, 538, Supt. of Documents, Washington, D.C.

(i) The level where the pressure is $p_0$ (= 101.33 cb) serves as the origin for measuring standard altitude, and is called the *base level.* The base level either may or may not coincide with sea level.

(ii) The standard temperature $T_p$ at the base level is 288°K (15°C). Up to the level where $z_p$ is 10,769 m, the standard temperature drops 6.5°C per (geometric) kilometer rise, corresponding to the constant lapse rate

$$\gamma = \frac{0.0065}{g_n} \text{ deg (dyn dm)}^{-1}. \tag{1}$$

At and above 10,769 m the standard temperature has the constant value 218°K (−55°C). Thus

$$T_p = \begin{cases} 288 - 0.0065 z_p & (z_p \leqq 10{,}769 \text{ m}) \\ 218 & (z_p \geqq 10{,}769 \text{ m}). \end{cases} \tag{2}$$

(iii) Gravity is assumed to have the standard value $g_n$ (= 9.80665 m s$^{-2}$) of section 1·07, and $R_d$ is assumed to be 287.076 kj t$^{-1}$ deg$^{-1}$.

We can obtain $p$ as a function of $z_p$ (below 10,769 m) by putting (1) into 4·18(7). We get

$$p = p_0 \left[ 1 - \frac{0.0065}{288} z_p \right]^{\frac{g_n}{0.0065 R_d}} \qquad (z_p \leqq 10{,}769 \text{ m}).$$

Substituting the constants from (iii) and using (2), we get

$$p = \left\{ \begin{matrix} p_0 (1 - 0.00002257 z_p)^{5.256} \\ p_0 \left( \dfrac{T_p}{288} \right)^{5.256} \end{matrix} \right\} \qquad (z_p \leqq 10{,}769 \text{ m}). \tag{3}$$

From (3) the pressure $p_a$ at the base of the isothermal layer is $p_a = p_0 (0.75694)^{5.256} = 0.23145 p_0 = 23.452$ cb. In the isothermal layer formula 4·24(3) yields the following:

$$\phi - \phi_a = 218 R_d \ln \frac{p_a}{p}.$$

Setting $\phi - \phi_a = g_n (z_p - 10{,}769)$ and $p_a = 23.452$, we can solve for $z_p$, obtaining

$$z_p = 10{,}769 + 6381.6 \ln \frac{23.452}{p} \qquad (z_p \geqq 10{,}769 \text{ m}). \tag{4}$$

To exhibit $p$ as the independent variable, we solve (2) and (3) for $T_p$ and $z_p$, and combine them with (4). Thus

$$T_p = \begin{cases} 288 \left( \dfrac{p}{p_0} \right)^{0.19028} & (p \geqq 23.452 \text{ cb}) \\ 218 & (p \leqq 23.452 \text{ cb}). \end{cases} \tag{5}$$

$$(6) \qquad z_p = \begin{cases} 44{,}308\left[1 - \left(\frac{p}{p_0}\right)^{0.19028}\right] & (p \geqq 23.452 \text{ cb}) \\ 10{,}769 + 6381.6 \ln \frac{23.452}{p} & (p \leqq 23.452 \text{ cb}). \end{cases}$$

Formulas (5) and (6) completely describe the standard atmosphere. They obscure the fact that this atmosphere has a constant lapse rate in its lower portions. On the other hand, they emphasize the fact that pressure is the independent variable to which both standard temperature and standard altitude are referred. Based on these formulas, there have been constructed tables of the U.S. standard atmosphere which are convenient for use in computations. (See, for example, N.A.C.A. *Technical Report* 538.)

Since, by (5), $T_p$ is a function of $p$, a sounding of the standard atmosphere may be plotted on any thermodynamic diagram. As explained in section 4·23, the standard altitude $z_p$ is proportional to the area on an emagram to the left of the sounding of the standard atmosphere between the isobars $p_0$ and $p$. The construction and study of such a diagram will answer most theoretical questions about the standard atmosphere and the pressure altimeter.

It should be observed that the definition of the U.S. standard atmosphere is not given in dynamic terms, since the lapse rate is originally expressed with geometrical meters instead of with dynamic height units. As a result formulas (5) and (6) are mutually consistent only when gravity has the standard value $g_n$. If gravity has a constant value $g$ other than $g_n$, the reader may show that formula (6) is a correct expression for altitude as a function of pressure in an atmosphere for which the temperature is equal to $T_p$ multiplied by $g/g_n$.

**4·31. The pressure altimeter.** In an airplane height is usually measured with a pressure altimeter. This instrument is an aneroid barometer whose dial is graduated in height units instead of pressure units. The scale is made with equal height units spaced uniformly around the dial. At its normal setting the mechanism is calibrated so that at each pressure $p$ the pointers indicate the standard altitude given by 4·30(6). At all levels in the standard atmosphere the altimeter with this setting will correctly indicate the true altitude above the base level defined in 4·30(i).

In practice it is desired to have the altimeter indicate altitude above sea level (briefly called *sea level altitude*). This is accomplished by rotating the height scale relative to the barometer and the pointers. If the altimeter is in the standard atmosphere, the height scale is rotated just

far enough to increase all height readings by the sea level altitude *of the base level.* After this is done, the altimeter will correctly indicate the sea level altitude of any level in the standard atmosphere. (In practice the height scale is fixed, and the rest of the mechanism is turned; the effect is identical with that just described.)

Before the height scale was turned, the instrument indicated *zero altitude* at the pressure $p_0$ (which is equal to 29.92 in. of mercury). In this position the " altimeter setting " is said to be 29.92. After the height scale was turned, the instrument indicated zero altitude at sea level. The pressure at which the instrument will read zero altitude is called the *altimeter setting.* It is usually expressed in inches of mercury, and in the standard atmosphere we have just seen that it is also the pressure at sea level.

The altimeter setting is the only pressure indication which is visible on the altimeter. It serves at all times to represent the amount by which the height scale has been rotated from its normal setting. When the altimeter setting $p_1$ is put in 4·30(6), it determines an altitude $z_{p_1}$ which may be positive or negative. No matter what the true atmosphere is like, a mechanically perfect altimeter with the altimeter setting $p_1$ will indicate at each pressure $p$ the corresponding standard altitude $z_p$ minus $z_{p_1}$.

In each airways weather station there is computed several times a day the altimeter setting which will cause an altimeter to indicate the true altitude of the field when the plane is resting on the runway. The reader may show from the last paragraph that the correct altimeter setting may be determined as follows:

(i) Determine the standard altitude $z_p$ of the field by putting the pressure at the field into 4·30(6).

(ii) Subtract the true altitude $z$ of the field from $z_p$, to obtain a height. Let this height be denoted by $z_{p_1}$.

(iii) Determine from 4·30(3) the pressure $p_1$ corresponding to the height $z_{p_1}$. This pressure is the altimeter setting. These operations may be performed quickly with the aid of tables of the standard atmosphere. In practice the whole procedure is incorporated into a single-entry table giving the altimeter setting $p_1$ for each pressure $p$ at the field.

It should be stressed that the altimeter setting for any one station depends only on the station pressure. In this respect it is very different from the variable reduction to a " sea level pressure " used as the pressure report for the synoptic maps.

**4·32. Altimeter errors.** Apart from mechanical and calibration errors a pressure altimeter is subjected to two types of errors which are

inherent in its design. The first arises when a plane lands at an airport with an altimeter setting which is incorrect for that airport. The second arises when a plane is high over the ground, if the intervening atmosphere is different from the standard atmosphere.

The first error is rather simple to visualize and measure. From 4·30(6) each millibar variation in $p$ represents (near $p_0$) a variation of between 8 and 9 m in $z_p$. Thus an altimeter will be wrong by 8 or 9 m for each millibar error in altimeter setting (about 3 m for each 0.01-in. error in altimeter setting). For example, suppose an altimeter was set correctly for a sea level field of take-off where the pressure was 1030 mb. Then on landing with the original setting at a sea level field where the pressure is 980 mb, the plane will hit ground when the altimeter indicates 420 m above sea level!

To explain the second error suppose that an altimeter is set correctly for a sea level station under the plane. Suppose the mean virtual temperature $T_m^*$ of the air column beneath the plane differs from the mean temperature $T_A$ of the standard atmosphere. Suppose also that gravity $g$ in the column differs from the value $g_n$ of the standard atmosphere. Then the altimeter will have an error which can be estimated from 4·24(3). Let the sea level pressure be $p_a$; let the plane be at the pressure $p_b$. Then the true dynamic height of the plane is

$$\phi = 287 T_m^* \ln \frac{p_a}{p_b}. \tag{1}$$

The altimeter will indicate an altitude corresponding at gravity $g_n$ to the dynamic height $\phi_A$ given by

$$\phi_A = 287 T_A \ln \frac{p_a}{p_b}. \tag{2}$$

Comparing (1) and (2), we see that

$$\phi = \frac{T_m^*}{T_A} \phi_A.$$

Hence the true altitude $z = \phi/g$ is given in terms of the indicated altitude $z_A = \phi_A/g_n$ by the formula

$$z = \frac{T_m^*}{T_A} \frac{g_n}{g} z_A \approx \frac{T_m^*}{T_A} z_A. \tag{3}$$

Since $T_A$ is not far from 280°K at the lower flight altitudes, we see from (3) that each 2.8°C departure of $T_m^*$ from $T_A$ will cause about a 1% error in the altimeter. If the actual air is colder than the standard atmosphere, the altimeter will read too high. If the actual air is warmer

than the standard atmosphere, the altimeter will read too low. Since $g$ never differs from $g_n$ by more than $\frac{1}{4}\%$ at flight levels, the maximum gravity error is equivalent to the error introduced by a variation in $T_m^*$ of merely 0.7°C. Thus the variation of gravity can usually be ignored in comparison with the variation of $T_m^*$.

The determination of $T_A$ in practice can be made exactly from tables. The accurate determination of $T_m^*$ is very difficult in flight, since the plane is constantly passing over new columns with unknown temperature distributions.

CHAPTER FIVE

# STABILITY OF HYDROSTATIC EQUILIBRIUM

**5·01. The parcel method.** In this chapter we shall develop methods for determining the vertical stability at any level of the atmosphere where hydrostatic equilibrium prevails. The level of the atmosphere which will be investigated is called the *reference level.*

First imagine that a small parcel of air is displaced infinitesimally upward or downward from this reference level. By studying the subsequent motion of the displaced parcel, we shall formulate certain criteria of stability: If the parcel tends to move back to the reference level, the atmosphere is said to be *stable* at that level; and if the parcel tends to move away from the reference level, the atmosphere is said to be *unstable* at that level. This method of characterizing the vertical stability is called the parcel method.

If the parcel were to mix with the surrounding air it would lose its identity, so we shall assume that the parcel is displaced *without mixing.* Moreover, although the displacement would actually disturb the environment near the parcel, we shall further assume that the environment remains undisturbed. These assumptions are certainly very artificial, for the parcel must actually stir up and mix with the air through which it moves. It would be better to examine a small continuous displacement of a whole region. Then the stability criteria would depend upon the increase or decrease of the entire motion subsequent to the initial displacement. However, such an analysis requires advanced hydrodynamical technique and moreover gives the same stability criteria as the parcel method. The simpler parcel method will therefore be used here.

It will be seen presently that the stability is determined by comparison of the densities of the parcel and of the surrounding air. Properties of the parcel will be denoted by primed symbols and properties of the environment *at the same level* will be denoted by unprimed symbols.

Any change of a thermodynamic property of the parcel is an individual variation, depending upon the process which the parcel undergoes and is designated by the differential symbol $d$ (see section 4·10). Although the environment is assumed undisturbed by the motion of the parcel, the properties of the environment will generally vary from level to level. Accordingly, as the parcel moves to new levels *its* environ-

ment undergoes a variation which then is a spatial variation and is designated by the geometrical differential symbol $\delta$ (see section 4·10).

At the reference level $\phi_0$ the parcel and its environment have exactly the same thermodynamic properties, for the parcel has yet to be separated from the environment. However, the properties of the displaced parcel at any other level $\phi$ will usually differ from the properties of the environment.

Since the environment is in hydrostatic equilibrium, the resultant buoyant force at any level is zero. Thus taking the $z$ component of equation 4·16(2), we have

$$0 = -g - \alpha \frac{\partial p}{\partial z}.$$

In general the parcel will have a vertical acceleration $\dot{v}_z = \ddot{z}$. By Newton's second law of motion this acceleration is equal to the resultant buoyant force per unit mass. We shall now assume that throughout the entire motion the parcel will adjust its pressure to the pressure of the environment. Thus

$$\ddot{z} = -g - \alpha' \frac{\partial p}{\partial z}.$$

Elimination of $\partial p/\partial z$ from the above equations gives

$$\ddot{z} = g \frac{\alpha' - \alpha}{\alpha}. \tag{1}$$

This relation equates the acceleration to the resultant buoyant force acting on unit mass of the parcel. The buoyant force is expressed in terms of the specific volumes of the parcel and the environment. This force is upward if the parcel is lighter than the environment ($\alpha' > \alpha$) and downward if the parcel is heavier than the environment ($\alpha' < \alpha$).

**5·02. Stability criteria.** The specific volume is not directly available from aerological data, so the buoyant force is more conveniently expressed by the virtual temperature. The equations of state 3·25(5) for the parcel and for the environment show that 5·01(1) may be written

$$\ddot{z} = g \frac{T^{*\prime} - T^*}{T^*}. \tag{1}$$

We shall investigate only infinitesimal displacements from the reference level $\phi_0$. The geometric height coordinate $z$ will be measured from this level, so the dynamic height of both the parcel and the environment above the reference level is $d\phi = \delta\phi = gz$. Let the virtual temperature at

$\phi_0$ be $T_0^*$. The virtual temperature variation in the environment is

$$T^* - T_0^* = \delta T^* = \frac{\delta T^*}{\delta \phi}\delta\phi = -\gamma^* g z. \tag{2}$$

Here the virtual temperature lapse rate $\gamma^*$ in the environment is defined by the spatial derivative

$$\gamma^* = -\frac{\delta T^*}{\delta \phi}.$$

An *individual virtual temperature lapse rate* $\gamma^{*\prime}$ of the parcel may also be defined by the individual or process derivative

$$\gamma^{*\prime} = -\frac{dT^{*\prime}}{d\phi}.$$

The change of the virtual temperature of the parcel is then

$$T^{*\prime} - T_0^* = dT^{*\prime} = \frac{dT^{*\prime}}{d\phi}d\phi = -\gamma^{*\prime} g z. \tag{3}$$

Subtraction of (2) from (3) gives

$$T^{*\prime} - T^* = g(\gamma^* - \gamma^{*\prime})z.$$

Equation (1) may then be written in the final form

$$\ddot{z} = \frac{g^2}{T^*}(\gamma^* - \gamma^{*\prime})z. \tag{4}$$

The reference level will be *stable*, *indifferent*, or *unstable* according to the following three conditions, read respectively from top to bottom:

$$\gamma^* \lessgtr \gamma^{*\prime}. \tag{5}$$

That is, the atmosphere is stable at the reference level if the acceleration and the displacement have opposite signs, so the parcel tends to move back to the reference level. The atmosphere is indifferent if the acceleration is zero. And it is unstable if the acceleration and the displacement have the same sign, so the parcel tends to move away from the reference level.

If the virtual temperature sounding curve is available, we can easily determine whether any level of the sounding is stable, indifferent, or unstable, once the individual or process virtual temperature lapse rate is known.

**5·03. The individual lapse rate.** The individual virtual temperature lapse rate in any process has been defined as

$$\gamma^{*\prime} = -\frac{dT^{*\prime}}{d\phi},$$

where $dT^{*\prime}$ is the change of the virtual temperature of a parcel lifted through the dynamic height $d\phi$. Since it is assumed that the parcel travels through an undisturbed environment, the dynamic height is measured in the environment. The environment is in hydrostatic equilibrium, so $\delta\phi = d\phi = -\alpha dp$. The individual virtual temperature lapse rate is then given by

$$\gamma^{*\prime} = \frac{1}{\alpha}\left(\frac{dT^{*\prime}}{dp}\right).$$

Here the derivative in parentheses is determined completely by the process, whereas the specific volume $\alpha$ refers to the environment. However, since we consider only an infinitesimal displacement from the reference level, where $\alpha' = \alpha$, the individual virtual temperature lapse rate for the parcel method depends only on the process. Thus

$$\gamma^{*\prime} = \frac{1}{\alpha'}\left(\frac{dT^{*\prime}}{dp}\right).$$

If we replace $T^{*\prime}$ by $T'$, the above argument will also apply to the individual lapse rate of temperature, $\gamma' = -dT'/d\phi$. As explained in 2·23 the temperature changes caused by radiation, conduction, or mixing are slow compared with the changes caused by the vertical motion of the parcel. Consequently the process performed by the parcel displaced vertically from its reference level is nearly adiabatic. In the following we shall consider the process to be strictly adiabatic. The process is then either an unsaturated or a saturated adiabatic process. The individual temperature lapse rate $\gamma'$ for an adiabatic process will be denoted by $\gamma_u$ for an unsaturated parcel and by $\gamma_s$ for a saturated parcel.

Since the parcel does not mix with its environment, the mixing ratio of an unsaturated parcel has the constant value $w_0$ throughout the displacement. Individual differentiation of

3·25(4) $$T^{*\prime} = (1 + 0.61w_0)T'$$

with respect to dynamic height gives for an unsaturated adiabatic process

(1) $$\gamma^{*\prime} = (1 + 0.61w_0)\gamma_u.$$

As explained in section 3·27 the process curves for an unsaturated adiabatic process nearly coincide with the dry adiabats. Therefore the lapse rate $\gamma_u$ of temperature along an unsaturated adiabatic process curve is almost equal to the dry adiabatic lapse rate $\gamma_d = 1/c_{pd}$. See 4·20(3). The lapse rate of virtual temperature along the unsaturated adiabats is

then given approximately by

(2) $$\gamma^{*\prime} \approx \gamma_u \approx \gamma_d \qquad \text{(unsaturated process)},$$

for the factor $1 + 0.61w_0$ in (1) is nearly equal to 1.

When a saturated parcel is displaced upward it will perform a saturation-adiabatic process. Since condensation occurs, the mixing ratio $w_s$ of the parcel decreases. Differentiation of equation 3·25(4) with respect to dynamic height then gives

(3) $$\gamma^{*\prime} = (1 + 0.61w_s)\gamma_s - 0.61T' \frac{dw_s'}{d\phi}.$$

The lapse rate of temperature along a saturation-adiabatic process curve is $\gamma_s$. The lapse rate $\gamma^{*\prime}$ may easily be visualized by constructing the virtual temperature curve of a saturated parcel whose image point follows a saturation adiabat. As the mixing ratio decreases the two curves become closer, so the virtual temperature of the parcel decreases more rapidly than the temperature of the parcel. This result is also evident from (3), for $dw_s'/d\phi$ is negative. The correction term $-0.61T'dw_s'/d\phi$ is then positive. In the lower troposphere this correction term may be as large as 10%. See equation 5·11(4). For rough calculations, however, we may make the approximation

(4) $$\gamma^{*\prime} \approx \gamma_s \qquad \text{(saturated process)}.$$

An exact formula for $\gamma_u$ and $\gamma_s$ will be given later in section 5·10.

In the following sections stability criteria will be presented in terms of the lapse rates of temperature $\gamma_d$ along a dry adiabat and $\gamma_s$ along a saturation adiabat, since these adiabats are usually drawn on meteorological thermodynamic diagrams. If the exact form of the stability criteria is wanted, the individual virtual temperature lapse rate $\gamma^{*\prime}$ must be computed.

**5·04. The lapse rate in the environment.** Although the lapse rates $\gamma^{*\prime}$ and $\gamma'$ for the process are always nearly equal, the lapse rates $\gamma^*$ and $\gamma$ in the environment may be quite different, for the vapor stratification in the atmosphere is arbitrary. Spatial differentiation of the relation

3·25(4) $$T^* = (1 + 0.61w)T$$

with respect to dynamic height gives

(1) $$\gamma^* = (1 + 0.61w)\gamma - 0.61T \frac{\delta w}{\delta \phi}.$$

When $\gamma^*$ in the stability conditions 5·02(5) is expressed by (1), we

find that the reference level is more stable than the temperature sounding indicates, if the mixing ratio increases with height; and it is less stable, if the mixing ratio decreases with height. In particular, the top of a cloud may be less stable than the temperature sounding indicates, especially if the cloud is below a dry inversion. For example, let us find what moisture distribution would make an isothermal atmospheric layer ($\gamma = 0$) have a virtual temperature lapse rate equal to the dry-adiabatic lapse rate ($\gamma^* = 1/c_{pd}$). Equation (1) then becomes

$$\frac{\delta w}{\delta \phi} = -\frac{1}{0.61 c_{pd} T}.$$

This variation is not too improbable, for the thickness $\Delta z$ of the layer having a constant variation of mixing ratio from the value $w$ at the bottom to the value 0 at the top is given by

$$\Delta z = \frac{0.61 c_{pd} T w}{g}.$$

For instance, the thickness of a layer saturated at the bottom and dry at the top, having a mean pressure of 90 cb and a mean temperature of 10°C, is 150 m. Such a layer might be found at the top of a stratus deck.

**5·05. Stability criteria for adiabatic processes.** The stability criteria 5·02(5) for an infinitesimal adiabatic displacement can now be assembled finally. If the parcel is unsaturated the three stability conditions are, from 5·03(2),

(1) $$\gamma^* \lessgtr \gamma_d.$$

And if the parcel is saturated the three stability conditions are, from 5·03(4),

(2) $$\gamma^* \lessgtr \gamma_s.$$

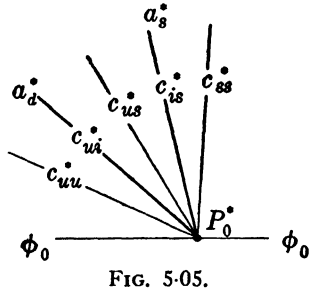


FIG. 5·05.

The graphical use of these criteria is illustrated in fig. 5·05, which represents a small section of a thermodynamic diagram. The virtual temperature at the reference level is represented by the point $P_0^*$. Through $P_0^*$ the dry and saturation adiabats $a_d^*$ and $a_s^*$ are drawn. Any virtual temperature sounding curve $c^*$ through $P_0^*$ may be classified with respect to these adiabats. The five possible classifications, illustrated in fig. 5·05 by the curves $c_{ss}^*$, $c_{is}^*$, $c_{us}^*$, $c_{ui}^*$, $c_{uu}^*$, are:

(*ss*) The sounding curve $c_{ss}^*$ is said to be *absolutely stable* if above the reference level it is warmer than the saturation adiabat $a_s^*$, that is, if

$\gamma^* < \gamma_s$; for then the reference level is stable no matter whether the air is saturated or unsaturated.

(*is*) The sounding curve $c^*_{is}$ is said to be *saturated indifferent* if it coincides with the saturation adiabat $a^*_s$, that is, if $\gamma^* = \gamma_s$; for then the reference level is indifferent if the air is saturated and stable if the air is unsaturated.

(*us*) The sounding curve $c^*_{us}$ is said to be *conditionally unstable* if it lies between the saturation adiabat $a^*_s$ and the dry adiabat $a^*_d$, that is, if $\gamma_d > \gamma^* > \gamma_s$; for then the reference level is unstable if the air is saturated and stable if the air is unsaturated.

(*ui*) The sounding curve $c^*_{ui}$ is said to be *dry indifferent* if it coincides with the dry adiabat $a^*_d$, that is, if $\gamma^* = \gamma_d$; for then the reference level is unstable if the air is saturated and indifferent if the air is unsaturated.

(*uu*) The sounding curve $c^*_{uu}$ is said to be *absolutely unstable* if above the reference level it is colder than the dry adiabat $a^*_d$, that is, if $\gamma^* > \gamma_d$; for then the reference level is unstable no matter whether the air is saturated or unsaturated.

Notice that these definitions refer only to the slope of the sounding curve $c^*$ at the reference level and do not give the actual stability at that level, because the stability depends upon whether the air is saturated or unsaturated.

**5·06. Stable oscillation.** If the reference level is stable, the acceleration of the parcel will counteract the displacement. Therefore the parcel will eventually stop and be driven back by the buoyant force to its equilibrium or reference level. However, its inertia will carry it past this level. Consequently the parcel will oscillate about the equilibrium level.

This can be shown analytically, for if the parcel is stable, a positive number $\nu^2$ can be defined as follows:

$$\nu^2 = \frac{g^2}{T^*}(\gamma^{*\prime} - \gamma^*).$$

Equation 5·02(4) may then be written

$$\ddot{z} + \nu^2 z = 0.$$

The solution of this second-order differential equation is well known. It is the equation for a simple harmonic oscillator. Thus

$$z = A \sin \nu t.$$

That is, the parcel oscillates about its equilibrium level ($z = 0$) with the amplitude $A$ and the circular frequency $\nu$. The period $\tau$ or time required

for one complete oscillation is

$$\tau = \frac{2\pi}{\nu} = \frac{2\pi}{g}\sqrt{\frac{T^*}{\gamma^{*\prime} - \gamma^*}}. \tag{1}$$

Evidently the more stable the reference level is, the smaller the period will be. As an example let us find the period of oscillation in a dry isothermal layer. We then have $\gamma^* = 0$, $\gamma^{*\prime} = 1/c_{pd}$, so (1) becomes

$$\tau = \frac{2\pi}{g}\sqrt{c_{pd}T_0}.$$

If the temperature $T_0$ is 0°C, the period is 335 sec. However, since the lapse rate is usually nearer the dry-adiabatic lapse rate, the period of oscillation is in general much longer.

**5·07. Finite displacement.** So far we have characterized the stability of the reference level for an infinitesimal displacement. We shall now investigate the stability of an atmospheric layer for a finite displacement of a parcel from its reference level. As before, we shall assume that the parcel does not disturb the environment and does not mix with the environment. These two assumptions are physically contradictory. If the parcel is small enough not to disturb the environment, it will rapidly mix and lose its identity. On the other hand, if the parcel is large enough to retain its identity throughout a finite displacement, its motion will cause compensating currents in the environment. Nevertheless, it is useful to examine this fictitious case as a first approximation to the theory of convection. Later in section 5·09 we shall allow for compensating motion in the environment.

The analysis of section 5·01 holds for any level $\phi$ reached by the displaced parcel. Therefore the equation

$$\frac{dv_z}{dt} = g\frac{\alpha' - \alpha}{\alpha} \tag{5·01(1)}$$

is valid for the parcel even after it has been displaced through a finite vertical distance. When the acceleration on the left-hand side of this equation is multiplied by the height increment $dz$, we find

$$dz\frac{dv_z}{dt} = v_z dv_z = d\left(\frac{v_z^2}{2}\right). \tag{1}$$

This is the change of the kinetic energy per unit mass of the parcel while it moves through the height $dz$. When the buoyant force on the right-hand side is multiplied by $dz$, we find

$$\frac{\alpha' - \alpha}{\alpha} g dz = \frac{\alpha' - \alpha}{\alpha} d\phi = -(\alpha' - \alpha)dp = dA. \tag{2}$$

This is the work done by the buoyant force on unit mass of the parcel while it moves through the height $dz$. As shown in fig. 5·07, $dA$ is the area on an $(\alpha, -p)$-diagram (or any other equivalent-area diagram such as the tephigram or the emagram) of the isobaric strip $dp$ between the virtual temperature sounding curves $c^{*\prime}$, $c^*$ for the process and for the environment respectively.

Since the expressions (1) and (2) are equal, we have by integration

$$(3) \qquad \tfrac{1}{2}(v_{zb}^2 - v_{za}^2) = -\int_{p_a}^{p_b} (\alpha' - \alpha)dp = A.$$

Thus the change of kinetic energy for any part of the finite displacement is equal to the area $A$ between the pressures $p_a$ and $p_b$ at the limits of the displacement, as shown in fig. 5·07. The area $A$ is positive if the process curve $c^{*\prime}$ is warmer than the sounding curve $c^*$, and negative if the process curve is colder. Therefore when a parcel ascends through a colder environment its kinetic energy and, hence, its rate of ascent increase. And when a parcel ascends through a warmer environment its kinetic energy and rate of ascent decrease.

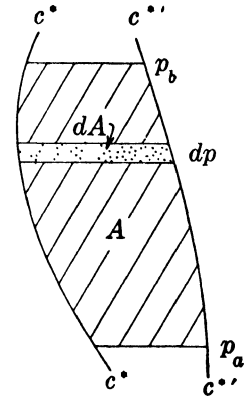



FIG. 5·07. Work performed on ascending parcel by buoyant force, shown on tephigram.

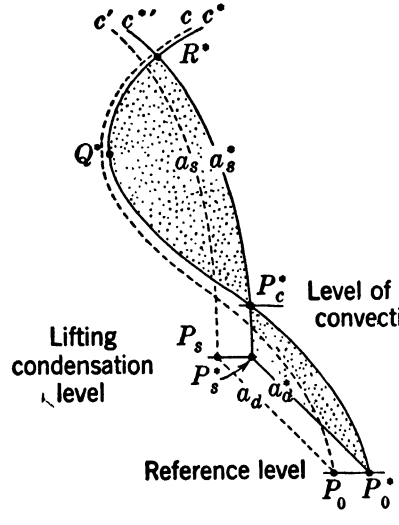



FIG. 5·08*a*. Latent instability, shown on tephigram.

**5·08. Latent instability.** We shall now examine the stability of a conditionally unstable layer with respect to a finite displacement. Fig. 5·08*a* shows such a layer schematically represented on a tephigram. Every level of the sounding curve $c^*$ from $P_0^*$ to $Q^*$ is conditionally unstable.

Consider the individual process curves $c'$, $c^{*\prime}$ of an unsaturated parcel displaced upward from the reference level $P_0$, $P_0^*$. The image point of the parcel will follow the dry adiabat $a_d$ upward from $P_0$ to the characteristic point $P_s$, where the parcel becomes saturated (see section 3·28).

The level where this point is reached is called the *lifting condensation level.* At the same time the virtual temperature image point of the parcel will follow the dry adiabat $a_d^*$ upward from $P_0^*$ to the virtual temperature characteristic point $P_s^*$. Since the sounding curve $c^*$ is conditionally unstable, the parcel ascends through warmer environment, so its kinetic energy and rate of ascent decrease. If the parcel did not receive a sufficiently strong impulse at the reference level to reach the level $P_s$, it would sink back toward the reference level. However, if the parcel is still ascending at the lifting condensation level, its image point will subsequently follow the saturation adiabat $a_s$ upward from $P_s$. At the same time its virtual temperature image point will follow the saturation adiabat $a_s^*$ upward from $P_s^*$.

Notice that the curves $c^*$, $c^{*\prime}$ intersect at the point $P_c^*$. The area $P_0^*P_s^*P_c^*$ represents the decrease of the parcel's kinetic energy during the ascent. If the kinetic energy of the initial impulse is less than this area, the parcel will sink back toward the reference level. But if the kinetic energy of the initial impulse is greater than this area, the parcel spontaneously will ascend beyond $P_c^*$ through a colder environment. Consequently the atmosphere is unstable with respect to the reference level if the initial impulse is strong enough for the parcel to reach the level $P_c^*$. This level is called the *level of free convection* with respect to the reference level. And the atmosphere above the level of free convection is said to be *latently unstable* with respect to the reference level (Normand, 1938).

Above the level of free convection the parcel will ascend through a colder environment and gain kinetic energy until it reaches the level $R^*$ where the curves $c^*$, $c^{*\prime}$ again intersect. The parcel will arrive at this level with kinetic energy equal to the area enclosed by the curves $c^*$, $c^{*\prime}$ plus the kinetic energy surplus at the level of free convection. At the expense of this energy it can penetrate into the stable region above $R^*$ until all its kinetic energy is consumed.

The level of free convection of a given reference level is determined by the point of intersection between the virtual temperature sounding curve and the saturation adiabat through the virtual temperature characteristic point. If the parcel is close to saturation at the reference level, the vertical distance to the lifting condensation level and also the distance to the level of free convection are small. So the kinetic energy of the initial impulse required to release the latent instability of the air at that level is also small. On the other hand, if the air at the reference level is far from saturation, the lifting condensation level is much higher and the corresponding saturation adiabat may not intersect the sounding curve, as indicated in fig. 5·08*b*. In this case no level of free convection and, hence, no latent instability exist with respect to the reference level.

The layers of latent instability, if any, are conveniently determined when both the virtual temperature sounding curve and the virtual temperature characteristic curve are plotted, as shown in fig. 5·08*c*. The *virtual temperature characteristic curve* $c_s^*$ connects the virtual temperature characteristic points $P_s^*$ corresponding to each point $P^*$ of

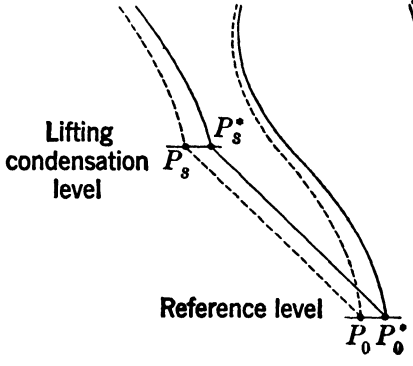



FIG. 5·08*b*.

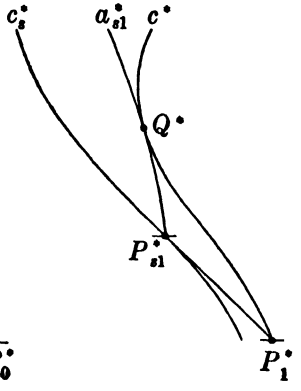



FIG. 5·08*c*.

$c^*$. The layer of latent instability is determined by the point $Q^*$ on $c^*$ at which a saturation adiabat is tangent. This saturation adiabat intersects the virtual temperature characteristic curve at some point $P_{s1}^*$ corresponding to the reference level $P_1^*$. Latent instability exists for all levels below the level $P_1^*$, for the saturation adiabats corresponding to these levels intersect the sounding curve $c^*$. However, latent instability does not exist for any level above the level $P_1^*$, for the corresponding saturation adiabats do not intersect the sounding curve $c^*$.

**5·09. The slice method.** One shortcoming of the parcel method is that the effect of compensating motion of the environment is neglected. We shall now allow for this effect by considering an extended region of the atmosphere at a given reference level. The method for studying such a region was first developed by J. Bjerknes (1933) and is called the slice method.

Let the region initially be completely saturated and also be homogeneous in all thermodynamic properties at any level near the reference level $\phi_0$. Within the region there may be several columns of ascending motion. In the remaining part of the region the air surrounding these columns will have a compensating downward motion, as indicated in fig. 5·09*a*. Let the total area with ascending motion be $A'$ and the average speed of ascent be $v_z'$. And let the total area with descending motion be $A$ and the average speed of descent be $v_z$. We shall further assume

that the mass ascending through the reference level $\phi_0$ in the time interval $dt$ is equal to the mass descending through $\phi_0$ in the same time interval.

These assumptions represent a simplified model of the atmosphere at a level of initial cumulus development. The ascending air will form clouds by saturation-adiabatic condensation. And the ascending motion in the cloud columns is compensated by descending motion in the sur-

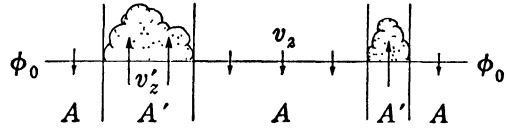



FIG. 5·09*a*.

rounding air. The atmosphere at the reference level $\phi_0$ will be called *stable* if the cumulus growth is retarded, *indifferent* if the cumulus growth is neither retarded nor accelerated, and *unstable* if the cumulus growth is accelerated.

In the time interval $dt$ an atmospheric slice of area $A$ and height $dz = v_z dt$ will be transported downward through the reference level. The volume of this slice is $dV = Adz$ and its mass is

$$dM = \rho A v_z dt = \rho A dz. \tag{1}$$

Substituting here $dz = d\phi/g$ and subsequently $\rho d\phi = -dp$, we have

$$dM = \frac{\rho A d\phi}{g} = -\frac{A dp}{g}. \tag{2}$$

The mass of the ascending slice may be obtained by a similar argument. Thus $dM'$ is given by equations similar to (1, 2) wherein symbols referring specifically to the ascending slice are primed.

Initially the thermodynamic properties are homogeneous throughout the reference level, so $\rho' = \rho$. Therefore, from (1, 2), the initial ratio $dM'/dM$ is equal to any one of the following expressions:

$$\frac{dM'}{dM} = \frac{A'v_z'}{Av_z} = \frac{A'dz'}{Adz} = \frac{A'd\phi'}{Ad\phi} = \frac{A'dp'}{Adp}.$$

Since the upward and downward transports of mass through $\phi_0$ are assumed equal, $dM' = dM$. Accordingly, we have from the above equations

$$\frac{A'}{A} = \frac{v_z}{v_z'} = \frac{dz}{dz'} = \frac{d\phi}{d\phi'} = \frac{dp}{dp'}. \tag{3}$$

For simplicity we shall assume that there is no horizontal advection

within the region, so local temperature changes must be caused entirely by vertical motion. As in the previous sections the individual temperature changes may be considered adiabatic. Consequently the ascending air will be cooled saturation-adiabatically, whereas the descending air will be heated dry-adiabatically. The individual lapse rate in the columns of ascending air is then $\gamma_s$, and the individual lapse rate in the descending air surrounding the cloud columns is $\gamma_d$.

So far nothing has been implied as to the distribution of temperature near the reference level except that the lapse rate $\gamma$ is the same both in the cloud columns and in the surrounding air. Although the analysis can be carried through for any value of $\gamma$, the most interesting case occurs when the reference level is conditionally unstable, that is, when $\gamma_d > \gamma > \gamma_s$. The following analysis will be confined to this case.

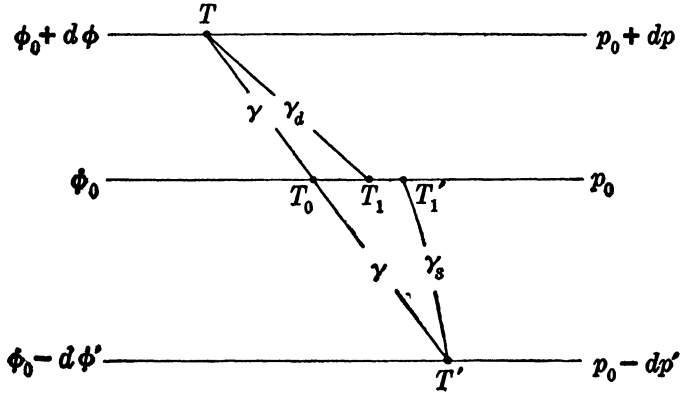



FIG. 5·09*b*.

As shown in fig. 5·09*b*, the sinking air which started from the level $\phi_0 + d\phi$ with the initial temperature $T = T_0 - \gamma d\phi$ descends dry-adiabatically and arrives at the reference level $\phi_0$ with the temperature

$$T_1 = T + \gamma_d d\phi = T_0 + (\gamma_d - \gamma)d\phi. \tag{4}$$

Since $\gamma_d > \gamma$, $T_1 > T_0$. Therefore at the reference level the region $A$ becomes warmer owing to the subsidence.

During the same time interval the ascending air which started from the level $\phi_0 - d\phi'$ with the initial temperature $T' = T_0 + \gamma d\phi'$ cools saturation-adiabatically and arrives at the reference level with the temperature

$$T_1' = T' - \gamma_s d\phi' = T_0 + (\gamma - \gamma_s)d\phi'. \tag{5}$$

Since $\gamma > \gamma_s$, $T_1' > T_0$. Therefore at the reference level the region $A'$ becomes warmer owing to release of latent heat.

As in the parcel method, the stability is determined by the buoyancy of the cloud columns relative to the surrounding air. Since both regions are initially saturated and at the same pressure, the buoyancy depends only upon the temperatures $T_1'$ and $T_1$. The atmosphere at the reference level is stable, indifferent, or unstable according to the following three conditions, read respectively from top to bottom:

$$T_1' \lesseqgtr T_1. \tag{6}$$

From (3) we have $d\phi \sim A'$ and $d\phi' \sim A$. Therefore, when equations (4, 5) are substituted in (6), the three stability conditions may be written

$$A(\gamma - \gamma_s) \lesseqgtr A'(\gamma_d - \gamma). \tag{7}$$

A useful form of (7) is obtained by evaluating the lapse rate $\gamma_i$ for which the convection is indifferent. This critical lapse rate is the weighted average of the lapse rates $\gamma_d$, $\gamma_s$. Thus

$$\gamma_i = \frac{A'\gamma_d + A\gamma_s}{A' + A}. \tag{8}$$

The final form of the three stability conditions is simply expressed in terms of the critical lapse rate $\gamma_i$ as follows:

$$\gamma \lesseqgtr \gamma_i. \tag{9}$$

This form of the stability conditions for the slice method is similar to the form of the stability conditions for the parcel method. However, in the parcel method the critical lapse rate is $\gamma_d$ if the air is unsaturated, and it is $\gamma_s$ if the air is saturated. Equation (8) shows that when the air is conditionally unstable the critical lapse rate for the slice method lies between these two extremes; that is, $\gamma_d > \gamma_i > \gamma_s$.

Evidently the slice method can be more generally applied than the parcel method. Indeed, the results of the parcel method may be obtained as special cases of the slice method. Let the area of the region $A' + A$ be constant. Then, as $A' \to 0$, each finite ascending column contracts into an infinitesimal filament ascending saturation-adiabatically through an undisturbed environment, and from (8) $\gamma_i \to \gamma_s$. As $A \to 0$, the finite descending region becomes an infinitesimal filament descending dry-adiabatically through an undisturbed environment, and from (8) $\gamma_i \to \gamma_d$. Therefore, since the lapse rate $\gamma$ of the region lies between $\gamma_s$ and $\gamma_d$, the cumulus convection is accelerated ($\gamma > \gamma_i$) if the areal ratio $A'/A$ is small enough. And the cumulus convection is retarded ($\gamma < \gamma_i$) if the reciprocal ratio $A/A'$ is small enough.

So far we have assumed that the regions of ascending and descending motion are given. Actually the extent of these regions can be deter-

mined only after the cumulus development starts. A perturbation with sufficiently narrow columns in an initially saturated reference level would be unstable. Moreover, the perturbation is more unstable, the narrower the columns. However, a very narrow ascending air column would rapidly be destroyed by turbulent mixing. Therefore the ascending columns must have a certain finite minimum cross section in order to *maintain* the upward convection. The column cross section actually selected by the perturbation must be small enough to be unstable and yet large enough not to be destroyed by the consequent convection.

As shown in fig. 5·09*b* the instability is insured by $T_1' > T_1$. The difference $T_1' - T_1$ required to maintain unstable convection may be quite small, whereas the difference $T_1 - T_0$ may be comparatively large. The effect of such convection would be to heat the reference level and all subsequent levels reached by the convective columns. This heating is supplied by release of latent heat of condensation in the ascending air and by subsidence in the descending air. Since all levels reached by the convection are heated, *heat is transported upward by the convective process.* This process is the most important means of transporting heat upward in the troposphere.

At the highest levels reached by the convection the heat is distributed horizontally from the tops of the ascending columns. The heat which is transported downward to the levels below by subsidence is thereby continually replenished by the latent heat released at the top of the convective region. Accordingly, the heating of the entire region affected by the convection is ultimately supplied by the latent heat of condensation released by the upward convection.

**5·10. Formulas for $\gamma_u$ and $\gamma_s$.** In section 5·03 certain unsaturated and saturated process lapse rates $\gamma_u$ and $\gamma_s$ were defined. For the purpose of estimating stability $\gamma_u$ can be closely enough approximated by $\gamma_d$, and $\gamma_s$ can be well enough estimated from a diagram. For other purposes, however, it is important to have exact formulas for these lapse rates. These will now be derived.

The adiabatic process for unsaturated air is given by

2·24(3) $$0 = c_p dT - \alpha dp,$$

where $c_p = c_{pd}(1 + 0.90w)$ is the specific heat of moist air at constant pressure. As in 5·03, the individual change of dynamic height is given by the hydrostatic equation: $d\phi = -\alpha dp$. Hence we have

(1) $$\gamma_u = -\frac{dT}{d\phi} = \frac{1}{c_p}.$$

This formula shows that when $w = 0$, $\gamma_u$ reduces to $1/c_{pd}$, i.e., to $\gamma_d$. See 4·20(3).

The value of $\gamma_s$ at any point in the atmosphere depends on which of the saturation-adiabatic processes (see 3·31, 3·32, 3·34) the lifted air parcel is presumed to follow. We shall give the formula for the pseudo-adiabatic process. According to 3·31(4) this process is described by the equation

$$-Ldw_s = (1 + w_s)(c_p dT - \alpha dp). \tag{2}$$

In order to evaluate $\gamma_s$, we must first express $dw_s$ in terms of $dT$ and $dp$. We note from 3·20(4) that

$$w_s = \frac{\epsilon e_s}{p - e_s}. \tag{3}$$

Differentiating (3) logarithmically, we find after collecting terms that

$$\frac{dw_s}{w_s} = \frac{p}{p - e_s}\left(\frac{de_s}{e_s} - \frac{dp}{p}\right). \tag{4}$$

But from (3) we see that

$$\frac{p}{p - e_s} = 1 + \frac{w_s}{\epsilon} = 1 + 1.61w_s. \tag{5}$$

Substituting (5) and Clapeyron's equation 3·11(4) into (4), we get

$$\frac{dw_s}{w_s} = (1 + 1.61w_s)\left(\frac{\epsilon L}{R_d}\frac{dT}{T^2} - \frac{dp}{p}\right).$$

This may be transformed further by noting that $R = R_d(1 + 0.61w_s)$:

$$\frac{dw_s}{w_s} = \frac{1 + 1.61w_s}{1 + 0.61w_s} \cdot \frac{1}{R_d T}\left[\frac{\epsilon L(1 + 0.61w_s)}{T} dT - \frac{RT}{p} dp\right].$$

When we simplify the right-hand side and use $p\alpha = RT$, we get

$$\frac{dw_s}{w_s} = \frac{(1 + w_s)}{R_d T}\left[\frac{\epsilon L(1 + 0.61w_s)}{T} dT - \alpha dp\right]. \tag{6}$$

This is the second relation between $dw_s$, $dp$, and $dT$ referred to in section 3·33. By putting (6) into (2), canceling $(1 + w_s)$, and collecting terms, we get

$$\left[c_p + \frac{Lw_s}{R_d T}\frac{\epsilon L(1 + 0.61w_s)}{T}\right] dT - \left[1 + \frac{Lw_s}{R_d T}\right] \alpha dp = 0.$$

We substitute $d\phi = -\alpha dp$, and introduce two abbreviations:

$$\mu = \frac{Lw_s}{R_d T}, \qquad \nu = \frac{\epsilon L(1 + 0.61w_s)}{c_p T} = \frac{\epsilon L}{c_{pd}(1 + 0.29w_s)T}. \tag{7}$$

We then get

$$-c_p \frac{dT}{d\phi} = \frac{1+\mu}{1+\mu\nu}. \tag{8}$$

Now $\gamma_s = -dT/d\phi$; and $1/\gamma_u = c_p$, by (1). Hence $-c_p(dT/d\phi) = \gamma_s/\gamma_u$. This ratio is denoted by $n$:

$$n = \frac{\gamma_s}{\gamma_u}. \tag{9}$$

We then get from (8) and (9):

$$n = \frac{1+\mu}{1+\mu\nu} \qquad \gamma_s = n\gamma_u. \tag{10}$$

This formula (10) is the desired formula expressing $\gamma_s$ in terms of the known meteorological variables of (1) and (7).

From (10) we may compute $n$ and hence $\gamma_s$ at any point on a diagram. It is seen that $0 < n < 1$. A typical value of $n$ for the lower troposphere is that determined for the state $T = 275°K$, $p = 90$ cb, where $w_s = 5 \times 10^{-3}$. From (7) we obtain $\mu = 0.159$, $\nu = 5.62$, whence from (10) $n = 0.61$. This corresponds to $\gamma_s = 0.00061$. This is a temperature drop of approximately 6°C per kilometer rise, which is accordingly used as a value of the saturation-adiabatic lapse rate for many rough calculations. The minimum value of $\gamma_s$ found in the atmosphere may be estimated as that at $T = 309°K$, $p = 100$ cb, $w_s = 40 \times 10^{-3}$, for which we compute $\gamma_s = 0.000325$.

Formula (10) is valid for either the rain stage or the snow stage of the pseudo-adiabatic process (see 3·30). The only difference is that in the snow stage the latent heat $L$ of evaporation in (7) should be replaced by the latent heat $L_{iv}$ of sublimation.

**5·11. Rate of precipitation.** A useful application of the saturation-adiabatic lapse rate is the evaluation of the amount of precipitation which falls from an ascending saturated layer. The assumption is made that the process is pseudo-adiabatic (see 3·30), so that *all* the condensed water falls out as precipitation. The method, given below, of finding the rate of precipitation was developed by Fulks (1935).

Consider a saturated sample of air containing one ton of dry air. It will contain $w_s$ tons of water vapor and thus its total mass is $(1 + w_s)$ tons. If this mass is lifted one meter, $-dw_s/dz$ tons of vapor will be condensed. *The amount of precipitation per ton of saturated air when lifted one meter* is therefore

$$-\frac{1}{1+w_s}\frac{dw_s}{dz}. \tag{1}$$

Consider next a vertical column of saturated air having the cross-sectional area of one square meter and the dynamic height of one dynamic decimeter. The volume of this column is $1/g$ cubic meters, and its mass is $\rho/g = 1/(\alpha g)$ tons. Let $P'$ be the number of tons of precipitation from this column when it is lifted one meter. From (1) we then have:

$$P' = -\frac{1}{(1+w_s)\alpha g}\frac{dw_s}{dz} = -\frac{1}{(1+w_s)\alpha}\frac{dw_s}{d\phi}. \tag{2}$$

To evaluate $dw_s/d\phi$ we divide 5·10(2) by $d\phi$:

$$-L\frac{dw_s}{d\phi} = (1+w_s)\left(c_p\frac{dT}{d\phi} - \alpha\frac{dp}{d\phi}\right). \tag{3}$$

By using $d\phi = -\alpha dp$, and $n = -c_p(dT/d\phi)$ from 5·10(9), we can solve (3) for $-dw_s/d\phi$:

$$-\frac{dw_s}{d\phi} = (1+w_s)\frac{(1-n)}{L}. \tag{4}$$

From (2) and (4) we get the final formula for $P'$:

$$P' = \frac{1-n}{\alpha L}, \tag{5}$$

where $n$ is given explicitly by 5·10(10). As a dimensional check of (5), we note that $P'$ is defined to be a mass, per dynamic unit column expressed in (meters)$^2$ × dynamic decimeters, per meter lift. Hence we should have

$$[P'] = \frac{[\mathrm{M}]}{[\mathrm{L}^2]\cdot[\mathrm{L}^2\,\mathrm{T}^{-2}]\cdot[\mathrm{L}]} = [\mathrm{ML}^{-5}\,\mathrm{T}^2].$$

The right side of (5) has these dimensions, since $n$ is a pure number.

We now define $P$ to be the rate of precipitation in millimeters per hour from a saturated layer 100 dyn m thick ascending at the speed of one meter per second. Obviously $P$ is independent of the area of the surface on which the precipitation falls, so we shall consider one square meter on the ground. Above this area are 1000 columns like that of the previous discussion. In one second they will rise one meter, and each will drop $P'$ tons of precipitation. In one hour they would at the same rate collectively provide $3.6 \times 10^6\, P'$ tons of precipitation. One ton of water in a unit column will have a height of one meter, or 1000 mm. Consequently, in one hour this 100-dyn m layer will give $3.6 \times 10^9\, P'$ mm of precipitation. We thus have from (5):

$$P = 3.6 \times 10^9 \frac{1-n}{\alpha L}\ \mathrm{mm\ hr^{-1}}. \tag{6}$$

Formula (6) is the practical form of the precipitation equation. In general, if the saturated layer were $\Delta H$ dynamic meters thick, rising at the speed of $v_z$ meters per second, then the rate of precipitation would be

$$\frac{v_z \Delta H}{100} P \text{ mm hr}^{-1}. \tag{7}$$

For the snow stage $L$ in (6) should be replaced by $L_{sv}$.

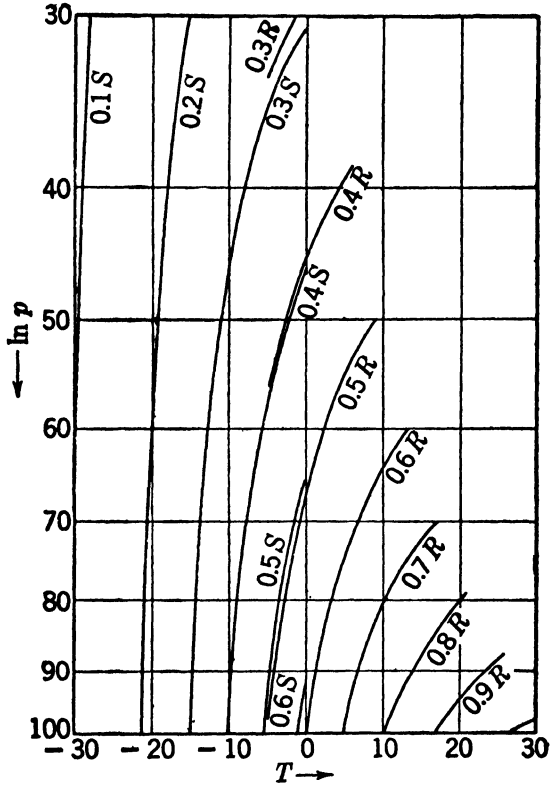



FIG. 5·12. Precipitation lines on emagram.

**5·12. Precipitation lines on the emagram.** Since both $n$ and $\alpha$ in 5·11(6) depend only on $p$ and $T$, it is possible to draw lines of constant $P$ on any thermodynamic diagram. They are shown in fig. 5·12 on an emagram, and the value of $P$ is given for each line. There are two separate families of lines. Those marked with $R$ are for the rain stage. Those marked $S$ are for the snow stage. Both sets of lines are due to Fulks.

We give a simple example of the use of the precipitation lines. Let us

suppose that a saturated isothermal layer extends between the pressure levels 900 mb and 600 mb. The temperature of the layer is 10°C, and it is known to have the vertical velocity 0.3 m $s^{-1}$. It is desired to estimate the resulting rainfall in millimeters per hour.

We break the layer up into the three sublayers 900–800 mb, 800–700 mb, and 700–600 mb. For each layer we perform the following calculations: (i) We determine its thickness $\Delta H$ in dynamic meters using any convenient method; (ii) we determine the value of $P$ at the midpoint of the sublayer from the precipitation lines; (iii) we determine the precipitation from that sublayer using formula 5·11(7). The resulting figures in (iii) are then added, to give the total rainfall in millimeters per hour. The calculation is summarized in the following table.

| Sublayer | $v_z$ (m $s^{-1}$) | $\Delta H$ (dyn m) | $P$ | $\frac{v_z \Delta H}{100} P$ |
|---|---|---|---|---|
| 900–800 mb | 0.3 | 960 | 0.72 | 2.1 |
| 800–700 mb | 0.3 | 1090 | 0.67 | 2.2 |
| 700–600 mb | 0.3 | 1250 | 0.60 | 2.3 |
| | | Total rainfall in mm $hr^{-1}$ = | | 6.6 |

In practice the determination of $v_z$ is quite difficult, and it limits the accuracy of the whole procedure. There is consequently little need of much accuracy in the determination of either $\Delta H$ or $P$.

CHAPTER SIX

# THE EQUATION OF MOTION

**6·01. Kinematics.** In chapter 4 we examined the atmosphere in a state of relative or hydrostatic equilibrium. That is, we considered the atmosphere when it is rotating with the earth. We know from experience that motion in the free atmosphere is much more complicated. In order to investigate this more complicated motion we must advert to kinematic and dynamic concepts.

The description of motion is called kinematics. Consider a moving point. Let its position $P$ be described from a reference frame which we may think of as a Cartesian coordinate system centered at some point $O$. $P$ is then specified by a coordinate triple $(x,y,z)$.

However, another and equivalent way of representing $P$ is to draw the directed vector length from $O$ to $P$. This vector is called the *position vector* of $P$ and is symbolized by $\mathbf{r}$. The $x,y,z$ components of $\mathbf{r}$ are merely the distances $x,y,z$. Hence

$$\mathbf{r} = x\mathbf{i} + y\mathbf{j} + z\mathbf{k}. \tag{1}$$

Here $\mathbf{i},\mathbf{j},\mathbf{k}$ may represent any set of rectangular unit vectors. In later applications we shall let $\mathbf{i},\mathbf{j},\mathbf{k}$ represent the standard system defined in 4·03.

**6·02. Velocity.** As the point moves along the path $c$ shown in fig. 6·02, it occupies different positions at different times. At the time $t$ let its position be $P$ and its position vector be $\mathbf{r} = \mathbf{r}(t)$. At the later time $t_1 = t + \Delta t$ let its position be $P_1$ and its position vector be $\mathbf{r}_1 = \mathbf{r}(t + \Delta t)$. Corresponding to the time difference $\Delta t = t_1 - t$, the position vector difference may be denoted by $\Delta\mathbf{r} = \mathbf{r}_1 - \mathbf{r}$. Since the vector difference $\mathbf{r}_1 - \mathbf{r}$ is the vector from the terminus of $\mathbf{r}$ to the terminus of $\mathbf{r}_1$, $\Delta\mathbf{r}$ is the vector from $P$ to $P_1$.

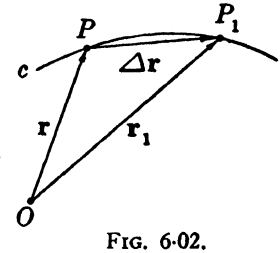


FIG. 6·02.

The quotient $\Delta\mathbf{r}/\Delta t$ is also a vector. It has the same direction and sense as $\Delta\mathbf{r}$. As the time increment becomes smaller, $P$ will approach $P_1$, and the quotient will approach a limiting value. This limiting value is defined to be the

velocity at $P$, and will be denoted by $\mathbf{v}$. We then have

$$\mathbf{v} = \lim_{t_1 \to t} \frac{\mathbf{r}_1 - \mathbf{r}}{t_1 - t} = \lim_{\Delta t \to 0} \frac{\Delta \mathbf{r}}{\Delta t}. \tag{1}$$

This vector limiting process is quite analogous to the familiar scalar process of differentiation. Hence the usual symbols for derivatives may be extended to vectors. So we may write

$$\mathbf{v} = \frac{d\mathbf{r}}{dt} = \dot{\mathbf{r}}, \tag{2}$$

where the dot placed above a symbol is equivalent to the operation $d/dt$ upon that symbol. We shall continue to use the differentiation symbol $d$ as we have used it here: *to denote variation with respect to a designated or individual point.*

The approach of $P_1$ to $P$ along the path $c$ not only defines the velocity, but also defines the tangent line to the path. Consequently the velocity must be along the tangent. We shall call the unit vector along the path in the direction of the motion the *unit tangent* and denote it by $\mathbf{t}$. Let $s$ represent a linear coordinate along the path, so that $ds = |d\mathbf{r}|$. The unit tangent is then defined by

$$\mathbf{t} = \frac{d\mathbf{r}}{|d\mathbf{r}|} = \frac{d\mathbf{r}}{ds}.$$

Since the unit tangent is the unit vector along the velocity, we have $\mathbf{v} = v\mathbf{t}$, where the numerical value of the velocity, called the *speed*, is

$$v = |\mathbf{v}| = \left|\frac{d\mathbf{r}}{dt}\right| = \frac{ds}{dt}. \tag{3}$$

The rectangular components of the velocity may be obtained by substituting the rectangular components of $\mathbf{r}_1$ and $\mathbf{r}$ into (1) and finding the limit. Since $\mathbf{i}$, $\mathbf{j}$, $\mathbf{k}$ are vectors fixed in the coordinate frame, the rate of change of the position vector may be expressed in terms of the rates of change of its components as follows:

$$\dot{\mathbf{r}} = \dot{x}\mathbf{i} + \dot{y}\mathbf{j} + \dot{z}\mathbf{k}.$$

Therefore the rectangular components of the vector derivative of a position vector are the scalar derivatives of the rectangular components of the position vector.

**6·03. Differentiation of a vector.** Any vector $\mathbf{a}$ which is a continuous single-valued function of the scalar variable $u$ may be represented as a position vector. Let the vector $\mathbf{a}$ be drawn from a given origin $O$.

As the variable $u$ increases, the terminus of $\mathbf{a}$ traces a continuous curve, called the *terminal curve*, similar to the path traced by the terminus of the position vector.

The vector derivative of $\mathbf{a} = \mathbf{a}(u)$ is defined as

$$\frac{d\mathbf{a}}{du} = \lim_{u_1 \to u} \frac{\mathbf{a}_1 - \mathbf{a}}{u_1 - u} = \lim_{\Delta u \to 0} \frac{\Delta \mathbf{a}}{\Delta u}, \tag{1}$$

where $u_1 = u + \Delta u$ and $\mathbf{a}_1 = \mathbf{a}(u + \Delta u)$. Evidently by definition $d\mathbf{a}/du$ is tangent to the terminal curve. Thus the derivative of a vector is easily visualized when the vector is represented as a position vector and the terminal curve is drawn.

By expanding $\mathbf{a}_1$ and $\mathbf{a}$ into rectangular components we get for the rectangular components of the derivative:

$$\frac{d\mathbf{a}}{du} = \frac{da_x}{du}\mathbf{i} + \frac{da_y}{du}\mathbf{j} + \frac{da_z}{du}\mathbf{k}. \tag{2}$$

Therefore the rectangular components of the vector derivative of $\mathbf{a}$ are the scalar derivatives of the rectangular components of $\mathbf{a}$.

The rules for differentiating functions, sums, and products involving vectors correspond to the rules for differentiating functions, sums, and products of scalars. That is,

$$\frac{d\mathbf{a}}{du} = \frac{d\mathbf{a}}{dw}\frac{dw}{du}, \qquad w = w(u), \tag{3}$$

$$\frac{d}{du}(\mathbf{a} + \mathbf{b}) = \frac{d\mathbf{a}}{du} + \frac{d\mathbf{b}}{du}, \tag{4}$$

$$\frac{d}{du}(\epsilon\mathbf{a}) = \frac{d\epsilon}{du}\mathbf{a} + \epsilon\frac{d\mathbf{a}}{du}, \tag{5}$$

$$\frac{d}{du}(\mathbf{a}\cdot\mathbf{b}) = \frac{d\mathbf{a}}{du}\cdot\mathbf{b} + \mathbf{a}\cdot\frac{d\mathbf{b}}{du}. \tag{6}$$

These rules are easily verified either by writing the derivatives as limits, according to (1), or by resolving the vectors into rectangular components and applying (2).

The rule (6) can be used to show that the derivative of a unit vector is normal to that vector. For differentiation of $\mathbf{a}\cdot\mathbf{a} = 1$ gives

$$\frac{d\mathbf{a}}{du}\cdot\mathbf{a} + \mathbf{a}\cdot\frac{d\mathbf{a}}{du} = 2\mathbf{a}\cdot\frac{d\mathbf{a}}{du} = 0.$$

This result could be anticipated geometrically, for the terminal curve of a unit vector is constrained to lie on the surface of a unit sphere. Since

$d\mathbf{a}/du$ is tangent to this terminal curve and consequently tangent to the sphere, it must be normal to $\mathbf{a}$.

All the definitions and results of this section also apply to partial derivatives symbolized by $\partial/\partial u$.

**6·04. Acceleration.** The position of a moving point has been described by the position vector $\mathbf{r} = \mathbf{r}(t)$ issuing from an origin $O$. As time passes, the terminal point of the position vector moves along the path $c$ with the velocity $\mathbf{v} = \mathbf{v}(t)$.

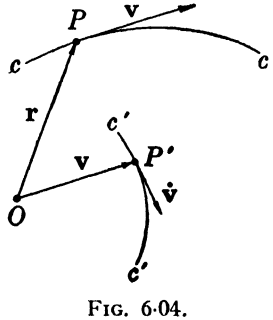


FIG. 6·04.

A clear picture of the variation of the velocity is obtained by transferring the origin of the vector $\mathbf{v}$ from the path point $P$ to the origin $O$, as shown in fig. 6·04. The terminal point $P'$ of the transferred velocity vector is called the *image point*. As time passes, this image point traces a terminal curve $c'$ called the *hodograph* of the velocity. To each instant $t$ there corresponds a definite point $P$ on the path $c$ and a definite image point $P'$ on the hodograph $c'$. $P$ represents the position of the moving point and $P'$ represents its velocity.

The velocity of a point is the individual rate of change $\dot{\mathbf{r}}$ of the position vector. The individual rate of change of the velocity $\dot{\mathbf{v}} = d\mathbf{v}/dt$ will be called the acceleration of the point. The acceleration is readily obtained from the hodograph. For, as shown in the figure, the point $P$ moves with the velocity $\dot{\mathbf{r}}$ along the path $c$ traced by $\mathbf{r}$. And the image point $P'$ moves with the velocity $\dot{\mathbf{v}}$ along the hodograph $c'$ traced by $\mathbf{v}$. Accordingly, *the acceleration of a moving point along the path is equal to the velocity of the image point along the hodograph.*

From 6·03(2) the rectangular components of the acceleration are given by

$$\dot{\mathbf{v}} = \dot{v}_x\mathbf{i} + \dot{v}_y\mathbf{j} + \dot{v}_z\mathbf{k}. \tag{1}$$

In the next section we shall derive another and more useful expression for the acceleration.

**6·05. Curvature.** When the relation $\mathbf{v} = v\mathbf{t}$ is differentiated we find

$$\dot{\mathbf{v}} = \dot{v}\mathbf{t} + v\dot{\mathbf{t}}. \tag{1}$$

Since the derivative of a unit vector is normal to that vector, $\dot{\mathbf{t}}$ and $\mathbf{t}$ are perpendicular. Consequently the acceleration has here been split into components tangential and normal to the path. We shall call the unit vector along the derivative of the unit tangent the *unit normal* and

denote it by **N**. That is,

$$\mathbf{N} = \frac{d\mathbf{t}}{|d\mathbf{t}|}. \tag{2}$$

All the normals to the unit tangent lie in the plane perpendicular to the path. To find the direction of the unit normal at a point $P$ on the path, we must examine the motion along the path in the neighborhood of $P$.

Suppose that the unit tangent $\mathbf{t}$ is drawn at $P$ as in fig. 6·05*a*. Let us select another point $P_1$ near $P$ and draw the unit tangent $\mathbf{t}_1$ at that point. The vectors $\mathbf{t}$ and $\mathbf{t}_1$ are of unit length. Therefore, as $P_1 \to P$, the length of the vector $\Delta\mathbf{t} = \mathbf{t}_1 - \mathbf{t}$ becomes numerically equal to the angle $\Delta\psi$ between $\mathbf{t}$ and $\mathbf{t}_1$. Thus

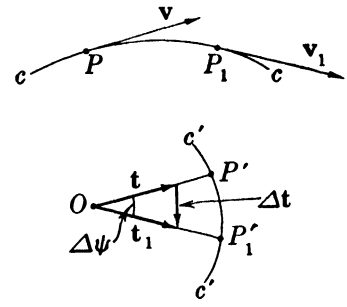



FIG. 6·05*a*.

$$\frac{|d\mathbf{t}|}{d\psi} = 1. \tag{3}$$

The rate of change of the unit tangent may be expressed by means of (2), (3), and 6·02(3) as

$$\dot{\mathbf{t}} = \frac{d\mathbf{t}}{dt} = \frac{d\mathbf{t}}{|d\mathbf{t}|}\frac{|d\mathbf{t}|}{d\psi}\frac{d\psi}{ds}\frac{ds}{dt} = \mathbf{N}\cdot 1\cdot K\cdot v, \tag{4}$$

where $K = d\psi/ds$ is called the *curvature* of the path $c$ at $P$. Curvature is a geometric rather than a kinematic concept: it is measured by the angular turn $\Delta\psi$ of the tangent through the arc length $\Delta s$. That is, the curvature of a curve at a point $P$ on the curve is defined as

$$K = \lim_{P_1 \to P} \frac{\Delta\psi}{\Delta s} = \frac{d\psi}{ds}. \tag{5}$$

Evidently this formal definition corresponds to the intuitive notion of curvature. For instance, as shown in fig. 6·05*b*, the curvature of a circle of radius $R$ is

$$K = \frac{d\psi}{ds} = \frac{d\psi}{Rd\psi} = \frac{1}{R}.$$

This result is important: *The curvature of a circle is the reciprocal of the radius of that circle.* A straight line may be regarded as a circle of infinite radius having zero curvature.

The path in the neighborhood of $P$ may always be replaced by a circle

having the same curvature as the path. Before constructing this circle let us first consider the construction of the tangent line at $P$. Choose a point $P_1$ on the path $c$ near $P$. The two points $P$ and $P_1$ determine a straight line. As $P_1 \to P$ this line approaches a limiting line tangent to the path at $P$.

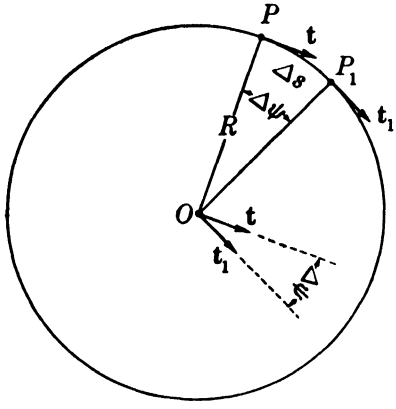



FIG. 6·05*b*. Curvature of a circle.

Consider now two distinct points, $P_1$ and $P_2$, on the path $c$ near $P$. The three points $P$, $P_1$, $P_2$ determine a circle. As $P_2 \to P_1 \to P$ this circle approaches a limiting circle called the *circle of curvature* to the path at $P$. The plane of this circle is called the *osculating plane.*

Suppose that the path contains the three points in the order $P$, $P_1$, $P_2$. The unit tangent $\mathbf{t}_1$ is defined by the approach of $P_2$ to $P_1$, and the unit tangent $\mathbf{t}$ by the approach of $P_1$ to $P$. Consequently, as $P_2 \to P_1 \to P$, $\mathbf{t}_1$ and $\mathbf{t}$ become coplanar with the osculating plane. Since both unit tangents are along the path, their difference is directed toward the center of the circle of curvature. This center will be called more briefly the *center of curvature.*

As $P_2 \to P_1 \to P$ the unit tangents $\mathbf{t}_1$ and $\mathbf{t}$ define the curvature of the path and also the curvature of the circle of curvature. Hence both curvatures are the same. Accordingly

$$K = \frac{1}{R}, \tag{6}$$

where $K$ is the curvature of the path, and $R$, called the *radius of curvature*, is the radius of the circle of curvature.

When the expression (4) for the rate of change of the unit tangent is substituted in (1), we find

$$\dot{\mathbf{v}} = \dot{v}\mathbf{t} + v^2 K\mathbf{N}.$$

The tangential component of the acceleration is called the *tangential acceleration.* It is numerically equal to the rate of change of the speed. Accordingly *a moving point speeds up or slows down only in the direction of motion.* Notice that $\dot{v}$ is not the magnitude of the acceleration.

The normal component of the acceleration is called the *centripetal acceleration*, for it is directed toward the center of curvature. The vector $\mathbf{K}$ of magnitude $K$ and directed toward the center of curvature will

be called the *vector curvature*. Thus, $\mathbf{K} = K\mathbf{N}$. Accordingly the centripetal acceleration is $v^2\mathbf{K}$.

The centripetal acceleration may be expressed in another form by extending the notion of angular speed from the rate of angular rotation along a fixed circle to the rate of angular rotation along the osculating circle. This generalized or instantaneous *angular speed*, denoted by $\omega$, is defined as

$$\omega = \frac{d\psi}{dt}. \tag{7}$$

As a consequence of this definition

$$v = \frac{ds}{dt} = \frac{ds}{d\psi}\frac{d\psi}{dt} = \frac{\omega}{K} = \omega R. \tag{8}$$

The vector $\mathbf{R}$ of magnitude $R$ and directed away from the center of curvature will be called the *vector radius of curvature*. Thus $\mathbf{R} = -R\mathbf{N}$. So the centripetal acceleration is $-\omega^2\mathbf{R}$.

When the centripetal acceleration is expressed by $v^2\mathbf{K}$ or $-\omega^2\mathbf{R}$, the acceleration becomes

$$\dot{\mathbf{v}} = \dot{v}\mathbf{t} + v^2\mathbf{K}, \tag{9}$$

$$\dot{\mathbf{v}} = \dot{v}\mathbf{t} - \omega^2\mathbf{R}, \tag{10}$$

respectively.

The unit tangent and the unit normal constitute an orthogonal system in which the expressions for velocity and acceleration are particularly simple. Any system so intimately connected with the motion will be called a *natural system*. And metric coordinates along the unit vectors of a natural system will be called *natural coordinates*. We shall make extensive use of such coordinates in the following.

**6·06. Reference frames.** Let us denote by $F$ the reference frame from which the motion of a point is described. The operations by which the position vector, the velocity, and the acceleration of the point have been obtained are defined only with respect to $F$. Suppose that the motion of the same point throughout the same interval of time is described from another reference frame $F_a$. With respect to $F_a$ a position vector, velocity, and acceleration may also be defined. In general the position vector and its derivatives observed from $F_a$ will differ from the corresponding vectors observed from $F$. For each frame may move and change relative orientation in any arbitrary manner.

Suppose that the frame $F$ is rigidly attached to the earth. Such a frame is called a *relative frame*. Quantities referred to the relative frame will be called *relative* and their symbols will carry no subscript.

Let the frame $F_a$ be attached to some point on the axis of the earth and be oriented so that the stars appear fixed. In this frame the axis of the earth also appears fixed. In dynamic meteorology such a frame is called an *absolute frame* (see 6·07). Quantities referred to the absolute frame will be called *absolute* and their symbols will be distinguished by the subscript $a$.

In practice the motion of the atmosphere is always referred to a relative frame. But, as we shall see in the following chapter, the dynamical description of the motion is referred to an absolute frame.

**6·07. Dynamics.** The motion of material points or particles is not arbitrary but depends in a definite way upon the presence of other matter. The formulation and consequences of this dependence constitute the science of dynamics. We shall not define or develop the fundamental dynamical concepts; we shall suppose that these notions are understood. Indeed, they have already been introduced and used in the preceding chapters.

If mass and force are understood, then dynamics can be founded upon *Newton's second law of motion*, the fundamental dynamical law. This law may be formulated as follows: *The resultant force acting upon a particle is proportional to the mass of the particle, and is proportional to the acceleration of the particle as observed from an absolute frame.* When units are properly chosen, as in the mts system, the acceleration and the resultant force per unit mass are equal.

Newton's second law should properly refer the motion to a frame located at the center of gravity of the solar system and fixed with respect to the stars. Although this refinement is required for astronomical calculations, it is unnecessary for the dynamics of the atmosphere. We shall consider here that a frame located at a point on the axis of the earth and fixed with respect to the stars is an absolute frame, valid for the statement of Newton's second law.

In the atmosphere the acting forces are the pressure force, the force of gravity, and the frictional force. Here we shall suppose that the frictional force is absent. Later in chapter 9 the effect of friction will be considered. The pressure force arises from the interaction of the air elements and is independent of the reference frame from which it is observed. However, as we have seen in 4·09, the force of gravity is measured upon the rotating earth and depends upon the rotation.

**6·08. The force of gravitation.** An observer fixed in absolute space, not rotating with the earth, would measure the force of gravitation rather than the force of gravity. The force of gravitation arises from the attraction between mass points and is given by Newton's law of universal

gravitation. The force of gravitation acting upon a unit mass at a distance $r$ from the center of the earth is directed toward the center, and its magnitude $g_a$ is given by

$$g_a = \frac{GM}{r^2}. \tag{1}$$

Here $G$ is the universal gravitational constant, and $M$ is the mass of the earth. $G$ has the dimensions $[M^{-1}L^3T^{-2}]$, so it has the same value in both mts and cgs units. This value is $6.658 \times 10^{-8}$. The mass of the earth has been found by astronomical measurements to be $5.988 \times 10^{21}$ tons.

Formula (1) holds only if the mass of the earth is symmetrically distributed about the center of the earth in homogeneous concentric spherical shells. Actually the earth is nearly an oblate spheroid of revolution slightly depressed at the poles. Moreover, the mass of the earth is asymmetrically distributed. Hence (1) cannot hold exactly. But it does give a good approximation to the actual force of gravitation.

Since the earth is a spheroid, the polar and equatorial radii are different. The polar radius is $a_P = 6357$ km, and the equatorial radius is $a_E = 6378$ km. A sphere with the radius $a = 6371$ km has very nearly the same volume and area as the earth. The value $a$ will be used for the mean radius of the earth. Introducing this value into (1), we find the mean value of the force of gravitation at the surface of the earth to be

$$g_a = \frac{GM}{a^2} = 9.822 \text{ m s}^{-2}. \tag{2}$$

The force of gravitation is directed toward the center of the earth. If it has a potential, the equipotential surfaces must then be spherical. The normal distance between two infinitesimally separated spherical surfaces is $\delta r$. Consequently, if a gravitational potential $\phi_a$ exists, it must satisfy the relation

$$\delta\phi_a = g_a \delta r.$$

When (1) is substituted for $g_a$, the existence of the gravitational potential $\phi_a$ is proved, for

$$\delta\phi_a = GM\frac{\delta r}{r^2} = -\delta\left(\frac{GM}{r}\right).$$

Thus, by integration,

$$\phi_a = -\frac{GM}{r} + C.$$

If the constant of integration $C$ is evaluated so that $\phi_a = 0$ at sea level at the poles, then

$$\phi_a = GM\left(\frac{1}{a_P} - \frac{1}{r}\right). \tag{3}$$

The gradient of the gravitational potential is the vector force of gravitation $\mathbf{g}_a$. Thus

$$\mathbf{g}_a = -\nabla\phi_a. \tag{4}$$

This force $\mathbf{g}_a$ is the force of gravitational attraction of the earth acting upon a particle of unit mass.

By the argument of 4·10 it can be shown that a gravitational potential $\phi_a$ exists for any distribution of mass. Consequently the gravitational force $\mathbf{g}_a$ is the gradient of this potential. That is, (4) holds for any distribution of the mass of the earth.

**6·09. The equation of absolute motion.** The mathematical formulation of Newton's second law of motion is known as the equation of absolute motion. The forces observed from the absolute frame acting upon a particle of unit mass are the gravitational force $\mathbf{g}_a$ and the pressure force.

In section 4·15 the pressure force per unit volume was shown to be $-\nabla p$. Consider the pressure force acting upon a parcel of mass $\delta M$ and of volume $\delta V$. This force is $-\delta V\nabla p$. The *pressure force per unit mass*, denoted by $\mathbf{b}$, is then

$$\mathbf{b} = -\frac{\delta V}{\delta M}\nabla p = -\alpha\nabla p. \tag{1}$$

Newton's second law requires that the absolute acceleration $\dot{\mathbf{v}}_a$ equal the resultant of the pressure force $\mathbf{b}$ and the gravitational force $\mathbf{g}_a$. Thus[¶]

$$\dot{\mathbf{v}}_a = \mathbf{b} + \mathbf{g}_a = -\alpha\nabla p - \nabla\phi_a. \tag{2}$$

This is the equation of absolute motion referred to unit mass. The equation of absolute motion referred to unit volume is obtained from (2) by multiplication with the density $\rho$. Thus

$$\rho\dot{\mathbf{v}}_a = -\nabla p - \rho\nabla\phi_a. \tag{3}$$

Although this equation is sometimes useful, hereafter the equation of absolute motion referred to unit mass will usually be intended when the equation of absolute motion is mentioned.

The equation of absolute motion (2) may be expressed as an equilibrium of forces by defining a force $\mathbf{f}_a$ equal and opposite to the absolute

acceleration. Thus

$$\mathbf{f}_a = -\dot{\mathbf{v}}_a. \tag{4}$$

This force $\mathbf{f}_a$ is called the *inertial force of reaction*. For it arises from the inertia of a particle moving relative to the absolute frame, and it completely balances the resultant of all the acting forces. So the equation of absolute motion may be stated

$$\mathbf{0} = \mathbf{b} + \mathbf{g}_a + \mathbf{f}_a. \tag{5}$$

That is, the resultant of all forces per unit mass, including the inertial force of reaction, is always zero. This formulation of Newton's second law is physically significant to an observer attached to the moving particle, for he is unable to distinguish between real forces and the inertial force of reaction. Accordingly, whenever forces are measured upon a body accelerating relative to the absolute frame, inertial forces appear.

The equation of absolute motion refers the acceleration to an absolute frame $F_a$. Since these equations express so simply the dynamic conditions which control the motion, the dynamics of a process is often better understood when the motion is referred to the absolute frame.

However, an observer fixed on the earth can express his observations more conveniently with respect to a relative frame $F$ fixed to the earth. In order to use the equation of motion, observations relative to $F$ must be referred to the absolute frame $F_a$. That is, we must know how motion as observed from a relative frame would appear from the absolute frame. Evidently this depends upon the motion of the relative frame with respect to the absolute frame.

**6·10. The acceleration of a point of the earth.** The earth rotates as a solid body from west to east with a constant angular speed which will be denoted by $\Omega$. $\Omega$ is then determined by the period of rotation of the earth with respect to the fixed stars. This period is called the *sidereal day* from the Latin word for star. Therefore, $\Omega$ is given by

$$\Omega = \frac{2\pi \text{ rad}}{1 \text{ sidereal day}}.$$

Since the earth moves around the sun, the sidereal day is different from the *solar day* or *day*, which is the period of rotation of the earth with respect to the sun. In one year, or approximately $365\frac{1}{4}$ solar days, the earth has rotated $365\frac{1}{4}$ times with respect to the sun. The earth has in one year also made one complete revolution in absolute space around the sun from west to east. Hence in one year the earth has made $366\frac{1}{4}$ revolutions with respect to the stars. Therefore

$$1 \text{ year} = 365\tfrac{1}{4} \text{ solar days} = 366\tfrac{1}{4} \text{ sidereal days}.$$

Consequently the angular speed of the earth is given by

$$\Omega = \frac{366\frac{1}{4} \cdot 2\pi \text{ rad}}{365\frac{1}{4} \text{ solar days}} = 7.292 \times 10^{-5} \text{ rad s}^{-1}. \tag{1}$$

We may consider that the particles of the earth form a space of points called *relative space*. This space may be extended to include every point which appears at rest when observed from a point of the earth. Every point of relative space rotates with the constant absolute angular speed $\Omega$ around the axis of the earth in a fixed circle of curvature centered on the axis. This circle is called a *zonal circle* and the plane of the circle, its osculating plane, is called a *zonal plane*. Since a point at rest in relative space moves with constant speed, its acceleration is purely centripetal and lies in the zonal plane, directed toward the axis of the earth. The absolute acceleration of a point fixed in relative space will be called the *acceleration of a point of the earth* and denoted by $\dot{\mathbf{v}}_e$. Then by 6·05(10)

$$\dot{\mathbf{v}}_e = -\Omega^2 \mathbf{R}. \tag{2}$$

The equal and opposite inertial force of reaction $\mathbf{f}_e$ is called the *centrifugal force of a point of the earth*. Thus,

$$\mathbf{f}_e = \Omega^2 \mathbf{R}. \tag{3}$$

So the equation of absolute motion for a particle at rest in relative space is, by 6·09(5),

$$\mathbf{0} = \mathbf{b} + \mathbf{g}_a + \mathbf{f}_e. \tag{4}$$

This is the equation of relative or hydrostatic equilibrium, expressed from the absolute frame. The same equation, expressed from the relative frame, has already been obtained in 4·16(2) and is

$$\mathbf{0} = \mathbf{b} + \mathbf{g}.$$

Evidently to an observer at rest in absolute space the pressure force is balanced by the force $\mathbf{g}_a + \mathbf{f}_e$. But to an observer at rest in relative space, the pressure force appears to be balanced by a single force, the force of gravity $\mathbf{g}$. Accordingly we have

$$\mathbf{g} = \mathbf{g}_a + \mathbf{f}_e. \tag{5}$$

That is, as stated in the last section, a moving observer is unable to distinguish between real and inertial forces.

On a given zonal circle the magnitude $f_e = \Omega^2 R$ of the centrifugal force is constant. The equiscalar surfaces of $R$ are cylinders of revolution coaxial with the axis of the earth. So by 4·13 the ascendent of $R$ is a

unit vector normal to those cylinders and directed away from the axis of the earth. Hence

$$\mathbf{R} = R\nabla R = \nabla(\tfrac{1}{2}R^2).$$

Since the angular speed of the earth is constant, the centrifugal force is the gradient of a *centrifugal potential* $\phi_e$. Thus

$$\mathbf{f}_e = -\nabla\phi_e,$$

where the centrifugal potential is given by

$$\phi_e = -\tfrac{1}{2}\Omega^2 R^2.$$

The equipotential surfaces of $\phi_e$ coincide with equiscalar surfaces of $R$; they are cylinders of revolution coaxial with the axis of the earth.

Since both the gravitational force and the centrifugal force are potential vectors, the force of gravity is also a potential vector. This was shown independently in chapter 4, where the potential of gravity was denoted by $\phi$. Equation (5) may then be rewritten in terms of potential vectors as

$$-\nabla\phi = -\nabla\phi_a - \nabla\phi_e = -\nabla(\phi_a + \phi_e).$$

This equation shows that the potentials $\phi$, $\phi_a$, and $\phi_e$ are related by

$$\phi = \phi_a + \phi_e. \tag{6}$$

The potential $\phi_a$ in (6) may refer to any distribution of the mass of the earth. If, in particular, the earth is regarded as made up of homogeneous spherical shells, then $\phi_a$ is given by 6·08(3), and (6) becomes

$$\phi = GM\left(\frac{1}{a_P} - \frac{1}{r}\right) - \tfrac{1}{2}\Omega^2 R^2. \tag{7}$$

The geopotential surfaces of constant $\phi$ are found graphically by drawing spherical surfaces for $\phi_a$ and cylindrical surfaces for $\phi_e$. Both surfaces are surfaces of revolution which are completely defined by their intersections with any plane through the axis of the earth, called a *meridional plane*. Consequently the surfaces of constant $\phi_a$, $\phi_e$, and $\phi$ are completely represented by their traces on a meridional plane. The lines of constant gravitational potential are circles concentric with the center of the earth. And the lines of constant centrifugal potential are straight lines parallel to the axis of the earth. The diagonal curves of unit values of these two sets of lines form the meridional geopotential lines.

The meridional traces of the potentials $\phi_a$, $\phi_e$, and $\phi$ are illustrated in fig. 6·10. Here the potential unit for which the traces are constructed is $10^7\ \mathrm{m^2\ s^{-2}}$. The shape of the geopotential surfaces has been exaggerated

by drawing for a centrifugal potential which represents an angular speed ten times that of the earth. Notice that the geopotential surfaces are inflated in the direction away from the axis of the earth. In that direction the centrifugal force becomes stronger and the gravitational force becomes weaker. Hence the distance between consecutive centrifugal potential traces decreases, and the distance between consecutive gravitational potential traces increases. Accordingly the geopotential surfaces far from the axis of the earth are nearly given by the cylindrical centrifugal potential surfaces, and the geopotential surfaces near the axis of the earth are nearly given by the spherical gravitational potential surfaces. Although the geopotential surfaces near the surface of the earth are actually inflated toward the equator, they are very nearly parallel, as explained in section 4·11.

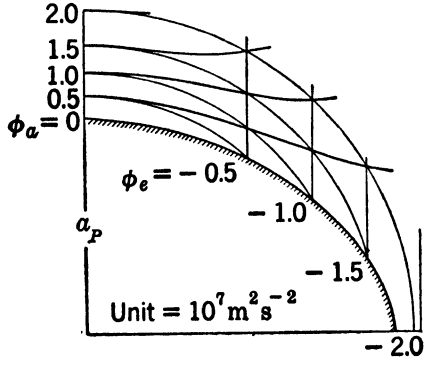



FIG. 6·10. Geopotential levels.

From (7) the surface $\phi = 0$ coincides with the surface of the earth at the poles. This geopotential surface is found to be very nearly ellipsoidal with a difference of 11 km between the polar and equatorial radii. The values $a_P$ and $a_E$ obtained from geodetic measurement show that the difference should be 21 km (see section 6·08). This discrepancy is due to the assumption that the mass of the earth is distributed in homogeneous concentric spherical shells. If, instead, $\phi_a$ in (6) represents the potential of a homogeneous oblate spheroid, the geopotential surfaces will be more nearly correct. The remaining discrepancy, due mainly to irregularities of mass distribution in the crust of the earth, is small.

**6·11. Zonal flow.** The equation of motion for a point rotating with the earth expresses the complete balance between the force of gravity and the pressure force. Accordingly, the isobaric surfaces must coincide with the geopotential surfaces. The ocean and the interior of the earth may be considered as viscous fluids rotating as a solid body with the absolute angular speed $\Omega$. So the isobaric surfaces in the earth and in the ocean are normal to the force of gravity. If the earth, the ocean, and the atmosphere rotate together as a solid body, the unit isobaric surfaces are then everywhere coincident with the geopotential surfaces. Since the thickness of an isobaric unit layer is proportional to the specific volume, the isobaric unit layers are very thin in the earth, thicker in the ocean, and much thicker in the atmosphere.

Let us now examine an atmosphere rotating around the axis of the earth with the absolute angular speed $\omega_a$. If $\omega_a$ is constant along each zonal circle and constant in time, the atmospheric flow is called *zonal.* In arbitrary zonal flow $\omega_a$ may vary from circle to circle. However, for simplicity we shall consider $\omega_a$ constant for all zonal circles.

In zonal flow the acceleration is purely centripetal, so the inertial force of reaction is a centrifugal force, given by

$$\mathbf{f}_a = \omega_a^2 \mathbf{R}. \tag{1}$$

And the equation of absolute motion is

$$0 = \mathbf{b} + \mathbf{g}_a + \mathbf{f}_a. \tag{2}$$

When the atmosphere and the earth rotate together as one body, we have $\omega_a = \Omega$ and therefore $\mathbf{f}_a = \mathbf{f}_e$. Equation (2) then becomes identical with equation 6·10(4) for relative or hydrostatic equilibrium.

Since the centripetal acceleration and the force of gravitation are meridional vectors, the pressure force and, consequently, the pressure gradient are also meridional vectors. Hence the isobaric surfaces must be normal to any meridional plane and are therefore surfaces of revolution about the axis of the earth. The whole pressure field is then completely determined by the *meridional isobars,* that is, by the lines in which the isobaric surfaces intersect a meridional plane.

The surfaces of constant gravitational potential appear as concentric circles in the meridional plane. Unless the absolute angular rotation is zero, the meridional isobars are depressed at the poles. This conclusion is illustrated by the vector diagram of the equation of motion for zonal flow in fig. 6·11*a*.

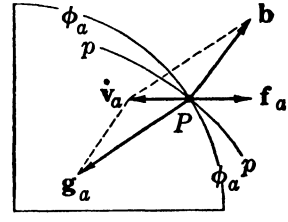



FIG. 6·11*a*. Meridional isobar in zonal flow.

The centrifugal force $\omega_a^2\mathbf{R}$ is the same for either sense of the absolute rotation about the axis of the earth. Consequently the isobaric surfaces will be the same for either sense of rotation of the same magnitude. Although the two senses of the absolute rotation of the atmosphere are dynamically indistinguishable, they may be distinguished kinematically according to the sense of the earth's rotation. When the atmosphere rotates zonally with the same sense as the earth, $\omega_a$ will be defined as positive. And when the atmosphere rotates with the opposite sense, $\omega_a$ will be defined as negative. In order to conform with later sign conventions this definition will apply only to the northern hemisphere. However, the results for constant zonal flow may easily be extended to

the southern hemisphere, for both the field of rotation and the pressure field are symmetric about the equator.

When $\omega_a$ is varied, the isobaric surfaces change orientation with respect to the surfaces of constant gravitational potential and of constant geopotential. In the diagrams of fig. 6·11*b* four orientations of the isobaric surfaces, represented by the meridional isobars, are illustrated. Only one quadrant of the meridional plane is shown in the diagrams. The isobaric pattern is symmetric both about the equator and the axis of the earth.

In diagram $b_0$ the absolute angular speed is zero, and the atmosphere is in absolute equilibrium. The isobaric surfaces then coincide with the spheres of constant gravitational potential. In all the other diagrams the isobaric surfaces are depressed at the poles.

In diagram $b_1$ the centrifugal force of the atmosphere is less than that of the earth. Therefore the isobaric surfaces are less depressed at the poles than are the geopotential levels, and any constant level has a belt of low pressure at the equator.

In diagram $b_2$ the centrifugal force of the atmosphere is the same as that of the earth. The pressure force is equal, but opposite in direction, to the force of gravity. Therefore the isobaric surfaces coincide with the geopotential levels.

In diagram $b_3$ the centrifugal force is greater than that of the earth. So the isobaric surfaces are more depressed at the poles than are the geopotential levels, and any constant level has a belt of high pressure at the equator.

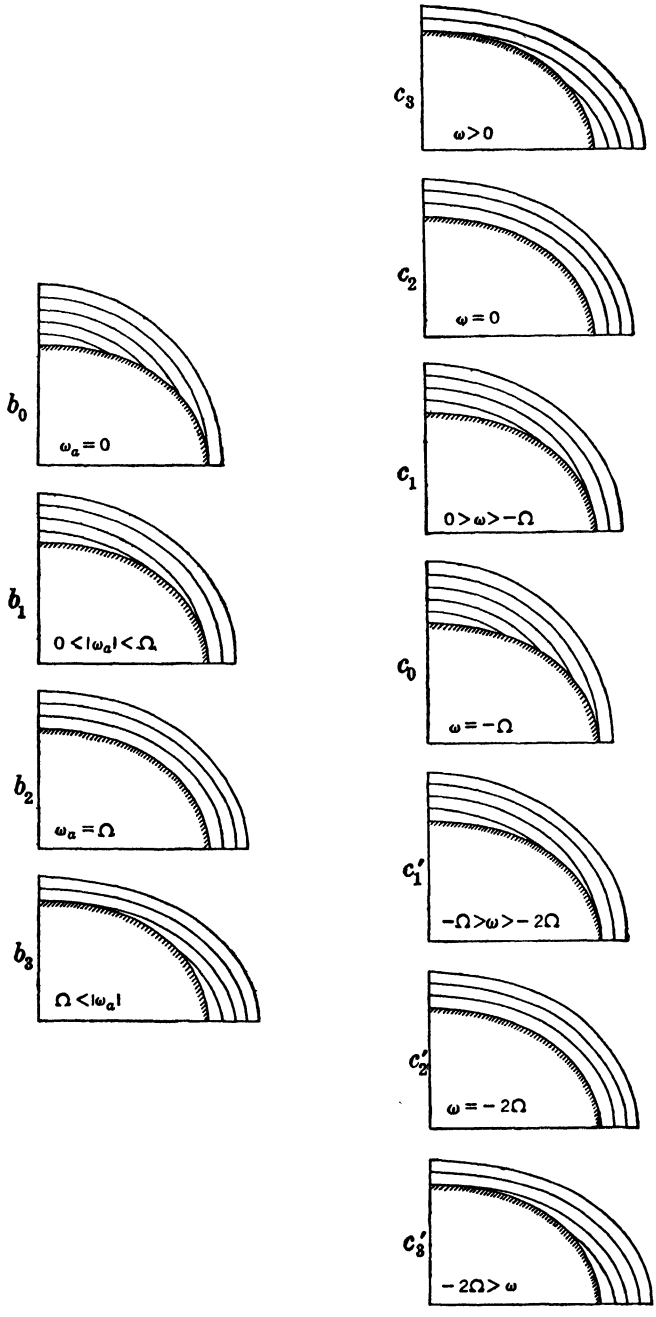
The absolute zonal rotation is observed from the earth as a relative zonal rotation with the relative angular speed $\omega$. Evidently the absolute angular speed $\omega_a$ is the algebraic sum of the positive angular speed $\Omega$ of the earth and the angular speed $\omega$ relative to the earth. Thus

$$\omega_a = \omega + \Omega. \tag{3}$$

When $\omega > 0$ the relative zonal wind blows from the west. When $\omega = 0$, the atmosphere is in relative or hydrostatic equilibrium. And when $\omega < 0$ the relative zonal wind blows from the east.

Relative zonal rotation in the same sense as the absolute rotation of the earth will be called *cyclonic*, and rotation in the opposite sense will be called *anticyclonic*. Zonal flow is then cyclonic when $\omega > 0$ and anticyclonic when $\omega < 0$. Later the terms cyclonic and anticyclonic will be generalized. However, the conventions adopted here for zonal flow in the northern hemisphere will still hold.

The diagrams $b_1$, $b_2$, $b_3$ of fig. 6·11*b* each represent both a positive and negative *absolute* rotation of the same strength. However, the pressure




FIGS. 6·11*b* and *c*. Pressure field in zonal flow.

field is not the same for positive and negative *relative* rotation of the same strength. In fig. 6·11*c* the diagrams of fig. 6·11*b* are redrawn in order of decreasing $\omega$. Diagrams $b_1$, $b_2$, $b_3$ correspond respectively to diagrams $c_1$, $c_2$, $c_3$ when the absolute rotation is positive, and to diagrams $c_1'$, $c_2'$, $c_3'$ when the absolute rotation is negative.

In diagram $c_2$ the relative angular speed is zero, and the atmosphere is in relative or hydrostatic equilibrium. The isobaric surfaces are then horizontal, so the pressure in any horizontal level is constant.

Diagram $c_3$ represents the only case of cyclonic or positive relative rotation. Relative to the horizontal levels the isobaric surfaces slope downward from the equator to the poles. So any horizontal pressure field has low pressure at the poles and a belt of high pressure at the equator. As the cyclonic rotation increases, the meridional slope of the isobaric surfaces becomes steeper, and the strength of the horizontal pressure field increases.

All the remaining diagrams in fig. 6·11*c* represent anticyclonic rotation of increasing strength taken in the order $c_1$, $c_0$, $c_1'$, $c_2'$, $c_3'$. Evidently anticyclonic flow is more complex than cyclonic flow. Diagram $c_1$ shows the anticyclonic rotation of moderate strength. Here the isobaric surfaces slope downward from the poles to the equator. So any horizontal pressure field has high pressure at the poles and a belt of low pressure at the equator.

When the strength of the anticyclonic flow is increased, the slope of the isobars becomes steeper, until, as shown in diagram $c_0$, the critical value $\omega = -\Omega$ is reached. Here the horizontal pressure field has a maximum strength with polar high pressure and equatorial low pressure, and the isobaric surfaces are spherical.

Diagram $c_1'$ shows that the horizontal pressure field again becomes weaker with further increase of the anticyclonic rotation. At the second critical value $\omega = -2\Omega$ the isobars become horizontal, as shown in diagram $c_2'$, so the pressure in any horizontal level is constant.

Diagram $c_3'$ shows the anticyclonic flow increased beyond the value $-2\Omega$. The isobaric surfaces then slope downward from the equator to the poles as in cyclonic flow. Any horizontal pressure field has low pressure at the poles and a belt of high pressure at the equator.

Zonal flow may be considered to have two centers: one at either pole. For cyclonic flow (see $c_3$) the centers always have low pressure in any horizontal level. And for anticyclonic flow of strength less than $-2\Omega$ ($c_1$, $c_0$, $c_1'$) the centers have high pressure in any horizontal level. But for anticyclonic flow of strength greater than $-2\Omega$ ($c_3'$), the centers again develop low pressure in any horizontal level.

Zonal anticyclonic flow of the types $c_1'$, $c_2'$, $c_3'$ would never occur in the

atmosphere. Although such anticyclonic flow is dynamically possible, no mechanism exists for generating absolute zonal rotation opposite to that of the earth.

Later, when arbitrary horizontal flow is examined, it will be helpful to return to this section, for any horizontal flow will be shown locally to be similar to zonal flow. However the dynamics of zonal flow is simpler and should first be clearly understood.

**6·12. Angular velocity.** In section 6·05 we defined the angular speed $\omega$ for an arbitrary motion of a point. The plane of rotation is the osculating plane, and the axis of rotation is the line normal to the osculating plane through the center of curvature. We shall now show how the rotation may be expressed vectorially.

The rotation is completely specified by the numerical value of the angular speed, the orientation of the axis, and the sense of the rotation. Hence, a vector of magnitude $\omega$ directed along the axis of rotation according to the right-handed screw rule (section 4·03) expresses all the necessary information about the rotation. This vector is called the angular velocity and will be denoted by $\boldsymbol{\omega}$. In particular, the angular velocity of the earth will be denoted by $\boldsymbol{\Omega}$. Since the earth rotates from west to east, $\boldsymbol{\Omega}$ is directed from south to north parallel to the axis of the earth.

The relation between the linear speed $v$ and the angular speed $\omega$ is $v = \omega R$. The vector $\mathbf{R}$ of magnitude $R$ is the radius vector directed from the center of curvature on the axis of rotation to the point whose motion is being considered. Let the radius vector from any point on the axis of rotation to the moving point $P$ be denoted by $\mathbf{r}$. And let $\theta$ ($\leqq \pi$) be the angle between the angular velocity $\boldsymbol{\omega}$ and the radius vector $\mathbf{r}$, as shown in fig. 6·12. The relation between the scalar radii $R$ and $r$ is then

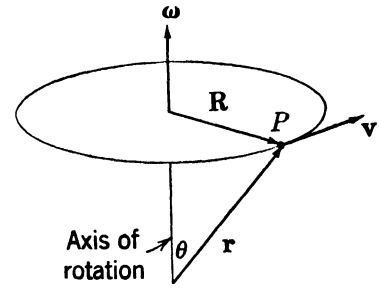


FIG. 6·12.

$$R = r \sin \theta.$$

The velocity $\mathbf{v}$ is a vector normal to the plane of $\boldsymbol{\omega}$ and $\mathbf{r}$. Its magnitude is

$$v = \omega R = \omega r \sin \theta.$$

And its sense is given by the right-handed rotation $\boldsymbol{\omega} \rightarrow \mathbf{r}$ through the angle $\theta$. Consequently the two vectors $\boldsymbol{\omega}$ and $\mathbf{r}$ define the velocity completely. Any vector similarly defined by two vectors is called the *vector product* of the two vectors.

**6·13. The vector product.** Let **a** and **b** be any two vectors, and let $\theta(\leqq \pi)$ be the angle between them. The vector product **v** of these two vectors is indicated by a cross between them. Thus

$$\mathbf{v} = \mathbf{a} \times \mathbf{b}.$$

The vector **v** is defined to be perpendicular to the plane through **a** and **b** and to have the magnitude

$$v = ab \sin \theta. \tag{1}$$

The sense of **v** is given by a right-handed rotation $\mathbf{a} \rightarrow \mathbf{b}$ through the angle $\theta$.

Let the vector **b** be projected into the plane perpendicular to **a**. This projection is a vector denoted by $\mathbf{b}_N$ in fig. 6·13*a*. Its magnitude, given by $b_N = b \sin \theta$, is the altitude of the parallelogram having the base **a**

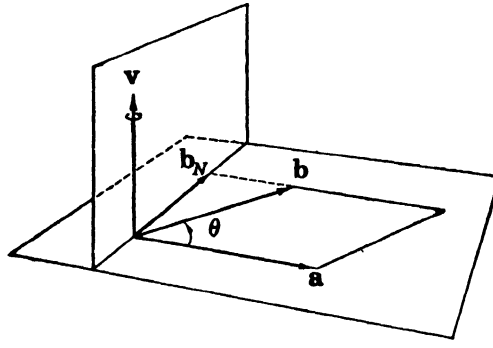



FIG. 6·13*a*. Vector product.

and the side **b**. So the numerical value of the vector product is equal to the area of the parallelogram, for $v = ab_N$. Hence the vector product may be considered as obtained by a positive rotation of $\mathbf{b}_N$ about **a** through a right angle and subsequent multiplication by $a$.

When the order of the two vectors in the vector product is reversed, a new vector product is obtained whose magnitude still is given by (1). However the rotation $\mathbf{b} \rightarrow \mathbf{a}$ is opposite to the rotation $\mathbf{a} \rightarrow \mathbf{b}$, so

$$\mathbf{b} \times \mathbf{a} = -\mathbf{a} \times \mathbf{b}. \tag{2}$$

Hence the vector product does not satisfy the commutative law but changes sign when the factors are permuted.

If the two vectors **a**, **b** are parallel, the area of the parallelogram is zero, and the vector product is zero. And if the two vectors are perpendicular, the vector product has the magnitude $v = ab$. Therefore the

vector products of the rectangular unit vectors are:

$$\begin{aligned} &\mathbf{i}\times\mathbf{i}=0, \quad &&\mathbf{j}\times\mathbf{j}=0, \quad &&\mathbf{k}\times\mathbf{k}=0, \\ &\mathbf{i}\times\mathbf{j}=\mathbf{k}, \quad &&\mathbf{j}\times\mathbf{k}=\mathbf{i}, \quad &&\mathbf{k}\times\mathbf{i}=\mathbf{j}. \end{aligned} \tag{3}$$

Although the vector product is not commutative, it is distributive with respect to addition. Thus

$$\mathbf{a}\times(\mathbf{b}+\mathbf{c})=\mathbf{a}\times\mathbf{b}+\mathbf{a}\times\mathbf{c}. \tag{4}$$

The proof for this is demonstrated geometrically in fig. 6·13*b*. All the vector products in (4) are in the plane normal to **a**. Suppose that this plane is the plane of the page and the vector **a** is directed toward the reader. The projection of **a** onto the page is the point labeled $A$. The vectors **b** and **c** project into the vectors $\mathbf{b}_N$ and $\mathbf{c}_N$ respectively. Since the triangular representation of the sum $\mathbf{b}+\mathbf{c}$ projects as a triangle, we have

$$(\mathbf{b}+\mathbf{c})_N=\mathbf{b}_N+\mathbf{c}_N. \tag{5}$$

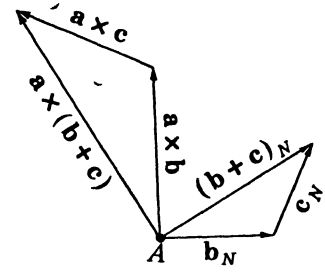


FIG. 6·13*b*.

The required vector products are obtained by positive rotation about **a** (counterclockwise in the diagram) of the vectors in (5) through a right angle and multiplication by $a$. The vector equality (5) is not affected by the operations of rotation and multiplication, so the distributive law (4) holds for the vector product.

With the aid of this law we can obtain the rectangular components of the vector product. Let the two vectors be resolved into components and unit vectors. When the vector product is expanded by the distributive law, and the vector products of the unit vectors **i**, **j**, **k** are reduced by (3), we find that the vector product $\mathbf{a}\times\mathbf{b}$ is given by

$$(a_yb_z-a_zb_y)\mathbf{i}+(a_zb_x-a_xb_z)\mathbf{j}+(a_xb_y-a_yb_x)\mathbf{k}.$$

This expansion may also be written as a determinant which is easier to remember. Thus

$$\mathbf{a}\times\mathbf{b}=\begin{vmatrix} \mathbf{i} & \mathbf{j} & \mathbf{k} \\ a_x & a_y & a_z \\ b_x & b_y & b_z \end{vmatrix}. \tag{6}$$

The change in sign of the vector product with the reversal of the order of the factors appears here as a property of the determinant. For the interchange of two rows changes the sign of the determinant.

The derivative of the vector product is obtained by differentiating (6). Thus

$$\frac{d}{du}(\mathbf{a}\times\mathbf{b})=\frac{d\mathbf{a}}{du}\times\mathbf{b}+\mathbf{a}\times\frac{d\mathbf{b}}{du}. \tag{7}$$

This rule accords with the usual process of differentiating a product. Notice, however, that the order of the factors in the vector product must be preserved.

**6·14. The scalar triple product.** Although only the properties of the vector product are required in this chapter, we shall later encounter the scalar product of a vector with a vector product. This scalar product is then of the type:

$$\mathbf{a}\cdot(\mathbf{b}\times\mathbf{c}) = \mathbf{a}\cdot\mathbf{v} = a_v v.$$

Since both factors in a vector product must be vectors, the parentheses enclosing the vector product in the above expression may be omitted. The scalar expression $\mathbf{a}\cdot\mathbf{b}\times\mathbf{c}$, involving three vectors, is called the scalar triple product.

Geometrically this scalar represents the volume of the parallelepiped having the three vectors **a**, **b**, **c** as edges. This is easily seen from fig. 6·14. The vector product $\mathbf{v} = \mathbf{b}\times\mathbf{c}$ is numerically equal to the area of the base parallelogram whose sides are **b** and **c**. The altitude of the parallelepiped above this base of area $v$ is the component $a_v$ of **a** normal to the base. So the volume of the parallelepiped is $a_v v$: the product of its base and altitude. But $a_v v$ is also the value of the scalar triple product.

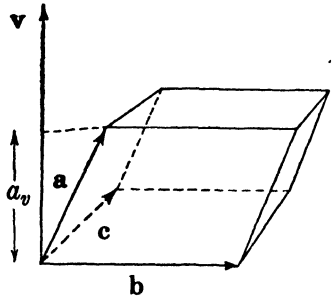


FIG. 6·14. Scalar triple product.

The scalar triple product is positive when **a** and **v** lie on the same side of the plane through **b** and **c**. If they lie on the opposite sides of this plane, the scalar triple product is negative. And if **a** lies in the plane the volume of the parallelepiped is zero, so the scalar triple product is also zero.

The volume of the parallelepiped may be obtained by considering any two of the vector edges **a**, **b**, **c** as bases. By the right-handed screw rule all the rotations $\mathbf{b}\to\mathbf{c}$, $\mathbf{c}\to\mathbf{a}$, $\mathbf{a}\to\mathbf{b}$ about **a**, **b**, **c** respectively have the same sense. Therefore,

$$\mathbf{a}\cdot\mathbf{b}\times\mathbf{c} = \mathbf{b}\cdot\mathbf{c}\times\mathbf{a} = \mathbf{c}\cdot\mathbf{a}\times\mathbf{b}. \tag{1}$$

Hence the scalar triple product does not change by cyclic permutation of its vectors. The non-commutative property of the vector product shows that the scalar triple product changes sign when the cyclic order of the vectors is altered. The scalar triple product is positive if the three vectors taken in cyclic order are relatively arranged as the axes of a right-handed coordinate system.

Since the order of the factors in a scalar product may be reversed, we obtain from (1)

$$\mathbf{a}\cdot\mathbf{b}\times\mathbf{c} = \mathbf{c}\cdot\mathbf{a}\times\mathbf{b} = \mathbf{a}\times\mathbf{b}\cdot\mathbf{c}. \tag{2}$$

Hence *the dot and cross can be interchanged without affecting the value of the scalar triple product.* Geometrically this result is evident from the diagram.

The scalar triple product may be expressed as a determinant of the rectangular components of the three vectors **a**, **b**, **c**. From 6·13(6) we find

$$\mathbf{a}\cdot\mathbf{b}\times\mathbf{c} = \mathbf{a}\cdot \begin{vmatrix} \mathbf{i} & \mathbf{j} & \mathbf{k} \\ b_x & b_y & b_z \\ c_x & c_y & c_z \end{vmatrix} = \begin{vmatrix} a_x & a_y & a_z \\ b_x & b_y & b_z \\ c_x & c_y & c_z \end{vmatrix}. \tag{3}$$

Here the properties of the scalar triple product appear as the properties of the determinant.

**6·15. The velocity of a point of the earth.** The concept of the vector product has been introduced for the purpose of expressing the velocity of rotation. We may now write

$$\mathbf{v} = \boldsymbol{\omega}\times\mathbf{r} = \boldsymbol{\omega}\times\mathbf{R}, \tag{1}$$

where **r** is a radius vector from any point on the axis of rotation, and **R** is the radius vector from the center of curvature.

In accordance with earlier conventions the absolute velocity of a point fixed in relative space will be called the *velocity of a point of the earth* and will be denoted by $\mathbf{v}_e$. This velocity is given by

$$\mathbf{v}_e = \boldsymbol{\Omega}\times\mathbf{r} = \boldsymbol{\Omega}\times\mathbf{R}, \tag{2}$$

where **r** is a position vector from any point on the axis of the earth, and **R** is the radius vector in the zonal plane.

The velocity of a point of the earth is by definition the time derivative of its position vector. Let the position vector be drawn from the axis

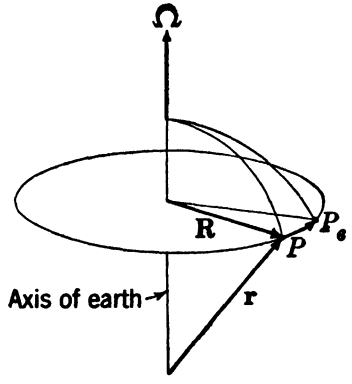



FIG. 6·15*a*.

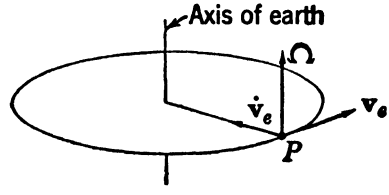



FIG. 6·15*b*.

of the earth as in fig. 6·15*a*. In the time interval $dt$ the point moves from $P$ to $P_e$ through the displacement $d_e\mathbf{r}$. The velocity of a point of the earth is then

$$\mathbf{v}_e = \frac{d_e\mathbf{r}}{dt}.$$

The acceleration of a point of the earth is obtained by repeating the time differentiation on $\mathbf{v}_e$. Thus

$$\dot{\mathbf{v}}_e = \frac{d_e \mathbf{v}_e}{dt}.$$

Introducing here the vector product (2) for $\mathbf{v}_e$, we find

$$\dot{\mathbf{v}}_e = \frac{d_e}{dt}(\boldsymbol{\Omega} \times \mathbf{r}) = \boldsymbol{\Omega} \times \mathbf{v}_e.$$

It was shown earlier, in 6·10(2), that the centripetal acceleration of a point of the earth is given by $-\Omega^2\mathbf{R}$. It is readily seen from fig. 6·15*b* that the vector product $\boldsymbol{\Omega} \times \mathbf{v}_e$ has the same value. This vector product, perpendicular to $\boldsymbol{\Omega}$ and to $\mathbf{v}_e$, is in the zonal plane and is directed toward the axis of the earth. And its magnitude is $\Omega v_e = \Omega^2 R$. Consequently $\dot{\mathbf{v}}_e = -\Omega^2\mathbf{R}$. This expression for the centripetal acceleration of a point of the earth has here been independently verified.

**6·16. Absolute and relative velocity.** In the last section we examined the absolute motion of a point of the earth. The motion is that of a particle at rest relative to the earth. We shall now examine an arbitrary

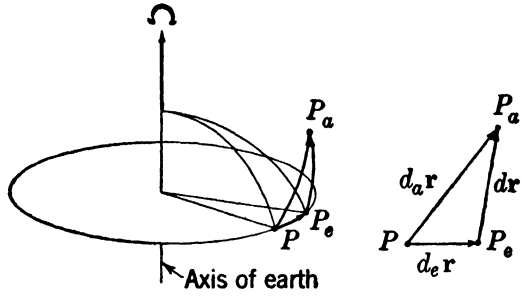



FIG. 6·16.

motion of a particle moving with respect to both an absolute and a relative frame.

Let the position of the particle be traced by a position vector $\mathbf{r}$ issuing from a point on the axis of the earth. Suppose the particle is located at the point labeled $P$ in fig. 6·16. During the time interval $dt$ let the point move to any arbitrary point $P_a$. In the same time interval the point of the earth coinciding with the initial position of the particle will rotate around the axis of the earth from $P$ to $P_e$. We have already denoted the displacement from $P$ to $P_e$ of a point of the earth by $d_e\mathbf{r}$. The displacement of the particle from $P$ to $P_a$, as observed from an absolute frame, will be denoted by $d_a\mathbf{r}$. And the displacement from $P_e$ to $P_a$, as observed

from a relative frame, will be denoted by $d\mathbf{r}$. The three displacements are shown in fig. 6·16. Evidently the absolute displacement is the vector sum of the displacement of the coinciding point of the earth and the relative displacement. Hence

$$d_a\mathbf{r} = d\mathbf{r} + d_e\mathbf{r}.$$

Dividing this equation by the time interval $dt$ required for the displacements, we find

$$\frac{d_a\mathbf{r}}{dt} = \frac{d\mathbf{r}}{dt} + \frac{d_e\mathbf{r}}{dt}. \tag{1}$$

The velocity of the coinciding point of the earth is

$$\mathbf{v}_e = \frac{d_e\mathbf{r}}{dt} = \boldsymbol{\Omega} \times \mathbf{r}.$$

So equation (1) may also be written:

$$\frac{d_a\mathbf{r}}{dt} = \frac{d\mathbf{r}}{dt} + \boldsymbol{\Omega} \times \mathbf{r}. \tag{2}$$

The rate of change with respect to the absolute frame of the position vector is by definition the absolute velocity,

$$\mathbf{v}_a = \frac{d_a\mathbf{r}}{dt}.$$

And the rate of change with respect to the relative frame of the position vector is the relative velocity,

$$\mathbf{v} = \frac{d\mathbf{r}}{dt}.$$

Consequently equation (2) may be written

$$\mathbf{v}_a = \mathbf{v} + \mathbf{v}_e = \mathbf{v} + \boldsymbol{\Omega} \times \mathbf{r}. \tag{3}$$

The absolute velocity of a particle is then equal to the vector sum of its relative velocity and the velocity of the coinciding point of the earth. The position vector $\mathbf{r}$ must issue from a point on the axis of the earth. For in the above derivation the origin of $\mathbf{r}$ must be fixed both in the absolute frame and in the relative frame.

**6·17. Absolute and relative acceleration.** In section 6·04 it was shown that the acceleration of a point moving along the path may be considered as the velocity of its image point moving along the hodograph. When a particle moves in an arbitrary path, the hodograph of the absolute velocity may be obtained by drawing the absolute velocity vector issuing from an origin on the axis of the earth. This vector may be con-

sidered as the position vector of the image point moving along the absolute hodograph. The relation between the absolute and relative velocities of the image point may then be obtained in the same fashion as for the real particle when $\mathbf{r}$ in equation 6·16(2) is replaced by $\mathbf{v}_a$. We then get

$$\frac{d_a\mathbf{v}_a}{dt} = \frac{d\mathbf{v}_a}{dt} + \Omega \times \mathbf{v}_a. \tag{1}$$

Let the absolute velocity be expressed as the sum of the relative velocity and the velocity of the coinciding point of the earth. Then $d\mathbf{v}_a/dt$ becomes

$$\frac{d}{dt}(\mathbf{v} + \mathbf{v}_e) = \frac{d}{dt}(\mathbf{v} + \Omega \times \mathbf{r}) = \frac{d\mathbf{v}}{dt} + \Omega \times \mathbf{v}.$$

And $\Omega \times \mathbf{v}_a$ becomes

$$\Omega \times (\mathbf{v} + \mathbf{v}_e) = \Omega \times \mathbf{v} + \Omega \times \mathbf{v}_e = \Omega \times \mathbf{v} + \mathbf{v}_e.$$

The rate of change with respect to the absolute frame of the absolute velocity is by definition the absolute acceleration,

$$\dot{\mathbf{v}}_a = \frac{d_a\mathbf{v}_a}{dt}.$$

And the rate of change with respect to the relative frame of the relative velocity is the relative acceleration,

$$\dot{\mathbf{v}} = \frac{d\mathbf{v}}{dt}.$$

Therefore when the expressions derived above for $d\mathbf{v}_a/dt$ and for $\Omega \times \mathbf{v}_a$ are added we find

$$\dot{\mathbf{v}}_a = \dot{\mathbf{v}} + 2\Omega \times \mathbf{v} + \dot{\mathbf{v}}_e. \tag{2}$$

This equation relates the absolute and relative accelerations. It shows that the acceleration of a particle with respect to an absolute frame may be considered as the sum of three accelerations. The first term is the acceleration of the particle with respect to a relative frame. The last term is the centripetal acceleration of the coinciding point of the earth. The middle term is called the *Coriolis acceleration*.

**6·18. Absolute and relative zonal flow.** A clear idea of the physical significance of the Coriolis acceleration, so called after its discoverer, is afforded by considering the special case of zonal flow. We have already discussed this simple type of flow (section 6·11). The relation between the absolute and the relative acceleration may be derived independently

for this motion without reference to the general theory. In accordance with the previous notation we shall let $\omega_a$ denote the absolute angular speed with sense and $\omega$ the relative angular speed with sense. These two angular speeds are related by $\omega_a = \omega + \Omega$.

The absolute centripetal acceleration of a particle is

$$\dot{\mathbf{v}}_a = -\omega_a^2 \mathbf{R},$$

and the relative centripetal acceleration is

$$\dot{\mathbf{v}} = -\omega^2 \mathbf{R}.$$

If the absolute centripetal acceleration is expanded we find

$$-\omega_a^2 \mathbf{R} = -(\omega + \Omega)^2 \mathbf{R} = -\omega^2 \mathbf{R} - 2\omega\Omega\mathbf{R} - \Omega^2 \mathbf{R},$$

or, by substitution of the absolute and relative centripetal accelerations,

$$\dot{\mathbf{v}}_a = \dot{\mathbf{v}} - 2\omega\Omega\mathbf{R} + \dot{\mathbf{v}}_e.$$

Comparison of this equation with 6·17(2) shows that the third term is the Coriolis acceleration; thus

$$2\boldsymbol{\Omega} \times \mathbf{v} = -2\omega\Omega\mathbf{R}.$$

This equation is readily verified with the aid of fig. 6·15*b*, when in that diagram $\mathbf{v}$ replaces $\mathbf{v}_e$.

**6·19. The equation of relative motion.** When flow in the atmosphere is observed from a relative frame, the absolute acceleration is obtained from the relative motion by the relation

6·17(2) $$\dot{\mathbf{v}}_a = \dot{\mathbf{v}} + 2\boldsymbol{\Omega} \times \mathbf{v} + \dot{\mathbf{v}}_e.$$

The equation of absolute motion is

6·09(2) $$\dot{\mathbf{v}}_a = \mathbf{b} + \mathbf{g}_a.$$

When the absolute acceleration is eliminated between these two equations, we find

$$\dot{\mathbf{v}} = \mathbf{b} - 2\boldsymbol{\Omega} \times \mathbf{v} + \mathbf{g}_a - \dot{\mathbf{v}}_e.$$

This equation has a clear meaning according to the principle of inertial forces: The acceleration relative to the earth is equal to the sum of all the forces, including the inertial forces arising from the absolute motion of the relative reference frame. The inertial force $-\dot{\mathbf{v}}_e$ has already been called the centrifugal force of a point of the earth. Moreover, it has been shown in 6·10(5) that the sum of the last two terms in the above equation constitutes the force of gravity $\mathbf{g}$. Hence,

**(1)** $$\dot{\mathbf{v}} = \mathbf{b} - 2\boldsymbol{\Omega} \times \mathbf{v} + \mathbf{g}.$$

The inertial force $-2\Omega \times \mathbf{v}$ is called the *Coriolis force.* This force is equal and opposite to the Coriolis acceleration. Since the Coriolis force acts normal to $\mathbf{v}$, it has no component along the relative motion. Consequently it cannot contribute to the speeding up or slowing down of a particle relative to the earth. For this reason the Coriolis force is often called the deflecting force. The Coriolis force will be denoted more briefly by $\mathbf{c}$,

$$\mathbf{c} = -2\Omega \times \mathbf{v}. \tag{2}$$

Equation (1) may then be written

$$\dot{\mathbf{v}} = \mathbf{b} + \mathbf{c} + \mathbf{g}. \tag{3}$$

This equation is called the equation of relative motion, for it expresses Newton's second law of motion with respect to observations from a relative frame. The equations of absolute and relative motion are completely equivalent. Both describe the same motion, but from a different viewpoint. And both yield the same physical result for any given problem. But when the problem admits of clear visualization in absolute motion, the equation of absolute motion is simpler to use, and the dynamics is easier to understand. For this reason zonal flow is described from the absolute frame. In general, however, the equation of relative motion is used, for it is usually too difficult to visualize a given relative flow from the absolute frame.

## CHAPTER SEVEN

# HORIZONTAL FLOW

**7·01. Horizontal flow.** Observations show that every large-scale current in the atmosphere is nearly horizontal. Appreciable vertical motion is usually confined to local convective currents, to boundary regions separating different air currents, or to mountainous regions where the air flow is influenced by topography. Regions of ascending air currents are often marked by the formation of clouds and precipitation due to lifting. These regions of vertical motion will be discussed later. We shall now examine flow which is strictly horizontal.

The equations of motion derived in the last chapter are certainly valid for horizontal flow. However, these equations do not account for the frictional forces acting near the surface of the earth. Consequently we may apply the results of this chapter on horizontal flow to real currents only when the flow occurs in the free atmosphere above the friction layer and when the regions of strong vertical motion are excluded.

The simplest type of horizontal flow is zonal. We shall find that many properties of zonal flow are also properties of arbitrary horizontal flow.

**7·02. Natural coordinates for horizontal flow.** The plane tangent to the level surface is called the *horizontal plane.* Evidently at the point of tangency this plane is normal to the force of gravity and to the unit vector $\mathbf{k}$ directed toward the local zenith. Since the unit tangent is in the horizontal plane, $\mathbf{t}$ and $\mathbf{k}$ are orthogonal.

In describing horizontal motion it will be convenient to introduce a unit vector orthogonal both to $\mathbf{t}$ and to $\mathbf{k}$. This vector is a horizontal vector normal to the motion and is called the *horizontal unit normal.* The horizontal unit normal will be denoted by $\mathbf{n}$, and the linear coordinate along it will be denoted by $n$. The three coordinates along the unit vectors $\mathbf{t}$, $\mathbf{n}$, $\mathbf{k}$ are then $s$, $n$, $z$ respectively. The sense of the horizontal unit normal will be chosen so that $\mathbf{t}$, $\mathbf{n}$, $\mathbf{k}$ is a right-handed triple having the same relative arrangement as $\mathbf{i}$, $\mathbf{j}$, $\mathbf{k}$. Accordingly the horizontal unit normal, viewed from the zenith, points to the left of the unit tangent.

Notice that the horizontal unit normal $\mathbf{n}$ is in the horizontal plane and directed to the left of the motion; whereas the space unit normal $\mathbf{N}$ is in the osculating plane and directed toward the center of space curvature.

The coordinate system described above constitutes a natural orthog-

onal coordinate system. When the flow is toward the east, this system coincides with the standard orthogonal coordinate system described in section 4·03. Both systems change orientation from point to point on any level surface. Hence they are valid only in the immediate neighborhood of the origin of the coordinates. For this reason they are called *local* coordinate systems.

**7·03. Standard and natural components.** The equation of relative motion is a vector equation. This equation is equivalent to three scalar equations along three non-coplanar lines. We shall resolve the equation of relative motion along the three natural coordinates $s$, $n$, $z$ and also along the three standard coordinates $x, y, z$. In both systems the vertical coordinate $z$ is, of course, the same.

Let $\mathbf{a}$ be an arbitrary vector. Let $\mathbf{l}$ be a unit vector along any line $l$. The projection of $\mathbf{a}$ along $l$ is $a_l\mathbf{l}$; see 4·05. Any vector is the sum of its projections along three perpendicular axes; see 4·06. So $\mathbf{a}$ is expressed in natural coordinates as

$$\mathbf{a} = a_s\mathbf{t} + a_n\mathbf{n} + a_z\mathbf{k},$$

and in standard coordinates as

$$\mathbf{a} = a_x\mathbf{i} + a_y\mathbf{j} + a_z\mathbf{k}.$$

The vector $\mathbf{a}$ may also be projected into any plane. This projection is a vector equal to the sum of the two projections of $\mathbf{a}$ along any two perpendicular lines in the plane. Let the vector projection of $\mathbf{a}$ in the horizontal plane be denoted by $\mathbf{a}_H$. This vector is then given by

$$\mathbf{a}_H = a_s\mathbf{t} + a_n\mathbf{n} = a_x\mathbf{i} + a_y\mathbf{j}.$$

Moreover, the vector $\mathbf{a}$ is equal to the sum of its projection in a plane and its projection along the normal to that plane. Thus

$$\mathbf{a} = \mathbf{a}_H + a_z\mathbf{k}.$$

The equation of relative motion

6·19(3) $$\dot{\mathbf{v}} = \mathbf{b} + \mathbf{c} + \mathbf{g}$$

expresses Newton's second law: The observed relative acceleration equals the resultant of all acting forces, including inertial forces due to the motion of the relative frame. The vectors in the equation of relative motion can be projected along any line or into any plane. The projected equation expresses Newton's second law along that line or in that plane: The relative acceleration projection equals the sum of all the force projections.

Therefore the equation of relative motion projected along the line $l$ is

(1) $$\dot{v}_l = b_l + c_l + g_l.$$

And the equation of relative motion projected into the horizontal plane is

(2) $$\dot{\mathbf{v}}_H = \mathbf{b}_H + \mathbf{c}_H.$$

Here $\mathbf{g}_H$ does not appear, for the force of gravity has no horizontal component.

**7·04. The acceleration.** The acceleration of a particle in arbitrary motion is

6·05(9) $$\dot{\mathbf{v}} = \dot{v}\mathbf{t} + v^2\mathbf{K}.$$

The vector curvature, directed toward the center of curvature and normal to the unit tangent, is then given by

(1) $$\mathbf{K} = K_n\mathbf{n} + K_z\mathbf{k}.$$

Therefore the acceleration becomes

$$\dot{\mathbf{v}} = \dot{v}\mathbf{t} + v^2K_n\mathbf{n} + v^2K_z\mathbf{k}.$$

The natural components for horizontal flow are then

(2) $$\dot{v}_s = \dot{v},$$

(3) $$\dot{v}_n = v^2K_n,$$

(4) $$\dot{v}_z = v^2K_z.$$

The horizontal and vertical components of the centripetal acceleration contain respectively the horizontal and vertical components of the vector curvature. These curvature components will now be examined in detail.

**7·05. Cyclic sense.** When the motion of a particle is horizontal, the path of that particle must lie in a level surface. Although a level surface is not exactly spherical (section 6·10), it may be considered spherical in so far as the geometry of the path is concerned.

The intersection between a sphere and an arbitrary plane is always a circle. If the plane passes through the center of the sphere, the circle is called a *great circle*. Otherwise, the circle is called a *small circle*. The circle cut by the osculating plane at any point of a spherical path is the circle of curvature at that point. Its axis of rotation is perpendicular to the osculating plane at the center of curvature and passes through the center of the earth.

Momentarily a particle moves along the circle of curvature about the axis of rotation. The particle may move with either cyclic sense along this circle. If the circle of curvature is a small circle, the cyclic sense

will be defined as *positive* when the particle appears *from the local zenith* to be moving counterclockwise, and as *negative* when the particle appears to be moving clockwise. This definition is illustrated in the left-hand ($c^+$) and right-hand ($c^-$) diagrams of fig. 7·05. The lower diagrams are

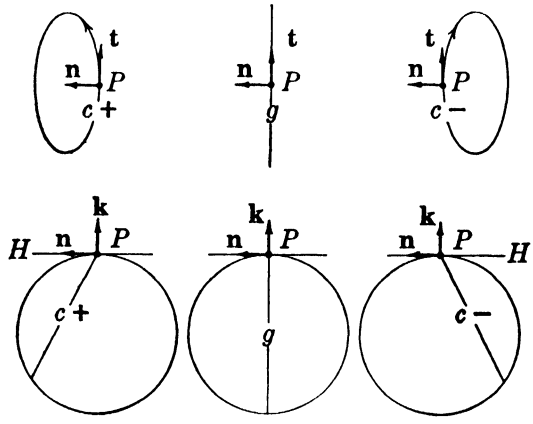



FIG. 7·05. Cyclic sense.

in the plane perpendicular to the path and show the particle at $P$ moving away from the reader. And the upper diagrams show the circle of curvature projected on the horizontal plane as it appears from the zenith at $P$.

If the circle of curvature of a particle is a great circle, the osculating plane passes through the local vertical. Consequently the path of the particle appears from the local zenith to be straight, as shown in the center diagram ($g$) of fig. 7·05. Flow momentarily along a great circle will be called *geostrophic*. Evidently geostrophic flow represents the transition between the positive and negative cyclic senses. So the cyclic sense of geostrophic flow may be defined either as positive or as negative.

In section 6·05 the quantities $\psi$, $K$, $R$, $\omega$ were defined as positive. However, for the discussion of horizontal flow it will be convenient to assign to them the cyclic sense as defined above. Accordingly in many of the equations of section 6·05 the symbols $\psi$, $K$, $R$, $\omega$ must be replaced by their absolute values. But this is not necessary in some equations, namely, in 6·05(5, 6, 7, 8).

Notice that the cyclic sense of rotation of a particle fixed to the earth is positive in the northern hemisphere and negative in the southern hemisphere. So $\Omega$ is positive in the northern hemisphere and negative in the southern hemisphere. For this reason the cyclic sense of zonal flow in

the southern hemisphere was not defined in section 6·11. However, all the equations of zonal flow so far introduced are valid in both hemispheres for either cyclic sense of rotation.

Internal consistency within this chapter requires that $\Omega$ have sense. That is, if the sense of angular rotation is distinguished by assigning cyclic sense to angular speeds, then, in particular, cyclic sense must be assigned to the angular speed of the earth. Accordingly the definitions and equations of this chapter apply to any horizontal flow in either hemisphere. However, since it is customary to regard $\Omega$ as positive, we shall strictly observe all the consequences of the cyclic sense convention in this chapter only.

**7·06. Angular radius of curvature.** Let $\theta$ be the acute angle ($\leqq \pi/2$) between the osculating plane and the horizontal plane. The angle $\theta$ will be called the *angular radius of curvature*, for, as shown in fig. 7·06*a*,

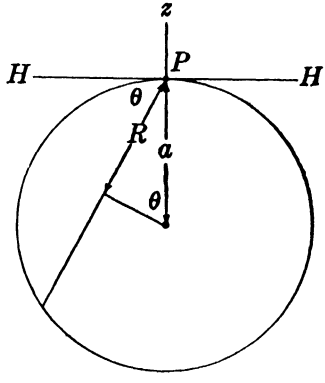



FIG. 7·06*a*. Angular radius of curvature.

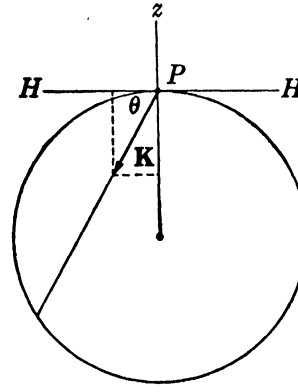



FIG. 7·06*b*. Natural components of **K**.

it is the angle subtended at the center of the earth by the radius of curvature. In particular, the angular radius of curvature for zonal flow is the colatitude.

The atmosphere may be considered as a thin blanket enveloping the earth. Whenever atmospheric flow is investigated, the distance to an air particle from the center of the earth is nearly equal to the mean radius of the earth. Consequently the radius of curvature subtending $\theta$ is $R = a \sin \theta$, and its reciprocal, the curvature, is

$$K = \frac{1}{a \sin \theta}. \tag{1}$$

This equation is valid for flow with either cyclic sense when we adopt the convention that $\theta$ *has the same sign as the cyclic sense.*

The vector curvature appears from the zenith to point to the left of flow with positive cyclic sense, and to the right of flow with negative cyclic sense. (See fig. 7·05.) The horizontal unit normal always points to the left of the flow, so the normal component $K_n = \mathbf{K}\cdot\mathbf{n}$ of the vector curvature has the same sign as the cyclic sense. It is seen from fig. 7·06*b* that the normal component of the vector curvature is

$$K_n = K \cos\theta. \tag{2}$$

Evidently this equation is valid for flow with either cyclic sense.

Since the center of curvature lies below the horizontal plane, the vertical component $K_z$ of the vector curvature is always negative. So, as shown in fig. 7·06*b*, this vertical component is

$$K_z = -K \sin\theta. \tag{3}$$

The curvature $K$ may be eliminated from the expressions for $K_n$ and $K_z$. When (1) is substituted in (2) and (3), we find

$$K_n = \frac{1}{a \tan\theta}, \tag{4}$$

$$K_z = -\frac{1}{a}. \tag{5}$$

We shall now show that these projections of the vector curvature of the spherical path are the curvatures of the corresponding projections of the spherical path.

**7·07. Horizontal curvature.** When the spherical path of a particle is projected onto the horizontal plane, a curve called the *horizontal path* is obtained. The curvature of this horizontal path is called the horizontal curvature and will be denoted by $K_H$.

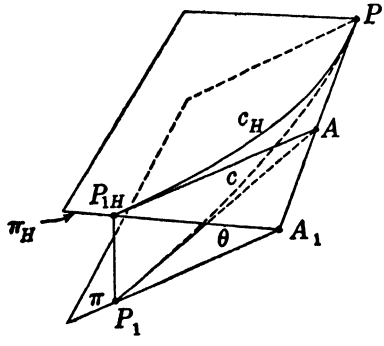



FIG. 7·07*a*. Horizontal curvature.

Consider an arc of an arbitrary spherical path $c$ near the point $P$; see fig. 7·07*a*. This arc may be thought of as being in the osculating plane $\pi$ of the spherical path at $P$. When the path $c$ is projected from $\pi$ onto the horizontal plane $\pi_H$ at $P$, we obtain the horizontal path $c_H$. The line of intersection between the planes $\pi$ and $\pi_H$ is the line $PAA_1$, tangent at the point $P$ both to $c$ and $c_H$. The two curves $c$ and $c_H$ define a cylinder normal to the horizontal plane $\pi_H$, whose generators are the

lines of projection from $c$ to $c_H$. The plane tangent to this cylinder along the generator $P_1P_{1H}$ intersects the tangent line at the point $A$. And the plane through the generator $P_1P_{1H}$ normal to the line $PAA_1$ intersects the line $PAA_1$ at $A_1$. The angle $P_1A_1P_{1H}$ is then the angle $\theta$ between the osculating plane and the horizontal plane.

The curvature of the spherical path $c$ at $P$ is by definition

6·05(5) $$K = \frac{d\psi}{ds},$$

where $d\psi = \angle A_1AP_1$ is the angular turn of the tangent to $c$ through the infinitesimal arc length $ds = PP_1$. Similarly the curvature of the horizontal path $c_H$ at $P$ is

(1) $$K_H = \frac{d\psi_H}{ds_H},$$

where $d\psi_H = \angle A_1AP_{1H}$ is the angular turn of the tangent to $c_H$ through the arc length $ds_H = PP_{1H}$.

As $P_1, P_{1H} \to P$, the arc length $ds$ along $c$ and $ds_H$ along $c_H$ become equal, so in the limit

(2) $$\frac{ds}{ds_H} = \frac{PP_1}{PP_{1H}} = 1.$$

And as $P_1, P_{1H} \to P$ the angles $d\psi$, $d\psi_H$ have the limiting ratio

$$\frac{d\psi_H}{d\psi} = \frac{AA_1 \cdot d\psi_H}{AA_1 \cdot d\psi} = \frac{A_1P_{1H}}{A_1P_1} = \cos\theta.$$

Therefore the horizontal curvature is given by

$$K_H = \frac{d\psi_H}{ds_H} = \frac{d\psi_H}{d\psi}\frac{d\psi}{ds}\frac{ds}{ds_H} = \cos\theta \cdot K \cdot 1.$$

And finally from 7·06(2) we find

(3) $$K_H = K\cos\theta = K_n.$$

Consequently, *the curvature of the horizontal projection of the path is equal to the horizontal component of the vector curvature.* So, from 7·06(4), the horizontal curvature may be expressed in terms of the angular radius of curvature as

(4) $$K_H = \frac{1}{a\tan\theta}.$$

Evidently the horizontal path is less strongly curved than the spherical path. The horizontal projection of the circle of curvature of a spherical

path is an ellipse (see fig. 7·05). The horizontal curvature is the curvature of this ellipse at the point $P$. However, the horizontal curvature may also be considered as the curvature of a circle, the *horizontal circle of curvature*, whose radius $R_H$ is the reciprocal of $K_H$. This radius is called the *radius of horizontal curvature* and is given by

$$R_H = a \tan \theta.$$

Notice that the smallest numerical value of the space curvature for horizontal flow is the curvature of a great circle. Since an arc of a great circle projects into a straight line on the horizontal plane, the horizontal curvature of a great circle is zero. Hence geostrophic flow, which is great circle flow on the earth, projects as linear flow in the horizontal plane. For this reason the cyclic sense of geostrophic flow is unimportant.

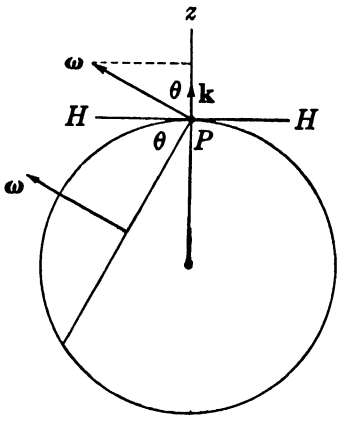



FIG. 7·07*b*. Vertical component of $\omega$.

The horizontal curvature has considerable practical importance because the meteorologist must work with plane maps of the earth. The curvature of a curve represented on a plane map of the earth is more nearly given by the horizontal curvature than by the space curvature, for a good map of the earth combines the horizontal plane projections at every point of the mapped region into a whole map with as little distortion as possible.

The horizontal curvature is closely associated with the component $\omega_z$ of the angular velocity about the local zenith. Fig. 7·07*b* shows that this component is

$$\omega_z = \omega \cos \theta. \tag{5}$$

Since, by (3), $K_H = K \cos \theta$, the relation

$$v = \frac{\omega}{K} = \omega R \qquad 6\text{·}05(8)$$

may be expressed as

$$v = \frac{\omega_z}{K_H} = \omega_z R_H. \tag{6}$$

Thus, as a particle moves along a spherical path with the angular speed $\omega$, its projection moves along the horizontal path with the angular speed $\omega_z$.

**7·08. Geodesic curvature.** Let $P_1$ and $P_2$ be any two distinct points on a surface $\sigma$. The shortest curve in $\sigma$ joining $P_1$ and $P_2$ is a *geodesic* of $\sigma$. Physically this geodesic can be visualized as the curve taken by a taut thread stretched between $P_1$ and $P_2$ on the convex side of a shell having the surface $\sigma$. If $\sigma$ is planar, the geodesics of $\sigma$ are straight line segments. And if $\sigma$ is spherical the geodesics of $\sigma$ are great circle arcs.

The geodesic curvature $K_g$ of a curve $c$ on $\sigma$ is defined as

$$K_g = \frac{d\psi_g}{ds},$$

where $d\psi_g$ is the angular turn of the geodesic, tangent to the curve, through the arc length $ds$. The construction of the angular turn between the geodesics $g$

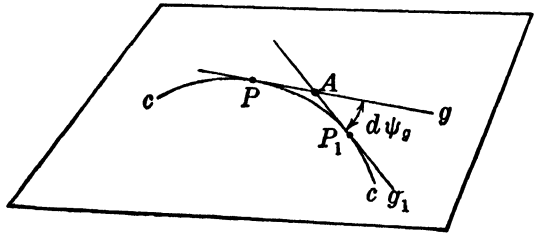



FIG. 7·08*a*.

and $g_1$, tangent to $c$ at $P$ and $P_1$ respectively, is illustrated in fig. 7·08*a* for a plane curve, and in fig. 7·08*b* for a spherical curve. Notice that the geodesic curvature is a generalized concept of curvature defined by an operation *entirely on the given surface.*

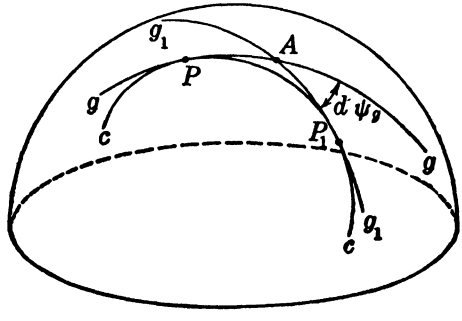



FIG. 7·08*b*.

If $\sigma$ is planar, evidently the geodesic curvature is the ordinary curvature. But if $\sigma$ is curved, the geodesic and ordinary curvatures are different. We shall now show that the geodesic curvature of a spherical curve is the horizontal curvature. Such a brief treatment will naturally be incomplete.

The spherical geodesics $g$ and $g_1$, represented in fig. 7·08*c*, are great circles whose planes intersect the horizontal plane tangent at $P$ in the straight lines

$g_H$ and $g_{1H}$ respectively. On the spherical surface $g$ and $g_1$ meet at $A$, and on the horizontal plane $g_H$ and $g_{1H}$ meet at $A_H$. As $P_1 \to P$, we see that $A, A_H \to P$ and that $d\psi_H, d\psi_g \to 0$. However, in the limit,

$$\frac{d\psi_g}{d\psi_H} = 1.$$

By 7·07(1, 2) we finally obtain

$$K_g = \frac{d\psi_g}{ds} = \frac{d\psi_g}{d\psi_H}\frac{d\psi_H}{ds_H}\frac{ds_H}{ds} = 1 \cdot K_H \cdot 1.$$

Consequently *the geodesic curvature of a spherical curve is equal to its horizontal curvature.* The curvature $K_H$, which occurs so often in the description of horizontal flow, may then be considered either as the geodesic curvature of the spherical path or as the planar curvature of the horizontal projection of the spherical path.

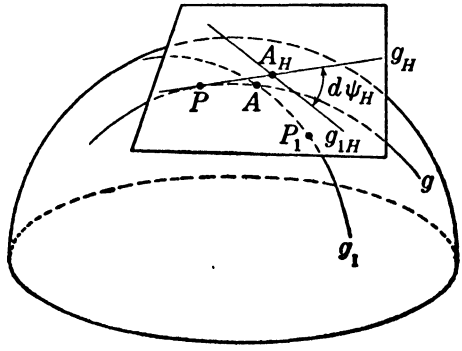



FIG. 7·08c.

**7·09. Vertical curvature.** Let the plane through the unit tangent and normal to the horizontal plane be called the *vertical plane.* When the spherical path is projected onto this vertical plane we obtain a curve called the *vertical path* whose curvature is the vertical curvature.

If the argument of section 7·07 is applied to the vertical path, we find that the curvature of the vertical path is equal to the vertical component of the vector curvature. Therefore the vertical curvature is $K_z$. Its reciprocal, the *radius of vertical curvature,* will be denoted by $R_z$. From 7·06(5) this radius is

$$R_z = -a.$$

Since $a$ is the radius of a great circle, *the spherical path projects into the vertical plane as an arc of a great circle no matter how strongly curved the spherical path may be.* Again we see how important is the notion of the great circle in horizontal flow.

In fig. 7·09 the three radii of curvature $R$, $R_H$, and $R_z$ are drawn to the

moving point $P$ from the centers of curvature $C$, $C_H$, and $C_z$ respectively. These centers are collinear points on the axis of rotation. The angular radius of curvature is then subtended both by $R$ and $R_H$.

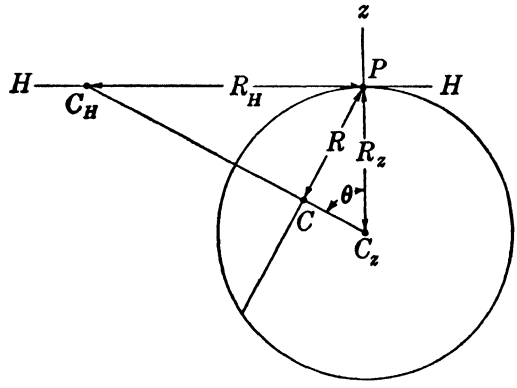



FIG. 7·09.

Since the horizontal and vertical components of the vector curvature represent curvatures, the horizontal and vertical components of the centripetal acceleration represent centripetal accelerations. As a particle moves along a spherical path, its projection in the horizontal plane moves along the horizontal path with the centripetal acceleration $K_H v^2$, and its projection into the vertical plane moves along the vertical path with the centripetal acceleration $K_z v^2$.

**7·10. The angular velocity of the earth.** The angular velocity of the earth is a vector parallel to the axis of the earth and extending northward. Since the natural coordinate system coincides with the standard coordinate system for a particle fixed to the earth, the simplest decomposition of $\Omega$ is afforded by standard coordinates. Moreover, we shall find that the natural coordinate components of $\Omega$ are not required.

Since the angular velocity of the earth is a meridional vector,

$$\Omega_x = 0. \tag{1}$$

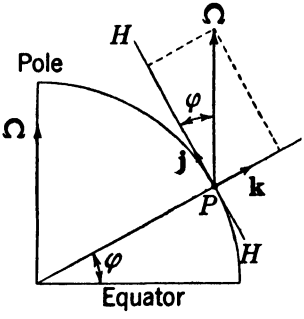



FIG. 7·10. Rectangular components of Ω.

The other standard components are in the meridional plane. Fig. 7·10 shows that these components are easily expressed in terms of the latitude $\varphi$. The component to the local north is

$$\Omega_y = |\Omega| \cos \varphi, \tag{2}$$

and the component along the local vertical is

(3) $$\Omega_z = |\Omega| \sin \varphi.$$

The vertical component of the earth's rotation is positive in the northern hemisphere and negative in the southern hemisphere. Equation (3) is valid in both hemispheres when the latitude angle $\varphi$ is considered positive in the northern hemisphere and negative in the southern hemisphere.

Since $\Omega$ is positive in the northern hemisphere and negative in the southern hemisphere, the component of the earth's rotation about the local zenith may also be written

(4) $$\Omega_z = \Omega \sin |\varphi|.$$

Evidently equation (2) is not altered by the sign of the latitude. The component of $\boldsymbol{\Omega}$ to the local north is always positive.

The components of the angular velocity of the earth are required for the decomposition of the Coriolis force.

**7·11. The Coriolis force.** The Coriolis force is given by the vector product

6·19(2) $$\mathbf{c} = -2\boldsymbol{\Omega} \times \mathbf{v}.$$

We shall evaluate this vector product in standard and natural components by using the determinant expression 6·13(6).

The Coriolis force may then be expressed in standard components by the determinant:

$$\mathbf{c} = -2 \begin{vmatrix} \mathbf{i} & \mathbf{j} & \mathbf{k} \\ 0 & \Omega_y & \Omega_z \\ v_x & v_y & 0 \end{vmatrix}.$$

Expansion of this determinant gives

$$\mathbf{c} = 2\Omega_z v_y \mathbf{i} - 2\Omega_z v_x \mathbf{j} + 2\Omega_y v_x \mathbf{k}.$$

So the standard components of the Coriolis force are:

(1) $$c_x = 2\Omega_z v_y,$$

(2) $$c_y = -2\Omega_z v_x,$$

(3) $$c_z = 2\Omega_y v_x.$$

And the Coriolis force may be expressed in natural components by the determinant:

$$\mathbf{c} = -2 \begin{vmatrix} \mathbf{t} & \mathbf{n} & \mathbf{k} \\ \Omega_s & \Omega_n & \Omega_z \\ v & 0 & 0 \end{vmatrix}.$$

Expansion of this determinant gives

$$\mathbf{c} = -2\Omega_z v\mathbf{n} + 2\Omega_n v\mathbf{k}.$$

So the natural components of the Coriolis force are:

$$c_s = 0, \tag{4}$$

$$c_n = -2\Omega_z v, \tag{5}$$

$$c_z = 2\Omega_n v. \tag{6}$$

Since the Coriolis force is normal to the velocity, the tangential component $c_s$ is zero. It is for this reason that the Coriolis force has been called the deflecting force.

The normal component $c_n$ is then the only horizontal component. The vertical component of the earth's angular velocity occurring in the expression for $c_n$ is positive in the northern hemisphere, zero at the equator, and negative in the southern hemisphere. Accordingly the horizontal Coriolis force as seen from the zenith acts to the right in the northern hemisphere, is zero at the equator, and acts to the left in the southern hemisphere.

Since the only horizontal component of the Coriolis force is normal to the flow, the horizontal vector component $\mathbf{c}_H$ is given by

$$\mathbf{c}_H = c_n\mathbf{n} = -2\Omega_z v\mathbf{n}.$$

We shall define the vector $\boldsymbol{\Omega}_z$, extending along the local vertical, by

$$\boldsymbol{\Omega}_z = \Omega_z\mathbf{k}.$$

Therefore the horizontal vector component of the Coriolis force may be written in the form

$$\mathbf{c}_H = -2\Omega_z v\mathbf{n} = -2\Omega_z v\mathbf{k}\times\mathbf{t} = -2\boldsymbol{\Omega}_z\times\mathbf{v}. \tag{7}$$

Finally, the vertical component $c_z$ is given either by (3) or by (6). Both expressions are, of course, the same. However the standard component form is more convenient to use.

**7·12. The pressure force and the force of gravity.** So far the components of two vectors in the equation of relative motion have been found. The other two vectors are the force of gravity and the pressure force. These forces are easily resolved.

The components of the force of gravity have already been obtained in 4·12(6). This force has no horizontal components, so $g_s$, $g_n$, $g_x$, $g_y$ are all zero. The only component of the force of gravity is in the vertical, so $g_z = \mathbf{g}\cdot\mathbf{k} = -g$.

The components of the pressure force may be obtained by reference to

section 4·15. When equation 4·15(4) is multiplied by the specific volume, we find for the component of the pressure force in the direction $l$

$$b_l = -\alpha \mathbf{l} \cdot \nabla p = -\alpha \frac{\partial p}{\partial l},$$

and the horizontal pressure force is

(1) $$\mathbf{b}_H = -\alpha \nabla_H p.$$

This horizontal force acts normal to the horizontal isobars toward lower pressure.

**7·13. The component equations of relative motion.** We have examined the standard and natural components of each vector in the equation of relative motion. The component equation along any line $l$ is

7·03(1) $$\dot{v}_l = b_l + c_l + g_l.$$

This equation shows that the relative acceleration component equals the sum of the force components. The components $\dot{v}_l$, $b_l$, $c_l$, $g_l$ have been obtained in the previous sections. They are assembled in the following table.

| $l$ | l | $\dot{v}_l$ | $b_l$ | $c_l$ | $g_l$ |
|---|---|---|---|---|---|
| $x$ | i | $\dot{v}_x$ | $-\alpha \frac{\partial p}{\partial x}$ | $2\Omega_z v_y$ | 0 |
| $y$ | j | $\dot{v}_y$ | $-\alpha \frac{\partial p}{\partial y}$ | $-2\Omega_z v_x$ | 0 |
| $z$ | k | $\dot{v}_z$ | $-\alpha \frac{\partial p}{\partial z}$ | $2\Omega_y v_x$ | $-g$ |
| $s$ | t | $\dot{v}$ | $-\alpha \frac{\partial p}{\partial s}$ | 0 | 0 |
| $n$ | n | $K_H v^2$ | $-\alpha \frac{\partial p}{\partial n}$ | $-2\Omega_z v$ | 0 |
| $z$ | k | $-\frac{v^2}{a}$ | $-\alpha \frac{\partial p}{\partial z}$ | $2\Omega_y v_x$ | $-g$ |

The standard component equations are given by the first three rows of the table. They are

(1) $$v_x = -\alpha \frac{\partial p}{\partial x} + 2\Omega_z v_y,$$

$$\dot{v}_y = -\alpha \frac{\partial p}{\partial y} - 2\Omega_z v_x, \tag{2}$$

$$v_z = -\alpha \frac{\partial p}{\partial z} + 2\Omega_y v_x - g. \tag{3}$$

These equations are displayed here for reference. They are often used in the investigation of atmospheric dynamics when it is desired to have the orientation of the coordinate system independent of the motion (see chapter 12).

However, we shall examine in detail only the natural component equations, given in the last three rows of the table. They are

$$\dot{v} = -\alpha \frac{\partial p}{\partial s}, \tag{4}$$

$$K_H v^2 = -\alpha \frac{\partial p}{\partial n} - 2\Omega_z v, \tag{5}$$

$$-\frac{v^2}{a} = -\alpha \frac{\partial p}{\partial z} + 2\Omega_y v_x - g. \tag{6}$$

These component equations along the natural coordinates $s$, $n$, and $z$ are called the *tangential*, *normal*, and *vertical* equations respectively. They will be discussed in the following sections.

**7·14. The vertical equation.** The vertical equation of relative motion equates the vertical centripetal acceleration to the sum of the vertical components of the acting forces. Thus,

$$\dot{v}_z = b_z + c_z - g.$$

The force of gravity occurring in this equation is the resultant vertical force measured by an observer fixed to the earth. However, if the observer moves horizontally relative to the earth the resultant vertical force which he measures is not equal to the force of gravity, for it also includes the vertical inertial forces due to the motion, namely, the vertical centrifugal force and the vertical Coriolis force. The resultant vertical force will be called the *virtual gravity*. Its magnitude $g^*$ is given by

$$g^* = g + \dot{v}_z - c_z = g - \frac{v^2}{a} - 2\Omega_y v_x.$$

A moving particle will be called "*heavier*," if $g^* > g$, and "*lighter*," if $g^* < g$.

The vertical centrifugal force is the centrifugal force which would be exerted on the projection of the particle moving along the vertical path.

Since the vertical path is an arc of a great circle, the effect of the vertical centrifugal force opposes the force of gravity, always making the particle lighter.

The vertical Coriolis force acts upward when the particle moves toward the east and downward when the particle moves toward the west. So its effect is to make the particle lighter for eastward motion and heavier for westward motion. Moreover, for a given horizontal velocity the effect of the vertical Coriolis force, being proportional to $\cos \varphi$, is zero at the poles and greatest at the equator.

Even for the strongest flow speeds (100 m $s^{-1}$) attained by the atmosphere the centrifugal and Coriolis correction terms to the force of gravity are small. The greatest error occurs in eastward flow at the equator. For $v = 100$ m $s^{-1}$ the centrifugal correction is then 0.0016 m $s^{-2}$. And the Coriolis correction is 0.0146 m $s^{-2}$. So the total error is 0.0162 m $s^{-2}$. When this error is compared with the mean value $g = 9.81$ m $s^{-2}$, we find that the correction terms are usually negligible for horizontal atmospheric flow. Hence $g^*$ *may usually be replaced by* $g$. That is,

$$g^* \approx g. \tag{1}$$

When the vertical equation is expressed in terms of the virtual gravity, we find

$$b_z = g^*. \tag{2}$$

The vertical pressure force is then completely balanced by the force of virtual gravity. (2) is called the *generalized hydrostatic equation.* When the relative flow is zero, $g^* = g$, and (2) becomes the hydrostatic equation.

For an atmosphere in horizontal motion height should be computed by the generalized hydrostatic equation. However, by (1) the hydrostatic equation is approximately satisfied. In fact, the error introduced by neglecting the inertial contributions to the virtual gravity is less than the unavoidable instrumental errors of the sounding equipment. Therefore the practical use of the hydrostatic equation in chapter 4 for computation of height is justified whenever the atmospheric flow is horizontal.

**7·15. The tangential equation.** The tangential equation of relative motion equates the change of speed to the tangential component of the pressure force. Thus

$$\dot{v} = b_s = -\alpha \frac{\partial p}{\partial s}. \tag{1}$$

A particle moving horizontally changes speed only when crossing horizontal isobars. *A particle moving toward lower pressure speeds up, and a particle moving toward higher pressure slows down.* Since a particle moving along a horizontal isobar is not subject to a tangential pressure force, it moves momentarily with constant speed. Horizontal flow along the isobars, and therefore normal to the pressure gradient, is called *gradient flow.* Gradient flow, accordingly, occurs at points where $\dot{v} = 0$, that is, at points of constant or extreme (maximum, minimum) speed.

If the flow at every point of the atmosphere were gradient flow, the horizontal isobars would everywhere be tangent to the wind direction. But in general the atmospheric flow is gradient only at isolated points. However, at any instant curves can be drawn which are everywhere tangent to the wind direction. Such curves are called *streamlines.* The streamlines give a snapshot of the flow direction throughout the entire atmosphere at a fixed time; they represent the *flow pattern* at that time. Usually this flow pattern varies from instant to instant. If the flow pattern is the same at every instant, the flow is called *steady.* The flow direction at every point is then independent of time.

We must make a clear distinction between a streamline and a path. A streamline is a curve tangent to the velocities of different air particles at a given instant, whereas a path is a curve tangent to the velocities of a given air particle at different instants. At a fixed time a streamline can be drawn through any given point of the atmosphere. Through the same point a path can also be drawn, namely, the path of the air particle which momentarily occupies that point. Since these two curves, the path and the streamline, have the same direction at the given point, they are tangent curves, but in general the two curves have different shapes. If the flow is steady, the path and the streamline through the given point coincide.

In the atmosphere the flow patterns are usually changing, so the streamlines and the paths have different shapes. However, horizontal currents in the atmosphere change speed rather slowly. When the current speeds up it flows slightly across the isobars toward lower pressure, and when the current slows down it flows slightly across the isobars toward higher pressure. The streamlines are therefore nearly along the isobars. This practical rule allows the horizontal pressure field to be drawn with considerable accuracy from a few scattered wind and pressure data. The relation between the streamlines and the isobars will be examined in more detail in chapter 12.

This discussion holds only for horizontal flow in the free atmosphere above the frictional layer. Near the surface of the earth the motion has

a component toward lower pressure as a consequence of friction. The flow under frictional forces will be treated in chapter 9.

**7·16. The normal equation.** The normal equation of relative motion equates the horizontal centripetal acceleration to the resultant of the normal pressure force and the horizontal Coriolis force. Thus

$$\dot{v}_n = b_n + c_n. \tag{1}$$

Although this equation clearly shows the dynamics of the flow, the kinematics is better understood when $\dot{v}_n$ and $c_n$ are expressed in terms of the speed. We then obtain from (1)

$$K_H v^2 + 2\Omega_z v - b_n = 0. \tag{2}$$

This equation is quadratic in $v$. Since $\Omega_z = |\Omega| \sin \varphi$, the speed depends on the horizontal curvature, the latitude, and the normal pressure force.

The latitude is by our convention (see section 7·10) positive in the northern hemisphere and negative in the southern hemisphere. The two latitudes $(\varphi, -\varphi)$ will be called *corresponding latitudes*. At corresponding latitudes the normal equation (2) gives the same speed $v$ for $\varphi$, $K_H, b_n$ in the northern hemisphere as for $-\varphi$, $-K_H$, $-b_n$ in the southern hemisphere. At corresponding latitudes, $(K_H, -K_H)$ will be called *corresponding horizontal curvatures*, and $(b_n, -b_n)$ will be called *corresponding normal pressure forces*.

These definitions of correspondence are equivalent to replacing $\mathbf{n}$ in the northern hemisphere by $-\mathbf{n}$ in the southern hemisphere. That is, *the direction to the left of the flow in the northern hemisphere corresponds to the direction to the right of the flow in the southern hemisphere.* The physical reason for this interchange is clear; the horizontal Coriolis force acts to the right of the flow in the northern hemisphere and to the left of the flow in the southern hemisphere. In corresponding flow the normal pressure force and the horizontal centripetal acceleration in both hemispheres have the same orientation with respect to the horizontal Coriolis force.

If the normal pressure force is opposite to the horizontal Coriolis force, the flow is called *baric*; and if the normal pressure force is along the horizontal Coriolis force, the flow is called *antibaric* (see fig. 7·16). In the northern hemisphere the flow is baric if low pressure lies to the left of the flow, and antibaric if low pressure lies to the right. In the southern hemisphere the flow is baric if low pressure lies to the right of the flow, and antibaric if low pressure lies to the left. Finally, if the normal pressure force is zero the flow is called *inertial*, for the only horizontal force, the horizontal Coriolis force, is an inertial force.

If the horizontal centripetal acceleration is opposite to the horizontal Coriolis force, the flow is called *cyclonic*; and if the horizontal centripetal

acceleration is along the horizontal Coriolis force, the flow is called *anticyclonic* (see fig. 7·16). In the northern hemisphere flow curved to the left is cyclonic and flow curved to the right is anticyclonic. In the southern hemisphere flow curved to the right is cyclonic and flow curved to the left is anticyclonic. Finally, if the horizontal centripetal acceleration is zero the flow is geostrophic.

The above definition of cyclonic and anticyclonic sense generalizes to arbitrary horizontal flow the definition given earlier for zonal flow. This generalization is more clearly exhibited by the following equivalent definition of cyclonic and anticyclonic sense, based upon the sense of the

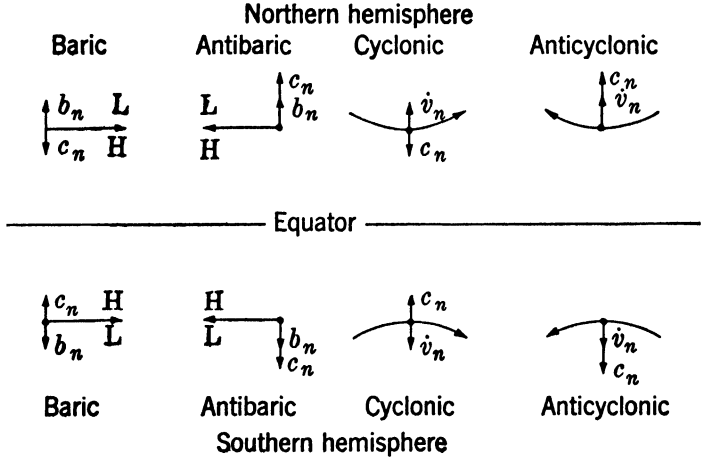



FIG. 7·16.

earth's rotation about the local zenith. *Flow which appears from the local zenith to have the same sense as the rotation of the earth about that zenith is cyclonic, and flow which appears to have the opposite sense is anticyclonic.* Both this definition and the definitions of positive (counterclockwise) and negative (clockwise) cyclic sense refer to the flow as it appears from the local zenith. That is, these definitions refer to the horizontal path of the flow. Cyclic sense is defined according to an arbitrary rule, whereas cyclonic sense and anticyclonic sense are defined according to the sense of a physically given rotation — the rotation of the earth about the local zenith.

Cyclonic flow and anticyclonic flow are defined according to the orientation of the horizontal centripetal acceleration with respect to the horizontal Coriolis force. Baric flow and antibaric flow are defined according to the orientation of the normal pressure force with respect to the horizontal Coriolis force. These definitions do not apply at the equator

where the horizontal Coriolis force is zero. However, even at the equator the definitions of geostrophic flow ($K_H = 0$) and of inertial flow ($b_n = 0$) apply.

Before examining the normal equation for arbitrary horizontal flow, we shall consider the three simple but physically important flow types which occur when one term of the normal equation is zero.

**7·17. Geostrophic flow.** Flow along a great circle is geostrophic. The horizontal curvature and the horizontal centripetal acceleration are then zero, so the normal pressure force is completely balanced by the horizontal Coriolis force. The two forces are equal and opposite, and the normal equation becomes

$$0 = b_n + c_n. \tag{1}$$

Since the normal pressure force is opposite to the horizontal Coriolis force, geostrophic flow is baric. That is, a geostrophic current has low pressure to the left in the northern hemisphere and low pressure to the right in the southern hemisphere. This rule, known as the *baric wind law*, was discovered empirically by Buys Ballot in 1857.

The geostrophic wind speed will be denoted by $v_g$. Solving equation (1) for this speed, we find

$$v_g = \frac{b_n}{2\Omega_z}. \tag{2}$$

Notice that geostrophic flow is the same for corresponding normal pressure forces at corresponding latitudes.

The dependence of the geostrophic wind upon the normal pressure force and the latitude is shown graphically in fig. 7·17*a*. Isopleths of $v_g$ are plotted against linear coordinates of $b_n$ and $\Omega_z$. The $v_g$ isopleths are straight lines radiating from the point $b_n = 0, \varphi = 0$ off the graph. Since the geostrophic wind becomes infinite at the equator for any non-zero normal pressure force, geostrophic flow cannot be realized in equatorial regions. So the graph is cut off at $\varphi = 30°$.

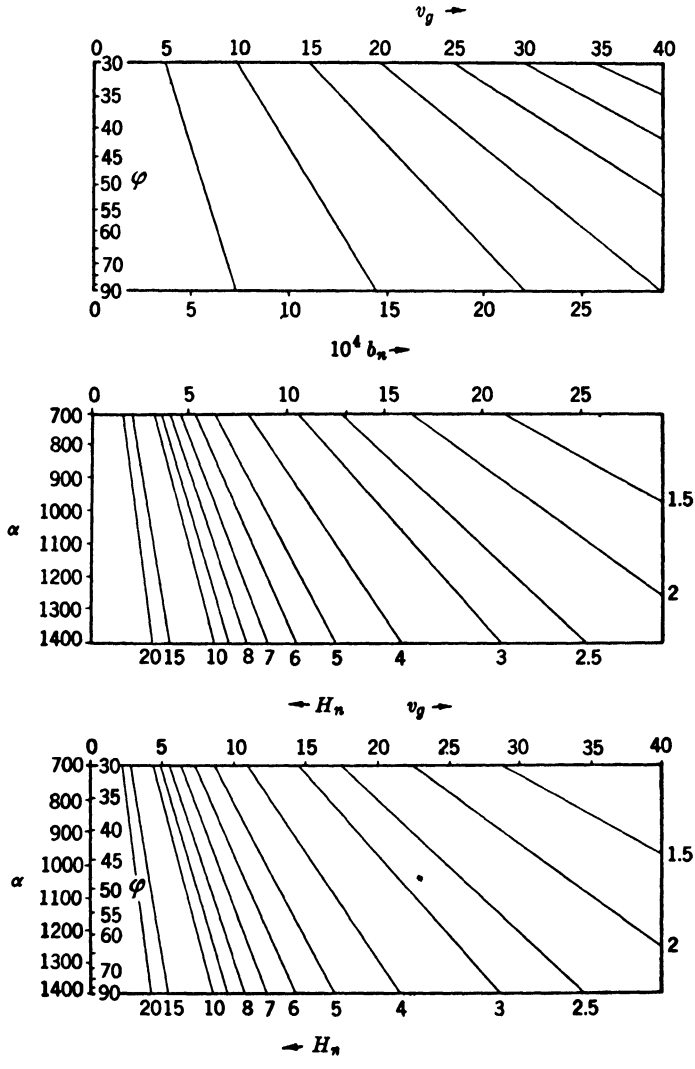
To evaluate the normal pressure force the horizontal pressure field must be known. Let the horizontal pressure field be represented by horizontal isobars drawn for the pressure interval $\Delta p$. The variation of pressure in the $n$ direction may be found by measuring the distance $\Delta n$ *normal to the flow* between consecutive isobars.

The most convenient unit of distance on a weather map is the degree of latitude. This unit is independent of the map projection. If the earth is regarded as a sphere of radius $a$, the degree of latitude has the constant length of $\pi a/180 = 111.1$ km. See 1·04(1).

Let the distance $\Delta n$, expressed in degrees of latitude, be $H_n$. Then

$\Delta n = 1.11 \times 10^5 H_n$. If $H_n$ is measured toward lower pressure between isobars drawn for 5-mb intervals, then $\Delta p = -0.5$, and

$$b_n = -\alpha \frac{\Delta p}{\Delta n} = 4.50 \times 10^{-6} \frac{\alpha}{H_n}. \tag{3}$$




Top: FIG. 7·17*a*; middle: FIG. 7·17*b*; bottom: FIG. 7·17*c*.

The graphical solution of this equation is shown in fig. 7·17*b*. Isopleths of $H_n$ are plotted against linear coordinates of $b_n$ and $\alpha$. The $H_n$ iso-

pleths are straight lines radiating from the point $b_n = 0$, $\alpha = 0$ off the graph.

When $b_n$ is eliminated from (2, 3), we find

$$H_n v_g \sin\varphi = 30.9 \frac{\alpha}{1000}. \tag{4}$$

This elimination of $b_n$ may be performed graphically in two operations: the first on fig. 7·17*a* and the second on fig. 7·17*b*. When these figures are superposed, the $v_g$ isopleths and the $H_n$ isopleths radiate from the same point. So both sets of isopleths may be represented by one set of lines. Fig. 7·17*c* shows the superposed graphs with one set of lines. These lines are drawn for integral values of $H_n$. They are labeled for $H_n$ along the bottom and right side. And they are labeled for $v_g$ along the top. The left side serves both as an $\alpha$ coordinate and a $\varphi$ coordinate.

Fig. 7·17*c* gives $v_g = v_g(\alpha, H_n, \varphi)$. $\alpha$ is not directly available from meteorological observations. From the equation of state we have

$$\alpha = \frac{R_d T^*}{p}. \tag{4·17(3)}$$

This equation is represented graphically in fig. 7·17*d*. Isopleths of $p$ are plotted against linear coordinates of $\alpha$ and $T^*$. The $p$ isopleths are straight lines radiating from the point $\alpha = 0$, $T^* = 0$ off the graph.

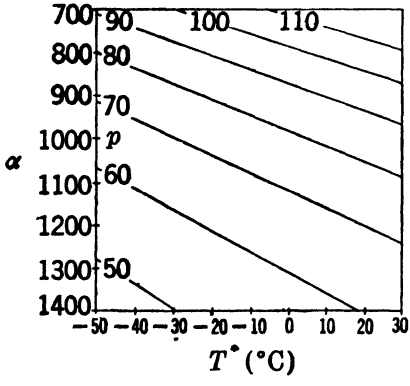



FIG. 7·17*d*. Graph of equation of state.

The complete practical solution $v_g = v_g(p, T^*, H_n, \varphi)$ is obtained by joining fig. 7·17*d* to the left side of fig. 7·17*c*. The resulting graph is shown in fig. 7·17*e*, and an example of the procedure is illustrated in fig. 7·17*f*. From the data $p = 100$ cb, $T^* = 0°C$, $H_n = 3°$, $\varphi = 45°$, the value $v_g = 11.4$ m s$^{-1}$ is obtained. The elimination of $b_n$ is shown in this diagram by the line labeled "$b_n$ = const" connecting the operations in the two superposed graphs.

In practical application the value of the speed is not so much required as the displacement of an air parcel from one weather map to the map twelve hours later. The unit of distance is again the degree of latitude. The total twelve-hour displacement in degrees of latitude is denoted by $D$. If the speed is constant throughout the twelve-hour interval

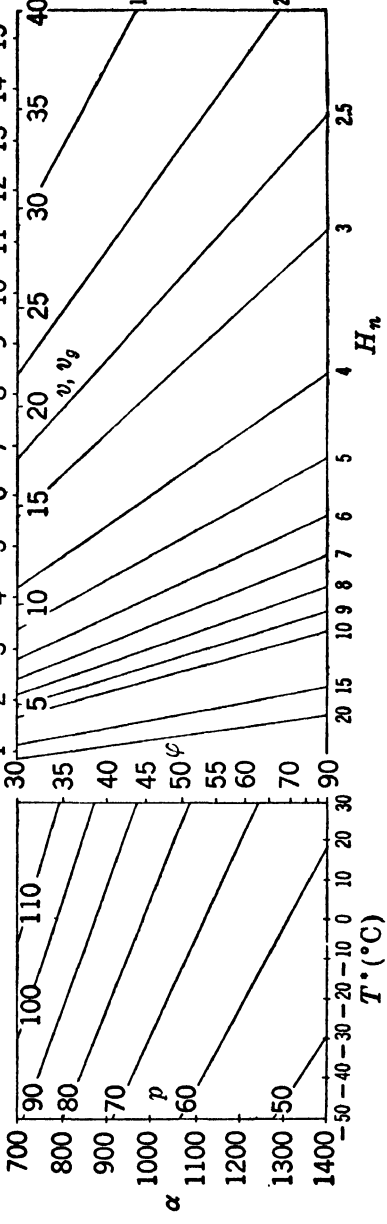



FIG. 7·17e.

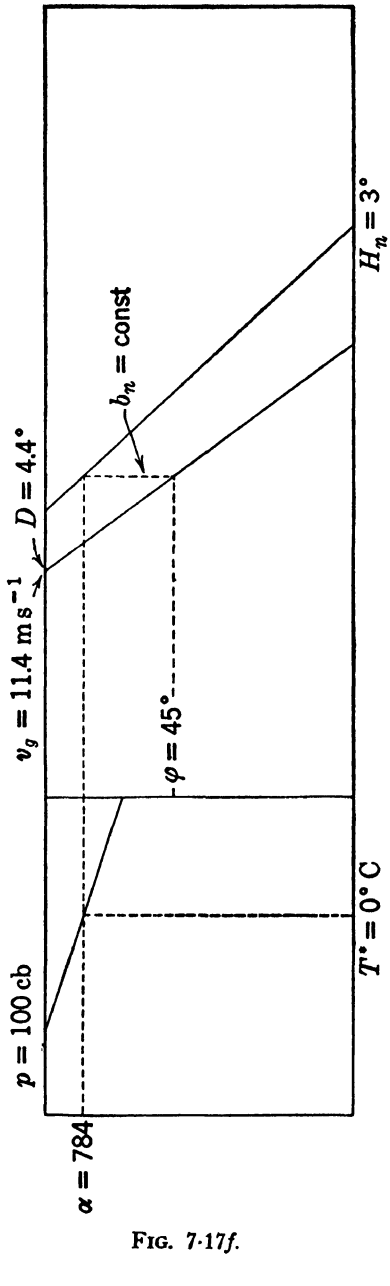



FIG. 7·17f.

between maps, $D$ is merely a constant multiple of $v$. Thus

$$D = \frac{12 \cdot 60 \cdot 60}{1.11 \cdot 10^5} v = 0.39v. \tag{5}$$

Even though the current speeds up or slows down, the value defined by (5) can be calculated. Evidently this value of $D$ is often more useful than is the value of $v$. A scale of $D$ has been placed along the $v_g$ scale in fig. 7·17*e*. The displacement in the above example is $D = 4.4°$.

**7·18. Inertial flow.** When the pressure force has no normal component, the horizontal flow is inertial. The horizontal centripetal acceleration is then equal to the horizontal Coriolis force, and the normal equation becomes

$$\dot{v}_n = c_n. \tag{1}$$

Both the centripetal acceleration and the Coriolis force are zero for a resting particle, so (1) is satisfied by

$$v = 0. \tag{2}$$

However, (1) also has a non-zero solution which will be denoted by $v_i$. This non-zero inertial wind speed is then given by

$$v_i = -\frac{2\Omega_z}{K_H}. \tag{3}$$

Since the horizontal centripetal acceleration is along the horizontal Coriolis force, inertial flow in both hemispheres is anticyclonic. An inertial current crossing the equator must then change cyclic sense. So inertial flow at the equator is geostrophic.

The graphical solution of (3) is shown in fig. 7·18*a*. Isopleths of $v_i$ are plotted against linear coordinates of $\Omega_z$ and $K_H$. The $K_H$ coordinate is labeled both in multiples of the curvature of a great circle and in degrees of angular radius of curvature. The $v_i$ isopleths are straight lines radiating from $\varphi = 0$, $K_H = 0$. They intersect any coordinate of constant latitude in a reciprocal $v_i$ scale. This fact will be useful later.

For inertial flow the angular speed of the horizontal projection of a particle is, from (3) and 7·07(6),

$$\omega_{zi} = v_i K_H = -2\Omega_z. \tag{4}$$

And the angular speed of inertial flow along a spherical path is, from 7·07(5),

$$\omega_i = \frac{\omega_{zi}}{\cos\theta} = -\frac{2\Omega_z}{\cos\theta}. \tag{5}$$

When the flow is zonal, the angular radius of curvature is the colatitude. Therefore $\cos\theta = \sin|\varphi|$, and (5) becomes $\omega_i = -2\Omega$ by 7·10(4). From (2), the angular speed of inertial flow may also be zero. Both results are verified in fig. 6·11$c_2$,$c_2'$. Inertial zonal flow occurs only when the isobaric and level surfaces coincide.

Inertial flow can be realized momentarily by a horizontal current flowing directly across horizontal isobars toward lower pressure. This

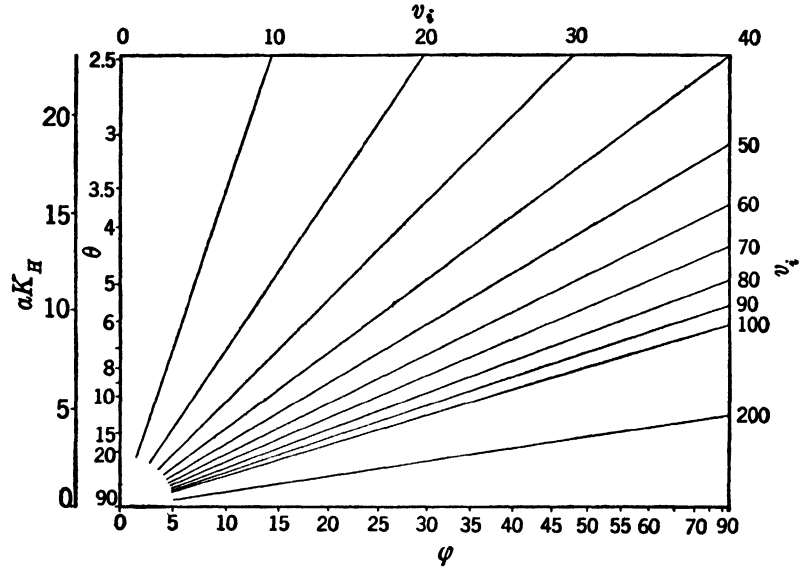



FIG. 7·18*a*. Graph of inertial wind speed.

current would curve anticyclonically and become baric. It would also speed up, for the pressure force at the moment of inertial flow would be wholly tangential.

However, as in zonal motion, inertial flow over an extended region can be realized only when an isobaric surface is level. Both the normal and the tangential pressure forces are then zero. And a current will move anticyclonically with constant speed in an inertial path. Since the magnitude of the earth's rotation about the local zenith is greater near the poles and zero at the equator, the curvature of the inertial path is also greater near the poles and zero at the equator.

An inertial path crossing the equator will oscillate about the equator between the corresponding latitudes $\varphi$, $-\varphi$, as shown in fig. 7·18*b*. An inertial path not crossing the equator will oscillate between two latitudes $\varphi_P$, $\varphi_E$, as shown in fig. 7·18*c*. The path will be looped, for the

curvature is greatest at the latitude $\varphi_P$ nearest the pole and least at the latitude $\varphi_E$ nearest the equator.

As $v_i \to 0$, the inertial path becomes more strongly curved, and the inertial circle of curvature shrinks to a point. The limiting *inertial period* $\tau_i$ required for the particle to rotate about this inertial circle centered at the latitude $\varphi$ is given by

$$\tau_i = \frac{2\pi}{|\omega_{zi}|} = \frac{2\pi}{2|\Omega_z|} = \frac{1}{2}\,\frac{\text{sidereal day}}{\sin|\varphi|}. \tag{6}$$

The particle completes one loop of the inertial path approximately in the inertial period $\tau_i$.

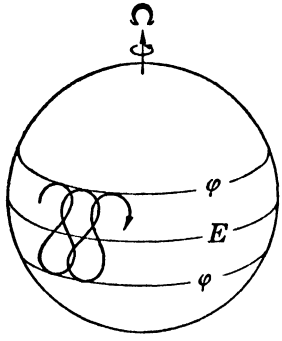



FIG. 7·18*b*.

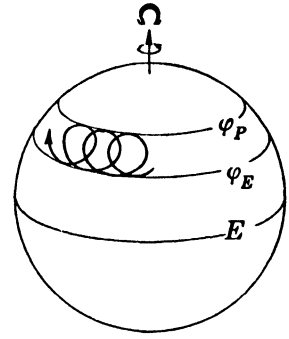



FIG. 7·18*c*.

The inertial period is simply related to the period of relative revolution of the plane of oscillation of a freely suspended pendulum. This plane maintains its orientation in space, while the earth rotates under it with the angular speed $\Omega_z$. It appears from the earth as if the pendulum plane rotates about the vertical in the opposite direction. The period of revolution of the pendulum plane is called the *pendulum day*, and is given by

$$\tau_p = \frac{2\pi}{|\Omega_z|} = \frac{\text{sidereal day}}{\sin|\varphi|}. \tag{7}$$

Evidently $\tau_p = 2\tau_i$, so the inertial period is one-half of the pendulum day.

**7·19. Cyclostrophic flow.** Whenever horizontal flow in the northern hemisphere is compared with horizontal flow in the southern hemisphere, the direction of the horizontal Coriolis force and the sense of the earth's rotation about the local zenith are important. At the equator both the horizontal Coriolis force and the earth's rotation about the zenith are zero, so the normal equation becomes

$$\dot{v}_n = b_n. \tag{1}$$

Unless the normal pressure force is zero, equatorial flow cannot be geostrophic. The circle of curvature is then a small circle, and the flow is called *cyclostrophic*. By (1) the center of horizontal curvature of a cyclostrophic current lies on the low-pressure side of the current.

When (1) is solved for the cyclostrophic wind speed $v_c$ we find

$$v_c^2 = \frac{b_n}{K_H}. \tag{2}$$

This equation is represented graphically in fig. 7·19. Isopleths of $v_c$ are plotted against linear coordinates of $b_n$ and $K_H$. These isopleths are straight lines radiating from the point $b_n = 0$, $K_H = 0$. The normal pressure force $b_n$ may be evaluated from the graphs for geostrophic flow.

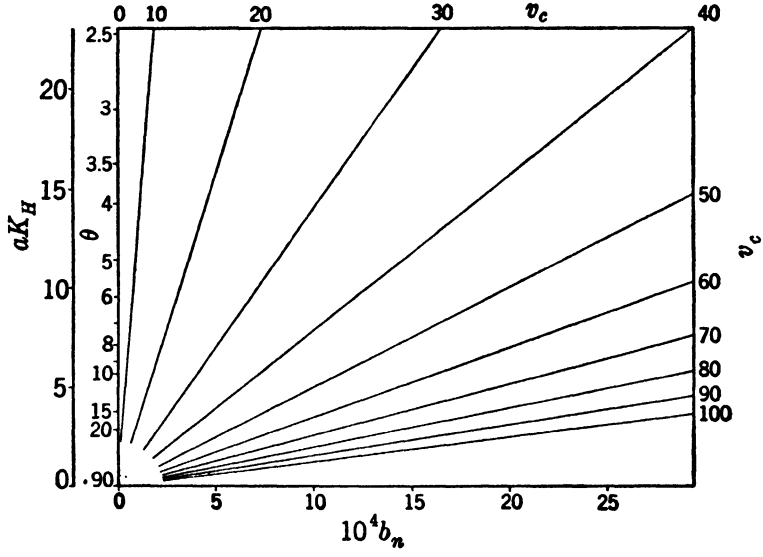



FIG. 7·19. Graph of cyclostrophic wind.

**7·20. Arbitrary horizontal flow.** The normal equation of horizontal motion is

$$v_n = b_n + c_n. \tag{7·16(1)}$$

We have examined this equation when one of the three terms is zero. In general all three terms are important.

In order to use the normal equation the direction of the flow or the rate of change of speed must be known. Let $\beta$ be the angle measured counterclockwise about the zenith from the horizontal pressure force $\mathbf{b}_H$ to the horizontal unit normal $\mathbf{n}$ as shown in fig. 7·20*a*. $\beta$ is also the angle

between the isobar $p$ and the flow direction $s$. Evidently the normal and tangential components of the pressure force are $b_n = b_H \cos \beta$ and $b_s = b_H \sin \beta$, respectively. Since $\dot{v} = b_s$, the normal pressure force may be expressed in terms of the horizontal pressure gradient and the rate of change of the speed as follows:

$$b_n^2 = b_H^2 - b_s^2 = b_H^2 - \dot{v}^2.$$

At points where the current is gradient $\beta$, $b_s$, and $\dot{v}$ are all zero; the current flows momentarily along the horizontal isobars with constant or extreme speed. In general the current overflows slightly across the isobars toward lower or higher pressure (see 7·15).

As shown in fig. 7·20*b* (valid for the northern hemisphere) a given wind speed is compatible with any normal pressure force at a given latitude. In the diagram $\dot{v}_n$, $b_n$, and $c_n$ are measured from the point $I$. Since $\varphi$ and $v$ are given, the horizontal Coriolis force is constant; $c_n$ extends to the right from $I$ to the fixed terminal point $G^-$.

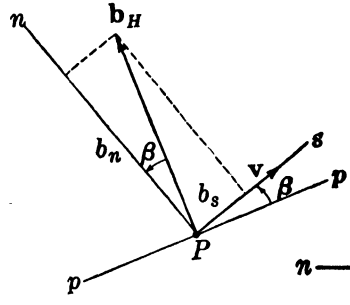



FIG. 7·20*a*.

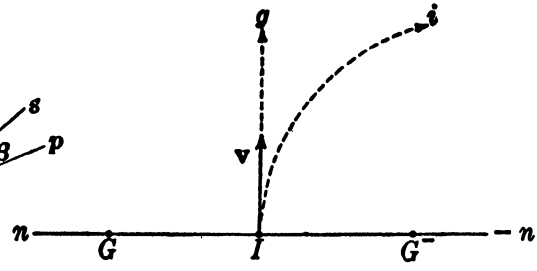



FIG. 7·20*b*.

Let the normal pressure force extend from $I$ to a variable terminal point $B$. If $B$ is at $I$ the flow is inertial, for $b_n = 0$. If $B$ is to the left of $I$, the flow is baric. And if $B$ is to the right of $I$, the flow is antibaric.

The horizontal centripetal acceleration $\dot{v}_n$ is determined by the normal equation as the sum of $b_n$ and $c_n$. The terminal point of $\dot{v}_n$ then lies to the right of $B$ by the length $c_n = IG^-$.

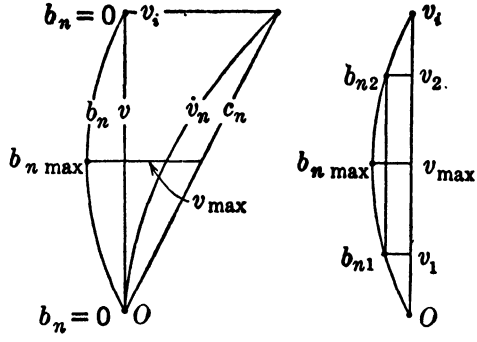
When $B$ is at $G$, the horizontal centripetal acceleration is zero; so $K_H = 0$ and the flow is geostrophic along the straight horizontal path $g$. If $B$ is to the left of $G$, the flow is cyclonically curved to the left of $g$. And if $B$ is to the right of $G$, the flow is anticyclonically curved to the right of $g$.

When $B$ is at $I$, the path is the inertial path $i$. When $B$ lies to the left of $I$ between $G$ and $I$, the flow is anticyclonically curved between $g$ and $i$. And when $B$ lies to the right of $I$, the flow is anticyclonically curved to the right of $i$.

It is clear that *cyclonic flow and geostrophic flow are always baric.* Anticyclonic flow is baric when the path is less curved than the inertial path, and antibaric when the path is more curved than the inertial path.

**7·21. Maximum speed.** We recognize in arbitrary horizontal flow many characteristics of zonal flow. Cyclonic flow and baric, inertial, and antibaric anticyclonic flow all appear in fig. 6·11*c*. Geostrophic flow also occurs, but only at the equator.

In zonal flow we found that the horizontal pressure field builds up to a maximum and then decreases as the angular speed increases anticyclonically. In the northern hemisphere this maximum field occurs when the relative angular speed has the value $-\Omega$. The pressure field in arbitrary anticyclonic flow behaves similarly, as illustrated for the northern hemisphere in fig. 7·21*a*. Here the latitude and the anticyclonic curvature are fixed. Hence $c_n$, $\dot{v}_n$, and consequently $b_n$ are determined only by the speed. The speed increases linearly along the line labeled $v$. The terminal points of the abscissas $c_n$, $\dot{v}_n$, and $b_n$ are plotted for all speeds between $v = 0$ and $v = v_i$. The horizontal Coriolis force acts to the right and is a linear function of the speed. So the terminal point of $c_n$ describes a straight line through $v = 0$. In anticyclonic flow the horizontal centripetal acceleration is directed to the right and is a quadratic function of the speed. So the terminal point of $\dot{v}_n$ describes a parabola through $v = 0$. When the speed is zero, $b_n$ is zero; and $b_n$ is also zero when the speed is inertial. Between these two speeds the horizontal pressure field is baric; $b_n$ rises parabolically to a maximum and then diminishes. The maximum occurs at one-half the inertial speed, as in zonal flow.




Left: FIG. 7·21*a*. Right: FIG. 7·21*b*. Maximum normal pressure force.

This result may be established analytically. When the normal equation is differentiated with respect to $v$ for a fixed curvature and latitude, we find

$$2K_H v + 2\Omega_z - \frac{\partial b_n}{\partial v} = 0.$$

The normal pressure force is a maximum when $\partial b_n/\partial v = 0$. The speed

at which this maximum occurs is denoted by $v_{max}$. From the above equation and 7·18(3) we have

$$v_{max} = -\frac{\Omega_z}{K_H} = \frac{v_i}{2}. \tag{1}$$

The angular speed of maximum flow is from 7·18(5)

$$\omega_{max} = v_{max} K = \frac{\omega_i}{2} = -\frac{\Omega_z}{\cos\theta}. \tag{2}$$

This result may be checked for the case of zonal flow. The angular radius of curvature is then the colatitude, and (2) becomes $\omega_{max} = -\Omega$ as required. The corresponding angular speed of the horizontal projection of the flow is from 7·18(4)

$$\omega_{zmax} = v_{max} K_H = \frac{\omega_{zi}}{2} = -\Omega_z. \tag{3}$$

For a given latitude and anticyclonic curvature the same normal pressure force ($b_{n1} = b_{n2}$) occurs at $v = v_1$ and at $v = v_2$, as shown in fig. 7·21*b*. That two speeds satisfy the normal equation is to be expected from the quadratic form of the equation. The diagram shows that $v_1$ and $v_2$ are symmetric about $v_{max}$. Hence

$$v_1 + v_2 = 2v_{max} = v_i. \tag{4}$$

Although both speeds $v_1$, $v_2$ are dynamically possible, only the smaller speed occurs in large-scale anticyclonic currents. The reason for this will be given later in section 11·15. There we shall examine the mechanism by which atmospheric circulation is generated.

The speed of a large-scale anticyclonic current must satisfy the relation

$$v \leqq v_{max}. \tag{5}$$

Anticyclonic speeds greater than $v_{max}$ will be called *abnormal*. Not only is the faster current in baric anticyclonic flow abnormal, but inertial currents and antibaric anticyclonic currents are also abnormal. Therefore antibaric flow and inertial flow seldom occur in the atmosphere. Even where an isobaric surface is level over an extended region, inertial flow as described in section 7·18 will not often develop; rather the entire region will have no wind. That is, when $b_n = 0$, the solution of the normal equation satisfying (5) is $v = 0$ rather than the abnormal solution $v = v_i$.

Equation (5) and its consequences apply only to large-scale anticyclonic flow in the atmosphere. All solutions of the normal equation are observed in small-scale mechanically produced vortices, in small-scale

atmospheric eddies produced by friction, and possibly in other small-scale atmospheric vortices.

**7·22. Solution of the normal equation.** The values of $v_g$, $v_i$, and $v_c$ can be computed from the equations

7·17(2) $$v_g = \frac{b_n}{2\Omega_z},$$

7·18(3) $$v_i = -\frac{2\Omega_z}{K_H},$$

7·19(2) $$v_c^2 = \frac{b_n}{K_H},$$

where $K_H$, $\Omega_z$, and $b_n$ refer to arbitrary horizontal flow. These speed values may be regarded not as the actual current speeds but as speed parameters characterizing arbitrary flow. As parameters, $v_g$, $v_i$, and $v_c$ need not satisfy the conditions required for geostrophic, inertial, or cyclostrophic flow. For example, although $v_i$ as a real current speed cannot be negative, $v_i$ is negative as a parameter describing cyclonic flow. The three parameters are not independent. They are linked by the relation

(1) $$v_c^2 = \frac{b_n}{K_H} = \frac{b_n}{2\Omega_z}\frac{2\Omega_z}{K_H} = -v_g v_i.$$

In terms of any two of these parameters, the normal equation

7·16(2) $$K_H v^2 + 2\Omega_z v - b_n = 0$$

may be simply expressed in three ways. Dividing the normal equation by $K_H$, we obtain the first relation:

(2) $$v^2 - v_i v - v_c^2 = 0.$$

When (1) is substituted into (2), we find the second relation:

(3) $$v^2 - v_i(v - v_g) = 0.$$

The third relation is derived from (2) by division with $v_c^2$ and subsequent substitution of (1):

(4) $$\frac{v^2}{v_c^2} + \frac{v}{v_g} - 1 = 0.$$

Since $v_g$, $v_i$, and $v_c$ have the same sign for corresponding flow in both hemispheres, the equations (2, 3, 4) are free from the arbitrary sign conventions of 7·16(2).

Each of the expressions (2, 3, 4) contains the unknown $v$ and two known parameters. Isopleths of $v$ can then be drawn in a diagram with any two parameters as coordinates. Usually atmospheric flow is strongly influenced by the pressure field. Near the equator the flow is almost cyclostrophic; in higher latitudes the flow is almost geostrophic. Therefore the most convenient graph for representing all latitudes is constructed from (4). However, if we are mainly concerned with the higher latitudes ($|\varphi| \geqq 30°$), (3) should be used. And in equatorial latitudes ($|\varphi| \leqq 30°$) (2) should be used.

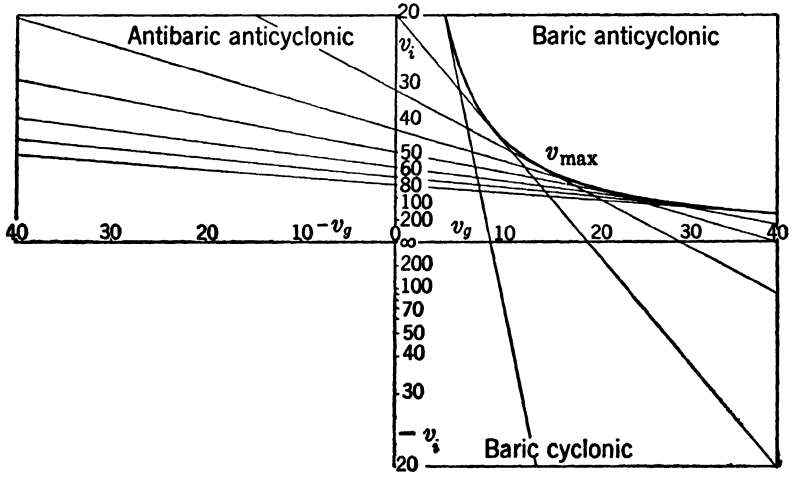



FIG. 7·22*a*.

In fig. 7·22*a* is shown the graph for (3), solving the normal equations in higher latitudes. The coordinates have been chosen so that the isopleths of $v$ will appear as straight lines. For this purpose the linear coordinates must be $v_g$ and $1/v_i$.

The only curved line in the diagram is the envelope of the isopleths. Every isopleth is tangent to the envelope at a point halfway between the intersections of the isopleth with the two axes. Since the $v_i$ scale is reciprocal, the $v_i$ coordinate of this tangent point is $v_i = 2v$. From 7·21(1) $v_i = 2v_{max}$; so any point on the envelope represents maximum anticyclonic flow. It also divides the isopleth into two branches. The lower branch represents the flow $v \leqq v_{max}$, and the upper branch represents the abnormal flow $v \geqq v_{max}$.

The diagram is divided into four quadrants. In the lower quadrants the flow is cyclonic ($v_i < 0$), and in the upper quadrants the flow is anticyclonic ($v_i > 0$). In the right quadrants the flow is baric ($v_g > 0$),

and in the left quadrants the flow is antibaric ($v_g < 0$). The positive horizontal axis represents geostrophic flow ($v = v_g$), and the positive vertical axis represents inertial flow ($v = v_i$).

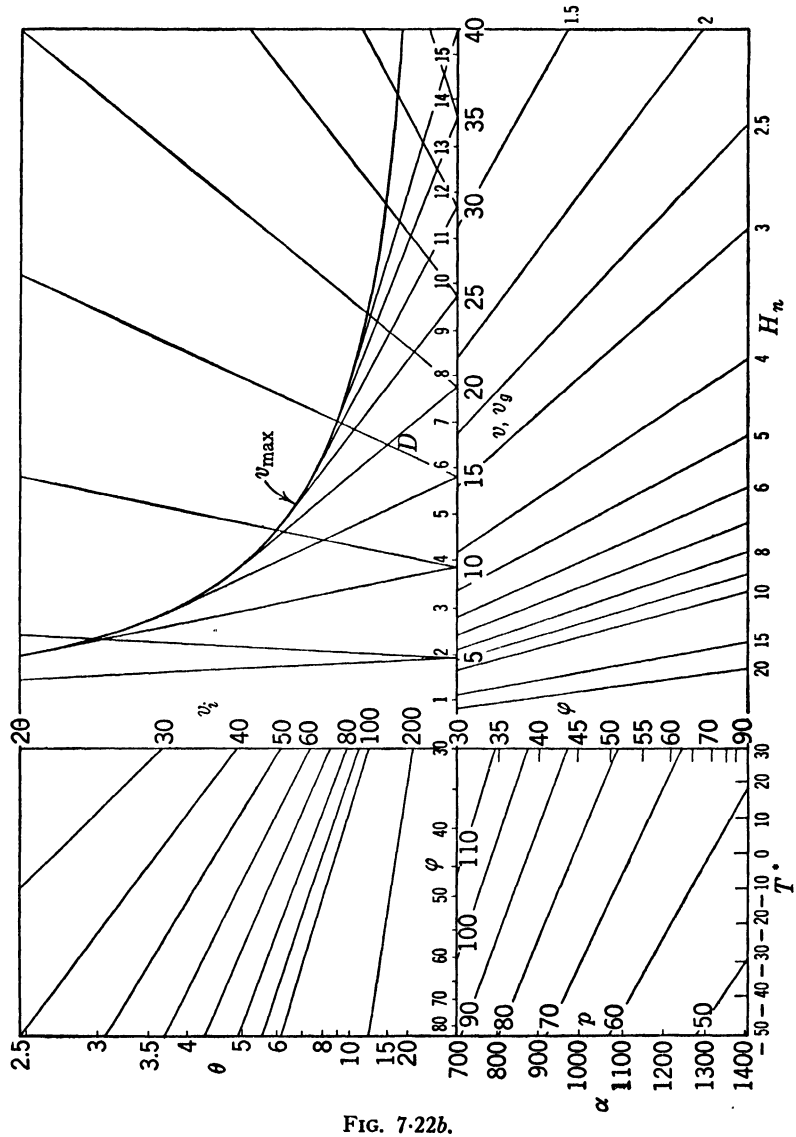



FIG. 7·22*b*.

Negative speeds have no physical significance and are not represented by isopleths on the diagram. As a result two regions of the diagram are not covered by isopleths. These regions represent impossible

flow. The lower left quadrant represents antibaric cyclonic flow. This type of flow is impossible, for, as indicated in section 7·20, cyclonic flow must be baric. The region to the upper right bounded by the envelope represents impossible baric anticyclonic flow for which $b_n > b_{n\max}$ (see fig. 7·21*b*).

We shall give the complete practical solution of the normal equation in the form (3). The independent variables are $p$, $T^*$, $H_n$, $\varphi$, and $\theta$. The required values for a current are $v$ and $D$.

For practical use the upper branches of the isopleths, representing abnormal anticyclonic flow, are deleted, so only the right-hand baric

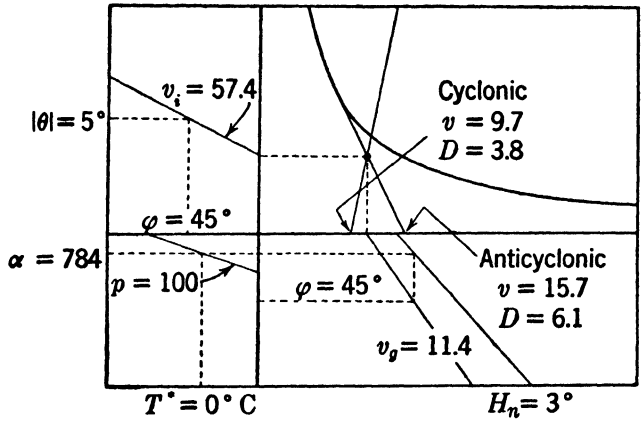



FIG. 7·22*c*.

quadrants remain. The lower cyclonic quadrant may be superposed over the upper anticyclonic quadrant by folding along the horizontal $v_g$ axis. The cyclonic isopleths then slope upward to the right, and the anticyclonic isopleths slope upward to the left. The parameter $v_g$ is found by joining fig. 7·17*e* to the bottom edge of the superposed quadrants. The parameter $v_i$ is found by turning fig. 7·18*a* over, cutting it in half along the coordinate $\varphi = 30°$, and joining the higher latitude half to the left-hand side of the superposed quadrants. Both joinings are permissible, for the $v_g$ isopleths intersect $\varphi = 30°$ in a linear $v_g$ scale, and the $v_i$ isopleths intersect $\varphi = 30°$ in a reciprocal $v_i$ scale. The resulting graph shown in fig. 7·22*b* gives $v = v(p, T^*, H_n, \varphi, \theta)$. An example of the procedure is illustrated in fig. 7·22*c* for the following data: $p = 100$ cb, $T^* = 0°C$, $H_n = 3°$, $\varphi = 45°$, $\theta = 5°$. The geostrophic speed and displacement are obtained as in fig. 7·17*f*. If the flow is cyclonic, then $v = 9.7$ m s$^{-1}$ and $D = 3.8°$. And if the flow is anticyclonic, then $v = 15.7$ m s$^{-1}$ and $D = 6.1°$.

In this example the cyclonic speed is less than the geostrophic value, and the anticyclonic speed is greater. The graph shows clearly that cyclonic flow is always subgeostrophic and that anticyclonic flow is always supergeostrophic. Analytically this result is obtained from (3), which shows that $v^2 = v_i(v - v_g) > 0$. For cyclonic flow ($v_i < 0$) we have $v < v_g$, and for anticyclonic flow ($v_i > 0$) we have $v > v_g$.

**7·23. Horizontal curvature of the streamlines.** The curvature $K_H$ is the horizontal curvature of the path of a particle. Since it is impossible to tag individual particles of air, the path cannot be observed directly. It is true that the approximate path may be inferred by successive displacements on consecutive weather maps. However, this method is both unsatisfactory and tedious. Fortunately the curvature of the path can be obtained from the streamline curvature. The horizontal streamlines are readily available on a synoptic constant-level weather map. They are curves everywhere tangent to the wind direction. The streamline and the path through a given point are both tangent to the velocity at that point. But in general the two curves have different curvatures.

The relation between the curvature of the path and the curvature of the streamline at an arbitrary point $P$ is obtained as follows: Let $\psi_H$ denote the angle, measured counterclockwise, from east to the projection of the wind direction on the horizontal plane at $P$. At a given time $\psi_H$ is a function $\psi_H = \psi_H(s_H)$, of the arc length $s_H$ along the horizontal projection of the streamline. If the flow pattern is steady, this function is the same at all times. If the flow pattern is changing, the wind direction at every point is also a function of time. The wind direction along the streamline through $P$ is then

$$\psi_H = \psi_H(s_H, t).$$

Consider now the particle initially at $P$. During the time element $dt$ this particle moves the infinitesimal distance $ds = ds_H$ along its path which is tangential to the streamline. The corresponding change of $\psi_H$ on the particle is then

$$d\psi_H = \frac{\partial \psi_H}{\partial s_H} ds_H + \frac{\partial \psi_H}{\partial t} dt. \tag{1}$$

The horizontal curvature of the path is defined by the angular turn of the wind along the horizontal projection of the path:

$$K_H = \frac{d\psi_H}{ds_H}. \tag{7·07(1)}$$

We shall denote the horizontal curvature of the streamline by $K_{HS}$.

This curvature is defined by the angular turn of the wind along the horizontal projection of the streamline at a fixed time:

$$K_{HS} = \frac{\partial \psi_H}{\partial s_H}. \tag{2}$$

The speed of the particle is $v = ds/dt = ds_H/dt$.

When (1) is divided by $ds_H$ and the above notations are introduced we find

$$K_H = K_{HS} + \frac{1}{v}\frac{\partial \psi_H}{\partial t}. \tag{3}$$

The expression $\partial \psi_H/\partial t$ is the *local turning of the wind* at the point $P$. In practice the local turning of the wind is determined by the wind recordings at a fixed station, or approximately by the wind change at the station between consecutive maps.

Equation (3) gives the path curvature in terms of the streamline curvature and the local turning of the wind. The two curvatures at a given point in the atmosphere are equal only if the wind direction at that point does not change. In particular, if the wind direction is independent of time at every point in the atmosphere, that is, if the flow is steady (see section 7·15), then the path and streamline curvatures are everywhere equal. This result confirms the previous statement that for steady flow the streamlines and paths coincide.

Since the atmosphere is actually characterized by changing flow patterns, the streamline and path curvatures are usually different. The two curvatures need not even have the same sign. We must then be careful about the usage of the words " cyclonic," " geostrophic," and " anticyclonic." Heretofore, we have characterized the flow of individual particles. However, in synoptic practice the flow is designated as cyclonic, geostrophic, or anticyclonic according to the instantaneous streamline pattern.

When (3) is substituted into the normal equation 7·16(2), we find

$$K_{HS}v^2 + \left(2\Omega_z + \frac{\partial \psi_H}{\partial t}\right)v - b_n = 0. \tag{4}$$

This relation may be expressed in the same form as the normal equation by letting the coefficient of the linear term be denoted by the symbol $2\Omega_{zS}$. Thus

$$2\Omega_{zS} = 2\Omega_z + \frac{\partial \psi_H}{\partial t}. \tag{5}$$

The normal equation then becomes

$$K_{HS}v^2 + 2\Omega_{zS}v - b_n = 0. \tag{6}$$

When the normal equation is expressed in the form (6), the coefficients can be evaluated directly from meteorological data. Since the horizontal streamlines almost coincide with the horizontal isobars, $K_{HS}$ may usually be replaced by the horizontal curvature of the horizontal isobars.

If the angular radius of curvature of the horizontal streamlines is denoted by $\theta_S$, the normal equation may be solved for $v = v(p,T^*,H_n,\Omega_{zS},\theta_S)$ by the methods and graphs introduced in the previous sections. The geostrophic, inertial, and cyclostrophic wind parameters must, however, be replaced by the fictitious parameters $v_{gS}$, $v_{iS}$, and $v_{cS}$ respectively. These new parameters are defined by the equations 7·17(2), 7·18(3), 7·19(2) wherein $\Omega_{zS}$ replaces $\Omega_z$ and $K_{HS}$ replaces $K_H$. In order to compute the values of $v_{gS}$, $v_{iS}$, and $v_{cS}$ graphically the linear $\Omega_z$ scale should be replaced by a linear $\Omega_{zS}$ scale, and $\Omega_{zS}$ itself must be computed from (5). However, only the coordinate labels of the graphs are changed; the graphical operations are the same.

CHAPTER EIGHT

# WIND VARIATION ALONG THE VERTICAL

**8·01. Geostrophic gradient flow.** We have stated in the last chapter that a horizontal current above the surface layer flows nearly along the horizontal isobars. In general the current overflows across the horizontal isobars toward lower or higher pressure (see section 7·15). But this overflow is usually so slight that the current is nearly gradient.

Moreover we have seen that cyclonic flow is subgeostrophic, and anticyclonic flow is supergeostrophic. Since a broad horizontal current above the surface layer is not often strongly curved, large-scale horizontal flow is approximately geostrophic, except in equatorial regions. Horizontal flow in the free atmosphere is then approximately geostrophic gradient flow.

In order to examine the wind variation along the vertical we shall assume that the flow is both geostrophic and gradient. The velocity of this flow will be denoted by $\mathbf{v}_g$ and will hereafter be called more briefly the geostrophic wind. Although only geostrophic flow will be investigated here, the deviation of this flow from any horizontal flow can be estimated qualitatively. If the actual wind velocity $\mathbf{v}$ is considered as the resultant of the velocity $\mathbf{v}_g$ and a deviation velocity, the following analysis applies only to the geostrophic velocity. However, since $\mathbf{v}$ is often nearly equal to $\mathbf{v}_g$, the analysis of geostrophic flow yields several important approximative rules.

The horizontal acceleration of a horizontal current is, from section 7·13,

$$\dot{\mathbf{v}}_H = \dot{v}\mathbf{t} + K_H v^2 \mathbf{n}.$$

When the current is both geostrophic ($K_H = 0$) and gradient ($\dot{v} = 0$), the horizontal acceleration $\dot{\mathbf{v}}_H$ is zero. Therefore the equation 7·03(2) of relative motion in the horizontal plane becomes

$$\mathbf{0} = \mathbf{b}_H + \mathbf{c}_H. \tag{1}$$

That is, the horizontal pressure force and the horizontal Coriolis force are in complete balance.

Since by 7·12(1) the horizontal pressure force is $-\alpha\nabla_H p$, and since by 7·11(7) the horizontal Coriolis force is $-2\boldsymbol{\Omega}_z \times \mathbf{v}$, equation (1) may be expressed as

$$2\boldsymbol{\Omega}_z \times \mathbf{v}_g = \mathbf{b}_H = -\alpha\nabla_H p. \tag{2}$$

The scalar form of this vector equation of geostrophic gradient flow is

$$2\Omega_z v_g = b_H. \tag{3}$$

Here $b_H$ occurs, rather than the $b_n$ of 7·17(2), for gradient flow is along the horizontal isobars.

**8·02. Isobaric slope.** The speed of a geostrophic gradient current determines the isobaric slope. Let the acute angle between an isobaric surface and the horizontal level be $\theta_p$. Then, as shown in fig. 8·02, the isobaric slope is

$$\tan\theta_p = \frac{b_H}{b_z} = -\frac{\delta z_p}{\delta n}. \tag{1}$$

Here $\delta z_p$ is† the rise of the isobaric surface above the horizontal level through the normal distance $-\delta n$.

Since $b_z = g^*$ and $b_H = 2\Omega_z v_g$, we also have, from 7·14(1),

$$\tan\theta_p = \frac{b_H}{g^*} \approx \frac{b_H}{g} = \frac{2\Omega_z v_g}{g}. \tag{2}$$

The isobaric slope is then determined dynamically by the strength of the geostrophic wind. Even for the strongest speeds occurring in the atmosphere the isobaric slope is small. For example, when $v_g = 100$ m s$^{-1}$ and $\varphi = 45°$ the isobaric slope is about 1/1000.

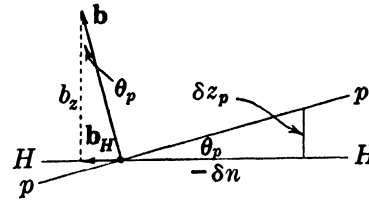


FIG. 8·02. Isobaric slope.

From the hydrostatic equation the dynamic thickness of an isobaric layer is given by the mean specific volume of the layer. The variation along the vertical of the isobaric slope and consequently of the geostrophic wind depends on the variation of the specific volume within the isobaric layer. If the specific volume has no variation within the isobaric layer, the layer is barotropic, and the two isobaric surfaces bounding the layer have the same slope. So the geostrophic wind does not change throughout the layer. But if the specific volume varies within the isobaric layer, the layer is baroclinic and is inflated in the direction of increasing specific volume. So the slope of the upper bounding isobaric surface differs from the slope of lower bounding isobaric surface. Accordingly the geostrophic wind varies along the vertical.

† The symbols $z_p$ and $T_p^*$ of this and the following section do not represent the same quantities as the symbols $z_p$ and $T_p$ of section 4·30.

**8·03. The thermal wind equation.** The above argument may be developed analytically by differentiating the geostrophic wind equation along the vertical with respect to dynamic height. Since the latitude is constant along the vertical, application of $\partial/\partial\phi$ to 8·01(2) gives

$$2\Omega_z \times \frac{\partial \mathbf{v}_g}{\partial \phi} = \frac{\partial \mathbf{b}_H}{\partial \phi}. \tag{1}$$

Here $\partial \mathbf{v}_g/\partial\phi$ is the variation or *shear* of the geostrophic wind along the vertical. The wind shear may be clearly visualized, as shown in fig. 8·03*a*, by drawing the vectors $\mathbf{v}_g$ for a given vertical at a given time, issuing from a common origin *O*. The terminal curve of $\mathbf{v}_g$ represents the distribution of wind along the vertical, with either dynamic or geometric height as the scalar variable. (See section 6·04.) This terminal curve will be called the *shear hodograph*. The wind shear is tangent to the shear hodograph and is directed toward increasing values of the height variable.

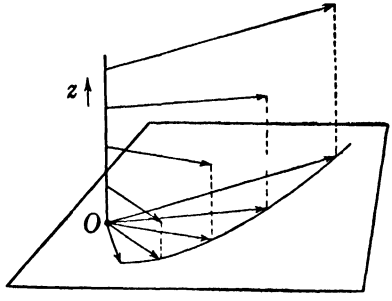



FIG. 8·03*a*. Hodograph of wind distribution along a vertical.

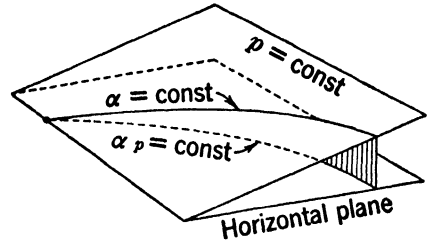



FIG. 8·03*b*. Definition of $\alpha_p$.

The variation of the horizontal pressure force along the vertical is

$$\frac{\partial \mathbf{b}_H}{\partial \phi} = \frac{\partial}{\partial \phi}(-\alpha \nabla_H p) = -\frac{\partial \alpha}{\partial \phi}\nabla_H p - \alpha \frac{\partial}{\partial \phi}\nabla_H p. \tag{2}$$

From the expressions 8·02(1, 2) for the isobaric slope we have

$$-\frac{\partial \alpha}{\partial \phi}\nabla_H p = \frac{1}{\alpha}\frac{\partial \alpha}{\partial \phi}\mathbf{b}_H = \frac{1}{\alpha}\frac{\partial \alpha}{\partial z}\frac{b_H}{g}\mathbf{n} = -\frac{1}{\alpha}\frac{\partial \alpha}{\partial z}\frac{\delta z_p}{\delta n}\mathbf{n}. \tag{3}$$

The partial differentiation symbols $\partial/\partial\phi$ and $\nabla_H$ are commutative. So, by the hydrostatic equation $\partial p/\partial\phi = -\rho$, we have

$$-\alpha \frac{\partial}{\partial \phi}\nabla_H p = -\frac{1}{\rho}\nabla_H \frac{\partial p}{\partial \phi} = \frac{\nabla_H \rho}{\rho} = -\frac{\nabla_H \alpha}{\alpha}. \tag{4}$$

When the horizontal volume gradient is expressed in the natural system and the equations (3, 4) are added, we find

$$\frac{\partial \mathbf{b}_H}{\partial \phi} = -\frac{1}{\alpha}\frac{\partial \alpha}{\partial s}\mathbf{t} - \frac{1}{\alpha}\left(\frac{\partial \alpha}{\partial n} + \frac{\partial \alpha}{\partial z}\frac{\delta z_p}{\delta n}\right)\mathbf{n}. \tag{5}$$

Consider now the projection into the horizontal plane of the isosteric lines drawn on an isobaric surface, as shown in fig. 8·03*b*. These lines define a horizontal field which will be denoted by $\alpha_p$. The ascendent $\nabla_H \alpha_p$ of this field will be called the *horizontal isobaric volume ascendent.* In the natural system this ascendent is expressed

$$\nabla_H \alpha_p = \frac{\delta \alpha_p}{\delta s}\mathbf{t} + \frac{\delta \alpha_p}{\delta n}\mathbf{n}.$$

Since $\mathbf{v}_g$ is along the horizontal isobars, the variations $\delta \alpha_p$ and $\delta \alpha$ along the wind are equal. Therefore,

$$\frac{\delta \alpha_p}{\delta s} = \frac{\partial \alpha}{\partial s}.$$

However, in the vertical plane normal to the wind direction the specific volume varies in both the $n$ and $z$ directions. That is, $\alpha = \alpha(n,z)$. So an arbitrary variation $\delta \alpha$ in the vertical $(n,z)$-plane is given by

$$\delta \alpha = \frac{\partial \alpha}{\partial n}\delta n + \frac{\partial \alpha}{\partial z}\delta z.$$

In particular, when the variation is taken along the isobaric surface, $\delta \alpha = \delta \alpha_p$ and $\delta z = \delta z_p$. Therefore,

$$\frac{\delta \alpha_p}{\delta n} = \frac{\partial \alpha}{\partial n} + \frac{\partial \alpha}{\partial z}\frac{\delta z_p}{\delta n}.$$

The above expressions for the natural components of the horizontal isobaric volume ascendent show that (5) may be written

$$\frac{\partial \mathbf{b}_H}{\partial \phi} = -\frac{\nabla_H \alpha_p}{\alpha}. \tag{6}$$

Consequently we have, from (1),

$$2\Omega_z \times \frac{\partial \mathbf{v}_g}{\partial \phi} = -\frac{\nabla_H \alpha_p}{\alpha}. \tag{7}$$

This is the mathematical formulation of the dependence anticipated qualitatively in the last section. Evidently the geostrophic wind has no shear through a barotropic layer, since $\alpha_p$ is constant for such a layer.

The specific volume is not immediately given by aerological data, so

for practical use (7) must be expressed in terms of the virtual temperature. Since the pressure variation along an isobaric layer is zero, logarithmic differentiation of the equation of state gives

$$\frac{\nabla_H \alpha_p}{\alpha} = \frac{\nabla_H T_p^*}{T^*}. \tag{8}$$

Therefore equation (7) for the geostrophic wind shear becomes

$$2\Omega_z \times \frac{\partial \mathbf{v}_g}{\partial \phi} = -\frac{\nabla_H T_p^*}{T^*}. \tag{9}$$

This relation, known as the *thermal wind equation*, could also have been anticipated qualitatively. For within an isobaric layer an increase of virtual temperature always occurs with an increase of specific volume. Therefore the layer is inflated in the direction of increasing temperature. Usually the virtual temperature correction is so small, in comparison with the spatial variation of temperature, that $T^*$ may be replaced by $T$. Although the following argument applies strictly only to the virtual temperature, we shall for convenience write $T$ for $T^*$.

**8·04. Isothermal slope.** The atmosphere is often analyzed synoptically by constructing the fields of the atmospheric variables in a series of constant-level charts. Although the horizontal temperature gradient is directly accessible from these charts, the isobaric horizontal temperature gradient, which occurs in the thermal wind equation, is not so easily available. We shall show in the next section that the difference between these two gradients is negligible. First, however, we shall derive another expression for the wind shear.

Equations 8·03(6, 8) may be combined to give

$$-\frac{\partial \mathbf{b}_H}{\partial \phi} = \frac{\nabla_H \alpha_p}{\alpha} = \frac{\nabla_H T_p}{T}. \tag{1}$$

Substituting here for $\partial \mathbf{b}_H/\partial\phi$, we have, from 8·03(2, 3, 4),

$$\frac{\nabla_H \alpha_p}{\alpha} = \frac{\nabla_H \alpha}{\alpha} - \frac{1}{\alpha}\frac{\partial \alpha}{\partial \phi}\mathbf{b}_H. \tag{2}$$

To express this equation in terms of the temperature instead of the specific volume, differentiate the equation of state logarithmically. We then find the following vector and scalar relations:

$$\frac{\nabla_H \alpha}{\alpha} = \frac{\nabla_H T}{T} - \frac{\nabla_H p}{p} = \frac{\nabla_H T}{T} + \frac{\mathbf{b}_H}{p\alpha};$$

$$\frac{1}{\alpha}\frac{\partial \alpha}{\partial \phi} = \frac{1}{T}\frac{\partial T}{\partial \phi} - \frac{1}{p}\frac{\partial p}{\partial \phi} = \frac{1}{T}\frac{\partial T}{\partial \phi} + \frac{1}{p\alpha}.$$

If these relations are substituted in (2), the term $\mathbf{b}_H/p\alpha$ occurs twice with opposite signs. From (1) the logarithmic volume and temperature ascendents are equal, so equation (2) becomes

$$\frac{\nabla_H T_p}{T} = \frac{\nabla_H T}{T} - \frac{1}{T}\frac{\partial T}{\partial \phi}\mathbf{b}_H. \tag{3}$$

Comparison of equations (2, 3) shows that each symbol $\alpha$ in (2) has been replaced in (3) by the symbol $T$.

The expression $(\partial T/\partial\phi)\mathbf{b}_H$ in (3) is determined by the isobaric slope, for, by 8·02(2), we have

$$\frac{\partial T}{\partial \phi}\mathbf{b}_H = \frac{\partial T}{\partial z}\frac{b_H}{g}\mathbf{n} = \frac{\partial T}{\partial z}\tan\theta_p\mathbf{n}.$$

Similarly the expression $\nabla_H T$ in (3) is determined by the isothermal slope. Let $\theta_T$ be the acute angle between the isothermal surface and the level surface. Moreover, let $\mathbf{n}_T$ be a horizontal unit vector, whose linear coordinate is $n_T$, normal to the horizontal isotherms and pointing toward colder air. The isothermal slope then depends upon the rise $\delta z_T$ of the trace in the $(n_T,z)$-plane of the isothermal surface above the horizontal level through the normal distance $\mp\,\delta n_T$. Thus

$$\tan\theta_T = \mp\frac{\delta z_T}{\delta n_T}.$$

The upper sign (minus) is required when the temperature decreases with height. This is the usual case in the atmosphere. However, in layers where the temperature increases with height, the lower sign (plus) is required.

The horizontal temperature ascendent is then given by

$$\nabla_H T = -\frac{\partial T}{\partial n_T}\mathbf{n}_T = -\frac{\partial T}{\partial z}\frac{\delta z_T}{\delta n_T}\mathbf{n}_T = \pm\frac{\partial T}{\partial z}\tan\theta_T\mathbf{n}_T,$$

where all variations are taken in the $(n_T,z)$-plane. When the above expressions for the isobaric and isothermal slopes are substituted in (3), we have

$$\frac{\nabla_H T_p}{T} = \frac{1}{T}\frac{\partial T}{\partial z}(\pm\tan\theta_T\mathbf{n}_T - \tan\theta_p\mathbf{n}).$$

Therefore the thermal wind equation 8·03(9) takes the form

$$2\Omega_z \times \frac{\partial \mathbf{v}_g}{\partial \phi} = -\frac{1}{T}\frac{\partial T}{\partial z}(\pm\tan\theta_T\mathbf{n}_T - \tan\theta_p\mathbf{n}): \tag{4}$$

According to this formula the geostrophic shear may be attributed

partly to the slope of the isobaric surface and partly to the slope of the isothermal surface. The isobaric slope is determined by the geostrophic speed and is always very small (see section 8·02). Since no similar dynamical control restricts the slope of the isothermal surface, any isothermal slope may occur in the atmosphere.

**8·05. The approximate thermal wind equation.** We shall now show that the part of the shear attributed to the slope of the isobars is so small that it may be neglected for practical purposes. Suppose that the isothermal surfaces are horizontal. Accordingly $\theta_T = 0$, and the shear may be attributed entirely to the isobaric slope. Division of the scalar form of 8·04 (4) by $2\Omega_z v_g = g \tan \theta_p$ then gives

$$\frac{1}{v_g}\frac{|\partial \mathbf{v}_g|}{\partial \phi} = \frac{1}{T}\frac{|\partial T|}{g\partial z} = \frac{1}{T}\frac{|\partial T|}{\partial \phi} = \frac{|\gamma|}{T}.$$

Here the magnitude of the shear is proportional to the lapse rate. The maximum lapse rate ordinarily found in the atmosphere is the dry adiabatic, $\gamma_d = 1/c_{pd}$. For this lapse rate the percentual wind shear is

$$\frac{1}{v_g}\frac{|\partial \mathbf{v}_g|}{\partial \phi} = \frac{1}{c_{pd}T} = 3.6\% \text{ per dyn km},$$

where the numerical percentage has been evaluated at $T = 0°C$. Even this maximum strength of the shear is extremely small; in fact it is smaller than the error of measurement of the wind. Consequently the part of the shear attributed to the isobaric slope may be neglected for all practical purposes. Therefore, by 8·04(3), a good approximation to the thermal wind equation is obtained when the horizontal isobaric temperature gradient is replaced by the horizontal temperature gradient. Thus the approximate form of equation 8·03(9) is

$$(1) \qquad 2\Omega_z \times \frac{\partial \mathbf{v}_g}{\partial \phi} = -\frac{\nabla_H T}{T}.$$

Whenever the horizontal temperature gradient gives appreciable geostrophic shear, the above approximate thermal wind equation may be used. Comparison of this equation with the equation of geostrophic flow 8·01(2) shows that the wind shear and the horizontal temperature gradient have the same relative orientation as the wind and the horizontal pressure gradient. So the following law, similar to the baric wind law, holds for the wind shear: *The geostrophic wind shear is directed along the horizontal isotherms, with low temperature to the left of the shear in the northern hemisphere, and with low temperature to the right of the shear in the southern hemisphere.*

This rule gives the direction of the geostrophic wind shear. For numerical computation of the strength of the shear (1) must be expressed in scalar form. In practical application the strength of the shear is measured by the magnitude $|\Delta \mathbf{v}_g|$ of the velocity variation through a finite layer of dynamic thickness $\Delta\phi = g\Delta z$. Let the mean temperature through the layer be $T$, and let $\Delta n_T$ be the distance between horizontal isotherms drawn for the interval $\Delta T$. The scalar form of (1) is then

$$\frac{2\Omega \sin \varphi}{g} \frac{|\Delta \mathbf{v}_g|}{\Delta z} = \frac{1}{T} \frac{|\Delta T|}{\Delta n_T}. \tag{2}$$

On upper level maps the horizontal isotherms are usually drawn for a temperature interval of 5°C. If the distance between isotherms, measured toward lower temperature and expressed in degrees of latitude, is $H_T$, then $\Delta n_T = 1.11 \times 10^5 H_T$ and $|\Delta T| = 5$. The deviation of the mean temperature of a layer in the troposphere from the value $T = 0$°C does not appreciably alter the value of the shear. Therefore equation (2) is approximately given by

$$H_T |\Delta \mathbf{v}_g| \sin \varphi = 11.1 \frac{\Delta z}{1000}.$$

In weather reports the upper winds are given for every 1000 ft along the vertical. The shear at any one of these levels is measured by the shear of the wind from the level 1000 ft lower to the level 1000 ft higher. Thus $\Delta z = 2000$ ft $= 610$ m. Moreover the speed is reported in miles per hour rather than in meters per second. Let $\Delta u_g$ be the magnitude of the geostrophic shear, expressed in miles per hour. From the conversion table in section 1·06 the shear $|\Delta \mathbf{v}_g|$ is then given by $\Delta u_g/2.237$. With these values for $|\Delta \mathbf{v}_g|$ and $\Delta z$, the above equations may be written

$$H_T \Delta u_g \sin \varphi = 15.1.$$

This form of the approximate thermal wind equation, first suggested by Neiburger, corresponds to equation 7·17(4) for the geostrophic wind.

Comparison of the formulas for the geostrophic wind and for the geostrophic wind shear show that the two equations are completely analogous. The geostrophic wind formula may be used to gauge the distance between horizontal isobars from wind reports. And the geostrophic wind shear formula may be used to gauge the distance between horizontal isotherms from wind shear reports. However, it should always be remembered that the practical use of these formulas is based on the assumption of geostrophic gradient flow. Although this type of flow is actually seldom realized, it often does give a fair approximation to the real flow in the free atmosphere above the friction layer.

**8·06. Analysis of the shear hodograph.** The wind distribution along the vertical at a meteorological station is obtained directly from a pilot balloon observation. From the drift of the pilot balloon the wind is determined at equally spaced levels — for instance, at every 1000 ft above sea level. The shear hodograph is constructed by marking the terminal points of the wind velocities drawn from the origin of a polar coordinate diagram. The consecutive terminal points are then connected by straight line segments as shown in fig. 8·06*a*. The real hodograph is, of course, a smooth curve. But it is not advisable to draw it with more details than the actual observations indicate, particularly if the hodograph has many irregularities and kinks. The terminal point of the surface wind is labeled *S*, and the succeeding terminal points of the upper level winds are labeled by numbers indicating the elevation of the wind levels in thousands of feet above sea level. Although the wind vectors are drawn here for illustration, they are usually omitted. The mean shear through each 1000-ft layer is represented by the directed segment from the terminal point of the wind at the bottom of the layer to the terminal point of the wind at the top of the layer.

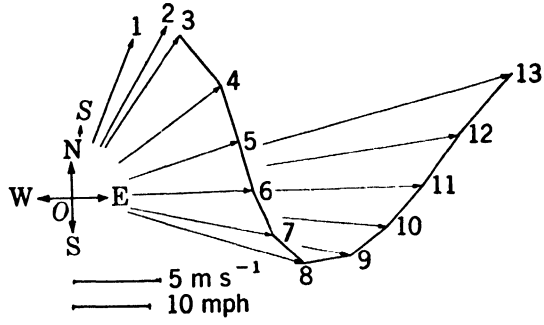



FIG. 8·06*a*.

Let fig. 8·06*a* represent the shear hodograph drawn from a pilot balloon observation taken in the northern hemisphere. Here the hodograph has not been drawn in the surface or friction layer $S \rightarrow 3$. For in the friction layer, usually about 3000 ft deep, the wind cannot be considered geostrophic. The wind distribution in the surface layer requires a separate analysis which will be presented in the next chapter. However, at higher levels the reported wind and the shear may often be assumed to be geostrophic. By the approximate thermal wind equation this shear is along the horizontal isotherms, with colder air to the left. Thus, in the layer $3 \rightarrow 8$ of the diagram the mean horizontal isotherms run approximately northwest-southeast, with colder air to the northeast

of the station. And in the layer 8 → 13 the mean horizontal isotherms run approximately southwest-northeast, with colder air to the northwest.

As pointed out by Rossby and collaborators, the shear hodograph shows qualitatively the horizontal direction toward the regions of maximum or minimum vertical stability. The direction of the mean horizontal isotherms for the two layers 3 → 8 and 8 → 13 has been indicated by two intersecting straight lines in the simplified shear hodograph shown in fig. 8·06*b*. In the four sectors bounded by these lines the vertical temperature distribution is different. In the sector opening toward the east warm air lies over cold air, so the vertical temperature distribu-

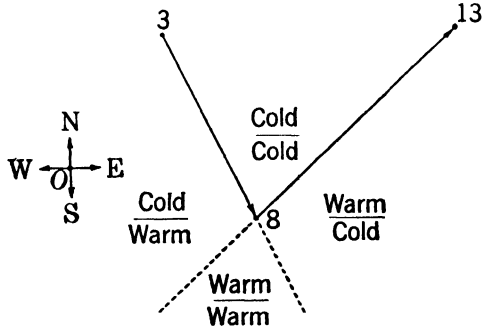



FIG. 8·06*b*.

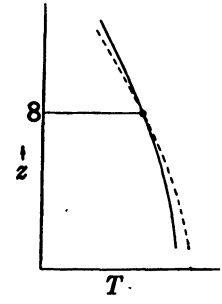



FIG. 8·06*c*.

tion is relatively stable. In the opposite sector opening toward the west, cold air lies over warm air, so the vertical temperature distribution is relatively unstable. Therefore, in this example the direction toward the region of maximum vertical stability is toward the east, along the shear at the level 8.

The following rule gives the direction toward the region of maximum or minimum vertical stability at a level where the shear hodograph is appreciably curved: *The shear points toward the region of maximum stability if the concave side of the hodograph encloses colder air, and points toward the region of minimum stability if the concave side encloses warmer air.* This rule, valid in both hemispheres, must be qualified further. At the level to which the rule applies the hodograph must be *significantly curved* as well as appreciably curved. That is, the level must lie between two fairly deep layers through which the hodograph is nearly straight, as in the example. The above qualified rule may be derived mathematically by differentiation of the thermal wind equation along the vertical $(\partial/\partial\phi)$.

Finally, the shear hodograph also shows qualitatively the tendency, or local change with time, of the stability along the vertical. In the lower

layer 3 → 8 of the shear hodograph (fig. 8·06*a*) the wind blows across the isotherms from a warmer region, so the temperature in that layer will rise. At the level 8 the wind blows along the isotherms, so the temperature of that level will not change. And in the upper layer 8 → 13 the wind blows across the isotherms from a colder region, so the temperature in that layer will fall. The consequent change of the vertical temperature distribution is illustrated in fig. 8·06*c*. The full-drawn sounding curve represents the temperature distribution along the vertical at the time of observation. As explained above, advection of temperature will change this temperature distribution toward the dashed sounding curve. Consequently the sounding will become less stable.

The following rule applies to the tendency of the vertical stability at a level where the shear is along the wind: *The sounding becomes less stable if the concave side of the hodograph encloses colder air, and becomes more stable if the concave side encloses warmer air.* This rule, valid in both hemispheres, applies only if the shear hodograph is both significantly and appreciably curved. It may be derived mathematically by local time differentiation of the thermal wind equation $(\partial/\partial t)$.

Both the above rules are useful in weather analysis and forecasting. By the first rule the distribution of vertical stability in space can be inferred from the shear hodograph. And by the second rule the local change of vertical stability with time can be inferred. However, these rules should be applied only where the shear hodograph is appreciably and significantly curved, and where the flow is approximately geostrophic gradient flow.

**8·07. Fronts.** We have examined the wind shear through an atmospheric layer in which the mass field, represented either by the specific

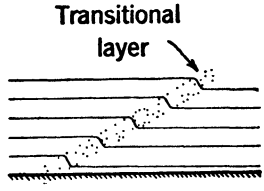



FIG. 8·07*a*.

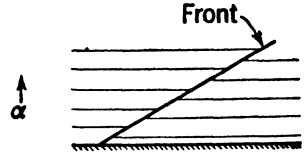



FIG. 8·07*b*.

volume or the density, varies continuously. We shall now examine the shear through a surface of discontinuity in the mass field. Such a surface is called a *frontal surface* or more briefly a *front*.

A real front in the atmosphere is never a sharp discontinuity. As shown in fig. 8·07*a*, it is a transitional layer with rapid but continuous variation of the specific volume or of the density. However, it is often

convenient to treat this transitional layer as a surface of discontinuity separating two air masses. At any point of the front the density undergoes an abrupt finite change from the lighter to the denser air mass. As shown in 8·07*b* the isosteric surfaces enter the frontal surface from one side, follow the front for a certain distance, and leave the frontal surface on the other side.

**8·08. The dynamic boundary condition.** Consider any point $P$ on the frontal surface of discontinuity. As $P$ is approached from within the dense air mass, the physical variables ($\rho$, $\alpha$, $p$, $T$, $\mathbf{v}$) approach definite values, which will be denoted by unprimed symbols. And as the point $P$ is approached from within the light air mass, the variables also approach definite but in general *different* values, which will be denoted by primed symbols. The difference of these two values, *the dense air mass value minus the light air mass value*, will be indicated by the symbol $\Delta$. Thus the density difference at the front separating two air masses is

$$\rho - \rho' = \Delta\rho > 0. \tag{1}$$

This condition can be taken as the definition of the front. In the special case where $\Delta\rho = 0$, the air mass discontinuity disappears, and the front is nonexistent.

Although the mass field is discontinuous at the front, dynamic principles require that the pressure field be continuous. That is, the pressure value at a given point on the front must be the same in both air masses. For otherwise the pressure gradient and pressure force would be infinite. Therefore, at any point in the frontal surface we have

$$\Delta p = 0. \tag{2}$$

This condition is known as the dynamic boundary condition.

The differentiation symbol $\delta$ has been used to denote variation at a fixed time between neighboring points of space. The variation of the pressure difference through a front between two neighboring points on the frontal surface is, from (2),

$$\delta(\Delta p) = \Delta(\delta p) = 0. \tag{3}$$

This equation expresses the dynamic boundary condition in differential form. It is valid only when the differentiation is taken in the frontal surface.

Let the differentiation be performed along the vector line element $\delta\mathbf{r}_F$ in the frontal surface. Then from 4·13(1) we obtain the following expression for the dynamic boundary condition:

$$\Delta(\delta p) = \Delta(\delta\mathbf{r}_F \cdot \nabla p) = \delta\mathbf{r}_F \cdot \Delta(\nabla p) = 0. \tag{4}$$

This equation shows that the frontal surface is perpendicular to the variation of the pressure gradient through the front. Let the variation of the pressure gradient be denoted by the vector **F**. Thus

$$\mathbf{F} = \Delta(-\nabla p) = -\nabla(\Delta p). \tag{5}$$

The dynamic boundary condition (4) requires that **F** be a vector perpendicular to the frontal surface, as illustrated in fig. 8·08*a*.

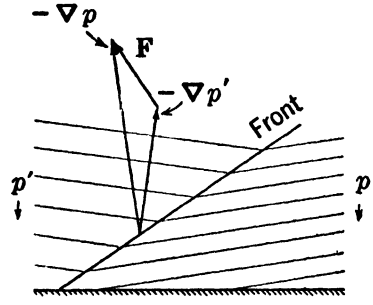



FIG. 8·08*a*. $\mathbf{F} = \Delta(-\nabla p)$.

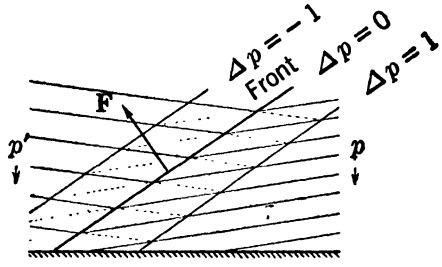



FIG. 8·08*b*. $\mathbf{F} = -\nabla(\Delta p)$.

The same result can be obtained differently, as illustrated in fig. 8·08*b*. First assume that the cold air mass extends beyond the front and that the pressure throughout the entire frontal region is given by the field $p$. Next assume that the warm air mass extends beyond the front and that the pressure throughout the entire frontal region is given by the field $p'$. The extended pressure fields $p$, $p'$ are represented in the diagram by dashed isobars dividing the frontal region into unit isobaric layers. Consider now the fictitious situation where both fields $p$, $p'$ are extended through the front. The two sets of isobaric units layers intersect each other and divide the frontal region into tubes of parallelogrammatic cross section. It is readily seen from the diagram that the unit surfaces of constant $\Delta p$ are the diagonal surfaces of these tubes. But according to (2) one of these surfaces, namely, $\Delta p = 0$, is the frontal surface. Therefore the frontal surface must be normal to the vector $\mathbf{F} = -\nabla(\Delta p)$, as shown by equation (5).

**8·09. Application of the dynamic boundary condition.** The general relation between the frontal surface and the pressure field is given by the dynamic boundary condition. Some of the consequences of this condition have already been explained. Further consequences will now be derived which may be applied directly to the weather map.

The difference between the two values of a physical quantity at a front has been indicated by the symbol Δ. The arithmetic mean of these two

values will be indicated by a superior bar ($\bar{}$). For instance, the mean value of the density at a front is $\bar{\rho} = (\rho + \rho')/2$.

Since $p = p'$ at a front, the equation of state $\rho = p/RT^*$ shows that the density and temperature differences through a front are related by

$$\frac{\Delta\rho}{\bar{\rho}} = 2\frac{\rho - \rho'}{\rho + \rho'} = 2\frac{T^{*\prime} - T^*}{T^{*\prime} + T^*} = -\frac{\Delta T^*}{\bar{T}^*}. \tag{1}$$

Hence, from 8·08(1) the virtual temperature difference $\Delta T^*$ is always negative. In the following we shall distinguish the air masses at the front by virtual temperature, rather than by density; we shall call the dense air mass cold and the light air mass warm. Henceforth we shall write $T$ for $T^*$ as in the thermal wind equations.

The front may be stable or unstable, depending upon the arrangement of the cold and warm air masses. The front is stable if the cold air flows in a wedge under the front and warm air flows above. And the front is unstable if the warm air flows in a wedge under the front and cold air flows above, for in this case thermal convection would immediately destroy the frontal discontinuity. Therefore we shall in the following consider only stable fronts.

The slope of the frontal surface may be obtained by the method used for the isobaric and isothermal slopes. Let $\theta_F$ be the acute angle between a frontal surface and a level surface. As shown in fig. 8·09*a*, the slope of a stable front with the cold air flowing below the front and the warm air flowing above is

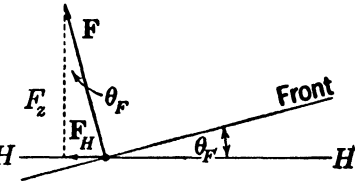



FIG. 8·09*a*. Frontal slope.

$$\tan\theta_F = \frac{F_H}{F_z}. \tag{2}$$

The horizontal and vertical components of $\mathbf{F}$ are obtained from the definition: $\mathbf{F} = -\Delta(\nabla p)$. Thus the vertical component $F_z$ is

$$F_z = \mathbf{F}\cdot\mathbf{k} = -\Delta(\nabla p\cdot\mathbf{k}) = -\Delta\left(\frac{\partial p}{\partial z}\right).$$

Since for all practical purposes the hydrostatic equation $\partial p/\partial z = -g\rho$ is valid, we have finally

$$F_z = g\Delta\rho \tag{3}$$

In order to find the horizontal component of $\mathbf{F}$, we shall introduce the horizontal orthogonal unit vectors $\mathbf{t}_F$, $\mathbf{n}_F$ whose linear coordinates are $s_F$, $n_F$ respectively. The two unit vectors will be oriented so that $\mathbf{t}_F$

is along the front with $\mathbf{n}_F$ to the left and pointing toward the warm air. For a stable front $\mathbf{n}_F$ is along the horizontal projection of $\mathbf{F}$. Thus

$$F_H = \mathbf{F}\cdot\mathbf{n}_F = -\Delta(\nabla p\cdot\mathbf{n}_F) = -\Delta\left(\frac{\partial p}{\partial n_F}\right) > 0, \tag{4}$$

so the slope of a stable front is given by

$$\tan\theta_F = -\frac{\Delta(\partial p/\partial n_F)}{g\Delta\rho} > 0. \tag{5}$$

The inequality (4) gives one condition that must be satisfied by the horizontal pressure field near a stable front. Since the vector $\mathbf{F}$ is normal to the front, a second condition may be obtained as follows:

$$\mathbf{F}\cdot\mathbf{t}_F = -\Delta(\nabla p\cdot\mathbf{t}_F) = -\Delta\left(\frac{\partial p}{\partial s_F}\right) = 0. \tag{6}$$

The two conditions (4): $\Delta(\partial p/\partial n_F) < 0$ and (6): $\Delta(\partial p/\partial s_F) = 0$, derived from the dynamic boundary condition, restrict the variation of the horizontal pressure field in the neighborhood of a front. Nine possible combinations of the two conditions are shown in fig. 8·09*b*. These diagrams show the front and the isobars in a level surface. The cold air covers the upper half of each diagram and the warm air covers the lower half.

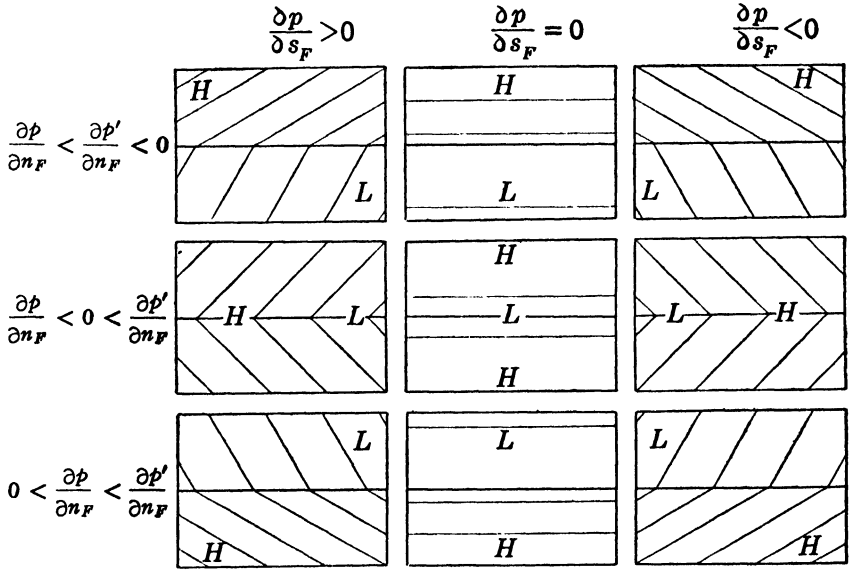



FIG. 8·09*b*. Nine possible horizontal pressure fields in the neighborhood of a front.

In the diagrams of the center column the horizontal pressure gradient has no component along the front, so the horizontal isobars are parallel to the front. In the diagrams of the left-hand column the horizontal pressure gradient has a component to the right along the front. And in the diagrams of the right-hand column the horizontal pressure gradient has a component to the left along the front. Notice that *the horizontal isobars intersecting the front have a kink pointing from low to high pressure.* This rule, valid in both hemispheres for any stable front, is extremely useful in the frontal analysis of constant-level weather maps.

**8·10. The kinematic boundary condition.** The dynamic boundary condition is a restriction on the pressure field at the front. There is also a restriction on the field of motion at the front, for the two air masses on either side of the front cannot move so that a void develops between them or so that they interpenetrate. That is, the velocity components $v_N$, $v'_N$ of the cold and warm air masses normal to the front are equal. Thus,

$$\Delta v_N = 0. \tag{1}$$

This condition is known as the kinematic boundary condition.

Let $\mathbf{N}_F$ be the unit vector along the vector $\mathbf{F}$, normal to the frontal surface. The velocity components $v_N$, $v'_N$ are respectively $\mathbf{v}\cdot\mathbf{N}_F$, $\mathbf{v}'\cdot\mathbf{N}_F$. So the kinematic boundary condition may be written

$$\Delta(\mathbf{v}\cdot\mathbf{N}_F) = \mathbf{N}_F\cdot\Delta\mathbf{v} = 0.$$

Multiplication of this equation by the magnitude $|\mathbf{F}|$ gives the following useful form of the kinematic boundary condition:

$$\Delta(\mathbf{v}\cdot\mathbf{F}) = \mathbf{F}\cdot\Delta\mathbf{v} = 0. \tag{2}$$

This equation requires that the velocity difference between the cold and warm air masses be *along* the front. That is, the two air masses may slide along the front with any tangential velocity difference.

The kinematic boundary condition is illustrated in fig. 8·10. Here the plane of the page represents any plane intersecting the front, and the arrows represent the projection of the velocities $\mathbf{v}$, $\mathbf{v}'$ into this plane. The arrangement of the nine diagrams corresponds to the arrangement of the nine diagrams in fig. 8·09*b*.

Since the front separates the two air masses, the speed of the front is given by the velocity component normal to the front. Therefore in the diagrams of the center column the front is stationary ($v_N = 0$), and in the diagrams of the right- and left-hand columns the front is moving ($v_N \neq 0$). A moving front actively pushed by the cold air mass ($v_N > 0$) is called a *cold front.* And a moving front actively pushed by the warm air mass ($v_N < 0$) is called a *warm front.* Consequently, the diagrams of

the left-hand column represent cold fronts, and the diagrams of the right-hand column represent warm fronts.

If the flow in the two air masses at the front is horizontal, $v_z = 0$. So, by expansion of the scalar product $\mathbf{v}\cdot\mathbf{F}$, the kinematic boundary condition (2) may be written

$$\Delta(\mathbf{v}\cdot\mathbf{F}_H) = \mathbf{F}_H\cdot\Delta\mathbf{v} = 0. \tag{3}$$

Here $\mathbf{F}_H$ is a horizontal vector normal to the front in the horizontal level. Moreover, if the front is stable $\mathbf{F}_H$ points toward the warm air mass. Therefore the unit vector $\mathbf{n}_F$ is along $\mathbf{F}_H$.

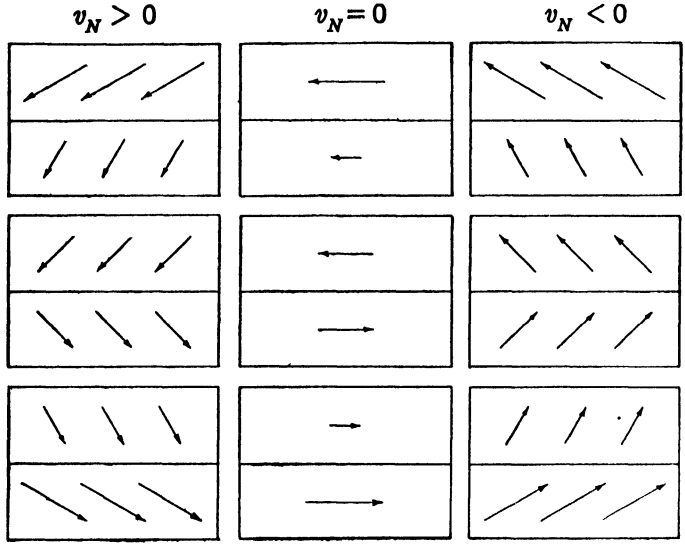



FIG. 8·10. Nine possible velocity fields in the neighborhood of a front in the northern hemisphere.

**8·11. Front separating two arbitrary currents.** The dynamic and kinematic dynamic boundary conditions apply to any front. Since well-defined moving fronts are always marked by extensive cloud systems, atmospheric flow near moving fronts cannot be horizontal. The vector $\mathbf{F}$ normal to the front is defined as the difference of the pressure gradient through the front. When the equation of motion is expressed in the absolute frame, we have from 6·09(2)

$$-\mathbf{F} = \Delta(\nabla p) = \Delta[\rho(\mathbf{g}_a - \dot{\mathbf{v}}_a)]. \tag{1}$$

And when the equation of motion is expressed in the relative frame, we have from 6·19(3)

$$-\mathbf{F} = \Delta(\nabla p) = \Delta[\rho(\mathbf{c} + \mathbf{g} - \dot{\mathbf{v}})]. \tag{2}$$

The frontal slope may be obtained by the method used in section 8·09 as the ratio between the horizontal and vertical components of $\mathbf{F}$. When the front separates two arbitrary currents the general formula for the frontal slope is too complicated for practical evaluation. However, the frontal slope is readily evaluated when the flow in the two air masses separated by the front is zonal or geostrophic. A front separating two constant zonal currents will be called a *zonal front*. A zonal front is a stationary surface of revolution about the axis of the earth, and is completely defined by its trace in a meridional plane. A front separating two geostrophic currents is called a *geostrophic front*. In section 8·13 we shall show that a geostrophic front also is stationary.

**8·12. The zonal front.** In zonal flow the absolute acceleration is, from section 6·11, $\dot{\mathbf{v}}_a = -\omega_a^2\mathbf{R}$. Therefore equation 8·11(1) becomes

$$-\mathbf{F} = \Delta[\rho(\mathbf{g}_a + \omega_a^2\mathbf{R})]. \tag{1}$$

Only small percentual variations of $\rho$ and $\omega_a$ will be considered here, so we may treat the symbol $\Delta$ as a differentiation symbol. Therefore, since $\mathbf{g}_a$ and $\mathbf{R}$ do not vary through the front, (1) may be written

$$-\mathbf{F} = \Delta\rho(\mathbf{g}_a + \bar{\omega}_a^2\mathbf{R}) + 2\bar{\rho}\bar{\omega}_a\Delta\omega_a\mathbf{R}. \tag{2}$$

To simplify this equation we shall define

$$\mathbf{g}_A = \mathbf{g}_a + \bar{\omega}_a^2\mathbf{R},$$
$$\beta = 2\bar{\rho}\bar{\omega}_a\Delta\omega_a.$$

The vector $\mathbf{g}_A$ will be called the *apparent gravity*, for to an observer moving zonally with the absolute angular speed $\bar{\omega}_a$ the force of apparent gravity replaces the force of gravity $\mathbf{g} = \mathbf{g}_a + \Omega^2\mathbf{R}$. Moreover, a surface $\phi_A$ normal to $\mathbf{g}_A$, called an apparent level, replaces the geopotential level $\phi$ normal to $\mathbf{g}$. Introducing the quantities $\mathbf{g}_A$ and $\beta$ into (2), we have

$$-\mathbf{F} = \mathbf{g}_A\Delta\rho + \beta\mathbf{R}. \tag{3}$$

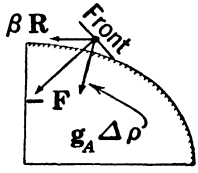
Since $\beta$ has the same sign as $\Delta\omega_a$, we may distinguish the following three cases according to the sign of $\Delta\omega_a$.

(i) $\Delta\omega_a < 0$. Here the warm air rotates faster than the cold air. The orientation of $-\mathbf{F}$ is shown in the upper diagram of fig. 8·12*a*, and the corresponding orientation of the stable zonal front is shown in the lower diagram. The cold air is then on the polar side of the front and the warm air is on the equatorial side. This is the usual geographical distribution of temperature.

(ii) $\Delta\omega_a = 0$. Here the angular speed does not vary through the front. The isobaric surfaces in both air masses and the frontal surface,

being normal to the apparent gravity, coincide with the apparent levels. The sea surface may be considered as a front separating the dense mass of water from the light mass of air. When the ocean and atmosphere have the same zonal rotation, the sea surface is an apparent level. And if, in particular, $\bar{\omega}_a = \Omega$, the sea surface is a geopotential level as indicated earlier.

(iii) $\Delta\omega_a > 0$. Here the cold air rotates faster than the warm air. The orientation of $-\mathbf{F}$ is shown in the upper diagram of fig. 8·12*b*, and the corresponding orientation of the stable zonal front is shown in the lower diagram. The cold air is then on the equatorial side of the front



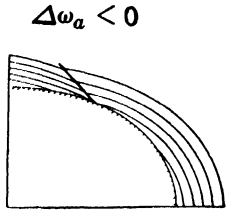
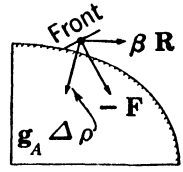




FIG. 8·12*a*.



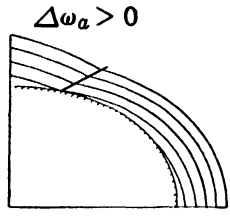




FIG. 8·12*b*.

and the warm air is on the polar side of the front. Although this is an unusual geographical distribution of temperature, such a front may develop in winter on the polar side of a cold continental region, with open water off the coast.

In all figures the apparent level has been shaded. If $\bar{\omega}_a = \Omega$ this apparent level may be taken as the surface of the earth. If $\bar{\omega}_a < \Omega$ the apparent level slopes downward toward the equator. And if $\bar{\omega}_a > \Omega$ the apparent level slopes downward toward the poles.

Notice that in both cases (i) and (iii) the stable zonal front has the faster rotating air on the equatorial side of the front and the slower rotating air on the polar side. Therefore the *horizontal shear* of the two zonal currents at the front is always cyclonic.

We shall now find the slope of the frontal surface with reference to the apparent level. Let $F_{AH}$ and $F_{Az}$ be the apparent horizontal and vertical components of the vector $\mathbf{F}$. The acute angle between the front and the apparent level will be denoted by $\theta_{AF}$. Therefore, in analogy to

8·09(2), the apparent frontal slope is given by

$$\tan \theta_{AF} = \frac{F_{AH}}{F_{Az}}.$$

Let the angle between the apparent level and the axis of the earth as shown in fig. 8·12*c* be denoted by $\varphi_A$, called the *apparent latitude.* The apparent horizontal and vertical components of **R** are then $R \sin \varphi_A$ and $R \cos \varphi_A$ respectively. Consequently we have for the apparent horizontal and vertical components of **F**, from (3):

$$F_{AH} = |\beta| R \sin \varphi_A;$$

$$F_{Az} = g_A \Delta\rho - \beta R \cos \varphi_A.$$

The frontal slope is then given by

$$\frac{1}{\tan \theta_{AF}} = \pm \frac{1}{\tan \varphi_A} + \frac{g_A \Delta\rho}{|\beta| R \sin \varphi_A}.$$

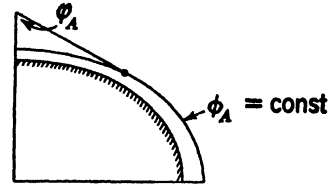



FIG. 8·12*c*. Apparent latitude.

Here the plus sign should be taken when $\Delta\omega_a < 0$, and the minus sign when $\Delta\omega_a > 0$. Usually the frontal angle $\theta_{AF}$ is small, compared with the apparent latitude $\varphi_A$, so the reciprocal of tan $\varphi_A$ may be dropped from the above equation. Thus

$$\tan \theta_{AF} = \frac{2\bar{\omega}_a \sin \varphi_A}{g_A} \frac{R|\Delta\omega_a|}{\Delta\rho} \bar{\rho}. \tag{4}$$

For practical use the density difference should be expressed by the temperature difference according to 8·09(1). Moreover, for all practical purposes the apparent level coincides with the geopotential level. So the final approximate form for the slope of a zonal front is

$$\tan \theta_F = \frac{2\Omega_z}{g} \frac{R|\Delta\omega_a|}{|\Delta T|} \bar{T}. \tag{5}$$

The two equations (4, 5) are always nearly equivalent. In particular, when $\bar{\omega}_a = \Omega$, they are exactly equivalent.

**8·13. The geostrophic front.** When the vectors in equation 8·11(2) are projected into the horizontal plane, we obtain

$$-\mathbf{F}_H = \Delta(\nabla_H p) = \Delta[\rho(\mathbf{c}_H - \dot{\mathbf{v}}_H)].$$

For geostrophic gradient flow, $\dot{\mathbf{v}}_H = \mathbf{0}$ and $\mathbf{c}_H = -2\Omega_z v_g \mathbf{n}$ (see section 7·11). Moreover, $\Omega_z$ does not change through the front. Consequently the above equation may be written

$$\mathbf{F}_H = 2\Omega_z \Delta(\rho v_g \mathbf{n}). \tag{1}$$

Let us form the scalar triple product $\mathbf{F}_H \cdot \mathbf{F}_H \times \mathbf{k}$. The volume of the parallelepiped having the three vectors $\mathbf{F}_H$, $\mathbf{F}_H$, $\mathbf{k}$ as edges is, of course, zero. Accordingly from (1) we have

$$0 = 2\Omega_z \Delta(\rho v_g \mathbf{F}_H \cdot \mathbf{n} \times \mathbf{k}).$$

The factor multiplying $\rho$ inside the parentheses may be simplified as follows:

$$v_g \mathbf{F}_H \cdot \mathbf{n} \times \mathbf{k} = v_g \mathbf{F}_H \cdot \mathbf{t} = \mathbf{F}_H \cdot \mathbf{v}_g.$$

By the kinematic boundary condition this factor has the same value on either side of the front, and consequently may be taken outside the symbol $\Delta$. Thus we have finally

$$2\Omega_z \mathbf{F}_H \cdot \mathbf{v}_g \Delta\rho = 0. \tag{2}$$

The density difference $\Delta\rho$ is by definition positive, so the scalar product $\mathbf{F}_H \cdot \mathbf{v}_g$ is necessarily zero except at the equator. Therefore the geostrophic flow is parallel to the front. Since the front moves only if the air masses have a velocity component normal to the front, *geostrophic flow in the two air masses separated by a front is possible only if the front is stationary.*

The slope of a stationary front separating two geostrophic currents may now be expressed by the geostrophic speed. From 8·09(2) the frontal slope is equal to the ratio $F_H/F_z$. The value of the vertical component $F_z$ is, from 8·09(3), $F_z = g\Delta\rho$. And since the unit vector $\mathbf{n}_F$ is along $\mathbf{F}_H$ for a stable front, the horizontal component $F_H$ is, from (1),

$$F_H = \mathbf{F}_H \cdot \mathbf{n}_F = 2\Omega_z \Delta(\rho v_g \mathbf{n} \cdot \mathbf{n}_F). \tag{3}$$

Since the unit vector $\mathbf{n}_F$ is 90° to the left of $\mathbf{t}_F$, and the unit vector $\mathbf{n}$ is 90° to the left of $\mathbf{t}$, the angle between $\mathbf{n}$ and $\mathbf{n}_F$ is also the angle between $\mathbf{t}$ and $\mathbf{t}_F$. Therefore

$$v_g \mathbf{n} \cdot \mathbf{n}_F = v_g \mathbf{t} \cdot \mathbf{t}_F = \mathbf{v}_g \cdot \mathbf{t}_F.$$

And the frontal slope is

$$\tan \theta_F = \frac{F_H}{F_z} = \frac{2\Omega_z}{g} \frac{\Delta(\rho \mathbf{v}_g)}{\Delta\rho} \cdot \mathbf{t}_F. \tag{4}$$

The slope of a stable front is always positive, so $\Delta(\rho \mathbf{v}_g) \cdot \mathbf{t}_F$ is positive in the northern hemisphere and negative in the southern hemisphere. Consider a stable geostrophic front in the northern hemisphere. The horizontal unit vector $\mathbf{t}_F$ is along the front, with warm air to the left and cold air to the right. Therefore, the vector difference of geostrophic momentum $\Delta(\rho \mathbf{v}_g)$ also must have warm air to the left and cold air to the right, as shown in the three diagrams of fig. 8·13*a*.

These diagrams show that *the horizontal shear of the geostrophic momen-*

*tum at a stable geostrophic front is always cyclonic.* We have already seen that a similar rule applies to a stable zonal front. Although the rule has been derived only for stationary fronts, observations show that it usually applies to moving fronts. For this reason the diagrams of fig. 8·10 have been drawn with cyclonic shear.

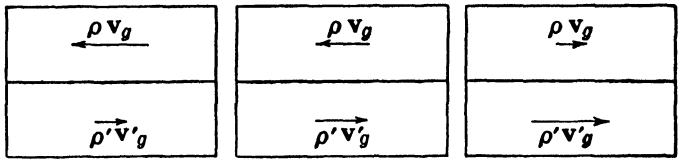



FIG. 8·13*a*. Shear of momentum at a geostrophic front.

We have shown in section 7·16 that the direction to the left of the flow in the southern hemisphere corresponds to the direction to the right of the flow in the southern hemisphere. Therefore, the direction of the arrows showing the geostrophic momentum in fig. 8·13*a* should be reversed in the southern hemisphere. However, the rule stated above is still valid.

A useful form for calculating the frontal slope is obtained by making the approximation

$$\Delta(\rho \mathbf{v}_g) = \bar{\mathbf{v}}_g \Delta\rho + \bar{\rho}\Delta\mathbf{v}_g.$$

Equation (4) then becomes

$$\tan\theta_F = \frac{2\Omega_z}{g}\left(\bar{\mathbf{v}}_g + \frac{\Delta\mathbf{v}_g}{\Delta\rho}\bar{\rho}\right)\cdot\mathbf{t}_F. \tag{5}$$

The magnitude of the first term on the right is, from 8·02(2), the slope $\tan\bar{\theta}_p$ of an isobaric surface in a geostrophic current with the speed $\bar{v}_g$. Consequently the magnitude of the second term on the right is, from 8·09(1), given by

$$|\tan\theta_F \pm \tan\bar{\theta}_p| = \frac{2\Omega_z}{g}\frac{|\Delta\mathbf{v}_g|}{|\Delta T|}\bar{T}. \tag{6}$$

Here the plus sign should be taken when the warm air has the larger speed, and the minus sign when the cold air has the larger speed.

The expression on the right of equation (6) is tabulated below for $\bar{T} = 0°C$ and for reasonable wind and temperature differences through a front at 45° latitude. These values indicate that the isobaric slope ($< 1/1000$) can be neglected for rough approximations. So the practical formula for the slope of a geostrophic front is

$$\tan\theta_F = \frac{2\Omega_z}{g}\frac{|\Delta\mathbf{v}_g|}{|\Delta T|}\bar{T}. \tag{7}$$

This formula, known as *Margules' formula*, is equivalent to the approximate expression 8·12(5) for the slope of a zonal front. Moreover, as we shall now show, Margules' formula also expresses the slope of a transitional frontal layer.

| $\lvert\Delta T\rvert$ | $\lvert\Delta \mathbf{v}_g\rvert$ | | |
|---|---|---|---|
| | 10 m s$^{-1}$ | 20 m s$^{-1}$ | 30 m s$^{-1}$ |
| 5°C | 1/175 | 1/88 | 1/58 |
| 10°C | 1/351 | 1/175 | 1/117 |

Real fronts in the atmosphere are transitional layers with rapid but continuous variation of the temperature and wind through the layer. If the flow throughout the transitional layer is geostrophic, the slope of a stationary transitional layer may be derived from the practical thermal wind equation.

We shall assume that the horizontal isotherms are parallel to the frontal layer. This assumption is not too restrictive, for the horizontal isosteres and isobars are almost parallel to a stationary front. The coordinate $n_T$ is then measured normal to the horizontal trace of the frontal layer. Therefore, as shown in fig. 8·13*b*, the slope of a stable transitional layer is given by

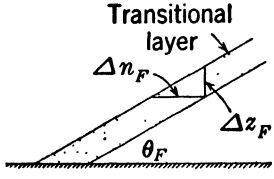



FIG. 8·13*b*.

$$\tan\theta_F = -\frac{\Delta z_F}{\Delta n_F} = -\frac{\Delta z_F}{\Delta n_T}.$$

When the geostrophic shear $\Delta \mathbf{v}_g/\Delta z_F$ is measured vertically through the frontal layer and the temperature variation $\Delta T$ is measured horizontally through the layer, the approximate thermal wind equation 8·05(2) may be written in the form

$$\tan\theta_F = \frac{\Delta z_F}{\Delta n_T} = \frac{2\Omega_z}{g}\frac{|\Delta \mathbf{v}_g|}{|\Delta \bar{T}|}\bar{T}.$$

This equation is Margules' formula for a transitional frontal layer. The wind variation through a continuous frontal layer has the same approximate form as the wind variation through a frontal surface of discontinuity.

CHAPTER NINE

# WIND VARIATION ALONG THE VERTICAL IN THE SURFACE LAYER

**9·01. Dynamics of friction.** The principles which have been derived in the two foregoing chapters are not applicable in the lowest layer of the atmosphere. The motion is here strongly influenced by friction and must be studied with an equation of motion in which the frictional force is included. The aim of this chapter is to determine how far up from the ground this frictional influence extends, and to find the main characteristics of the motion in the layers below, where friction operates.

Let the *frictional force per unit mass* be denoted by $\mathbf{m}$. The equation of motion in the layer of frictional influence next to the ground is then

$$\mathbf{v} = \mathbf{b} + \mathbf{c} + \mathbf{g} + \mathbf{m}. \tag{1}$$

The frictional force depends in a rather complicated way upon the state of the motion and the physical state of the atmosphere. The general problem of the effect of friction upon an arbitrary motion is not yet accessible to rigorous dynamical treatment. In what follows we shall, therefore, confine our discussion to the simple case of steady great circle flow.

**9·02. Steady great circle flow.** The state of motion to be considered in the surface layer is great circle flow, constant throughout each level, and having the proper variation in direction and magnitude from level to level. The problem will be to determine what the velocity variation with height must be if this flow shall remain steady under the influence of friction.

Since the motion is constant great circle flow, the horizontal acceleration is zero, and the horizontal equation of motion becomes

$$0 = \mathbf{b}_H + \mathbf{c}_H + \mathbf{m}_H. \tag{1}$$

The balance of these three forces is shown schematically in fig. 9·02*a*. The horizontal Coriolis force is expressed in terms of the velocity as follows:

$$\mathbf{c}_H = -2\boldsymbol{\Omega}_z \times \mathbf{v}. \tag{7·11(7)}$$

The motion may be resolved into one component equal to the geostrophic

velocity along the isobar, and an additional component which we shall call the *geostrophic deviation*, denoted by $\mathbf{u}$ (see fig. 9·02*a*). Thus

$$\mathbf{v} = \mathbf{v}_g + \mathbf{u}. \tag{2}$$

Substituting this in the expression for $\mathbf{c}_H$, we have

$$\mathbf{c}_H = -2\boldsymbol{\Omega}_z \times \mathbf{v}_g - 2\boldsymbol{\Omega}_z \times \mathbf{u}. \tag{3}$$

This equation gives the actual Coriolis force as the resultant of two vectors, one being the Coriolis force in a motion with the geostrophic wind, and the other the Coriolis force resulting from the deviation from the geostrophic wind. By definition the Coriolis force of the geostrophic wind is balanced by the pressure force:

$$\mathbf{b}_H = 2\boldsymbol{\Omega}_z \times \mathbf{v}_g. \qquad 8\cdot01(2)$$

Substituting this expression and (3) in (1), we obtain for the frictional force

$$\mathbf{m}_H = 2\boldsymbol{\Omega}_z \times \mathbf{u}. \tag{4}$$

This equation states that the deviation $\mathbf{u}$ of the actual wind from the geostrophic wind must be such that the Coriolis force resulting from the deviation will balance the frictional force. The three equations for

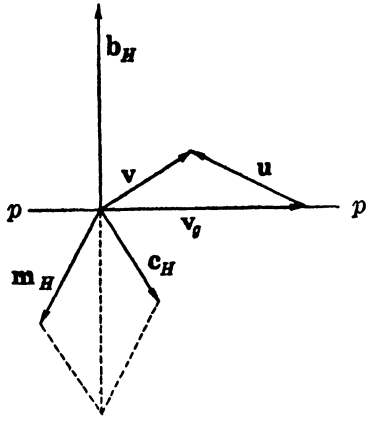



FIG. 9·02*a*.

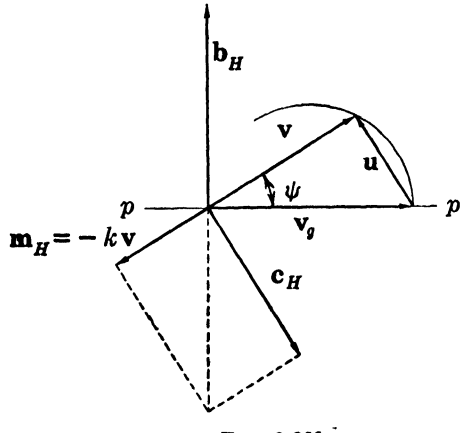



FIG. 9·02*b*.

$\mathbf{c}_H$, $\mathbf{b}_H$, $\mathbf{m}_H$ state: (i) that the force triangle, fig. 9·02*a*, is similar to the velocity triangle, with the factor of proportionality $2\Omega_z$ (taken equal to one in the diagram); (ii) that the force triangle is turned 90° to the right of the velocity triangle in the northern hemisphere.

Equation (4) is the basic equation for steady motion in the surface layer. When the proper expression for $\mathbf{m}_H$ is known, the geostrophic

deviation is obtained by integration, and the total motion is subsequently obtained from equation (2).

The first attempt to study the influence of friction between the atmosphere and the surface of the earth was made by Guldberg and Mohn in 1875. They assumed that the frictional force is directed opposite to the velocity and that its magnitude is proportional to the speed. The velocity triangle then becomes a right triangle, as shown in fig. 9·02*b*. If the factor of proportionality $k$ is assumed to decrease with height, the angle $\psi$ which the wind makes with the isobars has a maximum at the ground and decreases with elevation.

This solution explains in a qualitative way some of the observed features of the motion in the surface layer, notably that the wind has a component toward lower pressure. However, although it is true that the frictional force in a qualitative sense may be expected to act against the motion and tend to slow it down, there is no reason to believe that the expression for the frictional force is so simple as Guldberg and Mohn assumed. In order to derive a rational theory for atmospheric friction it becomes necessary to examine the physical mechanism of fluid resistance in some detail.

**9·03. The viscous stress.** Consider a layer of fluid enclosed between two rigid horizontal plates separated by a distance $z$, as in fig. 9·03*a*. The lower plate is at rest, and the upper plate is kept in steady horizontal motion with the velocity $\mathbf{v}$. When steady conditions are established, experiments show that the velocity of the fluid increases linearly from zero at the resting plate to the velocity $\mathbf{v}$ at the moving plate; in other words the shear is constant throughout the layer. This motion develops as a consequence of the viscosity or internal friction which arises from the irregular random motion of the fluid molecules.

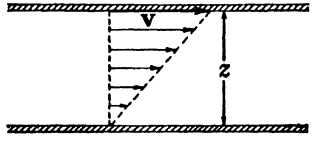



FIG. 9·03*a*.

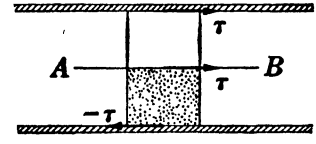



FIG. 9·03*b*.

Experiments show further that in order to keep the upper plate in steady motion it is necessary to apply a tangential force which is proportional to the velocity of the plate and inversely proportional to the distance $z$ between the two plates. If this force, referred to unit area of the plate, is denoted by $\tau$, we have

$$\tau \sim \frac{\mathbf{v}}{z}. \tag{1}$$

As no accelerations exist, the force on the upper plate is balanced by an equal and opposite force on the lower plate in order to keep it at rest, as shown in fig. 9·03*b*. Consider now a vertical column with unit cross section, extending from the lower plate to an arbitrary horizontal plane $AB$ between the two plates. The force $-\tau$ on the lower face of this column has to be balanced by a force $\tau$ on the top face of the column in the plane $AB$. This force, which is caused by the frictional interaction between the fluid layers on both sides of the plane, is called the *viscous stress*. In the ideal experiment described here we find that the viscous stress has the same value at every point in the fluid layer, and from (1) it is proportional to the constant shear in the layer.

Since the stress is caused by molecular action, it is evident that it can depend only on the velocity distribution in the immediate vicinity of the plane across which it acts. We may therefore generalize the above result to the case of horizontal motion which is constant on each horizontal plane, but where the velocity has an arbitrary variation along the vertical, as in fig. 8·03*a*. Also here we may expect that the stress at any level is proportional to the shear, $\partial v/\partial z$, at that level. Denoting the factor of proportionality by $\mu$, we have then

$$\tau = \mu \frac{\partial v}{\partial z}. \tag{2}$$

This relation, which was discovered by Newton, is called *Newton's formula* for the stress. The proportionality factor $\mu$ is called the *viscosity*. The viscosity is found to be a physical property of the fluid. It is independent of the velocity distribution, the dimensions of the system, and so forth.

**9·04. The viscosity of a perfect gas.** Since the stress is created by the molecular motion, we should be able to derive Newton's formula theoretically if the molecular motion is known. In a liquid fluid nothing is known of the molecular motion, but for a gas Newton's formula can be derived from the kinetic theory, as shown by Maxwell.

The kinetic theory states that the molecules of a gas move with a random distribution of velocities, and that the kinetic energy of this motion is the internal heat energy of the gas. Being random oscillation, such motion contributes nothing towards moving the gas as a whole. Let the molecules in addition to this random heat motion have an ordered streaming motion which is constant in planes parallel to $AB$ in fig. 9·04. Consider the conditions at the plane $AB$. As a result of the random heat motion, molecules from below will pass upward, and from above downward, each carrying along with them the

streaming momentum corresponding to the layer where they experienced their last impact. There is accordingly a transport of momentum through the plane, whereby the faster moving upper layer loses momentum, and the slower moving lower layer gains momentum. The process may be likened to the case of two trains moving in the same direction along parallel tracks, but with somewhat different speeds. If the passengers jump from one train to the other, the faster train will be slowed down, and the slower train will be accelerated. According to Newton's second law the rate of change of momentum is equivalent to a force exerted by the upper layer on the lower layer. This force is the viscous stress.

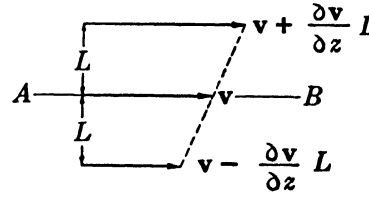


FIG. 9·04.

We shall now express this idea in mathematical form. Let $c$ be the average speed of the heat motion when the flow velocity is subtracted. Let $m$ be the mass of each molecule, and let $N$ be the number of molecules per unit volume. To simplify matters, assume that one-third of the molecules move perpendicular to the plane, one-half of this number $N/6$ moving downward, and the other half upward. The number passing downward per second through unit area is then $Nc/6$. These molecules experienced on an average their last collision at the distance of the *mean free path* $L$, and each has the streaming momentum $m[\mathrm{v} + (\partial \mathrm{v}/\partial z)L]$ characteristic of this level. Thus per unit area and time at the plane $AB$ we have:

$$\text{the downward momentum transport} = \tfrac{1}{6}Nmc\left(\mathrm{v} + \frac{\partial \mathrm{v}}{\partial z}L\right).$$

And by the same reasoning we have:

$$\text{the upward momentum transport} = \tfrac{1}{6}Nmc\left(\mathrm{v} - \frac{\partial \mathrm{v}}{\partial z}L\right).$$

The product $Nm$ is the mass per unit volume, or the density $\rho$. The net downward transport of momentum per unit area and time,

$$\tau = \tfrac{1}{3}\rho cL\frac{\partial \mathrm{v}}{\partial z}, \tag{1}$$

is the stress which the fluid above the plane exerts on the fluid below the plane. This equation is Newton's formula, 9·03(2), and gives for the viscosity the expression

$$\mu = \tfrac{1}{3}\rho cL. \tag{2}$$

This relation shows that the viscosity is a physical property of the fluid. Further, since $\rho L$ is constant for a given gas, the viscosity is independent of the density and hence of the pressure of the gas. Since the temperature is proportional to the square of the mean heat speed $c$, the viscosity is proportional to the square root of the temperature. The independence of pressure is well substantiated by experiments, but the increase with temperature is somewhat greater than this theory indicates.

**9·05. Viscosity of air and water.** Viscosity is measured by letting the fluid flow through a circular pipe under the influence of a known pressure gradient and recording the rate of discharge. Some values of the viscosity of air and water, obtained from such measurements, are given in table 9·05. The dimensions of viscosity are, from 9·04(2), $[\mu] = [ML^{-1}T^{-1}]$, and the numerical values in the table are in mts units.

TABLE 9·05

VISCOSITY IN MTS UNITS

| $T$°C | Air | Water |
|---|---|---|
| 0 | $1.7 \times 10^{-8}$ | $1.8 \times 10^{-6}$ |
| 100 | $2.2 \times 10^{-8}$ | $0.2 \times 10^{-6}$ |

In water the viscosity decreases rapidly with increasing temperature, as is generally true in all liquid fluids. In air the viscosity increases with temperature, in qualitative agreement with Maxwell's theoretical expression 9·04(2). However, it is seen that the actual increase is more rapid than the theory predicts. For both air and water the viscosity is practically unaffected by pressure changes, even up to 100 atmospheres.

The viscosity of air and water is quite small. For comparison the viscosity of glycerin at 20°C is about $9 \times 10^{-4}$ mts units.

**9·06. The frictional force.** In the special case of horizontal motion with shear the frictional force is readily expressed by the shearing stress. Consider a vertical column of unit cross section extending from the level $z$ to the level $z + \delta z$. See fig. 9·06. Let $-\boldsymbol{\tau}$ be the stress exerted on the bottom face by the fluid below, and $\boldsymbol{\tau} + (\partial\boldsymbol{\tau}/\partial z)\delta z$ the stress exerted on the top face of the column by the fluid above. These stresses may have different horizontal directions. The resultant of these stresses, $(\partial\boldsymbol{\tau}/\partial z)\delta z$, is the frictional force on the volume element $\delta V = \delta z$. The frictional force per unit volume is therefore $\partial\boldsymbol{\tau}/\partial z$, and the frictional force per unit mass is

$$\mathbf{m}_H = \alpha \frac{\partial \boldsymbol{\tau}}{\partial z}. \tag{1}$$

Note the analogy between this expression for the frictional force and the expression $-\alpha\nabla p$ for the pressure force. Like the pressure, the stress is defined as a force per unit area. The pressure gradient is the pressure force per unit volume, and similarly the variation of the stress per unit of height is the frictional force per unit volume. To obtain the corresponding forces per unit mass the volume forces are multiplied by the specific volume.

Only in the special case of horizontal motion with uniform velocity at each level has the frictional force the simple form (1). If the motion also has horizontal shear, tangential stresses on the vertical side faces of the fluid particles will result, and the horizontal gradients of these lateral stresses add to the frictional force. If the stress on a horizontal face is $\tau^z$, and the stresses on the vertical faces normal to the $x$ axis and the $y$ axis are respectively $\tau^x$ and $\tau^y$, it can be shown that the general expression for the frictional force is

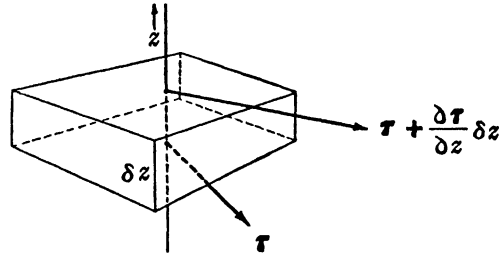



FIG. 9·06. Variation of the stress with height.

$$\mathbf{m} = \alpha\left(\frac{\partial \tau^x}{\partial x} + \frac{\partial \tau^y}{\partial y} + \frac{\partial \tau^z}{\partial z}\right). \tag{2}$$

The analogy with the expression for the pressure force is here complete. In all large-scale atmospheric currents the horizontal shear of the wind is extremely small in comparison with the vertical shear in the surface layer. The lateral stresses $\tau^x$ and $\tau^y$ are then correspondingly small, and the frictional force is in the first approximation given by the simple formula (1).

**9·07. Total mass transport in the surface layer.** When the expression 9·06(1) for the horizontal frictional force is introduced in the basic dynamic equation for steady motion in the surface layer, 9·02(4), we have

$$\alpha\frac{\partial \tau}{\partial z} = 2\Omega_z \times \mathbf{u}. \tag{1}$$

When this equation is multiplied by the density, we have

$$\frac{\partial \tau}{\partial z} = 2\Omega_z \times \rho\mathbf{u}.$$

Integrating this equation along a vertical extending from the ground,

where the stress is $\boldsymbol{\tau}_0$, to the top of the atmosphere, where the stress is zero, we have

$$-\boldsymbol{\tau}_0 = 2\boldsymbol{\Omega}_z \times \int_0^\infty \rho \mathbf{u} \delta z. \tag{2}$$

The integral on the right represents the total transport of mass resulting from the geostrophic deviation through a vertical column of unit cross section extending from the ground to the top of the atmosphere. Denoting this mass transport by $\mathbf{F}_u$,

$$\mathbf{F}_u = \int_0^\infty \rho \mathbf{u} \delta z, \tag{3}$$

equation (2) can be written

$$-\boldsymbol{\tau}_0 = 2\boldsymbol{\Omega}_z \times \mathbf{F}_u. \tag{4}$$

The physical interpretation of this equation is simple. Consider the total vertical column of air, having unit cross section and extending from the ground to the top of the atmosphere. No acceleration exists within this column, and the resultant of all the acting forces is therefore zero. The horizontal pressure forces acting on the column are balanced by the Coriolis forces which result from the geostrophic part of the motion. The only remaining external force is the stress $-\boldsymbol{\tau}_0$ exerted by the surface of the earth on the bottom face of the air column. To balance this stress the air in the column must have a motion in addition to the geostrophic wind (that is, a geostrophic deviation) such that the sum of the resulting Coriolis forces throughout the complete column is equal and opposite to the stress. The total mass transport of the geostrophic deviation is therefore directed at right angles to the surface stress and is proportional to the stress, in accordance with equation (4).

We may similarly define the mass transport $\mathbf{F}$ of the actual wind and the mass transport $\mathbf{F}_g$ of the geostrophic wind:

$$\mathbf{F} = \int_0^\infty \rho \mathbf{v} \delta z, \qquad \mathbf{F}_g = \int_0^\infty \rho \mathbf{v}_g \delta z. \tag{5}$$

When the equation $\mathbf{v} = \mathbf{v}_g + \mathbf{u}$ is multiplied by $\rho$ and the three terms are integrated from the bottom to the top of the atmosphere we have then

$$\mathbf{F} = \mathbf{F}_g + \mathbf{F}_u. \tag{6}$$

Equations (4) and (6) are illustrated by fig. 9·07.

A problem of considerable practical importance is that of evaluating the total transport of air across the isobars. According to (6) only the part $\mathbf{F}_u$ of the total mass transport contributes to the cross isobar transport. The component of $\mathbf{F}_u$ normal to the isobar can be evaluated from (4) when the direction and the magnitude of the surface stress $\boldsymbol{\tau}_0$ are known.

The surface stress is proportional to the wind shear immediately above the ground and is therefore directed along the wind at a short distance above the ground, say at the anemometer level where the surface wind is measured. It is rather plausible, and also borne out by theory (see H. U. Sverdrup: "Oceanography for Meteorologists," Prentice-Hall, 1942, p. 119) that the magnitude of the surface stress at any given station depends only upon the anemometer wind speed. The cross isobar transport can therefore be determined entirely from an observation of the surface wind when the direction of the isobar is known.

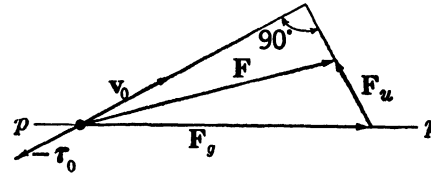



FIG. 9·07. Mass transports in a vertical column from the ground to the top of the atmosphere.

It should be noted that the above relation between the surface stress and the cross isobar transport does not involve any assumptions as to the wind distribution along the vertical.

**9·08. Wind distribution in the surface layer.** We shall now turn to the main problem of this chapter, namely to determine the wind distribution along the vertical in a steady straight current. To simplify the mathematical problem it will be assumed that the horizontal pressure force and, hence, the geostrophic wind have the same direction and magnitude at all levels, and further that the specific volume is independent of height. The latter assumption is not so serious a violation of actual conditions as it may seem, for it will be shown that the effect of friction is mainly confined to the lowest kilometer. Finally it will be assumed that the viscosity is independent of height. The justification of that assumption will be considered below.

When Newton's formula 9·03(2) for the stress is substituted in 9·07(1), we have

$$\alpha\mu \frac{\partial^2 \mathbf{v}}{\partial z^2} = 2\boldsymbol{\Omega}_z \times \mathbf{u}. \tag{1}$$

In this equation the height $z$ is the only independent variable. Differentiation with respect to height will in the remaining part of this section be denoted by primes. Since the geostrophic wind is assumed inde-

pendent of height, the variation with height of the actual wind is equal to the variation of the geostrophic deviation. Equation (1) can then be written

$$\alpha\mu\mathbf{u}'' = 2\Omega_z\mathbf{k}\times\mathbf{u}. \tag{2}$$

The three scalar parameters $\Omega_z$, $\alpha$, $\mu$ are, according to our assumptions, constant along the vertical. They are replaced by a single constant $\beta^2$, given by

$$\beta^2 = \frac{\Omega_z}{\alpha\mu}\,; \tag{3}$$

here $\beta^2$ is positive in the northern hemisphere and negative in the southern hemisphere. Then equation (2) takes the form

$$\mathbf{u}'' = 2\beta^2\mathbf{k}\times\mathbf{u}. \tag{4}$$

The solution of this homogeneous linear differential equation can be written down directly if the two-dimensional vector $\mathbf{u}$ is treated as a complex variable. A more elementary solution is given here. We introduce a natural system of reference $\mathbf{t}$, $\mathbf{n}$, $\mathbf{k}$ referred to the velocity $\mathbf{u}$, such that

$$\mathbf{u} = u\mathbf{t}. \tag{5}$$

The derivatives of the two unit vectors $\mathbf{t}$ and $\mathbf{n}$ are

$$\begin{aligned} \mathbf{t}' &= \theta'\mathbf{n}, \\ \mathbf{n}' &= -\theta'\mathbf{t}, \end{aligned} \tag{6}$$

where $\theta' = \partial\theta/\partial z$ represents the rate at which the vector $\mathbf{u}$ turns with increasing height. Differentiation of (5) gives for the shear of $\mathbf{u}$

$$\mathbf{u}' = u'\mathbf{t} + \theta' u\mathbf{n}. \tag{7}$$

The shear is here expressed as the sum of its natural components tangential and normal to the vector $\mathbf{u}$. There is a close formal analogy between this development for the shear and the development in section 6·05 for the acceleration, the only difference between the two being that one represents differentiation with respect to height and the other differentiation with respect to time. When (7) is differentiated once more, and the relations (6) are considered, we have

$$\mathbf{u}'' = [u'' - \theta'^2 u]\mathbf{t} + [\theta' u' + (\theta' u)']\mathbf{n}.$$

The vector product in (4) becomes

$$\mathbf{k}\times\mathbf{u} = u(\mathbf{k}\times\mathbf{t}) = u\mathbf{n}.$$

Substituting these expressions in (4), we obtain the two component equations

$$u'' = \theta'^2 u, \tag{8}$$

$$\theta' u' + (\theta' u)' = 2\beta^2 u. \tag{9}$$

The general solution of this simultaneous system (8, 9) is rather complicated. However, we are only interested in the special solution for which $u$ remains bounded as $z \to \infty$. This is the boundary condition for the system (8, 9). If it were violated, we should have infinitely high velocities at the top of the atmosphere, which is physically impossible.

To find the special solution, we first assume that $\theta'$ is constant. Then (9) takes the form

$$\theta' u' = \beta^2 u. \tag{10}$$

Differentiation of (10) gives

$$\theta' u'' = \beta^2 u'. \tag{11}$$

Elimination of $u$ between (8) and (10) gives

$$\theta' u'' = \frac{\theta'^4}{\beta^2} u'. \tag{12}$$

Comparison of (11) and (12) shows that $\theta'^4 = \beta^4$, whence for the system (8, 10) to be consistent we must have $\theta'^2 = \pm\beta^2$. Since $\theta'^2$ is positive by physical definition, the plus sign applies to the northern hemisphere and the minus sign applies to the southern hemisphere. Restricting the further discussion to the northern hemisphere, we see then that (10) takes the form

$$u' = \theta' u. \tag{13}$$

It is clear that (8) is a consequence of (13), so that the solution of the system (8, 13), i.e., the special solution of (8, 9) for constant $\theta'$, is obtained by solving (13) alone.

The solution of (13) is well known to be

$$u = u_0 e^{\theta' z}, \tag{14}$$

where $u_0$ is the value of $u$ at $z = 0$. Now, in order that $u$ be bounded as $z \to \infty$, we see from (14) that $\theta'$ must be negative. Since $\theta'^2 = \beta^2$, it follows that

$$\theta' = -\beta, \tag{15}$$

where $\beta$ is the positive root of $\beta^2$. We then have from (14) that

$$u = u_0 e^{-\beta z}. \tag{16}$$

Equations (15) and (16) give the northern hemisphere solution of the system (8, 13). It can be shown by more advanced methods *without any assumption about* $\theta'$ that (15, 16) is the only solution of the system (8, 9) that obeys the boundary condition at the top of the atmosphere.

In interpreting (16), the simplest condition would be that the velocity $\mathbf{v}$ at the ground be zero, whence from 9·02(2) $u_0 = |\mathbf{v}_g|$. However, the dynamical conditions at the ground are more complicated than assumed here and must be studied with an equation different from (4). The solution of (4) can therefore not be extended to the ground, but only to a somewhat higher level (say 10 m above the ground). This level may arbitrarily be taken to be the " anemometer level " where the surface wind is measured. Let $\mathbf{v}_0$ be the velocity at the anemometer level, and let $\mathbf{u}_0$ be the corresponding geostrophic deviation (see fig. 9·08); thus

$$\mathbf{v}_0 = \mathbf{v}_g + \mathbf{u}_0.$$

Hence, when the height $z$ is measured from the anemometer level, the $u_0$ of (16) is equal to $|\mathbf{u}_0| = |\mathbf{v}_0 - \mathbf{v}_g|$. The equation (16) then says that the magnitude of the geostrophic deviation decreases exponentially with

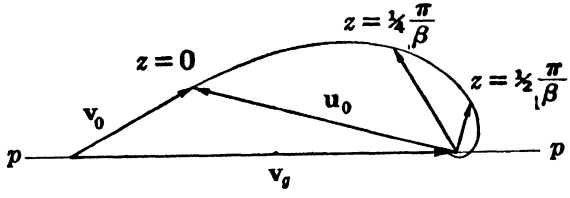



FIG. 9·08. Ekman spiral.

increasing height from the maximum value $u_0$ at the anemometer level.

The turning of the wind with height is given by (15). Here $\theta$ is the angle from an arbitrary fixed direction to the direction of $\mathbf{u}$. To simplify the formulas we shall measure the angle $\theta$ from the direction of $\mathbf{u}_0$ at the anemometer level, so that $\theta_0 = 0$. The integral of (15) is then

$$\theta = -\beta z. \tag{17}$$

The explicit solution at the anemometer level and above is given by combining equations (16) and (17); thus

$$u = u_0 e^{\theta} \quad \text{and} \quad \theta = -\beta z. \tag{18}$$

The geostrophic deviation turns linearly with height in a negative sense, and its magnitude decreases exponentially with the angle of turning. The equation (18) is the equation for the hodograph in polar coordinates. It is the well-known expression for the logarithmic spiral. The solution is known as the *Ekman spiral* after W. F. Ekman, who solved the corresponding problem for the surface layer of the ocean in 1902.

Fig. 9·08 illustrates schematically the velocity distribution in the layer next to the ground. It shows the velocity $\mathbf{v}_0$ and the geostrophic deviation $\mathbf{u}_0$ at the anemometer level, and also the hodograph of $\mathbf{u}$. The latter is, of course, also the hodograph of the total velocity $\mathbf{v}$. Two values of $\mathbf{u}$, for the angles $\theta = -\frac{1}{4}\pi$ and $\theta = -\frac{1}{2}\pi$, which correspond to the levels $z = \frac{1}{4}\pi/\beta$ and $z = \frac{1}{2}\pi/\beta$, are indicated in the diagram.

**9·09. Relation between surface velocity and geostrophic velocity.** The analysis in the preceding section does not give any information regarding the direction and magnitude of the surface wind (at the anemometer level).

The behavior of the surface wind is determined by the dynamics of the *bottom layer*, from the anemometer level down to the ground. The theory of this layer will not be treated in this book. It must suffice to mention a few of the results. It can be shown that the turning of the wind in the bottom layer is negligible, and so the wind and the shear of the wind have here *approximately the same direction*. Applying this at the anemometer level, we have

$$\mathbf{v}_0 = \kappa \mathbf{v}_0'. \tag{1}$$

The scalar factor of proportionality $\kappa$ depends upon the height of the anemometer level and the roughness of the ground. For example, if the anemometer level is at 10 m and the ground is open grassland, the proportionality factor is 55 m.

A well-known geometrical property of the logarithmic spiral is that the tangent at any point makes the constant angle of 45° with the radius vector. This is readily shown from the formula 9·08(7) for the shear. Substituting here for $u'$ and $\theta'$ from 9·08(13, 15) we find

$$\mathbf{v}' = \mathbf{u}' = -\beta u(\mathbf{t} + \mathbf{n}). \tag{2}$$

The shear is directed along the tangent of the hodograph. From (2) the shear is parallel to the vector $\mathbf{t} + \mathbf{n}$, which makes an angle of 45° with $\mathbf{t}$ and hence with the radius vector $\mathbf{u}$. Applying this result at the anemometer level, where from (1) the velocity and the shear are parallel, we find that the angle between the directions of $\mathbf{v}_0$ and $-\mathbf{u}_0$ is 45°, as shown in fig. 9·09. It follows then immediately from the diagram that $v_g \sin \psi_0 = v_g \cos \psi_0 - v_0$, or

$$v_0 = v_g (\cos \psi_0 - \sin \psi_0). \tag{3}$$

Another relation between the surface wind and the geostrophic wind is obtained as follows. The magnitude of the shear at the anemometer

level is, from (2),

$$|\mathbf{v}_0'| = \beta u_0 \sqrt{2}. \tag{4}$$

Taking the magnitude in equation (1) and substituting from (4), we find

$$v_0 = \kappa\beta u_0 \sqrt{2}. \tag{5}$$

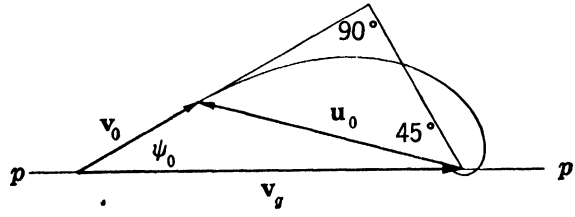



FIG. 9·09.

Further, by inspection of fig. 9·09,

$$v_g \sin \psi_0 = u_0 \sin 45° = \tfrac{1}{2} u_0 \sqrt{2}. \tag{6}$$

And finally when $u_0$ is eliminated from (5) and (6)

$$v_0 = 2\kappa\beta v_g \sin \psi_0. \tag{7}$$

This relation, together with the relation (3), determines the direction and magnitude of the surface wind. When the ratios between the two equations are taken, both $v_0$ and $v_g$ are eliminated and we find

$$\cot \psi_0 = 1 + 2\kappa\beta. \tag{8}$$

The angle $\psi_0$ between the surface wind and the isobar is thus less than 45°, which also is directly apparent from the diagram. The actual numerical value of the angle, and hence of the surface wind speed, depends upon the magnitude of the two parameters $\kappa$ and $\beta$.

**9·10. The geostrophic wind level.** The velocity distribution in fig. 9·08 agrees at least qualitatively with actual observations in a region with straight isobars over level ground. The surface wind is considerably smaller than the geostrophic wind, and it has a component across the isobars toward lower pressure. With increasing elevation the wind speed increases, and its direction approaches that of the geostrophic wind. The lowest level where the wind becomes parallel to the isobars is called the geostrophic wind level. As shown in fig. 9·10, this level is reached when the geostrophic deviation has turned an angle $\theta_H = -(\frac{3}{4}\pi + \psi_0)$. The height $H$ of the geostrophic wind level measured from the anemometer level is determined by $\theta_H = -\beta H$. When the

above value for $\theta_H$ is used, we find

$$H = \frac{1}{\beta}\left(\tfrac{3}{4}\pi + \psi_0\right) = \left(\tfrac{3}{4}\pi + \psi_0\right)\sqrt{\frac{\alpha\mu}{\Omega_z}}. \tag{1}$$

In the second expression to the right the value of $\beta$ has been introduced from 9·08(3). At the equator the height of the geostrophic wind level would become infinite. The physical reason for this is the fact that the

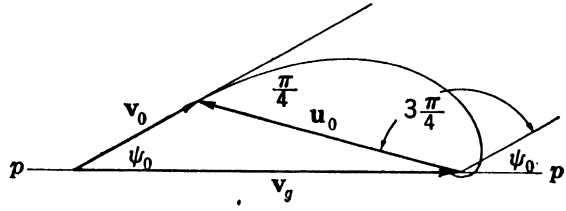



FIG. 9·10.

horizontal Coriolis force is zero at the equator, and hence no deflection of the motion can create forces which will balance the pressure force and the frictional force. The above discussion is therefore invalid close to the equator.

The height $H$ is proportional to $\sqrt{\mu}$ and hence increases with the viscosity of the air, which might be expected a priori. If the friction is caused by molecular action only, $\mu$ is the molecular viscosity. As an example take the 0°C value, $\mu = 1.7 \times 10^{-8}$ mts units, and $\alpha = 850$ m$^3$ t$^{-1}$. These values introduced in (1) give for the height of the geostrophic wind level at 40° latitude the value 1.6 m. Under the influence of molecular viscosity the layer of frictional influence in the atmosphere would only have a thickness of 1 to 2 m.

We know by experience that the geostrophic level is found much higher up. The height varies widely, depending on the nature of the surface of the earth and the stability of the air. A rough average value at 40° latitude is about 1500 m, or roughly one thousand times the value derived above. Substituted in (1), this value of the height would require that the viscosity be about $1.6 \times 10^{-2}$ mts units, or roughly one million times larger than the molecular value. It is evident from this that the internal friction is created by an enormously more powerful agent than the molecular motion. This agent is the atmospheric turbulence, and the viscosity which is found in the example above is the turbulent viscosity or *eddy viscosity* $\mu_e$.

**9·11. The eddy viscosity.** To complete the present discussion some qualitative remarks concerning the eddy viscosity will be made. It

appears that the main characteristics of turbulent flow can be described by considering the motion as the resultant of a certain *mean flow* and a random *eddy flow*, the latter giving no net transport of mass in any direction. This is evidently analogous to the molecular heat motion superimposed on the streaming flow of the air (section 9·04).

Consider the simple case where the mean flow is horizontal and is also steady and uniform in each horizontal level. The turbulent eddies will carry parcels of fluid from level to level, mixing rapidly into their new surroundings. The net result of this is a transport of *mean momentum* across the planes of constant mean flow. The slower streaming fluid on one side of the plane gains momentum at the expense of the faster streaming fluid on the other side. This momentum transport is equivalent to a tangential stress, called the *eddy stress*, across the planes of constant flow. It is equal to the rate of flow of momentum across unit area.

To obtain an expression for the eddy stress it is assumed that the parcels of air which are affected by the eddies *move a certain average distance l before they lose their identity and mix with their new environments.* The distance $l$ is called the *mixing length.* It corresponds to the mean free path of molecular motion, although its physical definition is less precise. Let $w$ be the average component of the eddy velocity perpendicular to the plane of constant flow. By reasoning similar to that in section 9·04 we find that the rate of momentum flow across unit area, and hence the eddy stress, is proportional to $\rho wl(\partial \mathbf{v}/\partial z)$, where $\mathbf{v}$ is the velocity in the mean flow. The factor of proportionality is usually included in the definition of the mixing length, so

$$\tau = \rho wl \frac{\partial \mathbf{v}}{\partial z}. \tag{1}$$

This formula for the eddy stress is analogous to Newton's formula for the molecular stress. It brings out the formal analogy between the dynamical action of molecular and eddy motion. The expression $\rho wl$ is dimensionally a viscosity and plays the role of viscosity in the above formula. It is therefore called the eddy viscosity and denoted by $\mu_e$:

$$\mu_e = \rho wl. \tag{2}$$

There is some similarity between this expression and Maxwell's formula 9·04(2) for the molecular viscosity. But, contrary to the molecular viscosity, the eddy viscosity is not a physical property. The mixing length depends upon the roughness of the ground, the distance from the ground, and also on the velocity distribution in the mean flow. The

vertical eddy component $\bar{w}$ depends upon the mixing length and the shear of the mean flow.

Several methods exist whereby the eddy viscosity and its distribution with height can be determined directly from the vertical wind distribution. From such determinations it is found that the eddy viscosity first increases from the ground upward, and then decreases again higher up. The actual values are found to vary within a wide range. Over a relatively level ground and with moderate stability the range is roughly from $0.5 \times 10^{-2}$ to $5 \times 10^{-2}$ mts units, with an average value of about $10^{-2}$. From the formula (2) this average value would correspond to a mixing length of 8 m and a vertical eddy velocity of 1 m $s^{-1}$.

The analysis of the frictional layer in the preceding sections is valid for a turbulent layer when the eddy viscosity is used, and when it is further assumed that the eddy viscosity is constant in the layer. See 9·08(1). The above remarks would indicate that the assumption of a constant eddy viscosity is unjustified. Nevertheless, the solution for a constant eddy viscosity having the average value of the layer is a useful first approximation to what actually happens.

CHAPTER TEN

# MECHANISM OF PRESSURE CHANGES

**10·01. Equation of continuity.** One important physical principle which has not yet been considered is that of the conservation of mass. This principle states that no fluid mass can be created or destroyed. Consider an arbitrary fixed volume bounded by a fictitious closed boundary at any place in an air current. Air will then flow through this

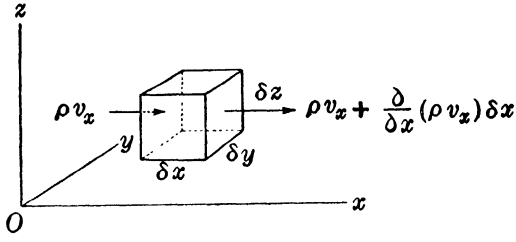



FIG. 10·01. Net inflow of mass along $x$ axis.

volume, passing in through the boundary from one side and escaping through the boundary on the other side. The principle of the conservation of mass requires that *the net inflow of mass into the fixed volume in a given time equal the increase of mass within the volume during the same time.*

To express this statement in mathematical form, let the fixed volume be an infinitesimal parallelepiped $\delta V = \delta x \delta y \delta z$, as in fig. 10·01. The net inflow along the $x$ axis into the volume $\delta V$ during the time element $dt$ is

$$(\rho v_x)\delta y \delta z dt - \left[\rho v_x + \frac{\partial}{\partial x}(\rho v_x)\delta x\right]\delta y \delta z dt = -\frac{\partial}{\partial x}(\rho v_x)\delta V dt.$$

Here $\rho v_x$ is a mean value for the area $\delta y \delta z$. Similar expressions are obtained for the net inflow along the $y$ axis and the $z$ axis. The sum of these three expressions represents *the total net inflow of mass into the volume $\delta V$ in the time $dt$*:

$$(1) \qquad -\left[\frac{\partial}{\partial x}(\rho v_x) + \frac{\partial}{\partial y}(\rho v_y) + \frac{\partial}{\partial z}(\rho v_z)\right]\delta V dt.$$

This inflow of mass must cause an increase of density in the volume element from the value $\rho$ at the time $t$ to the value $\rho + (\partial\rho/\partial t)dt$ at the time

$t + dt$. *The increase of mass in the volume* $\delta V$ *during the time* $dt$ *is therefore*

$$\left(\rho + \frac{\partial \rho}{\partial t}\, dt\right) \delta V - \rho \delta V = \frac{\partial \rho}{\partial t}\, \delta V dt. \tag{2}$$

The principle of the conservation of mass requires that the two expressions (1) and (2) be the same. When the factors $\delta V$ and $dt$ are divided out, we obtain the two equivalent expressions for the rate at which mass flows into a fixed unit volume. When these are equated we have

$$\frac{\partial \rho}{\partial t} = -\left[\frac{\partial}{\partial x}(\rho v_x) + \frac{\partial}{\partial y}(\rho v_y) + \frac{\partial}{\partial z}(\rho v_z)\right]. \tag{3}$$

This equation is known as the equation of continuity. The expression on the right can be written more conveniently in vector notation when the following convention is adopted. The operation symbol $\nabla$ used in 4·12 may be considered as a vector with the rectangular components $\partial/\partial x$, $\partial/\partial y$, $\partial/\partial z$. The part of equation (3) enclosed in brackets is then the scalar product of the vector operator $\nabla$ and the momentum vector $\rho\mathbf{v}$; thus

$$\nabla\cdot(\rho\mathbf{v}) = \frac{\partial}{\partial x}(\rho v_x) + \frac{\partial}{\partial y}(\rho v_y) + \frac{\partial}{\partial z}(\rho v_z). \tag{4}$$

The expression in (3) represents the rate of inflow or convergence of mass into unit volume. The quantity in (4), having the opposite sign, represents the outflow and is called the *divergence* of the vector $\rho\mathbf{v}$. It is sometimes denoted $\mathrm{div}(\rho\mathbf{v})$. Since $\rho\mathbf{v}$ represents the flow of mass the divergence $\nabla\cdot(\rho\mathbf{v})$ of this vector is called the *mass divergence.*

With the notation (4) the equation of continuity takes the form

$$\frac{\partial \rho}{\partial t} = -\nabla\cdot(\rho\mathbf{v}). \tag{5}$$

An alternative form of the equation of continuity will be derived in the next section.

**10·02. Divergence.** The compact vector expression for the mass divergence, $\nabla\cdot(\rho\mathbf{v})$, can be developed as follows:

$$\nabla\cdot(\rho\mathbf{v}) = \mathbf{v}\cdot\nabla\rho + \rho\nabla\cdot\mathbf{v}. \tag{1}$$

This formula is verified by performing the differentiation on the right in 10·01(4) and expressing the result in vector notation. Accordingly the divergence operator $\nabla\cdot$ follows the rules of differentiation when operating on the product of a vector and a scalar.

The first term on the right in (1) is the scalar product of the velocity

and the density ascendent. The second term on the right contains the expression

$$\nabla\cdot\mathbf{v} = \frac{\partial v_x}{\partial x} + \frac{\partial v_y}{\partial y} + \frac{\partial v_z}{\partial z}, \tag{2}$$

which is the divergence of the velocity field. The physical meaning of the velocity divergence is obtained as follows: Consider a moving element of air which at the time $t$ fills the rectangular space $\delta V = \delta x\delta y\delta z$ of fig. 10·01. At the time $t + dt$ this element will form an oblique parallelepiped whose angles differ infinitesimally from right angles. Its edges, to the first order in $dt$, are

$$\left(1 + \frac{\partial v_x}{\partial x}\,dt\right)\delta x, \qquad \left(1 + \frac{\partial v_y}{\partial y}\,dt\right)\delta y, \qquad \left(1 + \frac{\partial v_z}{\partial z}\,dt\right)\delta z.$$

The volume of the element at the time $t + dt$ is given, to the first order in $dt$, by the product of the three edges:

$$\delta V + \frac{d}{dt}(\delta V)dt = \left[1 + \left(\frac{\partial v_x}{\partial x} + \frac{\partial v_y}{\partial y} + \frac{\partial v_z}{\partial z}\right)dt\right]\delta x\delta y\delta z.$$

When we divide by $\delta V = \delta x\delta y\delta z$, we have

$$\frac{1}{\delta V}\frac{d}{dt}(\delta V) = \frac{\partial v_x}{\partial x} + \frac{\partial v_y}{\partial y} + \frac{\partial v_z}{\partial z} = \nabla\cdot\mathbf{v}. \tag{3}$$

This equation shows that the divergence of the velocity measures the rate of expansion per unit volume of the moving air elements. Equation (3) is a purely kinematic relation which is a consequence of the geometry of the motion.

If $\delta M = \rho\delta V$ is the mass of the moving element, we have on account of the conservation of mass that

$$\rho\delta V = \text{const.}$$

Upon logarithmic differentiation, we obtain

$$\frac{1}{\rho}\frac{d\rho}{dt} + \frac{1}{\delta V}\frac{d}{dt}(\delta V) = 0.$$

Substituting here for the divergence from (3), we have

$$\frac{d\rho}{dt} = -\rho\nabla\cdot\mathbf{v}. \tag{4}$$

This is the second form of the equation of continuity.

**10·03. Horizontal divergence.** Since the motion of the atmosphere is mainly horizontal, it is sometimes convenient to write the divergence

as the sum of the horizontal divergence,

$$(1) \qquad \nabla_H \cdot \mathbf{v} = \frac{\partial v_x}{\partial x} + \frac{\partial v_y}{\partial y},$$

and the vertical divergence, $\partial v_z/\partial z$. Thus according to **10·02(2)**

$$(2) \qquad \nabla \cdot \mathbf{v} = \nabla_H \cdot \mathbf{v} + \frac{\partial v_z}{\partial z}.$$

The physical significance of the horizontal divergence is similar to that of the three-dimensional divergence. Consider, at the time $t$, the small horizontal area $\delta A = \delta x \delta y$ which forms the base of the parallelepiped of fig. 10·01. Even though the motion may have a vertical component we shall assume that this area element moves in the horizontal plane with the horizontal velocity components. When the argument of the last section is repeated for this area we find

$$(3) \qquad \frac{1}{\delta A}\frac{d}{dt}(\delta A) = \nabla_H \cdot \mathbf{v}.$$

The horizontal divergence is then the rate of areal expansion per horizontal unit area of a fictitious element moving with the horizontal components of the motion. If the motion is strictly horizontal, the horizontal divergence is represented by the rate of areal expansion of the real fluid element per unit area.

**10·04. Individual and local change.** The change at a fixed point of a physical variable is called the *local* change of that variable. The local changes of pressure and temperature, for example, are those which are recorded by a barograph and a thermograph at a fixed station. The local rate of change is denoted by partial differentiation with respect to time, $\partial/\partial t$. The change which occurs on a given particle during its motion is called the *individual* change. The individual rate of change is denoted by the differentiation symbol $d/dt$, or by the dot symbol.

It is important to note the difference between the individual and the local rate of change. To find the relation between them, consider any one of the physical variables, for instance the density. In accordance with 4·04(3) the density field is analytically expressed as a function of the rectangular coordinates $x$, $y$, $z$, and the time $t$: $\rho = \rho(x,y,z,t)$. The variation of the density from the point $(x,y,z)$ at the time $t$ to an arbitrary neighboring point $(x + dx,\ y + dy,\ z + dz)$ at the time $t + dt$ is given by

$$(1) \qquad d\rho = \frac{\partial \rho}{\partial x}dx + \frac{\partial \rho}{\partial y}dy + \frac{\partial \rho}{\partial z}dz + \frac{\partial \rho}{\partial t}dt = d\mathbf{r} \cdot \nabla \rho + \frac{\partial \rho}{\partial t}dt.$$

This expression has general validity for arbitrary variations $d\mathbf{r}$ and $dt$. We shall, however, specialize it so that $d\mathbf{r}$ is the displacement during the time $dt$ of the particle which has the position $(x,y,z)$ at the time $t$. $d\mathbf{r}/dt = \mathbf{v}$ is then the velocity of the particle, and the corresponding $d\rho$ is the individual change; thus

$$\frac{d\rho}{dt} = \frac{\partial \rho}{\partial t} + \mathbf{v}\cdot\nabla\rho. \tag{2}$$

The individual rate of change is here expressed as the sum of the local rate of change and a second term, $\mathbf{v}\cdot\nabla\rho$, which is called the *advective* rate of change. The latter represents the change of density of the moving particle due to its motion into regions of different density. The formula (2) is readily verified for the following two special cases: (i) Equilibrium: The velocity is zero and therefore the advective change is zero. Every particle remains at rest and its individual change is identical to the local change in the field. (ii) Steady state: The field of density remains fixed in space and thus no local changes occur. The individual change on a particle can then only arise from a motion into a region of different density, i.e., from an advective change, in accordance with the formula. The relation between individual and local change has here been derived for the density. Obviously the derivation holds for any other physical variables in the atmosphere, vectors as well as scalars.

The equation of continuity offers a good illustration of the local and the individual change of density. In its first form, 10·01(5), it expresses the local change of density as the mass convergence into unit volume. In its second form, 10·02(4), it expresses the individual change of density in terms of the velocity convergence. That the two forms are equivalent follows from the fact that the one is transformed into the other when the relation (2) between the individual and local change is used. Substituting, for example, from (2) into the second form, 10·02(4), we have

$$\frac{\partial \rho}{\partial t} + \mathbf{v}\cdot\nabla\rho = -\rho\nabla\cdot\mathbf{v}$$

or, after rearrangement,

$$\frac{\partial \rho}{\partial t} = -(\mathbf{v}\cdot\nabla\rho + \rho\nabla\cdot\mathbf{v}) = -\nabla\cdot(\rho\mathbf{v}).$$

This is the first form of the equation of continuity, 10·01(5).

**10·05. Relative change in a moving pressure field.** The pressure field in a constant-level map moves over the map in a more or less regular way, and the internal change in shape and structure of the pattern is

usually slow and gradual. Certain features of the pressure field — for example, troughs, wedges, centers of high and low pressure — can be identified from one map to another. The first step in the preparation of a weather forecast is to determine the displacement of the pressure field during the time of the forecast period. The second step is to evaluate or estimate the changes which will occur in the meteorological variables relative to the moving pressure field during the same time.

These *relative* changes are related to the local changes by a formula similar to 10·04(2). To find this formula consider an identifiable point in the moving pressure pattern, for example, the point of intersection of a wedge line with one of the latitude circles. Let this identifiable point move through the displacement $d_i\mathbf{r}$ during the time interval $dt$. From 10·04(1) the relative change of density at this point during its displacement is

$$d_i\rho = d_i\mathbf{r}\cdot\nabla\rho + \frac{\partial\rho}{\partial t}\,dt. \tag{1}$$

The velocity of propagation of the pressure system is $d_i\mathbf{r}/dt = \mathbf{c}$, and therefore

$$\frac{d_i\rho}{dt} = \frac{\partial\rho}{\partial t} + \mathbf{c}\cdot\nabla\rho. \tag{2}$$

The relative change in the moving pressure field is thus the sum of the local change and the advective change due to the movement of the pressure field.

The formula (2) holds for the change of any physical variable. Of particular interest is the relative change of the pressure itself:

$$\frac{d_i p}{dt} = \frac{\partial p}{\partial t} + \mathbf{c}\cdot\nabla p. \tag{3}$$

The relative change of pressure, $d_i p/dt$, which indicates the deepening or filling of the pressure pattern, is thus expressed as the sum of the local pressure change and the convective change caused by the movement of the pressure pattern. The relation between the relative and the local change was first studied by Petterssen (1933). From the formula (3) Petterssen derived a number of kinematic formulas for the movement of troughs, wedges, and pressure centers. A comprehensive discussion of these formulas and of their application to weather forecasting is found in Petterssen's book " Weather Analysis and Forecasting."

**10·06. The pressure tendency.** In synoptic meteorology the local pressure change in the atmosphere is called the pressure tendency. The systematic study of the mechanism of local pressure changes was started

by J. Bjerknes in 1937. One important application of Bjerknes' theory is that it explains the pressure changes occurring during the development of the cyclone. This cyclone theory will be found in sections 10·17–10·20 below. First the tools of analysis must be developed, and some preliminary studies of simplified atmospheric models must be carried out. The treatment is essentially the same as that presented in a paper by J. Bjerknes and J. Holmboe.*

**10·07. The tendency equation.** The new tool of analysis introduced by Bjerknes in 1937 was the so-called tendency equation. This equation is obtained by a combination of the hydrostatic equation and the equation of continuity.

The hydrostatic equation is assumed to be valid in all aerological computations leading to the construction of the upper-level pressure maps. For their theoretical interpretation we can therefore safely take our start from the hydrostatic equation

4·16(3) $$-\delta p = \rho \delta \phi.$$

The pressure at any level $\phi$ is then obtained by integration of this equation from the level $\phi$ to the upper limit of the atmosphere $\phi = \infty$, where the pressure is zero; thus

(1) $$p = \int_{\phi}^{\infty} \rho \delta \phi.$$

The pressure is here represented as the weight of the vertical column of air of unit cross section extending from the level $\phi$ to the top of the atmosphere.

The local rate of change of the pressure at the level $\phi$ is evidently given by the change in weight of the vertical column. It is obtained by partial differentiation of (1) with respect to time:

(2) $$\left(\frac{\partial p}{\partial t}\right)_{\phi} = \int_{\phi}^{\infty} \frac{\partial \rho}{\partial t} \delta \phi.$$

The local rate of decrease of density is, from the equation of continuity 10·01(5), equivalent to the mass divergence:

$$-\frac{\partial \rho}{\partial t} = \nabla \cdot (\rho \mathbf{v}) = \nabla_H \cdot (\rho \mathbf{v}) + \frac{\partial}{\partial z} (\rho v_z).$$

The last expression on the right gives the mass divergence as the sum of horizontal and vertical mass divergence. When this is substituted in

* J. Bjerknes and J. Holmboe, "On the Theory of Cyclones," *Journal of Meteorology*, vol. I, No. 1 and 2, 1944.

equation (2), we have

$$\left(\frac{\partial p}{\partial t}\right)_\phi = -\int_\phi^\infty \nabla_H \cdot (\rho \mathbf{v}) \delta\phi + (g\rho v_z)_\phi. \tag{3}$$

The local pressure change at the level $\phi$ is here represented explicitly as the change in the weight of the vertical air column. This change is caused in part by horizontal divergence of mass above the level $\phi$ and in part by the vertical transport of mass through the base of the column.

Equation (3), known as the tendency equation, was derived by Margules (1904), but most of its practical applications date from 1937. The first term on the right will be referred to as the *divergence term*. In a qualitative sense we may visualize positive horizontal mass divergence as a horizontal spreading of air, and negative divergence, i.e., convergence, as a horizontal crowding of air. This makes the physical interpretation of the divergence integral in the tendency equation quite clear: Horizontal convergence increases the mass of air within the vertical column and shows up as a pressure rise at the base of the column. Horizontal divergence decreases the mass of air present within the column and makes the pressure fall at the base of the column. These effects are shown schematically in the left part of fig. 10·07.

Equally obvious is the meaning of the second term on the right in the tendency equation, which will be called the *vertical motion term*. An influx of air from below into the column increases the weight of air inside it and thereby also the pressure at its base. Correspondingly, an outflow of air downwards through the base of the column represents a loss of weight of the column and a decrease of pressure at the base. These effects are illustrated by the right part of fig. 10·07.

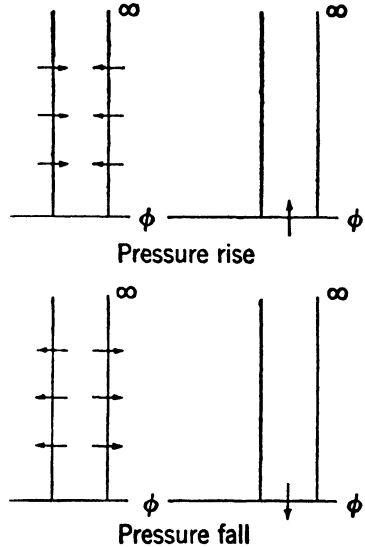


FIG. 10·07.

On a level part of the surface of the earth the vertical motion is zero and the tendency equation reduces to

$$\left(\frac{\partial p}{\partial t}\right)_0 = -\int_0^\infty \nabla_H \cdot (\rho \mathbf{v}) \delta\phi. \tag{4}$$

All large-scale pressure changes observed on the surface map (except special mountain effects) should be explicable in terms of this equation. The problem of finding the distribution of horizontal mass divergence will be discussed at some length in this chapter.

A modified form of the tendency equation can be used to compare the tendency at the ground (assumed to be horizontal) with the tendency at an arbitrary upper level $\phi$ of the same vertical column. When the tendency at the level $\phi$, equation (3), is subtracted from the tendency at the ground, equation (4), we find

$$(5) \qquad \left(\frac{\partial p}{\partial t}\right)_0 - \left(\frac{\partial p}{\partial t}\right)_\phi = -\int_0^\phi \nabla_H \cdot (\rho \mathbf{v}) \delta\phi - (g\rho v_z)_\phi .$$

The tendency at the level $\phi$ may be computed from this equation when the tendency at the ground, the vertical motion at the level $\phi$, and the horizontal mass divergence below the level $\phi$ are known. The practical solution of this problem is discussed further in the next section.

**10·08. The advective pressure tendency.** The divergence term in the modified tendency equation 10·07(5) may be separated into two parts. When the horizontal mass divergence is developed according to the formula 10·02(1), we have

$$\nabla_H \cdot (\rho \mathbf{v}) = \mathbf{v} \cdot \nabla_H \rho + \rho \nabla_H \cdot \mathbf{v},$$

and when the resulting expression on the right is substituted in 10·07(5), we find

$$(1) \qquad \left(\frac{\partial p}{\partial t}\right)_0 - \left(\frac{\partial p}{\partial t}\right)_\phi = -\int_0^\phi \mathbf{v} \cdot \nabla_H \rho \delta\phi - \int_0^\phi \rho \nabla_H \cdot \mathbf{v} \delta\phi - (g\rho v_z)_\phi .$$

It is plausible that horizontal divergence below a fairly low level is accompanied by descending motion at that level, and that horizontal convergence below the level is accompanied by ascending motion at that level. The second and the third term on the right in (1) then have opposite signs. The sum of these two terms is, by 10·02(4),

$$(2) \qquad \epsilon = -\int_0^\phi \rho \nabla_H \cdot \mathbf{v} \delta\phi - (g\rho v_z)_\phi = \int_0^\phi \left(\frac{d\rho}{dt} - v_z \frac{\partial \rho}{\partial z}\right) \delta\phi .$$

When the plausible assumption is made that the density of the air particles changes only as a result of their vertical displacements, the last integral to the right in (2) can be evaluated. It is then found that $\epsilon$ is proportional to the vertical stability of the air, and vanishes for an adia-

batic lapse rate. For the stability which normally occurs in the troposphere the joint contribution, $\epsilon$, from the second and third terms in (1) to the tendency difference can for rough approximations be neglected.

In the following discussion it will be assumed that the conditions are such that the quantity $\epsilon$ can be neglected in equation (1). That equation then reduces to

$$\left(\frac{\partial p}{\partial t}\right)_0 - \left(\frac{\partial p}{\partial t}\right)_\phi = -\int_0^\phi \mathbf{v}\cdot\nabla_H \rho \delta\phi. \tag{3}$$

The difference between the pressure tendencies at the ground and at the level $\phi$ represents the rate of change in the weight of the intermediate air column. According to (3) this change of weight is caused by the horizontal advection of air from regions of different density in the layers below the level $\phi$. Thus if the motion has a component from the region of denser air, $\mathbf{v}\cdot\nabla_H \rho < 0$ and the column becomes heavier. The pressure tendency evaluated from (3) will be called the advective pressure tendency.

Rossby has shown that the integral in (3) can be reduced to a simple form which can be evaluated from a pilot balloon observation, if it is assumed that the wind is geostrophic. The advective pressure change which is obtained on the basis of this assumption may be considered as a first approximation which is good in a broad and fairly straight current, but is less reliable in regions with strongly curved and rapidly changing streamline patterns. When the wind is assumed geostrophic, the approximate thermal wind equation 8·05(1) is valid; thus

$$2\boldsymbol{\Omega}_z \times \frac{\partial \mathbf{v}}{\partial \phi} = -\frac{\nabla_H \alpha}{\alpha} = \frac{\nabla_H \rho}{\rho}. \tag{4}$$

The isobaric horizontal gradients have here been replaced by the horizontal gradients, the two being always very nearly equal, due to the small inclination of the isobaric surface. When the value of $\nabla_H \rho$ from (4) is substituted in the integral of (3), we find

$$\left(\frac{\partial p}{\partial t}\right)_0 - \left(\frac{\partial p}{\partial t}\right)_\phi = -\int_0^\phi \rho \mathbf{v}\cdot 2\boldsymbol{\Omega}_z \times \delta\mathbf{v} = 2\boldsymbol{\Omega}_z \cdot \int_0^\phi \rho \mathbf{v} \times \delta\mathbf{v}. \tag{5}$$

The integral element in the first integral is a scalar triple product (see section 6·14). It changes sign when the cyclic order of the three vectors is changed. Since $2\boldsymbol{\Omega}_z$ is a constant vector along the vertical of integration, it may be taken outside the integral sign, giving the final expression on the right-hand side.

If $\bar{\rho}$ represents the mean density in the layer below the level $\phi$, equa-

tion (5) becomes

$$\left(\frac{\partial p}{\partial t}\right)_0 - \left(\frac{\partial p}{\partial t}\right)_\phi = 2\bar{\rho}\Omega_z \int_0^\phi \mathbf{v} \times \delta\mathbf{v}. \tag{6}$$

The integral has a simple geometrical interpretation and can be evaluated graphically from the hodograph of the wind shear (fig. 8·06*a*). The magnitude of $\mathbf{v} \times \delta\mathbf{v}$ is equal to twice the area $\delta A$ swept out by the horizontal wind vector $\mathbf{v}$ from the level $\phi$ to the level $\phi + \delta\phi$, as in fig. 10·08*a*. The integral from the ground to the level $\phi$ is thus twice the total *vector area* $\mathbf{A}$ swept out by the velocity between the two levels: see 11·13. Thus

$$\mathbf{A} = \tfrac{1}{2} \int_0^\phi \mathbf{v} \times \delta\mathbf{v}. \tag{7}$$

The vector $\mathbf{A}$ is directed along the vertical, upward if the wind turns to the left with increasing height, and downward if the wind turns to the right. Introducing (7) into (6) we find

$$\left(\frac{\partial p}{\partial t}\right)_0 - \left(\frac{\partial p}{\partial t}\right)_\phi = 4\bar{\rho}\Omega_z \cdot \mathbf{A} = 4\bar{\rho}\Omega_z A \ (\text{cb s}^{-1}). \tag{8}$$

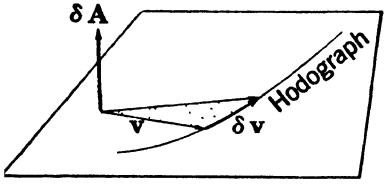



FIG. 10·08*a*. Vector area increment.

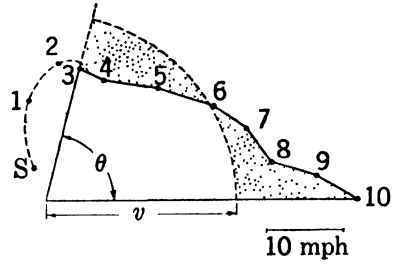



FIG. 10·08*b*. Equivalent sectorial area under hodograph.

In the last expression $A$ has always the same sign as the sense of turning of the wind with height. $A$ is an area in the hodograph plane and has the dimensions $[L^2T^{-2}]$ of velocity square. If mts units are used, the equation gives the tendency difference in centibars per second. In practical applications it is more convenient to express the tendency in millibars per three hours, and also to measure the velocity in miles per hour: 1 cb $s^{-1}$ = $1.08 \times 10^5$ mb $(3\ hr)^{-1}$, and 1 (mile $hr^{-1})^2$ = 0.200 $m^2\ s^{-2}$. Thus from (8)

$$\left(\frac{\partial p}{\partial t}\right)_0 - \left(\frac{\partial p}{\partial t}\right)_\phi = 8.64 \times 10^4 \bar{\rho}\Omega_z A \text{ mb } (3\text{ hr})^{-1}, \tag{9}$$

where $A$ is expressed in (miles $hr^{-1}$)$^2$. The formula is used primarily to compute the advective pressure tendency on an upper-level map, for instance the 10,000-ft map, from a pilot balloon observation and the known tendency at the ground. If we assume the value 922 $m^3$ $t^{-1}$ for the mean specific volume of the column from the ground to 10,000 ft, i.e., the value of $\alpha$ at $p = 850$ mb, $T = 273°K$, the formula takes the form

$$(10) \qquad \left(\frac{\partial p}{\partial t}\right)_0 - \left(\frac{\partial p}{\partial t}\right)_{10} = 6.83 \times 10^{-3} A \sin \varphi \text{ mb } (3 \text{ hr})^{-1}.$$

The practical procedure in computing the 10,000-ft advective pressure tendency from this formula is shown schematically in fig. 10·08*b*. The hodograph of the wind distribution along the vertical from the ground to the 10,000-ft level as obtained from a pilot balloon observation is plotted on a polar diagram. The points for the surface and each 1000 ft of elevation are marked $S$, 1, 2, $\cdots$, 10. The variation of the wind in the surface layer (schematically shown as an Ekman spiral) is primarily caused by friction. The density advection in this layer is not in accord with the simple formula (10), which was derived on the assumption that the wind is geostrophic. Although the advection in the frictional layer may be of some consequence, its contribution is omitted from the computation, since no simple technique is at hand for its evaluation. A rough average value for the geostrophic wind level over land is 3000 ft. The contribution to the advective pressure change between the geostrophic level and the 10,000-ft level is measured by the area under the hodograph between these levels. Instead of evaluating this area directly, we may evaluate the area of an equivalent circular sector. The circular arc has been drawn such that the two triangular areas are equal. The area of the circular sector is $\frac{1}{2}\theta\bar{v}^2$, where $\theta$ is the sectorial angle, measured in radians, and $\bar{v}$ is the mean speed of the layer measured in miles per hour. Introducing this value in the formula (10), we find

$$(11) \qquad \left(\frac{\partial p}{\partial t}\right)_0 - \left(\frac{\partial p}{\partial t}\right)_{10} = 3.42 \times 10^{-3} \theta \bar{v}^2 \sin \varphi \text{ mb } (3 \text{ hr})^{-1}.$$

The area $\frac{1}{2}\theta\bar{v}^2$ can be read off the diagram directly if lines of constant value of $\theta\bar{v}^2$ are drawn in the polar diagram. One such line is shown in fig. 10·08*c*. For a given latitude the tendency difference is directly proportional to the area. The lines of constant $\theta\bar{v}^2$ may therefore be drawn and labeled directly for unit values of the tendency difference, as shown in fig. 10·08*d*. The diagram has been computed for the latitude 40°. In practical use the diagram is drawn on transparent paper, or preferably a thin sheet of celluloid. When the pilot balloon hodograph has been plotted on a regular polar diagram the transparent area computer,

fig. 10·08*d*, is placed on top of it. If, in the northern hemisphere, the wind turns to the right with increasing height (warm air advection), the base line of the computer is placed along the 10,000-ft velocity vector.

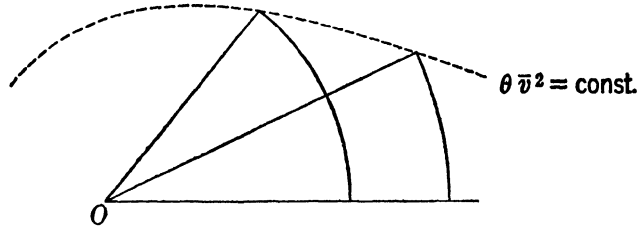



FIG. 10·08*c*. Line of constant sectorial area.

The area and hence the tendency difference is negative in this case. If the wind turns to the left (cold air advection), the base line of the area computer is placed along the 3000-ft velocity vector. The area and hence the tendency difference is positive in this case.

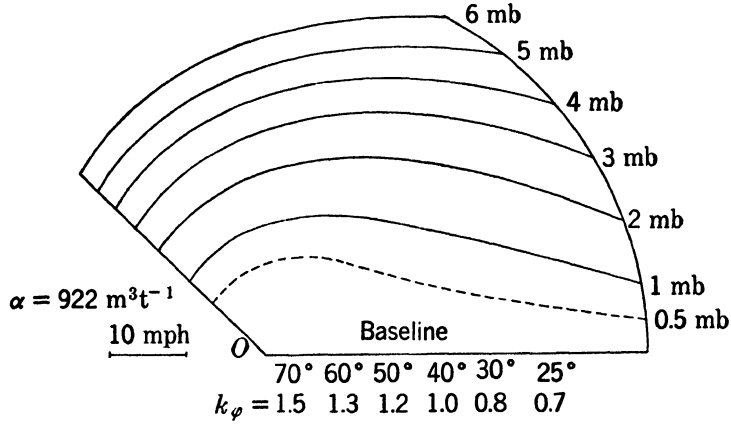



FIG. 10·08*d*. Area computer for advective pressure change.

If the computer is used for a station in another latitude $\varphi$, the values indicated by the computer must be multiplied by the factor $k_\varphi = \sin\varphi/\sin 40°$. The values of this correction factor for a number of latitudes are listed below the base line of the computer.

It should be noted that the 10,000-ft tendency as obtained by this method is only a first crude approximation. The method is based on the assumptions that the quantity $\epsilon$ in (2) is zero; that the wind is geostrophic; that advection in the frictional layer can be neglected; and that $1/\bar{\rho}$ is near $922\,\text{m}^3\,\text{t}^{-1}$.

**10·09. Relation between the horizontal divergence and the field of pressure.** The equation of motion implicitly contains the relation between the field of motion and the pressure field. By making suitable assumptions it is possible to estimate the distribution of the horizontal divergence directly from the horizontal pressure field.

In the layer of frictional influence near the surface of the earth the winds have a systematic component across the isobars from high to low pressure (chapter 9). Every " low " is then a region of horizontal mass convergence and every " high " a region of horizontal mass divergence, within the layer of friction. However, the layer of friction represents only about one-twentieth of the weight of the atmosphere, and any horizontal divergence in this layer may easily be overcompensated by horizontal divergence in the remaining nineteen-twentieths of the atmosphere.

In the free atmosphere, above the layer of frictional influence, the wind is in the first approximation geostrophic, blowing parallel to the isobars of the pressure map. Furthermore, at any given latitude the geostrophic wind is inversely proportional to the distance between the isobars. We can therefore think of the isobars of a constant-level pressure map as representing the horizontal motion of the air in the same level. The air flows along " isobaric channels " covering the strips between successive isobars. Where the channel is wide, the air flows slowly, whereas in the narrow parts of the channel the air flows rapidly. The product of the density $\rho$, the wind speed $v$, the channel width $\delta n$, and the *constant* channel depth $\delta z$ defines what may be called the *transport capacity* $\delta F$ of the isobaric channel:

$$\delta F = \rho v \delta n \delta z. \tag{1}$$

The transport capacity is practically constant for a reasonably straight channel which runs about west-east along a circle of latitude.

If the transport capacity of isobaric channels were constant all over the map there would be no convergence or divergence to produce pressure changes. Every isobaric channel would be like a well-regulated river with constant transport all along, so that no local accumulations or depletions would occur. However, this is fulfilled only approximately in the atmosphere, because the geostrophic wind is only a first approximation to reality. Actually the isobaric air channels change their transport capacity somewhat from point to point. The places of minimum transport capacity will then be " bottlenecks " in the flow of air. The air approaching a bottleneck will crowd horizontally and cause a *longitudinal* mass convergence in the current, whereas beyond the bottleneck there will be longitudinal mass divergence. To complete the list of

shortcomings of the geostrophic wind, the air does not follow strictly along the isobaric channels but overflows slightly from the one to the other. It overflows toward lower pressure when the air speeds up, and toward higher pressure when the air slows down. This also may cause horizontal mass divergence which will be referred to as *transversal* mass divergence. For brevity, we shall hereafter in chapter 10 write " divergence " instead of " mass divergence."

In the following, the longitudinal and transversal divergence will be evaluated quantitatively, or estimated qualitatively, for selected simple patterns of flow under the two general headings: (i) *wave-shaped flow patterns*, and (ii) *closed flow patterns*. These flow patterns, of course, correspond to wave-shaped isobar patterns and closed isobar patterns respectively. The former are mainly observed in the upper levels; the latter, in the lower levels of the traveling cyclones. The results from the study of these fundamental patterns will thus ultimately throw some light on the mechanism of the composite cyclonic disturbances.

**10·10. Longitudinal divergence in wave-shaped isobar patterns.** The type of wave-shaped isobar pattern to be studied is shown schematically in fig. 10·10*a*. The amplitude of the wave disturbance has a maximum in the middle of the pattern and tapers off to the north and to the south of this latitude. This resembles the usual pressure distribu-

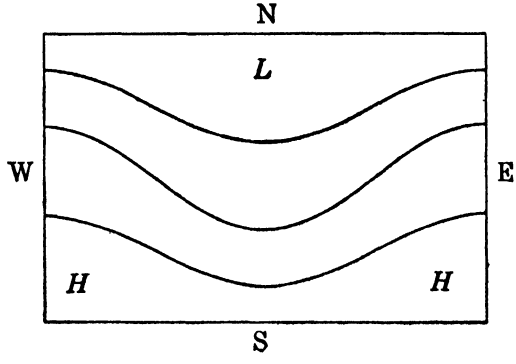



FIG. 10·10*a*. Wave-shaped isobar pattern.

tion on an upper-level map above a moving cyclone in the latitudes of the westerlies. In order to facilitate the discussion it has been assumed that the isobars are *symmetric with respect to the trough lines and the wedge lines, and that these lines are straight lines with north-south orientation.*

It follows from the symmetry of the pattern with respect to the trough lines and the wedge lines that these lines are the places of maximum or

minimum transport capacity of each isobaric channel. To estimate the distribution of longitudinal divergence, it is thus sufficient to evaluate the transport capacity of the isobaric channels at their southern bends (where they intersect the trough lines) and at their northern bends (where they intersect the wedge lines). From the place of minimum to the place of maximum transport capacity (along the direction of the current) there will be longitudinal divergence, and from the place of maximum to the place of minimum transport capacity there will be longitudinal convergence.

The trough lines and the wedge lines are not only the places of maximum or minimum transport capacity of the isobaric channels but are also the places of maximum or minimum speed. At such points the flow is gradient flow along the isobars, so that in the normal component equation of motion,

7·13(5) $$K_H v^2 + 2\Omega v \sin\varphi = -\frac{1}{\rho}\frac{\delta p}{\delta n},$$

$\delta n$ is measured normal to the isobar. Therefore $\delta n$ is the width of the isobaric channel bordered by the isobars $p$ and $p+\delta p$. In the following the horizontal curvature $K_H$ will be denoted by $K$. No ambiguity will arise, for only horizontal curvatures will be used.

Multiplying equation 7·13(5) by $\rho\delta n\delta z$ and introducing the notation $\delta F$ for the transport capacity from 10·09(1), we have

(1) $$\delta F(Kv + 2\Omega \sin\varphi) = -\delta p\delta z = \text{const.}$$

The channel depth $\delta z$ and the pressure difference across the channel $\delta p$ are both constant all along the isobaric channel. The transport capacity at the places with gradient flow is accordingly proportional to the reciprocal of the quantity $(Kv + 2\Omega \sin\varphi)$. The distribution of longitudinal divergence is therefore obtained by comparison of the values of this quantity at the places where the isobaric channel intersects the trough line and the wedge line.

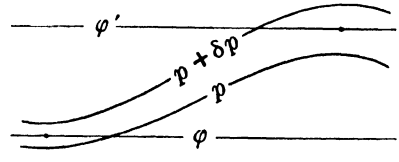



FIG. 10·10*b*. Isobaric channel from the pattern in fig. 10·10*a*.

Fig. 10·10*b* shows an arbitrary isobaric channel in the pattern of fig. 10·10*a*, bordered by the isobars with the pressures $p$ and $p+\delta p$. The channel has its cyclonic bend at the latitude $\varphi$ where it intersects the trough line, and its anticyclonic bend at the latitude $\varphi'$ where it intersects the wedge line. Obviously the relation $\varphi' > \varphi$ holds in all cases. In the following all the quantities at the cyclonic bend will be

denoted by unprimed symbols, and the corresponding quantities at the anticyclonic bend by primed symbols. Note that $\delta p < 0$.

The transport capacities $\delta F'$ and $\delta F$ at the two bends must satisfy one of the following three conditions

$$\delta F' \gtreqless \delta F. \tag{2}$$

The upper condition states that the bottleneck in the current is at the cyclonic bend of the isobaric channel. West of this bend air accumulates and causes longitudinal convergence; east of the bend there will be longitudinal divergence. The middle condition states that the transport capacities are the same at the two bends, so the longitudinal divergence is zero. The lower condition states that the bottleneck in the current is at the anticyclonic bend of the isobaric channel, so the flow has longitudinal convergence to the west of this bend and longitudinal divergence to the east of it.

According to equation (1) the conditions (2) can be written

$$Kv + 2\Omega \sin \varphi \gtreqless K'v' + 2\Omega \sin \varphi' \tag{2'}$$

or, after rearrangement of the terms,

$$Kv - K'v' \gtreqless 2\Omega (\sin \varphi' - \sin \varphi) = 4\Omega \cos \frac{\varphi' + \varphi}{2} \sin \frac{\varphi' - \varphi}{2}. \tag{3}$$

The angle $(\varphi' + \varphi)/2$ is the *central latitude* $\bar{\varphi}$, around which the isobaric channel winds, and the angle $(\varphi' - \varphi)/2$ is half of the difference in latitude between the northern and the southern bends of the channel. The latter may be called the *angular amplitude* of the isobar and is denoted by $\sigma_p$; thus

$$\bar{\varphi} = \frac{\varphi' + \varphi}{2}, \qquad \sigma_p = \frac{\varphi' - \varphi}{2}. \tag{4}$$

With these notations introduced, (3) takes the form

$$Kv - K'v' \gtreqless 4\Omega \cos \bar{\varphi} \sin \sigma_p. \tag{5}$$

This formula contains the horizontal curvatures of the air trajectories at the southern and the northern bends of the isobaric channel. These curvatures depend upon the shape of the streamlines and the speed of propagation of the wave disturbance.

The horizontal curvature $K$ of the path is related to the horizontal curvature $K_S$ of the streamline by the equation

$$Kv = K_S v + \frac{\partial \psi}{\partial t}, \tag{7·23(3)}$$

where $\partial\psi/\partial t$ is the local rate of turning of the wind. At any identifiable point in the moving pressure pattern the relative rate of turning of the wind is given by

10·05(2) $$\frac{d_i\psi}{dt} = \frac{\partial\psi}{\partial t} + \mathbf{c}\cdot\nabla\psi.$$

Let the identifiable point be the intersection between the trough line (or the wedge line) and one of the circles of latitude. The velocity $\mathbf{c}$ is then a zonal vector, tangential to the path at the troughline, and so $\mathbf{c}\cdot\nabla\psi = c(\partial\psi/\partial s)$. Furthermore the wind is always zonal at the trough line, so the relative turning of the wind, $d_i\psi/dt$, is zero. Accordingly, the local rate of turning of the wind at any point on the trough line or the wedge line is

$$\frac{\partial\psi}{\partial t} = -c\frac{\partial\psi}{\partial s} = -cK_S.$$

$\partial\psi/\partial s$ is by definition (see section 7·23) the horizontal curvature of the streamline. Substituting this expression for the local turning into the general formula 7·23(3), we have at the two bends

(6) $$\begin{aligned} Kv &= K_S(v - c), \\ K'v' &= K'_S(v' - c). \end{aligned}$$

Let $\bar{v}$ be the mean zonal wind in the isobaric channel, and let $\Delta v$ be the half difference of the speeds at the northern and southern bends. Thus:

(7) $$\bar{v} = \frac{v' + v}{2}, \qquad \Delta v = \frac{v' - v}{2}.$$

Introducing these in (6), we find

$$\begin{aligned} Kv &= K_S(\bar{v} - c) - K_S\Delta v, \\ K'v' &= K'_S(\bar{v} - c) + K'_S\Delta v. \end{aligned}$$

The difference between these expressions is

(8) $$Kv - K'v' = (K_S - K'_S)(\bar{v} - c) - (K_S + K'_S)\Delta v.$$

Substituting this in (5) and solving for $\bar{v} - c$, we have finally

(9) $$\bar{v} - c \gtreqless \frac{4\Omega\cos\bar{\varphi}\sin\sigma_p}{K_S - K'_S} + \frac{K_S + K'_S}{K_S - K'_S}\Delta v.$$

The expression on the right has the dimensions of a velocity. It is completely determined by the geographical location and geometry of the

pattern, and by the difference of wind speeds at the northern and southern bends of the isobar. We shall in the following refer to this quantity as the *critical speed* and denote it by $v_c$; thus

$$v_c = \frac{4\Omega \cos \bar{\varphi} \sin \sigma_p}{K_S - K'_S} + \frac{K_S + K'_S}{K_S - K'_S} \Delta v. \tag{10}$$

With this notation introduced, equation (9) takes the form

$$\bar{v} - c \gtreqless v_c. \tag{11}$$

$\bar{v} - c$ is the mean value of the zonal speed relative to the moving wave pattern, and will be called more briefly the *relative zonal wind.*

The three conditions (11) are equivalent to the three conditions (2) taken in the same order: Thus, if the relative zonal wind is *supercritical,* that is, greater than the critical speed, the bottleneck in the current is at the cyclonic bend of the isobaric channel, so the flow has longitudinal convergence to the west of the trough and longitudinal divergence to the east of the trough. If the relative zonal wind is *critical,* that is, equal to the critical speed, the transport capacities are the same at the two bends, so the longitudinal divergence is zero. If the relative zonal wind is *subcritical,* that is, less than the critical speed, the bottleneck in the current is at the anticyclonic bend of the isobaric channel, so the flow has longitudinal convergence to the east of the trough and longitudinal divergence to the west of the trough.

The expression (10) for the critical speed becomes much simpler when the curvature is numerically the same at the cyclonic and the anticyclonic bends, that is, when $K_S = -K'_S$. The second term on the right side of equation (10) is then equal to zero, and the critical speed is

$$v_c = \frac{2\Omega \cos \bar{\varphi} \sin \sigma_p}{K_S}. \tag{12}$$

So far no analytical expression has been specified for the streamlines or the isobars. The only restriction in the choice of isobaric pattern prescribes that the isobars should be symmetrical with respect to the north-south trough lines and wedge lines. The critical speed may be determined directly on the weather map from (10). If the curvatures at the two bends are numerically equal, we may use formula (12). This formula may be simplified still further when the streamlines are assumed to be sine curves.

**10·11. Critical speed in sinusoidal waves.** In order to treat the streamlines as simple sine curves, it is necessary to consider the surface of the earth as flat and the latitude circles as straight parallel lines in the

region between the two bends. A sinusoidal streamline can then be drawn winding between the latitudes $\varphi$ and $\varphi'$, as shown in fig. 10·11. In a standard system of coordinates with the origin at the point where the streamline intersects the central latitude at the time $t = 0$, this streamline has the equation

$$y = A_S \sin k(x - ct). \tag{1}$$

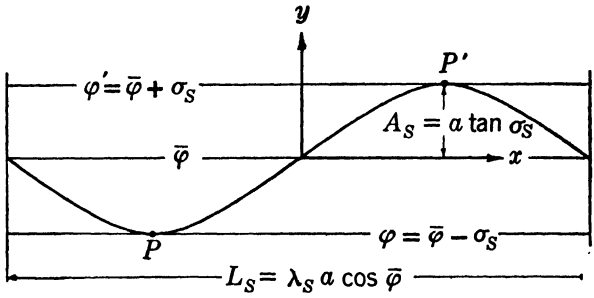



FIG. 10·11. Sinusoidal streamline.

Here $A_S$ is the amplitude and $c$ is the speed of the wave. If $L_S$ is the wave length, $k = 2\pi/L_S$ is called the *wave number* and represents the number of waves in the linear interval of $2\pi$ length units.

If the latitudinal amplitude of the streamline is denoted by $\sigma_S$, the linear amplitude $A_S$ on the horizontal plane is defined by projection as:

$$A_S = a \tan \sigma_S. \tag{2}$$

The linear wave length $L_S$ can be expressed by the angular wave length of longitude $\lambda_S$ as follows:

$$L_S = \lambda_S a \cos \bar{\varphi}.$$

The angular wave length defines an *angular wave number* $n = 2\pi/\lambda_S$, which gives the number of waves along the total circumference of the latitude circle. The relation between the linear wave number $k$ and the angular wave number $n$ is

$$k = \frac{2\pi}{L_S} = \frac{2\pi}{\lambda_S a \cos \bar{\varphi}} = \frac{n}{a \cos \bar{\varphi}}. \tag{3}$$

The curvature of the streamline is by definition the angular turn of its tangent per unit arc length along the streamline; thus

$$K_S = \frac{\delta \psi}{\delta s}. \tag{4}$$

If $\psi$ is the angle between the tangent and the $x$ axis, then

$$\tan \psi = \frac{\delta y}{\delta x}.$$

Differentiating this formula with respect to the arc length $s$, we have

$$\frac{1}{\cos^2 \psi} \frac{\delta \psi}{\delta s} = \frac{\delta}{\delta s}\left(\frac{\delta y}{\delta x}\right). \tag{5}$$

At the southern and northern bends, where the streamline is parallel to the $x$ axis, $\cos^2 \psi = 1$ and $\delta s = \delta x$. Therefore from (4) and (5) we have

$$K_S = \frac{\delta^2 y}{\delta x^2}.$$

When (1) is differentiated twice with respect to $x$, we find for the curvature of a sinusoidal streamline at the two bends

$$K_S = -k^2 A_S \sin k(x - ct) = \pm k^2 A_S. \tag{6}$$

In the last expression on the right the positive sign should be used at the southern bend and the negative sign at the northern bend.

By substituting in (6) the values for $A_S$ from (2) and for $k$ from (3), the curvature at the southern bend becomes

$$K_S = \frac{n^2 \tan \sigma_S}{a \cos^2 \bar{\varphi}}.$$

When this expression for $K_S$ is introduced in 10·10(12), we find for the critical speed in a sinusoidal flow pattern the expression

$$v_c = \frac{2\Omega a \cos^3 \bar{\varphi} \sin \sigma_p}{n^2 \tan \sigma_S}. \tag{7}$$

This formula was derived by Rossby (1939) from the principle of conservation of vorticity (see 12·05). It will follow from (7) and 12·05(12) that the amplitude factor $\sin \sigma_S / \tan \sigma_p$ is equal to one. This would indicate that the streamline amplitude is slightly larger than the isobar amplitude. However, in section 12·06 it will be proved that the two amplitudes are equal at the level of zero longitudinal divergence. This apparent error in the formula (7) comes from the fact that it has been derived by combining spherical and plane methods. The basic formula 10·10(12) is exact on a spherical level for a wave-shaped isobar with the same streamline curvature at the northern and the southern bends. This formula cannot be specialized to a curve in a " plane level " without causing a slight degree of inconsistency.

The critical speed in a sinusoidal flow pattern is thus a function of the latitude and the angular wave number. The critical speed is large for

long waves in low latitude, and small for short waves in high latitude. Some values of the critical speed, as computed from (7), are given in table 10·11.

TABLE 10·11

$v_c = (2\Omega a \cos^3\varphi)/n^2$(M S$^{-1}$) TABULATED

| $\varphi$ | $n$ | | | | |
|---|---|---|---|---|---|
| | 2 | 3 | 6 | 10 | 20 |
| 70° | 9.3 | 4.1 | 1.0 | 0.4 | 0.1 |
| 60° | 29.0 | 12.9 | 3.2 | 1.2 | 0.3 |
| 50° | 61.6 | 27.4 | 6.8 | 2.5 | 0.6 |
| 40° | 104 | 46.3 | 11.6 | 4.2 | 1.0 |
| 30° | 151 | 67.0 | 16.8 | 6.0 | 1.5 |
| 0° | 232 | 103 | 25.8 | 9.3 | 2.3 |

For long waves it seems unwarranted to consider the earth as flat and to neglect the curvature of the latitude circles. No detailed discussion of this question will be given here. It may suffice to mention that waves spanning over one-half to one-third of the circumference of the earth must be treated by spherical methods. Practical synoptic cases are more likely to deal with wave numbers around $n = 6$ or more (wave lengths 60° of longitude or less), and in such cases the difference between the flat and the spherical treatment seems to be insignificant.

**10·12. Transversal divergence in wave-shaped isobar patterns.** We now turn our attention to that part of the horizontal divergence which is caused by the overflow of mass from the one isobaric channel to the other, i.e., the transversal divergence. Fig. 10·12 shows the same idealized pressure pattern which was discussed in section 10·10. A qualitative estimate of the transversal divergence in this pressure pattern is obtained by considering the inflow and outflow of mass across the northern straight isobar $p = p_0 - 4$ (cb), and across the southern straight isobar $p = p_0$.

Suppose for a moment that the isobar pattern in fig. 10·12 is stationary. Particles at the northern edge of the pattern will then have their maximum speed while passing the longitudes of the wedges and minimum speed while passing the longitudes of the troughs. In order to change speed in that rhythm the particle must have a component toward high pressure while it slows down, i.e., from the wedge to the trough (see section 7·15). And it must have a component toward low pressure while it speeds up, i.e., from the trough to the wedge. The flow at the northern edge must therefore be as qualitatively indicated by the stream-

line (dotted line) in the diagram. The analogous analysis along the southern straight isobar leads to a streamline with opposite phase. There is thus outflow from the region east of the trough, both across the northern and the southern edge of the isobar pattern, and therefore transversal divergence from this region. And there is transversal convergence into the region west of the trough.

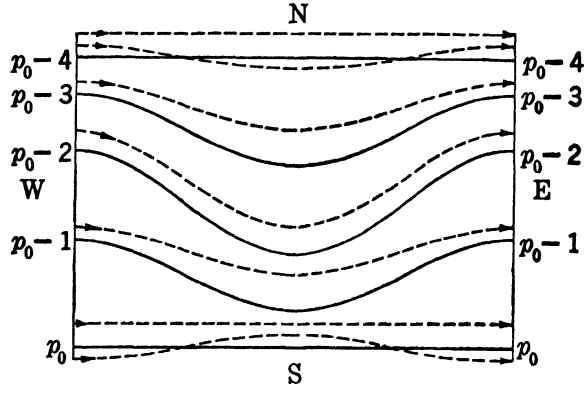



FIG. 10·12. Flow pattern for the isobar pattern in fig. 10·10*a*.

If the pressure system is moving, the same rule holds, provided that the system does not move eastward faster than the mean speed of the air, i.e., provided that the relative zonal wind is from the west. If the pressure system moves eastward with the mean zonal speed, the relative zonal wind is zero, and the transversal divergence of the flow pattern is zero. If the pressure system moves eastward faster than the air, the relative zonal wind is from the east; the particles at the northern edge of the frame slow down east of the trough (while being overtaken by the trough), and they speed up to the west of the trough (while being overtaken by the wedge). The streamlines at the northern and southern edges of the frame will then have the opposite phase from those shown in fig. 10·12 and consequently give transversal convergence into the region east of the trough and transversal divergence from the region west of it. These rules may be summarized as follows: *The transversal divergence and the relative zonal wind have the same sign in the region to the east of the trough, and have opposite signs in the region to the west of the trough.*

The above rule only gives the sign of the transversal divergence. The mean divergence over a given area is obtained by dividing the total outflow from that area by the area. The areas of outflow and inflow in the wave pattern, fig. 10·12, are proportional to the meridional distance between the northern and southern straight isobars. The transversal

divergence is therefore proportional to the reciprocal of the width of the pattern and is zero for a pattern of infinite lateral extent. All the isobars then have the same shape, and the longitudinal divergence is the total horizontal divergence.

**10·13. Total horizontal divergence associated with wave-shaped isobar patterns.** The total horizontal divergence is the sum of the longitudinal and the transversal divergence. The following three alternatives may occur:

1. $\bar{v} - c > v_c$: The relative zonal wind is from the west and is greater than the critical speed; the longitudinal and the transversal divergence are both positive to the east of the trough and are both negative to the west of the trough.

2. $\bar{v} - c < 0$: The relative zonal wind is from the east; the longitudinal and the transversal divergence are both negative to the east of the trough and are both positive to the west of it. In both cases 1 and 2 the two parts of the horizontal divergence have the same sign at any point of the flow pattern.

3. $v_c > \bar{v} - c > 0$: The relative zonal wind is from the west and is smaller than the critical speed; the longitudinal divergence is negative to the east of the trough and positive to the west of the trough; the transversal divergence is positive to the east of the trough and negative to the west of it. The two parts of the horizontal divergence then counteract each other throughout the field. For a certain value of the relative zonal wind less than the critical speed but larger than zero the longitudinal divergence is balanced by transversal convergence and the total horizontal divergence is zero.

The distribution with height of the horizontal divergence in an actual synoptic situation can be estimated with the aid of the above rules for longitudinal and transversal divergence. In general, the strength of the zonal circulation and hence also of the relative zonal circulation increases with height. In the region to the east of every trough and to the west of every wedge there is longitudinal divergence above the level where the relative zonal wind has the critical speed, and there is longitudinal convergence below that level. In the same region there is transversal divergence above the level where the relative zonal wind is zero, and transversal convergence below that level. Between the level of zero longitudinal divergence and the level of zero transversal divergence the two effects will have opposite signs. At some intermediate level the longitudinal and the transversal divergence are equal and opposite, and the total horizontal divergence is zero.

The distribution both of the longitudinal and the transversal diver-

gence depends upon the *relative* zonal wind and hence upon the speed of the wave. The speed of the wave prescribes the pressure tendency. The pressure tendency is, from the tendency equation 10·07(3), a direct consequence of the distribution of horizontal divergence. Thus the horizontal divergence, the speed of the wave, and the pressure tendency are interdependent: *The wave will travel with such a speed that the pressure tendencies arising from the displacement of the pressure pattern are in accordance with the field of horizontal divergence.*

The three-dimensional structure of the wave disturbance may be analyzed from this point of view. The conditions are fundamentally different in a barotropic and in a baroclinic current. Only the rather unreal barotropic case is as yet accessible to investigation by rigorous dynamical analysis. In order to gain the greatest possible experience we shall first examine the barotropic wave. Later we shall proceed to the qualitative analysis of the much more complicated conditions in the real atmospheric waves, which are always baroclinic.

**10·14. Barotropic waves in a westerly current.** To simplify matters we shall assume that the wave pattern has infinite lateral extent, so that all isobars have the same shape. The transversal divergence is then always zero, and the total horizontal divergence is equal to the longitudinal divergence.

In a barotropic current the isothermal surfaces coincide with the isobaric surfaces. The dynamic thickness of each isobaric layer is therefore constant throughout. The slope of all isobaric surfaces is then the same along any given vertical, and the geostrophic wind has no vertical shear (see section 8·03). The strength of the zonal circulation and the shape of the streamline pattern of the wave are therefore the same at every level.

The pressure tendency at the ground indicates whether the wave moves or not. If we assume that the surface of the earth is flat this tendency is

10·07(4) $$\left(\frac{\partial p}{\partial t}\right)_0 = -\int_0^\infty \nabla_H \cdot (\rho \mathbf{v}) \delta\phi.$$

The sign of the mass divergence is determined from the three conditions

10·10(11) $$\bar{v} - c \gtreqless v_c.$$

The mean zonal wind $\bar{v}$ has the same value at all levels in a barotropic current; the speed $c$ of the wave is characteristic of the entire wave and therefore independent of height; the critical speed $v_c$ is determined by the wave length and so is also independent of height. Thus the mass diver-

gence has the same sign throughout any vertical column. Fig. 10·14 illustrates the barotropic wave for each of the three conditions 10·10(11).

The diagram to the left represents a wave for which the relative zonal wind is supercritical,

$$\bar{v} - c > v_c. \tag{1}$$

The bottleneck in the current will then be at the cyclonic bend of every isobaric channel. Air is accumulated at all levels to the west of the trough, and is depleted at all levels to the east of the trough. At the

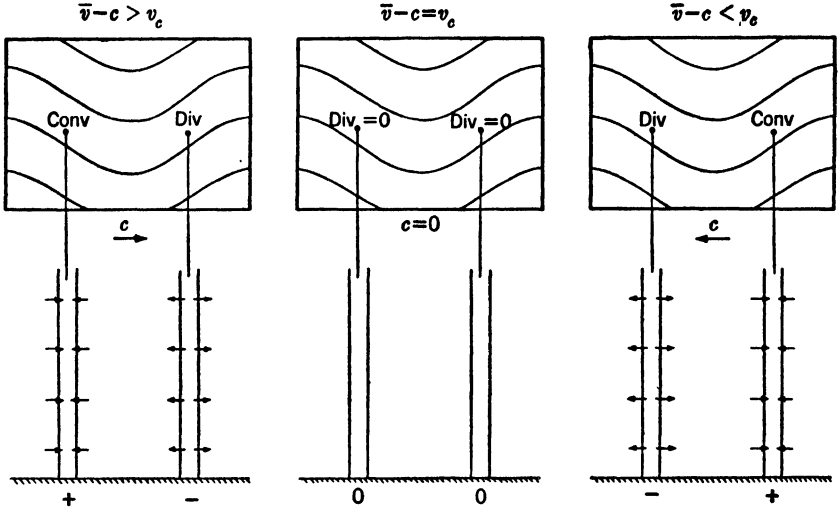



FIG. 10·14. Propagation of barotropic wave.

ground the pressure is therefore rising to the west of the trough and falling to the east of it. So the wave moves to the east ($c > 0$), and hence from (1) $\bar{v} > v_c$.

The center diagram represents a wave for which the relative zonal wind is critical,

$$\bar{v} - c = v_c. \tag{2}$$

The transport capacities are the same at the two bends of each isobaric channel. The entire flow is non-diverging and the pressure tendency at the ground is zero. So the wave is stationary ($c = 0$), and hence from (2) $\bar{v} = v_c$.

The diagram to the right represents a wave for which the relative zonal wind is subcritical,

$$\bar{v} - c < v_c. \tag{3}$$

The bottleneck in the current will then be at the anticyclonic bend of every isobaric channel. Air is accumulated at all levels to the east of the trough and is depleted at all levels to the west of the trough. At the ground the pressure is therefore rising to the east of the trough and falling to the west of it. So the wave moves to the west ($c < 0$), and hence from (3) $\bar{v} < v_c$.

The above results may be summarized as follows:

$$\bar{v} - c \gtreqless v_c, \tag{4}$$

$$c \gtreqless 0, \tag{5}$$

$$\bar{v} \gtreqless v_c. \tag{6}$$

We have shown that the three conditions (4) read from top to bottom imply the conditions (5) taken in the same order. The conditions (4) and (5) combined give the conditions (6). It is readily seen that any one of (4), (5), (6) implies the other two. Thus from (5, 6) the *barotropic wave moves eastward when the mean zonal wind is supercritical; it is stationary when the mean zonal wind is critical; it moves westward when the mean zonal wind is subcritical.*

For waves of finite width the transversal divergence is different from zero. The only reformulation of the above rules is, then, that the stationary, non-diverging wave occurs for a smaller value of the zonal wind than the critical speed.

The tendency at upper levels is given by the complete tendency equation

$$10\cdot07(3) \qquad \left(\frac{\partial p}{\partial t}\right)_\phi = -\int_\phi^\infty \nabla_H\cdot(\rho\mathbf{v})\delta\phi + (g\rho v_z)_\phi.$$

We have shown that the divergence has the same sign throughout any given atmospheric column, so the divergence term has the greatest magnitude at the ground and decreases with height. The vertical motion term is zero at the ground and increases in magnitude with height. In the special case of a homogeneous current ($\rho$ independent of $p$) the pressure tendency would be the same at all levels. Here the decreasing contribution from the divergence term with height is exactly balanced by the increasing contribution from the vertical motion term. In the more general barotropic case where the density decreases with height, both the pressure amplitude and the total tendency decrease upward. In this case the contribution from the divergence term must decrease more rapidly with height than the contribution from the vertical motion term increases.

The zero isallobars at all levels coincide with the trough lines and the

wedge lines. This means that the amplitude of the pressure wave does not change with time; in other words, the barotropic wave is a *stable* wave, which moves without any changes in its internal structure. This result is in complete accord with classical wave theory. The only destabilizing factor, shear, is absent in the barotropic wave, so the wave must be stable.

**10·15. The relative streamlines.** We shall now examine waves in a baroclinic westerly current. In a barotropic current the isotherms coincide with the isobars at all levels, but in a baroclinic current they will generally intersect the isobars. Therefore the structure of the wave will be different from level to level, and will also change with time.

The internal structure of a moving wave is deformed by the relative wind, that is, the wind as seen by an observer who moves along with the wave. The streamlines of this relative wind are the relative streamlines. Let **v** be the wind and **c** the velocity of propagation of the wave. The wind relative to the wave is then **v** − **c**. The relative streamlines are the streamlines of the velocity field **v** − **c**. See fig. 10·15*a*.

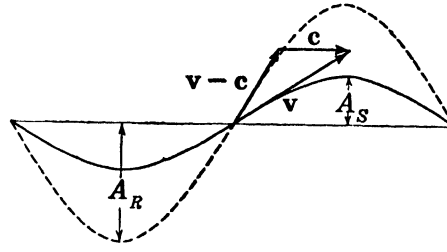



FIG. 10·15*a*. Streamline and relative streamline.

At the trough lines and the wedge lines of the streamline pattern both the real wind and the relative wind are zonal. These meridians are therefore also the trough or wedge lines of the relative streamline pattern. So both patterns have the same wave length, but their amplitudes are in general different. The streamlines are by definition everywhere tangential to the velocity. Let $\delta y_S$ and $\delta y_R$ be the respective meridional increments on the streamline and on the relative streamline, corresponding to the same zonal increment $\delta x$. The differential equations for the streamlines and the relative streamlines are then respectively

$$\frac{\delta y_S}{\delta x} = \frac{v_y}{v_x},$$

$$\frac{\delta y_R}{\delta x} = \frac{v_y}{v_x - c}.$$

Taking the ratio of these equations, we have

$$\frac{\delta y_S}{\delta y_R} = \frac{v_x - c}{v_x}. \tag{1}$$

The ratio on the right side in (1) is constant in the special case where, throughout the level, the zonal wind component $v_x$ has the constant value $v$ of the actual wind at the trough line and at the wedge line. Equation (1) may then be integrated. If the integration is taken from the inflection point (the central latitude) to the wedge line, we find

$$\frac{A_S}{A_R} = \frac{v - c}{v}. \tag{2}$$

When the wind speed $v$ at the trough line is different from the wind speed $v'$ at the wedge line, the ratio between the two amplitudes is not so simple as indicated by (2). However, if the difference $v' - v$ is small compared to the mean speed $\bar{v}$, it can be shown that the amplitude ratio has the approximate value

$$\frac{A_S}{A_R} = \frac{\bar{v} - c}{\bar{v}}. \tag{3}$$

Thus, in a wave where the variation in the zonal wind is not too large, the ratio of the streamline amplitude to the relative streamline amplitude is the same as the ratio of the mean relative zonal wind to the mean zonal wind.

Fig. 10·15*b* shows the streamline (full line) and the relative streamline (broken line) for three different values of the speed. In all three cases the streamline is the same. The relative streamline is obtained from the formula (3), or directly by inspection of the velocity vector diagrams in the figure. In the upper diagram the wave is stationary ($c = 0$), and the relative streamline coincides with the streamline, $A_S = A_R$. In the middle diagram the wave moves toward the right with a slower speed than the air. The relative streamline is here in phase with the streamline, but the amplitudes differ in the sense $A_S < A_R$. In the lower diagram the wave moves to the right with a greater speed than the air. In this case the relative zonal wind is negative, so the amplitudes $A_S$ and $A_R$ have opposite signs. The relative streamline is 180° out of phase with the streamline.

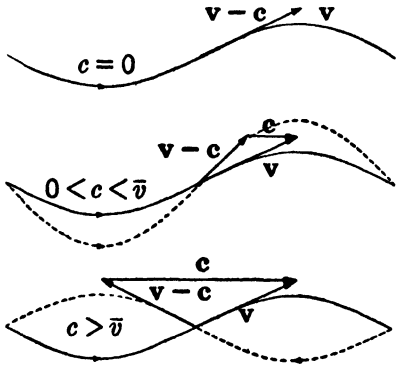



FIG. 10·15*b*.

A wave moving without change of shape appears stationary to an observer moving along with the wave. For such a wave the relative

streamlines are also the relative paths. The relative streamlines thus indicate the true meridional displacements of the air particles.

**10·16. Stable baroclinic waves.** A wave whose shape and internal structure do not change during its propagation will be called stable. We shall investigate whether stable waves can exist in a baroclinic current, and study the three-dimensional structure of such waves.

We shall assume that the motion is nearly horizontal and that the temperature of individual particles is conserved. If the relative streamlines were to intersect the isotherms, the temperature field relative to the moving wave would be deformed and the wave would not be stable. Therefore in a stable baroclinic wave *the relative streamlines must coincide with the isotherms.*

This rule implies that the isotherms have the same shape at all levels if the wind is assumed to be geostrophic. By the thermal wind equation, 8·05(1), the shear of the geostrophic wind is directed along the horizontal isotherms. Since, now, a stable wave moves with the same speed at all levels, the shear of the wind is also the shear of the relative wind. So the shear of the relative wind at any level is directed along the isotherms and, hence, along the relative streamlines at that level. Thus the relative wind does not turn with height, so *the relative streamlines have the same shape at all levels.*

This property of the relative streamlines, combined with the relation between the relative and the real streamlines, makes it possible to predict the whole three-dimensional structure of a stable baroclinic wave. The main features of such a wave are shown schematically in fig. 10·16. The central part of the diagram represents horizontal maps at four selected levels, with one streamline and one relative streamline drawn in each map. The relative streamlines (broken lines) have been given the same shape at all levels. The wave is assumed to move toward the east. The speed of the wave is the same at all levels. But on account of the baroclinic temperature field (warm to the south and cold to the north) the zonal wind increases with increasing height, as indicated in the left part of the diagram. At some level the speed of the zonal current must be equal to the speed of the wave. At that level the relative zonal wind is zero; from 10·15(3), $A_S = 0$, so the streamlines are straight. Below that level the air is being overtaken by the wave and the streamlines are 180° out of phase with the relative streamlines. Their amplitude increases with increasing depth below the level of straight streamlines. Above the level of straight streamlines the air overtakes the wave; the streamlines are in phase with the relative streamlines; and $A_S < A_R$.

When the streamlines are identified as isobars, it is readily seen that

the change of the pressure distribution from level to level is qualitatively in accord with the hydrostatic equation. The warm trough at low levels vanishes with height and is surmounted by a warm pressure wedge, whose isobar amplitude increases with height. Correspondingly, the cold pressure wedge at low levels vanishes with height, and is surmounted by a cold trough whose isobar amplitude increases with height.

We can now estimate the transversal, longitudinal, and total mass divergence in the various parts of the wave. This estimate, as applied to the column $AA$, is shown qualitatively in the three graphs to the right in fig. 10·16.

The transversal divergence is zero at the level where the relative zonal wind is zero ($\bar{v} = c$). Above that level the relative zonal wind is positive, so there is transversal divergence to the east of the trough and trans-

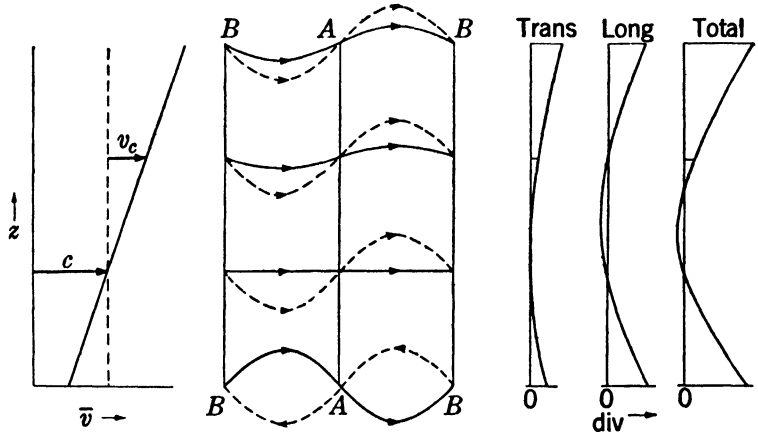



FIG. 10·16. Distribution of divergence in a stable baroclinic wave.

versal convergence to the west of it. Below the level where $\bar{v} = c$, the relative zonal wind is negative, so there is transversal convergence to the east of the trough and transversal divergence to the west of it. Therefore the column $AA$ has transversal divergence both above and below the level where $\bar{v} = c$.

The longitudinal divergence is zero at the level where the relative zonal wind is critical ($\bar{v} - c = v_c$). Above that level the relative zonal wind is supercritical, and the bottleneck is at the cyclonic bend. So there is longitudinal divergence to the east of the trough and longitudinal convergence to the west of it. Below the level where $\bar{v} - c = v_c$ the relative zonal wind is subcritical, and the bottleneck is at the anticyclonic bend. So there is longitudinal convergence to the east of the

trough and longitudinal divergence to the west of it. Therefore the column $AA$ has longitudinal divergence above the level where $\bar{v} - c = v_c$ and also below the level where $\bar{v} = c$. Between these levels the column $AA$ has longitudinal convergence, for the relative wind is subcritical, and the column is to the east of the trough.

The total horizontal divergence is obtained by addition of the transversal and longitudinal parts. For the column $AA$ it is positive at all levels except in a layer whose base is the level where $\bar{v} = c$, and whose top is below the level where $\bar{v} - c = v_c$.

If the level 0 is interpreted as a flat part of the earth's surface, it seems rather likely that divergence may dominate at $AA$, and convergence at $BB$. This would mean pressure fall at the base of column $AA$ and pressure rise at the base of $BB$. This again would make the pressure wave at the ground move westward, contrary to our initial assumption. The only place and time that a trough like that shown in fig. 10·16 could move eastward would then be while the trough is over a mountain range. The downward velocity on the lee side of the mountain could then be strong enough to overcompensate the effect of convergence in the column $BB$ above and produce pressure fall ahead of the trough. Likewise the upslope wind on the west side of the mountain could overcompensate the effect of the divergence in column $AA$ and produce pressure rise behind the trough.

If now the wave pattern moves eastward, columns like $AA$ with a preponderance of divergence will arrive over the lee side of the mountain. The influence of downward motion and divergence will add up in the tendency equation, and a strong pressure fall at the ground will result, which will continue on the lee side till columns with a preponderance of convergence arrive after the passage of the upper-level trough. This is equivalent to a deepening of the low-level trough over the lee slope of the mountain and a belated arrival of the following high-pressure wedge to the same region.

**10·17. The first formation of the baroclinic wave.** We are now ready to take up the fundamental problem in J. Bjerknes' theory of pressure changes. That problem, as mentioned in section 10·06, deals with the study of the mechanism of pressure changes in the moving cyclones. In what follows we shall discuss the incipient wave in the baroclinic westerly current, characterized by the usual decrease of temperature along the isobaric layers towards the pole. To simplify the discussion we shall assume that the wave disturbance has infinite lateral extent with zero transversal divergence. We shall see later that the results are in principle the same for waves with finite width.

The fields of longitudinal and transversal divergence have the zero lines along the troughs and along the wedges. Consequently, horizontal divergence does not explain the first formation and intensification of the wave disturbance. The only alternative is vertical motion, downward where the trough is formed and upward where the wedge is formed. This would explain why the wave pattern of upper isobars always forms with a definite phase lag, relative to the frontal wave disturbances in the lower atmosphere. The upward motion over the warm front surface creates the incipient upper wedge, and the downward motion behind the center at the ground creates the incipient upper trough.

The complete description of that process in terms of the equations of dynamics and thermodynamics is not yet within reach, so we must confine our treatment to qualitative reasoning. Let us consider two limiting cases:

1. The influence of the vertical displacement on the pressure change at the level $\phi$ is completely compensated by divergence or convergence in the air column above, so that everywhere

$$\left(\frac{\partial p}{\partial t}\right)_\phi = (g\rho v_z)_\phi - \int_\phi^\infty \nabla_H \cdot (\rho \mathbf{v}) \delta\phi = 0. \tag{1}$$

This is the usual assumption when the vertical stability is examined.

2. The influence of the vertical displacement on the pressure change at the level $\phi$ is not at all compensated by divergence or convergence in the air column above, so that everywhere

$$\left(\frac{\partial p}{\partial t}\right)_\phi = (g\rho v_z)_\phi. \tag{2}$$

The real case is likely to lie somewhere between (1) and (2) and will depend on the character of the initial undisturbed flow and the intensity and spatial extent of the vertical disturbance.

Fig. 10·17*a* illustrates case (1). The upper part represents a vertical west-east cross section through the center of the young frontal wave. The intersection with the frontal surface appears in the diagram as an approximate sine curve tangent to the ground. In the reference level the isobars were initially straight and parallel to the path of the incipient wave, so that the line $\phi\phi$ on the vertical cross section was an isobar in the initial stage. According to equation (1) the isobar $p = p_0$ stays in the position $\phi\phi$ also after the vertical motion has started. The isotherms in the reference level were initially straight and parallel to the isobars, so that $\phi\phi$ in the vertical cross section also was an initial isotherm. The

vertical displacement $\Delta\phi$ changes the temperature at the constant level $\phi$ by

$$\Delta T = -\Delta\phi(\gamma_d - \gamma), \tag{3}$$

where $\gamma_d$ is the dry adiabatic lapse rate, and $\gamma$ the actual lapse rate. The new isotherm position is consequently raised in the region of descent and lowered in the region of ascent.

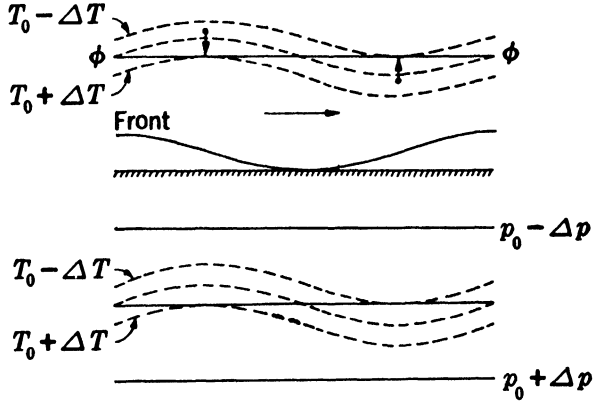



FIG. 10·17*a*. Vertical displacements with complete compensation by divergence in the air column above.

In the initial stage the isobaric surfaces slope gently down toward the pole and the isothermal surfaces slope the same way at a steeper angle. The isobaric surfaces stay fixed also in the perturbed state. However, the isothermal surfaces move up in the region of descent and down in the region of ascent, thereby maintaining their meridional slope. Consequently, the horizontal map in the reference level $\phi$ (lower part of fig. 10·17*a*) retains its straight west-east isobars also in the perturbed state. The isotherm $T = T_0$, at first straight west-east and coinciding with the isobar $p = p_0$, becomes sinusoidal in the new state. Isotherms to the north and south of $T = T_0$ behave similarly. They define a warm tongue extending northward in the region of descent, and cold tongue extending southwards in the region of ascent.

The case (2) is illustrated in fig. 10·17*b*. Since no horizontal divergence is present, no internal changes occur in the vertical air columns. They move up and down as solid columns. The vertical cross section (upper part of the diagram) shows how isobars and isotherms alike are lifted and lowered just as much as the air particles themselves. The lower part shows how sinusoidal isobars and isotherms result on the horizontal map in the reference level. The cold tongue coincides with the

pressure trough and the warm tongue with the pressure wedge. The north-south amplitude of the isobars is considerably greater than that of the isotherms, the reason being that the isobaric surfaces have a much smaller meridional slope than the isothermal surfaces.

Figs. 10·17*a* and *b* show only the initial effect of the lowering and raising of two adjacent portions of the baroclinic upper westerly current. After the upper wave has formed and the isobars and isotherms intersect

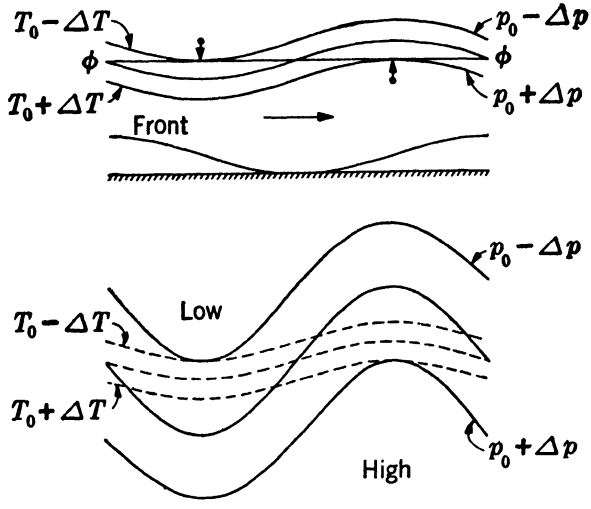



FIG. 10·17*b*. Vertical displacements without any compensation by divergence in the air column above.

on the upper-level map, the horizontal advection starts to move the isotherms. This process is shown in fig. 10·17*c*. The initial state has been selected as a compromise between the two limiting cases represented by figs. 10·17*a* and *b*. The initial isotherm in 10·17*c* has been made straight west-east, as a compromise between the sinusoidal isotherms with opposite phase in figs. 10·17*a* and *b*. This initial straight isotherm is numbered 0, and the subsequent positions reached by the same isotherm under the influence of horizontal advection relative to the wave are numbered 1, 2, · · ·, 6. We shall stipulate that the air moves eastward faster than the wave (the usual case in the upper air). The relative streamlines are then in phase with the isobars but have greater north-south amplitude (see fig. 10·15*b*). The result of the advection is obviously the formation of a warm tongue in the region of southerly wind components and a cold tongue in the region of northerly wind components. If the advection is allowed to continue undisturbed while the particles move one-quarter of the wave length, the warm tongue would

arrive at coincidence with the pressure wedge, and attain a north-south amplitude twice that of the relative streamlines. However, extrapolation of the isotherm advection so far ahead has little practical value because the isobars also change during the process.

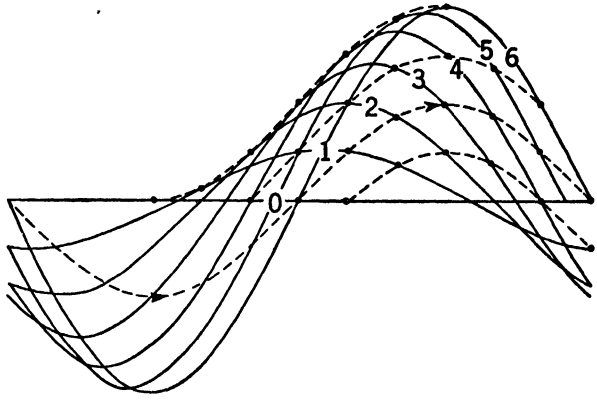



FIG. 10·17*c*. Horizontal advection of an initially straight isotherm.

Let us consider an early stage in the isotherm advection in fig. 10·17*c*, and look for the change to be expected in the isobar pattern. The lower

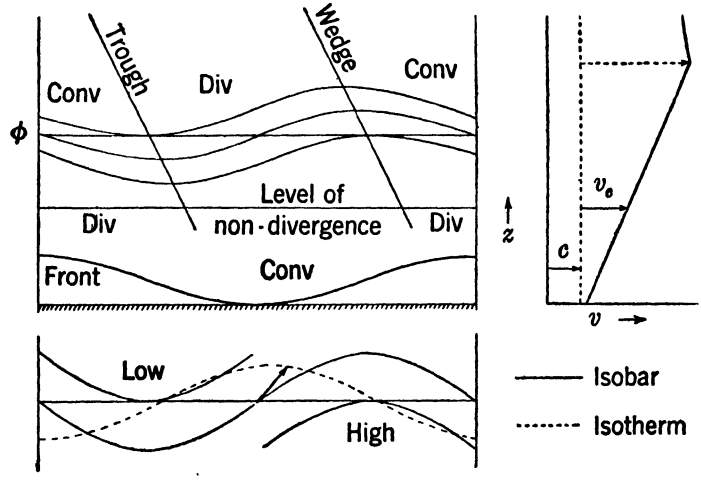



FIG. 10·17*d*. Structure of a young unstable wave in a baroclinic westerly current.

part of fig. 10·17*d* shows the horizontal map at the level $\phi$. The temperature and pressure waves are out of phase with each other, so the crests and troughs of the pressure wave must tilt, as shown in the upper

part of the figure. This upper diagram, representing the vertical cross section along the path of the wave, contains three successive isobars. The vertical distance between them is greatest in the warm tongue. The pressure crest therefore tilts westward (toward warm) with increasing height. And the pressure trough also tilts westward (toward cold) with height.

The variation of the zonal wind with height in the warm air immediately south of the polar front is shown in the right-hand diagram of fig. 10·17*d*. The zonal wind increases with height in the troposphere to a maximum value at the tropopause and decreases from there up. The wave is assumed to move with a slightly slower speed than the warm air at the surface. This choice is plausible, since the surface air always overtakes the wave and ascends over the warm front. The relative zonal wind then increases from a small positive value at the ground to a maximum value at the tropopause. Since the transversal divergence is zero, the flow is non-diverging at the level where the relative zonal wind is critical. The horizontal divergence ahead of the trough is positive above the level of non-divergence and negative below that level. In a westerly current of given strength the height of the level of non-divergence depends on the wave length. For short waves the level of non-divergence is low. As the wave length increases, the level of non-divergence is raised to greater heights until the tropopause is reached. For still longer waves no level of non-divergence exists.

Let us first examine a short wave whose level of non-divergence is below the reference level $\phi$, as indicated in the figure. Consider a vertical column of air extending upward from the reference level at the position of the trough line in that level. The pressure change at the base of this column indicates whether the trough is deepening or filling on the reference level map. First, the trough would deepen if the air continues to descend at the base of the column after the initial wave has developed. But, even if that downward motion has ceased, deepening would still continue if the integral of horizontal divergence in the column above the reference level shows depletion of air. Because of the westward tilt of the trough, the vertical column is east of the trough at all levels above the reference level. So the entire column has horizontal divergence, and the pressure tendency at its base is negative. Similar reasoning for the crest of the pressure profile shows that the pressure wedge on the map in the reference level must be building up, even though the upward motion which started the wedge may have ceased. Thus, *a baroclinic westerly current is dynamically unstable for waves whose level of non-divergence is sufficiently low, and tends to make these waves grow strong, however weak they may be at the start.*

Let us next consider long waves where no level of non-divergence exists. The relative zonal wind at all levels is then subcritical, so the flow has horizontal convergence at all levels ahead of the trough. The long waves therefore would move westward. However, such waves would have no opportunity to develop. Since the trough and the wedge would tilt westward, the pressure would rise in the trough and fall on the wedge at all levels, and the initial disturbance would be damped out. Therefore the baroclinic westerly current is stable for these long waves.

The waves which develop in the westerlies above the polar front always have finite lateral width and, consequently, have transversal divergence. The only way in which transversal divergence can influence the above result is to make the total horizontal divergence zero for a somewhat smaller value of the relative wind than the critical speed. Other things being equal, the transversal divergence therefore lowers the level of non-divergence, and makes the waves of finite width more unstable than the infinitely wide waves.

The same kind of dynamic instability exists whenever the temperature in a given isobaric surface decreases toward the left (right in the southern hemisphere) across the current, or, as it also may be expressed, whenever the speed of the current increases with height. The principal region of dynamical instability is thus the temperate region of westerlies. These westerlies are dynamically more unstable in winter than in summer. This explains, in a general way, the storminess in middle latitudes and its seasonal cycle.

If the direction of the horizontal temperature gradient is reversed in the preceding discussion, we obtain a system where the troughs and wedges tilt eastward with height. Any disturbance in this system will therefore be damped out. In the stratosphere of the temperate zone the westerlies decrease with height. So independently intensifying waves seem excluded in this region. In winter at latitudes greater than 60° the stratosphere temperature decreases toward the pole, so the westerlies must increase with height. In this region and season active wave formations may have their birth in the stratosphere and grow because of dynamic instability.

Easterly currents are dynamically unstable only when they flow between a warm high and a colder low. This involves a reversal of the normal meridional temperature gradient, and is hence very rare in high latitudes. However, such a reversal is normal in summer in the low latitudes between the thermal and the geographical equators. So the equatorial easterlies in summer (especially late summer) exhibit some dynamical instability. This is probably significant for the formation of tropical cyclones.

**10·18. Horizontal divergence in closed cyclonic isobar patterns.** The layers from the ground up to roughly 3 km elevation show more complicated pressure patterns than the higher layers. In the lower layers closed isobars around centers of high and low pressure frequently occur. Occasionally such closed pressure patterns also extend to layers well above 3 km.

The simplest closed low (or high) for theoretical treatment is the one with the center at the pole, surrounded by circular zonal isobars coinciding with circles of latitude. Any ring-shaped channel between two neighboring isobars will then follow a constant latitude and will therefore have the same transport capacity throughout. So there is no region of accumulation or depletion of air and no pressure changes will occur. The circular vortex centered at the pole is thus a possible steady state. In fact it also exists in the atmosphere permanently. The upper westerlies of the temperate latitudes are part of the huge cyclonic vortex centered at the pole. (At the ground the polar low is concealed, since the cold polar air contributes enough surplus weight in the lower layers to make the minimum of pressure disappear.)

If a low with concentric circular isobars is centered at some latitude away from the pole, the isobaric channels surrounding the center will not have equal transport capacity all around. Let us compare the transport capacity at the northernmost and southernmost points of the ring-shaped isobaric channel (fig. 10·18*a*). On account of the symmetry these points are places of maximum or minimum speed, where the wind is gradient wind. Assume for simplicity that the density is the same, and hence that the horizontal pressure force has the same value at the two points. When the normal component equation, 7·13(5), is differentiated with respect to latitude, keeping the curvature and the pressure force constant, we find

$$\frac{\partial v}{\partial \varphi} = -\frac{v\Omega \cos \varphi}{Kv + \Omega \sin \varphi}. \tag{1}$$

This shows that the gradient wind increases with decreasing latitude. The southernmost point of the ring-shaped isobaric channel has the maximum speed, and the northernmost point has the minimum speed. Since the isobaric channel has the same width at the two bends, the transport capacity is directly proportional to the wind speed. So the bottleneck of the channel is at the northernmost point. The whole western half of the vortex then exports more air to the eastern half than it receives in return. Air will be depleted from the western half of the vortex and accumulated in the eastern half. If the vortex extends with a vertical axis all the way up through the atmosphere, the pressure would

fall in its western part and rise in the eastern part. The low and the associated vortex would *move westward*. The stationary circular vortex reaching to the top of the atmosphere is thus impossible unless it is centered over the pole.

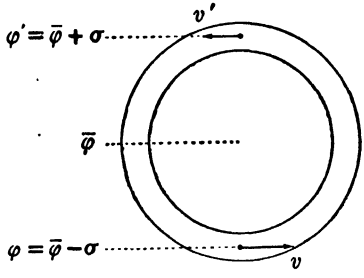



FIG. 10·18*a*. Concentric circular isobaric channel.

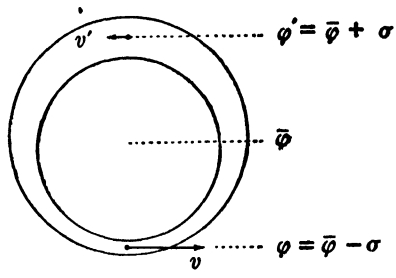



FIG. 10·18*b*. Eccentric circular isobaric channel.

The tendency for westward displacement of closed lows is counteracted if the pressure pattern is made eccentric, as shown in fig. 10·18*b*. The isobaric channel is narrow in the south and wide in the north. According to equation 10·10(1) the transport capacity, $\delta F = \rho v \delta n \delta z$, will be equal at the southernmost and northernmost points if

$$Kv + 2\Omega \sin \varphi = K'v' + 2\Omega \sin \varphi'. \tag{2}$$

If the central latitude $\bar{\varphi}$ and angular amplitude $\sigma_p$ are introduced from 10·10(4) and the subscript $(p)$ is dropped, (2) becomes

$$Kv - K'v' = 4\Omega \cos \bar{\varphi} \sin \sigma. \tag{3}$$

If the circular pressure pattern moves along the west-east direction, the relation between the curvature of the path and the curvature of the streamline at the southernmost point and the northernmost point of the isobaric channel is given by

$$\begin{aligned} Kv &= K_S(v - c), \\ K'v' &= K'_S(v' + c). \end{aligned} \tag{10·10(6)}$$

The circular isobar has the angular radius of curvature $\sigma$ and hence, in analogy to 7·07(4), its horizontal curvature is $K_p = 1/(a \tan \sigma)$. Since, now, the streamlines coincide very nearly with the isobars, we have approximately that $K_S = K'_S = K_p = 1/(a \tan \sigma)$, and consequently

$$Kv - K'v' = K_S(v - v' - 2c) = \frac{v - v' - 2c}{a \tan \sigma}.$$

When this expression is substituted in (3), we get the condition for equal

transport capacity at the southernmost and the northernmost points in a circular isobaric channel:

$$v - v' - 2c = 4\,\Omega\, a \cos\bar{\varphi} \sin\sigma \tan\sigma. \tag{4}$$

An isobaric pattern which in all isobaric channels satisfies equation (4) will be said to have the *critical eccentricity*, which makes the eastern and the western half of the vortex import equal amounts of air from each other during any given time. We see from (4) that, approximately,

$$v - v' - 2c = 4\,\Omega\, a\sigma^2 \cos\bar{\varphi}.$$

The values of $v - v' - 2c$ in (4) are given in table 10·18 for values of $\sigma$

TABLE 10·18

$(v - v' - 2c)$ IN M S$^{-1}$ FOR CRITICAL ECCENTRICITY

| $\bar{\varphi}$ | $\sigma$ | | | |
|---|---|---|---|---|
| | 1° | 5° | 10° | 20° |
| 90° | 0 | 0 | 0 | 0 |
| 80° | 0.1 | 2.5 | 9.9 | — |
| 70° | 0.2 | 4.9 | 19.4 | 79 |
| 60° | 0.3 | 7.1 | 28.4 | 116 |
| 50° | 0.4 | 9.1 | 36.6 | 149 |
| 40° | 0.4 | 10.9 | 43.6 | 177 |
| 30° | 0.5 | 12.3 | 49.3 | 200 |
| 20° | 0.5 | 13.3 | 53.5 | 217 |
| 10° | 0.6 | 13.9 | 56.0 | — |

up to 20°. The table shows what velocity difference there must be between the southernmost and the northernmost point of a stationary ring-shaped isobaric channel in order that the channel shall have equal transport capacities at the two points. The value of $v - v' - 2c$ for the critical eccentricity increases with increasing distance from the pole and increasing radius of the channel. A stationary low with exactly the critical eccentricity for all isobaric channels would have almost concentric isobars near the center and increasingly eccentric isobars toward the outskirts. Isobaric channels of 20° radius require impossible winds to have the critical eccentricity.

If the low moves toward the east, the values in the table must be augmented by twice the speed of the low to give the velocity difference $v - v'$ needed for critical eccentricity. If the low moves westward the tabulated values must be diminished by the same amount. So the critical eccentricity is accentuated if the low moves toward the east and less pronounced if the low moves toward the west.

The actual eccentricity of closed flow patterns on the map, as expressed by the difference in wind velocity at the southernmost and northernmost points of individual isobaric channels, may be compared with the tabulated values for the critical eccentricity. It will generally be found that closed circulations have subcritical eccentricity. That is, they do not have enough eccentricity to make the eastern half of the vortex export as much air to the western half as it receives in return.

The total accumulation or depletion of air in a half-vortex depends not only on the exchange of air with the other half of the vortex but also on the inflow or outflow across the limiting outer isobar. In an eccentric vortex, like that in fig. 10·18*b*, the flow of air from the velocity maximum in the south to the velocity minimum in the north would be associated with a slight component of motion across the isobar towards high pressure. This represents a depletion of air from the eastern half of the vortex. Corresponding reasoning for the western half shows an inflow across the outer isobar and accumulation of air in that part.

Thus eccentricity tends in two ways to deplete air from the eastern half of the vortex, and accumulate air in the western half, and thereby counteracts the latitude effect which makes the eastern half gain and the western half lose air. The flow is actually non-diverging for slightly subcritical eccentricity.

**10·19. Closed cyclonic isobar patterns surmounted by wave-shaped patterns.** The above treatment of the cyclonic vortices in temperate latitude tends to show that only those low-pressure patterns can move eastward which have packed isobars to the south and open isobars to the north of the center. The lower the latitude the greater the eccentricity required. However, that result is valid only for cyclones which reach with essentially the same closed isobaric patterns to the top of the atmosphere. The usual cyclone of the temperate latitudes has closed isobars only in the lowest 2 or 3 km of the atmosphere. Higher up it appears only as a trough in the upper west-east trend of the isobars. The treatment of such cyclones will show that, although a pattern of packed isobars to the south and open isobars to the north of the center is favorable for a rapid displacement eastward, such a pressure pattern is by no means necessary for the eastward displacement of the ordinary cyclone in temperate latitudes.

Fig. 10·19 represents a schematic picture of the processes which produce the pressure changes in the ordinary eastward moving cyclone in temperate latitudes. It has been assumed that $(v - v') < 4\Omega a\sigma^2 \cos\bar{\varphi} + 2c$. According to 10·18(4) this implies that the pressure distribution around the closed center in the lower atmosphere is not

sufficiently eccentric to cause a depletion of air in front of the center, and an accumulation of air behind. In the layers with closed isobars we have horizontal convergence in front of the cyclone and horizontal divergence in the rear. Higher up, where the cyclone is represented by a trough in the west-east isobars, there will, according to our earlier results, be horizontal divergence in front of the trough and horizontal convergence behind.

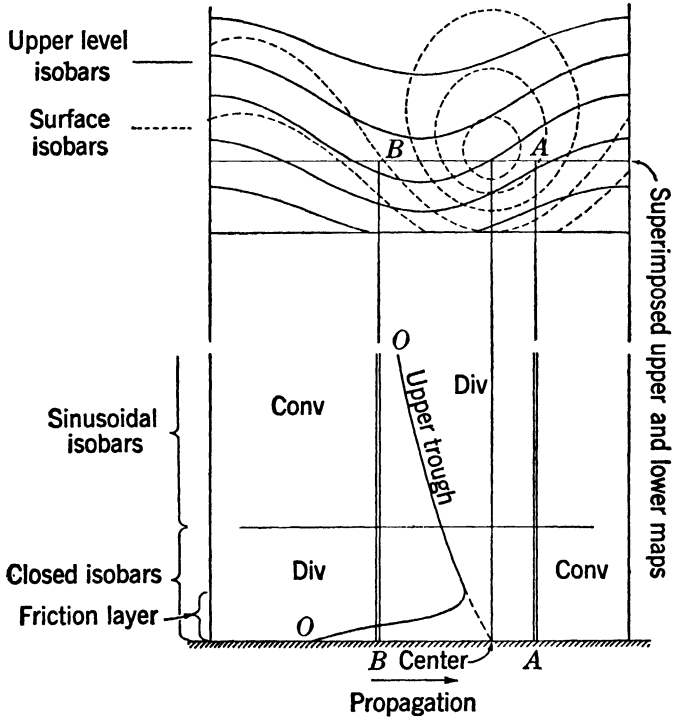



FIG. 10·19. Closed cyclonic isobar pattern surmounted by wave-shaped pattern.

A column fixed in space at *A* (while the air is flowing through it) will gain weight by the convergence in the lower layers and will lose weight by the divergence in the upper layers. In order that there shall be a net loss of weight of the whole column, more air must be removed in the upper layers than accumulates through convergence in the lower layers. The fall of pressure ahead of the cyclone depends on that.

A column fixed in space at *B* will gain some weight by the convergence in the friction layer, but will normally lose more than that by the divergence in the superjacent layers of closed isobars. Above the level where the closed center disappears, column *B* will gain weight by the conver-

gence prevailing behind the upper air trough. The net effect of the changes in weight of column $B$ should be positive, so as to give a rise in pressure behind the moving cyclone. Again this demands that the influence from the upper layers shall overcompensate the influence from the lower layers.

Fig. 10·19 explains in a qualitative way how centers of low can have falling pressure in front and rising pressure in the rear, although the analysis of the horizontal flow in the low layers shows accumulation of air in front of the center and depletion of air in the rear. The general west-east drift of centers of low is thereby explained very much in accordance with the old rule of thumb: The centers move along with the upper current. We now have obtained the physical explanation for this rule: The upper current provides for depletion of air in front of the center and accumulation of air behind the center.

Actually there is a phase difference between the upper trough and the cyclone center at the ground, the upper trough lagging a little. Because of that phase lag upper air divergence takes place vertically above the central area of the cyclone. If the upper air divergence at that place is strong enough to overcompensate the convergence of air into the cyclone center in the lower layers, there will be falling pressure at and around the center. In that case the cyclone is deepening. This process of intensification evidently depends on the phase lag and the backward tilt of the upper trough, which again (according to section 10·17) reverts to the vertical shear as the primary cause for wave instability.

It is furthermore evident from fig. 10·19 that deepening is most likely to occur if the pressure pattern changes from closed isobars to wave-shaped isobars at a relatively low level. This is characteristic of young cyclones. The first level to have closed isobars around a new cyclone is the surface level. As the cyclone grows it develops closed isobars at successively higher levels. The older the cyclone, the higher up will be the level of transition from closed to wave-shaped isobars, and the more the pressure changes will be influenced by the lower pattern of closed isobars. Finally the influence of the lower pattern will cancel or overcompensate that of the upper pattern, and the cyclone will stop or turn slightly retrograde. This, too, is very well corroborated by nature. Cyclones move fast eastward while they are young, but slow down when they get old and deep, sometimes even retrograding a little toward the west in their last phase.

It is interesting to note that the vortex in the surface layers, while being forced along by the influence of the " upper current," counteracts that displacement by piling up air in front. Thus if a vortex of given eccentricity is forced to move to the east, that eccentricity becomes the

more subcritical, the faster its eastward speed. In an eastward moving low the air will accumulate in the eastern half at the expense of the air in the western half, even though the same pressure pattern when stationary maintained non-divergence. This again means that the pressure fall in the front half and the rise in the rear half, both originating in the upper current, will be reduced respectively by the convergence and divergence in the lower layers. This effect increases with increasing eastward speed of the system and thus acts as a regulator of the speed.

The next step in the treatment of the pressure changes in moving cyclones should be to modify the circular isobars at the surface so as to accommodate fronts. Obviously there are a great many problems left for future work concerning the distribution of divergence in pressure fields with non-circular isobars delimiting more or less sharply defined troughs, etc. However, it is expected that the fundamental difference between the front and the rear of the moving cyclone, as represented in fig. 10·19, will remain as a background pattern upon which frontal effects are superimposed.

**10·20. Closed anticyclonic isobar patterns.** The analysis of pressure changes associated with moving highs can be carried out in analogy with the above analysis of the pressure changes in moving lows.

The anticyclone with concentric circular isobars is impossible as a steady state except when centered at the pole. At other latitudes steady-state anticyclones extending to high levels must have eccentric isobars, with the maximum pressure gradient on the polar side of the center. The usual moving anticyclone does not extend far from the ground as a system of closed isobars, but it is surmounted by a wedge. The upper wave-shaped flow pattern produces accumulation of air over the front half of the high and depletion of air over the rear half, and thereby makes it move eastward. The lower closed flow pattern produces the opposite effect, but it is overcompensated by the contribution of pressure change superimposed from the high layers. Since the upper wedge usually lags behind the position of the center of high at the ground, the upper flow pattern produces an accumulation of air over the central region of the high. If that accumulation of air is sufficient to overcompensate the outflow of air in the frictional layer near the ground, the high will intensify.

CHAPTER ELEVEN

# CIRCULATION AND VORTICITY

**11·01. Method of line integrals.** Many problems of atmospheric motion are studied quite conveniently by a special method which involves the application of line integrals. This method has a close analogy to the general method used in the mechanics of rigid bodies. In this field of science all internal deformations are neglected, and the body is studied as a rigid entity. The internal forces in the body, which appear in pairs, are thus eliminated from the problem.

Similarly, in hydrodynamics we may consider as an *entity* a group of fluid particles lying on a closed curve, and then neglect all differences between the particles in the group. The dynamics of such a group is determined by equations with one of the acting forces eliminated. These equations are much simpler than the general equation of motion.

**11·02. Line integral of a vector.** Each of the physical vectors, velocity, acceleration, and gravity, is defined at every point in the atmosphere. Let $\mathbf{a}$ denote any one of these vectors. In the field of $\mathbf{a}$ consider an arbitrary curve connecting an initial point with the position vector $\mathbf{r}_1$ and a terminal point with the position vector $\mathbf{r}_2$, fig. 11·02. Let this curve be divided into infinitesimal curve elements. Each curve element defines an infinitesimal vector $\delta\mathbf{r}$, whose sense is given by the direction from $\mathbf{r}_1$ to $\mathbf{r}_2$ along the curve. Since the curve is located in the field of $\mathbf{a}$, the vector $\mathbf{a}$ has at any given time a definite value at each point on the curve. When scalar multiplication of each of the elements $\delta\mathbf{r}$ by the corresponding vector $\mathbf{a}$ is performed, we obtain infinitesimal scalar products. The sum of these products defines by its limit the curvilinear integral (line integral) of the vector $\mathbf{a}$, which is denoted as follows:

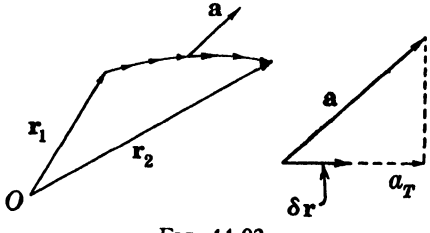


FIG. 11·02.

$$I = \int_1^2 \mathbf{a}\cdot\delta\mathbf{r}. \tag{1}$$

Mathematically there is no difference between this integral and those defined in ordinary calculus. Both are limits of sums of infinitesimal quantities. In (1) the integral element is the scalar product which, according to 4·07, may be written in any of the following scalar forms:

$$\mathbf{a}\cdot\delta\mathbf{r} = a_T\delta s = a\delta s\cos\theta = a_x\delta x + a_y\delta y + a_z\delta z. \tag{2}$$

We shall, however, prefer to use the compact expression (1).

It follows from (2) that only the tangential component $a_T$ of the vector is subjected to the integration. In the special case where the vector is the velocity, the integral (1) is known as the *procession* and is denoted by $P$; thus

$$P = \int_1^2 \mathbf{v}\cdot\delta\mathbf{r}. \tag{1'}$$

A similar terminology is used in the general case (1) where the physical nature of the vector is unspecified, and the integral (1) is called the *procession integral* of the vector **a**.

When the curve of integration in (1) is a closed curve, the initial and the terminal points will coincide, and the integral becomes a cyclic integral. Denoting the closed curve by $c$ we shall introduce for the curvilinear integral of **a** around the closed curve the notation

$$I = \int_c \mathbf{a}\cdot\delta\mathbf{r}. \tag{3}$$

In the special case when the vector is the velocity, this integral is called the *circulation*, and is denoted by $C$; thus

$$C = \int_c \mathbf{v}\cdot\delta\mathbf{r}. \tag{3'}$$

In the general case (3) the integral is called the *circulation integral* of the vector **a**.

It is important to keep in mind the complete generality of the integral defined above. The geometrical properties and the physical nature of the vector field may be completely arbitrary, and the curve of integration may have any shape and location in the field. Thus there is a priori no relation between the vector field and the curve, except that the entire curve must be within the region where the vector is defined. The physical interpretation of the integrals is evident in the special case where the vector is the velocity. The interpretations for other physical vectors are given in the following sections. The evaluation of the integrals can only be performed when the vector field and the curve of

integration are known. However, our aim is not to evaluate the integrals, but rather to develop general laws for their behavior. These laws make it possible to investigate further the dynamical relations between the motion and the fields of the physical variables.

**11·03. Line integrals of the equation of absolute motion.** We shall first consider absolute motion, where a simple physical interpretation of the results is possible. The equation of absolute motion can be written in the following two equivalent forms:

$$\dot{\mathbf{v}}_a = -\nabla\phi_a - \alpha\nabla p, \tag{1a}$$

$$\rho\dot{\mathbf{v}}_a = -\rho\nabla\phi_a - \nabla p, \tag{1b}$$

where in (1$a$) the equation is referred to unit mass, and in (1$b$) to unit volume.

Following the procedure outlined in the preceding section, we perform scalar multiplication of each of the vectors in these equations by the vector line element $\delta\mathbf{r}$ of an arbitrary curve in the atmosphere. According to 4·13(1) the scalar products of the potential vectors are

$$\nabla\phi_a\cdot\delta\mathbf{r} = \delta\phi_a, \qquad \nabla p\cdot\delta\mathbf{r} = \delta p; \tag{2}$$

here $\delta\phi_a$ and $\delta p$ are the variations respectively in the potential of gravitation and in pressure from the initial to the terminal point of the vector element $\delta\mathbf{r}$. Thus the result of the scalar multiplication in (1) is

$$\dot{\mathbf{v}}_a\cdot\delta\mathbf{r} = -\delta\phi_a - \alpha\delta p, \tag{3a}$$

$$\rho\dot{\mathbf{v}}_a\cdot\delta\mathbf{r} = -\rho\delta\phi_a - \delta p. \tag{3b}$$

Each of the expressions may be integrated along the curve from an initial point 1 to a terminal point 2 on the curve. We thus obtain the following relations between the procession integrals of the vectors in the equation of motion:

$$\phi_{a2} - \phi_{a1} = -\int_1^2 \alpha\delta p - \int_1^2 \dot{\mathbf{v}}_a\cdot\delta\mathbf{r}, \tag{4a}$$

$$p_2 - p_1 = -\int_1^2 \rho\delta\phi_a - \int_1^2 \rho\dot{\mathbf{v}}_a\cdot\delta\mathbf{r}. \tag{4b}$$

The first of these equations is the dynamic generalization of the barometric height formula.

Each of the equations (4) remains a full equivalent of the equation of motion, as long as we have free choice of the curves. This generality is

lost when the curves are subjected to special conditions, but in return we obtain useful special theorems. We shall consider two such specializations:

1. *Equilibrium curves.* In any field of motion an infinite number of curves may be drawn normal to the acceleration. These curves are called equilibrium curves. If the integrals (4) are taken along an equilibrium curve, the equations reduce to the hydrostatic forms:

$$\phi_{a2} - \phi_{a1} = -\int_1^2 \alpha \delta p, \tag{5a}$$

$$p_2 - p_1 = -\int_1^2 \rho \delta \phi_a. \tag{5b}$$

Thus the barometric height formula, which is approximately fulfilled for an arbitrary curve, is fulfilled exactly along the equilibrium curves. These curves may, under special simple conditions, be rather easy to determine. For example, for steady zonal motion the only acceleration is the centripetal acceleration, so that one system of equilibrium curves consists of the lines parallel to the axis of the earth; another system consists of the circles of latitude.

2. *Isobaric curves and horizontal curves.* If the curve in (4*a*) lies in an isobaric surface, and the curve in (4*b*) in a level surface of $\phi_a$, the equations reduce to

$$\phi_{a2} - \phi_{a1} = -\int_1^2 \dot{\mathbf{v}}_a \cdot \delta \mathbf{r}, \tag{6a}$$

$$p_2 - p_1 = -\int_1^2 \rho \dot{\mathbf{v}}_a \cdot \delta \mathbf{r}. \tag{6b}$$

The first of these formulas indicates that the isolines of $\phi_a$ on an isobaric surface run normal to the isobaric component of the acceleration; the other, that the isobars in a level surface of $\phi_a$ run normal to the component of the acceleration in that surface.

**11·04. Primitive circulation theorems in absolute motion.** We shall next consider the case where the line integrals in the two equations 11·03(4) are taken along a closed curve. The initial and terminal points of the integration are then identical, and the procession integrals become

circulation integrals; thus:

$$(1a) \qquad \int_c \dot{\mathbf{v}}_a \cdot \delta\mathbf{r} = -\int_c \alpha \delta p,$$

$$(1b) \qquad \int_c \rho \dot{\mathbf{v}}_a \cdot \delta\mathbf{r} = -\int_c \rho \delta \phi_a.$$

These equations connect the circulation of the vectors $\dot{\mathbf{v}}_a$ and $\rho\mathbf{v}_a$ with cyclic integrals of the physical variables. In (1$a$) the potential of gravitation is eliminated, and in (1$b$) the pressure is eliminated. They are known as the circulation theorems and were derived by V. Bjerknes in 1898. Both theorems are fundamental for the study of physical hydrodynamics.

The theorem (1$b$) has been given a useful mechanical interpretation by E. Höiland (1939). He considers a closed fluid tube with the infinitesimal constant cross section $\delta A$ and applies the theorem (1$b$) to a curve which is the central line in this tube. If we multiply (1$b$) by the constant $\delta A$ and introduce $-\delta\phi_a = -\nabla\phi_a \cdot \delta\mathbf{r} = \mathbf{g}_a \cdot \delta\mathbf{r}$, we have:

$$(2) \qquad \int_c \delta A \rho \dot{\mathbf{v}}_a \cdot \delta\mathbf{r} = \int_c \delta A \rho \mathbf{g}_a \cdot \delta\mathbf{r}.$$

Let $\dot{v}_T$ and $g_{aT}$ denote the components of the acceleration and the gravitation tangential to the tube in the direction of the vector element $\delta\mathbf{r}$. With these notations equation (2) takes the form:

$$(2') \qquad \int_c \dot{v}_T (\rho \delta A \delta s) = \int_c g_{aT} (\rho \delta A \delta s),$$

or, since $\rho \delta A \delta s = \delta M$ is the mass contained in the tubular volume element $\delta V = \delta A \delta s$:

$$(2'') \qquad \int_c \dot{v}_T \delta M = \int_c g_{aT} \delta M.$$

This equation, which is equivalent to the circulation theorem (1$b$), clearly reveals the analogy between this theorem and the equation of motion of a rigid body. By considering the particles in a closed tubular fluid filament we have a mechanica system for which the pressure forces have no resultant in the direction tangential to the filament. The integral of the mass multiplied by the acceleration tangential to the filament is therefore determined by the gravitation alone. Höiland calls the integral $\int_c \dot{v}_T \delta M$ the *total mass acceleration* along the filament. In this terminology the circulation theorem (1$b$) can be stated as follows: *An arbitrary closed fluid filament with constant cross section has a total mass*

*acceleration along itself equal to the resultant of the force of gravitation along the filament.* This theorem is particularly important in the study of the stability of steady flow.

The theorem (1*a*) can be given a similar mechanical interpretation by considering a closed fluid filament of cross section $\delta A$, where $\rho\delta A$ is a constant along the filament. The particles composing this fluid filament represent a mechanical system where the resultant of gravitation tangential to the filament is zero. Another interpretation of the circulation theorem (1*a*), which has been of great importance for the development of modern meteorology, has been given by V. Bjerknes. This interpretation will be discussed in the following section.

**11·05. The theorem of solenoids.** It was shown in section 4·23 that the pressure integral $-\int\alpha\delta p$ has a simple graphical representation in the $(\alpha,-p)$-diagram. Corresponding values of pressure and specific volume along a vertical curve in the atmosphere define a certain curve in the $(\alpha,-p)$-diagram, or in the emagram, as in fig. 4·23. This curve, known as the sounding curve, represents the vertical curve in the atmosphere, and shows how the fields of pressure and mass are distributed along this vertical.

Consider now an arbitrary geometrical curve in the atmosphere. At any given instant this curve may be represented in the $(\alpha,-p)$-diagram by a curve which is determined by the distribution of pressure and mass along the atmospheric curve. We shall refer to the latter as the *image curve* of the atmospheric curve. When the atmospheric curve is closed, its image curve is also closed. The pressure integral $-\int_c\alpha\delta p$ in the circulation theorem 11·04(1*a*) is equal to the area enclosed by the image curve, and its sign is determined by the sense of the integration around this curve. The sign is positive if the integration has the sense of the rotation from the positive $\alpha$ axis to the negative $p$ axis, and negative if the integration has the opposite sense.

The isobaric unit layers in the atmosphere are represented in the $(\alpha,-p)$-diagram by horizontal stripes of unit width, and the isosteric unit layers are represented by vertical stripes of unit width. Taken both together the isobaric and isosteric unit surfaces divide the atmosphere into a system of tubes with parallelogrammatic cross sections. These unit tubes are known as the *pressure-volume solenoids* or the $(\alpha,-p)$-solenoids. Each solenoid in the atmosphere is represented by a unit square in the $(\alpha,-p)$-diagram, as shown in fig. 11·05*a*. The sign of the unit square is positive when the integration along its edge has the sense of the rotation from the positive $\alpha$ axis to the negative $p$ axis. Correspondingly a positive sense may be assigned to the solenoid, defined by the right-

handed rotation (through an angle less than 180°) from the volume ascendent $\nabla\alpha$ to the pressure gradient $-\nabla p$. (In fig. 11·05*a* the solenoids are directed out from the paper.)

Consider an arbitrary closed curve in the atmosphere and the corresponding image curve in the $(\alpha,-p)$-diagram. The two curves are denoted respectively by $c$ and $c'$ in fig. 11·05*a*. The area enclosed by the

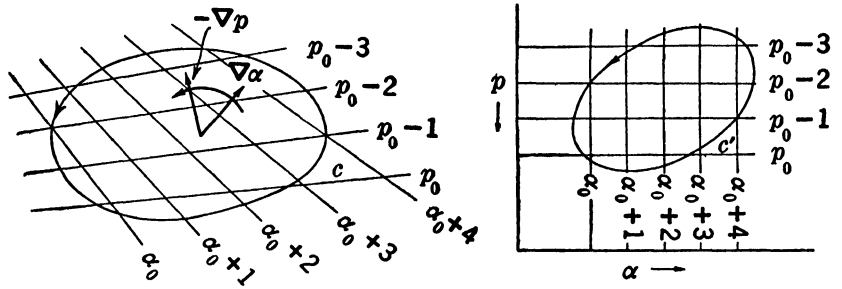



FIG. 11·05*a*. Pressure-volume solenoids enclosed by atmospheric curve, and equivalent area on $(\alpha,-p)$-diagram.

image curve $c'$ equals the number of unit squares contained within the curve. And since the integral $-\int_c \alpha\delta p$ is equal to this area, it is also equal to the number of pressure-volume solenoids embraced by the atmospheric curve $c$. The solenoids are counted algebraically. If their sense, as defined above, is the same as the sense of integration along the curve, they are counted positive; if their sense is opposite, they are counted negative. In fig. 11·05*a* the sense of integration indicated by the arrow on the curve is the sense of the solenoids. The solenoids are in this case counted positive, and the integral $-\int_c \alpha\delta p$, taken in the indicated sense, is accordingly positive. Had the integration been taken in the opposite sense, the solenoids would have been counted negative. Denoting the algebraic number of solenoids embraced by an arbitrary closed curve in the atmosphere by $N_{\alpha,-p}$, we can write

$$-\int_c \alpha\delta p = N_{\alpha,-p}. \tag{1}$$

This is the theorem of solenoids. When this theorem is combined with the circulation theorem 11·04(1*a*), we obtain

$$\int_c \dot{\mathbf{v}}_a\cdot\delta\mathbf{r} = N_{\alpha,-p}. \tag{2}$$

In this form the circulation theorem can be stated: *Along an arbitrary closed curve in the atmosphere the absolute acceleration has at any time a circulation equal to the algebraic number of pressure-volume solenoids*

*embraced by the curve. The circulation has the same sense as the solenoids, the sense of the rotation from volume ascendent to pressure gradient.*

This interpretation of the circulation theorem was given by V. Bjerknes. It does not reveal the underlying mechanical principle as clearly as Höiland's interpretation. But the solenoid theorem has great practical advantages, particularly in the science of synoptic meteorology, where the physical fields are represented graphically by their unit layers, so the solenoids are directly accessible.

As an example consider the ideal case shown in fig. 11·05*b*. The diagram to the left represents a meridional cross section through the lower troposphere, symmetric with respect to the axis of the earth. It shows schematically the mean distribution of pressure and mass in winter. The isobaric surfaces are drawn for every 10 cb, the isosteric surfaces for every 100 $m^3\ t^{-1}$. The mts-solenoids are thus obtained by increasing the number of isobars ten times, and the number of isosteres one hundred times. The solenoids are in this case annular tubes parallel to the circles of latitude, and their sense is from east to west. Consider the closed atmospheric curve 1231, composed of the isobaric segment 12, the isosteric segment 23, and the vertical segment 31 along the axis of the earth.

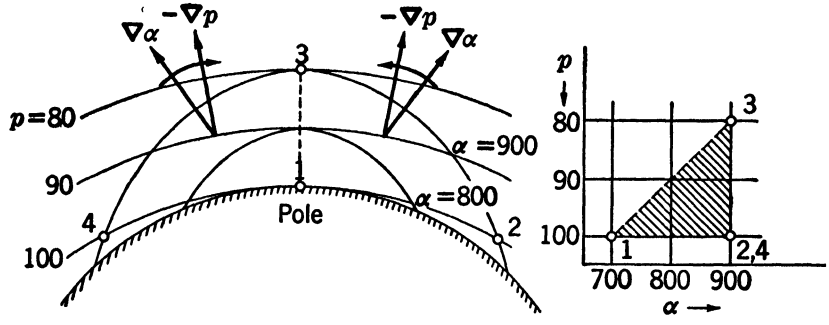



FIG. 11·05*b*. Idealized distribution of solenoids in meridional cross section.

The corresponding image curve in the $(\alpha,-p)$-diagram, to the right in fig. 11·05*b*, is the triangle enclosing the shaded area. We shall now apply the circulation theorem (2) to this curve, integrating along the curve with the sense indicated by the numbers. The area of the image curve is then positive, and the solenoids embraced by the atmospheric curve have the same sense as the integration, the sense of the rotation from volume ascendent to pressure gradient. Both results show that the acceleration has a circulation along the curve in the direction indicated by the numbers. The same result is obtained when the circulation theorem is applied to the curve 1431.

Consider finally the atmospheric curve 12341, whose image curve is the broken line 12321, which has zero area. The acceleration has no circulation along this curve. This result is also obtained directly from the theorem of solenoids. The solenoids to the right of the axis have the same sense as the integration and are counted positive. The solenoids to the left of the axis have opposite sense and are counted negative. Due to the symmetry there are equal numbers of positive and negative solenoids, so the total algebraic number of solenoids embraced by the curve 12341 is zero.

The above example shows that the information which can be gained from the theorem is greatly influenced by the selection of the curve. The curves 1231 or 1431 give the useful information that the acceleration has a tangential resultant along these curves in the direction indicated by the numbers. The curve 12341 gives the trivial result of no tangential resultant. One guiding principle for the selection of the curve is that it should embrace only solenoids of the same sign. Only with such curves can the full dynamical effect of the solenoids be estimated.

**11·06. Practical forms of the theorem of solenoids.** Since pressure and specific volume are the physical variables which enter directly into the atmospheric equations, the pressure-volume solenoids give the simplest rules when applied to dynamical problems. This is analogous to the fact that the $(\alpha,-p)$-diagram is the simplest thermodynamical diagram for the study of thermal energy transformations.

In practical meteorology the $(\alpha,-p)$-diagram is replaced by the emagram or the tephigram, which have the important meteorological variables as their coordinates. Similarly, the pressure-volume solenoids may be replaced by the pressure-temperature solenoids or the temperature-entropy solenoids. The relations between these three kinds of solenoids are the same as the relations between the $(\alpha,-p)$-diagram, the emagram, and the tephigram. If the same closed atmospheric curve is plotted in these three diagrams, the areas enclosed by the corresponding image curves in the diagrams are proportional; thus

$$(1) \qquad -\int_c \alpha \delta p = R_d \int_c \ln p \, \delta T = -c_{pd} \int_c \ln \theta \, \delta T.$$

The first integral is the pressure integral in the circulation theorem and is equal to the number of $(\alpha,-p)$-solenoids embraced by the atmospheric curve. The second and third integrals in (1) may be given a similar interpretation.

The second integral is equal to the area enclosed by the image curve in the emagram. It is positive if the integration has the sense of the

rotation from the negative $\ln p$ axis to the negative $T$ axis. This area is also equal to the number of $(-\ln p, -T)$-solenoids defined by the isothermal unit layers and the unit layers of $\ln p$. The sense of these solenoids is defined by the rotation $-\nabla p \rightarrow -\nabla T$ from pressure gradient to temperature gradient. The number of these solenoids embraced by the atmospheric curve will be denoted by $N_{-\ln p,-T}$.

The third integral is equal to the area enclosed by the image curve in the tephigram and is therefore also equal to the number of $(\ln \theta, -T)$-solenoids. These solenoids are defined by the isentropic and the isothermal unit layers and have the sense of the rotation $\nabla(\ln \theta) \rightarrow -\nabla T$ from entropy ascendent to temperature gradient. The number of these solenoids which are embraced by the atmospheric curve will be denoted by $N_{\ln \theta,-T}$. Introducing these notations in (1), we obtain

$$N_{\alpha,-p} = R_d N_{-\ln p,-T} = c_{pd} N_{\ln \theta,-T}. \tag{2}$$

The three kinds of solenoids in (2) are always parallel. The pressure-volume solenoid is by definition parallel to the line of intersection of the isobaric and the isosteric surface, along which both pressure and specific volume are constant. From the equation of state the temperature is constant along this line, and from Poisson's equation the potential temperature is also constant along the same line.

In synoptic analysis the isobars and isentropes are drawn for unit values of $p$ and $\theta$. The determination of the solenoids in (2) requires the isobars and isentropes for unit values of $\ln p$ and $\ln \theta$. To overcome this practical inconvenience, consider one of the temperature-entropy solenoids, defined by two isothermal surfaces with the temperature difference $\Delta T = 1°$, and two isentropic surfaces with the entropy difference $\Delta(\ln \theta) = 1$. The variation $\Delta\theta$ in potential temperature through the isentropic unit layer is given approximately by $\Delta\theta/\bar{\theta} = \Delta(\ln \theta) = 1$, or $\Delta\theta = \bar{\theta}$, where $\bar{\theta}$ is a mean potential temperature in the layer. Accordingly, an isentropic unit layer contains $\bar{\theta}$ potential temperature unit layers, and one temperature-entropy solenoid contains $\bar{\theta}$ temperature-potential temperature solenoids. Denoting by $N_{\theta,-T}$ the number of the latter solenoids embraced by the atmospheric curve, we then have

$$N_{\theta,-T} = \bar{\theta} N_{\ln \theta,-T}, \qquad N_{-p,-T} = \bar{p} N_{-\ln p,-T}. \tag{3}$$

The second expression is obtained by a similar consideration of the $(-\ln p, -T)$-solenoids. When the expressions (3) are introduced in (2), we have

$$N_{\alpha,-p} = \frac{R_d}{\bar{p}} N_{-p,-T} = \frac{c_{pd}}{\bar{\theta}} N_{\theta,-T}. \tag{4}$$

This gives the relations between the number of pressure-volume solenoids, pressure-temperature solenoids, and temperature-potential temperature solenoids which are embraced by the same atmospheric curve. In a dry atmosphere the solenoids are defined by the real temperature and potential temperature. In a moist atmosphere the virtual temperature and virtual potential temperature must be used; see 3·28.

Practical forms of the circulation theorem are obtained when the second and third expressions in (4) are introduced in the fundamental theorem 11·05(2); thus

$$\int_c \dot{\mathbf{v}}_a \cdot \delta\mathbf{r} = \frac{R_d}{\bar{p}} N_{-p,-T} = \frac{c_{pd}}{\bar{\theta}} N_{\theta,-T}. \tag{5}$$

When the unit isotherms, and the unit isobars or the unit potential isotherms have been drawn in a vertical cross section through the atmosphere, one of these theorems may be used to obtain a general idea of the distribution of the acceleration in the cross section. For rough estimates, the numerical factors $(R_d/\bar{p})$ and $(c_{pd}/\bar{\theta})$ are obtained from mean values of $p$ or $\theta$ within the curve. The variation in the factor $(c_{pd}/\bar{\theta})$ is small within the lower half of the troposphere where the range of potential temperature is about 270°–330°. A rough average value of $(c_{pd}/\bar{\theta})$ is thus 3.3, which gives the approximate rule: Each temperature-potential temperature solenoid contains about 3 pressure-volume solenoids.

The formulas (5) are used only for qualitative estimates of the distribution of the acceleration when the physical variables are represented graphically by their unit layers. When the solenoid number is wanted more accurately, it is determined by integration around a " rectangular " curve composed of two isobaric and two vertical curve segments. According to (1) we have for any closed atmospheric curve

$$N_{\alpha,-p} = -R_d \int_c T\delta(\ln p). \tag{6}$$

The two isobaric curve segments give no contribution to the integral on the right. Along the vertical segments of the curve the integral is identical to the barometric height formula. Let $p_1$ and $p_2$ be the pressures respectively on the lower and the upper isobar, and let $A$ and $B$ denote the colder and the warmer vertical, having respectively the mean temperatures $T_{mA}$ and $T_{mB}$. Denoting by $\phi_A$ and $\phi_B$ the dynamic thicknesses of the isobaric layer $(p_1 \to p_2)$ at the two verticals $A$ and $B$, we see from 4·24(3) that

$$|N_{\alpha,-p}| = R_d(T_{mB} - T_{mA}) \ln \frac{p_1}{p_2} = \phi_B - \phi_A. \tag{7}$$

With the aid of the second expression the number of solenoids is conveniently evaluated. The problem has been reduced to the determination of the dynamic heights of the two verticals. The last expression in (7) shows that the number of solenoids contained in the isobaric layer between the two verticals is equal to the variation in dynamic thickness of the layer, or the *dynamic inflation* of the isobaric layer. In the special case of an isobaric unit layer this result is obtained directly from 4·16(5), which contains the rule that the dynamic thickness of the isobaric unit layer is equal to $\alpha$. The dynamic inflation of the isobaric unit layer from $A$ to $B$ is $\alpha_B - \alpha_A$, which evidently is equal to the number of solenoids in the layer between $A$ and $B$.

Table 11·06 has been computed from the formula (7), with the pressure

TABLE 11·06

NUMBER OF PRESSURE-VOLUME SOLENOIDS

| $p_2$ cb | $T_{mB} - T_{mA}$ | | | | |
|---|---|---|---|---|---|
| | 1° | 10° | 20° | 30° | 40° |
| 30 | 346 | 3,455 | 6,910 | 10,365 | 13,820 |
| 60 | 147 | 1,466 | 2,932 | 4,398 | 5,864 |
| 90 | 30 | 303 | 605 | 908 | 1,210 |
| 100 | 0 | 0 | 0 | 0 | 0 |

on the lower isobar at the standard value $p_1 = 100$ cb. The table gives the number of solenoids contained in a curve bounded by this lower isobar, an upper isobar of pressure $p_2$ and two verticals with the mean temperature difference $T_{mB} - T_{mA}$.

As an example consider a closed meridional curve having one vertical at the pole, the other at the equator, and having the upper isobar $p_2 = 30$ cb and the lower isobar $p_1 = 100$ cb. This curve will embrace the majority of the solenoids of the troposphere. In winter the difference of mean temperature between the two verticals is about 40°. It is seen from the table that the corresponding number of solenoids is 13,820. This result also signifies that the isobaric layer 100–30 cb has a dynamic inflation of 1382 dyn m from the pole to the equator.

**11·07. Dynamic balance of steady zonal motion.** The utility of the circulation theorem 11·05(2) for the study of atmospheric motion may be illustrated by considering steady zonal motion. This field of motion is sometimes referred to as a circular vortex. The absolute acceleration is here the centripetal acceleration $-\omega_a^2\mathbf{R}$. For an arbitrary curve in the

circular vortex the circulation theorem becomes

$$-\int_c \omega_a^2 \mathbf{R}\cdot\delta\mathbf{r} = N_{\alpha,-p}. \tag{1}$$

We shall first examine the distribution of the solenoids in the circular vortex. It was shown in section 6·11 that the pressure field is symmetric about the axis of the earth. It is easy to see that the mass field is also symmetric about the axis. Since the isobaric surfaces are surfaces of revolution, the pressure gradient $-\nabla p$ has a constant magnitude along any one of the circles of latitude. According to the equation of motion the pressure force per unit mass $-\alpha\nabla p$ is constant in magnitude along each latitude circle. The specific volume is the ratio of the magnitudes of the pressure force and the pressure gradient. Hence, $\alpha = |\alpha\nabla p|/|\nabla p|$ is constant along each latitude circle, which proves that the isosteric surfaces are surfaces of revolution about the axis of the earth. The solenoids are therefore annular tubes parallel to the circles of latitude.

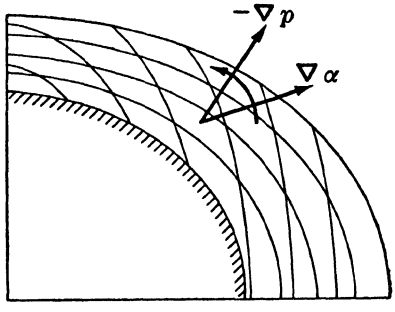



FIG. 11·07*a*. Solenoids in balanced zonal motion.

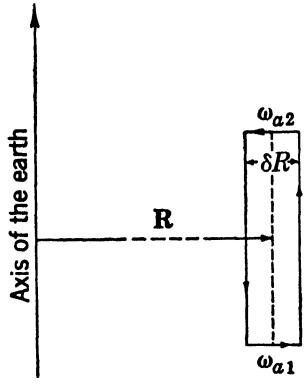



FIG. 11·07*b*. Circulation theorem applied to rectangular meridional curve.

The sense of the solenoids is determined by the rotation from volume ascendent to pressure gradient. Under normal conditions the cold and heavy masses are located in the polar region, as shown in fig. 11·07*a*. In this normal atmospheric vortex with a cold core the solenoids are in the northern hemisphere directed from east to west. In the abnormal vortex with a warm core the solenoids have the opposite sense.

From the circulation theorem (1) the tangential resultant of the centripetal acceleration along any closed meridional curve has the same sense as the solenoids. Consider first the normal vortex with a cold core. Let the meridional curve be a rectangle, with sides parallel and

perpendicular to the axis, fig. 11·07*b*. The " height " of the rectangle in the direction of the axis is arbitrary, but its width normal to the axis is infinitesimal, denoted by $\delta R$. Let further $\omega_{a2}$ and $\omega_{a1}$ denote the angular speed at the top and the base of the rectangular curve. (Here " up " and " down " refer to the equatorial plane.) Since the axial sides of the rectangle are equilibrium lines (perpendicular to the acceleration), they give no contribution to the circulation integral in (1). Thus, when the integration has the sense of the solenoids,

$$(\omega_{a2}^2 - \omega_{a1}^2)R\delta R = N_{\alpha,-p}. \tag{2}$$

The solenoid number is positive, so $\omega_{a2}^2 > \omega_{a1}^2$. The rectangular curve may be placed anywhere in the meridional plane; therefore throughout the vortex the angular speed increases with increasing distance from the equatorial plane. When a similar analysis is applied to the abnormal vortex with a warm core, we find that the angular speed decreases with increasing distance from the equatorial plane. When the specific volume is constant within each isobaric layer, the vortex contains no solenoids and is said to be barotropic. The angular speed is constant along any line parallel to the axis in the barotropic vortex. When " height " refers to the equatorial plane, the above results may be condensed into the following rule. *The strength of rotation in the circular vortex increases with height when its core is cold, decreases with height when its core is warm, and the rotation is independent of height when the vortex is barotropic.*

It is possible to derive these rules directly from simple physical reasoning. When the circulation integral in (1) is transferred to the right-hand side,

$$0 = \int_c \omega_a^2 \mathbf{R}\cdot\delta\mathbf{r} + N_{\alpha,-p}, \tag{3}$$

the theorem becomes an equation of equilibrium. The two terms on the right must be balanced for any meridional curve if the vortex shall be maintained as a steady state. Consider the dynamical effect of each of the terms in the normal atmospheric vortex with the cold core, as illustrated in fig. 11·07*c*. The solenoids tend to produce a " direct " meridional circulation around the solenoids: the heavier masses in the polar region tend to sink down and spread out southward along the surface of the earth, with a compensating northward flow aloft of the lighter masses from the equator. This circulation is prevented by the circulation of the centrifugal force. The strength of the zonal circulation and hence the centrifugal force increases with " height," so the centrifugal forces tend to produce a " retrograde " circulation around the solenoids. The action is similar to that of a centrifugal pump. The heavy

masses near the axis are prevented from sinking by the " centrifugal suction " arising from the stronger intensity of the vortex aloft. When the action of the solenoids and the action of the centrifugal suction have the same intensity everywhere in the vortex, no meridional circulation will arise, and the motion remains steady. The balance of the vortex is thus established by a complete adjustment between the mass field and the field of motion. It is important to note that the balance is controlled only by the variation in angular speed parallel to the axis. The variation of angular speed in the radial direction may be arbitrary.

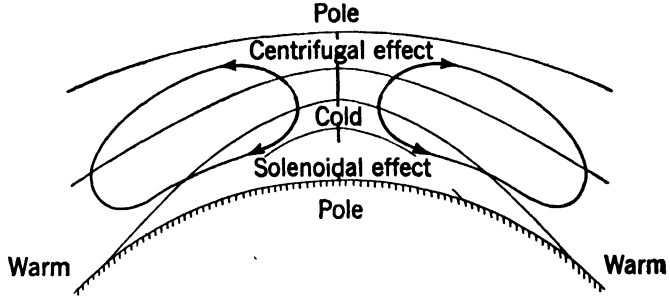



FIG. 11·07*c*. Dynamic balance of zonal motion.

We may finally consider the case where the atmosphere initially moves as a circular vortex, but where the initial distribution of angular speed and mass is such that the equation (3) is not satisfied. This vortex is unbalanced and a meridional circulation will result in the direction of the dominating effect. When the solenoidal effect dominates, that is, when the heavy masses are raised too much in the polar region, a " direct " circulation around the solenoids results. When the centrifugal suction dominates, that is, when the angular speed increases too rapidly with " height," a " retrograde " circulation against the solenoids results. During the subsequent meridional circulation both the solenoidal effect and the centrifugal effect are modified, and the question arises whether the motion approaches the steady state of a balanced vortex. This problem is intimately connected with that of the *stability* of the circular vortex. It can be shown that the stability depends primarily upon the variation of angular speed in the radial direction.

**11·08. Thermal wind in zonal motion.** The rules for the dynamical balance of (absolute) zonal motion are in qualitative agreement with the rules derived in section 8·03 for the variation of the wind with height. In the vortex with the cold core, where the isobaric temperature gradient is directed towards the pole, the west wind increases with " height," so the shear of the wind is directed toward the east in accordance with the

thermal wind formula. It is possible to derive a thermal wind formula for the shear of the wind in zonal motion directly from the circulation theorem, 11·07(1). For this purpose the solenoid number is replaced by the pressure integral 11·05(1); thus

$$(1) \qquad -\int_c \omega_a^2 \mathbf{R}\cdot\delta\mathbf{r} = -\int_c \alpha\delta p.$$

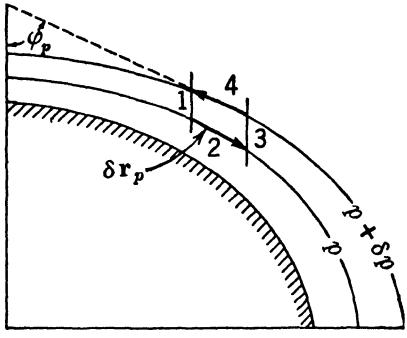



FIG. 11·08. Evaluation of thermal wind in zonal motion.

The theorem is applied to an infinitesimal meridional curve, consisting of two isobaric curve elements (2 and 4), and two equilibrium line elements (1 and 3) parallel to the axis, as shown in fig. 11·08. The sense of the integration is indicated by the numbers. Both integrals in (1) are easily evaluated for this curve.

The pressure integral vanishes along the isobaric elements 2 and 4, and the equilibrium line elements give the contribution

$$(2) \qquad -\int_c \alpha\delta p = -\alpha_3\delta p + \alpha_1\delta p = -(\alpha_3 - \alpha_1)\delta p = -\left(\frac{\delta\alpha}{\delta s}\right)_p \delta s_p \delta p.$$

Here $\delta s_p$ is the length, measured southward, of the isobaric elements 2 and 4. Since (2) is taken along equilibrium lines we have from 11·03(5$a$) $\delta\phi_a = -\alpha\delta p$, where $\delta\phi_a$ is the variation in the potential of gravitation from the lower to the upper isobar along the equilibrium lines 1 or 3. The potential of the centrifugal force is constant along the equilibrium lines, so from 6·10(6) $\delta\phi_a = \delta\phi$, where $\delta\phi$ is the corresponding variation in geopotential along the equilibrium line. Introduced in (2) this gives

$$(2') \qquad -\int_c \alpha\delta p = \frac{1}{\alpha}\left(\frac{\delta\alpha}{\delta s}\right)_p \delta s_p \delta\phi.$$

The acceleration integral on the left in (1) vanishes along the equilibrium lines. The isobaric curve elements ($\delta\mathbf{r}_2 = -\delta\mathbf{r}_4 = \delta\mathbf{r}_p$) give the contribution

$$(3) \qquad -\int_c \omega_a^2 \mathbf{R}\cdot\delta\mathbf{r} = (\omega_{a4}^2 - \omega_{a2}^2)\mathbf{R}\cdot\delta\mathbf{r}_p = \left(\frac{\delta\omega_a^2}{\delta\phi}\right)_R \delta\phi \mathbf{R}\cdot\delta\mathbf{r}_p.$$

The vector element $\delta\mathbf{r}_p$ is directed southward along the isobaric layer. Let $\varphi_p$ denote the angle between the isobar and the axis of the earth.

Then $\mathbf{R}\cdot\delta\mathbf{r}_p = R\delta s_p \sin\varphi_p$, so (3) takes the form

$$(3') \qquad -\int_c \omega_a^2 \mathbf{R}\cdot\delta\mathbf{r} = 2\omega_a \sin\varphi_p R\left(\frac{\delta\omega_a}{\delta\phi}\right)_R \delta\phi\delta s_p.$$

Here $R\delta\omega_a = \delta v$ is the variation in linear velocity along the equilibrium line from the lower to the upper isobar. When (2′) and (3′) are introduced in (1), we obtain

$$(4) \qquad 2\omega_a \sin\varphi_p\left(\frac{\delta v}{\delta\phi}\right)_R = \frac{1}{\alpha}\left(\frac{\delta\alpha}{\delta s}\right)_p.$$

This formula expresses quantitatively the result which was derived in the previous section: If the specific volume increases southward along the isobaric layer (vortex with cold core) the west wind increases with the distance from the equatorial plane.

Equation (4) gives the rate of increase of the west wind with the distance from the equatorial plane as a function of the rate of inflation of the isobaric layer. This formula is similar to equation 8·03(7), which gives the shear of the geostrophic wind with increasing height. However, whereas 8·03 (7) and the subsequent thermal wind formulas are approximate, based upon the assumption that the hydrostatic equation is valid, equation (4) is an exact result. Since $\omega_a$ never departs appreciably from $\Omega$, and the isobars are very nearly horizontal, we have approximately $\omega_a \sin\varphi_p \approx \Omega \sin\varphi = \Omega_z$. Assuming further that the velocity variation can be measured along the local vertical, instead of along the direction parallel to the axis of the earth, we have from (4)

$$(5) \qquad \frac{2\Omega_z}{g}\frac{\partial v}{\partial z} = -\frac{1}{\alpha}\frac{\partial\alpha}{\partial y} = -\frac{1}{T}\frac{\partial T}{\partial y},$$

which agrees with the approximate thermal wind equation 8·05(1).

**11·09. Circulation theorems in developed form.** The primitive circulation theorems are valid for arbitrary closed curves, when the integration along the curve is performed *at a fixed time.* The analysis of the mass distribution in zonal motion offers only one example of the numerous problems of a similar nature which may be successfully investigated with the aid of these theorems. The theorems reveal various characteristics of the *instantaneous* situation in the atmosphere. The primitive circulation theorems can therefore be characterized as *diagnostic* theorems.

More specialized theorems can be obtained by application of the circulation theorems to individual fluid curves consisting of the same fluid particles at all times. These *individual* circulation theorems make it

possible to estimate changes in the motion from one instant to the next, and can therefore be characterized as *prognostic* theorems.

**11·10. Transformation of the acceleration integral for closed individual curves.** An individual curve is defined as a curve which, once chosen, will always later consist of the same fluid particles. Let $\delta\mathbf{r}$ be a vector line element of such a curve. This element will move with the fluid and during the motion will generally change its length and orientation. If $\delta\mathbf{r}$ is the vector element (see fig. 11·10) at the time $t$, its position at the time $t + dt$ is determined by the displacements of its endpoints during the time element $dt$. It follows directly from the diagram, when we follow the two vector paths $A$ to $B$, that

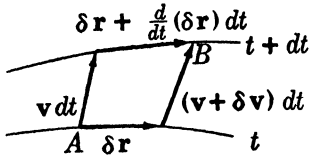


FIG. 11·10.

$$\mathbf{v}dt + \delta\mathbf{r} + \frac{d}{dt}(\delta\mathbf{r})dt = \delta\mathbf{r} + (\mathbf{v} + \delta\mathbf{v})dt. \tag{1}$$

Hence

$$\frac{d}{dt}(\delta\mathbf{r}) = \delta\mathbf{v}, \tag{2}$$

where $\delta\mathbf{v}$ is the variation of $\mathbf{v}$ at the time $t$ from the initial to the terminal point of the vector element $\delta\mathbf{r}$. The result (2) also follows directly from the fact that the two operations $d/dt$ and $\delta$ are independent and therefore interchangeable.

With the aid of (2) the acceleration integral in the primitive circulation theorem 11·04(1$a$) can be transformed. The integral element in this integral may be developed as follows:

$$\dot{\mathbf{v}}\cdot\delta\mathbf{r} = \frac{d}{dt}(\mathbf{v}\cdot\delta\mathbf{r}) - \mathbf{v}\cdot\frac{d}{dt}(\delta\mathbf{r}). \tag{3}$$

Substitution from (2) in the last term on the right gives

$$\dot{\mathbf{v}}\cdot\delta\mathbf{r} = \frac{d}{dt}(\mathbf{v}\cdot\delta\mathbf{r}) - \mathbf{v}\cdot\delta\mathbf{v} = \frac{d}{dt}(\mathbf{v}\cdot\delta\mathbf{r}) - \delta\left(\frac{v^2}{2}\right). \tag{3'}$$

The last step is evident, since $\delta(v^2) = \delta(\mathbf{v}\cdot\mathbf{v}) = 2\mathbf{v}\cdot\delta\mathbf{v}$. When (3′) is integrated around an arbitrary individual curve, the integral of the total differential $\delta(v^2/2)$ vanishes, and we have

$$\int_c \dot{\mathbf{v}}\cdot\delta\mathbf{r} = \int_c \frac{d}{dt}(\mathbf{v}\cdot\delta\mathbf{r}) = \frac{d}{dt}\int_c \mathbf{v}\cdot\delta\mathbf{r}. \tag{4}$$

The geometrical summation $\int_c$ and the time differentiation $d/dt$ are inde-

pendent for the same reason as in (2) and are therefore interchangeable. The last integral in (4) is by definition the circulation $C$. Using this notation (4) becomes

$$\int_c \dot{\mathbf{v}} \cdot \delta \mathbf{r} = \frac{dC}{dt}. \tag{5}$$

This important theorem was derived in 1869 by Lord Kelvin. It can be stated as follows: *The circulation integral of the acceleration taken around a closed individual fluid curve is equal to the rate of change of the circulation of the curve.* From this theorem Kelvin derived another theorem concerning the physical nature of the circulation.

**11·11. Individual circulation in absolute motion.** Kelvin's theorem holds both for absolute and relative motion. We shall apply it to the circulation theorem for absolute motion, 11·05(2). Substituting here from 11·10(5), we find for a moving fluid curve

$$\frac{dC_a}{dt} = N_{\alpha,-p}. \tag{1}$$

This is the theorem of individual circulation in absolute motion.

The theorem was originally developed by Lord Kelvin for the special case of a fluid whose density is a function of the pressure only, $\rho = \rho(p)$. Accordingly the density and, hence, the specific volume are constant on every isobaric surface. The isobaric and the isosteric surfaces coincide throughout the field, so no solenoids exist. Such a fluid is called *autobarotropic* (its mass field is automatically determined by the pressure field). In general, a fluid like the atmosphere is not autobarotropic, since the density depends not only upon the pressure but also upon the temperature and the humidity. Since an autobarotropic fluid contains no solenoids, theorem (1) reduces to

$$\frac{dC_a}{dt} = 0 \quad \text{or} \quad C_a = C_{a0}. \tag{2}$$

$C_{a0}$ is the initial circulation of the fluid curve and $C_a$ its circulation at an arbitrary later instant. Theorem (2) states: *The absolute circulation of a closed fluid curve is conserved in an autobarotropic fluid.* This theorem is the hydrodynamical equivalent of the law of conservation of angular momentum in elementary mechanics.

The complete theorem (1) was later developed by V. Bjerknes (1898) and can be stated as follows: *The rate of change of the absolute circulation of a closed individual fluid curve is equal to the number of pressure-volume solenoids embraced by the curve.* This theorem is equivalent to the

theorem in the mechanics of rigid bodies stating that the rate of change of the angular momentum of a system is equal to the resultant moment of the acting forces.

**11·12. Circulation of the latitude circles in zonal motion.** To illustrate the circulation theorem, 11·11(1), we shall examine the changes of the zonal circulation in a balanced circular vortex, when the vortex is disturbed by a symmetric perturbation. It was shown in section 11·07 that the solenoids in the circular vortex are annular tubes around the axis of the earth. Let the vortex be disturbed by a vortex ring perturbation, such that the particles on each parallel circle are given meridional impulses of equal strength and direction. This perturbation will not destroy the axial symmetry of the motion. Fluid curves which coincided with the circles of latitude before the perturbation are still circles of latitude after the perturbation, expanded from their original position at certain levels and contracted at other levels. Consequently the solenoids will remain annular tubes about the axis. So the expanding and contracting circles will never embrace solenoids and, from the theorem 11·11(1), their absolute circulation remains individually constant. Thus

$$\frac{dC_a}{dt} = 0 \quad \text{or} \quad C_a = \text{const.} \tag{1}$$

The absolute circulation of the latitude circle in zonal motion is

$$C_a = \int_c \mathbf{v}_a \cdot \delta\mathbf{r} = 2\pi R v_a = 2\pi R^2 \omega_a. \tag{2}$$

Substituting this expression in (1) we find

$$R^2 \omega_a = \text{const.} \tag{3}$$

This result resembles the law of conservation of angular momentum for a single particle. It could have been derived directly from this principle, for the moment about the axis of the forces acting on the fluid circle is zero. Equation (3) gives the simple rule that the absolute angular speed of an expanding or contracting circle changes in inverse proportion to the square of its radius.

**11·13. Relation between absolute and relative circulation.** The absolute circulation and the relative circulation are defined by the expressions

$$C_a = \int_c \mathbf{v}_a \cdot \delta\mathbf{r}, \qquad C = \int_c \mathbf{v} \cdot \delta\mathbf{r}. \tag{1}$$

The absolute and relative velocities are related by

6·16(3) $$\mathbf{v}_a = \mathbf{v} + \boldsymbol{\Omega} \times \mathbf{r},$$

where $\mathbf{r}$ is the position vector from an origin on the axis of the earth. We perform scalar multiplication of the three vectors in this equation by the vector line element $\delta\mathbf{r}$ of a closed fluid curve $c$ and integrate around the curve. Introducing the expressions (1) we find

(2) $$C_a = C + \int_c \boldsymbol{\Omega} \times \mathbf{r} \cdot \delta\mathbf{r}.$$

The integral on the right is the absolute circulation of the curve considered momentarily fixed to the earth. In the scalar triple product under the integral sign the dot and the cross may be interchanged (see section 6·14): $\boldsymbol{\Omega} \times \mathbf{r} \cdot \delta\mathbf{r} = \boldsymbol{\Omega} \cdot \mathbf{r} \times \delta\mathbf{r}$. Each integral element is then the scalar product of the constant vector $\boldsymbol{\Omega}$ and the vector $\mathbf{r} \times \delta\mathbf{r}$, so $\boldsymbol{\Omega}$ can be taken outside the integral sign. Thus

(3) $$C_a = C + \boldsymbol{\Omega} \cdot \int_c \mathbf{r} \times \delta\mathbf{r}.$$

This integral is the vector sum of the vector elements $\mathbf{r} \times \delta\mathbf{r}$ taken around the curve. When the curve $c$ lies in a plane the geometrical meaning of this *vector integral* is obtained as follows. Let the plane of the curve shown in fig. 11·13*a* intersect the axis of the earth at the point $O$, which

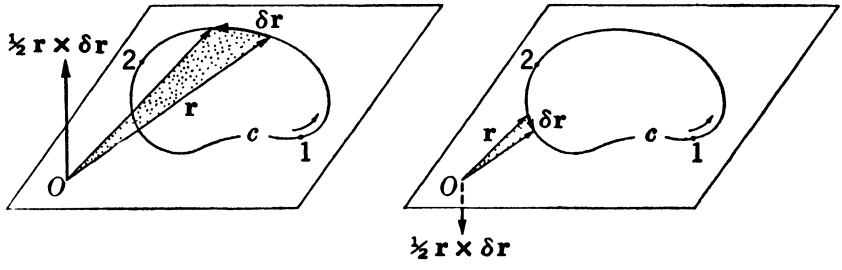



FIG. 11·13*a*. Vector area of closed curve.

may be chosen as the origin of the vector $\mathbf{r}$. The vector product $\mathbf{r} \times \delta\mathbf{r}$ is directed normal to the plane and is numerically equal to the area of the parallelogram formed by the two vectors. Thus the vector $\frac{1}{2}\mathbf{r} \times \delta\mathbf{r}$ has the magnitude of the shaded triangular area defined by the two vectors. The integral of the vector $\frac{1}{2}\mathbf{r} \times \delta\mathbf{r}$ taken along the upper branch of the curve from the point 1 to the point 2 is therefore a vector normal to the plane of the curve, having the same sense as the integration, and numerically equal to the sectorial area under the branch $1 \rightarrow 2$ of the curve.

The integral from 2 to 1 along the lower branch of the curve is a vector with opposite sense, having the magnitude of the sectorial area under the branch $2 \rightarrow 1$ of the curve. The total integral around the whole curve is therefore a vector normal to the plane of the curve, with the same sense as that of the integration, and numerically equal to the area enclosed by the curve. This vector is called the *vector area* of the curve and will be denoted by $\mathbf{A}$, where $A$ is the enclosed area. Accordingly we have

$$\mathbf{A} = \tfrac{1}{2} \int_c \mathbf{r} \times \delta\mathbf{r}. \tag{4}$$

This result, here derived for a plane curve, can be shown to hold generally for any skew curve, where $\mathbf{r}$ may be taken from an arbitrary origin. $\mathbf{A}$ is then a vector normal to the plane on which the projection of the curve encloses a maximum area, and is numerically equal to this area. When (4) is introduced in (3), we have

$$C_a = C + 2\boldsymbol{\Omega} \cdot \mathbf{A}. \tag{5}$$

This equation gives the relation between absolute and relative circulations on the earth.

Equation (5) can be verified directly for the special case of zonal motion. Consider one of the latitude circles with radius $R$, and perform the integration in the circulation integrals from west to east. The absolute circulation is

$$C_a = \int_c \mathbf{v}_a \cdot \delta\mathbf{r} = 2\pi R v_a = 2\pi R^2 \omega_a. \tag{6}$$

And the relative circulation is

$$C = \int_c \mathbf{v} \cdot \delta\mathbf{r} = 2\pi R v = 2\pi R^2 \omega. \tag{7}$$

The vector area $\mathbf{A}$ of the latitude circle is parallel to the axis of the earth, directed toward the north, and its magnitude is $\pi R^2$. Thus

$$2\boldsymbol{\Omega} \cdot \mathbf{A} = 2\pi R^2 \Omega. \tag{8}$$

Substituting the three expressions (6, 7, 8) in (5) and dividing out the factor $2\pi R^2$, we find $\omega_a = \omega + \Omega$, which verifies the theorem.

The sign of the scalar product in (5) is determined by the angle between the two vectors $\boldsymbol{\Omega}$ and $\mathbf{A}$. The sense of the vector $\mathbf{A}$ is determined by the sense of integration along the curve, which is open for choice. We shall now choose the sense of integration so that it has the

same sense as the rotation of the earth, as shown in fig. 11·13*b*. With this choice the angle between $\Omega$ and **A** is always acute (except when the plane of the curve is parallel to the axis of the earth). Let $\Sigma$ be the positive area enclosed by the equatorial projection of the curve. The scalar product $\Omega \cdot \mathbf{A}$ is then always a positive quantity equal to $\Omega\Sigma$, which introduced in (5) gives

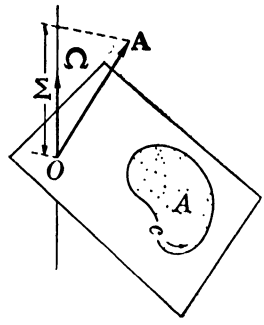



FIG. 11·13*b*. Equatorial projection of area of closed curve.

$$C_a = C + 2\Omega\Sigma. \tag{9}$$

Since the sense of integration has been chosen, a unique sign convention for the circulation is introduced: Circulation with the same sense as the rotation of the earth is positive, and circulation with the opposite sense is negative. For horizontal curves which do not intersect the equator the circulation is then *cyclonic* in both hemispheres if it has the same sense as the rotation of the earth, and *anticyclonic* if it has the opposite sense.

**11·14. Individual circulation relative to the earth.** The theorem for the change in relative circulation is obtained by time differentiation of equation 11·13(9); thus

$$\frac{dC_a}{dt} = \frac{dC}{dt} + 2\Omega \frac{d\Sigma}{dt}.$$

Substituting here for $dC_a/dt$ from 11·11 (1) and solving for $dC/dt$, we find

$$\frac{dC}{dt} = N_{\alpha,-p} - 2\Omega \frac{d\Sigma}{dt}. \tag{1}$$

With the chosen sense of integration the solenoidal term is positive when the sense ($\nabla\alpha \rightarrow -\nabla p$) of the solenoids is the same as the rotation of the earth, and is negative when the solenoids have the opposite sense.

Equation (1) is the theorem of circulation relative to the earth of an individual fluid curve. It is the most important of the circulation theorems for the study of atmospheric motion and is in usual meteorological language referred to simply as the *circulation theorem*. It can be stated as follows: *The rate of change of the circulation relative to the earth of an arbitrary closed fluid curve is determined by two effects: (i) the solenoid effect will tend to change the circulation in the sense of the solenoids by an amount per unit time equal to the number of solenoids embraced by the curve. (ii) The inertial effect will tend to decrease the circulation by an*

*amount per unit time proportional to the rate at which the projected area of the curve in the equatorial plane expands.*

This theorem holds for any closed fluid curve if the effect of friction is neglected. By appropriate choice of the curve many types of atmospheric motion which are too complicated for complete analytical treatment can be examined qualitatively.

It should be noted that the inertial term vanishes when the relative motion is zero. So the primary origin of the circulation (both absolute and relative) is the dynamic action of the solenoids. The effect of the inertial term is to modify relative circulation which already exists. This modification is of importance for every large-scale motion of the atmosphere.

The significance of the inertial term becomes clear when we consider curves which embrace no solenoids. This will be the case for any curve in an autobarotropic fluid, but the results will hold with rough approximation for horizontal curves, since in general few solenoids intersect the horizontal levels. In this case equation (1) may be integrated, and the circulation theorem becomes

$$C - C_0 = 2\Omega(\Sigma_0 - \Sigma). \tag{2}$$

This equation gives the following rule: A closed fluid curve, moving from one position into another, gains (or loses) an amount of circulation which is proportional to the decrease (or increase) in the area enclosed by the equatorial projection of the curve. For horizontal curves which do not intersect the equator the rule is simply: *The curve gains cyclonic circulation while its equatorial projection contracts, and it gains anticyclonic circulation while its equatorial projection expands.*

**11·15. Circulation of the circles in a local vortex.** The rule at the end of the preceding section explains in a qualitative way how cyclonic and anticyclonic circulations are generated in the atmosphere. It is a well-known empirical fact that a cyclone with closed isobars in the lower layers has horizontal convergence toward the central region, and consequently ascending motion with clouds and precipitation in the central part of the cyclone. Therefore all closed horizontal curves embracing the cyclone center contract and gain cyclonic circulation. Similarly the air over an anticyclone subsides and spreads out horizontally in the lower layers. So horizontal curves embracing the anticyclone center will expand and gain anticyclonic circulation.

Although these qualitative rules for the generation of cyclonic and anticyclonic circulations are similar, there is an important difference between the two processes when they are compared quantatively. To

demonstrate this difference we shall examine the following idealized model: The cyclone (or anticyclone) is assumed to have circular concentric streamlines with a uniform speed on each streamline. This model may be called a *local circular vortex*. We shall further assume that symmetrical convergence toward (or divergence from) the central region occurs in the vortex, and examine the change of circulation of the contracting (or expanding) fluid circles. If no solenoids intersect the horizontal levels, the circulation of the fluid circles changes in accordance with the theorem 11·14(2); thus

$$C + 2\Omega\Sigma = \text{const.} \tag{1}$$

Although the result will be valid in both hemispheres, we shall in the following restrict the discussion to a local vortex in the northern hemisphere. Let $R$ denote the radius of an arbitrary circle in the vortex, and let $\omega$ be the relative angular speed on this circle. The circulation around the circle is then

$$C = 2\pi R^2\omega. \tag{2}$$

Positive values of $\omega$ mean cyclonic circulation and negative values mean anticyclonic circulation. The area enclosed by the circle is $A = \pi R^2$, and the equatorial projection of the area (see fig. 11·15) is

$$\Sigma = A \sin\varphi = \pi R^2 \sin\varphi, \tag{3}$$

where $\varphi$ is the latitude of the axis of the vortex. Substituting these values of $C$ and $\Sigma$ in (1) and dividing out the constant factor $2\pi$, we find

$$R^2(\omega + \Omega_z) = \text{const.} \tag{4}$$

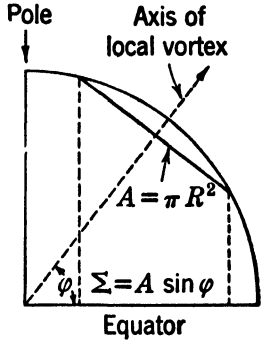



FIG. 11·15. Equatorial projection of circle in local vortex.

In the special case where the axis of the local vortex coincides with the axis of the earth this equation is identical to 11·12(3). Equation (4) gives the corresponding law for a vortex in arbitrary latitude: On a given fluid circular streamline, which expands or contracts because of symmetric horizontal divergence or convergence, the quantity $(\omega + \Omega_z)$ is inversely proportional to the square of the radius.

If the vortex has horizontal convergence toward the axis, the circles contract and $\omega$ increases, so the vortex gains cyclonic circulation. As the convergence continues, the radius of the contracting circle approaches zero, and from (4) $\omega + \Omega_z \to \infty$, or $\omega \to \infty$. Thus the cyclonic angular speed will increase indefinitely if the convergence continues to operate.

If the vortex has horizontal divergence out from the central region, the circles expand and $\omega$ decreases, so the vortex gains anticyclonic circulation. If the expansion were to continue until the radius approaches infinity, we should have from (4) $\omega + \Omega_z \to 0$, or $\omega \to -\Omega_z$. Actually the expansion can never proceed so far, so the anticyclonic angular speed which is generated by horizontal divergence is always numerically smaller than the critical value $-\Omega_z$. This limiting value corresponds to the anticyclone with the maximum strength of the horizontal pressure field, as was shown in section 7·21.

**11·16. Vorticity.** Any horizontal area $A$ bounded by a closed curve may be divided by two families of curves into infinitesimal elements $\delta A$, as shown in fig. 11·16. The sum of the circulations around the boundaries of these elements, taken all in the same sense, is equal to the circulation around the original boundary of the whole area. For in the sum the procession along each side common to two elements comes in twice — once for each element, but with opposite sense — and therefore disappears from the result. There remain then only the processions along those sides which are part of the original boundary. Thus, if $C$ denotes the circulation around the original boundary of $A$, and $\delta C$ denotes the circulation around an arbitrary element $\delta A$, we have

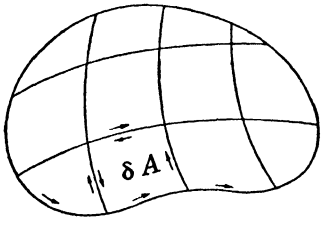


FIG. 11·16. Addition of circulation.

$$C = \int_A \delta C, \tag{1}$$

where the summation is extended over all the elements $\delta A$.

The limit of the ratio of the circulation $\delta C$ around an infinitesimal element to the area $\delta A$ of that element is called the vorticity, and is denoted by $\zeta$. Thus

$$\zeta = \frac{\delta C}{\delta A}. \tag{2}$$

In a rough sense the vorticity is the circulation around unit horizontal area. When $\delta C$ is eliminated from (1) by means of (2), we have

$$C = \int_A \zeta \delta A. \tag{3}$$

This theorem, given by Stokes (1854), states: *The circulation around a closed horizontal curve bounding any finite area $A$ is equal to the integral of the vorticity taken over the area $A$.*

The two-dimensional theorem stated here is only a special case of Stokes's theorem. The general three-dimensional theorem has the same form as (3) and is valid for an arbitrary surface in space bounded by a closed curve. The vorticity is then a vector and the scalar quantity $\zeta$, as defined by (2), is the component of the vector vorticity along the normal of the surface element $\delta A$. For horizontal areas and curves the quantity $\zeta$, which in the following will be called the vorticity, is actually the vertical component of the vector vorticity.

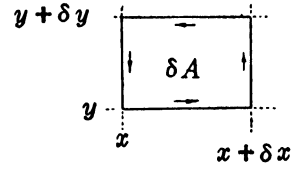


FIG. 11·17.

**11·17. The vorticity in rectangular coordinates.** Let the horizontal element of area be the infinitesimal rectangle $\delta A = \delta x \delta y$ shown in fig. 11·17. The circulation $\delta C$ around this element, taken in the sense of the positive $z$ axis (that is, with positive cyclic sense), is the sum of the processions along each of the four sides:

$$\delta C = v_x \delta x + \left(v_y + \frac{\partial v_y}{\partial x}\,\delta x\right)\delta y - \left(v_x + \frac{\partial v_x}{\partial y}\,\delta y\right)\delta x - v_y \delta y,$$

which reduces to

$$\delta C = \left(\frac{\partial v_y}{\partial x} - \frac{\partial v_x}{\partial y}\right)\delta x \delta y. \tag{1}$$

Dividing both sides by the area $\delta A = \delta x \delta y$, we have from 11·16(2) that

$$\zeta = \frac{\delta C}{\delta A} = \frac{\partial v_y}{\partial x} - \frac{\partial v_x}{\partial y}. \tag{2}$$

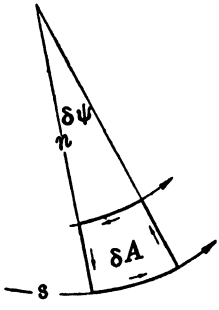


FIG. 11·18.

Equation (2) gives the analytical expression for the vorticity in rectangular coordinates.

**11·18. The vorticity in natural coordinates.** Next let the horizontal surface element be the infinitesimal area defined by two *streamlines* and two straight lines normal to the lower streamline, as in fig. 11·18. In the figure the two normals are extended in the horizontal plane to their point of intersection, which is the center of horizontal curvature of the lower streamline. Let $v$ be the speed on the lower streamline, and let $s, n$ be natural coordinates, as in 7·02. The circulation around this surface element, taken in the positive sense as shown by the arrows, is

$$\delta C = v R_S \delta\psi - \left(v + \frac{\partial v}{\partial n}\,\delta n\right)(R_S - \delta n)\delta\psi.$$

When the multiplication is performed, this expression reduces to

$$\delta C = \left( \frac{v}{R_S} - \frac{\partial v}{\partial n} + \frac{1}{R_S} \frac{\partial v}{\partial n} \delta n \right) R_S \delta\psi \delta n. \tag{1}$$

The third term in the parentheses approaches zero with $\delta n$. Thus, when both sides of the equation are divided by the area of the element, $\delta A = R_S \delta\psi \delta n$, we have

$$\zeta = \frac{\delta C}{\delta A} = vK_S - \frac{\partial v}{\partial n}, \tag{2}$$

which is the analytical expression for the vorticity in natural coordinates. According to this formula the vorticity manifests itself at any point in a horizontal current by the curvature of the streamlines, or by the horizontal rate of shear, or both. In absence of shear the vorticity has the same sign as the curvature. In a straight current the vorticity is positive if the speed increases to the right of the current, and negative if the speed increases to the left.

In the special case where the motion is a constant rotation with the angular speed $\omega$ about a vertical axis, the streamlines are concentric circles. The speed is here $v = \omega R_S$, and the rate of shear is $-\partial v/\partial n = \partial v/\partial R_S = \omega$. Substituting these values in (2) we find

$$\zeta = 2\omega. \tag{3}$$

In the field of constant rotation the vorticity is constant throughout and is equal to twice the angular speed of rotation. It can be shown that the vector vorticity in this case is a vector along the axis and is equal to twice the angular velocity.

**11·19. Absolute and relative vorticity.** The relation between absolute and relative circulations is given by the equation 11·13(5). If the curve is the edge of an infinitesimal horizontal surface element $\delta A$, and the absolute and relative circulations are denoted respectively by $\delta C_a$ and $\delta C$, we have

$$\delta C_a = \delta C + 2\boldsymbol{\Omega} \cdot \boldsymbol{\delta A}. \tag{1}$$

Here $\boldsymbol{\delta A}$ is the vector area of the surface element. Defining the circulation as positive when it has the same sense as the positive vertical, we have in both hemispheres $\boldsymbol{\delta A} = \delta A \mathbf{k}$. Substituting this in (1), and dividing the whole equation by $\delta A$, we find that

$$\zeta_a = \zeta + 2\boldsymbol{\Omega} \cdot \mathbf{k} = \zeta + 2\Omega_z. \tag{2}$$

With the sign convention chosen here, the absolute and relative vorticities are positive in both hemispheres when their sense is that of the positive

vertical. This sign convention is in accordance with the one introduced in chapter 7 for the angular speed. Accordingly, cyclonic vorticity is positive in the northern hemisphere and negative in the southern hemisphere. It should be noted that this sign convention is different from the one used for the circulation in 11·13(9) and subsequently for the circulation theorem in 11·14(1). In those formulas the circulation with the cyclic sense of the earth's rotation was positive. That gave the simplest rules for circulation of curves with an arbitrary orientation in space. In the northern hemisphere the two conventions are the same; in the southern hemisphere they are opposite.

If the atmosphere is at rest, the relative vorticity is everywhere zero. The absolute vorticity about the vertical is in this case $2\Omega_z$, and the vector vorticity can be shown to be $2\Omega$; see 11·18(3). In the general case the absolute vorticity is the sum of the vorticity relative to the earth and the absolute vorticity of the earth.

**11·20. The theorem of absolute vorticity.** From the theorems of circulation of individual moving curves equivalent theorems for the vorticity of individual moving particles may be derived. Consider an infinitesimal horizontal surface element $\delta A$ in a horizontal or nearly horizontal current. If the surface element is part of the fluid, its boundary will remain a closed curve moving with the fluid, and its absolute circulation $\delta C_a$ will change in accordance with the general theorem 11·11(1). Since the element is horizontal, the solenoids may be neglected, and the theorem takes the form

$$\frac{d}{dt}(\delta C_a) = 0. \tag{1}$$

Since $\delta A$ is infinitesimal, we have from 11·16(2)

$$\delta C_a = \frac{\delta C_a}{\delta A}\delta A = \zeta_a \delta A. \tag{2}$$

Substitution of (2) in (1) gives

$$\frac{d}{dt}(\zeta_a \delta A) = 0$$

or, when the differentiation is performed,

$$\frac{1}{\zeta_a}\frac{d\zeta_a}{dt} + \frac{1}{\delta A}\frac{d}{dt}(\delta A) = 0. \tag{3}$$

The second term is the rate of horizontal expansion of the moving ele-

ment per unit area. From 10·03(3) this is the horizontal divergence $\nabla_H \cdot \mathbf{v}$. Hence equation (3) can be written

$$\frac{d\zeta_a}{dt} = -\zeta_a \nabla_H \cdot \mathbf{v}. \tag{4}$$

This theorem is equivalent to the theorem 11·11(2) for horizontal motion. It states that the rate of change of the absolute vorticity of a moving element is proportional to its horizontal divergence. It should be noted that the theorem is exact only when the motion is strictly horizontal and the fluid autobarotropic. However, all large-scale atmospheric currents are so nearly horizontal, and the number of solenoids which intersect the horizontal levels are so few that the theorem can be used with sufficient accuracy at levels above the layer of friction. The theorem (4) is a special case of the famous vorticity theorem of Helmholtz (1858). The physical significance of Helmholtz' theorem, which involves the vector vorticity, is in every respect equivalent to that of the circulation theorem, 11·11(1).

**11·21. The theorem of relative vorticity.** When the expression 11·19(2) for the absolute vorticity is substituted in the theorem 11·20(4) we have

$$\frac{d}{dt}(\zeta + 2\Omega_z) = -(\zeta + 2\Omega_z)\nabla_H \cdot \mathbf{v}. \tag{1}$$

This is the theorem of relative vorticity. For horizontal motion it is equivalent to the theorem of relative circulation 11·14(2) and can also be derived directly from this theorem. The theorem (1) was derived by Rossby (1938) and has been used extensively by him and others for the analysis of the flow pattern in stationary and moving atmospheric waves.

Although the circulation theorem has a much simpler form and can be stated in brief and precise terms, the vorticity theorem has great advantages, particularly for the investigation of the structure of horizontal flow. The main reason is that the vorticity can be expressed analytically in terms of the velocity components, as in 11·17(2), or in terms of the curvature and shear of the flow pattern, as in 11·18(2).

The vorticity theorem (1) takes a convenient form when the differentiation is performed on the latitude term $2\Omega_z$. We have

$$\frac{d}{dt}(2\Omega_z) = 2\Omega \frac{d}{dt}(\sin\varphi) = 2\Omega \cos\varphi \frac{d\varphi}{dt}. \tag{2}$$

Here $d\varphi$ is the change of latitude of the moving particle during the time

element $dt$. Introducing the linear meridional displacement $dy = ad\varphi$, we have

$$\frac{d\varphi}{dt} = \frac{1}{a}\frac{dy}{dt} = \frac{v_y}{a}. \tag{3}$$

This is valid in both hemispheres when the $y$ axis points to the north (the standard system), and when $\varphi$ is counted positive in the northern hemisphere and negative in the southern hemisphere. Substituting (3) in (2), we have

$$\frac{d}{dt}(2\Omega_z) = \frac{2\Omega \cos\varphi}{a} v_y. \tag{4}$$

The vorticity theorem (1) can therefore be written

$$\frac{d\zeta}{dt} = -\frac{2\Omega \cos\varphi}{a} v_y - (\zeta + 2\Omega_z)\nabla_H \cdot \mathbf{v}. \tag{5}$$

If the horizontal flow is non-diverging, equation (5) becomes

$$\frac{d\zeta}{dt} = -\frac{2\Omega \cos\varphi}{a} v_y. \tag{6}$$

The factor $(2\Omega \cos\varphi)/a$ is positive in both hemispheres, so the vorticity decreases when the particle moves north and increases when the particle moves south. This rule is equivalent to the result already obtained in section 11·14 from the circulation theorem: When the particle, considered as a small horizontal disk, moves toward the pole its equatorial projection increases, and it gains anticyclonic vorticity. When the particle moves toward the equator its equatorial projection decreases, and it gains cyclonic vorticity.

**11·22. Air current crossing the equator.** As an example of the use of the vorticity theorem, consider a non-diverging current crossing the equator. Near the equator we have approximately $\cos\varphi = 1$, so 11·21(6) becomes

$$\frac{d\zeta}{dt} = -\frac{2\Omega}{a} v_y. \tag{1}$$

If the current crosses the equator from south to north, the vorticity of the particles moving with the current will decrease in both hemispheres. If the vorticity is zero at the southern origin of the current, the particles will arrive in the northern hemisphere with negative vorticity, which here is observed as anticyclonic. If the current crosses the equator from north to south, the particles will arrive in southern latitudes with posi-

tive vorticity, which here means anticyclonic vorticity. Therefore air which has newly crossed the equator has a tendency to show anticyclonic vorticity. According to 11·18(2) this vorticity shows up in the current as anticyclonic curvature or anticyclonic shear. In a broad current the shear is generally small, and the vorticity appears mainly as anticyclonic curvature of the current. A good example of this effect is found in the summer monsoon in India. As the thermal low develops over the Asiatic continent, a branch of the south-east trade wind of the southern hemisphere is forced to bend northward. As this current crosses the equator, it bends anticyclonically and arrives over India as a monsoon from the southwest.

**11·23. Air current crossing a mountain range.** If a broad and fairly straight current of air crosses a mountain range, it is well known from weather maps that a trough develops in the streamlines on the lee side of the mountain. This deformation of the current is easily explained in a qualitative sense from the vorticity theorem.

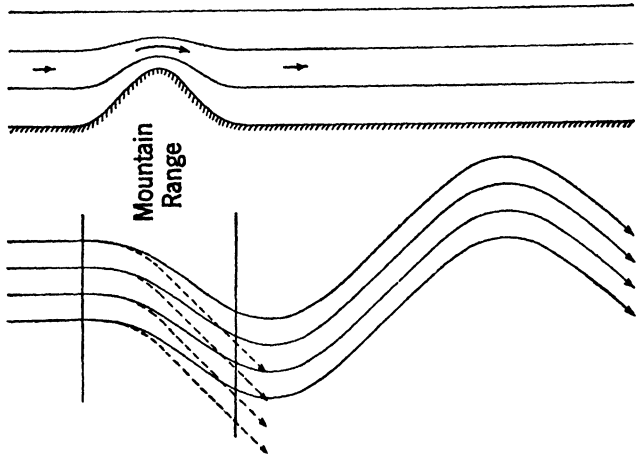



FIG. 11·23. Air current crossing a mountain range.

For simplicity it will be assumed that the current is a straight zonal current flowing from west to east, and that there is no horizontal shear in the current. Let this current be obstructed by a mountain range running normal to the current, as in fig. 11·23. Although the results will be valid in both hemispheres, we shall consider only the conditions in the northern hemisphere. We shall neglect the influence of friction in the surface layer and shall study the pure inertial effect caused by the presence of this obstacle. An air particle near the ground will flow uphill on the windward side and descend on the lee side of the mountain.

If the stratification of the air is stable, the flow at higher levels will be less modified by the obstacle, and above a certain level the deformation is negligible. The air below this level is subjected to vertical shrinking and horizontal divergence during its approach to the crest of the mountain, and to vertical stretching and horizontal convergence during its descent on the lee side of the mountain. The corresponding changes of the vorticity during the crossing are given by the vorticity theorem 11·21(5):

$$\frac{d\zeta}{dt} = -\frac{2\Omega \cos\varphi}{a} v_y - (\zeta + 2\Omega \sin\varphi)\nabla_H \cdot \mathbf{v}. \tag{1}$$

Since the current is zonal, $v_y = 0$, and the theorem reduces to

$$\frac{d\zeta}{dt} = -(\zeta + 2\Omega \sin\varphi)\nabla_H \cdot \mathbf{v}. \tag{2}$$

Hence the air particles gain anticyclonic vorticity on the windward side of the mountain, where the horizontal divergence is positive, and they gain cyclonic vorticity on the lee side of the mountain, where the horizontal divergence is negative. Since the current arrives at the obstacle without curvature or shear, and hence without any vorticity, the air particles acquire increasing anticyclonic vorticity during their climb. They pass over the crest of the mountain with a maximum of anticyclonic vorticity, which they subsequently lose during their descent on the lee side.

If the current and the mountain have infinite lateral extent to the north and to the south, no horizontal shear develops during the crossing. Thus the vorticity can show up only as a change of curvature of the current as indicated in fig. 11·23: increasing anticyclonic curvature on the windward side, maximum of anticyclonic curvature on the crest, and decreasing anticyclonic curvature on the lee side.

If equation (2) were valid during the entire crossing, the particles would lose exactly the same amount of vorticity during the descent as they gained during the ascent, and the current would leave the mountain as the straight current indicated by the broken streamlines. However, as soon as the anticyclonic turning begins, the particles obtain a velocity component toward the south, and the subsequent deformation of the current is controlled by the complete vorticity theorem, equation (1). Since $v_y < 0$, the latitude term is positive during the entire crossing. It counteracts the effect of the divergence until the crest is reached, but it cannot reverse the sign of this effect. Beyond the crest the latitude term and the divergence term have the same sign. The particles thus gain more vorticity during their descent than they lost during the ascent,

and the current will leave the mountain with cyclonic curvature, as indicated by the full streamlines in the figure.

In the absence of other kinds of divergence beyond the mountain range, the vorticity is from then on controlled only by the change in latitude. As a consequence the current gains cyclonic vorticity and curvature as long as the particles move south, that is, until the wind becomes a pure west wind. At this point the current has a maximum of cyclonic curvature and will consequently bend north. As the particles move north they lose their cyclonic vorticity and subsequently gain anticyclonic vorticity, so that the current eventually bends back anticyclonically again, and so on.

The effect of the mountain range upon an air current crossing it is thus to generate a stationary wave in the current beyond the mountains, beginning with a cyclonic trough immediately behind the mountain. Only this first cyclonic trough is usually well developed on the weather maps. The rest of the wave train is probably damped out by friction and other kinds of horizontal divergence which have not been considered here.

The stationary wave which develops in a current crossing a mountain range must evidently satisfy the tendency equation 10·07(3). Since the wave is stationary the pressure tendency must be zero throughout; thus

$$0 = -\int_{\phi}^{\infty} \nabla_H \cdot (\rho \mathbf{v}) \delta\phi + (g\rho v_z)_{\phi}. \tag{3}$$

The vertical motion at any point must have just the right value to balance the effect of divergence in the vertical column above the point. In a qualitative sense it is seen that this condition is satisfied. The upslope wind on the west side of the mountain will cancel the effect of the horizontal divergence in the vertical column above, and likewise the downslope wind on the lee side of the mountain will cancel the effect of the horizontal convergence in the vertical columns in this region.

**11·24. Non-diverging wave-shaped flow pattern.** In section 10·10 we made use of the concept of transport capacity in isobaric channels to examine the conditions for longitudinal mass divergence in wave-shaped patterns. In particular, we obtained the critical condition for zero longitudinal mass divergence by this *transport method.* A similar result may be derived from the vorticity theorem, as shown by Rossby. In this section we shall consider some of the physical implications of this *vorticity method,* and also attempt to bring out the points of similarity and difference between the two methods.

Consider a westerly current without horizontal shear, upon which is superimposed a wave disturbance of infinite lateral extent. The streamline amplitude is then independent of latitude. In such a wave the transversal divergence (section 10·12) is zero, and the total horizontal divergence is equal to the longitudinal divergence. We shall assume that there exists a level where the velocity divergence is zero and examine the conditions at that level.

We first note that, since both the transversal divergence and the longitudinal divergence are zero at that level, the zonal velocity component must be constant throughout the level, having the value $v$ of the actual speed at the trough line and the wedge line. Fig. 11·24 shows an

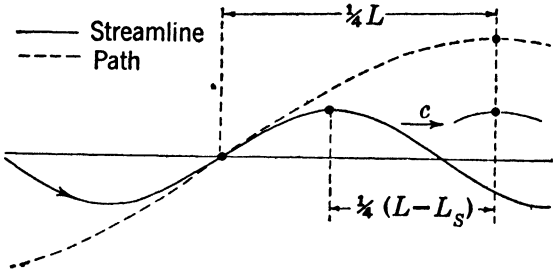



FIG. 11·24.

arbitrary streamline at the level of non-divergence, and also the path of the particle which at the time of the diagram is located at the inflection point of the streamline. The relation between the wave length $L_S$ of the streamline and the wave length $L$ of the path is obtained as follows: Let $T$ be the period during which the particle traverses one complete wave length of its path; thus

$$L = vT. \tag{1}$$

The particle arrives at the northern bend of the path after the time $\frac{1}{4}T$. The arrival of the particle at this point is simultaneous with the arrival of the streamline crest, because the wind must be from the west on this meridian at that time. Therefore the wave, moving with the speed of propagation $c$, travels the distance $\frac{1}{4}(L - L_S)$ during the time $\frac{1}{4}T$; hence

$$L - L_S = cT. \tag{2}$$

Taking the ratio between (2) and (1) and rearranging, we find

$$\frac{L_S}{L} = \frac{v - c}{v}. \tag{3}$$

The relation between the amplitude $A_S$ of the streamline and the amplitude $A$ of the path is obtained by considering the relative streamlines. As stated at the end of section 10·15, the relative streamlines are also the relative paths, and they therefore indicate the true meridional displacement of the air particles. So the amplitude $A_R$ of the relative streamline is equal to the amplitude $A$ of the path. From 10·15(2) we have then

$$\frac{A_S}{A} = \frac{v - c}{v}. \tag{4}$$

Accordingly, the amplitudes of the streamline and the path have the same ratio as their wave lengths, the ratio being that of the relative zonal wind to the actual zonal wind.

At the level of non-divergence the vorticity theorem 11·21(1) becomes

$$\frac{d}{dt}(\zeta + 2\Omega \sin \varphi) = 0.$$

According to this theorem the absolute vorticity, $\zeta + 2\Omega \sin \varphi$, remains constant for any given individual particle while it moves along the path. Since the current has no shear at the trough line and at the wedge line, the relative vorticity $\zeta$ at these lines is, from 11·18(2),

$$\zeta = vK_S.$$

Equating the absolute vorticity of the particle at the southern bend $P$ of the path (where the particle passes the longitude of the trough line) to its value at the northern bend $P'$ of the path (where the particle passes the longitude of the wedge line), we have

$$vK_S + 2\Omega \sin \varphi_P = vK'_S + 2\Omega \sin \varphi_{P'}. \tag{5}$$

This formula resembles 10·10(2′) for the transport capacity in a wave-shaped isobaric channel. When the longitudinal divergence is zero that formula becomes

$$Kv + 2\Omega \sin \varphi_S = K'v + 2\Omega \sin \varphi_{S'}. \tag{6}$$

$\varphi_S$ and $\varphi_{S'}$ are the latitudes respectively of the northern and the southern bends of the isobaric channel (assumed coincident with the streamline).

Although the two formulas (5) and (6) are similar, they are the statements of different physical principles. The vorticity formula (5) is satisfied when the horizontal velocity divergence is zero and the current is barotropic. This formula contains the curvatures of the streamline and equates the absolute vorticity at the southern and northern bends of the *path* at the times when the moving particle occupies these points.

The transport formula (6) is satisfied when the longitudinal mass divergence is zero. This formula contains the curvatures of the path and equates the transport capacities at the southern and northern bends of a *streamline* at one fixed time.

In general the two principles are not equivalent, for zero mass divergence usually does not mean zero velocity divergence. However, in the special case considered here the two formulas (5, 6) are equivalent. To show this we first rearrange the terms and write the two formulas as follows:

$$(7) \qquad (K_S - K'_S)v = 2\Omega\ (\sin\varphi_{P'} - \sin\varphi_P) = 4\Omega\cos\bar{\varphi}\sin\sigma_P,$$

$$(8) \qquad (K - K')v = 2\Omega\ (\sin\varphi_{S'} - \sin\varphi_S) = 4\Omega\cos\bar{\varphi}\sin\sigma_S.$$

$\bar{\varphi}$ is the central latitude of the streamline and the path, and $\sigma_P$, $\sigma_S$ are the angular amplitudes respectively of the path and the streamline. Taking the ratio between (7) and (8), we find

$$(9) \qquad \frac{K - K'}{K_S - K'_S} = \frac{\sin\sigma_S}{\sin\sigma_P}.$$

The formulas 10·10(6) give the kinematic relations which exist between the curvatures of the streamline and the path at the two bends. Substituting in (9) for $K$ and $K'$ from 10·10(6), we find:

$$(10) \qquad \frac{\sin\sigma_S}{\sin\sigma_P} = \frac{v - c}{v}.$$

A comparison of this formula with (4) would seem to indicate that (10) is slightly incorrect. The error is however only apparent. As in formula 10·11(7), the apparent error comes from a combination of spherical and plane methods. The two formulas (5, 6) are valid on a spherical level. When they are applied to streamlines and paths in a "plane level," for which the formula (4) is derived, a slight inconsistency will result.

The formula (9) is then correct at a level of non-divergence, and accordingly the two formulas (5, 6) are consistent. Later, in chapter 12, it will be shown how the condition for non-divergence is derived directly from the vorticity theorem.

**11·25. Export.** The vector area **A** of a closed curve was defined in section 11·13 as a vector normal to the plane of the curve and numerically equal to the area enclosed by the curve. Consider any closed fluid curve which moves along in a current. During a time element $dt$ a vector line element $\delta\mathbf{r}$ of the curve sweeps over the vector area $\mathbf{v}dt \times \delta\mathbf{r}$. The rate at

which the vector area of the curve changes is accordingly

$$\frac{d\mathbf{A}}{dt} = \int_c \mathbf{v} \times \delta\mathbf{r}. \tag{1}$$

This result can also be obtained by differentiation of equation 11·13(4).

We shall apply (1) to any horizontal curve in a *horizontal* atmospheric current. Taking the integration in the cyclic sense of the positive vertical, we have for such curves that $\mathbf{A} = A\mathbf{k}$, where $A$ is the area enclosed by the curve. Performing scalar multiplication in (1) with the vertical unit vector $\mathbf{k}$, and interchanging the dot and the cross in the scalar triple product under the integral, we find

$$\frac{dA}{dt} = \int_c \mathbf{k} \times \mathbf{v} \cdot \delta\mathbf{r}. \tag{2}$$

Let $\mathbf{n}$ be a horizontal unit vector normal to the curve, directed out from the region enclosed by the curve, and let $\delta s$ be the length of the vector element $\delta\mathbf{r}$. Then $\delta\mathbf{r} \times \mathbf{k} = \mathbf{n}\delta s$, and accordingly

$$\mathbf{k} \times \mathbf{v} \cdot \delta\mathbf{r} = \mathbf{v} \cdot \delta\mathbf{r} \times \mathbf{k} = \mathbf{v} \cdot \mathbf{n}\delta s = v_n \delta s. \tag{3}$$

It follows then that only the velocity component $v_n$ normal to the curve is subjected to the integration in (2). The integral in (2) is called the *export*, and will be denoted by $E$. Thus by definition

$$E = \int_c \mathbf{k} \times \mathbf{v} \cdot \delta\mathbf{r} = \frac{dA}{dt}. \tag{4}$$

There is a close mathematical analogy between the export and the circulation. Both are represented by line integrals around a closed curve, one integrating the normal component of the velocity and the other the tangential component.

The export has an additive property similar to that of the circulation, 11·16(1). Let the area $A$ which is enclosed by the curve be divided into infinitesimal elements $\delta A$ by two families of curves, as in fig. 11·16. The sum of the exports $\delta E$ from these elements is equal to the export $E$ through the original boundary of the whole area. For in the sum the transport through each side common to two elements comes in twice — once for each element — and therefore disappears from the result. There remain then only the transports through those sides which are parts of the original boundary, and consequently

$$E = \int_A \delta E. \tag{5}$$

The export $\delta E$ from the element $\delta A$ is, from (4), given by $\delta E =$

$d(\delta A)/dt$. And the export per unit area has the limiting value

$$\frac{\delta E}{\delta A} = \frac{1}{\delta A}\frac{d}{dt}(\delta A) = \nabla_H \cdot \mathbf{v}. \tag{6}$$

The expression on the right is, from 10·03(3), the horizontal divergence of the velocity field. When $\delta E$ is solved from (6) and substituted in (5), we obtain:

$$E = \int_A \nabla_H \cdot \mathbf{v}\,\delta A. \tag{8}$$

This theorem was derived by Gauss (1813) and states: *The export through a closed horizontal curve bounding an area is equal to the integral of the horizontal divergence over that area.*

The two-dimensional theorem stated here is only a special case of Gauss's theorem. The general three-dimensional theorem states that the export through a closed surface bounding a region is equal to the volume integral of the divergence over that region.

**11·26. Irrotational vectors.** A vector **a** is called *irrotational* in a given region if, for all closed curves in that region, the circulation integral of the vector is zero:

$$\int_c \mathbf{a} \cdot \delta\mathbf{r} = 0. \tag{1}$$

We have shown earlier that the circulation integral of a potential vector $\nabla\varepsilon$ is zero for any closed curve in the field of $\varepsilon$. The potential vector is accordingly irrotational. We shall now prove the converse statement, namely, that *any irrotational vector* **a** *is potential.* That is, we shall prove that the vector **a** can be represented as the ascendent of a scalar function $\varepsilon$, which is called the *potential* of **a**.

Consider an arbitrary closed curve in the field of the irrotational vector **a**. Any two points $P_0$ and $P$ on this curve divide the curve into two branches. Since the circulation integral (1) is zero, the procession integral of **a** from $P_0$ to $P$ along one branch is the negative of the procession integral from $P$ to $P_0$ along the other branch. The integral from $P_0$ to $P$ has accordingly the same value along both branches of the closed curve. Since the closed curve is arbitrary, we conclude that the procession integral of an irrotational vector is independent of the path. Let $P_0$ be a fixed point and $P$ a variable point. For any path from $P_0$ to $P$, the integral

$$\varepsilon = \int_{P_0}^{P} \mathbf{a} \cdot \delta\mathbf{r} \tag{2}$$

is then independent of the path. The integral $\varepsilon$ is therefore a function only of the position of the variable point $P$. The total differential of $\varepsilon$ is from (2)

$$\delta\varepsilon = \mathbf{a}\cdot\delta\mathbf{r}, \tag{3}$$

where $\delta\varepsilon$ is the variation of $\varepsilon$ through the displacement $\delta\mathbf{r}$. But, according to 4·13(1), the total differential of the scalar function $\varepsilon$ can also be written

$$\delta\varepsilon = \nabla\varepsilon\cdot\delta\mathbf{r}. \tag{4}$$

Since (3) and (4) hold for every direction of $\delta\mathbf{r}$, we have

$$\mathbf{a} = \nabla\varepsilon, \tag{5}$$

which proves the statement made at the outset.

The irrotational vector has thus two fundamental properties: (i) Its circulation integral around every closed curve is zero. (ii) It can be expressed as the ascendent (or gradient) of a scalar function, called the potential of the irrotational vector. Either one of these properties might be used as the definition of irrotational.

**11·27. Velocity potential.** It was shown in section 11·11 that the absolute circulation of individual fluid curves is conserved in an autobarotropic fluid. If the motion of such a fluid is started from absolute rest, the circulation of any fluid curve is initially zero and will then remain zero during the subsequent motion. The velocity is therefore an irrotational vector, and so the motion is called irrotational. For such a motion there exists, as shown in the preceding section, a scalar function $\varphi$, such that

$$\mathbf{v}_a = -\nabla\varphi. \tag{1}$$

The function $\varphi$ is called the *velocity potential.* Therefore irrotational flow also is called potential flow.

The above considerations lead to the following important conclusion: If an autobarotropic fluid (without friction) is started from rest, its motion is potential at any later time.

The existence of a potential makes the study of the motion rather simple. This is because the potential is a single scalar function, whereas the components of the velocity are a set of three scalar functions. The study of the motion of autobarotropic fluids has for this reason been brought to a high level of perfection in the field of classical hydrodynamics. However, the atmosphere is in general baroclinic, and the solutions of potential flow have therefore only limited interest for meteorology.

**11·28. Stream function.** Another application of the irrotational vector, which is useful for the study of atmospheric motion, will now be discussed. Consider any *horizontal* current in the atmosphere, and assume that in this current a level exists where the horizontal divergence of the velocity is zero. From Gauss's theorem 11·25(8) the export through any closed curve in that level is zero. Therefore, from 11·25(4),

$$\int_c \mathbf{k} \times \mathbf{v} \cdot \delta \mathbf{r} = 0 \tag{1}$$

for every closed horizontal curve in the level of non-diverging flow. The horizontal vector $\mathbf{k} \times \mathbf{v}$ is then irrotational at the level of non-divergence and, as shown in section 11·26, there exists a scalar function $\psi$ at that level such that

$$\mathbf{k} \times \mathbf{v} = -\nabla \psi. \tag{2}$$

The velocity is perpendicular to the vector $-\nabla\psi$, and is therefore everywhere parallel to the lines of constant $\psi$. These lines are consequently the streamlines, and the function $\psi$ is for this reason called the *stream function.* We have then the following important rule: *If a level of non-divergence exists in a horizontal current, the motion at that level can be described by a scalar stream function which is constant along the streamlines.* The stream function was introduced in this way by Lagrange (1781) and is sometimes called Lagrange's stream function. The stream function has, from (2), the dimensions

$$[\psi] = [v][\mathrm{L}] = [\mathrm{L}^2\mathrm{T}^{-1}]. \tag{3}$$

The variation of the stream function from streamline to streamline is obtained by integration of (2). If $P_0$ is a fixed point on the streamline $\psi_0$ and $P$ is a variable point, the value of $\psi$ at $P$ is given by

$$\psi_0 - \psi = \int_{P_0}^{P} \mathbf{k} \times \mathbf{v} \cdot \delta \mathbf{r} = \int_{P_0}^{P} v_n \delta s.$$

In the second integral $v_n$ represents the velocity component normal to the path of integration; see 11·25(3). The variation of the stream function from streamline to streamline accordingly measures the velocity transport in the channel between the two streamlines. That this transport is constant all along the channel is just another statement of the fact that the flow is non-diverging.

The existence of a stream function in a surface of non-diverging flow holds quite generally without any restriction as to the shape of the surface. The stream function may always be expressed analytically in

terms of curvilinear coordinates in the surface. If the levels are considered as spherical, the stream function in a level of non-diverging flow is most conveniently expressed in spherical coordinates. If only a limited region of the earth is considered, the level may in the first approximation be assumed a plane surface. The stream function can then be expressed as a function of the rectangular coordinates $x$, $y$ of the standard Cartesian system. In this case the rectangular components of (2) become

$$v_x = -\frac{\partial \psi}{\partial y}, \qquad v_y = \frac{\partial \psi}{\partial x}. \tag{4}$$

As a check we may substitute these values for the velocity components in the Cartesian expression for the horizontal divergence,

$$\nabla_H \cdot \mathbf{v} = \frac{\partial v_x}{\partial x} + \frac{\partial v_y}{\partial y}. \tag{10·03(1)}$$

It is seen that the horizontal divergence is zero when the velocity field satisfies the conditions (4).

The Cartesian expression for the vorticity is given by

$$\zeta = \frac{\partial v_y}{\partial x} - \frac{\partial v_x}{\partial y}. \tag{11·17(2)}$$

At a level of non-divergence where the velocity field is represented by a stream function $\psi$, the vorticity may be expressed in terms of the stream function. When the values (4) of the velocity components are substituted, we find that

$$\zeta = \frac{\partial^2 \psi}{\partial x^2} + \frac{\partial^2 \psi}{\partial y^2}. \tag{5}$$

If the vorticity is equal to zero, (5) becomes Laplace's differential equation for two dimensions. Accordingly, the flow at the level of non-divergence is irrotational if the stream function satisfies Laplace's equation.

CHAPTER TWELVE

# THEORY OF WAVES IN A ZONAL CURRENT

**12·01. The atmospheric equations.** The final goal of dynamic meteorology is the theoretical prediction of the weather, that is, from dynamic theory to determine the state of the atmosphere at some future time when its initial state is known. We are still far from the solution of this most general problem in atmospheric dynamics.

According to a fundamental mathematical principle a problem has no definite solution unless the number of independent equations is equal to the number of unknown variables. The unknown future state of the atmosphere is described by the velocity and the three physical variables of state. To solve for the vector variable $\mathbf{v}$ and the three scalar variables $p$, $\alpha$, $T$, one vector equation and three scalar equations are required. The one vector equation is the equation of motion. The three scalar equations are: the equation of continuity, the equation of state, and the equation of energy. The solution of the general problem of atmospheric motion calls for the integration of these simultaneous atmospheric equations.

However, the atmosphere is much too complex a " fluid system " to allow complete integration of the atmospheric equations with our present knowledge. Not only is it heterogeneous and of variable composition due to condensation and evaporation, but it is also a " thermally active " fluid continually receiving or losing heat. The atmospheric heat exchange is maintained primarily by radiation and condensation, which both depend upon the amount of water vapor in the air. The spatial distribution of the water vapor is continually being changed by the motion of the atmosphere. The motion, on the other hand, is primarily caused by the thermal action of heating and cooling and thus depends upon the moisture distribution. This interdependence between the motion and the distribution of water vapor leads to insurmountable mathematical difficulties in any complete theoretical analysis of atmospheric motion. However, some knowledge about the dynamic behavior of the atmosphere can be gained without complete integration.

The earlier chapters in this book illustrate one type of theoretical approach. A number of simple dynamic rules were developed from the several atmospheric equations. These rules were used to study the

motion which is actually observed in the atmosphere. The problem was to understand the observed behavior of the atmosphere and explain the evolution of the weather in terms of these dynamic rules. The study of wave motion in the westerlies in chapter 10 is a good example of this type of mixed theoretical-empirical approach.

If we wish to study the atmosphere with strictly theoretical methods, we must make some simplifying assumptions. Actually the equation of energy introduces an additional variable: the heat imparted to the moving particle. This would require further equations from the field of conduction and radiation of heat. It is therefore customary to eliminate the heat from dynamic problems by assuming that the changes of state of the air are prescribed. The temperature may then be eliminated from the equations of energy and state. The resulting equation, which gives the specific volume (or density) of the air particles as a function of their pressure, is called the equation of *piezotropy*, and an atmosphere whose physical behavior is restricted in this way is called a piezotropic atmosphere. For example, if the air particles are restricted to adiabatic changes the piezotropic equation is Poisson's equation. It should be noted that no work is performed by the air in a piezotropic atmosphere. The equation of piezotropy is for each particle represented by a line in the thermodynamic diagram. The particle can perform only processes along that line, and hence no cyclic process encloses any area. Therefore the piezotropic atmosphere, which is the only case as yet accessible to rigorous dynamic analysis, is thermally inactive.

Even for the piezotropic atmosphere we find that the complete integration of the atmospheric equations is too difficult. However, we already know one simple solution of the atmospheric equations, namely, steady zonal motion; see 11·07. Here the fields of pressure and mass are symmetric about the axis of the earth, and the air moves along the circles of latitude without any changes of state. The equations of continuity, state, and energy are then automatically satisfied. And the equation of motion is satisfied when the variation of the wind in the direction of the axis has the value prescribed by the solenoids; see 11·08(4). This solution also has great practical value, for it represents the first approximation to the motion actually observed in the atmosphere, when the variations arising from the asymmetric distribution of continents and oceans are eliminated. The moving cyclones and anticyclones which cause the daily changes in the weather are superimposed on this zonal motion. We know that these disturbances have closed circulation only in the lowest part of the atmosphere, and that in upper levels they are surmounted by wave-shaped flow patterns superimposed on the general westerly current. We also know that these upper waves

initially have small amplitudes, so that the wave motion may be regarded as a small perturbation superimposed on a steady zonal current.

The first step in a rational theory of atmospheric motion is therefore the study of wave-shaped perturbations with small amplitudes superimposed on a zonal current. In this problem the general atmospheric equations are reduced to linear equations which can be treated with relatively simple mathematical methods. V. Bjerknes has developed the general form of the linear atmospheric *perturbation equations* for small perturbations superimposed upon a completely arbitrary motion. With the aid of these perturbation equations H. Solberg and later C. L. Godske and B. Haurwitz have solved a large number of atmospheric problems — in particular, problems connected with wave motion in a sloping frontal surface separating two zonal currents. The solutions of these problems have thrown much light upon the dynamics of the formation and development of cyclones. A complete treatment of the perturbation theory, and some aspects of the dynamic cyclone theory is given in *Physikalische Hydrodynamik*,* chapters 7–13.

In the present chapter we shall consider only waves in a zonal current without internal frontal discontinuities. The complete solution of waves in a barotropic zonal current is discussed in sections 12·05–12·07. The dynamics of wave motion in baroclinic currents is discussed qualitatively later in section 12·08.

**12·02. Autobarotropy.** An atmospheric current has been called *barotropic* when the surfaces of constant specific volume (the isosteric surfaces) coincide with the isobaric surfaces throughout the current. In the general *baroclinic* case the isosteric surfaces intersect the isobaric surfaces, and the current contains solenoids.

In the barotropic case the geometric distribution of density is determined completely by the pressure distribution. Accordingly there exists for each barotropic situation a relation of the form $\rho = \rho(p)$, known as *the equation of barotropy*. For example, an atmospheric layer in hydrostatic equilibrium and having a constant lapse rate of virtual temperature is barotropic. Its equation of barotropy is given by 4·18(6) when the virtual temperature is eliminated by means of the equation of state.

Both barotropic and baroclinic currents may be specified to be piezotropic; that is to say, the physical changes of the individual moving particles may be prescribed by an equation of piezotropy (section 12·01). A current which at a given moment is barotropic does not, in general,

* V. Bjerknes, J. Bjerknes, H. Solberg, and T. Bergeron, *Physikalische Hydrodynamik*, Springer, Berlin, 1933.

remain barotropic even if its changes are piezotropic. Assume, for instance, that the air within a dry atmospheric layer in hydrostatic equilibrium changes state adiabatically. The layer is then both barotropic and piezotropic. When this layer is disturbed, it will remain barotropic if the lapse rate is dry adiabatic. But for any other value of the lapse rate the layer will become baroclinic.

In general a barotropic atmosphere will not remain barotropic unless its equation of barotropy is identical to its equation of piezotropy. If this condition is satisfied, the atmosphere is said to be *autobarotropic*. The corresponding equation of autobarotropy describes both the geometric distribution of the mass field in terms of the pressure field at any given time and also the physical change of each individual air particle during its motion. Simple examples of autobarotropy are: (i) an incompressible homogeneous atmosphere, (ii) an adiabatic atmosphere with adiabatic changes of state, (iii) an isothermal atmosphere with isothermal changes of state.

The barotropic currents which are investigated in the following sections are always assumed to be autobarotropic. For convenience they will nevertheless be referred to simply as barotropic currents.

**12·03. Boundary conditions.** In order to obtain explicit solutions of the atmospheric equations boundary conditions must be introduced.

At an internal boundary (or frontal surface) separating one air mass from another air mass with different motion and physical properties two boundary conditions must be satisfied, namely, the dynamic and the kinematic boundary conditions; see sections 8·08, 8·10. The solutions of cyclone waves in the polar front must satisfy both these boundary conditions.

At an external boundary or free surface the kinematic boundary condition is automatically satisfied, for the motion of a free surface is not restricted. The dynamic boundary condition at a free surface requires simply that the pressure be zero. The only free surface of the atmosphere is its outer limit.

At a fixed rigid boundary the dynamic boundary condition is automatically satisfied, for the fixed boundary can take up any pressure exerted by the fluid. The kinematic boundary condition at a fixed boundary requires that the velocity component normal to the surface be zero. The only rigid boundary of the atmosphere is the surface of the earth. On a level part of the surface of the earth the boundary condition is therefore that the vertical motion is zero.

In the single layer problem to be discussed below the only two boundary conditions to be satisfied are then: (i) $p = 0$ at the top of the atmosphere, (ii) $v_z = 0$ at the surface of the earth.

**12·04. Sinusoidal waves in a westerly current.** Some of the properties of waves in a westerly current were derived in chapter 10 with the aid of the transport method and the tendency equation. We shall now derive these results more rigorously by solving the atmospheric equations for small perturbations of a zonal current. We shall frequently refer to the earlier results during the development in the following sections. Whenever possible we shall use the same notations as in chapter 10.

In chapter 10 it was unnecessary to specify the analytical expression for the streamlines or the isobars. The results hold on a spherical earth for any wave-shaped flow pattern symmetrical about the north-south trough and wedge lines. Only in section 10·11 was the theory specialized to a sinusoidal wave on a flat earth. In the following we shall restrict our investigation to simple harmonic waves with sinusoidal streamline patterns. For such waves we shall be able to undertake a more complete quantitative analysis than was ever possible in chapter 10, and the mathematical treatment can be extended to levels of diverging flow.

Although much of the theory has been developed for a spherical earth by Haurwitz, we shall, in order to simplify the mathematical treatment, assume that the earth is flat. That is, as in 10·11, we shall consider a limited region of the earth where the levels may with sufficient accuracy be assumed to be horizontal planes. Within such a region the circles of latitude will be considered as parallel straight lines.

As in chapter 10, we shall first examine waves in a barotropic westerly current, and later proceed to the study of waves in the more real baroclinic westerly current.

**12·05. Waves in a barotropic current.** It was shown in section 11·07 that the speed of a barotropic zonal current has no variation in the direction parallel to the axis of the earth. The speed may have any variation normal to the axis. We shall now consider a barotropic westerly current which has no horizontal shear. Therefore in any given level the current has the same speed at all latitudes. It follows then that the current has the same speed at all levels within the region we consider.

In this barotropic current we shall examine a sinusoidal wave disturbance which has infinite lateral extent, so that all the streamlines have the same amplitude. We shall first assume that a level of non-divergence exists and study the motion at that level. The wave-shaped flow pattern at the level of non-divergence can be described by a stream function (section 11·28). Introducing a standard Cartesian system of coordinates, we shall show that this stream function has the form

$$\psi = -v[y - A_S \sin k(x - ct)]; \tag{1}$$

where $A_S$ is the streamline amplitude; $k = 2\pi/L_S$ is the wave number

(see 10·11); and $c$ is the speed of the wave. The constant factor $v$ must have the dimensions of a velocity to make the expression for the stream function dimensionally correct; see 11·28(3). It will be shown presently that $v$ is the speed of the undisturbed current.

At the time $t = 0$ an arbitrary streamline $\psi = \text{const}$ in the flow pattern (1) intersects the $y$ axis at the ordinate $y_0 = -\psi/v$. Substituting the value $\psi = -vy_0$ in (1) and dividing out the constant factor $v$, we find the equation for the streamlines:

$$y - y_0 = A_S \sin k(x - ct). \tag{2}$$

The different streamlines are obtained by assigning different values to $y_0$. They are all congruent sine curves. The streamline passing through the origin at the time $t = 0$ is the same as that examined in section 10·11.

The rectangular velocity components corresponding to the stream function (1) are obtained from the expressions 11·28(4). We find

$$\begin{aligned} v_x &= v, \\ v_y &= vkA_S \cos k(x - ct). \end{aligned} \tag{3}$$

The zonal velocity component has the constant value $v$ throughout the level of non-divergence. Hence the westerly current has the same speed in all latitudes, in accordance with the assumption made at the outset.

The paths of the individual air particles in the moving flow pattern (2) are obtained by integration of the simultaneous system

$$\begin{aligned} \frac{dx}{dt} &= v, \\ \frac{dy}{dt} &= vkA_S \cos k(x - ct). \end{aligned} \tag{4}$$

The $x$ equation can be integrated independently of the $y$ equation. The air particles which are on the $y$ axis at the time $t = 0$ have at any later time $t$ the abscissa

$$x = vt. \tag{5}$$

Substitution of this value of $x$ in the $y$ equation gives $dy/dt = vkA_S \cos k(v - c)t$. This equation can now be integrated. The air particle which has the ordinate $y_0$ on the $y$ axis at the time $t = 0$ has at any later time $t$ the ordinate

$$y = y_0 + \frac{v}{v - c} A_S \sin k(v - c)t. \tag{6}$$

The equations (5, 6) give the position of the particle with the initial

coordinates $(0,y_0)$ as a function of time. When the time is eliminated, we have

$$y - y_0 = \frac{v}{v-c} A_S \sin \frac{v-c}{v} kx. \tag{7}$$

This is the equation for the paths of the particles which cross the $y$ axis at the time $t = 0$. All the paths are congruent sine curves with the amplitude $A = A_S v/(v-c)$ and the wave length $L = L_S v/(v-c)$. This is in accordance with the more general formulas 11·24(3, 4).

The vorticity of the velocity field (3) is obtained from 11·17(2). We have

$$\zeta = \frac{\partial v_y}{\partial x} - \frac{\partial v_x}{\partial y} = -vk^2 A_S \sin k(x - ct). \tag{8}$$

The vorticity of the flow pattern (2) is thus independent of latitude. Its maximum cyclonic value, $vk^2 A_S = vK_S$, occurs at the trough line, and its maximum anticyclonic value, $-vk^2 A_S = vK_S'$, at the wedge line; see 10·11(6). The vorticity is zero halfway between these lines, where the streamline has zero curvature.

We shall now examine what restrictions the vorticity theorem imposes upon the flow pattern (2). For non-diverging barotropic flow the vorticity theorem is

$$\frac{d\zeta}{dt} + \frac{2\Omega \cos \varphi}{a} v_y = 0. \tag{11·21(6)}$$

The individual change of the vorticity may be separated into local and advective change by 10·04(2). Since the motion is horizontal we have

$$\frac{d\zeta}{dt} = \frac{\partial \zeta}{\partial t} + \mathbf{v}\cdot\nabla\zeta = \frac{\partial \zeta}{\partial t} + v_x \frac{\partial \zeta}{\partial x} + v_y \frac{\partial \zeta}{\partial y}. \tag{9}$$

When the value (8) for the vorticity is substituted in the three terms on the right side in (9), and the indicated differentiation is performed, we find

$$\frac{d\zeta}{dt} = (c - v)vk^3 A_S \cos k(x - ct) = -k^2(v - c)v_y. \tag{10}$$

With this value for $d\zeta/dt$ the vorticity theorem becomes

$$-k^2 \left( v - c - \frac{2\Omega a \cos^3 \varphi}{n^2} \right) v_y = 0. \tag{11}$$

In the parentheses the angular wave number $n$ has been substituted for the linear wave number $k$ from 10·11(3).

If the value of $v$ satisfies equation (11), the stream function (1) represents a moving wave-shaped flow pattern of such a nature that the individual particles retain constant absolute vorticity. Of all the flow patterns represented by (1), only the special one which also satisfies (11) has physical reality. This solution, characterized both by non-divergence and conservation of individual absolute vorticity, requires that the west wind relative to the moving wave have the critical speed:

$$v - c = \frac{2\Omega a \cos^3 \varphi}{n^2} = v_c. \tag{12}$$

This result, obtained by Rossby, is approximately the same as that derived from the transport method; see 10·11(7) and 10·10(11). The earlier result holds for the level of zero longitudinal divergence, which in the present case of an infinitely wide wave is the level of zero horizontal divergence.

Since the west wind must have the same speed at all levels in a barotropic current, equation (12) is satisfied at every level if it is satisfied at any one level. Therefore, as stated in section 10·14, if a level of non-divergence exists in a barotropic current, the entire flow is non-diverging. The pressure tendency is then zero at every point in the field, so the wave is stationary ($c = 0$). Therefore in a barotropic current the condition (12) is satisfied for a stationary wave only.

Conversely, if the barotropic wave moves, the flow has horizontal divergence at all levels, and at no level can the velocity field be represented by a stream function. However, if the wave has the same streamline amplitude in all latitudes, we shall show that the velocity field at a level of diverging flow is given by

$$\begin{aligned} v_x &= \bar{v} + \Delta v \sin k(x - ct), \\ v_y &= \bar{v} k A_{S0} \cos k(x - ct). \end{aligned} \tag{13}$$

Here $\bar{v}$ is the mean zonal wind; $\bar{v} + \Delta v$ and $\bar{v} - \Delta v$ are the wind speeds at the wedge and trough lines, respectively. As in 10·10(7), $\Delta v$ may be either positive or negative. Both $\bar{v}$ and $\Delta v$ are assumed to be independent of latitude. The significance of the amplitude factor $A_{S0}$ will be explained presently.

Since the streamline by definition is tangent to the velocity, the differential equation for the streamlines is

$$\frac{\delta y}{\delta x} = \frac{v_y}{v_x}. \tag{14}$$

When the velocity components (13) are substituted in (14), this equa-

tion can be integrated. The explicit equation for the streamlines of the velocity field (13) is found to be

$$y - y_0 = A_{S0} \frac{\bar{v}}{\Delta v} \ln \left[ 1 + \frac{\Delta v}{\bar{v}} \sin k(x - ct) \right]. \tag{15}$$

Here as in (2) $y_0$ is the ordinate where the streamline intersects the $y$ axis at the time $t = 0$. The amplitude $A'_S$ of the northern bend measured from the latitude $y = y_0$ is different from the amplitude $A_S$ of the southern bend. The two amplitudes are

$$\begin{aligned} A'_S &= A_{S0} \frac{\bar{v}}{\Delta v} \ln \left( 1 + \frac{\Delta v}{\bar{v}} \right), \\ A_S &= -A_{S0} \frac{\bar{v}}{\Delta v} \ln \left( 1 - \frac{\Delta v}{\bar{v}} \right). \end{aligned} \tag{16}$$

Evidently all the streamlines in the field (13) have the same amplitudes. If the horizontal divergence is small, $|\Delta v|$ is small compared with $\bar{v}$. We then have to the first order of approximation from (16) that $A'_S = A_S = A_{S0}$, and from (15) that

$$y - y_0 = A_S \sin k(x - ct). \tag{16'}$$

The streamlines are then approximately the same as the sinusoidal streamlines (2) at a level of non-divergence. The diverging velocity field (13) thus approaches the non-diverging velocity field (3) when $\Delta v \to 0$.

The zonal velocity amplitude $\Delta v$ is evidently proportional to the difference in transport across the trough line and the wedge line and is therefore a qualitative indication of the horizontal divergence in the current. The relation between $\Delta v$ and $\nabla_H \cdot \mathbf{v}$ is obtained by substitution of the velocity components (13) in the Cartesian expression 10·03(1) for $\nabla_H \cdot \mathbf{v}$. We then find that

$$\nabla_H \cdot \mathbf{v} = \frac{\partial v_x}{\partial x} + \frac{\partial v_y}{\partial y} = \Delta v k \cos k(x - ct), \tag{17}$$

or when $v_y$ is substituted from (13),

$$\nabla_H \cdot \mathbf{v} = \frac{\Delta v}{\bar{v}} \frac{v_y}{A_{S0}}. \tag{18}$$

This formula shows that the divergence is zero at the trough line and wedge line and has a maximum or minimum value halfway between these lines.

Another expression for the horizontal divergence is obtained from the

vorticity theorem 11·21(5):

$$-(\zeta + 2\Omega_z)\nabla_H \cdot \mathbf{v} = \frac{d\zeta}{dt} + \frac{2\Omega \cos \varphi}{a} v_y. \tag{19}$$

It is readily seen from (8) that the diverging field (13) has the same vorticity as the non-diverging field (3). The individual vorticity change in the field (13) is then given by the following equation similar to equation (10):

$$\frac{d\zeta}{dt} = -k^2(v_x - c)v_y. \tag{20}$$

Substituting this expression in (19) and introducing the critical speed $v_c = (2\Omega a \cos^3 \varphi)/n^2$, we find

$$(\zeta + 2\Omega_z)\nabla_H \cdot \mathbf{v} = k^2(v_x - c - v_c)v_y. \tag{21}$$

This formula confirms the results obtained from the conditions 10·10(11). In the region to the east of the trough ($v_y > 0$) the longitudinal divergence has the same sign as the deviation $v_x - c - v_c$ of the relative zonal wind from the critical speed. The formula (21) gives the quantitative expression from which the longitudinal divergence can be evaluated when the deviation $v_x - c - v_c$ is known.

When the ratio is taken between (21) and (18), we find

$$(\zeta + 2\Omega_z)\Delta v = \bar{v}k^2 A_{S0}(v_x - c - v_c).$$

Substituting here the value of $v_x$ from (13), we obtain

$$2(\zeta + \Omega_z)\Delta v = \bar{v}k^2 A_{S0}(\bar{v} - c - v_c). \tag{22}$$

This equation demonstrates the physical limitations of the theory presented here. From (8) the vorticity is given by

$$\zeta = -\bar{v}k^2 A_{S0} \sin k(x - ct), \tag{22'}$$

a function of $(x - ct)$. All the other quantities in (22) are constants along any given latitude. Equation (22) is then wrong, unless the velocity components of the wave disturbance in (13) are small. If the two amplitude factors $\Delta v$ and $A_{S0}$ are small of the first order, the product $\zeta \Delta v$ becomes small of the second order and may be dropped from (22). We then have:

$$2\Omega_z \Delta v = \bar{v}k^2 A_{S0}(\bar{v} - c - v_c), \tag{23}$$

which is now consistent. The simple harmonic wave motion (13) is therefore, strictly speaking, physically possible only when the velocity components due to the wave disturbance are infinitesimal. Nevertheless, it is reasonable to assume that the theory holds approximately also for waves of not too large finite amplitude.

**12·06. The pressure field in the barotropic wave.** When the motion is specified, the pressure field can be obtained from the equation of motion. The field of motion in the barotropic wave in the preceding section is given analytically in terms of the standard Cartesian components $x,y$. Accordingly, we shall use the Cartesian components of the equation of motion:

7·13(1) $$-\alpha \frac{\partial p}{\partial x} = \frac{dv_x}{dt} - 2\Omega_z v_y,$$

7·13(2) $$-\alpha \frac{\partial p}{\partial y} = \frac{dv_y}{dt} + 2\Omega_z v_x.$$

The individual time derivatives of the velocity components are separated into local and advective derivatives by 10·04(2). Since the motion is horizontal, we have:

(1)
$$\frac{dv_x}{dt} = \frac{\partial v_x}{\partial t} + \mathbf{v}\cdot\nabla v_x = \frac{\partial v_x}{\partial t} + v_x \frac{\partial v_x}{\partial x} + v_y \frac{\partial v_x}{\partial y},$$
$$\frac{dv_y}{dt} = \frac{\partial v_y}{\partial t} + \mathbf{v}\cdot\nabla v_y = \frac{\partial v_y}{\partial t} + v_x \frac{\partial v_y}{\partial x} + v_y \frac{\partial v_y}{\partial y}.$$

*Non-diverging flow:* We shall first examine the pressure field of the barotropic wave 12·05(2) at a level of non-divergence. When the velocity components 12·05(3) of this wave are substituted in the three terms on the right side in the equations (1) and differentiations are performed, we find the components of the acceleration at the level of non-divergence:

(2)
$$\frac{dv_x}{dt} = 0,$$
$$\frac{dv_y}{dt} = -(v - c)vk^2 A_S \sin k(x - ct).$$

The acceleration has no component in the $x$ direction, so the total acceleration is everywhere directed along the $y$ axis.

At the inflection points of the streamlines, halfway between the trough line and the wedge line, the acceleration is zero. This result may also be anticipated from earlier knowledge, if we for a moment imagine the acceleration separated into tangential and normal components. A particle at the inflection point on a streamline is from 12·05(7) also at the inflection point of its path. So the curvature of the path and hence the normal acceleration are zero. Furthermore, $v_y$ has an extreme value at the inflection point. So the actual speed of the air has the maximum

value $v(1 + k^2A_S^2)^{\frac{1}{2}}$ at this point, and hence the tangential acceleration is zero. The flow at an inflection point on a streamline is then both geostrophic and gradient. Consequently the isobars are parallel to the streamlines at the points of inflection on the streamline.

At the trough and wedge lines the acceleration has its extreme values. At the trough line it is

$$\left(\frac{dv_y}{dt}\right)_{\text{trough}} = (v - c)vk^2A_S = v^2K, \tag{3}$$

and at the wedge line it has the same numerical value, with negative sign. At every point on these lines the acceleration is directed normal to the path, so the tangential acceleration is zero. This also follows from the fact that the air speed has the minimum value $v$ at the trough and wedge lines. At these lines the paths 12·05(7) have, from 10·11(6), the curvature $d^2y/dx^2$. At the trough line the curvature is $K = (v - c)k^2A_S/v$. This verifies the last expression on the right in (3), the normal acceleration. Thus the tangential acceleration is zero, so the isobars are parallel to the streamlines at the trough and wedge lines. Hence these lines are also the trough and wedge lines of the pressure pattern.

The acceleration field (2) thus immediately reveals several characteristics of the pressure field at the level of non-divergence. The isobars are in phase with the streamlines, and have the same wave length. They

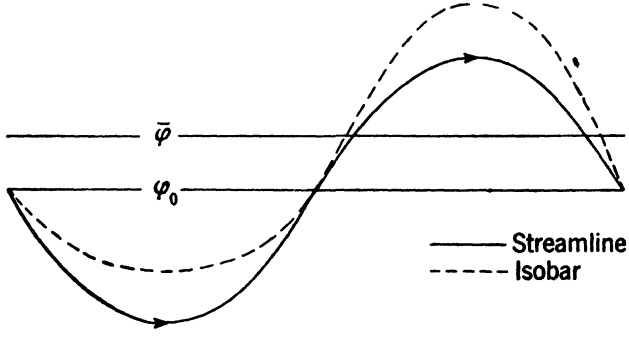



FIG. 12·06*a*. Isobar in sinusoidal non-diverging current.

are parallel to the streamlines at the points of inflection on the streamlines. The speed of the air has a minimum at the trough and wedge lines, and a maximum halfway between these lines, at the inflection points. Therefore air approaching the trough and wedge lines flows across the isobars toward higher pressure, and air leaving these lines flows across the isobars toward lower pressure. A pressure field which

satisfies these specifications is shown qualitatively by the isobar in fig. 12·06*a*. The isobar is, of course, only roughly sinusoidal.

The analytical expression for the pressure field is obtained when the acceleration components (2) and the velocity components 12·05(3) are substituted in the component equations of motion. We find then

$$
\begin{aligned}
-\alpha \frac{\partial p}{\partial x} &= -2\Omega_z v k A_S \cos k(x - ct), \\
-\alpha \frac{\partial p}{\partial y} &= -(v - c) v k^2 A_S \sin k(x - ct) + 2\Omega_z v.
\end{aligned} \tag{4}
$$

We shall first integrate these equations for the special case of a homogeneous and incompressible current. Later it will be shown how the result is modified for an arbitrary barotropic current.

At any given time the pressure variation $\delta p$ between any two neighboring points separated by the horizontal vector element $\delta \mathbf{r}$ is given by

$$
\delta p = \nabla_H p \cdot \delta \mathbf{r} = \frac{\partial p}{\partial x} \delta x + \frac{\partial p}{\partial y} \delta y. \tag{5}
$$

Let $p_0$ denote the pressure at the origin at the time $t = 0$. The pressure at the same time at any other point $(x,y)$ in the level is obtained by taking the line integral of $\delta p$ along any path from the origin to the point $(x,y)$. The integration is particularly simple when the path is taken along the $y$ axis from the origin (0,0) to the point $(0,y)$, and from there parallel to the $x$ axis to the point $(x,y)$. We note that $\delta x = 0$ along the first part of this path (which coincides with the $y$ axis), and that $\delta y = 0$ along the second part of the path (which is parallel to the $x$ axis). The line integral of (5) from the origin to the point $(x,y)$ is then

$$
p - p_0 = \int_{(0,0)}^{(0,y)} \frac{\partial p}{\partial y} \delta y + \int_{(0,y)}^{(x,y)} \frac{\partial p}{\partial x} \delta x. \tag{6}
$$

When this equation is multiplied by the constant factor $-\alpha$ and the expressions (4) are introduced, both integrals are easily evaluated. The results written in the reverse order are:

$$
\alpha(p_0 - p) = -2\Omega_z v A_S \sin k(x - ct) + 2\Omega v a (\cos \varphi_0 - \cos \varphi), \tag{7}
$$

where $\varphi_0$ and $\varphi$ are the latitudes respectively of the origin and the ordinate $y$.

The expression (7) may be checked by differentiating it partially with respect to $x$ and $y$, and comparing the results with (4). The partial derivative of (7) with respect to $x$ gives the $x$ component of (4). But

the partial derivative of (7) with respect to $y$ is

$$-\alpha \frac{\partial p}{\partial y} = -\frac{2\Omega \cos \varphi}{a} vA_S \sin k(x - ct) + 2\Omega_z v.$$

To make this expression the same as the $y$ component of (4), we must have:

$$(v - c)k^2 = \frac{2\Omega \cos \varphi}{a} = v_c k^2. \tag{8}$$

This condition has already been derived twice earlier, first by the transport method 10·10(11), and then in the last section 12·05(12) by the vorticity method.

The condition $v - c - v_c = 0$ at the level of non-divergence is thus derived here independently for the third time, and this time directly from the equations of motion (4). Only when the value of $v$ satisfies this condition will the velocity field 12·05(3) represent a solution of the equation of motion. Only then will the velocity field be adjusted to a pressure field (7) which is dynamically possible and consistent with the motion.

When the condition $v - c - v_c = 0$ is satisfied, equation (7) gives the analytical expression for the pressure field in a homogeneous wave. For an arbitrary barotropic wave the development is similar. The equation of autobarotropy gives $\alpha$ as a function of $p$. We may therefore define a function $\pi$ of $p$ as follows:

$$\pi(p) = \int_0^p \alpha \delta p. \tag{9}$$

The function $\pi$ is called the *barotropic pressure function*. It is equal to the dynamic elevation of the top of the atmosphere above the point with the pressure $p$. We have $\delta\pi = \alpha\delta p$, and therefore $\partial\pi/\partial x = \alpha\partial p/\partial x$, $\partial\pi/\partial y = \alpha\partial p/\partial y$. When these expressions are substituted in (4) the integration may be carried out exactly as in the homogeneous case, and we find the following equation similar to equation (7):

$$\pi_0 - \pi = -2\Omega_z v A_S \sin k(x - ct) + 2\Omega va (\cos \varphi_0 - \cos \varphi). \tag{10}$$

Here $\pi_0 = \pi(p_0)$ is the value at the origin at the time $t = 0$. An isobar, $\pi = \text{const}$, of the barotropic field (10) has the same shape as the corresponding isobar in the homogeneous field (7). Only the spacing of the isobars is different.

Consider the isobar $p_0$ passing through the origin at the time $t = 0$; from (7) it has the equation:

$$2\Omega a (\cos \varphi - \cos \varphi_0) = -2\Omega_z A_S \sin k(x - ct).$$

Introducing $A_S = a \tan \sigma_S$ and dividing out the factor $2\Omega a$, we find

$$\cos \varphi - \cos \varphi_0 = -\tan \sigma_S \sin \varphi \sin k(x - ct). \tag{11}$$

Since the origin may be placed in any latitude, this equation holds for any isobar in the field. Equation (11) confirms the earlier results as to the relation between the pressure pattern and the flow pattern: The two patterns are in phase and have the same wave length. The equation shows further that the shape of the isobar is independent of $v$ and $c$. Therefore, the shape of the pressure pattern is completely determined by the shape of the flow patterns, and it is independent of the propagation of the flow pattern and the intensity of the flow.

To investigate how much the pressure pattern deviates from the flow pattern, we shall determine the latitudes of the southern and northern bends of the isobar (11). As in 10·10, we denote these latitudes respectively by $\varphi$ and $\varphi'$. At the two bends we have then from (11):

$$\begin{aligned} \cos \varphi - \cos \varphi_0 &= \tan \sigma_S \sin \varphi, \\ \cos \varphi' - \cos \varphi_0 &= -\tan \sigma_S \sin \varphi'. \end{aligned} \tag{12}$$

Subtracting the lower from the upper equation, and introducing the notation of 10·10(4), we find:

$$2 \sin \bar{\varphi} \sin \sigma_p = 2 \tan \sigma_S \sin \bar{\varphi} \cos \sigma_p,$$

or

$$\tan \sigma_p = \tan \sigma_S. \tag{13}$$

The isobars and the streamlines have the same amplitudes at a level of non-divergence.

If the wave is stationary this result follows immediately from a fundamental theorem by Bernoulli. This theorem is most conveniently derived from the tangential equation of motion: Using the formula 10·04(2), the tangential acceleration is expressed as the sum of the local and the advective changes:

$$\frac{dv}{dt} = \frac{\partial v}{\partial t} + \mathbf{v} \cdot \nabla v.$$

In steady flow no local changes occur, so $\partial v/\partial t = 0$. The component of $\nabla v$ along $\mathbf{v}$ is $\partial v/\partial s$, so the advective change is $\mathbf{v} \cdot \nabla v = v \partial v/\partial s$. We substitute this value of the tangential acceleration in 7·13(4) and find

$$v \frac{\partial v}{\partial s} = -\alpha \frac{\partial p}{\partial s}.$$

Introducing from (9) the barotropic pressure function $\pi$ we have

$\alpha\partial p/\partial s = \partial\pi/\partial s$. The above equation then becomes:

$$\frac{\partial}{\partial s}\left(\frac{v^2}{2}+\pi\right)=0. \tag{14}$$

This is *Bernoulli's theorem* in differential form. It may be stated as follows: *When a barotropic fluid has any steady horizontal motion the sum of the kinetic energy per unit mass and the barotropic pressure function has no variation along the streamlines.* The theorem is named after Daniel Bernoulli (1700–1783), who founded the science of hydrodynamics.

We shall now apply Bernoulli's theorem to the stationary barotropic wave. Since the speed is the same at the southern and northern bends of the streamline, the barotropic pressure function also has the same value at these points. So the same isobar passes through both bends of the streamline and has accordingly the streamline amplitude. Bernoulli's theorem also shows that the streamlines have their highest pressure at the trough and wedge where the speed is minimum, and their lowest pressure at the inflection points where the speed is maximum; see fig. 12·06*a*. The pressure drop along the streamline from trough (or wedge) to inflection point is given by:

$$\bar{\alpha}\Delta p = \tfrac{1}{2}v_{y0}^2 = \tfrac{1}{2}(vkA_S)^2.$$

For example, at a level where $v = 10\ \mathrm{m\,s^{-1}}$, $\bar{\alpha} = 1000\ \mathrm{m^3\,t^{-1}}$, a wave at 60° lat having $n = 6$, $\sigma_S = 5°$ would have a pressure variation $\Delta p = 0.5$ mb along its streamlines. The deviation of the isobar from the streamline in a stationary wave may be estimated by this method.

The deviation of the pressure pattern from the flow pattern is obtained more directly from the equations (12), which hold for both a moving and a stationary wave. When these equations are added we find

$$2\cos\bar{\varphi}\cos\sigma_p - 2\cos\varphi_0 = -2\tan\sigma_S\cos\bar{\varphi}\sin\sigma_p.$$

We substitute here from (13) $\sigma_S = \sigma_p$, and find after rearrangement of the terms:

$$\cos\bar{\varphi} = \cos\varphi_0\cos\sigma_p. \tag{15}$$

The central latitude $\bar{\varphi}$ of the isobar is accordingly north of the latitude $\varphi_0$, as indicated in fig. 12·06*a*. Equation (15) holds for any isobar in the field. The isobar passing through the inflection points of an arbitrary streamline deviates at the trough and wedge from that streamline by the amount $\bar{\varphi} - \varphi_0$. The values of $\bar{\varphi} - \varphi_0$ for different latitudes and amplitudes are shown in table 12·06*a*, computed from (15). The value of $\bar{\varphi} - \varphi_0$ is a good indication of the deviation of the pressure pattern from the flow pattern. In a given latitude the deviation is determined com-

pletely by the amplitude of the isobar and is independent of the wave length, the wind speed, and the speed of the wave. In high latitudes the deviation of the two patterns is negligible. In low latitudes the deviation is appreciable, particularly when the amplitude is large.

TABLE 12·06*a*

$\bar{\varphi} - \varphi_0$ TABULATED

| $\sigma_p$ | $\varphi_0$ | | | |
|---|---|---|---|---|
| | 10° | 30° | 50° | 70° |
| 5° | 1.2° | 0.4° | 0.2° | 0.1° |
| 10° | 4.1° | 1.5° | 0.7° | 0.3° |
| 15° | — | 3.2° | 1.6° | 0.7° |

It was shown in section 10·14 that the non-diverging barotropic wave must be stationary. It may therefore seem unnecessary to investigate its pressure field as if it were a moving wave. However, the results derived above will hold approximately at a level of non-divergence in a baroclinic wave. We shall therefore need the general derivation for moving waves later in the study of the baroclinic waves.

*Diverging flow:* We shall now examine the pressure field in the moving barotropic wave, which has horizontal divergence at all levels. It has been shown that the velocity field at any level in such a wave is given by 12·05(13) when the two amplitude factors $|\Delta v|$ and $A_{S0}$ are sufficiently small. For small $|\Delta v|$ the amplitude factor $A_{S0}$ becomes the streamline amplitude $A_S$; see 12·05(16). In the following development we shall accordingly write $A_{S0} = A_S$ and drop all terms containing squares or products of $\Delta v$ and $A_S$. The streamlines of the wave 12·05(13) are given by 12·05(15). For infinitesimal amplitudes this expression becomes

$$y - y_0 = A_S \sin k(x - ct). \tag{16}$$

The flow pattern has simple sinusoidal streamlines as in the case of non-diverging flow.

The pressure field is obtained from the equations of motion. We first substitute the velocity field 12·05(13) in (1) and find the corresponding acceleration field:

$$\begin{aligned} \frac{dv_x}{dt} &= (\bar{v} - c)\Delta v k \cos k(x - ct), \\ \frac{dv_y}{dt} &= -(\bar{v} - c)\bar{v}k^2 A_S \sin k(x - ct). \end{aligned} \tag{17}$$

These expressions and the velocity components are introduced in the component equations of motion, which then become:

$$
\begin{aligned}
-\alpha\frac{\partial p}{\partial x} &= [(\bar{v}-c)\Delta v - 2\Omega_z\bar{v}A_S]k\cos k(x-ct),\\
-\alpha\frac{\partial p}{\partial y} &= -[(\bar{v}-c)\bar{v}k^2A_S - 2\Omega_z\Delta v]\sin k(x-ct) + 2\Omega_z\bar{v}.
\end{aligned}
\tag{18}
$$

These equations may now be integrated exactly like the equations (4), and we find an equation similar to (10):

$$\pi_0 - \pi = [(\bar{v}-c)\Delta v - 2\Omega_z\bar{v}A_S]\sin k(x-ct) + 2\Omega a\bar{v}\,(\cos\varphi_0 - \cos\varphi), \tag{19}$$

where $\pi$ is given by (9). The partial derivative of (19) with respect to $x$ gives the $x$ equation (18). The partial derivative of (19) with respect to $y$ is the same as the $y$ equation (18) only when

$$2\Omega_z\Delta v = \bar{v}k^2A_S(\bar{v}-c) - \bar{v}A_S\frac{2\Omega\cos\varphi}{a} = \bar{v}k^2A_S(\bar{v}-c-v_c). \tag{20}$$

But this is the earlier condition 12·05(23), derived from the vorticity theorem. Only when the parameters in the velocity field 12·05(13) satisfy this condition does that field represent a solution of the equation of motion.

We substitute in (19) the value of $\Delta v$ from (20) and introduce two abbreviations:

$$\xi = \frac{k}{2\Omega_z} = \frac{n}{\Omega a\sin 2\varphi}, \tag{21}$$

$$\eta = \xi^2(\bar{v}-c)(\bar{v}-c-v_c). \tag{22}$$

The resulting equation

$$\pi_0 - \pi = -2\Omega_z\bar{v}(1-\eta)A_S\sin k(x-ct) + 2\Omega a\bar{v}\,(\cos\varphi_0 - \cos\varphi) \tag{23}$$

gives the barotropic pressure function in the wave with the velocity field 12·05(13). We shall now study the relation between the flow pattern (16) and the pressure field (23) in this wave.

For the isobar $\pi_0$ through the origin at $t = 0$ we find, similar to (11),

$$\cos\varphi - \cos\varphi_0 = -(1-\eta)\tan\sigma_S\sin\varphi\sin k(x-ct). \tag{24}$$

This equation differs from (11) only in the amplitude factor $(1-\eta)$. When the development subsequent to (11) is repeated for (24), we find

$$\tan\sigma_p = (1-\eta)\tan\sigma_S, \tag{25}$$

$$\cos\bar{\varphi} = \cos\varphi_0\cos\sigma_p. \tag{26}$$

The deviation $\bar{\varphi} - \varphi_0$ between the central latitudes of a streamline and the isobar passing through its inflection points is from (26) and (15) the same in the diverging and the non-diverging wave.

The amplitudes are equal when $\eta = 0$, that is, when the relative zonal wind either is zero or has the critical speed $v_c$. In the first case both amplitudes are zero; see 10·15(3). In the second case the flow is non-diverging and (25) reduces to (13). For supercritical and for negative relative zonal wind ($\eta > 0$) the streamline amplitude is larger than the isobar amplitude. For subcritical, positive relative zonal wind ($\eta < 0$) the streamline amplitude is smaller than the isobar amplitude; see fig. 12·06*b*.

For any given value of the relative wind the magnitude of the amplitude difference is determined by the factor $\xi^2$ in $\eta$. The values of $\xi$ for different latitudes and wave numbers are shown in table 12·06*b*. For a

TABLE 12·06*b*

$\xi = n(\Omega a \sin 2\varphi)^{-1}$ M$^{-1}$ S, TABULATED

| $\varphi$ | $n$ | | | | |
|---|---|---|---|---|---|
| | 2 | 3 | 6 | 10 | 20 |
| 45° | 0.0043 | 0.0064 | 0.0129 | 0.0216 | 0.0431 |
| 40°, 50° | 0.0044 | 0.0066 | 0.0132 | 0.0219 | 0.0438 |
| 30°, 60° | 0.0050 | 0.0075 | 0.0149 | 0.0249 | 0.0498 |
| 20°, 70° | 0.0067 | 0.0101 | 0.0201 | 0.0335 | 0.0671 |
| 10°, 80° | 0.0126 | 0.0189 | 0.0378 | 0.0630 | 0.1260 |

given wave length the minimum value of $\xi$ occurs at 45° lat and its variation in the belt from 30° to 60° lat is quite small. To estimate the value of $\eta$ in this range of latitudes, consider a case where the relative zonal wind and its deviation from the critical speed both have the order of magnitude 10 m s$^{-1}$. For a relatively long wave ($n = 6$) $\eta$ is then about 0.02. For a short wave ($n = 20$) $\eta$ is about 0.2. We shall show in the next section that $\eta$ is usually very small in the barotropic wave. So the amplitude difference is therefore negligible. However, the above analysis also holds approximately at a level of diverging flow in a baroclinic wave. Since the wind increases with height in these waves, both the relative wind and its deviation from the critical value may be large at high levels. Here $\eta$, and hence the amplitude difference, may be appreciable, particularly for short waves in very high or very low latitudes.

It remains to show how the isobar runs at the inflection points of the streamline. Let $\psi_S$ and $\psi_p$ denote the angles which the streamline and the isobar make with the $x$ axis at these points. Differentiation of (16)

and (24) gives at the inflection point east of the trough:

$$\tan \psi_S = \left(\frac{\delta y}{\delta x}\right)_0 = kA_S,$$

$$\tan \psi_p = \left(\frac{a\delta\varphi}{\delta x}\right)_0 = (1-\eta)kA_S;$$

therefore

$$\tan \psi_p = (1-\eta)\tan \psi_S. \tag{27}$$

Accordingly, the angle $\psi_S - \psi_p$ has the same sign as $\eta$. For non-diverging flow ($\eta = 0$) the isobar is parallel to the streamline at the inflection point in accordance with the earlier result. For supercritical and for negative relative zonal wind ($\eta > 0$) the air at the inflection point

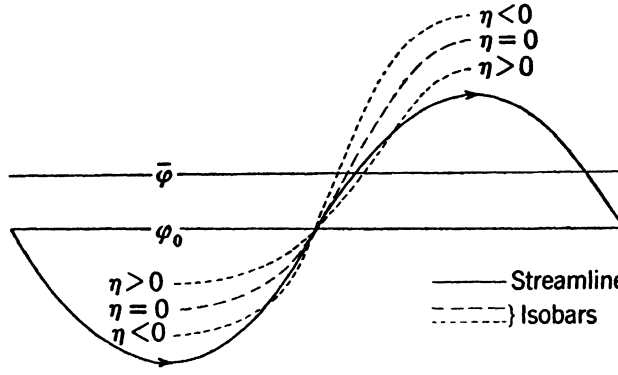



FIG. 12·06*b*. Isobars in sinusoidal diverging current.

east of the trough flows across the isobar toward higher pressure. And for subcritical, positive relative zonal wind ($\eta < 0$) the air at that point flows across the isobars toward lower pressure. The three cases are shown schematically in fig. 12·06*b*. Since $\eta$ is very small in the barotropic wave, the isobars are here nearly parallel to the streamlines at the inflection point.

**12·07. The speed of propagation of the barotropic wave.** In the analysis in the preceding section not all the atmospheric equations at our disposal have been used. The equations of state and of thermal energy are automatically accounted for by the equation of autobarotropy. Besides this condition only the horizontal component of the equation of motion has been considered so far. The remaining equations are the vertical (hydrostatic) equation and the equation of continuity. These equations enable us to find the speed of propagation of the barotropic wave.

It was shown in section 10·07 how the hydrostatic equation and the equation of continuity combine into the tendency equation. We shall first evaluate the pressure tendency *at the surface of the earth.* The tendency equation is here

10·07(4) $$\frac{\partial p}{\partial t} = -\int_0^\infty \nabla_H \cdot (\rho \mathbf{v}) \delta\phi.$$

Note that by writing the tendency equation in this form we make use of the boundary condition $v_z = 0$ at the *lower boundary* of the atmosphere. We separate the mass divergence into two terms, as follows:

$$\nabla_H \cdot (\rho \mathbf{v}) = \rho \nabla_H \cdot \mathbf{v} + \mathbf{v} \cdot \nabla_H \rho.$$

It was stated in the preceding section that the isobars, and hence the isosteres, are very nearly parallel to the streamlines in the barotropic wave, so $\mathbf{v} \cdot \nabla_H \rho \approx 0$. The justification of this approximation is discussed at the end of this section. Substituting from 12·05(17) for the horizontal velocity divergence we find then

$$\nabla_H \cdot (\rho \mathbf{v}) = \rho \Delta v k \cos k(x - ct).$$

The value of $\Delta v$ is given by 12·06(20). It was shown at the outset in section 12·05 that the barotropic current has the same speed at all levels. That makes $\Delta v$ also the same at all heights. The tendency at the surface is therefore

(1) $$\frac{\partial p}{\partial t} = -\Delta v k \cos k(x - ct) \int_0^\infty \rho \delta\phi.$$

From the hydrostatic equation we have $\rho\delta\phi = -\delta p$. Hence the integral in (1) is equal to the pressure, $p$, at the ground. Note that we here make use of the boundary condition $p = 0$ at the *upper boundary* of the atmosphere.

We multiply equation (1) by $-\alpha$, introduce from 4·19(5) $\alpha p = R_d T^* = \phi_h$, and from 12·06(9) the barotropic pressure function $\pi$. We then get

(2) $$-\frac{\partial \pi}{\partial t} = \phi_h \Delta v k \cos k(x - ct),$$

where $\phi_h$ is the dynamic height of the homogeneous atmosphere.

Partial differentiation of 12·06(23) with respect to time gives on the other hand

(3) $$-\frac{\partial \pi}{\partial t} = 2\Omega_z \bar{v} A_S c(1 - \eta) k \cos k(x - ct).$$

Since the two expressions (2, 3) must be the same, we have the condition:

$$\phi_h \Delta v = 2\Omega_z \bar{v} A_S c(1 - \eta). \tag{4}$$

Earlier we derived the condition

$$2\Omega_z \Delta v = k^2 \bar{v} A_S (\bar{v} - c - v_c). \tag{12·06(20)}$$

Only when the parameters in the velocity field 12·05(13) satisfy both these conditions does that field represent a solution of the complete set of atmospheric equations for a barotropic wave.

We now take the ratio of the two dynamical conditions above and introduce $\xi$ from 12·06(21). The resulting equation is

$$\phi_h \xi^2 (\bar{v} - c - v_c) = c(1 - \eta). \tag{5}$$

Note that the complete set of atmospheric equations and also the boundary conditions at the bottom and at the top of the atmosphere were needed to derive this equation. Equation (5) then represents the complete solution for a wave in a barotropic zonal current. It gives $c$ implicity as a function of latitude, wave number, and zonal wind speed. However, since $\eta$ contains $c^2$, (5) is a cubic equation in $c$ and therefore rather difficult to discuss in its present form. To facilitate the discussion we transform it as follows: First we multiply (5) by $(\bar{v} - c)$ and introduce $\eta$ from 12·06(22). We then get

$$\phi_h \eta = c(\bar{v} - c)(1 - \eta),$$

or

$$[\phi_h + c(\bar{v} - c)]\eta = c(\bar{v} - c).$$

We now substitute again for $\eta$ and divide out the factor $(\bar{v} - c)$. The resulting equation is:

$$c = \xi^2 [\phi_h + c(\bar{v} - c)](\bar{v} - c - v_c) \qquad \text{(exact)}. \tag{6}$$

The numerical value of $\phi_h = R_d T^*$ is about $280^2$ m$^2$s$^{-2}$, whereas $c(\bar{v} - c)$ certainly must be less than say $28^2$ m$^2$s$^{-2}$. The value of $c$ with an error of less than 1% is therefore

$$c = \xi^2 \phi_h (\bar{v} - c - v_c). \tag{7}$$

This equation confirms the qualitative rules derived earlier in section 10·14. The wave is stationary ($c = 0$) when the zonal wind has the critical speed. The wave moves toward the east ($c > 0$) when the zonal wind is supercritical and toward the west ($c < 0$) when the zonal wind is subcritical. Equation (7) shows further that $c$ is proportional to $\bar{v} - c - v_c$. From 12·05(18, 23), that means that the speed of the wave is proportional to the horizontal divergence in the current, which is just what the tendency equation predicts in a qualitative sense.

Solving finally for $c$ from (7), we have

$$c = (\bar{v} - v_c)\frac{\xi^2\phi_h}{1 + \xi^2\phi_h} \qquad \text{(first approximation)}. \tag{8}$$

Rossby (1939) derived essentially the same formula as (8). The mts values of $\xi$ for different latitudes and wave numbers are given in table 12·06*b*. Corresponding values of the non-dimensional factor in (8) are given in table 12·07. The table has been computed for $\phi_h =$

TABLE 12·07

$\xi^2\phi_h(1 + \xi^2\phi_h)^{-1}$ TABULATED

| $\varphi$ | $n$ | | | | |
|---|---|---|---|---|---|
| | 2 | 3 | 6 | 10 | 20 |
| 45° | 0.59 | 0.76 | 0.93 | 0.97 | 0.99 |
| 40°, 50° | 0.60 | 0.77 | 0.93 | 0.97 | 0.99 |
| 30°, 60° | 0.66 | 0.81 | 0.94 | 0.98 | 0.99 |
| 20°, 70° | 0.78 | 0.89 | 0.97 | 0.99 | 1.00 |
| 10°, 80° | 0.93 | 0.97 | 0.99 | 1.00 | 1.00 |

$280^2 = 78{,}400\ \mathrm{m^2\ s^{-2}}$, which corresponds to a surface temperature of about 273°K. However, the values in the table can be used safely for any observed surface temperature. The table shows that the non-dimensional factor in (8) is considerably smaller than 1 for long waves in middle latitudes, but the factor rapidly approaches 1 for shorter waves. For waves of the same order of magnitude as those actually observed in the atmosphere (wave lengths 60° of longitude or less) the wave moves approximately in accordance with the simple formula

$$c = \bar{v} - v_c \qquad \text{(second approximation)}.$$

The barotropic waves move then approximately as though the flow were non-diverging. Physically, this means that the deviation from non-divergence required to move the barotropic waves along with the speed $c$ is a small fraction of $c$ if the wave is short but is a considerable fraction of $c$ for very long waves. The values of $v_c$ were given in table 10·11.

It remains to find the value of $\eta$ for the barotropic wave. We substitute in (5) for $c$ from (6) and divide out the factor $\xi^2(\bar{v} - c - v_c)$. We find then

$$\phi_h = (1 - \eta)[\phi_h + c(\bar{v} - c)]$$

or, when we solve for $\eta$,

$$\eta = \frac{c(\bar{v} - c)}{\phi_h + c(\bar{v} - c)}. \tag{9}$$

Since $c(\bar{v} - c)$ usually is less than 1% of $\phi_h$, $\eta$ will be smaller than 0.01. Therefore the isobars have practically the same amplitudes as the streamlines and they are very nearly parallel to the streamlines at the inflection points. This makes permissible the neglect of the horizontal density advection $\mathbf{v}\cdot\nabla_H\rho$ in the tendency equation, which is the only physical approximation made in this section.

**12·08. Waves in a baroclinic current.** The atmosphere is always more or less baroclinic, with cold and heavy masses in the polar regions, and with warm and light masses in the equatorial region. The isobaric layers are accordingly inflated in the direction from the poles to the equator. In the case of zonal symmetry the undisturbed zonal current increases in intensity with increasing distance from the equatorial plane in accordance with the exact formula:

11·08(4) $$2\omega_a \sin\varphi_p \left(\frac{\delta\bar{v}}{\delta\phi}\right)_R = \frac{1}{\alpha}\left(\frac{\delta\alpha}{\delta s}\right)_p .$$

We shall consider only the belt of latitudes which has west winds at the surface of the earth. Within this belt the west wind increases in all latitudes with increasing distance from the equatorial plane. In the direction normal to the axis the speed may have any variation. To simplify matters we shall assume that the wind is constant throughout each horizontal level. The vertical shear of the wind, $\partial\bar{v}/\partial\phi$, is then also constant throughout each level. Since the isobaric surfaces are nearly horizontal we have further $\omega_a \sin\varphi_p \approx \Omega_z$. The above formula becomes then approximately:

11·08(5) $$\frac{\partial\bar{v}}{\partial\phi} = -\frac{1}{2\Omega_z}\frac{1}{T}\frac{\partial T}{\partial y} = \frac{1}{2\Omega a}\frac{\partial(\ln T)}{\partial(\cos\varphi)},$$

which is identical to the thermal wind formula for the geostrophic wind. The assumption of a constant wind throughout each level therefore prescribes the variation of the temperature with latitude to be as follows:

$$\ln T = \ln T_P + \beta\cos\varphi.$$

$T_P$ is the temperature at the pole and $\beta = 2\Omega a\partial\bar{v}/\partial\phi$.

If a harmonic wave disturbance is superimposed on this baroclinic westerly current, the resulting velocity field at an arbitrary level is given by

(1) $$v_x = \bar{v} + \Delta v \sin k(x - ct),$$
$$v_y = \bar{v}kA_S \cos k(x - ct).$$

The symbols have the same meaning as in 12·05(13). For small $|\Delta v|$ we have shown from 12·05(16) that $A_S$ is the streamline amplitude.

The streamlines of the velocity field (1) are, from 12·05(16′),

$$y - y_0 = A_S \sin k(x - ct). \tag{2}$$

Just as in 12·05(22′), we find that the velocity field (1) has the vorticity

$$\zeta = -\bar{v}k^2 A_S \sin k(x - ct). \tag{3}$$

And, just as in 12·05(17), we find that the velocity field (1) has the divergence

$$\nabla_H \cdot \mathbf{v} = \Delta v k \cos k(x - ct). \tag{4}$$

If the motion (1) shall be dynamically possible, the expressions (3, 4) for the vorticity and the divergence must satisfy the vorticity theorem 11·21(5):

$$-(\zeta + 2\Omega_z)\nabla_H \cdot \mathbf{v} = \frac{d\zeta}{dt} + \frac{2\Omega \cos \varphi}{a} v_y. \tag{5}$$

It should be noted that this theorem is exact only when no solenoids intersect the horizontal level; see 11·20. In the undisturbed baroclinic current the solenoids are directed along the latitude circles and do not intersect the levels. When the baroclinic current is disturbed by the wave perturbation the field of solenoids is modified too. But the solenoids will remain approximately horizontal and very few will intersect the levels. The vorticity theorem (5) therefore applies, in the first approximation, to the velocity field (1) of the baroclinic wave. When the values (3, 4) of the vorticity and the divergence are substituted in (5), and higher order terms are neglected, we find that:

$$2\Omega_z \Delta v = \bar{v}k^2 A_S(\bar{v} - c - v_c). \tag{6}$$

When $\Delta v$ satisfies this equation, the velocity field (1) represents a flow pattern which is physically possible at all levels. The critical speed $v_c$ (see table 10·11) is determined by the wave length and the latitude and has the same value at all levels. The strength of the relative zonal circulation, $\bar{v} - c$, increases with height in the baroclinic westerlies. If it is assumed that the wave moves with a slightly lower speed than the air at the ground, the relative zonal wind increases from a small positive value at the ground to a maximum value at the tropopause. The deviation $\Delta v$ is zero and the flow is non-diverging at the level where the relative zonal wind has the critical value, $\bar{v} - c - v_c = 0$. Above the level of non-divergence the relative zonal wind is supercritical, and $\Delta v > 0$. The bottleneck of the flow is then at the cyclonic trough, which therefore has divergence to its east. Between the level of non-divergence and the ground the relative zonal wind is subcritical, and $\Delta v < 0$. The

bottleneck of the flow is here at the anticyclonic wedge, and the flow has convergence to the east of the trough.

The pressure field in the wave with the velocity field (1) is obtained by the procedure outlined in section 12·06. Just as in 12·06(24), we find for the isobar through the origin at the time $t = 0$ the equation:

$$\cos\varphi - \cos\varphi_0 = -(1-\eta)\tan\sigma_S \sin\varphi \sin k(x-ct), \tag{7}$$

where

$$\eta = \xi^2(\bar{v}-c)(\bar{v}-c-v_c). \tag{8}$$

The relation between the amplitudes of the streamline and the isobar is:

$$\tan\sigma_p = (1-\eta)\tan\sigma_S. \tag{9}$$

The relation between the central latitude $\varphi_0$ of the streamline and the central latitude $\bar{\varphi}$ of the isobar passing through its inflection points is:

$$\cos\bar{\varphi} = \cos\varphi_0 \cos\sigma_p. \tag{10}$$

The deviation between the isobars and the streamlines at the inflection points is given by 12·06(27):

$$\tan\psi_p = (1-\eta)\tan\psi_S. \tag{11}$$

The relation between the pressure pattern and the flow pattern at the various levels of the baroclinic wave is readily obtained from the three formulas (9, 10, 11). The deviation between the two patterns depends

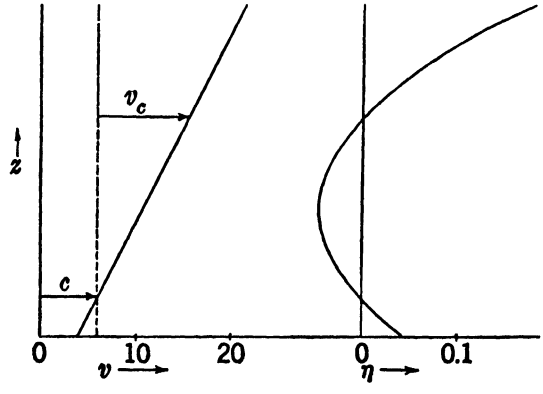



FIG. 12·08.

upon the value of $\eta$. From (8) $\eta$ is zero at the level where the relative zonal wind is zero and at the level of non-divergence, where the relative zonal wind has the critical speed. At these levels the isobars are tangential to the streamlines at the points halfway between the troughs

and the wedges, and the two patterns have exactly the same amplitudes.

Above the level of non-divergence and below the level where the relative zonal wind is zero $\eta$ is positive. And in the layer between those two levels $\eta$ is negative; fig. 12·08. The corresponding deviation of the isobars from the streamlines is as indicated schematically in fig. 12·06*b*.

In the barotropic waves the relative zonal wind never deviates much from the critical speed. So $\eta$ is always small, and the pressure pattern coincides approximately with the flow pattern at all levels in the barotropic waves. In the baroclinic waves, on the other hand, the relative zonal wind may be considerably greater than the critical speed at levels high above the level of non-divergence; see fig. 12·08. At these levels the magnitude of $\eta$ becomes appreciable, and therefore the departure of the pressure pattern from the flow pattern is no longer negligible. As a general rule the deviation between the two patterns is most pronounced at high levels when the level of non-divergence is low and the current is strongly baroclinic.

The above remarks throw some light upon the dynamics of the baroclinic waves and on their three-dimensional structure. The principal problem remaining to be solved for these waves is the determination of their velocity of propagation. To solve that problem the tendency equation would have to be integrated for the baroclinic wave. The integration was rather simple for the barotropic wave, because the horizontal divergence is independent of height and the flow patterns at all levels are in phase. In the baroclinic waves not only does the horizontal divergence vary with height, but the troughs and wedges will in general tilt with height because of the asymmetry between the temperature field and the pressure field; see fig. 10·17*d*. The points along a vertical column will therefore have different positions relative to the flow pattern at different levels. This makes the integration of the tendency equation for the baroclinic waves very difficult. When we have successfully performed the integration, the velocity of propagation of the baroclinic wave can be determined, and the conditions for dynamical instability of the waves, as derived by qualitative reasoning in section 10·17, can be obtained.

# INDEX


Abnormal flow, 162, 202, 204
Absolute acceleration, 170
Absolute circulation, 313
Absolute circulation theorem, 313
Absolute frame, 152
Absolute instability, 131
Absolute motion, 151
  equation of, 154
Absolute stability, 130
Absolute temperature, 11, 34
Absolute velocity, 168
Absolute vorticity, 322
  theorem of, 323
Acceleration, 3, 148
  absolute and relative, 170
  centripetal, 150
    in horizontal path, 183
    in vertical path, 183
    in zonal flow, 159, 171
    of a point of the earth, 156, 168, 170
  Coriolis, 170
  dimensions of, 3
  in horizontal path, 183
  in vertical path, 183
  in zonal flow, 159, 171
  natural components of, 151, 175
  of gravity, 88
  of a point of the earth, 156, 168, 170
  tangential, 150, 175, 189
  units of, 6
Adiabatic heating, 68
Adiabatic process, 27, 64, 67
  of dry air, 28
  of unsaturated moist air, 64
  pseudo-, 68, 69
  reversible saturation-, 68, 70
  saturation-, 72
Adiabats, 28
  dry, 29
  on emagram, 36, 37
  on Stüve diagram, 30
  on tephigram, 39
  saturation, 72
  unsaturated, 65, 139
Advection, of density, 259
  of temperature, 220, 279, 285
Advective pressure tendency, 258
Advective rate of change, 254
Air, composition of, 16
  dry, *see* Dry air
  moist, *see* Moist air
  saturated, 62
  unsaturated, 62, 65
($\alpha$,$-p$)-diagram, 18, 29, 300
Altimeter (pressure), 121
Altimeter errors, 122
Altimeter setting, 122
Altitude, sea level, 121
  standard, 119
Amplitude, angular, 266
    of isobar, 266, 351, 354
    of path, 331
    of streamline, 269, 331, 351, 354
  of path, 330, 343
  of relative streamline, 277, 330
  of streamline, 269, 330, 345
Anemometer level, 241, 244
Angular amplitude, *see* Amplitude, angular
Angular radius of curvature, 177, 183, 289
Angular speed, 151
  in inertial flow, 196
  in zonal flow, 160
  of the earth, 155, 177
Angular velocity, 3, 163
  of the earth, 163, 183
    components of, 183
    vertical component of, 184, 191
  vertical component of, 180
Angular wave number, 269
Antibaric flow, 190, 204
Anticyclone, abnormal, 162, 202, 204
  of maximum strength, 162, 201
  structure of, 294
Anticyclonic circulation, 317, 318
Anticyclonic flow, 191, 204, 207
  zonal, 160

Anticyclonic sense, 191, 317, 323
Anticyclonic vorticity, 323
Apparent gravity, 227
Apparent latitude, 229
Apparent level, 227
Arc length, 149
Area, 2
  on thermodynamic diagrams, 19, 35, 37, 39, 109, 133, 301
  under hodograph, 260
  vector, 260, 315, 316
Area computer for advective pressure change, 262
Ascendent, 97
  isobaric volume, 213
  volume, 301
Atmosphere, baroclinic, 102
  barotropic, 102, 340
  composition of, 16
  dry-adiabatic, 106
  homogeneous, 102, 105
  isothermal, 107
  normal, 8
  U. S. standard, 119
  with constant lapse rate, 104
Atmospheric column, weight of, 103, 286
Atmospheric equations, 337
Atmospheric process, 27, 337
Autobarotropy, 313, 339
Avogadro's law, 14

Bar, 6
Baric flow, 190, 201, 204
Baric wind law, 192
Baroclinic atmosphere, 102
Baroclinic current, 286
Baroclinic wave, 279, 360
  dynamic instability of, 286
  formation of, 281
  mass divergence in, 280, 285
  pressure changes in, 281
  speed of, 274
  stable, 274
Barometer, 7, 121
Barometric height formula, 103, 297
Barotropic atmosphere, 102, 340
Barotropic current, 341
Barotropic layer, 211
Barotropic pressure function, 350
Barotropic wave, 274, 341
  mass divergence in, 274
  pressure changes in, 274, 276, 357
  pressure field in, 347
  speed of, 276, 356
Barye, 5
Base level, 120
Bergeron's theory of precipitation, 55
Bernoulli's theorem, 352
Bjerknes, J., convection theory of, 135
  cyclone theory of, 256, 281
Bjerknes, V., circulation theorem of, 299, 302, 313, 317
  hydrostatic tables of, 111
Boiling point, normal, 50, 51
Boiling temperature, 50
Boundary conditions, 221, 225, 244, 340, 357
  dynamic, 221, 340
  kinematic, 225, 340
Boyle's law, 12
Buys Ballot's law, 192

Calorie, 21
Calorimeter, 20
Cartesian (rectangular) components of a vector, 85, 174
Cartesian coordinates, 83
Center of curvature, 150
Centibar, 5, 7
Centigrade, 11
Centrifugal force of a point of the earth, 89, 156
Centrifugal potential, 157
Centripetal acceleration, 150
  in horizontal path, 183
  in vertical path, 183
  in zonal flow, 159, 171
  of a point of the earth, 156, 168, 170
Cgs units, 5, 6
Channel, isobaric, 263
  isobaric unit, 100
Characteristic curve, 135
Characteristic point, 67, 76, 133
Charles's law, 12
Circle, curvature of, 149
  great, 175, 180, 181, 182, 233
  inertial, 198
  of curvature, 150
  of horizontal curvature, 180

Circle, small, 175
  zonal, 156
Circular frequency, 131
Circular vortex, 308
  local, 319
Circulation, 296
  absolute, 313
  anticyclonic, 317, 318
  cyclic sense of, 317
  cyclonic, 317, 318
  in meridional plane, 309
  in zonal flow, 314
  rate of change of, 313, 317
  relative, 315, 317
Circulation integral, 296
Circulation theorem, 317
  absolute, 313
  individual, 311
  of Bjerknes, 299, 302, 313, 317
  of Kelvin, 313
  primitive, 298
  relative, 317
Clapeyron's equation, 49, 50–1
Closed flow patterns, 264, 288, 294
  mass divergence in, 291
Column, atmospheric, weight of, 103, 286
Component equations of relative motion, 186
Components of vector, 85
  natural, 151, 174
  rectangular, 85, 174
Composition of dry air, 16
Condensation, 41, 68, 72, 77
Condensation level, lifting, 134
Conditional instability, 131
Conservation, of energy, 21, 91
  of mass, 250
Continuity, equation of, 250, 252, 337
Convection, cumulus, 136
  level of free, 134
Convergence, *see* Divergence
Cooling, adiabatic, 68
  isobaric, 72
  super-, 55
Coordinates, local, 174
  natural, 151, 173
  rectangular or Cartesian, 83
  standard, 83
Coriolis acceleration, 170
Coriolis force, 172, 184
  components of, 184
  horizontal, 185
Corresponding curvatures, 190
Corresponding latitudes, 190
Corresponding normal pressure forces, 190
Critical constants, for permanent gases, 43
  for water substance, 42
Critical eccentricity, 290
Critical lapse rate, 138
Critical point, 50, 51
Critical speed, 268, 271, 344
Critical state, 42
Critical temperature, 41
Cumulus convection, 136
Curvature, 149
  angular radius of, 177, 183, 289
  center of, 150
  circle of horizontal, 180
  corresponding, 190
  cyclic sense of, 176, 190
  geodesic, 181
  horizontal, 178, 182, 265
    of streamline and path, 207, 267
  of circle, 149
  of sinusoidal streamline, 270
  radius of, 150
  radius of horizontal, 180
  vector, 151
  vertical, 182
Cyclic sense, 176
  of circulation, 317
  of curvature, 176, 190
  of the earth's rotation, 177
  of vorticity, 323
Cyclone, structure of, 292
Cyclonic circulation, 317, 318
Cyclonic flow, 190, 204, 207
  zonal, 160
Cyclonic sense, 191, 317, 323
Cyclonic vorticity, 323
Cyclostrophic flow, 199
Cyclostrophic speed, 199, 203

Dalton's law, 15
Day, sidereal, 155
  solar, 155
Decimeter, dynamic, 94

Degree, absolute, (°K), 11
centigrade (°C), 11
Fahrenheit (°F), 12
of latitude, 5, 192
Del ($\nabla$), 95, 251
Density, 3, 9
local change of, 253
of water, 5, 44
Density advection, 259
Derivative, individual, 146, 253
local (time-), 253
of a vector, 146, 165, 251, 312
Deviation, geostrophic, 234, 244
Dew point temperature, 77
Diagrams, thermodynamic, 34
($\alpha$,$-p$)-diagram, 18, 29, 300
emagram, 35
height evaluation on, 115
important criteria of, 35
precipitation lines on, 143
saturation adiabats on, 74
Stüve, 30, 35
($T$,$e$)-diagram, 49
tephigram, 38, 74
vapor lines on, 61, 74
Differentials, exact, 32, 92
geometric ($\delta$), 92, 126
individual ($d$), 92, 125, 146
inexact, 32
process ($d$), 92, 125
Differentiation, logarithmic, 26
of a vector, 146, 165, 312
divergence-, 251
Dimensions, 2
Distributive law, for scalar product, 87
for vector product, 165
Divergence, 251
frictional, 263
horizontal, 253, 324, 333
mass, 251
horizontal, 256
in baroclinic wave, 280, 285
in barotropic wave, 274
in closed flow patterns, 291
in tendency equation, 257
longitudinal, 263, 268, 331
transversal, 264, 271
Dry-adiabatic atmosphere, 107
Dry-adiabatic lapse rate, 107, 129
Dry-adiabatic layer, height of, 110
Dry-adiabatic process, 28
Dry adiabats, 29
Dry air, composition of, 16
equation of state of, 13
molecular weight of, 17
Poisson's constants for, 28, 31
specific gas constant of, 14, 16
specific heats of, 25
Dry stage, 62
Dynamic boundary condition, 221, 340
Dynamic decimeter, 94
Dynamic height, 94
computation of, 114, 115, 117
by dry-adiabatic layer, 110
by isothermal layer, 111
on emagram, 109
Dynamic instability, 286
Dynamic meter, 95
Dyne, 5

Earth, acceleration of a point of, 156, 168, 170
angular speed of, 155, 177
angular velocity of, 163, 183
mass of, 153
radius of, 153
shape of, 153, 158
velocity of a point of, 167
Earth's rotation, sense of, 177, 191
Eccentricity, critical, 290
Eddy stress, 248
Eddy viscosity, 247
Ekman spiral, 244
Emagram, 35
height computation on, 117
precipitation lines on, 143
Väisälä scales on, 115
Energy, 3, 21
conservation of, 21, 91
dimensions of, 3
equation of, 22, 337
internal, 23
kinetic, 132
potential, 91
specific, 3, 94
units of, 6
English units, 7
Entropy, 33
specific, 33, 46

Equation, Clapeyron's, 49, 50–1
hydrostatic, 101, 188
normal, 187, 190, 203
of absolute motion, 154
of continuity, 250, 252, 337
of energy, 22, 337
of relative equilibrium, 101, 156
of relative motion, 171, 174, 337
components of, 186
projections of, 174
of state, 12, 337
of dry air, 14
of mixture of perfect gases, 15
of moist air, 63
of perfect gas, 13
of water vapor, 44
Poisson's, 28
tangential, 187, 188, 351
tendency, 256
thermal wind, 212, 214, 216, 311
vertical, 187
Equations, atmospheric, 337
component, of relative motion, 186
of horizontal flow, 186, 187, 188, 203
perturbation, 339
Equilibrium, equation of relative, 101, 156
hydrostatic, 102
indifferent, 127, 131, 138
mechanical, 88
of zonal motion, 308
phase, 42, 48, 50
pressure in relative, 97
relative, 101, 102, 156
stable, 127, 130, 138
thermal, 10
unstable, 127, 130, 138
Equilibrium curves, 298
Equiscalar surface, 83, 96
Equiscalar unit layer, 97
Equivalent potential temperature, 76
Equivalent temperatures, 77
Erg, 5
Evaporation, latent heat of, 47
Evaporation curve, 50, 51
Evaporation temperature, 50
Exact differential, 32, 92
Export, 331

Fahrenheit degree, 12
Field, 81
scalar, 83
First law of thermodynamics, 21
Flow, antibaric, 190, 204
anticyclonic, 191, 204, 207
baric, 190, 201, 204
cyclonic, 190, 204, 207
cyclostrophic, 199
geostrophic, 176, 192, 233, 245, 263
geostrophic gradient, 210, 348
gradient, 189, 265, 348
great circle, 233
horizontal, 173
equations of, 186, 187, 188, 203
inertial, 190, 196, 200
irrotational, 333
potential, 334
steady, 189, 208, 352
zonal, 158, 170, 306
Flow pattern, 189
closed, 264, 288, 294
wave-shaped, 264, 328, 341
Force, 3
centrifugal, of a point of the earth, 89, 156
Coriolis, 172, 184
components of, 184
horizontal, 185
frictional, 233, 238
inertial, 155, 156, 171, 172
of gravitation, 88, 152
of gravity, 88, 156
components of, 96, 185
pressure, per unit mass, 88, 97, 154
components of, 186
horizontal, 186
horizontal normal, 190, 200
per unit volume, 99
Frame, reference, absolute, 152
relative, 151
Frequency, circular, 131
Frictional divergence, 263
Frictional force, 233, 238
Front, 220
boundary conditions at, 221, 225, 340
geostrophic, 227, 229
pressure distribution at, 224
shear at, 228, 231
slope of, 223, 229, 231
wind distribution at, 226, 231

Front, zonal, 227
Frontal surface, 220

Gas constant, specific, 13, 15
for dry air, 14, 16
for mixtures, 16
for moist air, 63, 67
for water vapor, 44
universal, 15
Gases, perfect, 13, 15, 24, 25
equation of state of, 13
laws of, 12
mixture of, 15
specific heats of, 25
permanent, 11, 43
Gauss's theorem, 333
Generalized hydrostatic equation, 188
Geodesic, 181
Geodesic curvature, 181
Geometric differential ($\delta$), 92, 126
Geopotential, 93, 157
Geopotential level, 92
Geopotential unit layer, 94
Geostrophic deviation, 234, 244
Geostrophic flow, 176, 192, 233, 245, 263
Geostrophic front, 227, 229
Geostrophic gradient flow, 210, 348
Geostrophic speed, 192, 203
Geostrophic velocity, 210, 233–4
Geostrophic wind level, 246
Geostrophic wind shear, 212, 216, 231
Gradient, 97
horizontal pressure, 100
pressure, 99
temperature, 216
Gradient flow, 189, 265, 348
geostrophic, 210, 348
Gradient wind diagram, 205
Gravitation, force of, 88, 152
Newton's law of universal, 88, 153
potential of, 153
Gravity, acceleration of, 88
apparent, 227
force of, 88, 156
components of, 96, 185
potential of (geopotential), 93, 157
standard, 8, 120
virtual, 187
Great circle, 175, 180, 181, 182
flow on, 233

Hail stage, 68
Heat, 20
mechanical equivalent of, 22
latent, of evaporation, 47
of melting, 47
of sublimation, 47
of transformation, 46
specific, 21
at constant pressure, 23
at constant volume, 23
of dry air, 25
of ice, 43
of moist air, 64, 67, 139
of water, 44
of water vapor, 45
Heat capacity, 21
Heat transport, vertical, 139
Heating, adiabatic, 68
isobaric, 72
Height, dynamic, 94
computation of, 114, 115, 117
by dry-adiabatic layer, 110
by isothermal layer, 111
on emagram, 117
of homogeneous atmosphere, 103, 106, 357
Helmholtz' vorticity theorem, 324
Hodograph, 148
area under, 260
of moving particle, 148
shear, 212, 218
Höiland's theorem, 299
Homogeneous atmosphere, 102, 105
height of, 103, 106, 357
Horizontal Coriolis force, 185
Horizontal curvature, 178, 182, 265
circle of, 180
radius of, 180
Horizontal divergence, 253, 324, 333
Horizontal flow, 173
equations of, 186, 187, 188, 203
Horizontal (geopotential) levels, 92
Horizontal path, 178
Horizontal plane, 173
Horizontal pressure force, 186
Horizontal pressure gradient, 100
Horizontal shear, 322
Horizontal unit normal, 173
Horizontal vector projection (vector component), 174

Humidity, relative, 58
specific, 57
saturation, 58
Humidity variables, 57
Hydrostatic equation, 101
generalized, 188
Hydrostatic equilibrium, 102
stability criteria for, 127, 130, 138
Hydrostatic tables, Bjerknes, 111
U. S. Weather Bureau, 114

Ice, thermal properties of, 43
Image curve, 300
Image point, 66, 76, 133, 148
Indifferent equilibrium, 127, 131, 138
convectional, 138
dry-, 131
saturated-, 131
Individual circulation theorem, 311
Individual derivative, 146, 253
Individual differential ($d$), 125, 146
Individual lapse rate, 128, 139
Inertial circle, 198
Inertial flow, 190, 196, 200
Inertial force, 155, 156, 171, 172
Inertial path, 198, 200
Inertial period, 198
Inertial speed, 196, 203
Inexact differential, 32
Instability, 127, 130, 138
absolute, 131
conditional, 131
convectional, 138
dynamic, 286
latent, 134
shear, 277, 286
Integral, circulation, 296
line, 19, 32
of a vector, 295, 296
Integrating factor, 34
Internal energy, 23
Irrotational flow, 333
Irrotational vector, 333
Isentropic, 34; *see also* Adiabatic process
Isobaric channel, 100, 263
transport capacity of, 263
Isobaric heating, 72
Isobaric layer, standard, 111
unit, 82, 102
Isobaric process, 20
Isobaric slope, 211
Isobaric surface, 82, 102, 111, 211
standard, 111
Isobaric unit channel, 100
Isobaric unit layer, 82
dynamic thickness of, 102
Isobaric volume ascendent, 213
Isobars, 32, 100
and streamlines, 189, 200, 270, 272, 289, 348, 356, 362
closed patterns of, 264, 288, 294
horizontal, 100
at front, 224
in zonal flow, 160
on sea level map, 82
wave-shaped patterns of, 264, 272, 351
Isopleths, of cyclostrophic speed, 199
of geostrophic speed, 195
of gradient speed, 204
of inertial speed, 197
on thermodynamic diagrams, 35, 36, 39, 61, 73, 74
Isosteric process, 20
Isosteric surface, 82, 102
Isotherm advection, 220, 279, 285
Isothermal atmosphere, 107
Isothermal layer, height of, 111
Isothermal slope, 214
Isothermal surface, 82, 215, 283
Isotherms, 32
in stable baroclinic wave, 279
of perfect gas, 20
of water substance, 40, 41, 56

Joule, 6
Joule's experiment, 22
Joule-Thomson effect, 24

Kelvin, 11
circulation theorem of, 313
Kilojoule, 6
Kinematic boundary condition, 225, 340
Kinematics, 145
Kinetic energy, 132
Kinetic theory of gases, 236

Lapse rate, 104, 129
critical, 138
dry-adiabatic, 107, 129

Lapse rate, individual, 128, 139
saturation-adiabatic, 129, 139, 141
unsaturated adiabatic, 129, 139
Latent heat, of evaporation, 47
of melting, 47
of sublimation, 47
of transformation, 46
variation of, 47
Latent instability, 134
Latitude, 183, 184
apparent, 229
corresponding, 190
degree of, 5, 192
Length, dimension of, 2
units of, 5, 7
Level, anemometer, 241, 244
apparent, 227
base, 120
geopotential, 92
geostrophic wind, 246
lifting condensation, 134
of free convection, 134
of non-divergence, 273, 280, 285, 363
sea, 93, 94, 228
Level surface, 92
apparent, 227
Line integral, 19, 32
of a vector, 295, 296
Local circular vortex, 319
Local coordinates, 174
Local (time-) derivative, 253
Logarithmic differentiation, 26
Longitudinal divergence, 263, 268, 331

Magnus' formula, 52
Margules' formula, 232
Mass, conservation of, 250
dimension of, 2
units of, 5, 7
Mass divergence, 251
horizontal, 256
in baroclinic wave, 280, 285
in barotropic wave, 274
in closed flow pattern, 291
in tendency equation, 257
longitudinal, 263, 268, 331
transversal, 264, 271
Mass transport in surface layer, 239
Mass variables, 9
Maximum anticyclonic pressure field, 162, 201
Maximum speed (anticyclonic), 201, 204
Maxwell's theory of viscosity, 237
Mean free path, 237
Mechanical equilibrium, 88
Mechanical equivalent of heat, 22
Melting, latent heat of, 47
Melting point, normal, 53
Melting pressure, 53
Melting temperature, 53
Meridional isobars in zonal flow, 159, 161
Meridional plane, 157
circulation in, 309
Meter, 4
dynamic, 95
Metric ton, 5
Millibar, 7
Mixing length, 248
Mixing ratio, 57
saturation, 58
Mixture of perfect gases, 15
Moist air, 9, 15, 57
equation of state of, 63
saturated, 62
specific gas constant of, 63
specific heats of, 64
thermal properties of, 57, 62
Moisture variables, 57
Molar volume, 14
Mole, ton, 14
Molecular viscosity, 237
Molecular weight, 14
of dry air, 17
of mixture of perfect gases, 17
of water vapor, 44
Momentum, 3, 6
shear of geostrophic, 231
Momentum transport, vertical, 237, 248
in surface layer, 240
Motion, component equations of relative, 186
equation of absolute, 154
equation of relative, 172, 174, 337
horizontal, 173
irrotational, 334
projected equations of relative, 175
turbulent, 248
vertical, 131, 132, 136, 142, 257, 283
zonal, 158, 170, 306

Mts units, 4, 6

Natural component equations of motion, 186
Natural components, of acceleration, 151, 175
  of vector, 174
Natural coordinates, 151, 173
Natural unit vectors, 151, 173
Newton's formula for viscous stress, 236
Newton's law of universal gravitation, 88, 153
Newton's second law of motion, 152, 155, 172, 174
Normal, horizontal unit, 173
  unit, 148
Normal atmosphere, 8
Normal boiling point, 50, 51
Normal equation, 187, 190, 203
Normal melting point, 53
Normal pressure force, 190, 200
Number of solenoids, 306

Oscillation, stable vertical, 131
Osculating plane, 150
  of spherical path, 175, 177, 178

Parcel method, 125
Partial pressure, 15, 59, 64
Path, 147
  amplitude of, 330, 343
  and streamline, 189, 207, 266, 329, 342
  curvature of, 149
  horizontal, 178
  horizontal curvature of, 178, 266, 331, 348
  inertial, 198, 200
  mean free, 237
  of process, 18
  vertical, 182
  wave length of, 329, 343
Pendulum day, 198
Perfect gases, 13, 15, 24, 25
  equation of state of, 13
  laws of, 12
  mixture of, 15
  specific heats of, 25
Period, inertial, 198
  of stable oscillation, 132
Permanent gases, 11, 43
Perturbation equations, 339
Phase, change of, 46, 49
Phase equilibrium, 42, 48, 50
Phases of water substance, 42, 50, 56
Piezotropy, 338, 340
Poisson's constants, 28
  for dry air, 28, 31
  for moist air, 65, 67
Poisson's equation, 28
Position vector, 145
Potential, 96, 333
  centrifugal, 157
  geo-, 93, 157
  gravitational, 153
  of gravity (geopotential), 93, 157
  thermodynamic, 48
  velocity, 334
Potential energy, 91
Potential flow, 334
Potential temperature, 31, 66
  equivalent, 76
  virtual, 66
  wet bulb, 76
Precipitation, 68, 141
  Bergeron's theory of, 55
Precipitation lines on emagram, 143
Pressure, 10
  dimension of, 3
  melting, 53
  partial, 15, 59, 64
  saturation vapor, 40, 48, 57
  sea level, 122
  standard, 8
  units of, 3, 6, 7
  vapor, 40, 58, 61
Pressure dynamic height curve, 114, 116, 118
Pressure force, per unit mass, 88, 97, 154
    components of, 186
    horizontal, 186
    normal, 190, 200
  per unit volume, 99
Pressure gradient, 99
  components of, 100
  horizontal, 100
Pressure tendency, 255
  advective, 258
Primitive circulation theorem, 298
Process, adiabatic, 27, 64, 67
  atmospheric, 27, 337

Process, cyclic, 19
dry-adiabatic, 31
isobaric, 20, 72
isosteric, 20
isothermal, 19
path of, 18
physical, 18
piezotropic, 338, 340
pseudo-adiabatic, 68, 69
reversible saturation-adiabatic, 68, 70
saturation-adiabatic, 72
unsaturated adiabatic, 64
Process curve, 108
Process differential ($d$), 92, 125
Procession, 296
Product, scalar, 87
scalar triple, 166
vector, 164
Projection of a vector, 174
Propagation, speed of, 255
Pseudo-adiabatic process, 68, 69
Psychrometric formula, 79

Radiation, effect on atmospheric process, 27
Radius, of curvature, 150
angular, 177, 183, 289
horizontal, 180
vector, 151
of earth, 153
Rain stage, 68
Rectangular components, of vector, 85, 174
of vector product, 165
Rectangular (Cartesian) coordinates, 83
Rectangular unit vectors, 86
Reference frame, absolute, 152
relative, 151
Regelation, 54
Relative acceleration, 170
natural components of, 175
Relative change in moving pressure field, 254
Relative circulation, 314, 317
Relative circulation theorem, 317
Relative equilibrium, 101, 102, 156
equation of, 101, 156
pressure in, 97
Relative frame, 151
Relative humidity, 58
Relative motion, component equations of, 186
equation of, 171, 174, 337
Relative streamline, 277
Relative velocity, 169
Relative vorticity, 322
theorem of, 324
Relative zonal wind, 268
Resultant of vectors, 84, 86
Reversible saturation-adiabatic process, 68, 70
Right-handed screw rule, 83
Rossby, 67
vorticity theorem of, 324
Rotation, 83, 151, 163, 175

Saturated moist air, 62
Saturated stage, 62
Saturation, super-, 55
Saturation-adiabatic lapse rate, 129, 139, 141
Saturation-adiabatic process, 72
reversible, 68, 70
Saturation adiabats, 72
on diagram, 74
Saturation mixing ratio, 58
Saturation specific humidity, 58
Saturation vapor pressure, 40, 48, 57
over ice, 52
over water, 50
Scalar, 83
Scalar field, 83
Scalar product, 87
Scalar triple product, 166
Screw rule, right-handed, 83
Sea level, 93, 94, 228
Sea level altitude, 121
Sea level pressure, 122
Second (solar), 5
Sense, anticyclonic, 191, 317, 323
cyclic, 176
of circulation, 317
of curvature, 176, 190
of earth's rotation, 177
of vorticity, 323
cyclonic, 191, 317, 323
Shear, frontal, 228, 231
horizontal, 322
of geostrophic wind, 212, 216, 231
Shear hodograph, 212, 218

Shear instability, 277, 286
Sidereal day, 155
Sinusoidal flow pattern, 269, 341
Slice method, 135
Slope, frontal, 223, 229, 231
  isobaric, 211
  isothermal, 214
Small circle, 175
Snow stage, 68
Solar day, 155
Solar second, 5
Solenoids, 300, 303
  in zonal motion, 307, 361
  number of, 306
  pressure-temperature, 303
  pressure-volume, 300
  temperature-entropy, 303
  theorem of, 301
Sounding curve, 103, 108, 130
Specific, 3
Specific energy, 3, 94
  units of, 6, 94
Specific entropy, 33, 46
Specific gas constant, 13, 15
  for dry air, 14, 16
  for mixtures, 16
  for moist air, 63, 67
  for water vapor, 44
Specific heat, 21
  at constant pressure, 23
  at constant volume, 23
  of dry air, 25
  of ice, 43
  of moist air, 64, 67, 139
  of water, 44
  of water vapor, 45
Specific humidity, 57
  saturation, 58
Specific volume, 3, 6, 9
Speed, 146
  angular, 151
    of earth, 155
  critical, 268, 271, 344
  cyclostrophic, 199, 203
  geostrophic, 192, 203
  inertial, 196, 203
  maximum anticyclonic, 201, 204
  of barotropic wave, 276, 356
  of propagation, 255
  of wave, 269
Speed, rate of change of, 150, 189
  subcritical, 268
  subgeostrophic, 207
  supercritical, 268
  supergeostrophic, 207
Spiral, Ekman, 244
Stability, *see also* Instability
  absolute, 130
  convectional, 138
  criteria in hydrostatic equilibrium, 127, 130, 138
  region of, 219
  tendency of, 220
Stable equilibrium, 127, 130, 138
Stable vertical oscillation, 131
Stable wave, 277
  baroclinic, 279
Stage, dry, 62
  hail, 68
  rain, 68
  saturated, 62
  snow, 68
  unsaturated, 62
Standard altitude, 119
Standard atmosphere (U. S.), 119
Standard component equations of relative motion, 186
Standard components of vector, 85, 174
Standard coordinates, 83
Standard gravity, 8, 120
Standard isobaric layers, 111
Standard isobaric surface, 111
Standard temperature, 119
State, 9
  critical, 42
  equation of, 12, 337
    of dry air, 14
    of mixture of perfect gases, 15
    of moist air, 63
    of perfect gas, 13
    of water vapor, 44
  triple, 41, 42
Steady flow, 189, 208, 352
Stokes's theorem, 320
Stream function, 335
Streamline, 189
  amplitude of, 269, 330, 345
  and path, 189, 207, 266, 329, 342
  horizontal curvature of, 207, 267, 289, 322, 330

Streamline, relative, 277
sinusoidal, 269, 329, 342, 348
Streamlines and isobars, 189, 200, 270, 272, 289, 348, 356, 362
Stress, eddy, 248
viscous, 235
Stüve diagram, 30, 35
Subcritical speed, 268
Subgeostrophic speed, 207
Sublimation, latent heat of, 47
Sublimation curve, 49, 50, 53
Sublimation temperature, 52
Supercooling, 55
Supercritical speed, 268
Supergeostrophic speed, 207
Supersaturation, 55
Surface, equiscalar, 83, 96
frontal, 220
isobaric, 82, 102, 111, 211
isosteric, 82, 102
isothermal, 82, 215, 283
level (geopotential), 92
thermodynamic, 56
Surface layer, 233
mass transport in, 240

($T$,$e$)-diagram, 49, 50
Tangent, unit, 146, 173
Tangential acceleration, 150, 175, 189
Tangential equation, 187, 188, 351
Temperature, 10, 34
absolute, 11, 34
dew point, 77
dimension of, 2, 12
equivalent, 77
equivalent potential, 76
evaporation, 50
melting, 53
potential, 31, 66
sublimation, 52
thermodynamic definition of, 34
virtual, 63, 67
virtual potential, 66
wet bulb, 77, 78
wet bulb potential, 76
Temperature gradient, 216
Temperature scales, 12
Tendency, advective pressure, 258
of vertical stability, 220
pressure, 255
Tendency equation, 256
Tephigram, 38, 74
Terminal curve (of vector), 147
Thermal equilibrium, 10
Thermal wind equation, 212, 214, 216, 311
Thermal wind in zonal flow, 309
Thermodynamic definition of temperature, 34
Thermodynamic diagrams, 34
($\alpha$,$-p$)-, 18, 29, 300
emagram, 35
height evaluation on, 115
important criteria of, 35
precipitation lines on, 143
saturation adiabats on, 74
Stüve, 30, 35
($T$,$e$)-, 49
tephigram, 38, 74
vapor lines on, 61, 74
Thermodynamic potential, 48
Thermodynamic surface of water substance, 56
Thermodynamics, first law, of 21
Time, dimension of, 2
units of, 5, 155
Ton (metric), 5
Ton mole, 14
Transformation, latent heat of, 46
Transformation temperature, 48
Transport, of mass in surface layer, 239
vertical heat, 139
vertical momentum, 237, 248
Transport capacity of isobaric channels, 263
Transversal divergence, 264, 271
Triple point, 50, 51, 53
Triple product, scalar, 166
Triple state, 41, 42
Turbulence, 248

Unit channel, isobaric, 100
Unit layer, equiscalar, 97
geopotential, 94
isobaric, 82, 102
Unit normal, 148
horizontal, 173
Unit tangent, 146
Unit vectors, 85
natural, 151, 173

Unit vectors, rectangular, 86
Units, cgs, 5, 6
  English, 7
  mts, 4, 6
Universal gas constant, 15
Unsaturated adiabat, 65, 139
Unsaturated-adiabatic lapse rate, 129, 139
Unsaturated-adiabatic process, 64
Unsaturated air, 62
  adiabatic process of, 65
Unsaturated stage, 62
Unstable equilibrium, 127, 130, 138
U. S. standard atmosphere, 119
U. S. Weather Bureau hydrostatic tables, 114

Väisälä scales on emagram, 115
Vapor, water, equation of state of, 44
    specific gas constant of, 44
    specific heats of, 45
Vapor lines on diagram, 61, 74
Vapor pressure, 40, 58, 61
  saturation, 40, 48, 57
    over ice, 52
    over water, 50
Variables, moisture, 57
  physical, 9, 32
    fields of, 82
Vector(s), 85
  components of, 85
  differentiation of, 146, 165, 251, 312
  irrotational, 333
  line integral of, 295, 296
  natural components of, 174
  position, 145
  potential, 96, 333
  projections of, 174
  rectangular components of, 85, 174
  resultant of, 84, 86
  scalar product of, 87
  scalar triple product of, 166
  unit, 85
  vector product of, 164
Vector area, 260, 315, 316
Vector curvature, 151
Vector product, 164
  components of, 165
Vector radius of curvature, 151
Velocity, 3, 145; *see also* Speed
Velocity, absolute, 168
  angular, 3, 163
    of the earth, 163, 183
  dimensions of, 3
  geostrophic, 210, 233–4
  geostrophic deviation, 234, 244
  hodograph of, 148
  of a point of the earth, 167
  of propagation, 255
  relative, 168
  units of, 6
Velocity potential, 334
Vertical curvature, 182
Vertical equation, 187
Vertical heat transport, 139
Vertical momentum transport, 237, 248
Vertical motion, in cumulus convection, 136
  in long waves, 283
  in stable oscillation, 131
  kinetic energy of, 132
Vertical path, 182
Vertical plane, 182
Virtual gravity, 187
Virtual potential temperature, 66
Virtual temperature, 63, 67
Viscosity, eddy, 247
  molecular, 236, 237
Viscous stress, 235
Volume, 2, 9
  molar, 14
  specific, 3, 6, 9
Volume ascendent, 301
  isobaric, 213
Vortex, circular, 308
    local, 319
Vorticity, 320
  absolute, 322
  anticyclonic, 323
  cyclonic, 323
  in natural coordinates, 321
  in rectangular coordinates, 321
  relative, 322
  sense of, 323
  theorem of absolute, 323
  theorem of relative, 324
Vorticity theorem, of Helmholtz, 324
  of Rossby, 324

Water, density of, 5, 44

Water, thermal properties of, 44
Water substance, critical constants for, 42
  isotherms of, 40, 41, 56
  phases of, 42, 50, 56
  thermodynamic surface of, 56
Water vapor, equation of state of, 44
  molecular weight of, 44
  specific heats of, 45
Wave, baroclinic, 279, 360
    dynamic instability of, 286
    formation of, 281
    speed of, 274
  barotropic, 274, 341
    pressure field in, 347
    speed of, 276, 356
  pressure changes in, 274, 276, 281, 357
  speed of, 269
Wave length, 269
  of streamline and path, 329, 343
Wave number, 269
  angular, 269
Wave-shaped flow pattern, 264, 328, 341
Weight, molecular, 14
    of dry air, 17
    of mixture of perfect gases, 17
    of water vapor, 44
  of atmospheric column 103, 286
Wet bulb potential temperature, 76
Wet bulb temperature, 77, 78
Wind, cyclostrophic, 199
  geostrophic, 192, 210
  gradient, 189, 200
  relative zonal, 268
  shear of, 212, 218, 322
  thermal, 212, 309
  zonal, 160
Wind distribution in the surface layer, 241
Wind shear in the surface layer, 244
Work, 3, 5, 6, 7
  in thermodynamics, 17
  of gravity, 91

Zonal circle, 156
Zonal flow, 158, 170, 306
  absolute and relative, 158, 170
  acceleration in, 159, 171
  angular speed in, 160
  circulation in, 314
  equilibrium of, 308
  pressure field in, 161
  solenoids in, 307, 361
  thermal wind in, 309
Zonal front, 227
Zonal plane, 156
Zonal wind, relative, 268